

ARC FURNACE AND SHUNT REACTIVE COMPENSATION MODELLING

FOR VOLTAGE FLICKER REDUCTION

Thesis submitted in accordance with the requirements of

the University of Liverpool for the degree of

Doctor in Philosophy

by

Ian Christopher Davis

December 1985



IMAGING SERVICES NORTH

Boston Spa, Wetherby
West Yorkshire, LS23 7BQ
www.bl.uk

BEST COPY AVAILABLE.

VARIABLE PRINT QUALITY



IMAGING SERVICES NORTH

Boston Spa, Wetherby
West Yorkshire, LS23 7BQ
www.bl.uk

MISSING PRINT

SUMMARY

This thesis describes the modelling of a 56MVA electric arc furnace installation and its high voltage supply from 275kV. Models were constructed both in the laboratory, and mathematically using a mainframe digital computer. In both cases an investigation of the supply voltage distortion was carried out, with the disturbances that cause complaint from other consumers at the lowest distortion level being identified as the visible flickering of tungsten filament lamps. Model static shunt reactive compensators were applied to each system model, in order to reduce the voltage flicker annoyance levels caused by a given arc furnace demand.

Both arc furnace models utilised digital recordings of 33kV three-phase currents to reproduce measured supply voltage distortion.

The laboratory model system had a three-phase rating of 452VA, using an AIM-65 8-bit microcomputer and commercial power amplifiers to draw non-sinusoidal currents from a 175V supply.

The mathematical model used the same 1.8 sec data span of recorded current data to generate distorted supply voltage waveforms. The step-by-step solution of differential equations allowed a theoretical performance study of a six-pulse static shunt compensator.

Different thyristor-controlled reactor (TCR) schemes were applied to the laboratory arc furnace model, with fast phase angle control of conduction achieved with a voltage-integral algorithm using Intel 8088 16-bit microprocessor. The TCR control methods are fully described, with theoretical and experimental performance studies.

The results use power spectrum analysis and an internationally recognised flickermeter to show that the compensation methods reduced flicker levels, giving an improvement factor of 40 percent.

ACKNOWLEDGEMENTS

I gratefully record my obligation to my supervisor, Mr D R Turner, for his sustained guidance and encouragement with the work contained in this thesis, and to Professor J D Parsons for the use of the facilities of the Department of Electrical Engineering and Electronics.

I would like to make special acknowledgements to Mr P H Ashmole, Mr G E Gardner, Mr W B Jervis and their colleagues at the Central Electricity Generating Board for providing financial and technical support throughout the period of this research project.

Members of the University of Liverpool's staff have helped in many ways, and amongst them I wish especially to thank Dr C G Goodyear, for an insight to the frequency domain, Mr P Watkinson, Mr A Noble and Mr K Meador, who showed patience and understanding, and the staff of the computer laboratory.

Finally, thank you Claire, for your dedication and perseverance.

This work was supported by the Science and Engineering Research Council with the Central Electricity Generating Board under the CASE award scheme.

CONTENTS

	<u>PAGE</u>
I INTRODUCTION	1
1.1 THE ARC FURNACE LOAD	2
1.1.1 Electrical Supply to Arc Furnaces	2
1.1.2 Supply Voltage Distortion	2
1.2 SHUNT REACTIVE COMPENSATION	4
1.2.1 Compensation for Arc Furnaces	4
1.2.2 Thyristor Controlled Reactors for Flicker Reduction	5
1.3 DIGITAL COMPUTER CONTROL OF POWER EQUIPMENT	6
1.3.1 Applications of Digital Control	6
1.3.2 Digital Control of Thyristor Switches	7
1.3.3 Microprocessor Control of a TCR Compensator	7
1.4 MODELLING	8
1.4.1 Physical Modelling of Static Compensators	8
1.4.2 Digital Modelling of Compensator Systems and Flicker	9
II MODELLING OF AN ARC FURNACE	10
2.1 REQUIREMENTS FOR A PHYSICAL MODEL	11

CONTENTS (cont'd)

	<u>PAGE</u>
2.2 THE SYSTEM TO BE MODELLED	13
2.2.1 The Templeborough Installation and its Supply	13
2.2.2 Measurements made at 33kV	17
2.2.3 Selection of Data	18
2.3 THE PHYSICAL MODEL	22
2.3.1 The Model's Supply	22
2.3.2 Line Current Reproduction	22
2.3.3 Impedance Scaling	34
2.3.4 Safety Sequence	44
2.4 RESULTS	45
2.4.1 Line Current Waveforms	46
2.4.2 Voltage Waveforms	46
2.4.3 Power Spectra of Voltage Waveforms	48
III FLICKER AND ITS REDUCTION	59
3.1 FLICKER	60
3.1.1 V_f - A Flicker Voltage	50
3.1.2 Frequency Dependence of Flicker	60
3.1.3 Annoyance Levels	62

CONTENTS (cont'd)

	<u>PAGE</u>
3.2 THE ELECTRIC ARC FURNACE AS A FLICKER SOURCE	65
3.2.1 The Arc Furnace Melt Cycle	65
3.2.2 Composition of Melt Baskets	68
3.2.3 Operators and Electrode Control Systems	68
3.2.4 Voltage Distortion due to an Electric Arc Furnace Installation	69
3.3 FLICKER LEVELS ON A PARTICULAR FURNACE SUPPLY AND ITS LABORATORY MODEL	73
3.3.1 Study for the Templeborough Installation	73
3.3.2 Study for the Physical Model	76
3.4 FLICKER REDUCTION	79
3.4.1 Shunt Reactive Compensation	79
3.4.2 The Rating of a Reactive Compensator	82
3.4.3 Control of Static Shunt Reactive Compensators	90
3.4.4 Performance of Installed Reactive Compensators	94
IV A SIX-PULSE THYRISTOR-CONTROLLED REACTOR	97
4.1 THE LABORATORY MODEL THYRISTOR-CONTROLLED REACTOR	98
4.1.1 Modelling Requirements	98
4.1.2 Control Requirements	108

CONTENTS (cont'd)

	<u>PAGE</u>
4.2 MICROPROCESSOR CONTROL	112
4.2.1 System Operations	112
4.2.2 Sampling	114
4.2.3 The Control Algorithm	118
4.2.4 Control Variables	123
(i) Sample Loop Delay	123
(ii) Reference Sinusoid	125
(iii) Integration Limit	129
4.3 STEADY-STATE TUNING AND PERFORMANCE	132
4.3.1 Thyristor Firing and Conduction Limits	132
4.3.2 Phase Balancing	134
4.3.3 Steady-State Reactive Compensation Theory	135
(i) Open Circuit Voltage Control	139
(ii) Shunt Load TCR Compensation	142
4.4 USE OF THE TCR UNDER NON-SINUSOIDAL CONDITIONS	150
V SIX PULSE TCR RESULTS	152
5.1 STEADY STATE TCR COMPENSATOR PERFORMANCE	154
5.1.1 Open Circuit Voltage Control	154
5.1.2 Shunt Load Compensation	158

CONTENTS (cont'd)

	<u>PAGE</u>
5.2 ANALYSIS OF VOLTAGE DISTORTION	162
5.2.1 Spectral Analysis	162
5.2.2 Data Logging	164
5.3 TCR PERFORMANCE WITH THE ARC FURNACE MODEL	166
5.3.1 Frequency Domain Study of Compensator Action	166
5.3.2 Time Domain Study of Compensator Action	177
5.4 ESI FLICKERMETER STUDIES	183
5.4.1 The Use of the Digital Flickermeter	183
5.4.2 Arc Furnace Model without TCR Compensator	185
5.4.3 Arc Furnace Model with TCR Compensator	185
VI A TWELVE-PULSE THYRISTOR-CONTROLLED REACTOR	189
6.1 MODELLING AND CONTROL	191
6.1.1 Modelling Requirements	191
6.1.2 Conduction Patterns	193
6.1.3 Control Requirements	193
6.1.4 Control Variables	199
(i) Sample Loop Delay	199
(ii) Reference Sinusoid	200
(iii) Integration Limit	201

CONTENTS (cont'd)

	<u>PAGE</u>
6.2 STEADY-STATE TUNING AND PERFORMANCE	202
6.2.1 Thyristor Firing and Conduction Limits	202
6.2.2 Steady-State Reactive Compensation Results	202
6.3 TWELVE-PULSE TCR PERFORMANCE WITH THE ARC FURNACE MODEL	206
VII COMPUTATIONAL MODELLING AND ANALYSIS	214
7.1 THE PRINCIPLE OF THE COMPUTATIONAL MODEL	215
7.1.1 The System to be Modelled	215
7.1.2 Measured and Calculated Currents and Voltages	216
7.1.3 Inputs to the Arc Furnace Model	220
7.1.4 Phase Angle ' δ '	220
7.2 Y- Δ TRANSFORMER CURRENT AND VOLTAGE TRANSFORMATIONS	222
7.2.1 Current Transformation	222
7.2.2 Voltage Transformation	224
7.2.3 Current Derivative Transformation	225

CONTENTS (cont'd)

	<u>PAGE</u>
7.3 PERFORMANCE OF THE COMPUTATIONAL ARC FURNACE MODEL	226
7.3.1 Results Comparison Using Power Spectra	226
7.3.2 Results Comparison in the Time Domain	229
7.3.3 Demodulation	230
7.4 COMPUTATIONAL MODELLING OF A TCR COMPENSATOR	238
7.4.1 TCR Compensator Circuit Definitions	238
7.4.2 The Differential Equations of Compensator Currents	240
7.4.3 Step-by-Step Solution of Compensator Differential Equations	243
7.4.4 Compensator Control	244
7.4.5 Results from the Computer Model Compensator	246
VIII DISCUSSION, CONCLUSIONS AND FURTHER WORK	253
8.1 DISCUSSION	254
8.1.1 The Laboratory Arc Furnace Model	254
(i) Current Waveform Reproduction	254
(ii) Voltage Waveform Reproduction	256

CONTENTS (cont'd)

	<u>PAGE</u>
8.1.2 The Laboratory TCR Model	257
(i) The Six-Pulse TCR Compensator	257
(ii) The Twelve-Pulse TCR Compensator	259
8.1.3 Data Analysis	260
8.1.4 Mathematical Modelling	261
8.2 CONCLUSIONS	263
8.3 FURTHER WORK	264
REFERENCES	265
APPENDIX A: Short Circuit Power of 56MVA Arc Furnace	276
APPENDIX B: Recovery of CEGB Data from Magnetic Tape Storage	279
APPENDIX C: Cubic Spline Curve-Fitting and its Application	283
APPENDIX D: AIM-65 Microcomputer Operation and Program Listings	297
APPENDIX E: Safe-Start Sequence for the Laboratory Model	310
APPENDIX F: Six-Pulse TCR Control Program	313

CONTENTS (cont'd)

	<u>PAGE</u>
APPENDIX G: FORTRAN Spectrum Analysis Package	323
APPENDIX H: Data Logging	336
APPENDIX J: Computational Arc Furnace Model- Program Listing	341
APPENDIX K: Twelve-Pulse TCR Control Program Listing	359
APPENDIX L: Published Papers	367

GLOSSARY AND ABBREVIATIONS

- α The phase angle between voltage peak and start of inductive current conduction. Units: Degrees.
- α The phase angle between voltage zero-crossing and start of inductive current conduction. Units: Degrees.
- ϵ The phase angle between voltage zero-crossing and start of 'first-stage' inductive current conduction in the twelve-pulse TCR only. Units: Degrees.
- δ The phase angle by which arc furnace busbar voltage lags 'infinite busbar' voltage. Units: Degrees.
- σ A phase angle used for calculation of voltage depression. Equal to $(180^\circ - \alpha)$. Units: Degrees.
- ω Angular frequency, $2\pi f$. Units: Radians/sec.
- ω_c Filter cut-off frequency. Units: Radians/sec.
- Δ A three-phase circuit connection arrangement.
- p.c. Percent.
- p.f. Power factor.
- p.u. Per unit.
- Ⓐ Preceeds a hexadecimal number.
- ACE Association of Chief Engineers (UK)
- ADC Analogue to digital converter.
- C Three-phase TCR compensator rating. Units: VA.

GLOSSARY AND ABBREVIATIONS (cont'd)

- [C] A three-phase transformation matrix.
- $[C_t]$ The transposed matrix of [C].
- CEGB Central Electricity Generating Board (UK)
- CIGRE Centre International des Grandes Reseaux Electriques
- CIRED Conference International des Reseaux Electrique de Distribution
- CVRY The time series values of computationally calculated $v_R - v_Y$.
- D Sample loop delay. Units: Seconds.
- DAC Digital to analogue converter.
- DCVRY The time series of computationally demodulated values of calculated $v_R - v_Y$.
- DFT Discrete Fourier transform.
- DMVRY The time series of computationally demodulated values of recorded $v_R - v_Y$.
- E A continuous integration sum. Units: Volt seconds.
- EDF Electricite de France
- EPROM Erasable programmable read-only memory.
- ERA Electrical Research Association (UK)
- ESI Electricity Supply Industry (UK)

GLOSSARY AND ABBREVIATIONS (cont'd)

F	Arc furnace three-phase rating. Units: VA.
FFT	Fast Fourier transform.
F_N	Nyquist frequency. Units: Hertz.
F_S	Sampling frequency. Units: Hertz.
FSD	Full scale deflection.
IEE	The Institution of Electrical Engineers (UK)
IEEE	The Institute of Electrical and Electronic Engineers (USA)
IMP	Flicker improvement factor.
I_{RYB}	The vector representing the three-phase currents i_R, i_Y and i_B .
i_{TH}	Thyristor holding current. Units: Amperes.
i_{TL}	Thyristor latching current. Units: Amperes.
L_C	The inductance connected in each branch of a three-phase TCR. Units: Henries.
LIMIT	Discrete sample integration limit. Units: Volts.
M	Mutual inductance. Units: Henries.
MUSDU	Multi-user microprocessor system development unit.
MVRY	The time series recordings of $v_R - v_Y$ stored and used computationally.

GLOSSARY AND ABBREVIATIONS (cont'd)

N	Transformer voltage ratio.
N_q	Quantisation noise. Units: dB w.r.t. signal level.
PCC	Point of common coupling.
R	Resistance. Units: Ohms.
RAM	Random access memory.
S_c	Fault level. Units: VA.
S_t	Short circuit power. Units: VA.
SGT	Super-grid transformer (275/33kV).
TCR	Thyristor controlled reactor.
TNA	Transient network analyser.
UIE	Union International Electrotechnic
VIA	Virtual interface adaptor.
V_{RMS}	RMS voltage. Units: Volts.
v	Instantaneous voltage.
v_f	Flicker voltage. Units: Volts.
V_{fg}	Gauge point fluctuation voltage.
v_R	A constant sinusoid used for reference in an integration process.

GLOSSARY AND ABBREVIATIONS (cont'd)

- V_t Short circuit voltage depression. Units: Percent.
- VDU Visual display unit.
- X Reactance. Units: Ohms.
- Z Complex impedance $R + jX$. Units: Ohms.

CHAPTER ONE

INTRODUCTION

1.1 THE ARC FURNACE LOAD

1.1.1 Electrical Supply to Arc Furnaces

1.1.2 Supply Voltage Distortion

1.2 SHUNT REACTIVE COMPENSATION

1.2.1 Compensation for Arc Furnaces

1.2.2 Thyristor Controlled Reactors for
Flicker Reduction

1.3 DIGITAL COMPUTER CONTROL OF POWER EQUIPMENT

1.3.1 Applications of Digital Control

1.3.2 Digital Control of Thyristor Switches

1.3.3 Microprocessor Control of a TCR
Compensator

1.4 MODELLING

1.4.1 Physical Modelling of Static
Compensators

1.4.2 Digital Modelling of Compensator
Systems and Flicker

1.1 THE ARC FURNACE LOAD

1.1.1 Electrical Supply to Arc Furnaces

Arc furnace installations have a well-established reputation as sources of harmonic and sub-harmonic disturbances of the supply system voltage^[1,2,3]. Being rapidly fluctuating loads, their large electrical rating requires that they be connected at points on the supply system having a low source impedance. The allowable level of resulting voltage distortion is fixed by the electricity supply authority; customers proposing to install such plant face not only the capital cost of their own equipment, but also the costs incurred by the supply authority in strengthening or segregating the supply to that installation. These costs, for arc furnaces up to 40MVA, were debated as early as 1963 during the discussion period following an IEE symposium on transient, fluctuating and distorting loads^[2,3,4,5]. At that time, the sum of £300,000 was agreed reasonable to achieve suitable segregation.

This economic factor has naturally made necessary a precise calculation of the level of segregation required, in conjunction with a detailed study to define acceptable levels of supply voltage distortion.

The UK Electricity Council issued guidelines in 1970 in the form of an Engineering Recommendation P7/2, 'Supply to Arc Furnaces'^[6] that is now well known. The UK Association of Chief Engineers (of the supply industry) followed this document with their own detailed report^[7], which explored the subject in greater depth.

1.1.2 Supply Voltage Distortion

The voltage distortion effect of the arc furnace load has been the subject of discussion and research for over twenty years^[3]. This type of distortion causes annoyance by the visible flickering of tungsten filament lamps. This occurs even at low levels of voltage distortion, due to the fourth power relationship between voltage and light output.

In the UK, Dixon, Kendall and Thomas have published results of many studies^[4,5,8,9] into the annoyance effects of such lamp flicker caused by different types of supply voltage distortion. In 1963 Kendall advocated the need for a flicker meter and its proper application, and further research into the nature of arc furnace voltage distortion followed^[10,11,12,13], with work towards the development of a flicker meter being carried out both in the UK^[14,15,16] and abroad^[17,18]. Internationally, the 'Union International Electrothermie' (UIE) has co-ordinated the efforts towards flicker evaluation through its Disturbances Study Committee (DSC), and its flicker measuring methods working group published a valuable review of arc furnace disturbances^[19] and found common agreement for a flicker measuring method^[20], resulting in the internationally standardised flicker meter now used by the UK Electricity Supply Industry (ESI)^[16].

1.2 SHUNT REACTIVE COMPENSATION

Shunt reactive compensation techniques are well established as a means of controlling power system voltages^[21,22,23]. Mechanical switching of inductors and capacitors could only compensate for relatively slow reactive load variations, and a faster response was obtained by excitation control of synchronous rotating machines^[24].

Rapidly fluctuating loads, particularly the arc furnace, demanded a speed of response even faster than could be obtained from the synchronous compensator, and in the early 1960s static compensator systems utilising saturated iron^[25,26] were installed at arc furnace installations with some success^[27,28,29,30].

1.2.1 Compensation for Arc Furnaces

The UK Electricity Council published a document 'Compensators for Arc Furnaces'^[31], which with other review documents^[19,32,33,34,35] identified thyristor-switched reactive devices as having potential for flicker compensation duties, with the general reservation that practical experience at that time was limited and their performance had then to be established.

A large amount of research and application of thyristor-controlled reactive compensators followed, with early success for transmission system voltage control. The literature contains many detailed reports of such work, and many of those up to 1982 are referenced in a bibliography of static VAR compensators, published by the IEEE^[36].

1.2.2 Thyristor Controlled Reactors For Flicker Reduction

The control systems utilised to obtain the required compensator performance vary between manufacturers. The reactive compensator theory and control methods applicable to flicker reduction have been included in many publications [32,37,38,39,40,41,42], but evidence of the successful application of thyristor-controlled equipment for flicker reduction is not so widespread. Those schemes which show flicker improvement [43,44,45,46] use thyristor-controlled reactors as the variable VAR element, with fixed capacitors for filtering and power factor improvement. Measurement methods used to demonstrate their efficacy comprise both power spectrum analysis and different 'flickermeter' equipment.

The successful control methods are rarely presented in detail, for sound commercial reasons. However, a digital control system can be made flexible enough to allow its application to a variety of different control strategies. This digital approach, using minicomputers or microprocessors, offers the capability for greatest speed and accuracy of control.

1.3 DIGITAL COMPUTER CONTROL OF POWER EQUIPMENT

This research project makes extensive use of modern digital techniques for the control of laboratory power equipment. To show that such work may be of use in the environment for which it is eventually intended, a brief review of previous applications follows.

1.3.1 Applications of Digital Control

The many advantages of using computer control, for almost any scheme, are now well-known and widely accepted. Primary reasons for their wide application are:

- (i) Arithmetic processing power and accuracy
- (ii) Flexibility
- (iii) Cost
- (iv) Ease of monitoring and data logging

Initial applications to power equipment included simple sequence controllers and data loggers, and early problems of size, component reliability and electromagnetic interference and isolation have now been largely overcome. The last five years have seen the development of an extremely wide range of low cost robust programmable logic controllers for process control in an industrial environment, and dedicated systems are easily designed for high speed control of specific equipment such as power equipment protection and control^[47,48,49,50] and HVDC Converter Control^[51,52,53,54].

1.3.2 Digital Control of Thyristor Switches

Fibre-optic isolation techniques, effective electromagnetic screening and 'hardening' of sensitive equipment now allows digital controllers working at ground potential to control thyristor switch assemblies at voltages in excess of 33kV.

Thyristor technology has advanced rapidly, allowing simpler and more effective switch assemblies to be built. Recent advances include symmetric and asymmetric light-triggered thyristors, controlled turn-on, gate-assisted turn-off, and voltage break-over protection [55,56,57,58,59,60].

1.3.3 Microprocessor Control of a TCR Compensator

A microprocessor controller has not, to the author's knowledge, yet been applied to a full-scale TCR compensator scheme. A control system is presented in this thesis, and the available technology demonstrated in other engineering schemes may be suitably applied to this system.

1.4 MODELLING

Historically, modelling has been used by researchers to overcome difficulties in understanding caused by the size or complexity of the real system. Scale models, with all parameters under the control of the researcher, give savings in both the cost of equipment and the time required for the solution of a problem.

More recently, the advent of the digital computer has allowed researchers to extend mathematical modelling to include the most complex of systems.

These two types of modelling - physical and mathematical - have been represented in various studies into shunt static compensation techniques and the nature of voltage flicker.

1.4.1 Physical Modelling of Static Compensators

Cooper and Yacimini presented a review of modelling methods at the 1979 IEE seminar, 'Reactive Compensation in Power Systems'^[51], and concluded that small scale physical modelling of thyristor controlled devices was a valuable study method, whilst warning of a reduced X/R ratio and the need for a wide frequency response.

Many papers show how Transient Network Analysers (TNAs) can be applied for physical modelling of static compensators and networks^[62,63,64,65], but the TNA is not generally applied to an evaluation of static compensator performance for voltage flicker reduction. A difficulty appears to be the generation of a suitably distorted voltage waveform, accurately reproducing the frequency components causing flicker effect.

The results of other forms of static compensator physical modelling have recently been presented^[66,67], and this thesis treats aspects of this work in greater depth.

1.4.2 Digital Modelling of Compensator Systems and Flicker

The advent of the digital computer allowed the study of network transient phenomena by the step-by-step solution of differential equations. Domme[68,69,70,71] has published widely on this subject, and he demonstrates how various system components may be represented in the differential equations^[68] of a general numerical model. The computational step-width is identified as an important factor in non-linear circuit solutions^[69] and frequency dependence of components, especially lines, is accommodated using convolution between the frequency domain and the time domain^[71]. The frequency dependence of parameters in digital models is further discussed by Budner^[72] and Marti^[73], while Feero, Juvet and Long^[74] give a study of the mathematical modelling of power system components.

Particular cases of computer modelling applied to static compensators are few^[13,75,76]. Arc furnace load modelling has been attempted^[76,77,78,79] and both of these subjects are explored further in this thesis.

Digital models studying voltage flicker^[13,14,76,80] have used either voltage waveforms synthesised from low frequency sinusoids, or they have utilised recordings of arc furnace currents to aid the study of the flicker effect.

The basis for work in this thesis is that in order to model system voltage disturbances, the use of measurements of real arc furnace currents will offer the most realistic tests of performance for any model static compensator. This principle is applied for both a physical model in the laboratory and a mathematical model on a digital computer.

CHAPTER TWO
MODELLING OF AN ARC FURNACE

2.1 REQUIREMENTS FOR A PHYSICAL MODEL

2.2 THE SYSTEM TO BE MODELLED

2.2.1 The Templeborough Installation and its Supply

2.2.2 Measurements made at 33kV

2.2.3 Selection of Data

2.3 THE PHYSICAL MODEL

2.3.1 The Model's Supply

2.3.2 Line Current Reproduction

2.3.3 Impedance Scaling

2.3.4 Safety Sequence

2.4 RESULTS

2.4.1 Line Current Waveforms

2.4.2 Voltage Waveforms

2.4.3 Power Spectra of Voltage Waveforms

2.1 REQUIREMENTS FOR A PHYSICAL MODEL

The aim of modelling an arc furnace and its electrical supply is simply to reproduce in the laboratory the type of voltage disturbances found in the full-scale case. If this can be done successfully, then any modifications made in the laboratory having an effect on the voltage fluctuations should have a full-scale parallel. In particular a means of reducing those voltage disturbances causing tungsten-filament lamp flicker by means of shunt compensation may be sought. Synthesized currents may have some value for investigating the annoyance factors of different combinations of disturbances at different frequencies, but for a practical study involving current compensation, it must be necessary to use load currents modelling actual currents as closely as possible, to make the results most relevant.

In its broadest terms, the Templeborough system to be modelled comprises:

(i) From the supply system:

An 'infinite busbar', or supply having a source impedance which is very low compared to the impedances of the components that it supplies. Thus the supply voltage is practically independent of the current drawn from it.

(ii) At the 'furnace busbar':

A load, drawing non-sinusoidal currents described by recordings made at this voltage. These are not the furnace line currents, but the currents drawn by the primary of the 33kV/500 V furnace transformer.

(iii) Between (i) and (ii) above:

A complex impedance representing the lumped parameters of components between the 'infinite busbar' and the load.

The infinite busbar can be modelled simply by using a suitable low-impedance, three phase supply. The load will require some device or devices that, when driven by a continuous signal derived from the recordings of the currents at 33kV, will faithfully reproduce the waveform at a suitable magnitude of current in each of the three phases.

The impedances present between supply and load can be modelled using components with values of complex impedance such that, for given base levels of current and voltage, their per unit impedance is as close as possible to that found in the full scale system.

2.2 THE SYSTEM TO BE MODELLED

In June of 1977 the System Technical Branch of the CEGB Headquarters organised a programme of measurements on an arc furnace supply at 33kV. The measurements were made at the Templeborough 275kV/33kV substation, which supplied six arc furnaces having a collective nameplate rating of 360MVA.

The aim of the exercise was to investigate the supply voltage 'flicker' fluctuations (see Chapter III) and harmonics produced by arc furnace operation. The three-phase current waveforms were recorded simultaneously with the voltage waveforms, and a record of relevant stages in the arc furnace melt cycles was kept. The varying electrical characteristics of single and multi-furnace operation could, therefore, be obtained.

2.2.1 The Templeborough Installation and its Supply

The six arc furnace transformers are supplied at 33kV from five 275/33kV supergrid transformers (SGTs) local to the steelworks. The SGTs are connected to the 275kV Sheffield ring between the Brinsworth and Pitsmoor switching stations (Figure 2.1).

The fault level on the Sheffield 275kV ring was 8500MVA, the system reactance being:

$$X_s = \frac{\text{Base VA}}{\text{Fault Level}}$$

$$= 1.18\text{p.c. on } 100\text{MVA base}$$

The fault level at the 33kV 'furnace busbar' is governed by the configuration of SGT transformers connected to it. Measurements (detailed further in 2.2.3 below) were taken on the left hand side of the split 33kV busbar shown in Figure 2.1. This enables a simplified supply diagram to be drawn (Figure 2.2) which also shows the impedances of each component.

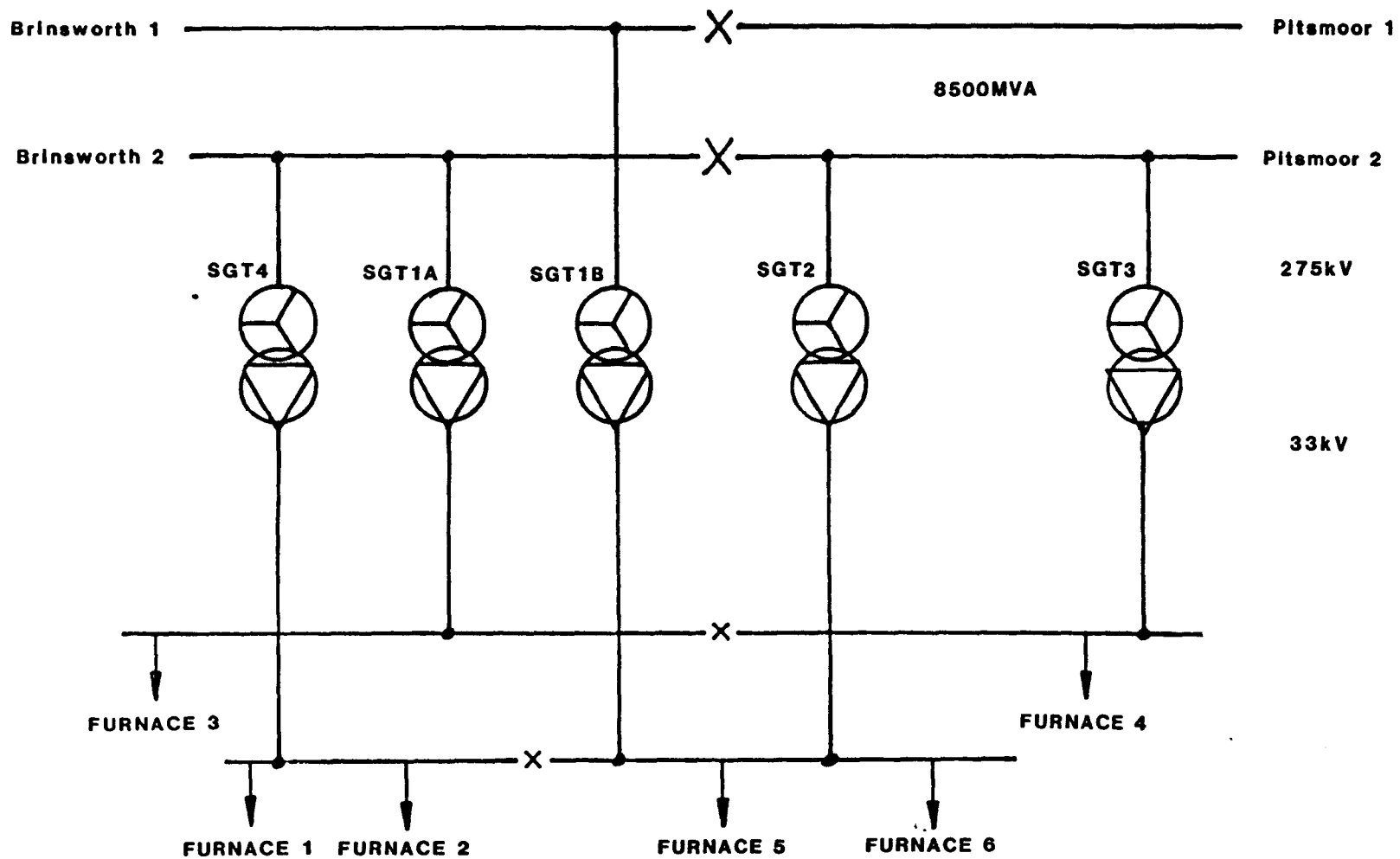


Fig. 2.1 : Templeborough arc furnace installation - supplies from 275kV

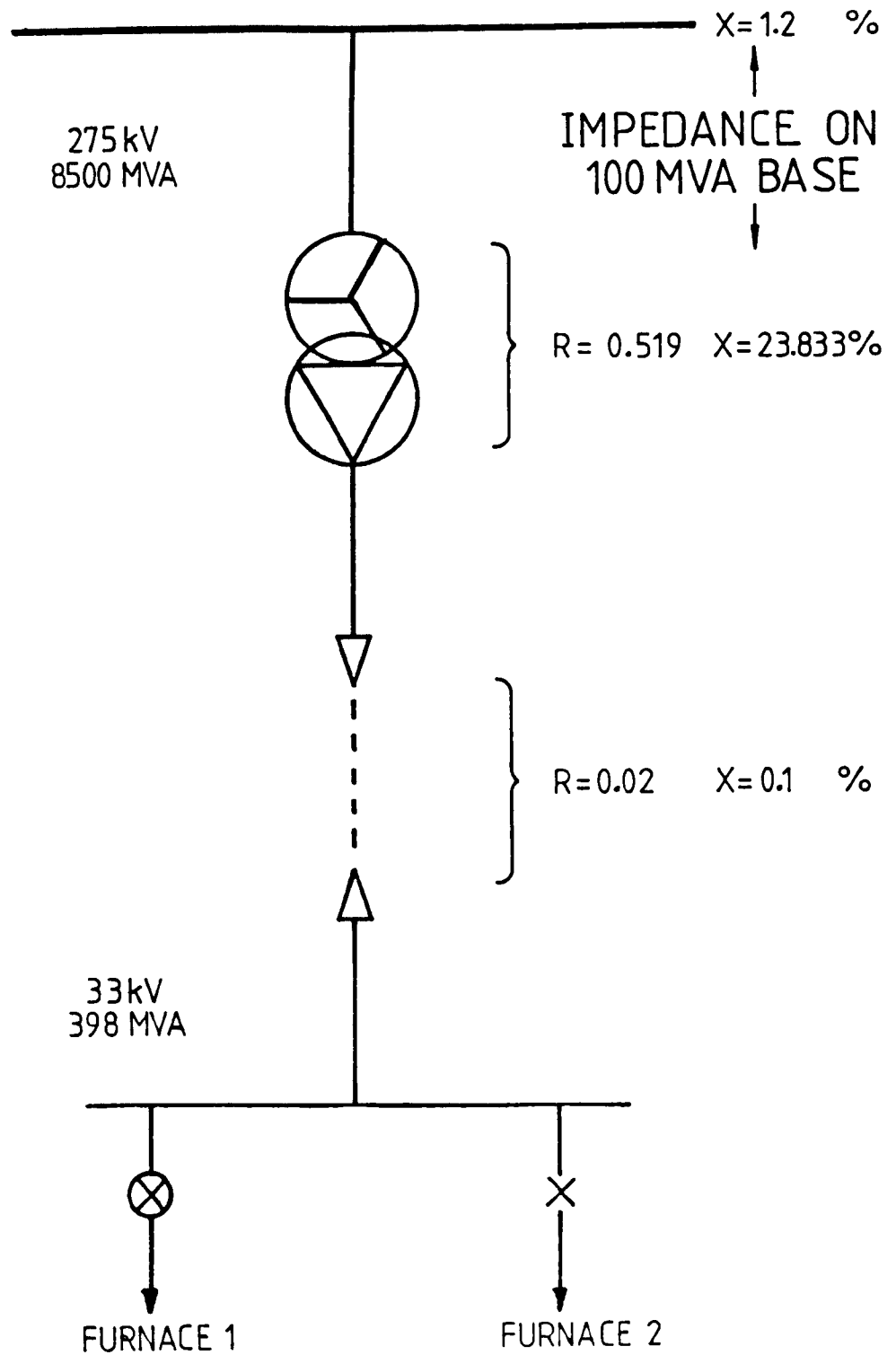


Fig. 2.2 : Simplified supply diagram for Templeborough furnaces 1 & 2

The total system impedance for the 33kV busbar is therefore:

$$\begin{aligned} Z_{\text{tot}} &= (0 + j 1.2)\text{p.c.} && 275\text{kV supply} \\ &+ (0.519 + j 23.833)\text{p.c.} && \text{SGT 4} \\ &+ (0.02 + j 0.1)\text{p.c.} && 33\text{kV cable} \end{aligned}$$

$$Z_{\text{tot}} = 0.539 + j 25.133\text{p.c. on 100MVA base}$$

The X/R ratio, or 'Q factor' for the supply circuit is then:

$$\underline{Q = 46.6}$$

The individual furnace 33kV/500 V Δ - Δ transformers are not considered here because there are no records for the currents and voltages in the secondary circuits.

Also not shown in Figures 2.1 and 2.2 is a Y-Y connected earthing transformer for the 33kV circuit. This transformer has a high impedance connected from the primary star-point to earth, to ensure that the otherwise isolated system does not depart from an earth reference. This transformer was judged to be unimportant in that its contribution towards the source impedance and its effects on current imbalances were negligible.

There were no connections to other consumers at 33kV, therefore the Point of Common Coupling (PCC) is at 275kV.

The short circuit level, S_C , of the furnace installation is shown in Appendix A to be 87.46MVA. The importance of this value relative to the fault level at the point of common coupling is discussed further in Part 3.3, with particular emphasis on the voltage flicker levels that are to be expected.

2.2.2 Measurements made at 33kV

Data acquisition at the Templeborough installation was by means of a digital recording and measuring (DREAM) system which has been widely used in power system studies^[81,82].

The equipment and its possible operating modes are described in great detail in CEGB internal documents and need not be repeated here. However, the principal features of the mode used at Templeborough are:

- (i) Simultaneous sampling of eight analogue signals every 800 microseconds.
- (ii) Each sample has 15 data bits plus one sign bit. Quantisation noise is thus -90dB relative to the full scale signal.
- (iii) Digital storage on magnetic tape in blocks of 2048 Bytes up to a maximum of 30 MBytes per tape.

Long-term studies may be made using repetitive short samples, but for this application a continuous stream of data was recorded, the length of which is limited only by the magnetic tape spool capacity.

Recordings of line current were made using current transformers (CTs) developing a voltage across resistors for conversion to a digital value.

Y-connected 33kV/110V voltage transformers (VTs) supplied the three phase voltages for ADC conversion. It could not be ascertained whether the star point of these VTs was connected to any neutral or earth reference. The continually changing imbalance of the system voltages and a floating star point may then have given rise to measurement of 'phase' voltages unrepresentative of the true system phase voltages.

To eliminate the possibility of studying misleading voltage measurements, the equivalent line voltages were calculated for every set of data samples. These derived line voltages were then independent of any neutral reference, and would give a true measurement of the three phase system voltages.

2.2.3 Selection of Data

Study of the reproduction of large amounts of Templeborough data by chart recorder at CEGB headquarters revealed a particularly interesting section. The record corresponded to one 56MVA furnace operating in isolation from others, and effectively supplied through its own supergrid transformer (SGT).

The data for this period was transferred to magnetic tape for use at Liverpool University. Appendix B describes in detail the operations required to recover analogue data from the digital magnetic tape recordings supplied to the University. The voltage and current recordings used for the studies are shown in Figures 2.3 (a),(b) and (c).

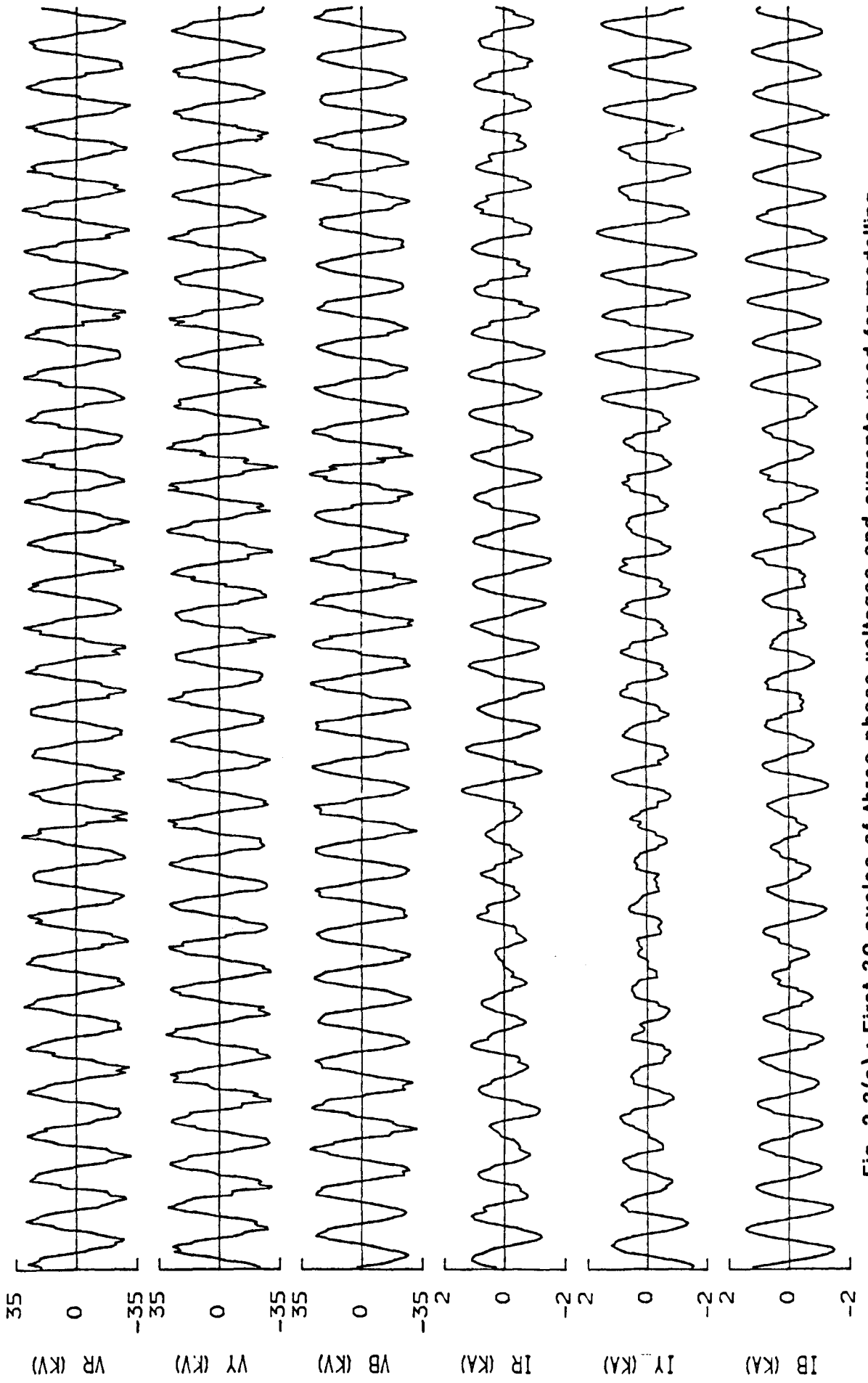


Fig. 2.3(a) : First 30 cycles of three phase voltages and currents used for modelling

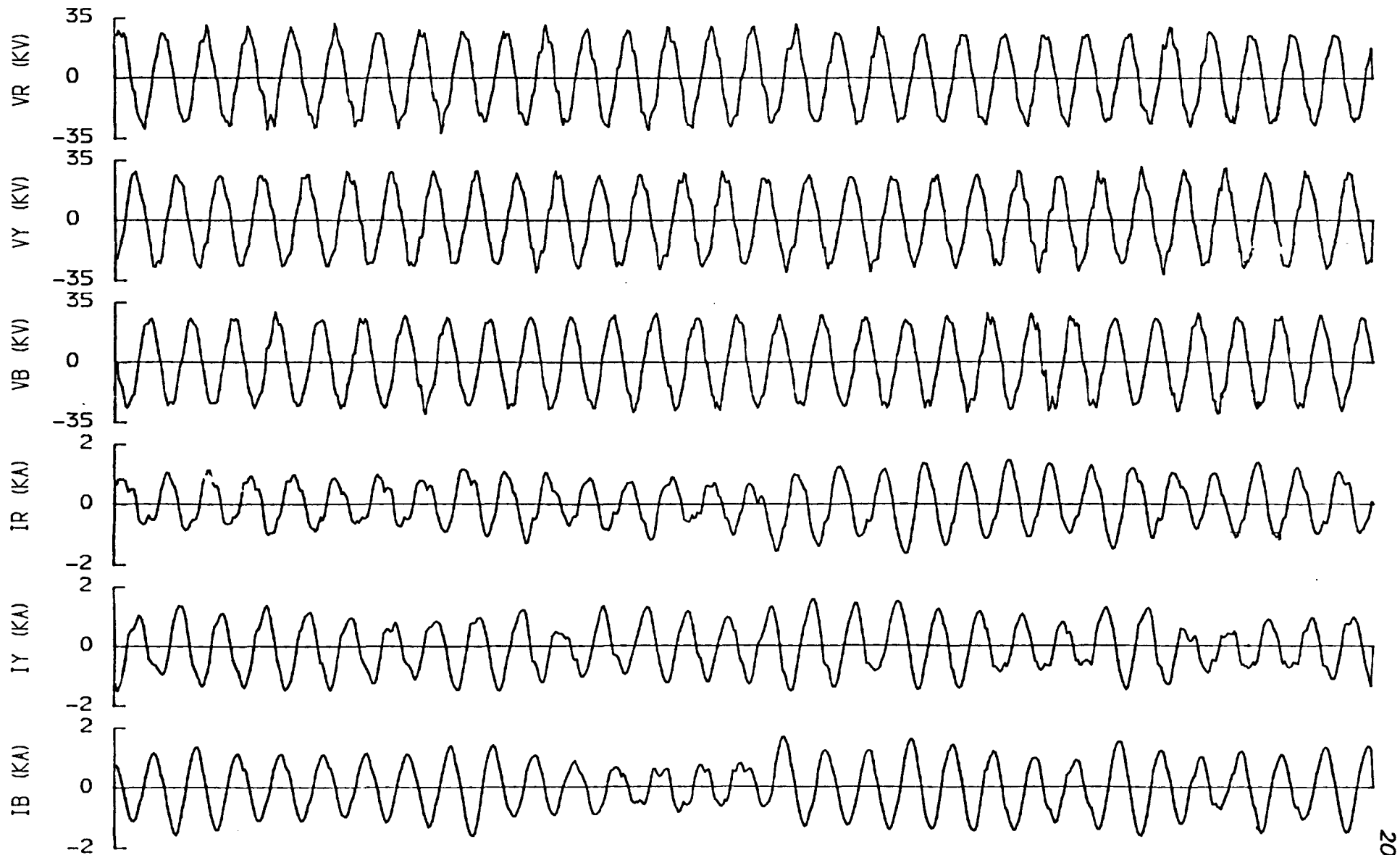


Fig. 2.3(b) : Second 30 cycles of three phase voltages and currents used for modelling

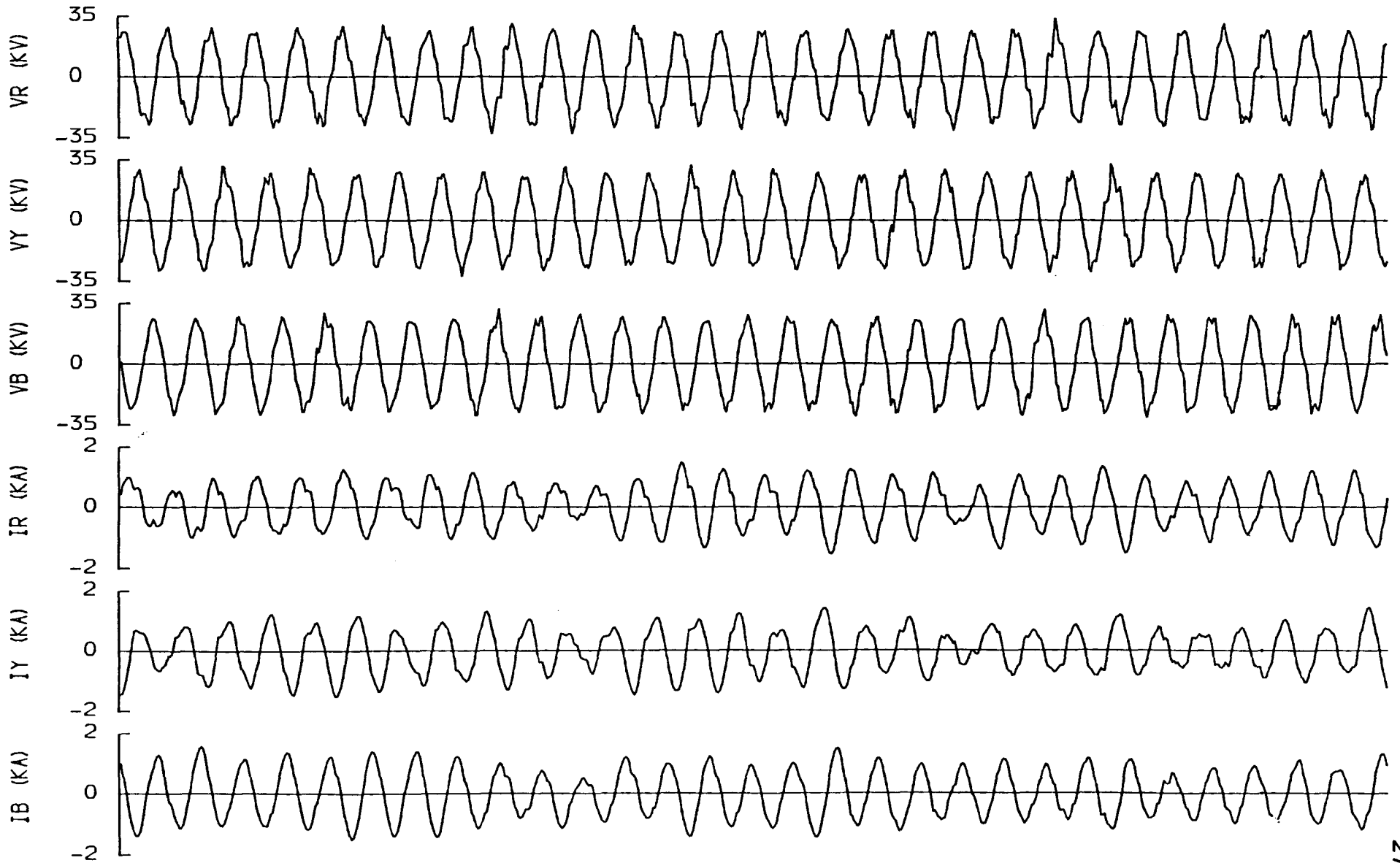


Fig. 2.3(c) : Final 30 cycles of three phase voltages and currents used for modelling

2.3 THE PHYSICAL MODEL OF ARC FURNACE AND SUPPLY

Section 2.1 above discusses, in broad terms, the requirements for a laboratory model. The methods used to fulfill those requirements will now be presented.

2.3.1 The Model's Supply

Modification of the laboratory 200 V three-phase supply to that shown in Figure 2.4 provided a source with a per-phase impedance of

$$Z_s = (0.0165 + j 0.0073) \text{ Ohms}$$

This impedance, with an X/R ratio of 0.4, is not intended to model exactly the real 275kV Sheffield ring. The impedance is, however, of such a low value that it will be almost negligible compared to the impedances of the equipment it is to supply (2.3.3 below).

2.3.2 Line Current Reproduction

It was desired that a scale model of a particular arc furnace installation should be subjected to the same form of non-sinusoidal currents that the real installation suffered. This demanded a variable impedance capable of very fast response - in fact the frequency response had to be at least within the range 20-80Hz to allow the critical 0-30Hz modulations of the 50Hz carrier to be impressed upon the system, without distortion away from the driving signal. The driving signal would, of course, be derived from the recordings of the on-site current measurements at 33kV.

A feasibility study was undertaken, using a professional audio power amplifier as a 'current sink'. Using such a device for the variable load offered the advantages of easily controllable gain that would be practically uniform from 20Hz to 20kHz, and a short development time for the prototype system.

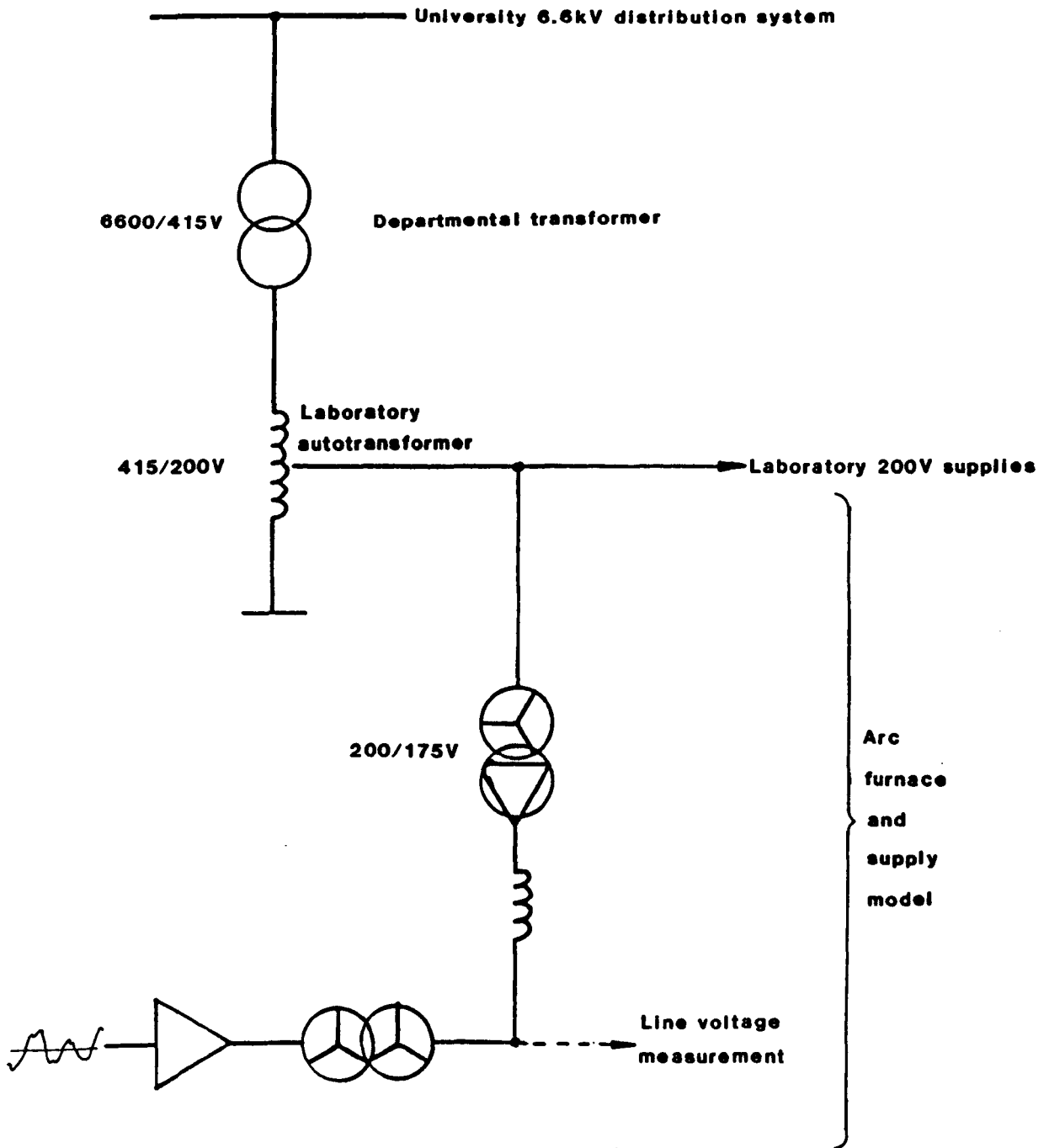


Fig. 2.4 : The laboratory supply from 6.6kV

An analogue input to the power amplifier was required, which would represent the line current waveform at 33kV. The necessary data was available on magnetic tape, and this was transferred via punched paper tape to a flexible microcomputer system dedicated to driving the power amplifier input. This method allowed many different sections of data to be applied to the variable load, including waveforms purely synthesized on the mainframe computer for test purposes.

The results of the feasibility study were encouraging^[66], and an extension to three-phase operation was undertaken.

The block diagrams illustrating the system used for the three-phase arc furnace model are given in Figure 2.5 (a),(b),(c).

A problem identified early in the project was the 800 microsecond sampling period used for the CEGB measurements and recordings. Although sufficiently small for data analysis, with a Nyquist frequency of 625Hz, the step lengths for current waveform reproduction were large. Figure 2.6 illustrates the step waveform produced with no smoothing.

Physical smoothing with low-pass filter networks could not achieve a suitable waveform. The data was therefore modified on the mainframe computer before punch tape output. Various interpolation and curve-fitting procedures were studied, and the method of least-squares cubic-spline approximation used to obtain three extra data points between each pair of recorded values. This reduced the time between data points from 800 microseconds to 200 microseconds. The computational principles and their practical application are further detailed in Appendix C.

The interpolation routines could easily be adjusted to produce any number of data points from the original samples. The obvious restriction, apart from punch tape length, was the capacity of the microcomputer memory.

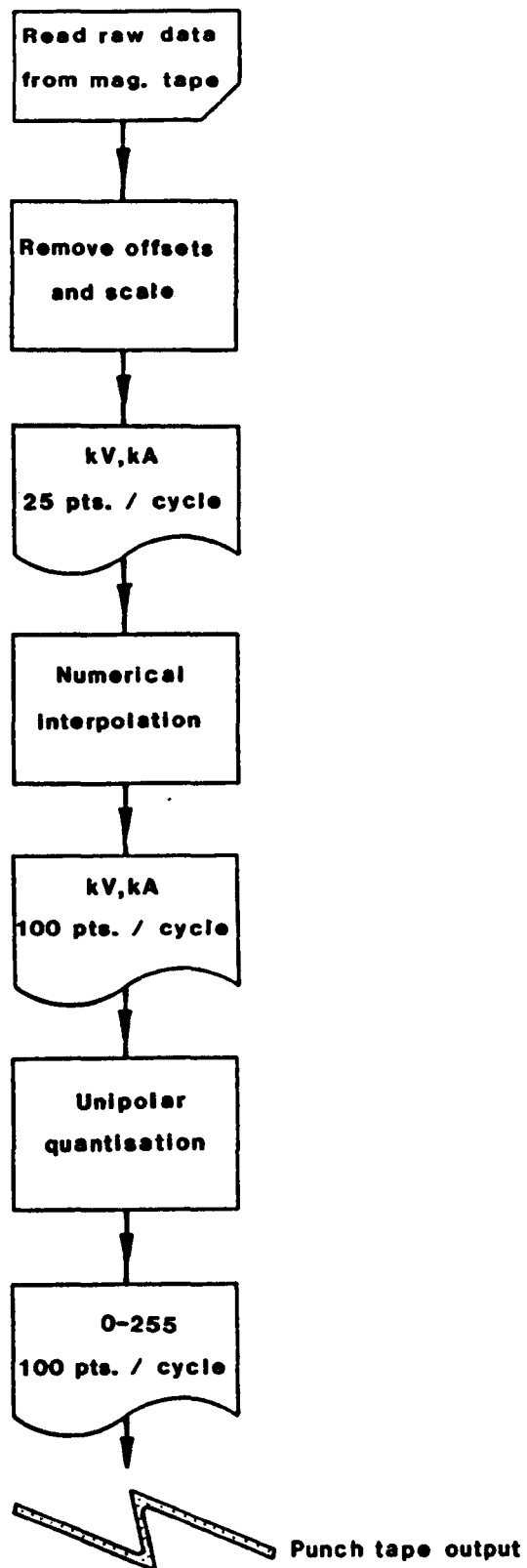


Fig 2.5(a) : Arc furnace model - mainframe computer data processing

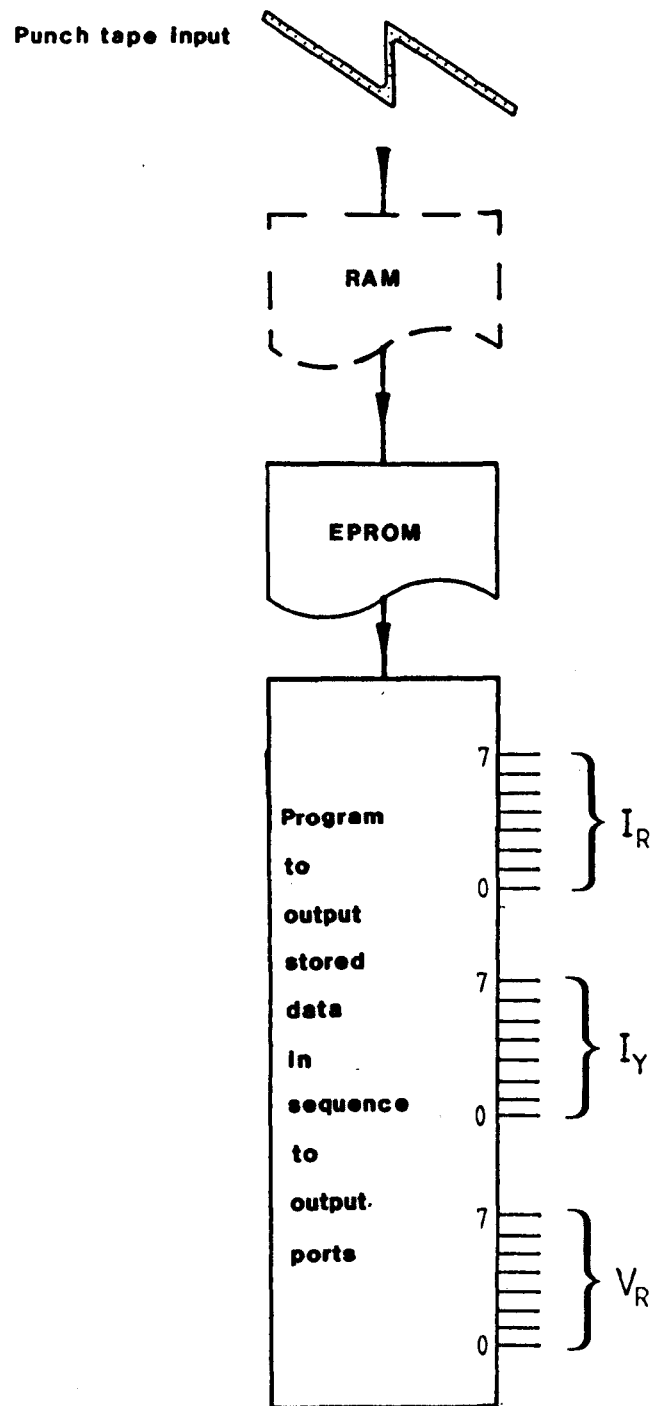
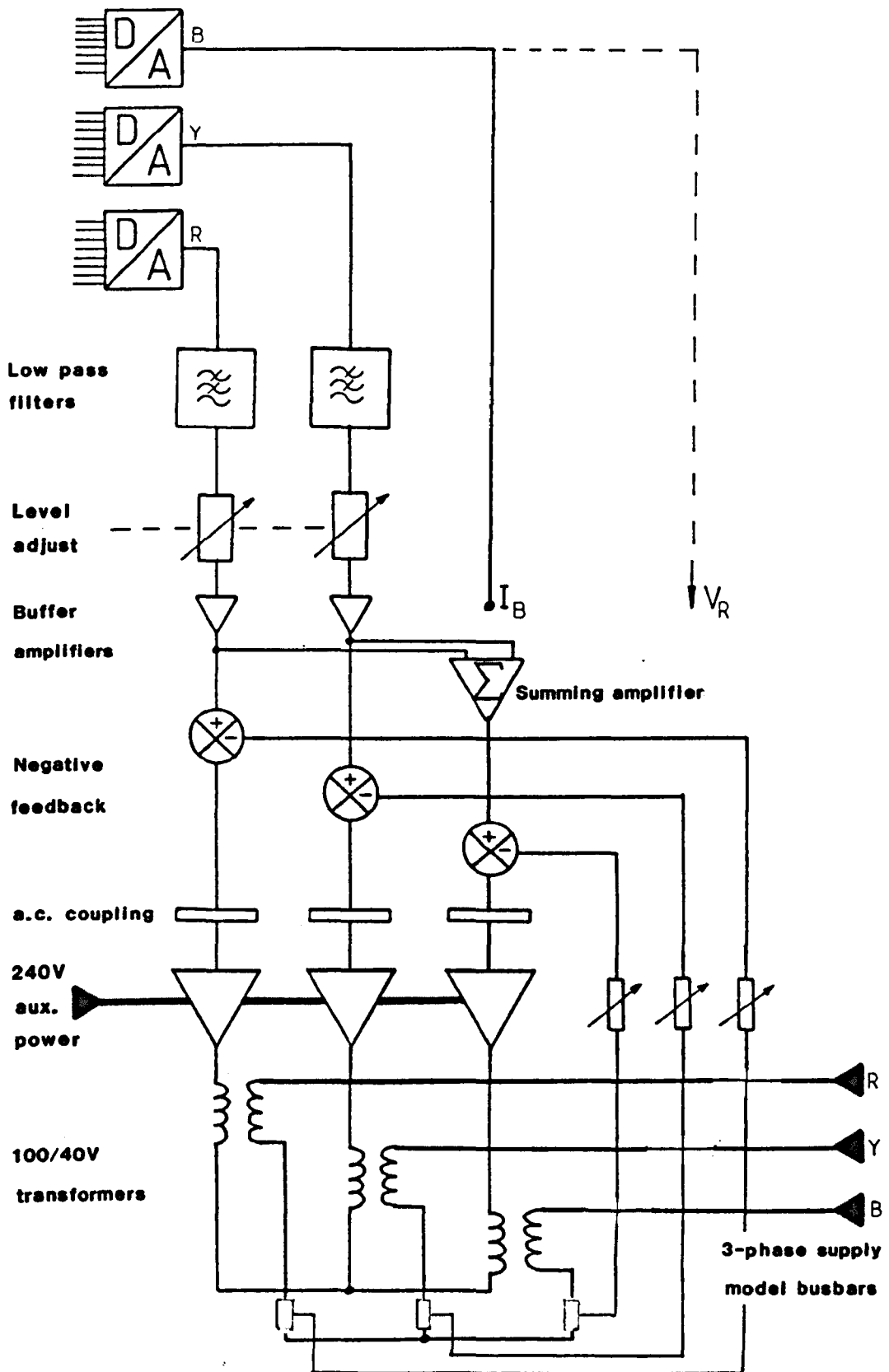


Fig. 2.5(b) : Arc furnace model - use of data by microcomputer



**Fig. 2.5(c) : Arc furnace model -
signal conditioning and current amplification**

The microcomputer chosen for this feasibility study, and subsequently used in the full laboratory mode, was the Rockwell AIM-65 system [81,84,85]. Its features are:

- (i) 8080 microprocessor driven at 4MHz
- (ii) 64K bytes of addressable memory
- (iii) ROM resident 8K byte monitor program for single-key entry and manipulation
- (iv) ROM resident 8K byte 8080 assembler
- (v) Single line display, thermal printer and full size keyboard

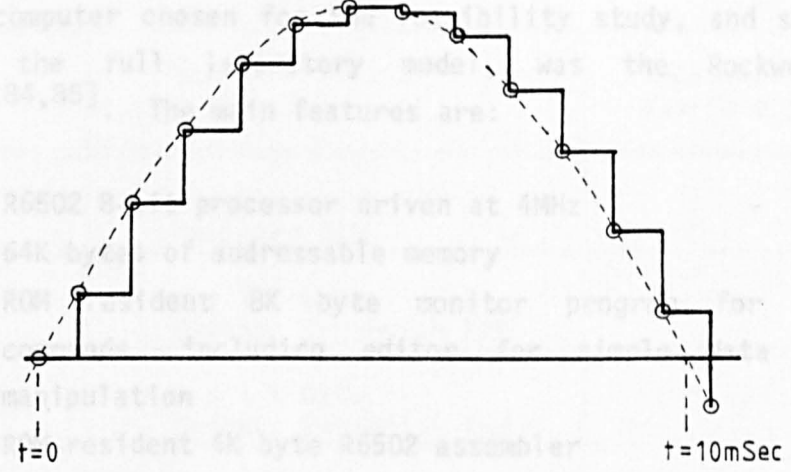


Fig. 2.6 : 800 microsecond quantisation of a 50 Hz waveform

A Data Plus multi-purpose expansion board [86] provided 16K bytes of dynamic RAM and two 8082 Virtual Interface Adaptors (VIAs) each providing two independent 8 bit I/O ports.

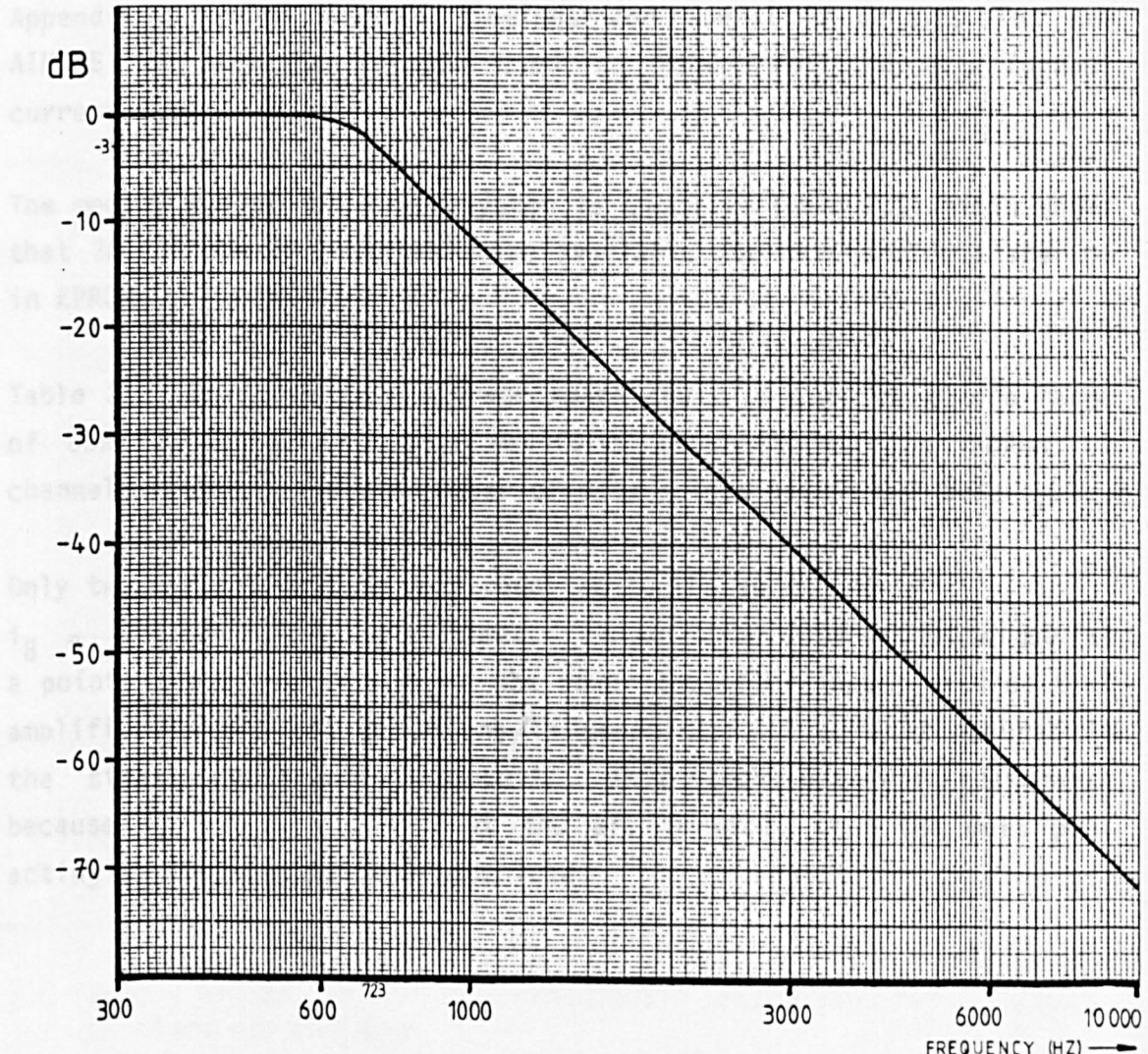


Fig. 2.7 : Low pass filter cut-off characteristics

The microcomputer chosen for the feasibility study, and subsequently used in the full laboratory model, was the Rockwell AIM-65 system^[83,84,85]. The main features are:

- (i) R6502 8-bit processor driven at 4MHz
- (ii) 64K bytes of addressable memory
- (iii) ROM resident 8K byte monitor program for single-key commands, including editor for simple data entry and manipulation
- (iv) ROM-resident 4K byte R6502 assembler
- (v) Single line display, thermal printer and full-size keyboard

A Dram Plus multi-purpose expansion board^[86] provided 16K bytes of dynamic RAM and two R6522 Virtual Interface Adaptors (VIAs) each providing two independent 8 bit I/O ports.

Appendix D gives program listings and operating details for the AIM-65 microcomputer system used to regenerate the arc furnace current waveforms.

The memory map of the final system is shown in Table 2.1. This shows that 28,672 memory locations were available for waveform data storage in EPROM.

Table 2.2 shows how this storage space could be used to give a range of 50Hz cycles of recorded waveforms depending on the number of channels required and the number of data points output per 50Hz cycle.

Only two current outputs were required to the model, since $i_B = -(i_R + i_Y)$ at all times. Using this summing technique at a point in the system near to the power amplifier inputs ensured that amplifiers would not be acting in opposition if a fault occurred in the signal conditioning circuit. This technique was reasonable because $i_R + i_Y + i_B = 0$ at the arc furnace, with the melt pool acting as the star point of the load.

Address	Use	Locations for Waveform Storage
0000 0FFF	4 x 1 K byte On-board RAM	-
1000 1FFF	4 x 1 K byte Dynamic Expansion RAM	-
2000 2FFF	4 x 1 K byte Dynamic Expansion RAM	-
3000 3FFF	4 x 1 K byte Dynamic Expansion RAM	-
4000 4FFF	4 x 1 K byte Dynamic Expansion RAM	-
5000 5FFF	2 x R6522 VIA	-
6000 6FFF	1 x 4 K byte EPROM	0 - 4,095
7000 7FFF	1 x 4 K EPROM	4,096 - 8,191
8000 8FFF	1 x 4 K EPROM	8,192 - 12,287
9000 9FFF	1 x 4 K EPROM	12,288 - 16,383
A000 AFFF	AIM-65 Printer, key- board, display, I/O etc	-
B000 BFFF	1 x 4 K byte EPROM	16,384 - 20,479
C000 CFFF	1 x 4 K byte EPROM	20,480 - 24,575
D000 DFFF	1 x 4 K byte EPROM	24,576 - 28,671
E000 EFFF	AIM-65 Monitor	-
F000 FFFF	AIM-65 Monitor	-

Table 2.1 Memory Map of the AIM-65 microcomputer system used for waveform reproduction

No. of Channels	Number of Data Points Per Cycle					
	25	50	75	100	125	150
2	573	286	191	143	114	95
3	382	191	127	95	76	63
4	286	143	95	71	57	47

Table 2.2 Showing maximum number of complete 50Hz cycles of recorded data that could be output using only 28 K bytes of EPROM for storage

Frequency wrt ω_c	$0.1 \omega_c$	$0.25 \omega_c$	$0.5 \omega_c$	ω_c
Phase	-12°	-29°	-60°	-135°

Table 2.3 Phase response of a -60 dB/decade low-pass active filter
 $\omega_c = 723\text{Hz}$

A third output channel from the microcomputer was allowed for in the memory considerations. This was used:

- (i) To output the recorded i_B for comparison with the i_B derived as described above.
- (ii) To output the recorded V_R for phase and form comparison with the model's V_R .

Spline interpolation was used for each channel, to give 100 points per cycle from the original 25 points per cycle. This was sufficient to give a smooth waveform after low pass filtering of the DAC output waveform. The low pass filter used had the passband characteristics shown in Figure 2.7.

This filter characteristic was found necessary in order to eliminate severe oscillations, which occurred in early models at the data output frequency of 5kHz. The filter circuit diagram is given in Figure 2.8. It comprises a -40dB/decade Butterworth cascaded with a -20dB/decade low pass active filter. The phase response of such a filter is important, and is given in Table 2.3. The 50Hz current fundamental is at $0.07\omega_c$, and the varying amplitude modulation components of the distorted 50Hz signal may be phase-shifted by many degrees. Close inspection of the signal waveforms before and after filtering showed that the effect of this phase delay was extremely slight.

The continuous output from the signal conditioning circuits was fed to the inputs of three commercial power amplifiers. The maximum rating of the 'arc furnace model' was determined by the rating of these power amplifiers. Figure 2.9 shows the limits of VI output available^[87]. It can be seen that the maximum continuous a.c. power falls-off rapidly above 100 volts and 20 amps when current flow matches voltage polarity. The high inductive current component measured at 33kV presented the possibility of driving current in opposition to the voltage applied to the amplifiers, and the quadrants of Figure 2.9 show the de-rating necessary.

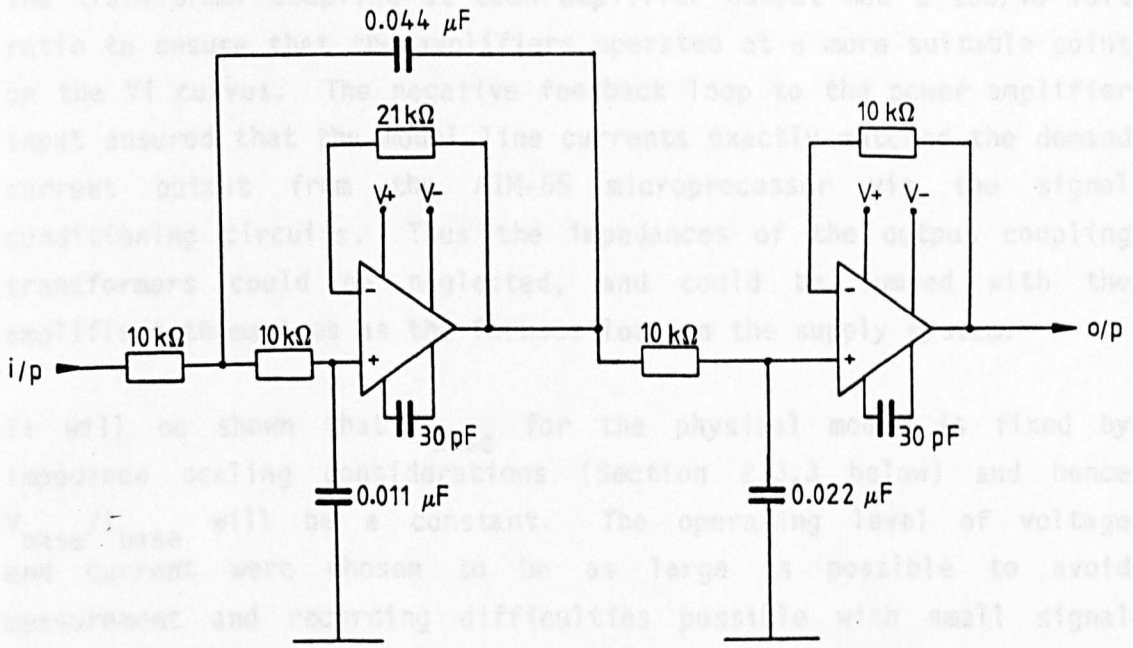


Fig. 2.8 : -60dB/decade low pass filter circuit diagram

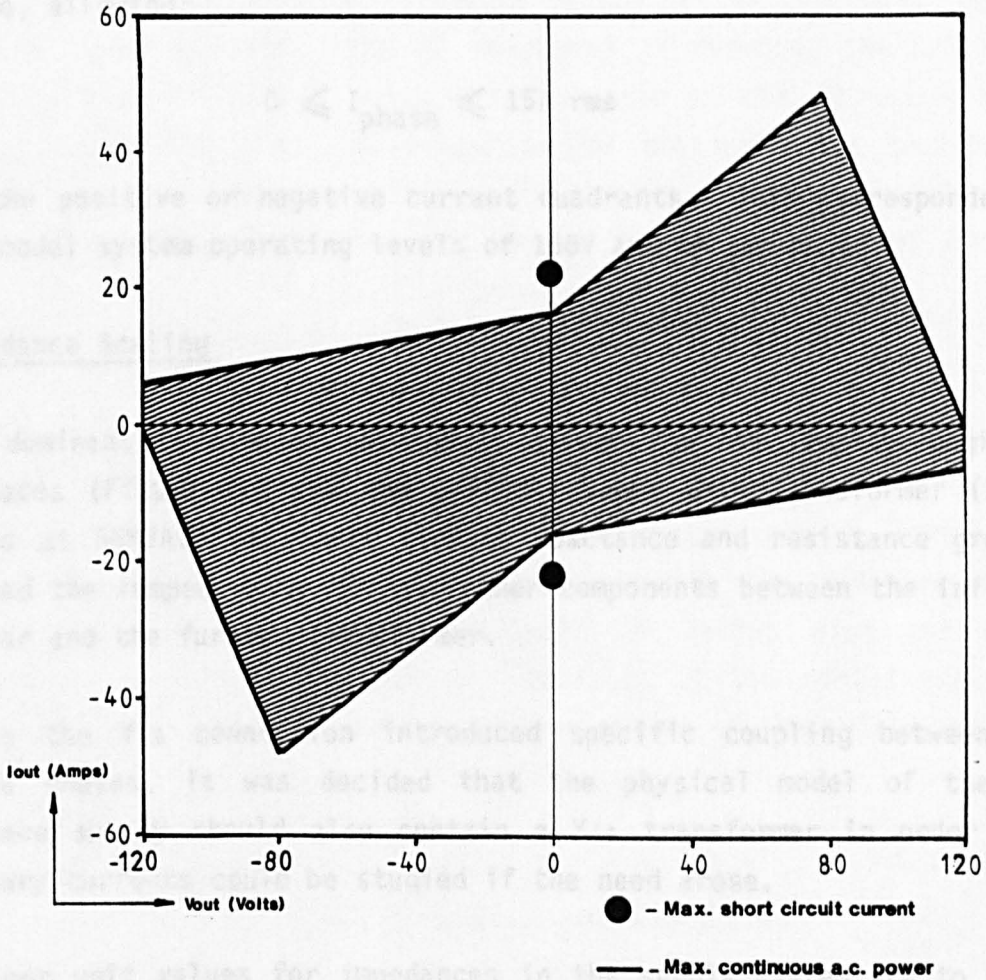


Fig. 2.9 : Power amplifier VI output curves

The transformer coupling at each amplifier output had a 100/40 Volt ratio to ensure that the amplifiers operated at a more suitable point on the VI curves. The negative feedback loop to the power amplifier input ensured that the model line currents exactly matched the demand current output from the AIM-65 microprocessor via the signal conditioning circuits. Thus the impedances of the output coupling transformers could be neglected, and could be lumped with the amplifiers themselves as the furnace load on the supply system.

It will be shown that Z_{base} for the physical model is fixed by impedance scaling considerations (Section 2.3.3 below) and hence $V_{\text{base}}/I_{\text{base}}$ will be a constant. The operating level of voltage and current were chosen to be as large as possible to avoid measurement and recording difficulties possible with small signal levels and thyristor switching.

$V_{\text{phase}}=40\text{V rms}$ lies well within the amplifiers continuous operation curve, allowing:

$$0 \leq I_{\text{phase}} \leq 15\text{A rms}$$

in the positive or negative current quadrants. This corresponded to the model system operating levels of 100V and 6A per phase.

2.3.3 Impedance Scaling

The dominant feature of the supply system for the Templeborough arc furnaces (Figure 2.1) is the 275/33kV Super Grid Transformer (SGT), rated at 56MVA. Its short circuit reactance and resistance greatly exceed the lumped value for all other components between the infinite busbar and the furnace transformer.

Since the Y- Δ connection introduced specific coupling between the three phases, it was decided that the physical model of the arc furnace supply should also contain a Y- Δ transformer in order that primary currents could be studied if the need arose.

The per unit values for impedances in the supply system are to bases of 33kV and 100MVA, giving a base value of line current of 1.75kA.

Suitable model system operating levels were chosen as 100V and 3A per phase to ensure that the power amplifiers^[87] would be well within their operating range. Setting base values of $V_L=175V$ and $I_L=3A$ gives

$$\begin{aligned} \text{3-phase VA base} &= \sqrt{3} (V_L \text{ base}) (I_L \text{ base}) \\ &= \underline{909.3VA} \end{aligned}$$

$$\begin{aligned} \text{and } Z_{\text{base}} \text{ (per phase)} &= \frac{(V_L \text{ base})^2}{\text{3-phase VA base}} \\ &= \underline{33.67 \text{ Ohms}} \end{aligned}$$

These base values were used to specify equipment with impedances suitable to model the real system.

The ratio of resistance to reactance of the SGT is $Q = 45.9$. As the physical size of such items of equipment is reduced, the X/R ratio also reduces - a typical value for equipment of 1000 VA rating being approximately 10. The specifications for the model Y- Δ transformer emphasized a maximum value for short-circuit resistance which would approximately equal the per unit value of resistance found for the real SGT.

$$\text{i.e. } R_{sc} \text{ max} = 0.00519 \text{ p.u.} \times 33.67 \text{ Ohms} = \underline{0.174 \text{ Ohms}}$$

Ideally X_{sc} would then be 8.02 Ohms (representing 0.2383 p.u.) but the much reduced X/R ratio for the model transformer will give X_{sc} considerably less than this. This difference between actual and desired reactance could then be overcome with the addition of an inductance with low series resistance in series with the model transformer. Fine adjustment of the value of the series reactance gave a suitable lumped parameter representation of the supply system.

For the 200/175V Y- Δ transformer:

$$R_{sc} = 0.124 \text{ Ohms per phase wrt } 175V$$

$$X_{sc} = 0.069 \text{ Ohms per phase wrt } 175V \text{ at } 50Hz$$

For each additional line choke:

$$R_{\text{series}} = 0.80 \text{ Ohms}$$

$$X_{\text{series}} = 9.36 \text{ Ohms at 50Hz}$$

Thus the impedance of the line choke dominates, and the X/R ratio of the lumped parameters is 10.2. The magnetising current of the Y- Δ transformer was found to be 0.8 Amps and non-sinusoidal at rated voltage. It is therefore important that the series line chokes are not inserted between the Y- Δ transformer and the low impedance supply, since considerable distortion of the voltage waveform results. With the Y- Δ transformer primary connected directly to the low impedance supply, its magnetising current can be safely ignored.

Although the model's X/R ratio is a factor of four lower than that of the Templeborough system, the inductive reactance remains the dominant component. The ratio of lumped inductive reactances was used to determine the exact base value for line current as follows:

For the Templeborough System

Lumped impedance

to infinite busbar = SGT impedance + supply impedance

$$= (0.00519 + j0.2383) + (0.0 + j0.01) \text{ p.u.}$$

$$= (0.00519 + j0.2483) \text{ p.u.}$$

To bases of 100MVA, 33kV, 1.749kA

For the Analogue Model

$$\begin{aligned}
 \text{Lumped impedance} &= \text{Line choke} + \text{Y-}\Delta \text{ transformer} + \text{supply} \\
 \text{to secondary of} & \quad \text{impedance} \quad \text{impedance} \quad \text{impedance} \\
 \text{6.6kV transformer} & \\
 &= (0.8 + j9.36) + (0.124 + j0.069) \\
 & \quad + (0.0165 + j0.0073) \quad \text{Ohms wrt 175V} \\
 &= (0.9405 + j9.436) \quad \text{Ohms wrt 175V}
 \end{aligned}$$

Let $j9.436$ Ohms at 175V represent $j0.2483$ p.u. to bases of 100MVA and 33kV.

$$\text{Therefore, } Z_{\text{base}} \text{ for the model} = \frac{X \text{ Ohms}}{X \text{ p.u.}} = j38.0 \text{ Ohms}$$

$$\text{Then } VA_{\text{base}} = \frac{(V_{\text{Lbase}})^2}{Z_{\text{base}}} = \frac{(175\text{V})^2}{38.0} = 805.90\text{VA}$$

$$\text{And } I_{\text{base}} = \frac{VA_{\text{base}}}{\sqrt{3} (V_{\text{Lbase}})} = \frac{805.90}{\sqrt{3}(175.0)} = 2.659 \text{ Amps}$$

This is only slightly less than the base current value of 3A initially chosen for the model.

The magnitude of the input signal to the amplifiers was adjusted until the first peak of the model yellow phase line current, I_{γ} , representing 1.1978 kA, was:

$$\begin{aligned}
 & 1.1978\text{kA} \times \frac{I_{\text{baseMODEL}}}{I_{\text{baseSYSTEM}}} \\
 & = 1.1978\text{kA} \times \frac{2.659\text{A}}{1.749\text{kA}} \\
 & = 1.81 \text{ Amps}
 \end{aligned}$$

As shown in Figure 2.10.

The signal conditioning circuits and amplifier gains were each adjusted to give exactly balanced amplification for each phase under steady-state sinusoidal conditions.

A circle diagram is shown in Figure 2.11 for the laboratory 200V 3-phase supply at the receiving end. This diagram gives the lumped supply impedance for the model, and demonstrates how reactive power flow is due to the magnitude of the voltage difference along the line rather than the phase angle between sending and receiving end.

Figure 2.12 shows that currents drawn from the supply have frequency components in the range -20dB to -50dB, relative to the fundamental, in the band 1-100Hz. The power spectrum to 600Hz is shown in Figure 2.13, with peaks visible at 3rd, 5th, 7th, 9th and 11th harmonic frequencies.

Macedo^[88] investigated the characteristics of supply impedances, highlighting the possibility of resonant nodes at frequencies up to 19th harmonic. Components of current at such nodes would produce disproportionate voltage fluctuations and would need to be recognised in any study. Calculations^[89] for the real Templeborough system showed that such nodes existed at 6th and 17th harmonic (Figure 2.14), due to the combination of system capacitance and inductance.

Any disproportionate voltage fluctuations arising at these frequencies are, however, well outside the range of those necessary for lamp flicker analysis.

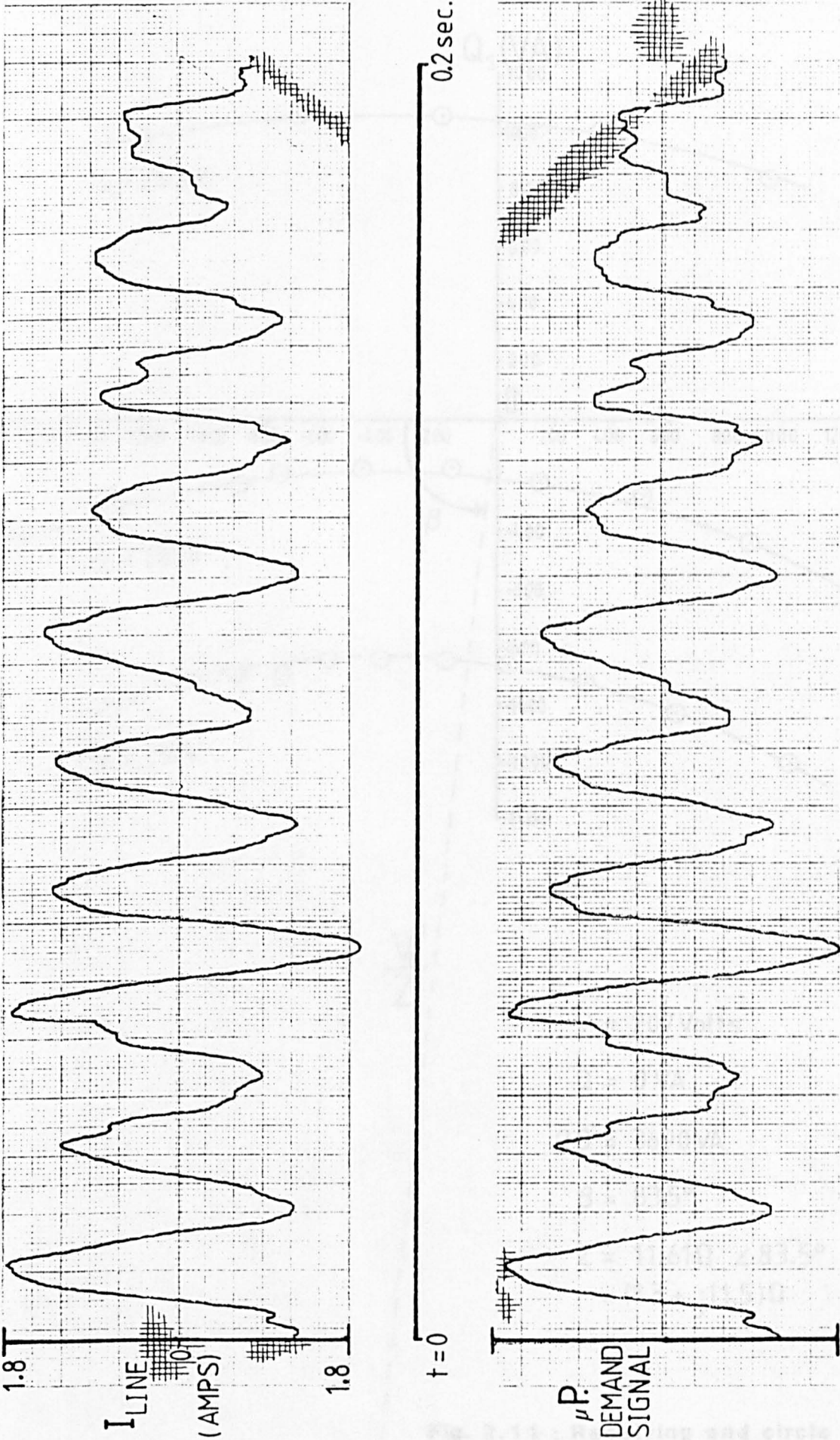


Fig. 2.10 : Comparison of demand signal and model line current

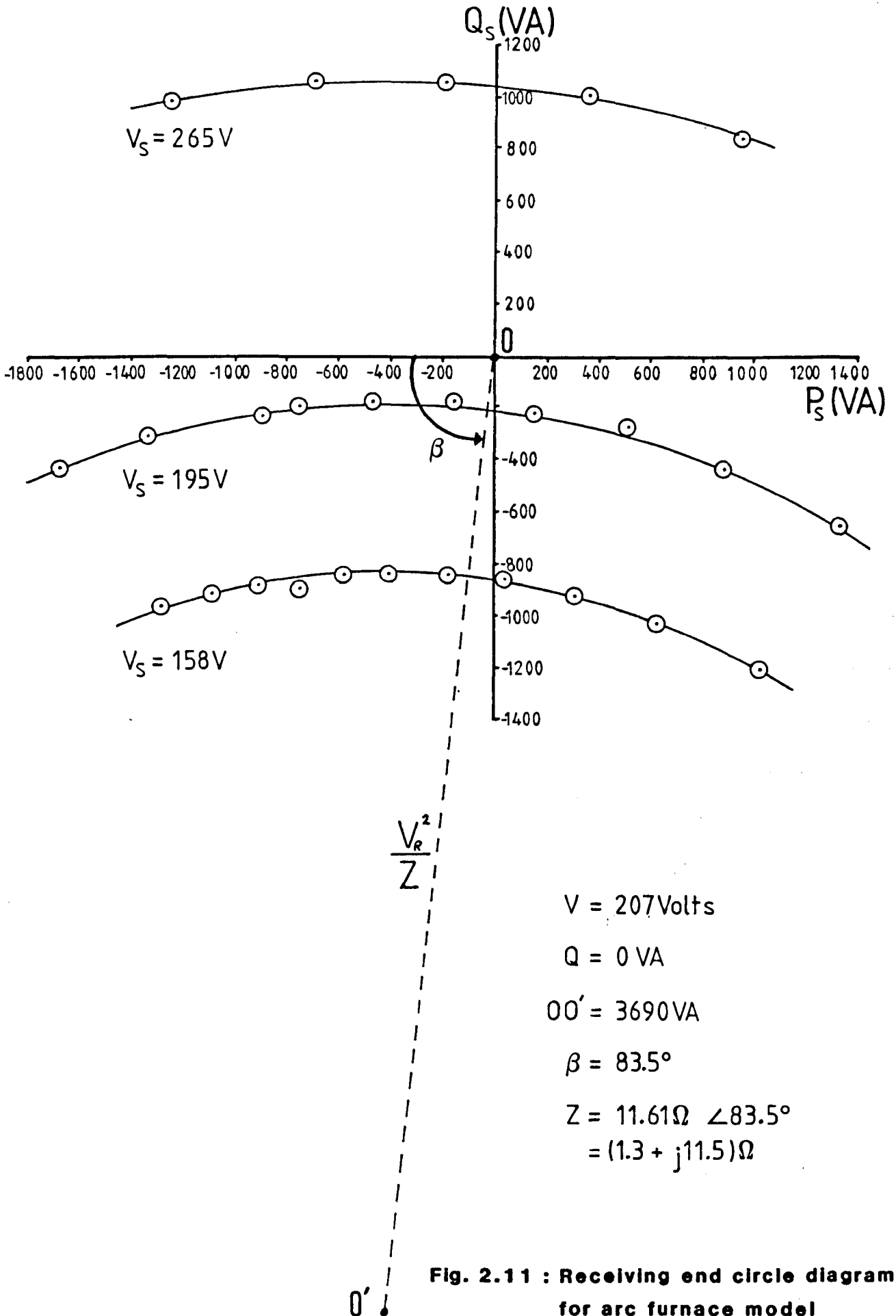


Fig. 2.11 : Receiving end circle diagram for arc furnace model

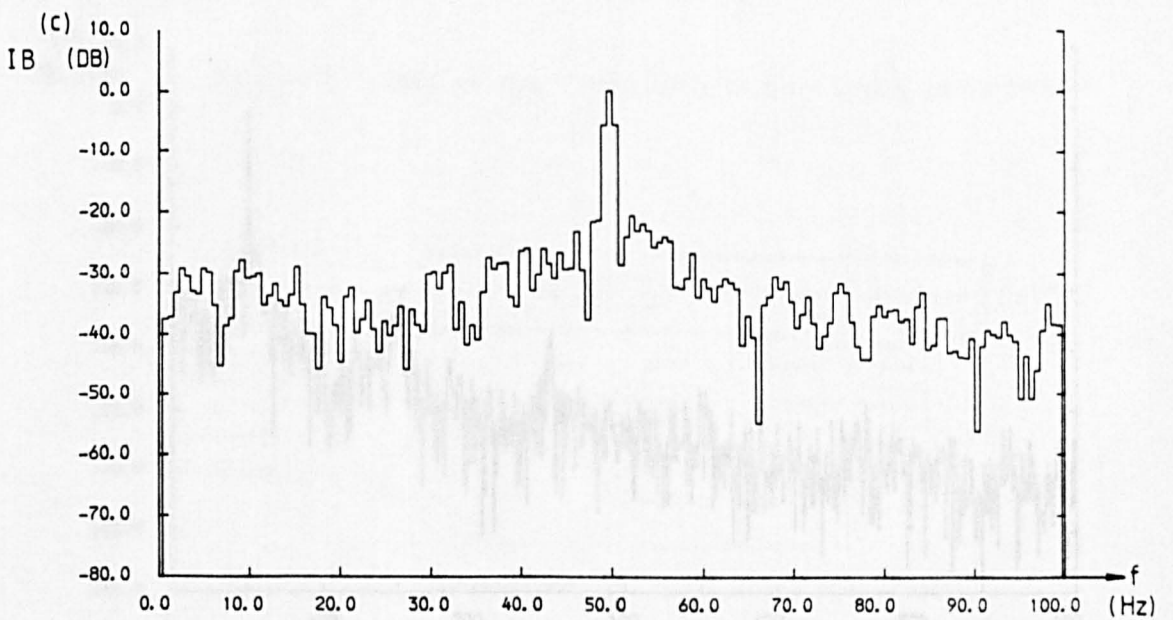
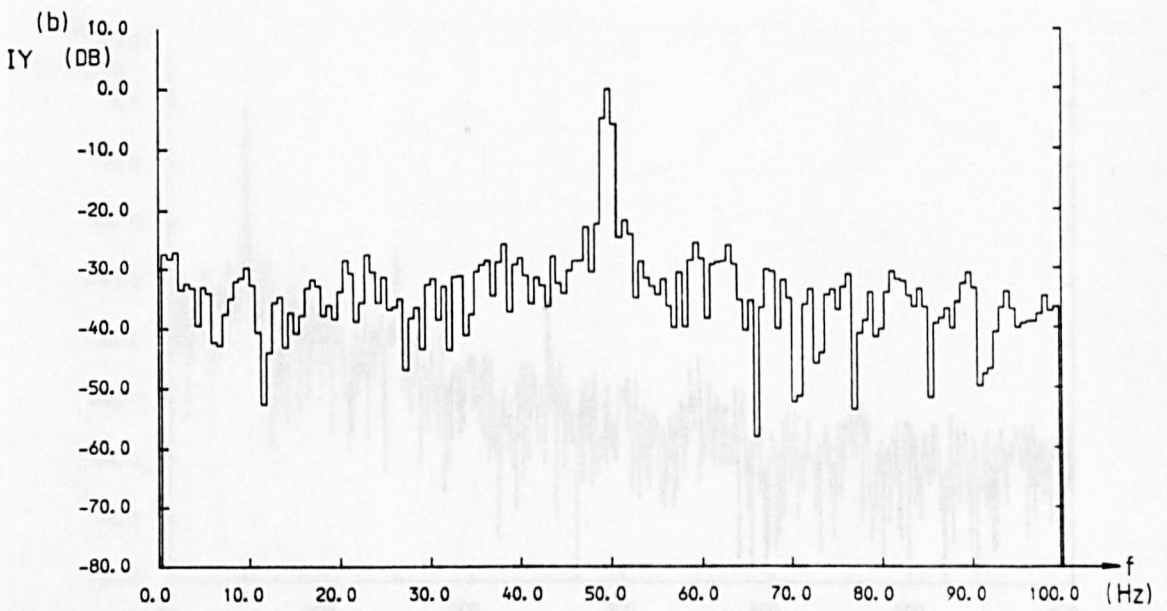
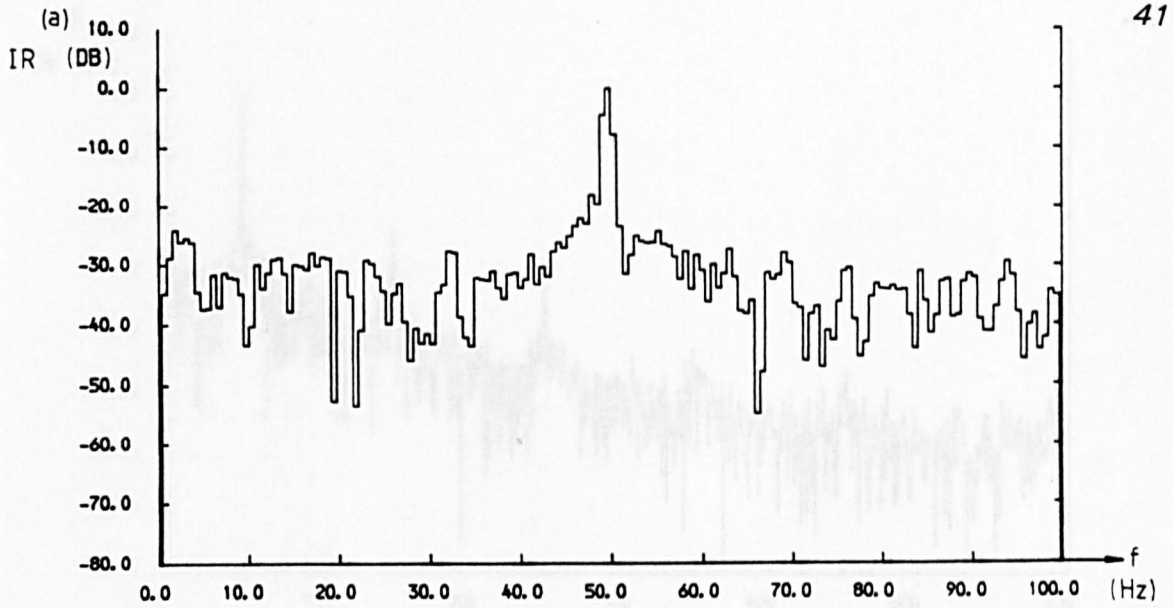


Fig. 2.12 : 0-100Hz power spectra of recorded arc furnace three phase currents

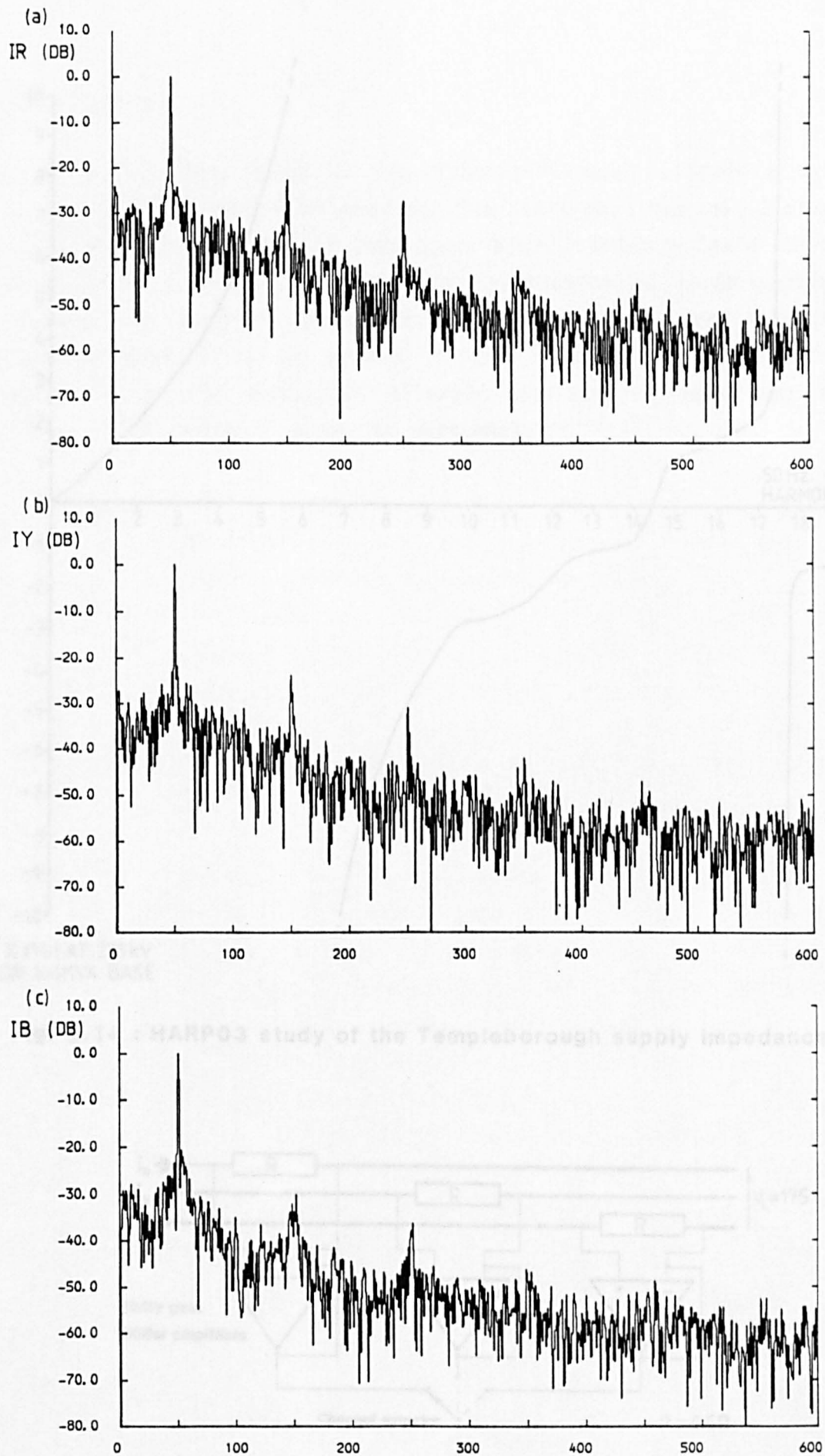


Fig. 2.13 : 0-600Hz power spectra of recorded arc furnace three phase currents

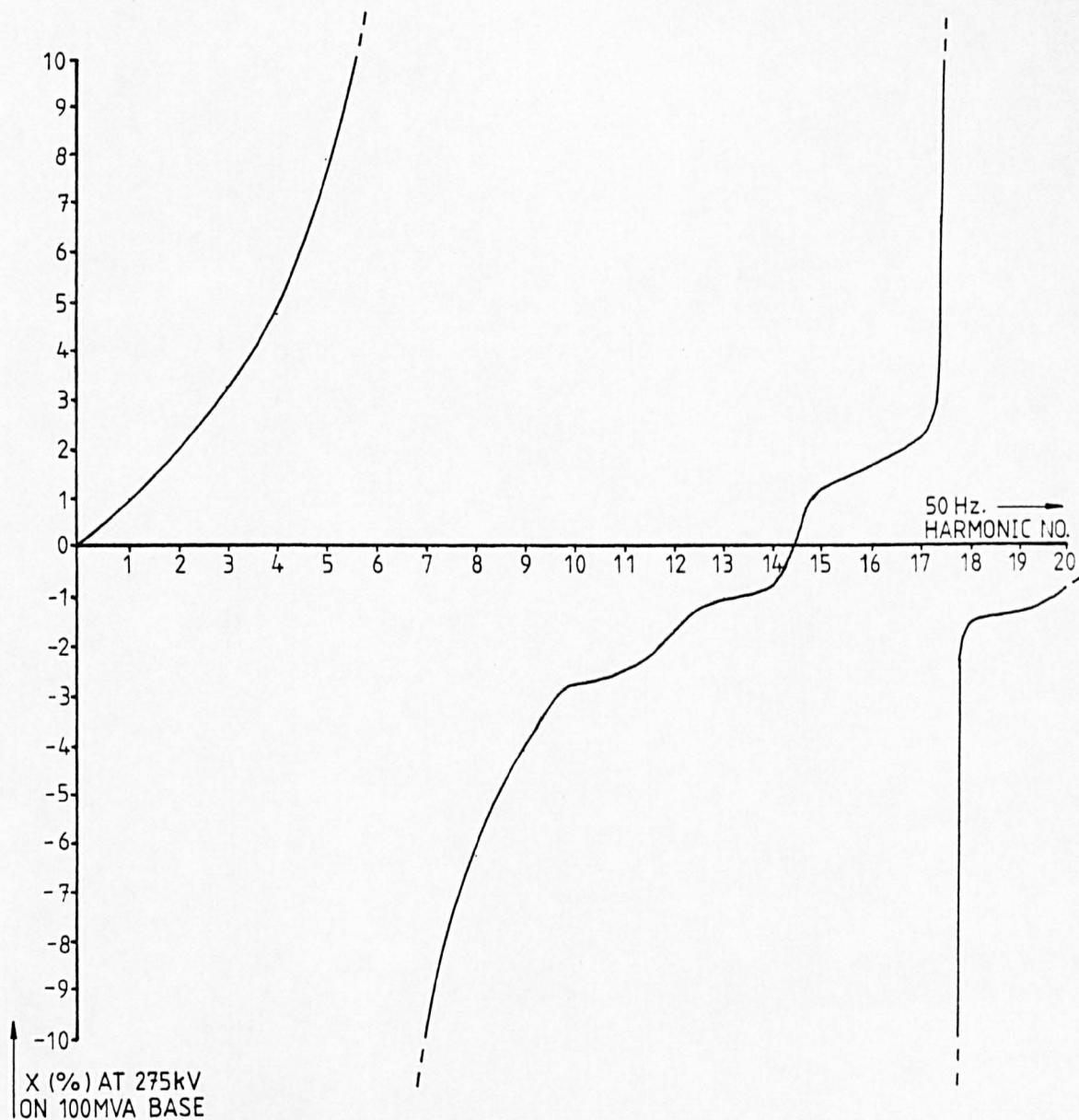


Fig. 2.14 : HARP03 study of the Templeborough supply impedance

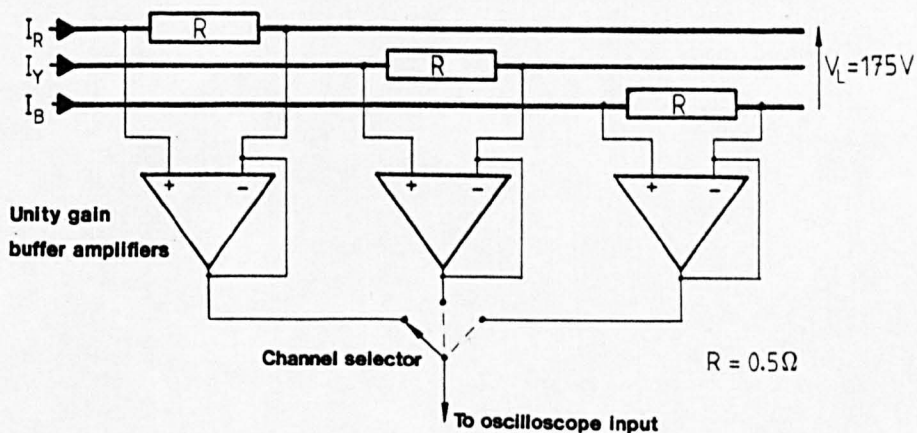


Fig. 2.15 : Method used for measurement of line current

2.3.4 Safety Sequence

The particular arrangement of the laboratory model allowed a safe sequence of events to be followed for its start-up. Appendix E gives a schematic of the complete laboratory model, and the 'safe-start' sequence. This sequence avoided the application of large voltage transients or current surges to the equipment, thus allowing protective devices to be graded to the relatively low operating levels. A safety contactor allowed complete disconnection of supplies in the event of danger to personnel.

2.4 RESULTS

Measurement of the characteristics of non-sinusoidal waveforms may be attempted in a number of ways. Modern oscilloscopes have now replaced high speed chart recorders for most applications, and digital measurement techniques enable large amounts of data to be stored and retrieved easily.

The study of the success of the laboratory model in reproducing arc furnace supply characteristics was undertaken in three stages.

- (i) The accuracy with which the line currents produced by the power amplifiers compared with those line currents measured at 33kV at the Templeborough installation
- (ii) The voltage fluctuations at 175V that the model line currents produced, again compared to those measured at 33kV
- (iii) The frequency components of the currents and voltages described above.

Section 2.3.2 describes how the same stream of data is continually cycled through to drive the model's power amplifiers. This meant that the model was operating in a continuous mode, and different measurements could be taken sequentially using the same recording equipment. For (i) and (ii) above, where the measured quantities were studied as a function of time, it was essential that some common time reference be available for comparison between non-concurrent recordings. This was achieved using a short triggering pulse output from the microcomputer driving the power amplifiers. The pulse was output only at the beginning of each complete cycle of the 1.78 second data stream. Further details of this synchronising pulse output may be found in Appendix D.

2.4.1 Line Current Waveforms

Laboratory recordings of the model waveforms were made using a 0.5 Ohm resistive shunt in each line of the model. The voltage thus developed was fed directly to the AC coupled input of a Gould digital storage oscilloscope. The full specification of this instrument is given in Reference [90].

Figure 2.15 details the recording method. A Bryants 25000 flat bed X-Y plotter was used to present the results in a suitable A4 format.

Figure 2.16 shows the first five 50Hz cycles of the red, yellow and blue line current waveforms with the data points output from the microcomputer memory presented adjacent to the measurement of line current for direct comparison.

The fine stepped effect on both waveforms is a characteristic of the digital storage oscilloscope and plotter, and should not be confused with the output of quantised data at 5kHz from the microcomputer. The low pass filter described in Section 2.3.2 attenuates this 5kHz component, and possible phase errors due to this filter are not apparent in the results.

The magnitude of the line currents was determined by the setting of the 'level adjust' potentiometers (Appendices D and E). In practice the first peak of the yellow line current waveform was always carefully set to equal 1.8 Amps.

Then = $1.8\text{A} \times 0.5\ \text{Ohms} = 0.9\ \text{Volts}$ to oscilloscope

2.4.2 Voltage Waveforms

The laboratory model was normally made to cycle over 89 complete 50Hz cycles of digitally stored data, this being the limit of that which could be stored in the microcomputer memory.

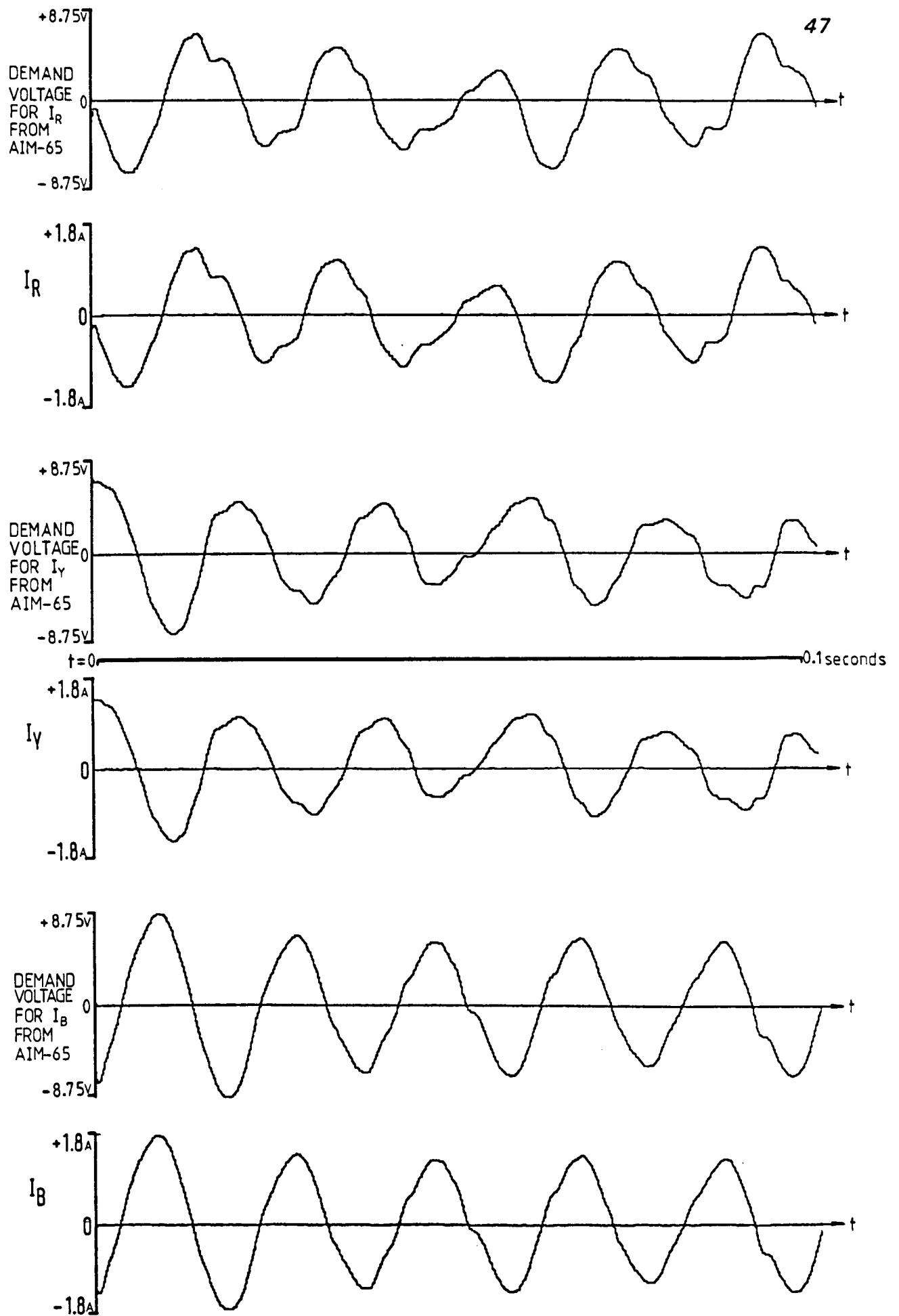


Fig. 2.16 : First 5 cycles of arc furnace model line current

Presentation of results in the time domain in a suitable format suffers in that:

- (i) To show all 89 cycles loses much useful detail.
- (ii) Showing only one or two cycles may be criticised for being unrepresentative.

Figures 2.17(a),(b) show the line voltage V_B-V_R with the model current off and at rated magnitude respectively. There is little value in presenting the open circuit voltage in the fashion of Figure 2.17(a) again, now that it has been shown to be a steady sinusoid. Figure 2.18 repeats Figure 2.17(b), with the open circuit voltage level now only indicated by a straight line. The low frequency fluctuations imposed on V_{BR} are clearly evident from the varying level of the voltage peaks.

Figures 2.19 and 2.20 show the corresponding variations for V_R-V_Y and V_Y-V_B respectively.

The form of Figure 2.17 is repeated for the first 2.5 cycles only in Figure 2.21. This shows clearly the voltage fluctuations due to the arc furnace model within each cycle for V_R-V_Y .

Figures 2.22 and 2.23 give the corresponding variations for V_Y-V_B and V_B-V_R respectively.

Figure 2.24 shows the phase relationship between line voltage and current in the laboratory model for each of the three phases.

2.4.3 Power Spectra of Voltage Waveforms

The voltage waveforms presented in Section 2.4.2 clearly show distortion from a sinusoidal form. A precise evaluation of the distortion is difficult when the 50Hz fundamental is present, and the 'flicker voltage', V_f , may be obtained if this fundamental frequency is removed.

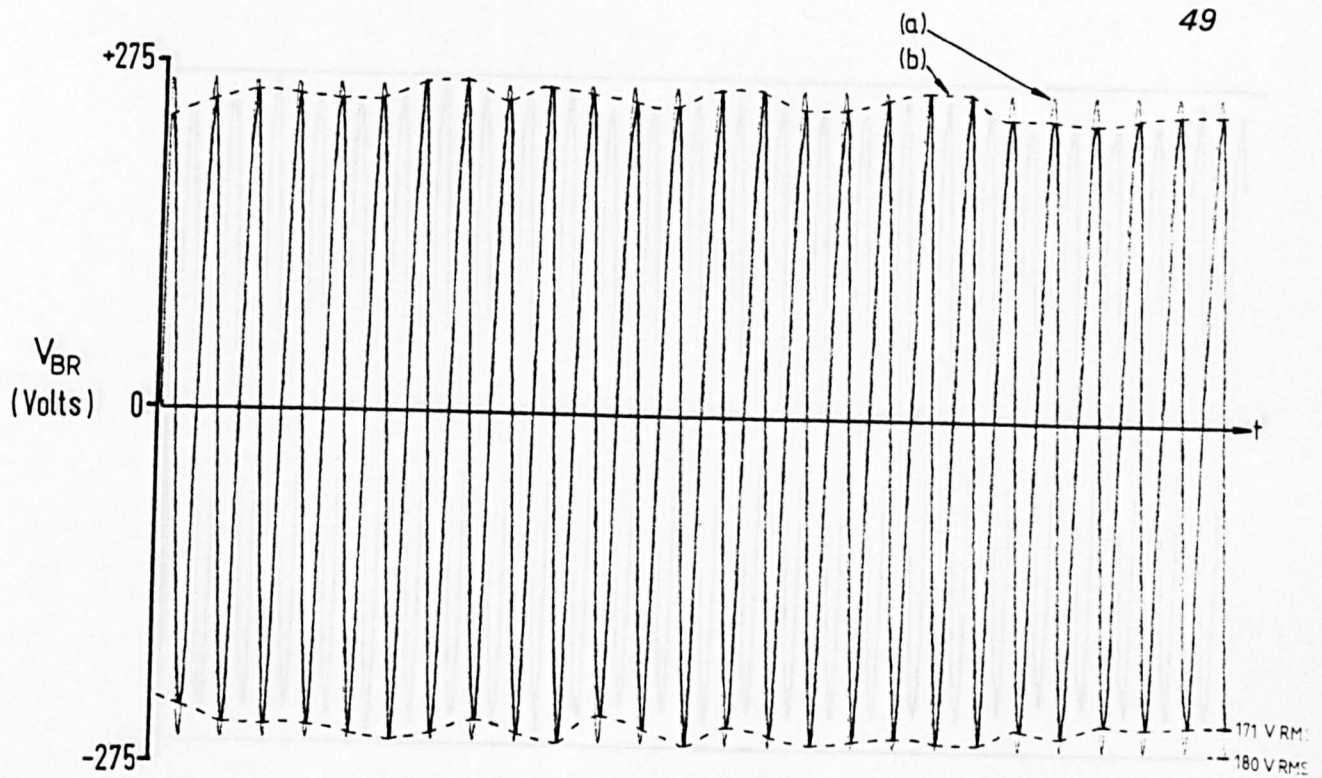


Fig. 2.17(a) : Arc furnace model open circuit line voltage V_{br}
(b) : V_{br} with arc furnace model operating

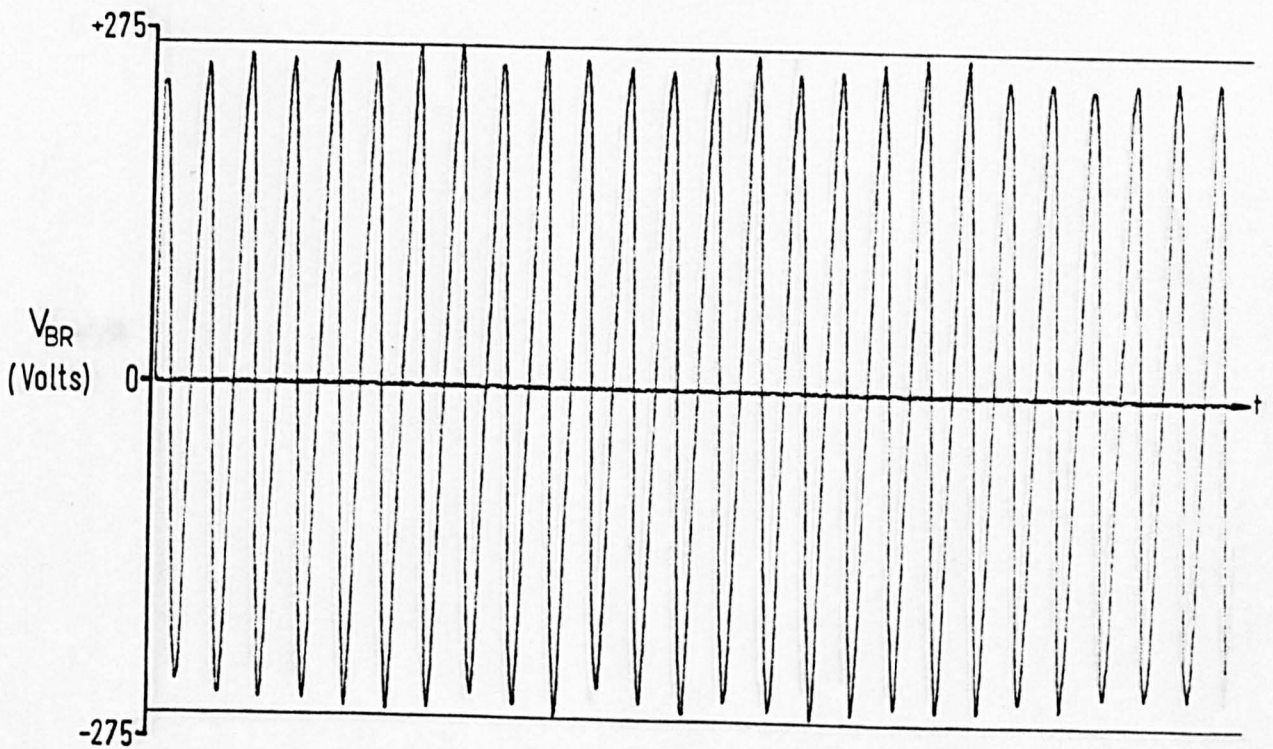


Fig. 2.18 : V_{br} with arc furnace model operating

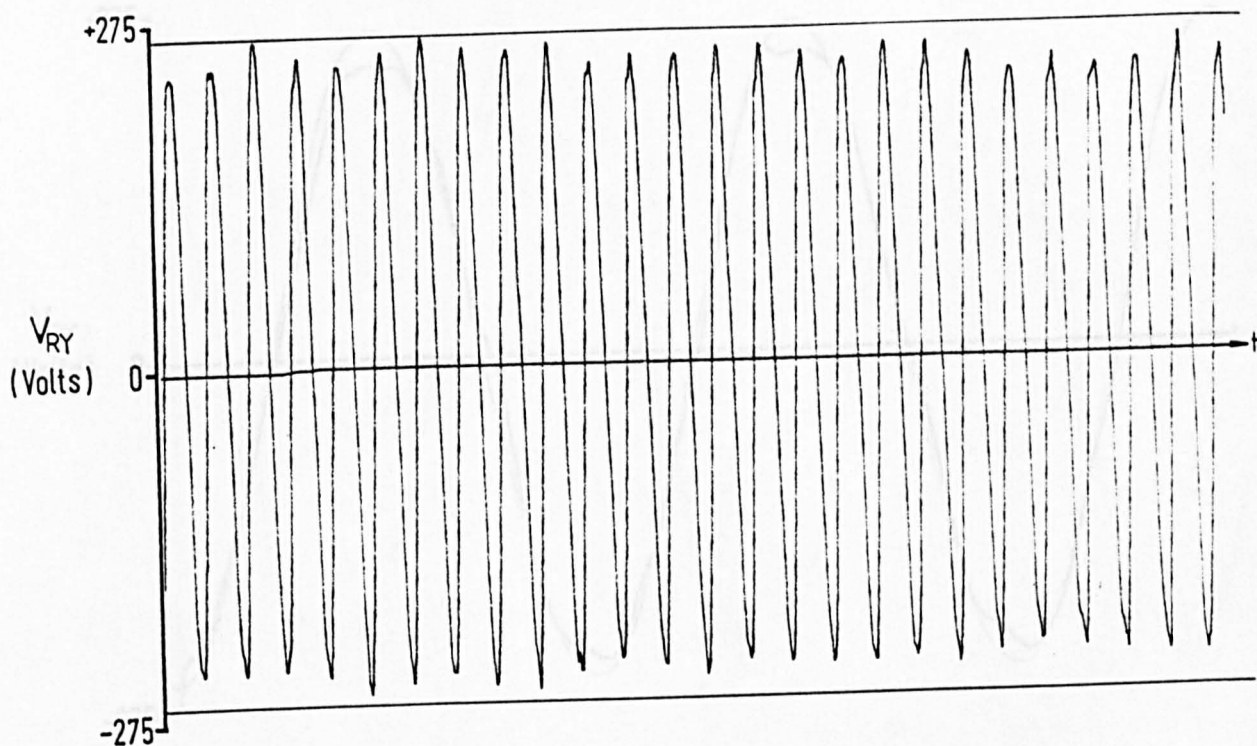


Fig. 2.19 : V_{ry} with arc furnace model operating
 ry

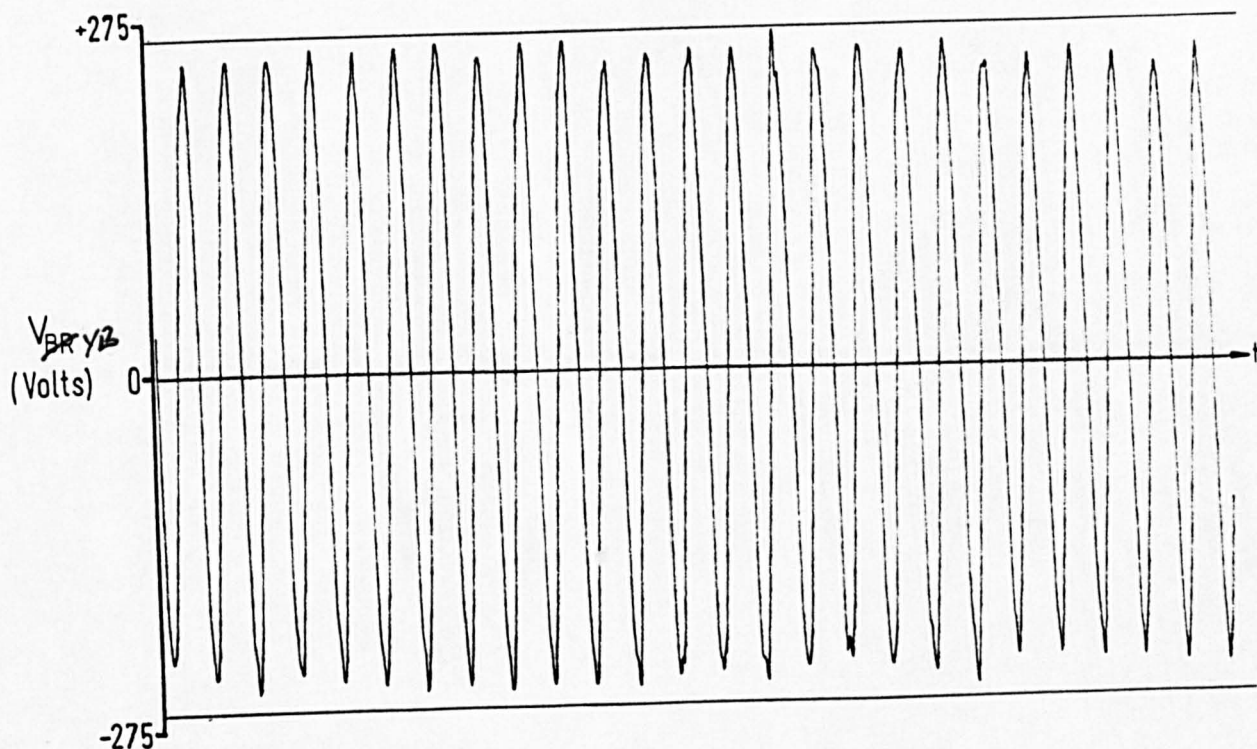


Fig. 2.20 : V_{YB} with arc furnace model operating
 YB

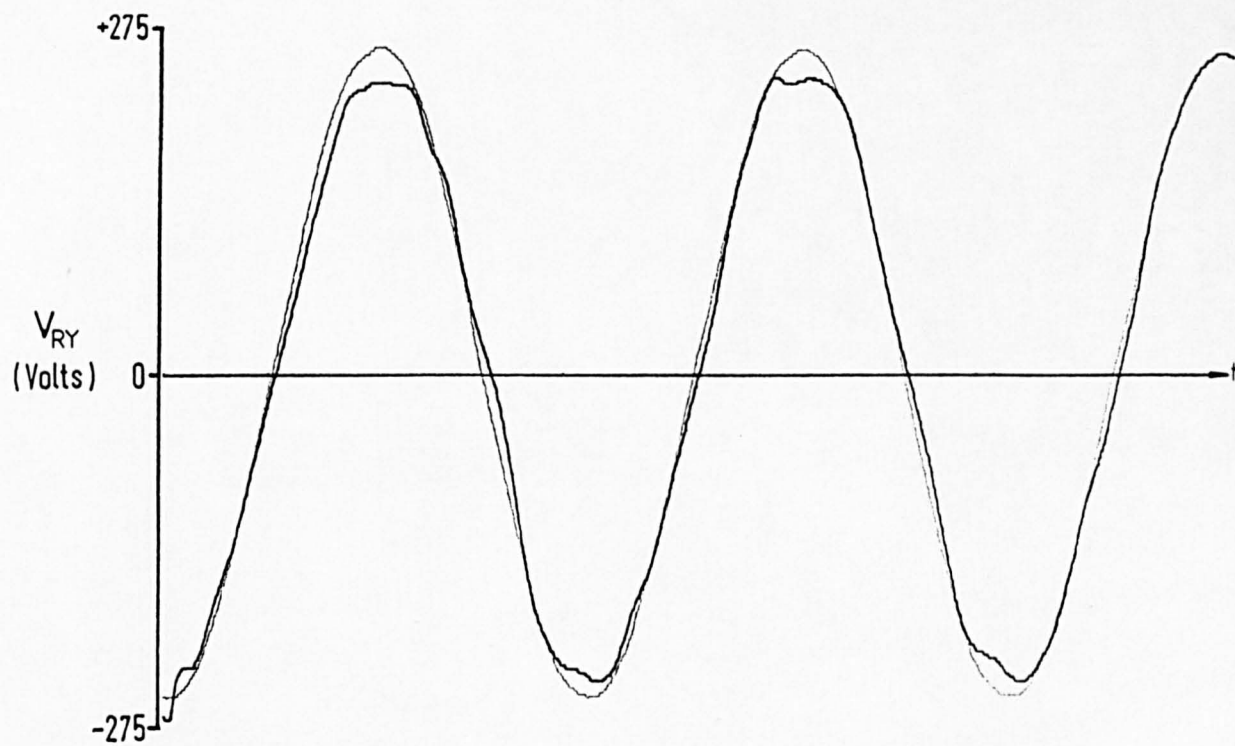


Fig. 2.21 : Detail of distorted V_{br}
 ry

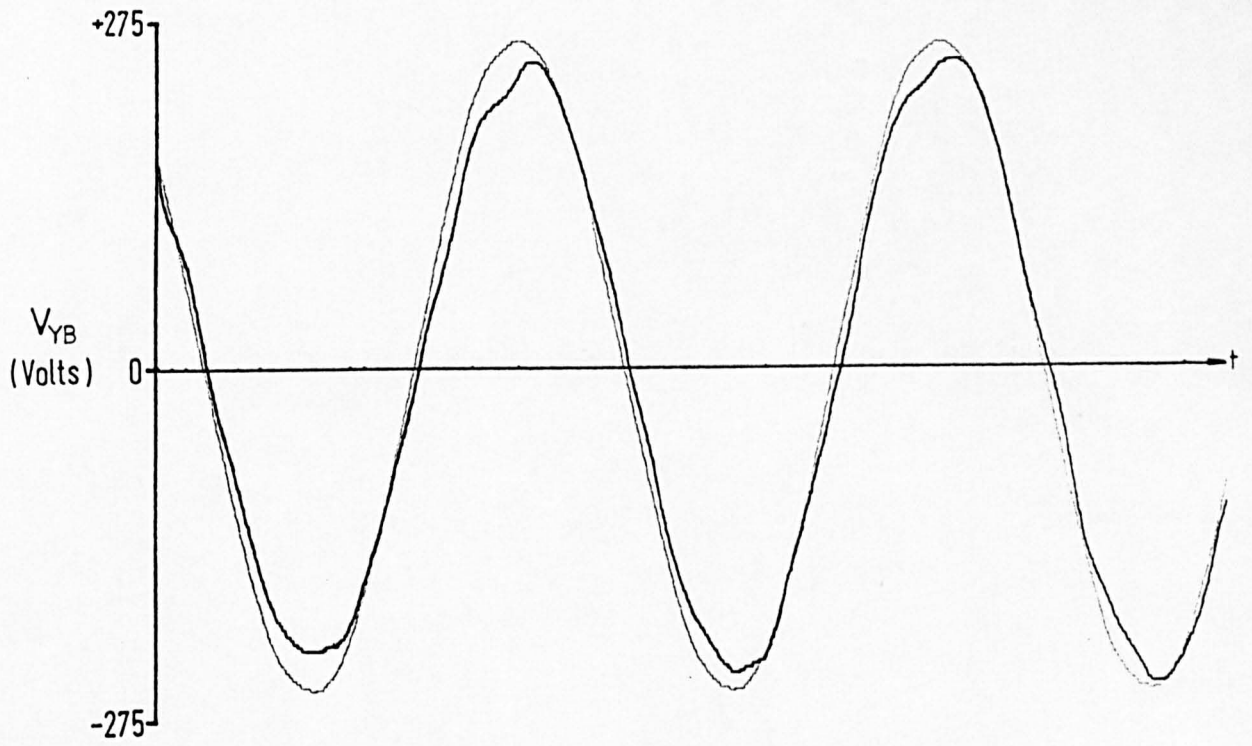


Fig. 2.22 : Detail of distorted V_{Yb}

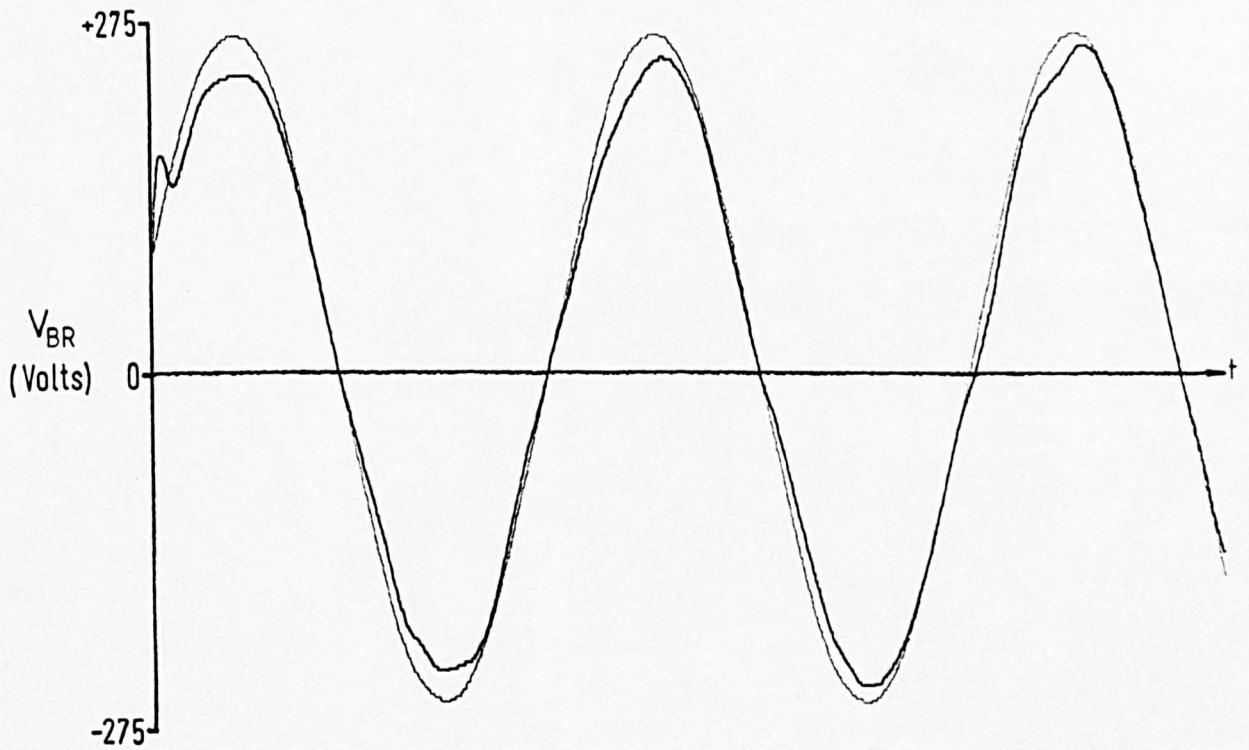


Fig. 2.23 : Detail of distorted V_{Yr}
 br

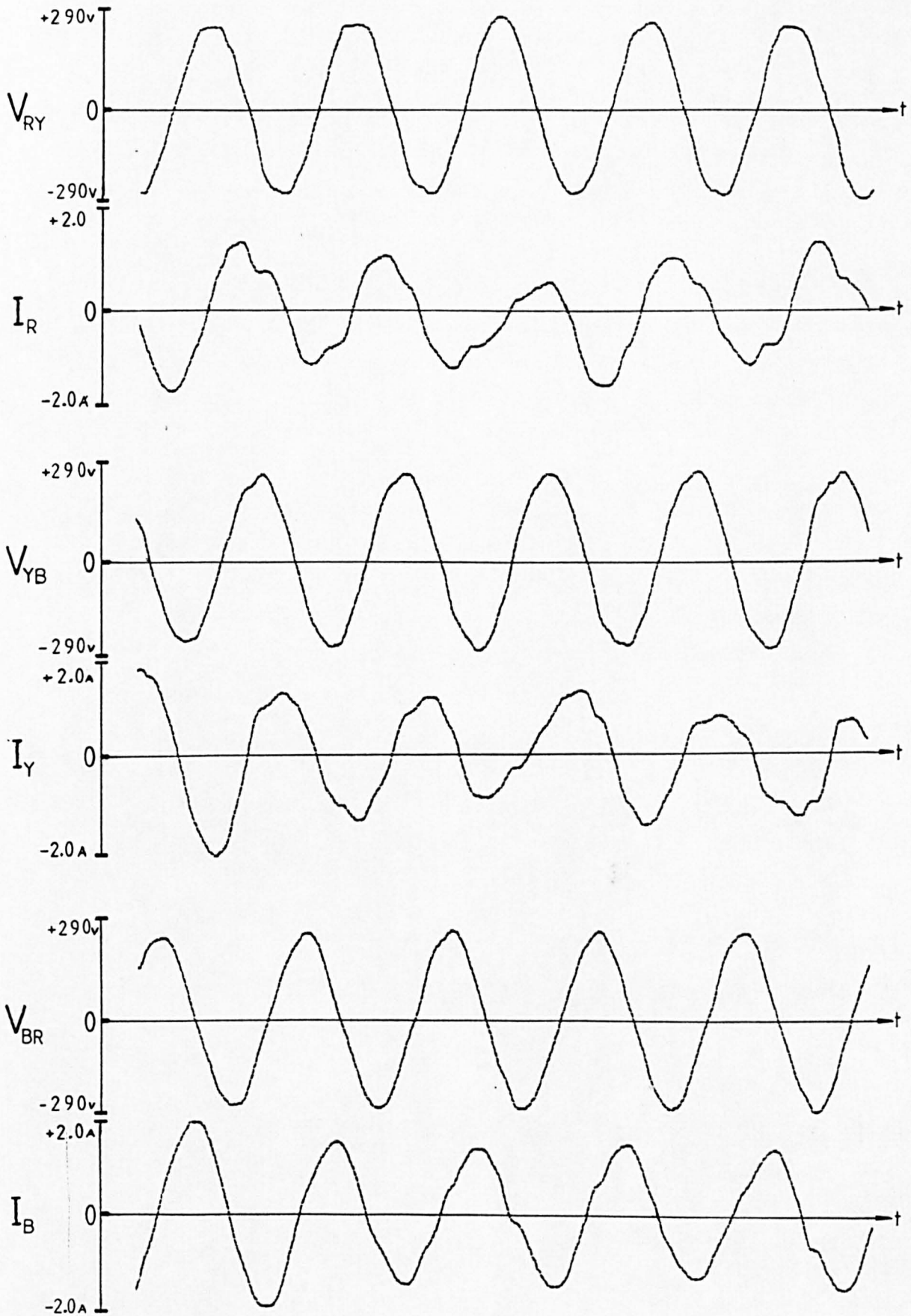


Fig. 2.24 : Arc furnace model three phase voltages and currents

The relevance of V_f in these studies is described further in Part 3.1, and Section 8.4.3 studies the results from a digital model in both the full form and the demodulated form. It is shown that analysis of the power spectral density can give valuable information about the continuous signal in the time domain. A large number of power spectra are used for performance studies in Chapter V, and Section 5.2.1 discusses further the procedures available for obtaining a power spectrum, and explains the techniques chosen for the laboratory.

The aim here is simply to present power spectra of the time domain signals seen in 2.4.2 above, in order to demonstrate the laboratory model's ability to reproduce distorted voltages which model those occurring in the full size system.

Each spectrum gives a measure of the power of frequency components which make up the continuous signal. The power components at different frequencies are presented in decibels (dBs) relative to the power in the fundamental component at 50Hz. Measurements were made using a commercial spectrum analyser^[118] with output to an X-Y flat-bed plotter.

Figure 2.25 shows the power spectrum to 250Hz of a laboratory signal generator producing only a 50Hz sinusoid. The 3rd harmonic component is visible at approximately -60dB relative to the fundamental, and noise is present across the spectrum between -75dB and -80dB.

Figure 2.26 gives the equivalent power spectrum of the open circuit laboratory supply line voltage. The 2nd, 3rd, 4th and 5th harmonic components are clearly shown above the same noise levels of approximately -75dB.

Figure 2.27 shows the power spectrum to 500Hz of the line voltage distorted by operation of the arc furnace model at the rated level of current. Disturbances across the whole spectrum are evident between -45dB and -65dB, and the magnitude of the harmonic voltages is also increased slightly by components in the current waveform of the furnace model.

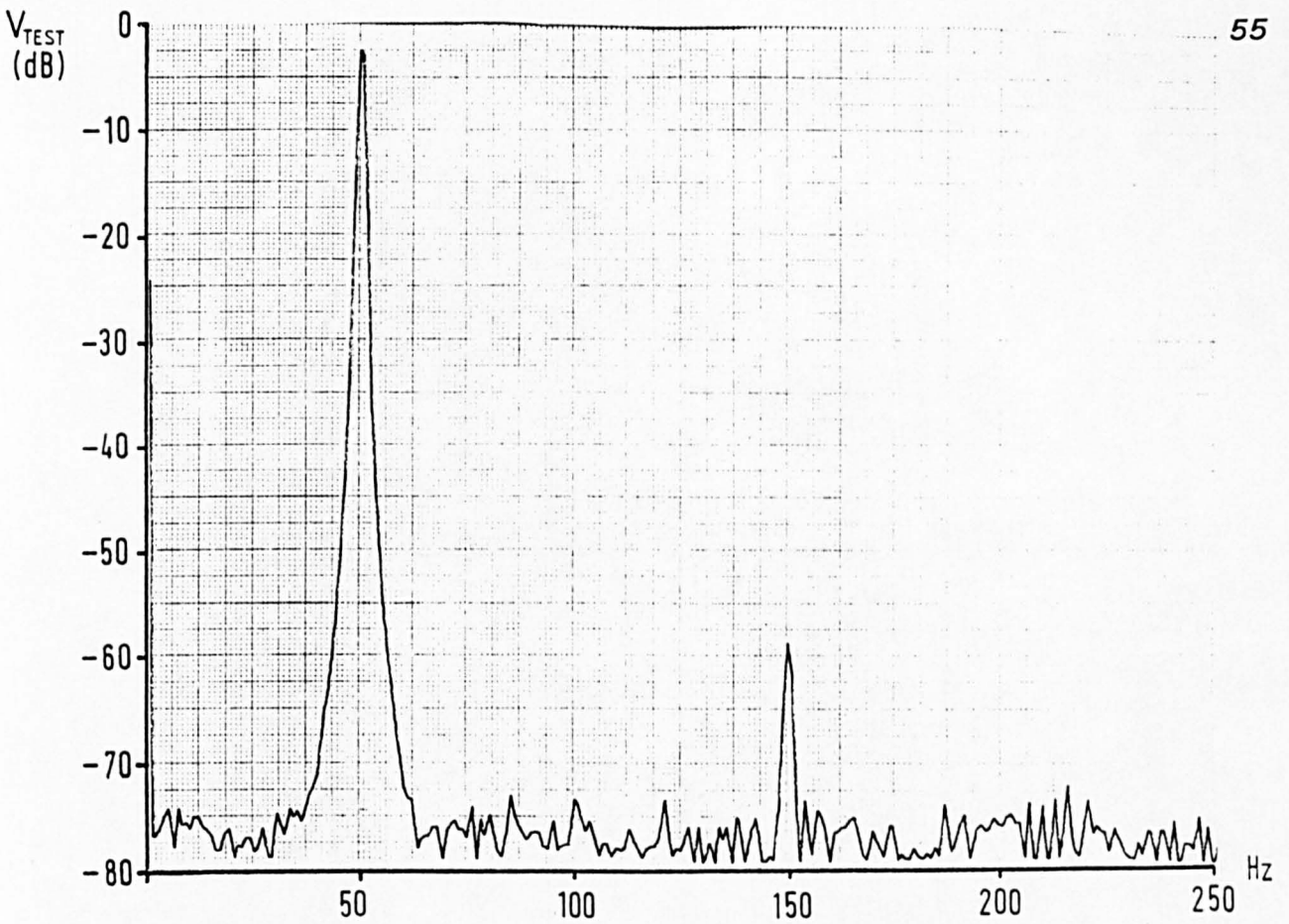


Fig. 2.25 : Power spectrum of 50Hz test sinusoid

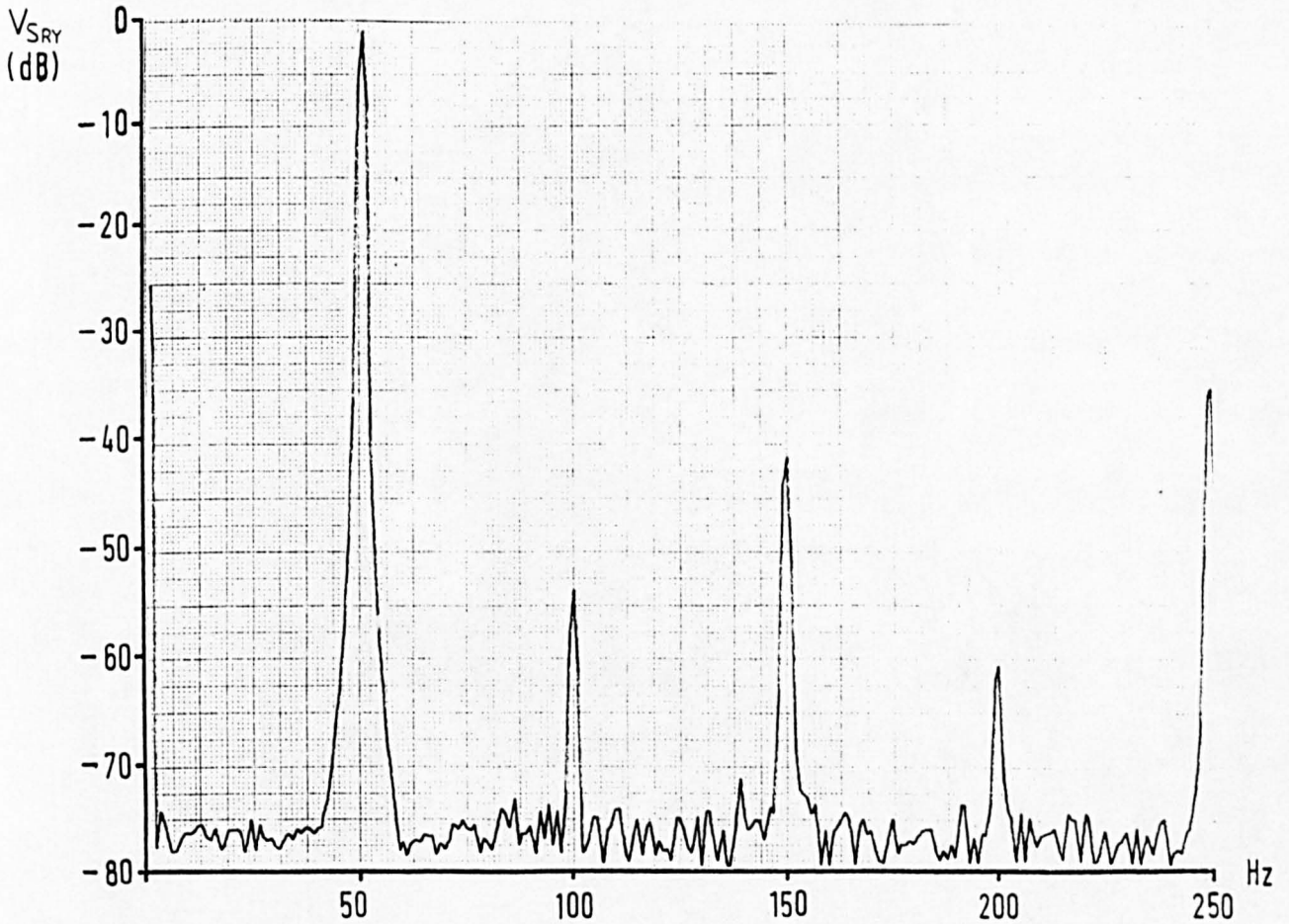


Fig. 2.26 : Power spectrum of open circuit supply line voltage

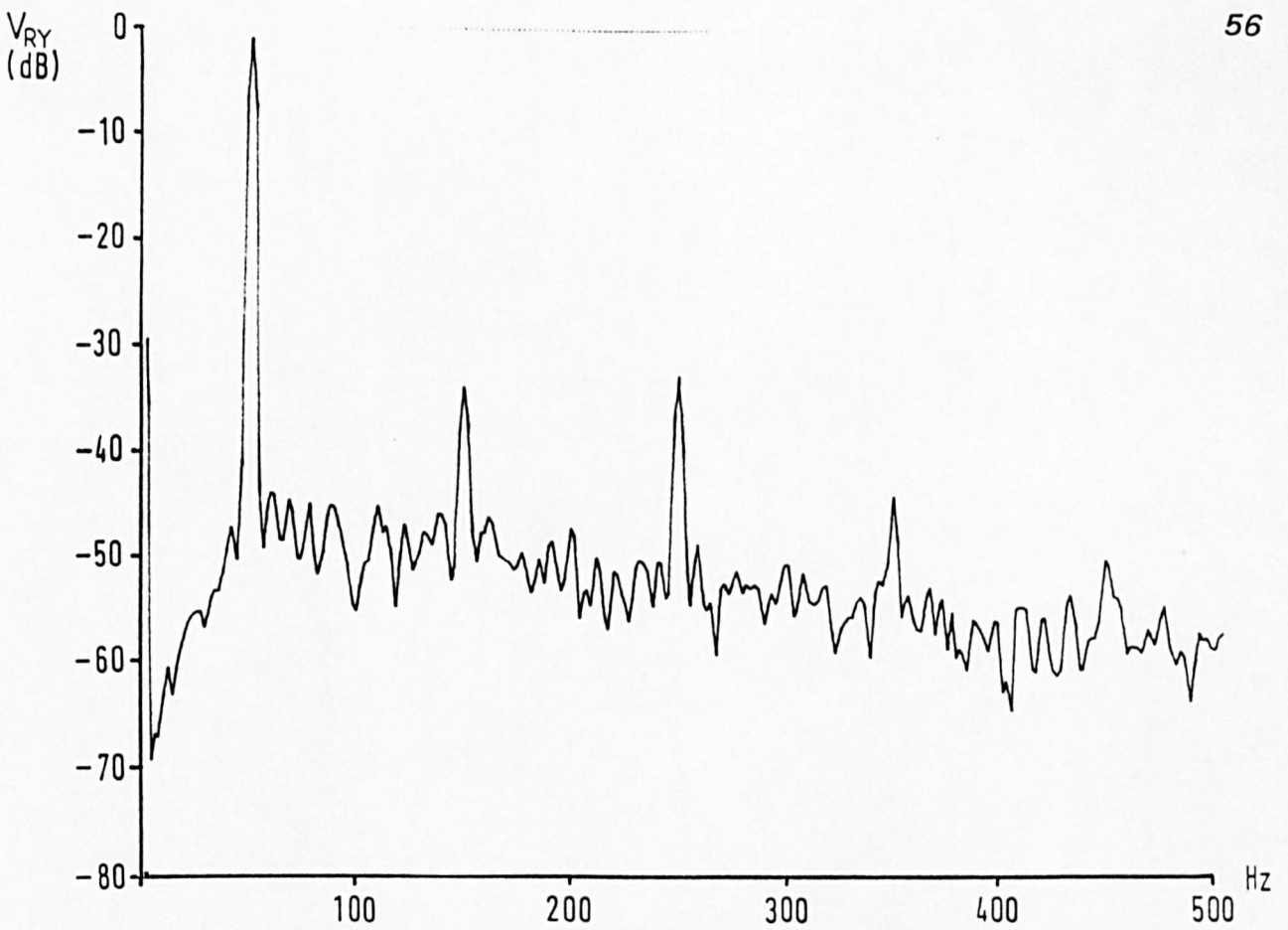


Fig. 2.27 : Arc furnace model V_{ry} power spectrum to 500Hz

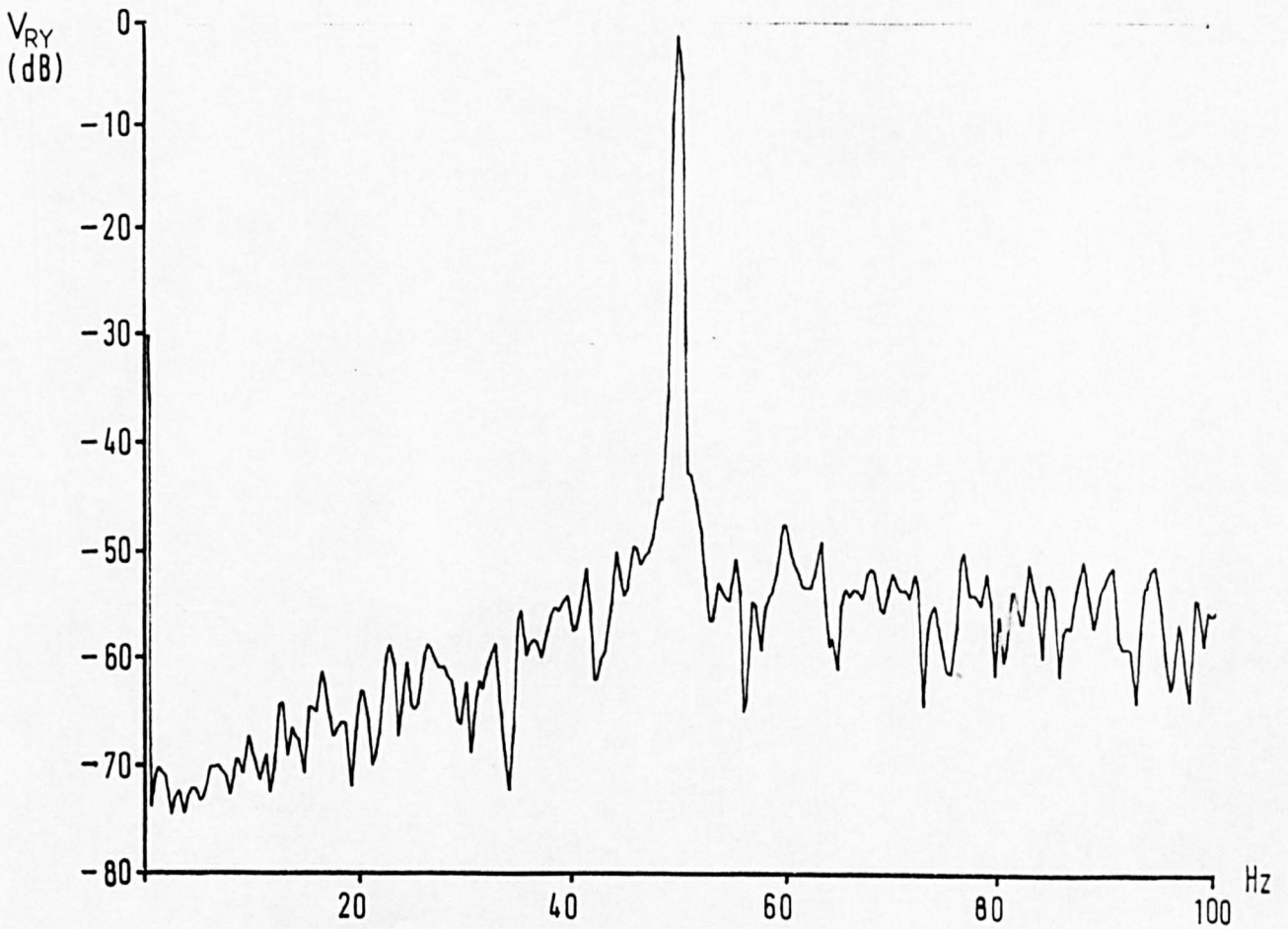


Fig. 2.28 : Arc furnace model V_{ry} power spectrum to 100Hz

Chapter III shows that modulation frequencies between 1Hz and 30Hz are of primary interest for the investigation of tungsten filament lamp flicker. The power from these modulating frequencies will lie in the sidebands above and below the 50Hz 'carrier' signal. These are shown more clearly in Figure 2.28 - the disturbance levels of between -50dB to -70dB in the power spectrum will correspond to voltage components between -25dB and -35dB relative to the 50Hz voltage waveform.

Figures 2.27 and 2.28 may be compared with Figures 2.29 and 2.30 which show the corresponding power spectra of the line voltage recordings made at 33kV. This comparison illustrates the success of the model in reproducing the voltage disturbances evident at the Templeborough installation.

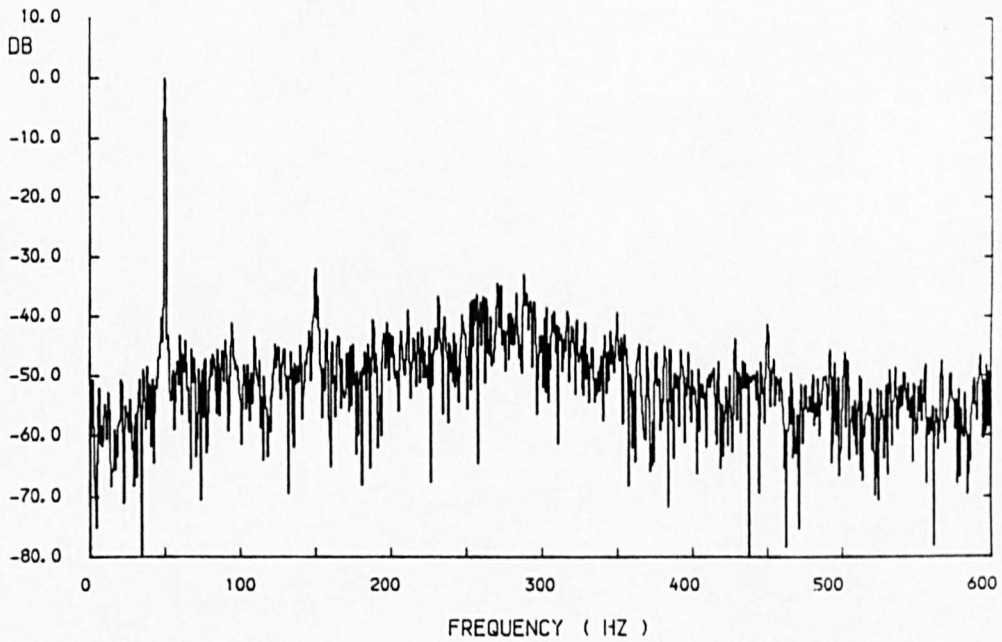


Fig. 2.29 : 0-600Hz power spectrum of CEGB recorded Vry

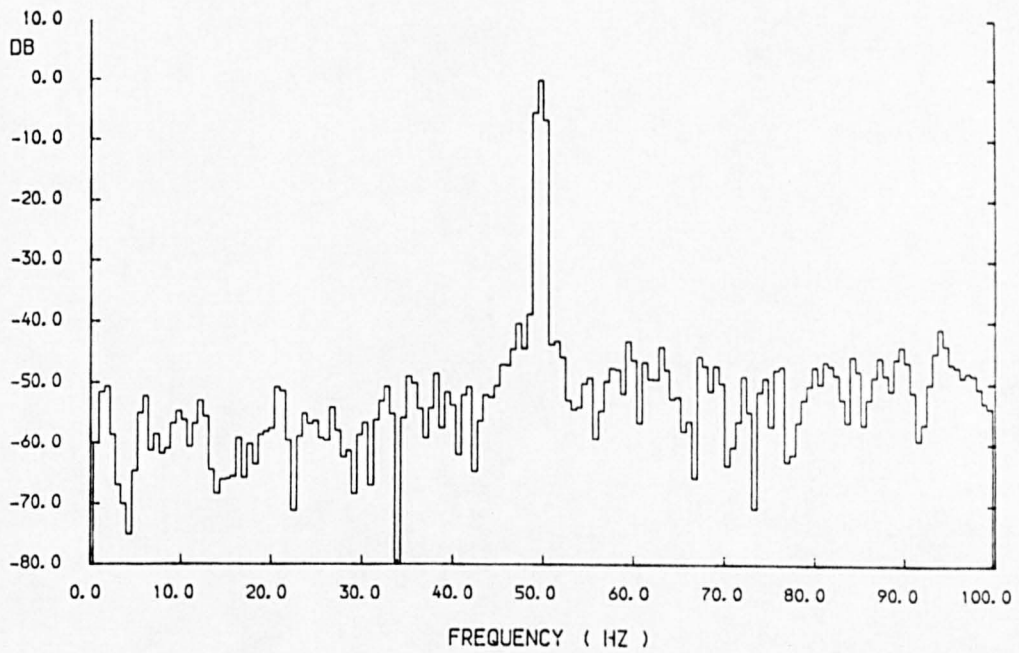


Fig. 2.30 : 0-100Hz power spectrum of CEGB recorded Vry

CHAPTER THREE

FLICKER AND ITS REDUCTION

3.1 FLICKER

- 3.1.1 V_f - A Flicker Voltage
- 3.1.2 Frequency Dependence of Flicker
- 3.1.3 Annoyance Levels

3.2 THE ELECTRIC ARC FURNACE AS A FLICKER SOURCE

- 3.2.1 The Arc Furnace Melt Cycle
- 3.2.2 Composition of Melt Baskets
- 3.2.3 Operators and Electrode Control Systems
- 3.2.4 Voltage Distortion due to an Electric Arc Furnace Installation

3.3 FLICKER LEVELS ON A PARTICULAR FURNACE SUPPLY AND ITS LABORATORY MODEL

- 3.3.1 Study for the Templeborough Installation
- 3.3.2 Study for the Physical Model

3.4 FLICKER REDUCTION

- 3.4.1 Shunt Reactive Compensation
- 3.4.2 The Rating of a Reactive Compensator
- 3.4.3 Control of Static Shunt Reactive Compensators
- 3.4.4 Performance of Installed Reactive Compensators

3.1 FLICKER

The flickering of tungsten filament lamps due to distortion of the supply voltage waveform is not a new phenomenon. A survey in 1956^[1] associated the occurrence of flicker with arc furnace installations connected to the power supply system. Since that time there have been significant advances in the understanding of how various factors in a distorted supply voltage effect flicker perception and annoyance^[2-20]. Naturally, an understanding of the causes of lamp flicker perception is useful when its reduction is being considered.

3.1.1 V_f - A 'Flicker Voltage'

Dixon and Kendall^[8] used the concept of a 'flicker voltage', V_f , in their studies of annoyance factors for different combinations and magnitudes of frequencies superimposed on the supply voltage waveform. If the distorted waveform is considered as a 50Hz 'carrier' frequency that is amplitude modulated by any combination of other frequencies, then V_f represents the arithmetic sum of those frequency components in the time domain. Figures 3.1(a),(b) show a graphical representation of V_f that is often used.

V_f can be obtained in practice using 50Hz notch filters with passband and cut-off characteristics to suit the levels and frequencies of modulation voltage that are to be studied. Digital filtering techniques may also be employed where suitable processing capability is available.

3.1.2 Frequency Dependence of Flicker

A distorted supply voltage waveform may easily be synthesised - methods include repetitive load switching, on-line computation and electronic modulation techniques^[13]. V_f can then be simply restricted to a single frequency that may be varied at will.

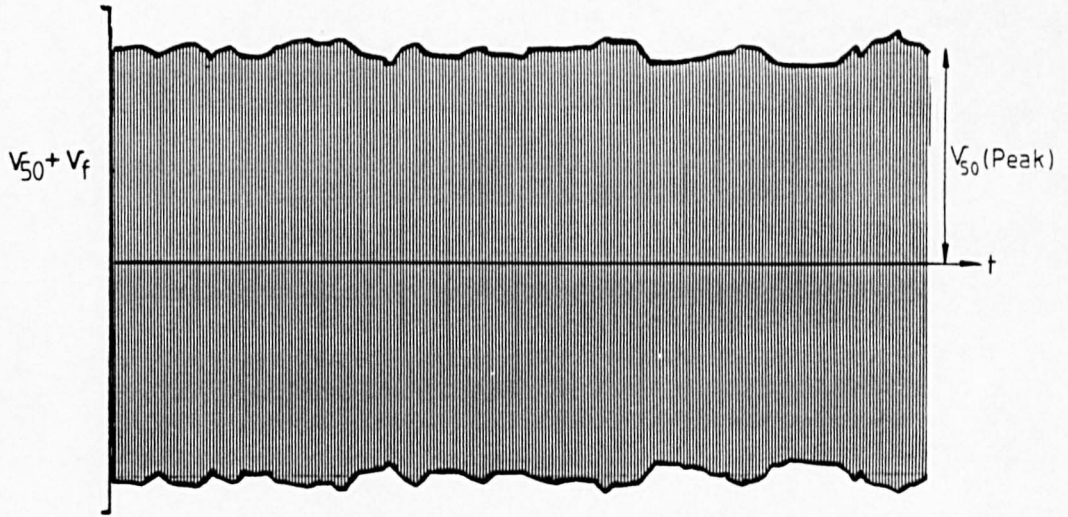


Fig. 3.1(a) : Amplitude modulated 50Hz supply waveform



Fig. 3.1(b) : Flicker voltage V_f from demodulation

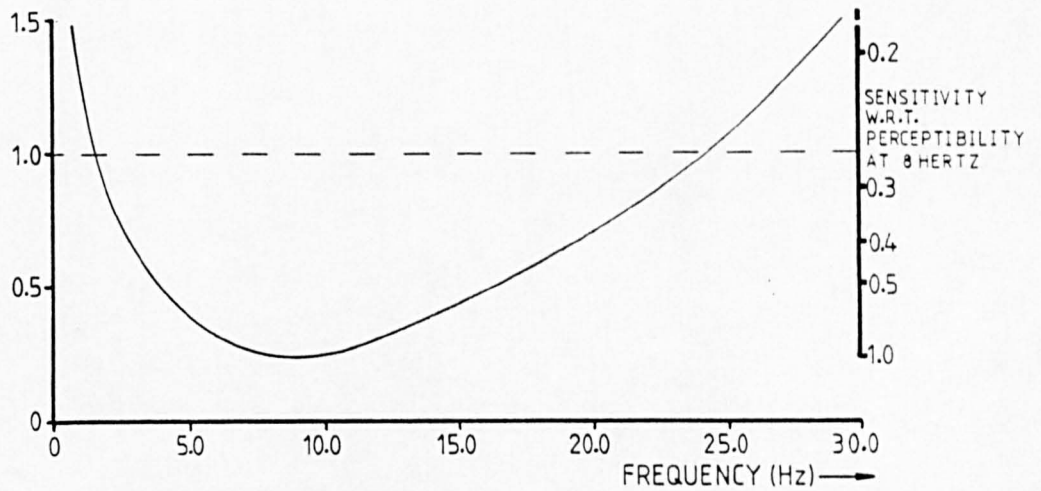


Fig. 3.2 : Normalised sensitivity to flicker frequency

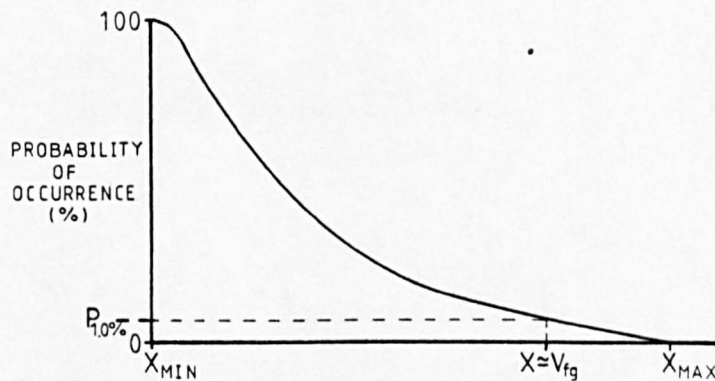


Fig. 3.3 : Example of a cumulative probability curve

The magnitude of V_f that gives an annoying level of lamp flicker at a given frequency is highly subjective, it is also related to the environment and activity of the subjects. Research has enabled a weighting curve to be produced^{[5],[7],[14],[16]} (Fig. 3.2). This curve represents the transfer function of lamp + eye + brain, with a distorted voltage as the input and physiological response to lamp flicker as the output. It is clear that flicker voltages with frequencies in the range 2-20Hz will cause greatest complaint if the level of V_f is constant.

Flicker voltages with frequencies outside of this range cannot be neglected if the relative magnitude of V_f is large at such frequencies.

The flicker voltage, V_f , will rarely be a sinusoid at a single frequency. Any $v_f(t)$ can, however, be represented by its spectrum of sinusoids in the frequency domain $v_f(\omega)$ ^[91,92]. The annoyance effect of non-sinusoidal $v_f(t)$ can thus be evaluated using the magnitudes of its individual frequency components.

3.1.3 Annoyance Levels

No mention has yet been made of the magnitude of V_f . Since V_f is a measure of the distortion of a sinusoidal supply voltage V_{fund} , it is logical to relate V_f to V_{fund} . The UK Electricity Council's 1970 Recommendations^[6] use the ratio of RMS quantities, but increasing use is being made of the definition

$$V_f(\text{p.c.}) = \frac{V_f \text{ (peak to peak volts)}}{V_{fund} \text{ (peak volts)}} \times 100\text{p.c.}$$

which is used by the UIE^[19].

In most cases $V_f(t)$ is not a periodic function but is a stochastic process - random within certain statistical bounds. In such cases an observation lasting only a short time may not be representative of the continuous signal, and the question of how to treat successive observations becomes important. The accepted method in the UK for analysis of flicker measurements is to generate a Cumulative Probability Function (CPF)^[14,16].

Figure 3.3 shows an example of a CPF - the ordinate is a percentage probability that the abscissa (the measured quantity) corresponding to a point on the curve will be equalled or exceeded. The percentage probability is based purely on all observations within some time period. Thus all of the observations exceed the lowest measured value, and the probability that this lowest measured value will be exceeded is 100p.c.,

i.e. $P_{100p.c.} = X_{min}$

The UK Electricity Council's recommendation^[6] is that the RMS ratio $V_f(p.c.)$ be used as the measured quantity. The value of V_f then corresponding to $P_{1.0p.c.}$ is defined as V_{fg} , the gauge-point fluctuation voltage. Obviously for different levels of supply voltage distortion V_{fg} will take a different value. The recommendation^[6] is that the limits for V_{fg} be set at:

$$\begin{aligned} V_{fg} &= 0.25p.c. \text{ for network voltages up to } 132kv \\ V_{fg} &= 0.20p.c. \text{ for networks above } 132kv \end{aligned}$$

These values were chosen in view of tests^[7] which showed how a continuous level of fluctuation voltage related to subjective flicker perception:

$V_f = 0.20\text{p.c.}$	-54.0dB	Just perceptible, but not annoying
$V_f = 0.25\text{p.c.}$	-52.0dB	Obvious, but not annoying
$V_f = 0.30\text{p.c.}$	-50.5dB	Uncomfortable or intolerable
$V_f > 0.30\text{p.c.}$	-50.5dB	Intolerable

Later studies^[14,16] have shown the importance of frequency-weighting the measured value V_f , and of using more figures from the CPF (e.g. $P_{0.1\text{p.c.}}$, $P_{1.0\text{p.c.}}$, $P_{3.0\text{p.c.}}$, $P_{10.0\text{p.c.}}$) for a more accurate representation of the flicker severity factor of a distorted supply voltage waveform.

3.2 THE ELECTRIC ARC FURNACE AS A FLICKER SOURCE

The non-sinusoidal nature and imbalance of three-phase currents drawn by an arc furnace has already been illustrated, using a block of data from the CEGB recordings, (Fig. 2.3). The severity of these current fluctuations for a given furnace installation is not constant, but a function of several factors:

- (i) The point in the arc furnace melt-cycle.
- (ii) The type of material to be melted down, and its movement within the furnace crucible.
- (iii) The combined effects of electrode control apparatus and human operator actions.

The consequent disturbances of the supply voltage waveform experienced by other consumers will then depend on:

- (iv) The point from which their electrical supply is derived (the Point of Common Coupling).
- (v) The impedances present between furnace installation, consumer and the 'infinite busbar'.

Each of the above points are now examined in more detail.

3.2.1 The Arc Furnace Melt-Cycle

The melt-cycle is defined as the sequence of events normally followed in order to produce usable molten steel from solid constituents. The start of the cycle sees the first 'basket' of metal dropped into the furnace crucible. The electrodes lower and arcs are struck between them and the surface of the metal.

As the electric arc bores down into the heap of metal, the electrodes are lowered. When the electrode tips are below the top of the metal, maximum voltage is applied via the on load tap changer. For this 'bore-down' stage the arcs are now long and maximum energy is transferred to the scrap surrounding the arcs (Figure 3.4(a)). The full power 'bore-down' is continued until much of the metal lies in a molten pool. The arc is then extinguished and a second basket of metal is added. The 'bore-down' process is repeated, then medium power is used when there is little metal projecting from the molten pool - this reduces wear on the refractory lining of the furnace, which would otherwise be exposed to the full power output from the arcs (Figure 3.4(b)).

When all of the metal has been liquified, a sample of the melt indicates how the metal can be refined to give the quality of steel required. Chemical additions are made and refining is carried out with very low power input to the molten pool (Figure 3.4(c)).

Example times for the above processes for a 100 Tonne, 70MVA furnace are^[121]:

First Basket Bore-down	30 mins
Second Basket Bore-down	25 mins
'Medium Power' melting	10 mins
Refining	20 mins

The most severe fluctuations in furnace current occur during the two 'bore-down' periods when large pieces of metal may fall in the immediate region of each arc, which will be operating at full power. Phase to phase short circuit and/or single phase open circuit conditions lasting for several seconds may arise, and the cycle-by-cycle current waveform is mainly non-repetitive, reflecting varying arc length after the extinguishment and re-striking of the arc around current-zero.

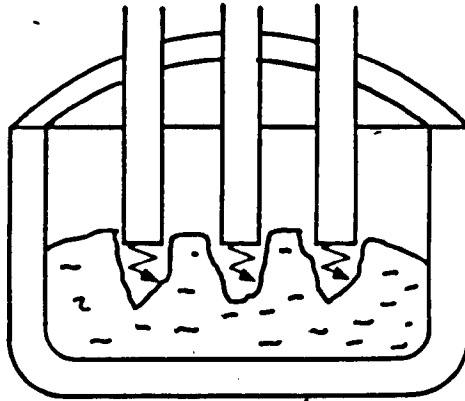


Fig. 3.4(a) : Arc furnace crucible - bore down

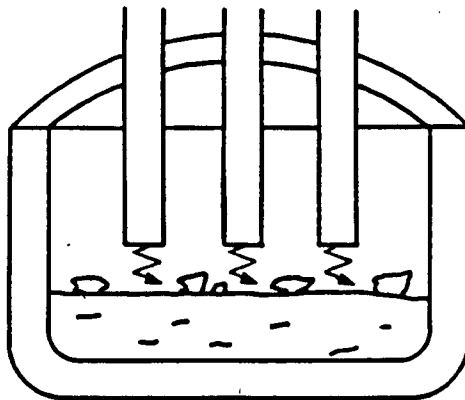


Fig. 3.4(b) : Arc furnace crucible - medium power

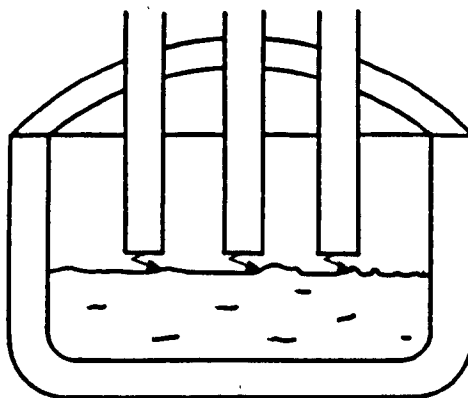


Fig. 3.4 : Arc furnace crucible - refining

3.2.2 Composition of Melt-Baskets

Each basket of metal to be melted may contain a mixture of the following types of scrap metals:

- (i) Turnings - From industrial machining process.
- (ii) 'Fragmentised' medium duty steel structures.
- (iii) Rod or Billets - probably produced at the same steelworks.
- (iv) Slag scrap collected from previous melts.
- (v) 'No. 1' scrap - an assortment of heavy and medium duty steel previously cut to fit into crucible.
- (vi) Plate iron.
- (vii) 'Bales' - a clean scrap steel compressed into large blocks.

The composition of particular baskets is varied to suit the grade of steel required, and to a lesser extent the relative quantities available^[121].

Turnings or 'swarf' will give the most consistent arc behaviour and hence the smallest current variations. 'bales' of compressed steel take longest to melt down and their movement in the crucible can create severe fluctuations in arc current.

3.2.3 Operators and electrode control systems

Automatic electrode control systems are used on all but the smallest of arc furnaces. Their primary function is to keep the arc current near constant for a given electrode voltage. If the electrode voltage is increased, a larger arc can be sustained and the power input to the furnace is greater.

Short circuits in the furnace cause the electrodes to be withdrawn, open circuits cause them to be lowered. The methods of control need not be discussed here since there is much information in the literature^[93,94].

Operators in the furnace control room will manipulate furnace transformer on-load tap changers and circuit breakers, and utilise electrode controllers to progress through the melt cycle in a way that they see fit. Thus additional variations will exist for different melt-cycles.

Further information on almost every aspect of electric arc furnace operations is given by Robiette^[93].

3.2.4 Voltage Distortion due to an Arc Furnace Installation

A load drawing a non-sinusoidal current from a sinusoidal supply e.m.f. will cause distortion of the voltage at its terminals provided there is some impedance present in the current path.

Figure 3.5 shows a representation of a power system supplying an arc furnace installation and other consumers. The 'point of common coupling' (PCC) is defined^[6] as the electrical point nearest to the arc furnace installation to which other consumers are connected.

On a large power system, the reactive components of impedances usually exceed the corresponding resistive components by a factor of at least 20, thus if

$$Z_s = R_s + jX_s \quad \text{and} \quad Z_f = R_f + jX_f$$

$$\text{then} \quad Z_s \approx jX_s \quad \text{and} \quad Z_f \approx jX_f$$

Where Z_s and Z_f represent the system and furnace impedances respectively. The corresponding phasor diagram for $I = I_s = I_f$ lagging V_0 by a phase angle θ is shown in Figure 3.6. Clearly if $V_{af} \gg IX_{tot}$ then the arithmetic difference, ΔV , between the voltages V_0 and V_{af} can be written:

$$\Delta V_{af} \approx I \sin \theta X_{tot}$$

$$\text{and} \quad \Delta V_{PCC} \approx I \sin \theta X_s$$

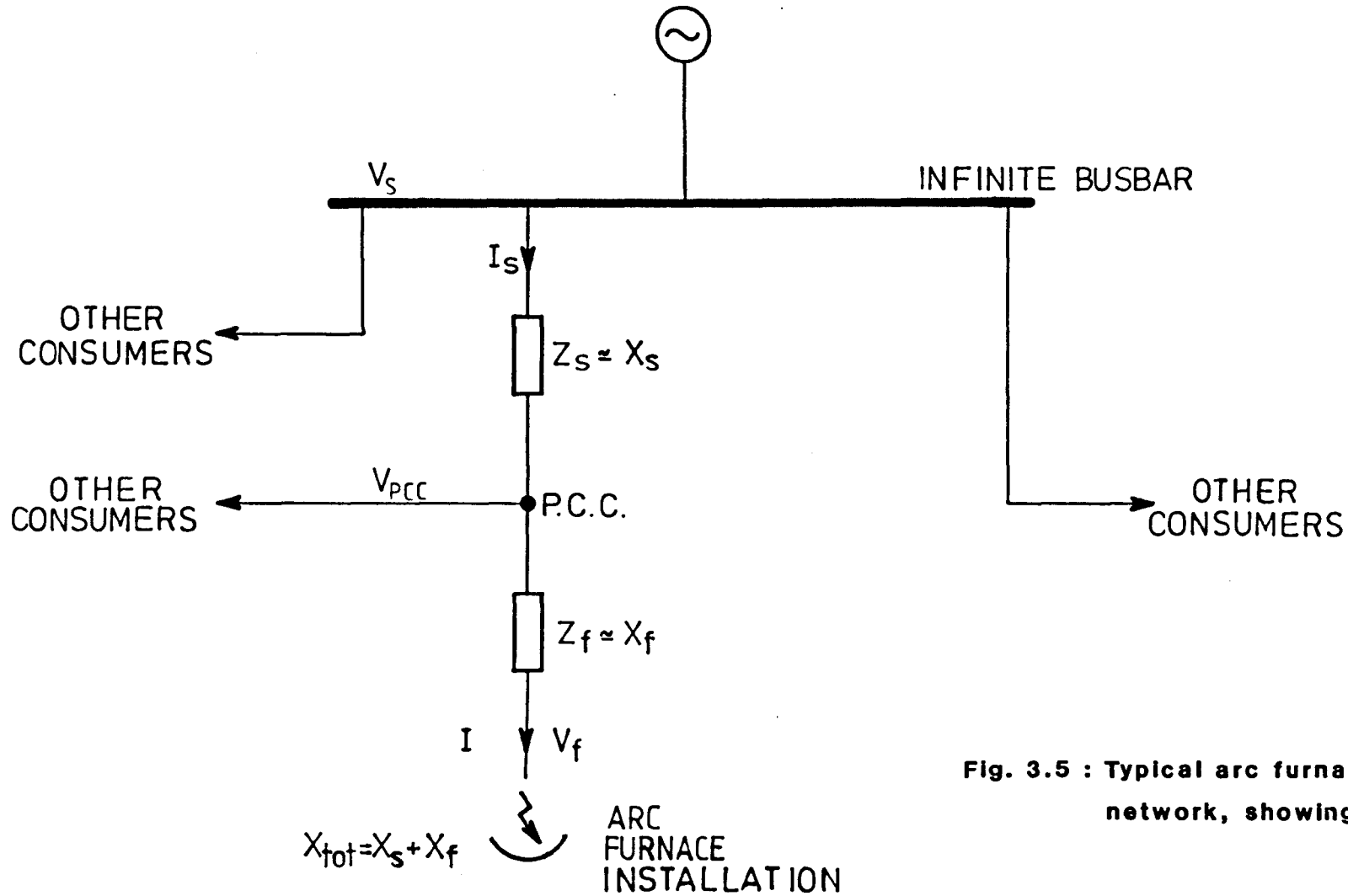


Fig. 3.5 : Typical arc furnace supply network, showing PCC

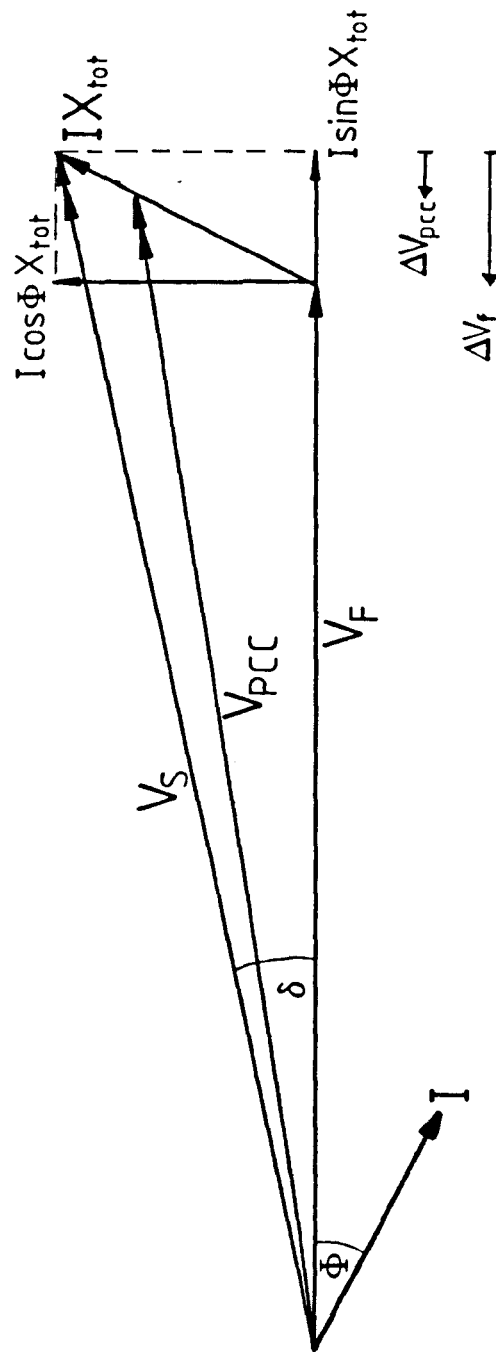


Fig. 3.6 : Phasor diagram for voltages at system, PCC and furnace installation

Thus the voltage fluctuations at the point of common coupling are primarily due to variations in the reactive component of I.

Arc furnaces operate at a power factor of 0.7-0.8 at full load [93] i.e. $I \sin \phi \approx 0.6I$. Thus the reactive component of $I(t)$ is not negligible. The measurements of $i(t)$ (Figure 2.3) were shown to have power spectral density components at levels between -25dB and -45dB in the critical modulation band of 0-30Hz (Figure 2.12) - the effect of these current fluctuations is further studied below.

3.3 FLICKER LEVELS ON A PARTICULAR FURNACE SUPPLY AND ITS MODEL

A method for predicting the severity of perceived tungsten filament lamp flicker from a knowledge of the arc furnace and supply system details is contained in the UK Electricity Council Recommendations on arc furnaces and their supply^[6]. Firstly, this method will be applied to the Templeborough power system used for the CEGB measurements (see Section 2.1.1), and secondly to the laboratory model of that system. Impedances in each network may be represented in the form used in reference [6], and repeated in Figure 3.7.

The results may then be related to measured values of the flicker voltage, V_f .

3.3.1 Study for the Templeborough Installation

The voltage depression caused at a point on the supply network to an arc furnace installation is primarily dependent upon two quantities:

- (i) The short-circuit power of the arc furnace,
- and (ii) The fault level at the point of study.

A quantity V_t , the Short-Circuit Voltage Depression, is defined^[6] as:

$$V_t = \frac{S_t}{S_c} \times 100\text{p.c.}$$

Where S_t and S_c are the furnace short-circuit power and fault level at the point of common coupling respectively. The precise definition of these quantities and a discussion of typical values is given in detail in Reference [6] and need not be repeated here.

The short-circuit power, S_t , of the arc furnace can be either measured directly or calculated from other data^[6]. A general method for performing this calculation given in Reference [6] is followed in Appendix A. This gives:

$$\underline{S_t = 87.46\text{MVA}}$$

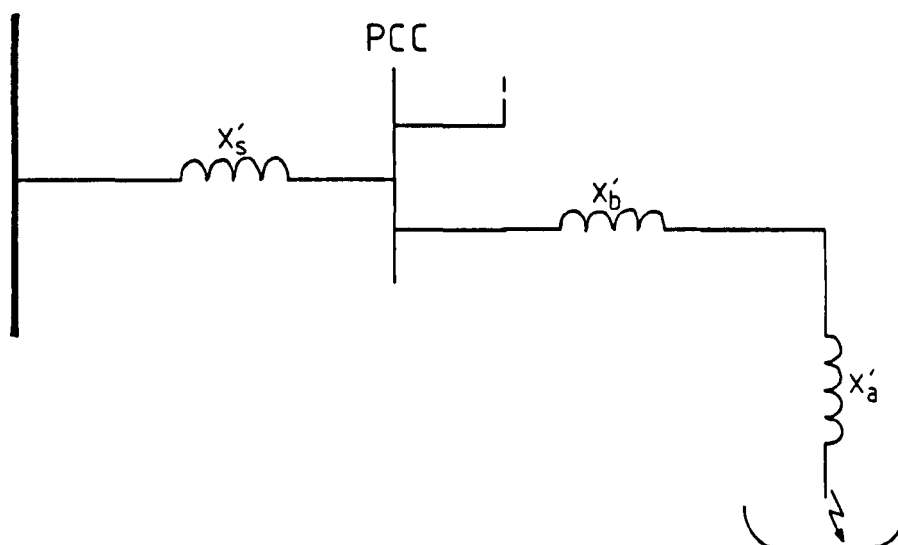


Fig. 3.7 : Electricity Council notation for arc furnace supply system

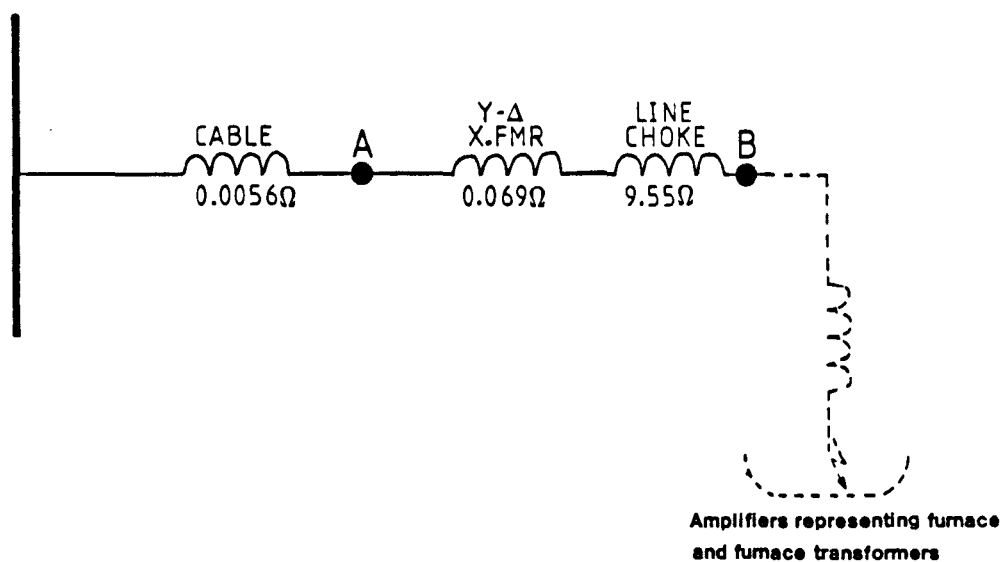


Fig. 3.8 : One line diagram of the laboratory arc furnace model supply

It will be useful to note the 33kV short circuit current here:

$$I_{sc} = \frac{87.46 \times 10^6}{\sqrt{3} \times (33 \times 10^3)} = 1.53\text{kA or } \underline{0.875\text{p.u.}}$$

S_c , the fault level for the point of calculation of V_t is easily found:

$$\text{At 275kV } S_c = \frac{100}{X_s'} = 8500\text{MVA, giving } V_t (275\text{kV}) = 1.03\text{p.c.}$$

$$\text{At 33kV } S_c = \frac{100}{X_s' + X_b'} = 400\text{MVA, giving } V_t (33\text{kV}) = 21.87\text{p.c.}$$

V_{fg} can now be predicted from V_t :

$$V_{fg} = k_s V_t$$

where the 'severity factor', k_s , is usually in the range 0.09 to 0.15 with a mean at 0.12^[6].

Thus for $k_s =$	0.09,	0.12,	0.15
$V_{fg} (275\text{kV}) =$	0.093p.c.,	0.123p.c.,	0.154p.c.
$V_{fg} (33\text{kV}) =$	1.97p.c.,	2.62p.c.,	3.28p.c.

It will be noted that the theoretical value of V_{fg} at 275kV is well below the flicker perceptibility threshold of 0.20p.c. described in Section 3.1.3. Tests conducted by the Electrical Research Association (ERA)^[6] for the same system support this, in so far as there were no complaints from consumers with the PCC at 275kV.

3.3.2 Study for the Physical Model

If the Templeborough system has been modelled with sufficient accuracy, then the model's values of V_{fg} will be identical to those found in the preceding section. It will be useful to give an analysis for the physical model, so that the relevance of different impedances may be appreciated.

In section 3.3.1 the furnace short-circuit current, I_{sc} , was shown to be 0.875p.u. If the model's current base has been scaled correctly, this will be equivalent to a current of:

$$\begin{aligned} I_{sc} &= 0.875 \text{p.u.} \times I_{\text{base}} \\ &= 0.875 \text{p.u.} \times 2.659 \text{A} \\ &= 2.33 \text{A} \end{aligned}$$

For $V_L = 1.0 \text{p.u.} = 175 \text{v}$, the short-circuit power is therefore:

$$S_t = \sqrt{3} (175)(2.33) = \underline{706 \text{VA}}$$

Figure 3.8 gives a one line representation of the model, with all ohmic impedances referred to 175 volts. Point A corresponds to the 275kV point of common coupling whilst point B corresponds to the 33kV busbar.

The model's bases will be repeated here for reference:

$$V_{\text{base}} = 175 \text{V}, \quad X_{\text{base}} = 38.0 \text{ Ohms}, \quad I_{\text{base}} = 2.659 \text{A}, \quad VA_{\text{base}} = 805.9 \text{VA}$$

$$X_s' = 0.0056 \text{ Ohms} = \frac{0.0056}{38.0} \text{ p.u.}$$

$$= 0.00015 \text{ p.u. to the model's bases}$$

$$X_b' = 0.069 + 9.55 \text{ Ohms} = \frac{9.619}{38.0} \text{ p.u.}$$

$$= 0.2531 \text{p.u. to the model's bases}$$

Then the Fault Level at A is:

$$S_{CA} = \frac{805.9}{0.00015} = 5.37\text{MVA}$$

and at B:

$$S_{CB} = \frac{805.9}{0.2531} = 3184\text{VA}$$

These values are calculated using reactive impedance components only, as for the full scale system. However, the X/R ratio for the system is large - typically 20 or more, against the models' X/R ratio of approximately 10. The error in S_c introduced by not taking account of resistances is thus -0.5p.c. for the model compared to -0.1p.c. for the real system. Although small, these errors should be borne in mind.

To find the short circuit voltage depression, V_t , at A and B:

$$V_t = \frac{S_t}{S_c}$$

Therefore, $V_{tA} = \frac{706}{5.37 \cdot 10^6} = 0.013\text{p.c.}$

$$V_{tB} = \frac{706}{3184} = 22.8\text{p.c.}$$

and using $V_{fg} = k_s V_t$

for $k_s =$	0.09,	0.12,	0.15
V_{fgA}	= 0.0012p.c.,	0.0016p.c.,	0.0020p.c.
V_{fgB}	= 2.05p.c.,	2.74p.c.,	3.42p.c.

Thus the short-circuit voltage depression at B accurately represents that in the real system at 33kV.

(The real system has $V_t = 1.05\text{p.c.}$ at 275kV
and $V_t = 21.87\text{p.c.}$ at 33kV)

This is reasonable if the voltage fluctuations at the 33kV busbar are to be studied - although in the case of Templeborough this was not the PCC. The disturbance levels at point B (Figure 3.8) will be much higher than those found to be 'just annoying' since the theoretical V_{fg} is approximately 2.0p.c. compared with the 0.25p.c. limit^[6].

If flicker compensation at this level can be achieved, then any improvement factor will still hold true for voltage disturbances further away from the flicker source.

Figure 2.30 showed the power spectral density of the red-yellow line voltage derived from the CEBG recordings at 33kV. The section of data corresponds to those 90 cycles used by the physical model, and it was presented in Section 2.4.3 to allow comparison of 33kV and modelled line voltage power spectra.

Communication theory^[92] would present the power spectrum of a simple amplitude modulated carrier wave as sidebands symmetrical about the carrier frequency. The total signal power P_{TOT} is related to the carrier power P_c and the modulation index 'm' as:

$$P_{TOT} = P_c \left(1 + \frac{m^2}{2} \right)$$

with power $\frac{P_c m^2}{4}$ in each sideband.

The arc furnace non-sinusoidal current's power spectra (Figure 2.12) show reasonable symmetry about the 50Hz fundamental frequency. But the corresponding power spectra for the distorted supply voltage (Figure 2.28) show that the frequency components in the upper sideband have slightly higher powers than the frequency components in the lower sideband. Such an effect may be caused by a system impedance that varies in the range 0-100Hz, with a shunt inductance component becoming relevant at very low frequencies.

3.4 FLICKER REDUCTION

Chapter I introduced a variety of methods for reducing the levels of flicker at a PCC. Each method achieves a reduction in the flicker voltage, V_f , as a proportion of the 50Hz fundamental. This objective may be achieved either by reducing the impedance across which V_f is generated, or by altering the components of the currents that generate V_f . It is worthwhile to remember here that V_f may be resolved into many frequency components, with those centred around 8Hz having annoying effects at very low levels.

Once it has been decided to attempt flicker reduction by connection of a device in parallel with a varying load, careful thought must be given both to the characteristics of the load and to the requirements for the shunt-connected compensator.

3.4.1 Shunt Reactive Compensation

The electrical supply to high power installation is generally of such a rating that the Q factor of the equipment is greater than 20. It can easily be shown (Section 3.3.2) that for sinusoidal conditions it is the contribution of the reactive component of the current that dominates in the voltage drop across an impedance $Z = R + jX$ where $X/R \geq 20$ (Figure 3.6).

It is for this reason that REACTIVE compensation has been accepted and used for the control of voltage changes due to large fluctuating loads.

Miller^[95] provides an excellent reference text on a wide variety of reactive compensation techniques. He and others^[43,44,45,46] identify the Thyristor Controlled Reactor (TCR) as being able to offer the performance necessary for arc furnace voltage flicker reduction.

Point on wave control of thyristor firing results in non-continuous inductive currents in each TCR branch (Figure 3.9). Control of the firing angle ' α ' thus controls the compensator load on the power system.

When the arc furnace demand is high, often approaching short circuit, the shunt compensator demand is set low. The compensator demand is then set high to compensate for a low furnace demand.

Ideally then, the changes in furnace demand will be inversely matched by the balancing TCR. The magnitude and phase of the current drawn from the supply will then be constant. For the case where the balancing is achieved by an inductive system, the current drawn from the supply will remain constant at the maximum value drawn by the furnace installation, i.e. short circuit. This will be at extremely poor power factor (≈ 0.1), and may therefore require further reactive compensation in the form of fixed capacitor banks at the load.

Such capacitor banks simply shift the mean reactive power demand of the dynamically balanced load nearer to zero, thus lowering the magnitude of current through the supply impedance and increasing the load voltage. In practice the fixed capacitors will have values calculated to create a tuned circuit with existing inductances, to act as harmonic filters.

A circuit tuned to absorb harmonic current components is often necessary, due to the non-continuous form of TCR branch conduction.

Fourier analysis of the TCR branch current waveform shown in Figure 3.9 enables the RMS value of the n^{th} harmonic current component to be calculated^[95] as:

$$I_n = \frac{4}{\pi} I_0 \left[\frac{\sin(n+1)\alpha}{2(n+1)} + \frac{\sin(n-1)\alpha}{2(n-1)} - \cos\alpha \left(\frac{\sin n\alpha}{n} \right) \right]$$

Where

$$I_0 = \frac{V}{X_L} \quad \text{and } n = 3, 5, 7, 9, \dots$$

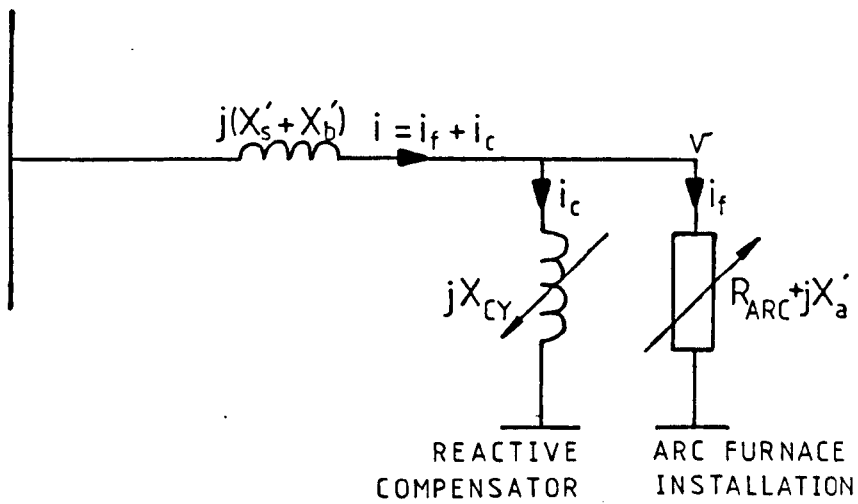


Fig. 3.9(a) : Shunt reactive compensation principle

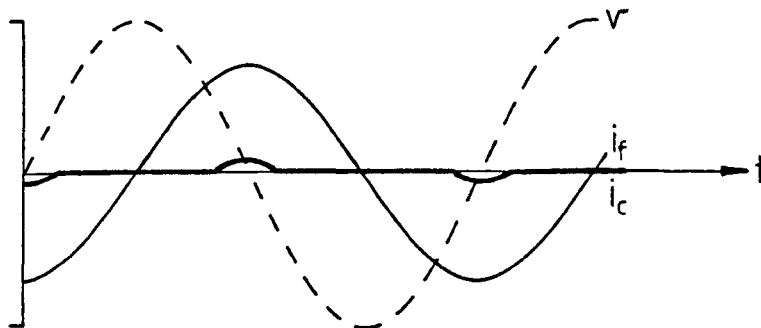


Fig. 3.9(b) : High furnace demand and low compensator demand

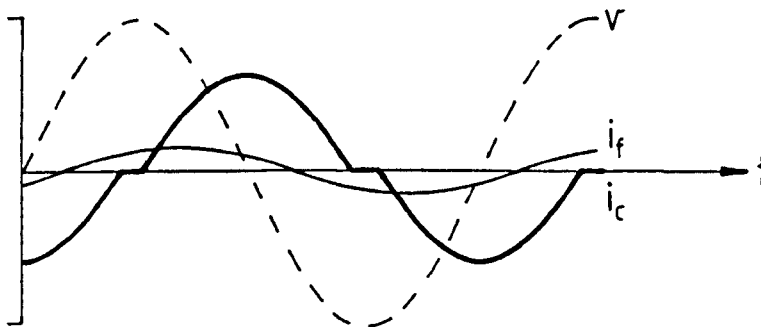


Fig. 3.9(c) : Low furnace demand and high compensator demand

Maximum amplitudes are then 5.05, 2.59, 1.05 percent for 5th, 7th and 11th harmonic currents respectively. The total harmonic content is a maximum of approximately 5 percent, occurring at $\alpha \approx 20^\circ$.

Several stages of Y-connected capacitor banks may then be used, each rated for a different harmonic frequency [37,96,97,98]. Using a TCR to balance the rapid variations in reactive power demand by the arc furnace then has the advantages of:

- (a) Continuous control of compensating currents between zero and maximum values.
- (b) Fast variation in demand - changes in the conduction angle may be made every 50Hz half cycle.

3.4.2 The Rating of a Reactive Compensator

Having understood the principle of shunt reactive compensation using a TCR, we must decide the details of its construction - in particular its rating. Any compensator equipment will be connected in parallel with an arc furnace installation to achieve a given flicker 'improvement factor', IMP, defined as:

$$\text{IMP} = \left[1 - \frac{\text{Compensated Flicker Voltage}}{\text{Uncompensated Flicker Voltage}} \right] \times 100\%$$

Flicker severity is itself a function of both the system fault level and the furnace installation short circuit power (Part 3.3), and the TCR VAR rating is then proportional to:

- (a) The required improvement factor.
- (b) The arc furnace installation's short circuit MVA.
- (c) The supply system fault level.

Furthermore, compensator performance is inextricably linked to its method of control. TCR rating may be calculated from theory exactly in accordance with (a),(b),(c) above and yet be unable to give any flicker improvement, solely due to its method of phase angle control.

It was decided to investigate the method of control of a three-phase TCR rated adequately for full reactive power compensation. Subsequent refinements in the phase angle control system could then offer the substantial benefit of reduction in TCR rating for a given improvement factor.

The Templeborough arc furnace installation has direct relevance to this project, and will therefore be studied between the two extremes of arc furnace operation: Open circuit to short circuit. If a TCR's operating range extends to both of these conditions, then a control system will have available the resources to match the most onerous fluctuations of the arc furnace load.

Not all electrical parameters are known. We are able to give the exact electrical representation of the furnace supply as far as the furnace transformer, and it is known that the arc is equivalent to a variable resistance^[93,99,100], therefore the equivalent circuit of Fig. 3.10(a) is missing only the unknown values of R_u and X_u . R_k and X_k are the lumped known parameters of the furnace installation's supply.

They were given in Section 3.2.1 as:

$$\begin{aligned} X_s' &= 1.2\text{p.c.} \\ X_b' &= 23.833\text{p.c.} & R_b' &= 0.519\text{p.c.} \\ X_a' &= 89.3\text{p.c.} \end{aligned}$$

on 100MVA base, giving a furnace short-circuit level of 87.46MVA.

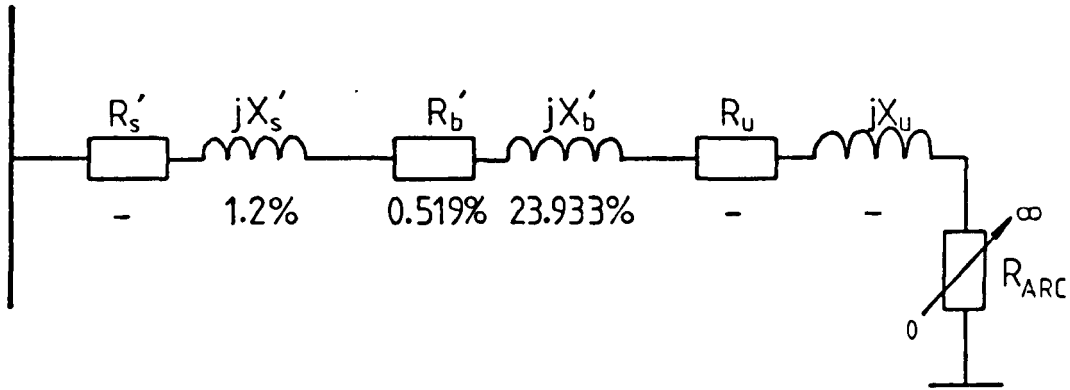


Fig. 3.10(a) : Templeborough supply one line diagram with percentage impedances to 100MVA base

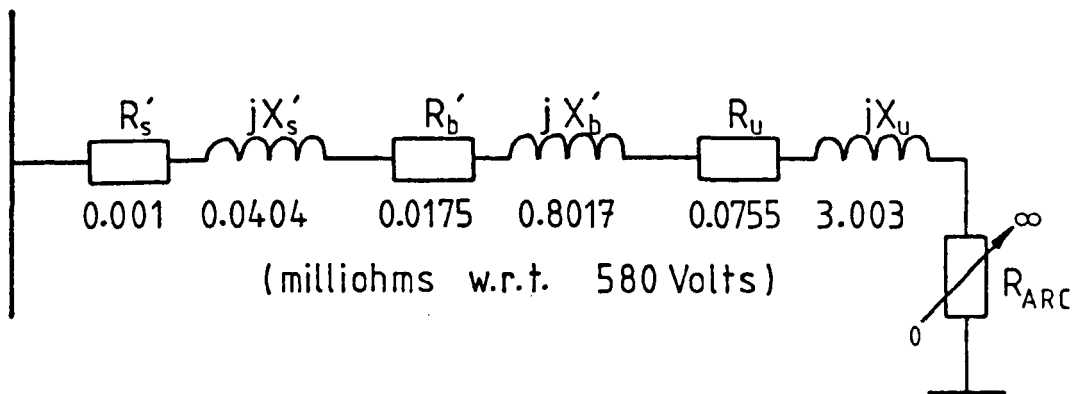


Fig. 3.10(b) : Templeborough supply one line diagram with derived equivalent ohmic impedances

Only values of reactance are used in the short-circuit level calculations^[6], since resistive components are generally relatively small and often unknown. An analysis including circuit resistive components, however, will be of great benefit in understanding circuit power factor and other parameters.

Knowing the furnace short-circuit level, S_t , and letting the furnace transformer secondary voltage be V_{LV} , then the arc current has a range of tens of thousands of amps:

For $V_{base} = V_{LV} = 580V$, and $VA_{base} = 100MVA$:

$$Z_{base} = 3.364\text{milliohms}$$

We know that the X/R ratio of the supply transformer is approximately 45, therefore assume $X/R \approx 40$ for the complete supply system to the furnace.

$S_t = 87.46MVA$, and $V_{LV} = 580V$ gives:

$$I_{sc} = 87,060 \text{ Amps } \angle 88.6^\circ \text{ lagging}$$

Therefore the total supply impedance will be:

$$\begin{aligned} Z_{tot} &= 3.846\text{milliohms } \angle 88.6^\circ \\ &= 0.094 + j3.845\text{milliohms} \end{aligned}$$

The values for X_s' , X_b' and R_b' are known and were given above.

Their corresponding ohmic values are:

$$\begin{aligned} X_s' &= 0.0404\text{milliohms} \\ X_b' &= 0.8017\text{milliohms} & R_b' &= 0.0175\text{milliohms} \end{aligned}$$

then $X_u = 3.003\text{milliohms}$

Let $R_s' = \frac{X_s'}{40} = 0.001 \text{ milliohms}$

then $R_u = 0.075 \text{ milliohms}$

The equivalent circuit so derived is given as Fig. 3.10(b). This one-line diagram shows per phase values, therefore:

$$\begin{aligned} \text{VA} &= \sqrt{3} (580) I \\ \text{Arc Power} &= 3 I^2 R_{\text{ARC}} \\ \text{Supplied Power} &= \text{Arc Power} + 3 I^2 (R_u + R_b') \\ \text{Supplied VAR}_s &= 3 I^2 (X_b' + X_u) \\ \text{Power Factor} &= \frac{\sum R}{\sum Z} \end{aligned}$$

The quantities are plotted against circuit current in Figure 3.11, and the equivalent 'circle diagram' from the same results is shown in Figure 3.12.

Figure 3.11 shows that maximum power transfer to the arc furnace installation occurs at 61kA, 0.707p.f. and 61MVA. In practice this point is not within the normal operating range^[93]. The full load working current for the 56MVA furnace is shown to be at a p.f. of approximately 0.8.

Furnace reactive power swings are:

$$\begin{aligned} \text{Open circuit to short circuit} &= 87\text{MYAR}, 1.6 \times \text{Furnace Rating} \\ \text{Normal operating range} &= 35\text{MYAR}, 0.63 \times \text{Furnace Rating} \end{aligned}$$

A survey of published ratings of TCR type shunt compensators installed for arc furnace voltage flicker reduction is summarised in Table 3.1. The range of compensator rating (C) to furnace rating (F), C/F, varies between 1.1 and 0.37. Unfortunately these ratios cannot be correlated with details of the system fault levels, nor with any measured improvement factor, since such information is often excluded from published work.

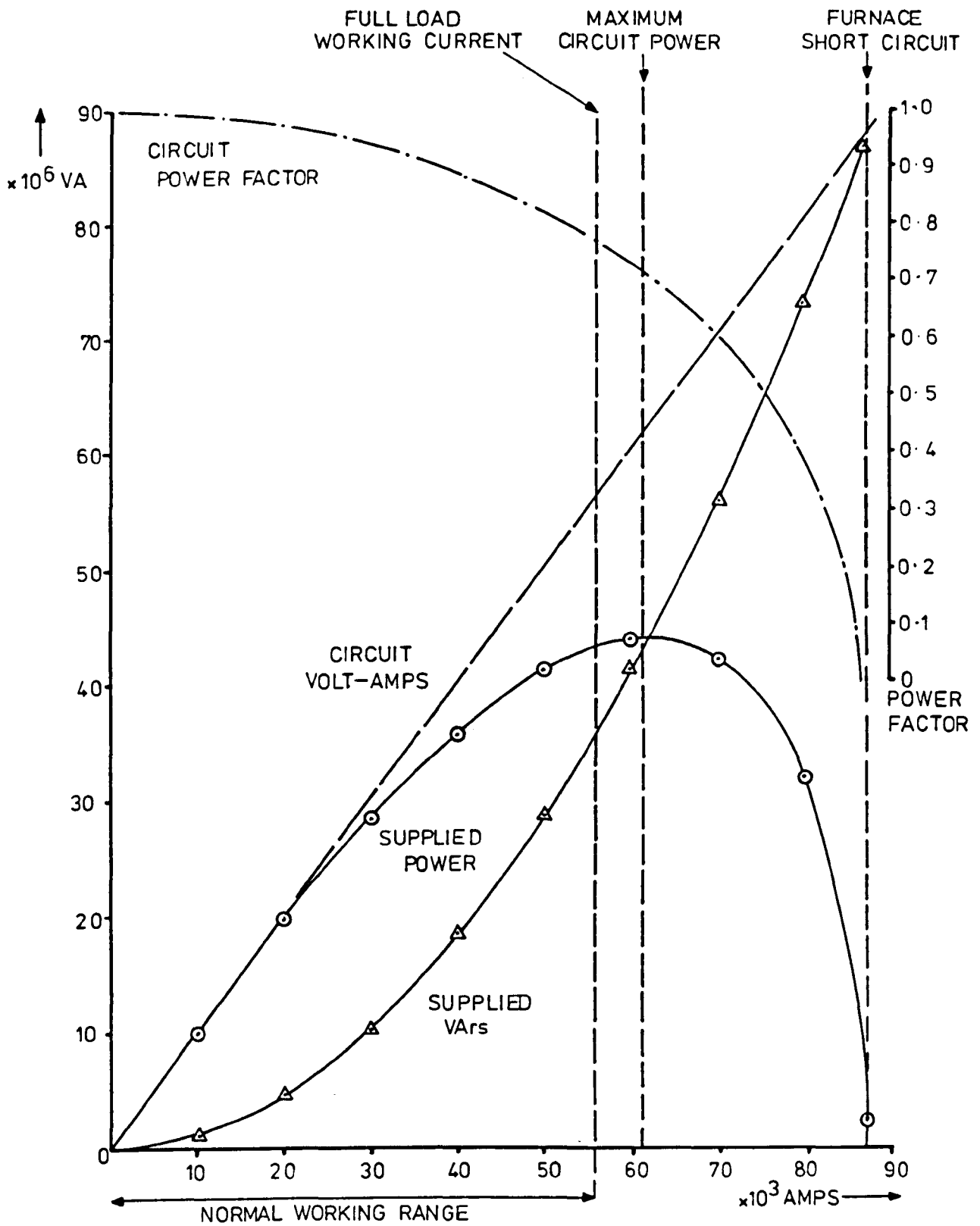


Fig. 3.11 : Arc furnace parameters as a function of current

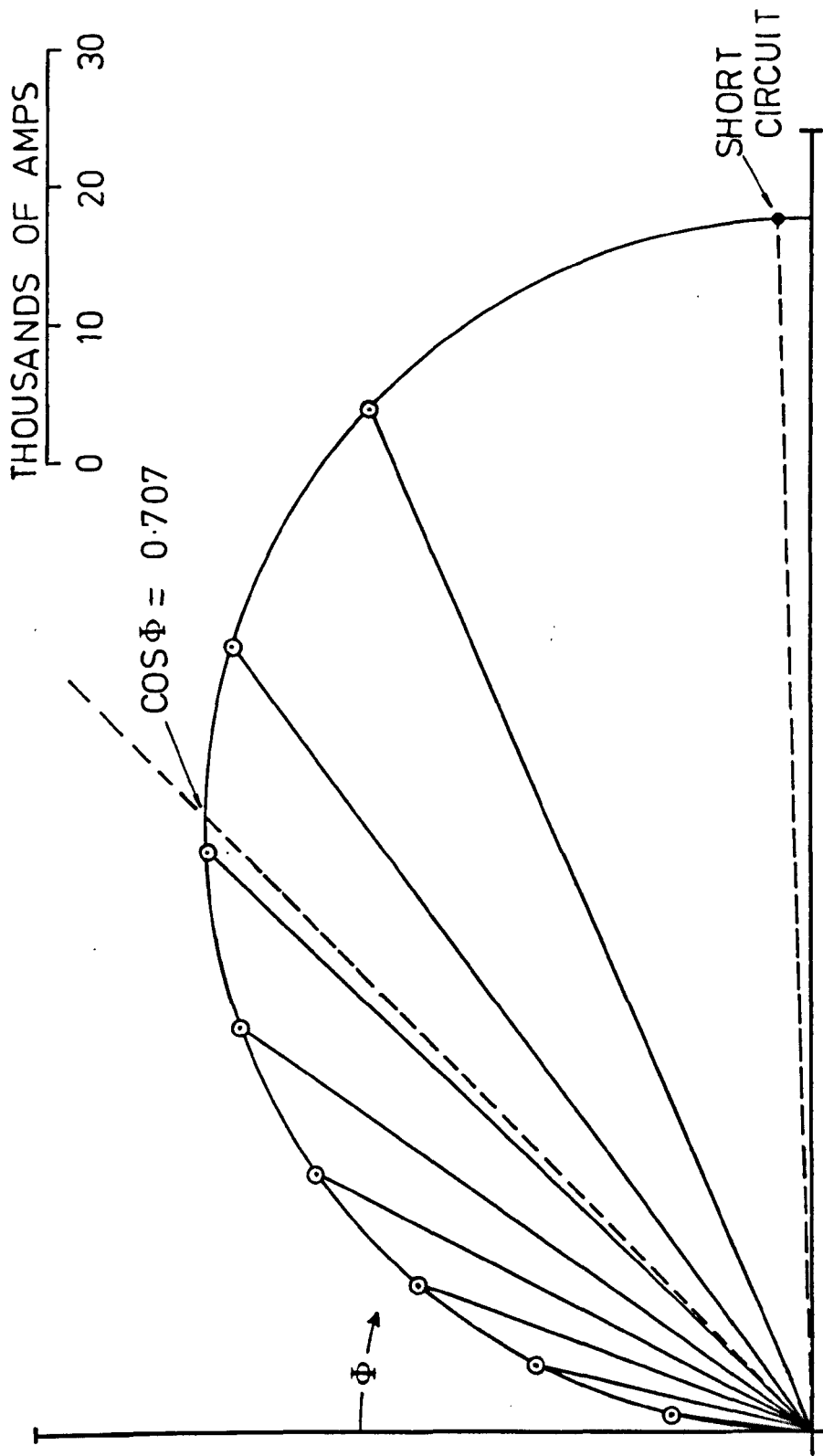


Fig. 3.12 : Arc furnace circle diagram

ITEM	DATE	FURNACE INSTALLATION		REACTIVE COMPENSATOR		MANUFACTURER	REF
		CAPACITY (TONNES)	RATING (MVA)	FIXED MVA	TCR MVA		
1.	1973	50	30	-	18	Nissin Electric Company	[43]
2.	1974	30	18	-	20		[43]
3.	1975	50	30	-	25		[43]
4.	1976	20 + 50	10 + 36	-	18		[43]
5.	1976	20 + 20	12 + 12	-	9		[43]
6.	1976	20 + 15 + 15	12 + 6.25 + 6.25	-	12		[43]
7.	1977	30 + 15	-	-	23		[43]
8.	1978	60 + 40 + 20	25 + 25 + 12	36	30	Oy Nokia Ab	[44]
9.	1978	100 + 100	72 + 72	146	120	Mitsubishi	[45]
10.	1978	20	4.6 + 15	14.7	9.5	EDF	[45]
11.	1981	-	65 + 65	-	65 + 65	-	[104]

Table 3.1 : Summary of published details of installed TCR schemes for arc furnace static shunt compensation

Figure 3.11 shows that the reactive power swing over the normal working range of the arc furnace is $0.63 \times$ Furnace MVA rating, and this MVA value was used for the initial TCR compensator study (Section 4.1.1).

3.4.3 Control of Static Shunt Reactive Compensators

The function of the control system, for a compensator incorporating thyristor-switched reactors or capacitors, is simply to control conduction in the compensator limbs by means of point on wave switching. This principle has been used successfully for many years, where closed-loop systems effect control of static compensators for transmission line voltage support [37,38,39,101,102].

The simplest closed-loop system will compare a rectified measured system voltage with same d.c. reference signal. The derived error signal is then used by a proportional control section to determine TCR firing angles [102].

Other feedback parameters, such as currents and reactive power, may be added and used by a more complex firing angle controller [63]. The controller may refer to a pre-set relationship between system admittance and compensator susceptance to set the thyristor firing angles [38,101]. Positive and negative sequence voltages are easily calculated from the three-phase system voltages, and have found use in some systems, where phase imbalance is to be corrected by an overall three-phase controller rather than by three individual systems [38,39].

In any such closed loop control system, the control loop will take a finite time to respond to system changes, and the delay may comprise:

- (a) T_D , a pure time delay or 'transport delay' between a control system's 'decision' and the required action.
- (b) T_C , the time constant of the control system.

In the context of voltage support for large systems, where compensation may be for widely distributed loads, such time delays rarely cause control difficulties. Indeed the response may be heavily damped deliberately to avoid instability of the large system.

When investigating the response of closed-loop systems, classical control theory^[103] enables Laplace transforms to be used to great benefit. In particular, the transfer function of the system will show the response of the output, C, for any input, R.

For a time constant, T_C , $C(t) = \frac{K}{T_C} \exp[-t/T_C] R(t)$

the Laplace transform is $C(s) = \frac{K}{1 + sT_C} R(s)$

Where K is the open loop gain of the system.

Adding a pure time delay modifies the transfer function to:

$$\frac{C(t)}{R(t)} = \frac{K}{T_C} \exp[-(t-T_D)/T_C]$$

with Laplace transform:

$$\frac{C(s)}{R(s)} = \frac{K}{1 + sT_C} \exp[-sT_D]$$

This transfer function may then be used to represent TCR compensator feedback control^[40,126]. If the input to the control system is an uncompensated reference flicker signal $R(t)$, and the response of the system is the controlled output $C(t)$, then the flicker improvement factor, IMP, may be expressed as:

$$\text{IMP} = 1 - \frac{\text{Compensated Flicker Voltage}}{\text{Uncompensated Flicker Voltage}} = 1 - \frac{C(t)}{R(t)}$$

The Laplace transform above then gives:

$$\text{IMP} = 1 - \frac{C(s)}{R(s)} = 1 - \frac{K}{1 + sT_C} \exp[-sT_D]$$

in the frequency domain.

The steady state gain and phase of the control system may be found by substituting for $s = j\omega$ in the transfer function, giving:

$$\frac{K}{1 + j\omega T_C} \exp[-j\omega T_D]$$

$$= \frac{K}{1 + \omega^2 T_C^2} (\cos\omega T_D - \omega T_C \sin\omega T_D) - j(\sin\omega T_D + \omega T_C \sin\omega T_D)$$

Ashmole^[32,40] shows how the compensator improvement factor varies with frequency for different values of compensator time constant T_C .

T_C and T_D will vary according to the closed loop control scheme used. The 'transport delay', T_D , may be reduced practically to 5 milliseconds for most compensator schemes, but the time constant, T_C , is generally longer. T_C will be affected by filtering, sampling or processing circuitry, and a value of $T_C = 20$ milliseconds would be considered as fast compensator closed loop control.

Given values of T_C and T_D , the gain and phase of the control system's transfer function may be calculated over a range of operating frequencies. Results from such calculations are plotted in polar form in Figure 3.13 with per unit gain and phase angle shown for $T_C = 5, 10, 20$ milliseconds for fixed $T_D = 5$ milliseconds. Each characteristic shows that reasonable gain may be obtained with phase delays of up to $\pi/2$ radians. Positive feedback is encountered in the third quadrant.

Most important for flicker frequency compensation is effective attenuation in the 0-30Hz disturbance frequency range. Figure 3.13 shows clearly that true negative feedback is only obtained up to 15Hz for $T_C = 20$ milliseconds, compared to 28Hz when $T_C = 5$ milliseconds. The corresponding frequencies at which positive feedback is encountered are 55Hz and 65Hz respectively. System gain at the critical frequency of 8Hz for $T_C = 20$ milliseconds is only 65p.c. of that given by a system with $T_C = 5$ milliseconds.

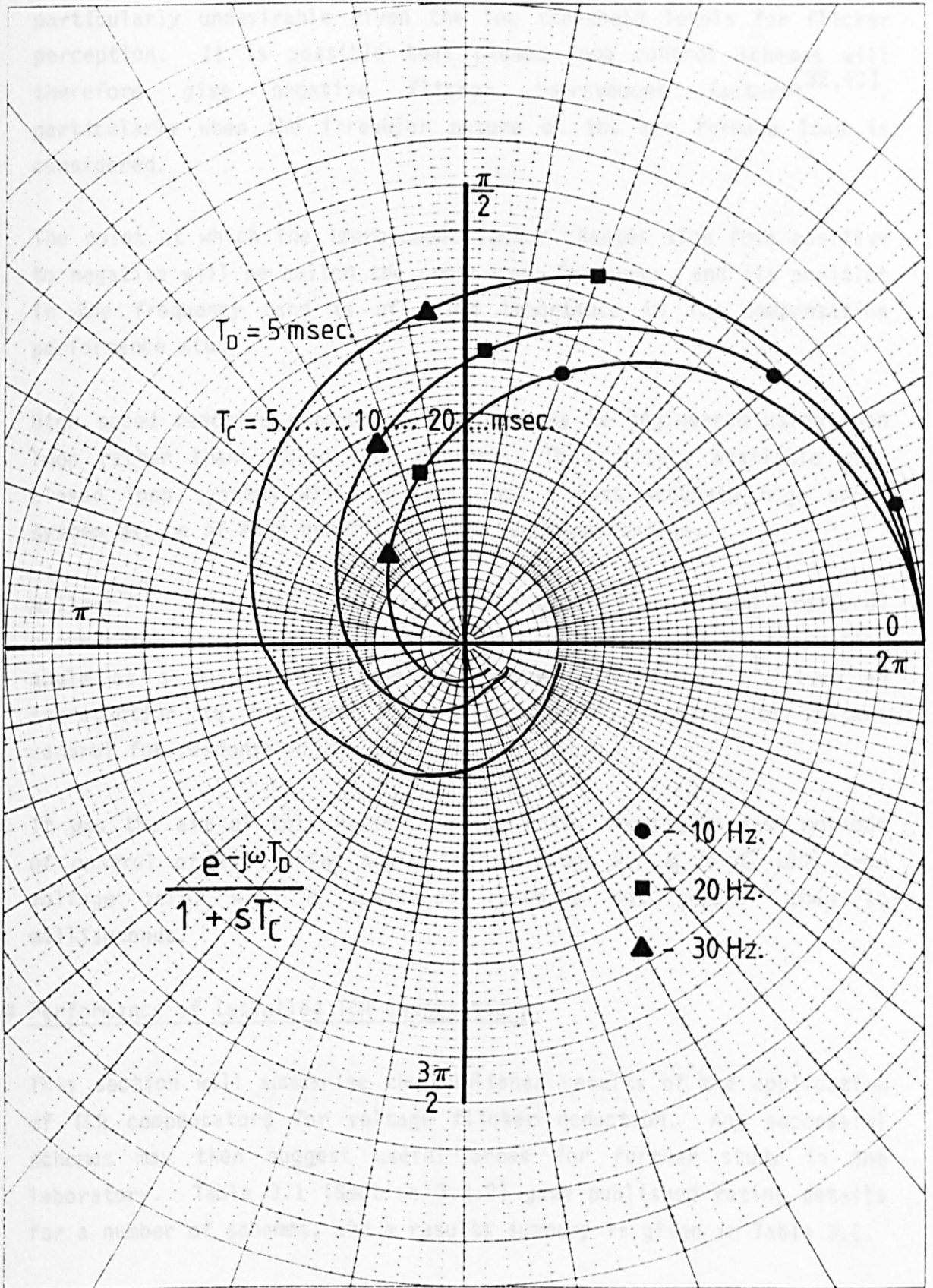


Fig. 3.13 : Polar plot for control system gain and phase

In practice, $T_C = 5.0$ milliseconds would prove difficult to obtain, and amplification of higher frequencies of distortion are particularly undesirable given the low threshold levels for flicker perception. It is possible that closed loop control schemes will therefore give negative flicker improvement factors^[32,40], particularly when the irregular nature of the arc furnace load is considered.

The point at which the improvement factor changes sign from positive to negative will be called the cross-over frequency, and its position in the frequency band is of prime importance in any compensation performance study.

High speed reactive compensator systems may be engineered using open loop rather than closed loop control. The accuracy available with closed loop systems will be lost, but a less accurate high speed system may be of more benefit for flicker compensation.

Miller^[95] describes one form of open loop (feed forward) compensator control that requires pre-programming of TCR conduction angle as a function of load admittance, and Cooper^[41] gives an introduction to two open loop schemes using integral of voltage control for response within one 50Hz half cycle.

It was the aim of this research project to investigate fast methods of control of TCR firing angle in the range $90^\circ \leq \alpha \leq 180^\circ$ from voltage zero, with a speed of response not greater than 10 milliseconds.

3.4.4 Performance of Installed TCR Compensators

This section will summarise the published results of the application of TCR compensators for voltage flicker reduction. Any successful schemes may then suggest useful areas for further study in the laboratory. Table 3.1 (Section 3.4.2) gave published rating details for a number of schemes, and a results summary is given in Table 3.2.

Ref. from Table 3.1 and Manufacturing	Control Method	Results	Flicker Measurement Method
1. 2. 3. 4. Nissin Electric Company[43] 5. 6. 7.	TCR thyristor firing when a reference voltage is exceeded by a signal proportional to busbar voltage plus furnace current. 90° phase lag may be incorporated. Claimed TD = 5mSec.	Flicker suppression factors between 0.22 and 0.59 for different arc furnace installations. Cross-over frequency = 15Hz.	Both ΔV_{10} flicker-meter and power spectrum analysis of voltage.
8. Oy Nokia Ab.[44]	Open loop; TCR thyristor firing after measurement of VAR within each half cycle. Claimed speed response LT 10msecs.	Power factor improvement from 0.87 to 0.99. Max. RMS voltage fluctuations reduced from 7 percent to 1 percent.	None
9. Mitsubishi[21]	Open loop; TCR thyristor firing after calculation of reactive component of load current and comparison with a preset characteristic for each half cycle.	Frequency independent 'flicker' voltage improvement ratios up to 65 percent. Frequency characteristics show flicker voltage attenuation up to 20Hz.	Custom 'flicker-meter' equipment and Power Spectrum analysis of voltage.
10. EDF[46]	Details not given.	Reduction in Q flicker modulation frequencies. Cross-over frequency at 26Hz.	Power spectrum analysis of system reactive power fluctuations.

Table 3.2 : Summary of published TCR flicker compensation results based on schemes listed in table 3.1

There are schemes offering reasonable evidence of a reduction of the power in flicker modulation frequencies, they use fast open loop control methods measuring both busbar voltage and load current. Multiplication or addition of these parameters is then used for comparison with a pre-set characteristic or level^[43,45].

This process is restricted to each half cycle, and thus speeds of response between 5 milliseconds and 10 milliseconds are claimed.

The highest cross-over frequency evident is at approximately 20Hz^[45], but none of the schemes studied use an internationally recognised flicker meter to obtain an improvement factor.

CHAPTER FOUR

A SIX-PULSE THYRISTOR-CONTROLLED REACTOR

4.1 THE LABORATORY MODEL THYRISTOR CONTROLLED REACTOR

4.1.1 Modelling Requirements

4.1.2 Control Requirements

4.2 MICROPROCESSOR CONTROL

4.2.1 System Operations

4.2.2 Sampling

4.2.3 The Control Algorithm

4.2.4 Control Variables

- (i) Sample Loop Delay
- (ii) Reference Sinusoid
- (iii) Integration Limit

4.3 STEADY-STATE TUNING AND PERFORMANCE

4.3.1 Thyristor Firing and Conduction Limits

4.3.2 Phase Balancing

4.3.3 Steady-State Reactive Compensation Theory

- (i) Open Circuit Voltage Control
- (ii) Shunt Load TCR Compensation

4.4 USE OF THE TCR UNDER NON-SINUSOIDAL CONDITIONS

4.1 THE LABORATORY MODEL THYRISTOR CONTROLLED REACTOR

Section 3.4.2 gave a VA rating for a shunt reactive compensator to suit the laboratory arc furnace model. Such a small scale model will have inherent differences in performance from any full size compensator, and these differences should be understood.

The main advantage of a small scale model is flexibility at low cost, and a major objective of this research project was to allow many different control methods to be studied for a given compensator arrangement. The arrangement of the reactances and thyristor switch circuits is given below, with a brief study of the principles of variable phase inductive conduction.

4.1.1 Modelling Requirements

Full scale Thyristor Controlled Reactors (TCRs) presently have three-phase ratings up to 120MVA^[45], and current thyristor technology allows direct connection of thyristor switch assemblies to 33kV^[44,45]. In such equipment series voltage sharing is necessary, and parallel current sharing with built-in redundancy is operationally desirable. For modelling purposes these switch assemblies may be represented by a single low cost thyristor of a suitable rating, that has the required turn-on and turn-off characteristics.

The rating of the uncontrolled three-phase shunt reactor shown in Figure 4.1 is simply:

$$C = \frac{3V_L^2}{\omega L_C} \text{ VAR}$$

Figure 4.2 shows how the compensator rating, C, varies with L_C for a 175V, 50Hz system. ~~Also shown are the equivalent reactive power swings of the arc furnace model.~~

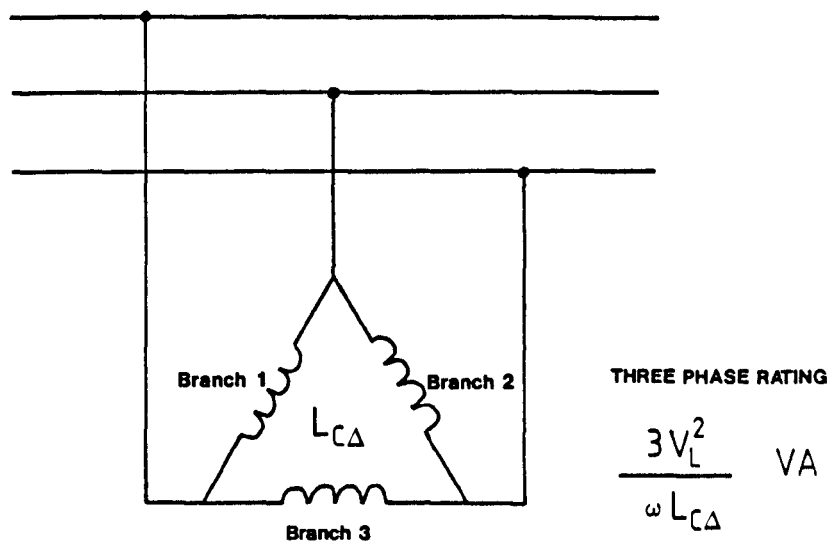


Fig. 4.1 : A fixed delta-connected shunt reactive compensator

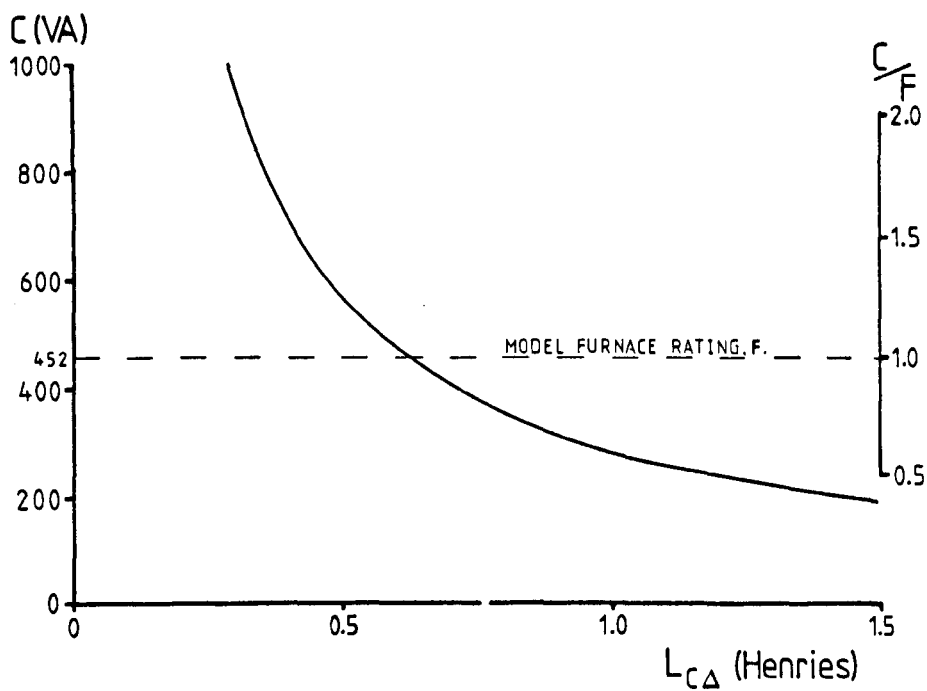


Fig. 4.2 : Compensator 3-phase rating as a function of branch inductance

The reactive power swings in the normal working range of the arc furnace model can be met by a compensator rating, C, of 0.63 times the model furnace rating, F, of 452VA (Section 3.4.2).

A coil having 1.0 Henry of inductance gives a compensator rating, C, of 286.5VA and then $C/F = 0.63$.

The coils used in the compensator branches were specially wound in copper strip to give an X/R ratio high with respect to their operating VA. An adjustable air gap between C-cores was designed to avoid saturation of the laminated iron cores, and facilitate changing of inductance values using an adjustable clamping system.

The impedances in the compensator branches were then:

$$\begin{aligned} \text{Branch 1,} & \quad Z_1 = (0.70 + j333.01) \\ \text{Branch 2,} & \quad Z_2 = (0.69 + j333.32) \\ \text{Branch 3,} & \quad Z_3 = (0.70 + j324.84) \end{aligned}$$

The high X/R ratio of 475 minimises any resistive losses in the compensator, and the current waveform will follow that predicted by the theory for pure inductances.

The voltage across each branch is $v = V \sin \omega t$

where $V_{\text{RMS}} = 175$ volts and $V = 175 \sqrt{2}$

$$\frac{di}{dt} = \frac{v}{L}$$

hence, for symmetrical current flow $i = -\frac{V}{\omega L} \cos \omega t$

$$\text{i.e.} \quad i = -I \cos \omega t$$

where $I_{\text{RMS}} = \frac{175}{\omega L}$ and $I = \frac{175}{\omega L} \sqrt{2}$

If conduction is delayed by some angle ' α ' from the point of uncontrolled current zero crossing, which corresponds to the symmetrical voltage peak, then the current waveform becomes non-sinusoidal as shown in Figure 4.3. (The voltage waveform shown is for reference only, and all amplitudes are normalised with respect to a sinusoidal peak value of 1.0).

The effects of such a conduction pattern with increasing α are:

- (a) Decreasing I_{RMS} .
- (b) Decreasing peak current, I .
- (c) Increasing harmonic components.
- (d) Decreasing $\frac{di}{dt}$ at the beginning of the conduction period.

The equation of the current waveform can be found by considering one half cycle (Figure 4.4). The constant term $I_0 \sin \alpha$ needs to be subtracted during conduction from the sinusoidal value.

$$\text{Hence, } i = (I_0 \sin \omega t - I_0 \sin \alpha) \quad \text{for } \alpha < \omega t < (\pi - \alpha)$$

$$\begin{aligned} \text{Whence, } I_{RMS} &= \sqrt{\frac{1}{T} \int_0^{\pi} (I_0 \sin \omega t - I_0 \sin \alpha)^2 dt} \quad \text{for } T = \pi / \omega \\ &= I_0 \sqrt{\frac{2}{\pi} \left[\frac{(\pi - \alpha)}{2} \left(\frac{1}{2} + \sin^2 \alpha \right) - \frac{3 \sin 2\alpha}{4} \right]} \end{aligned}$$

$$\text{Also, } I = I_0 (1 - \sin \alpha) \quad \text{for } 0 \leq \alpha \leq \frac{\pi}{2}$$

$$\text{And, } \left. \frac{di}{dt} \right|_{\alpha} = \frac{V \cos \alpha}{L} \quad \text{for } 0 \leq \alpha \leq \pi/2$$

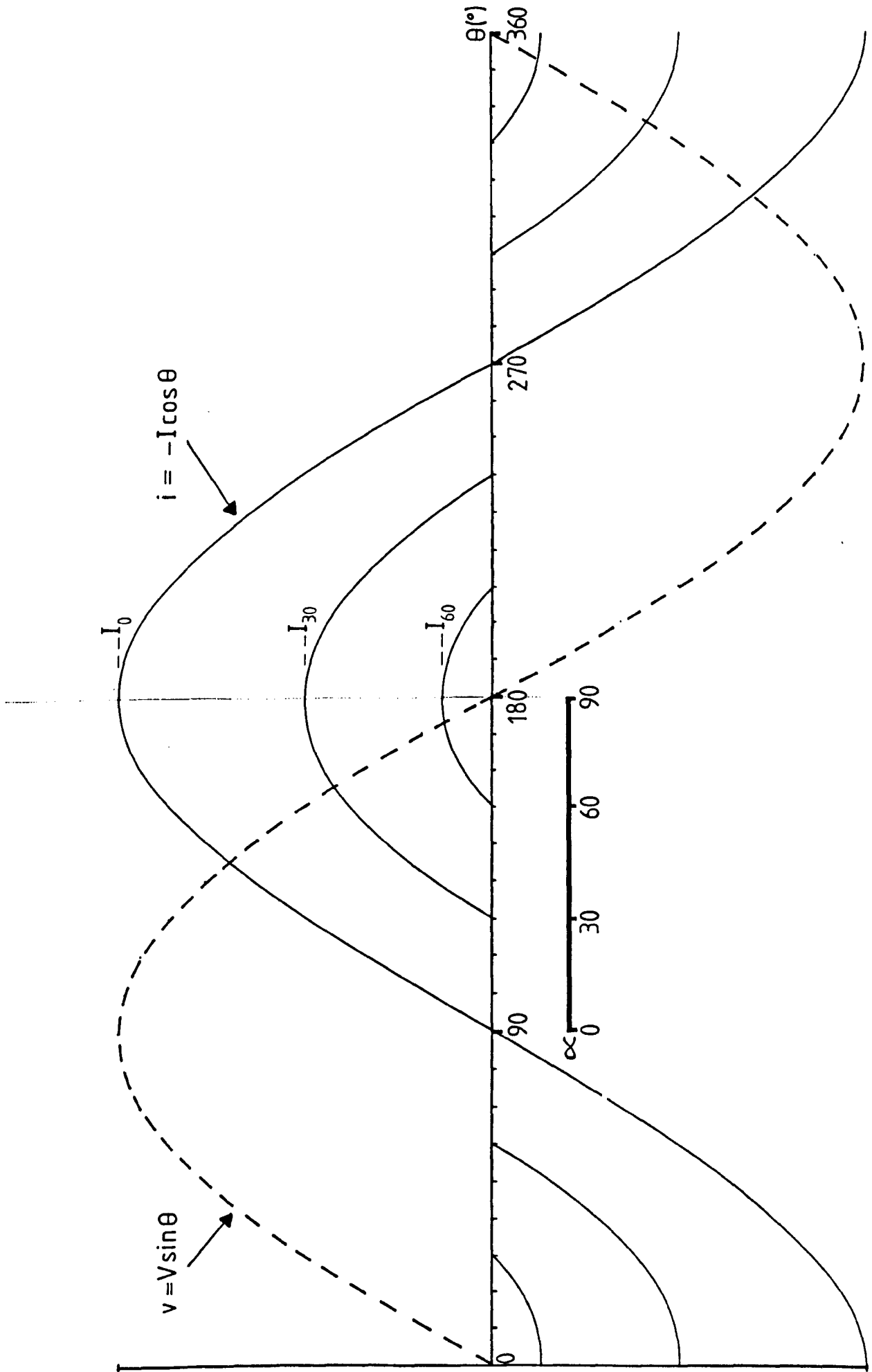
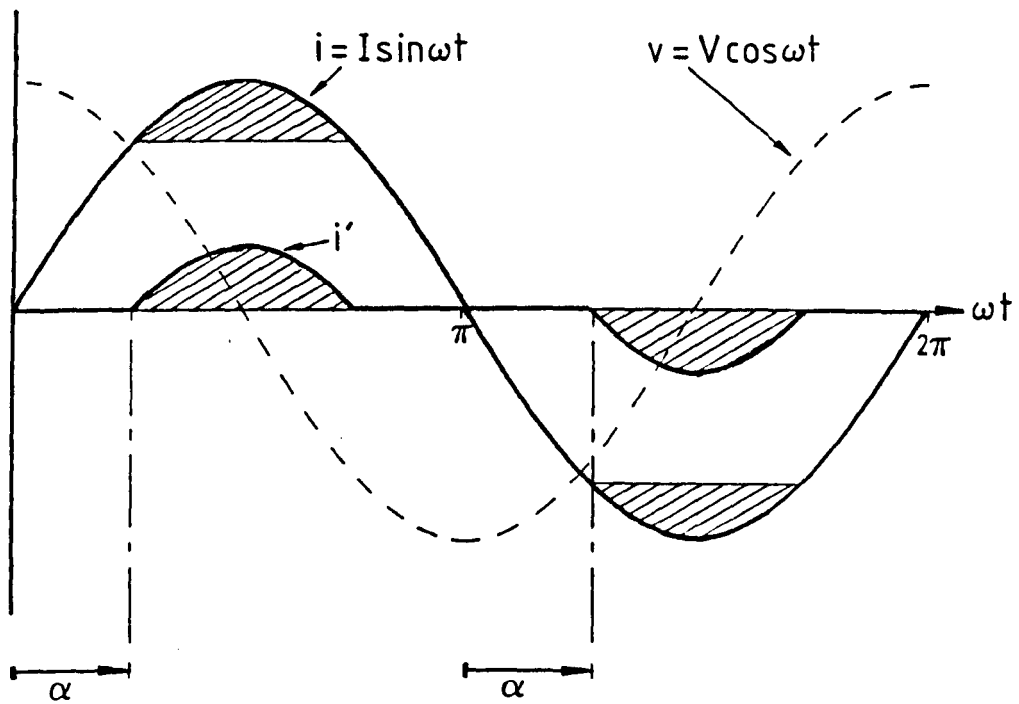


Fig. 4.3 : Conduction patterns resulting from phase angle control of inductive current



$$\begin{aligned}
 i' &= 0 && \text{for } 0 \leq \omega t \leq \alpha \\
 & && \& \pi - \alpha \leq \omega t \leq \pi + \alpha \\
 & && \& 2\pi - \alpha \leq \omega t \leq 2\pi \\
 i' &= (I \sin \omega t - I \sin \omega t) && \text{for } \alpha < \omega t < \pi - \alpha \\
 & && \& \pi + \alpha < \omega t < 2\pi - \alpha
 \end{aligned}$$

Fig. 4.4 : Firing angle ' α '

Figure 4.5 shows I_{RMS} for $0 \leq \alpha \leq 90^\circ$ normalised with respect to I_0 .

Figure 4.6 shows the variation of peak current I , normalised with respect to I_0 , for $0 \leq \alpha \leq 90^\circ$.

Section 3.4.1 briefly described the components of current occurring at harmonic frequencies when the current waveform is non-continuous, as shown in Figure 4.4. Such harmonic components will, of course, be generated by a laboratory TCR model. It was decided initially not to apply shunt-connected capacitors to the laboratory model. Harmonic current generation would then be studied as a separate exercise, and suitable capacitors connected at a later stage for the dual purpose of harmonic filtering and power factor correction.

di/dt at the point of start of conduction is of interest because thyristors are to be the devices controlling conduction. Their turn-on characteristics are not negligible, and it must be established that anti-parallel connection of thyristors in each compensator branch allows continuous control of the current in each branch. Figure 4.7 gives the notation used for references to the compensator Δ -connected components.

For symmetrical conduction about the voltage zero point it is necessary for the branch current to have reached the thyristor latching current, i_{TL} before the voltage zero.

Conduction will then continue until the current falls below the thyristor holding current, i_{TH} (Figure 4.8). Thus the line voltage, the branch inductance and the thyristor characteristics possibly present restrictions on the maximum value of α that may be used in practice.

Figure 4.9 gives I for values of α near to the voltage zero crossing point for $V_2 = 175V$ and $L_C = 1.0H$.

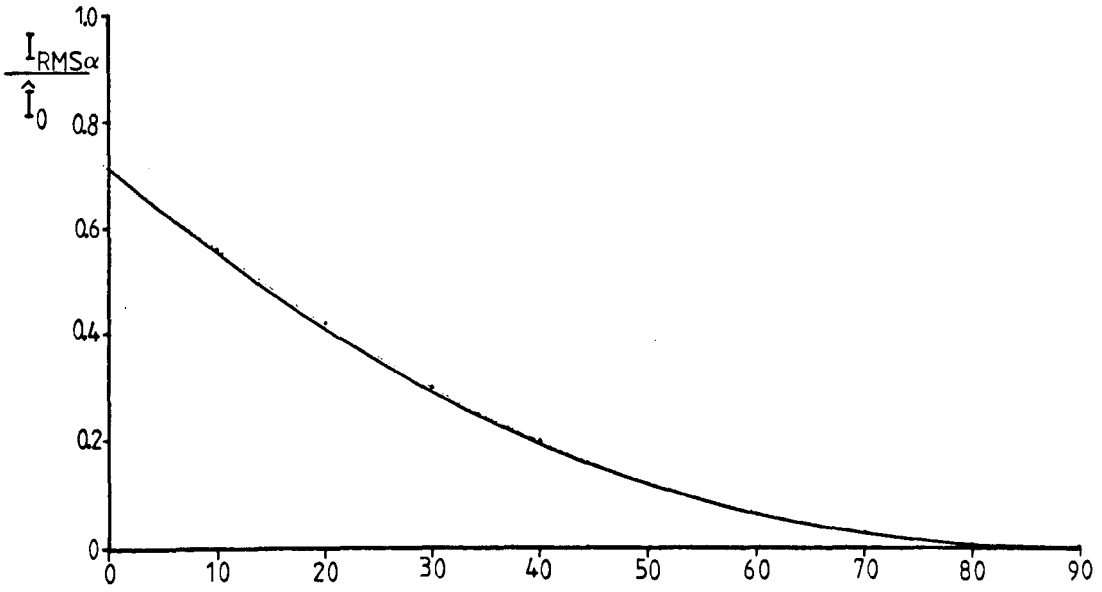


Fig. 4.5 : Variation of RMS current as a function of ' α '

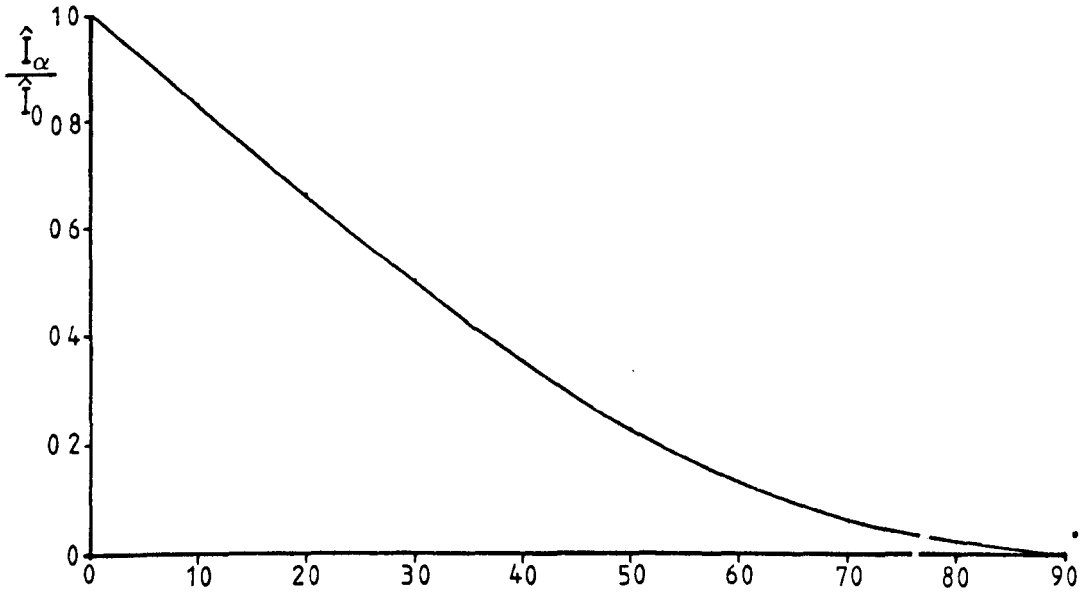


Fig. 4.6 : Variation of peak current as a function of ' α '

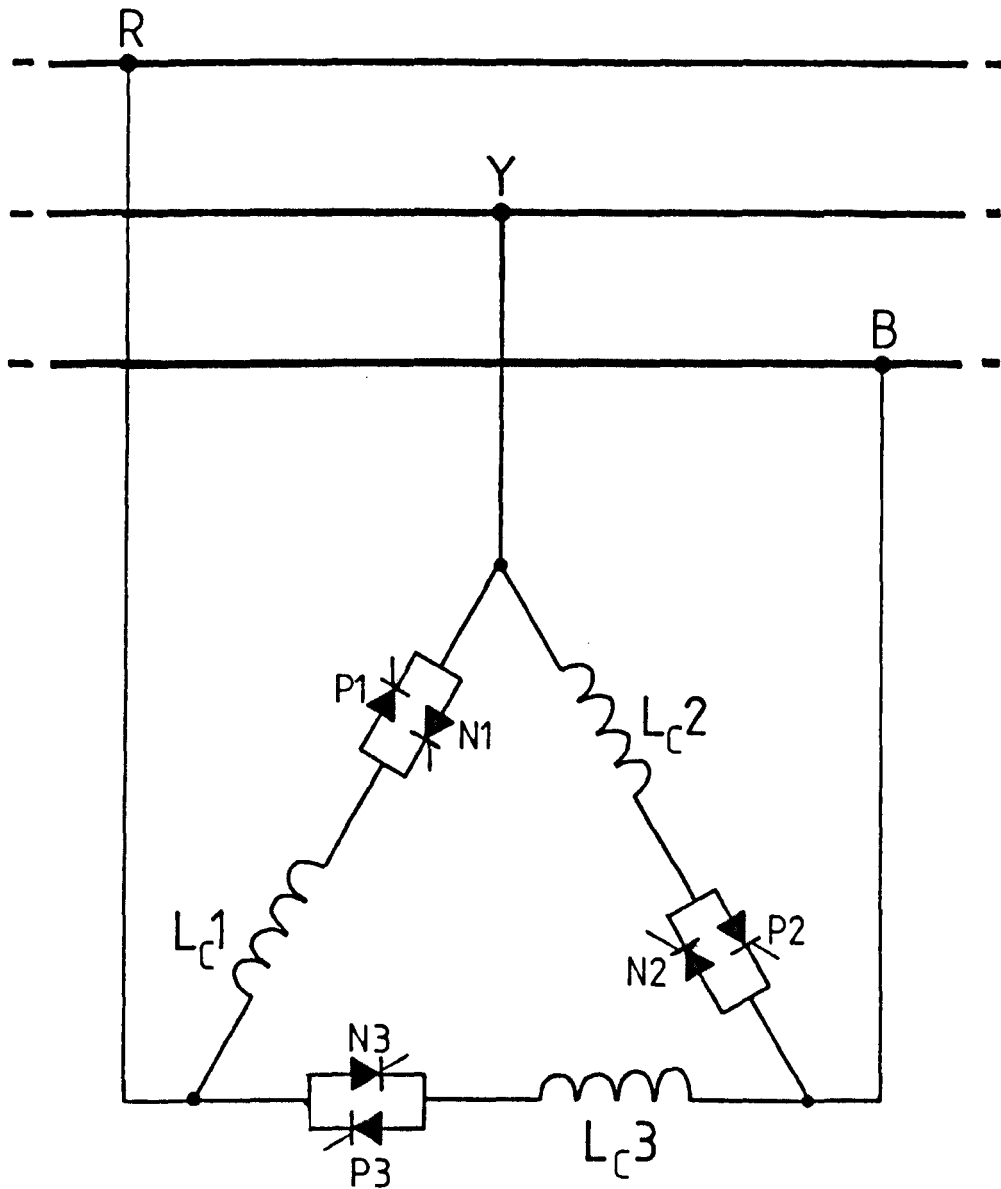


Fig. 4.7 : Laboratory 6-pulse TCR arrangement

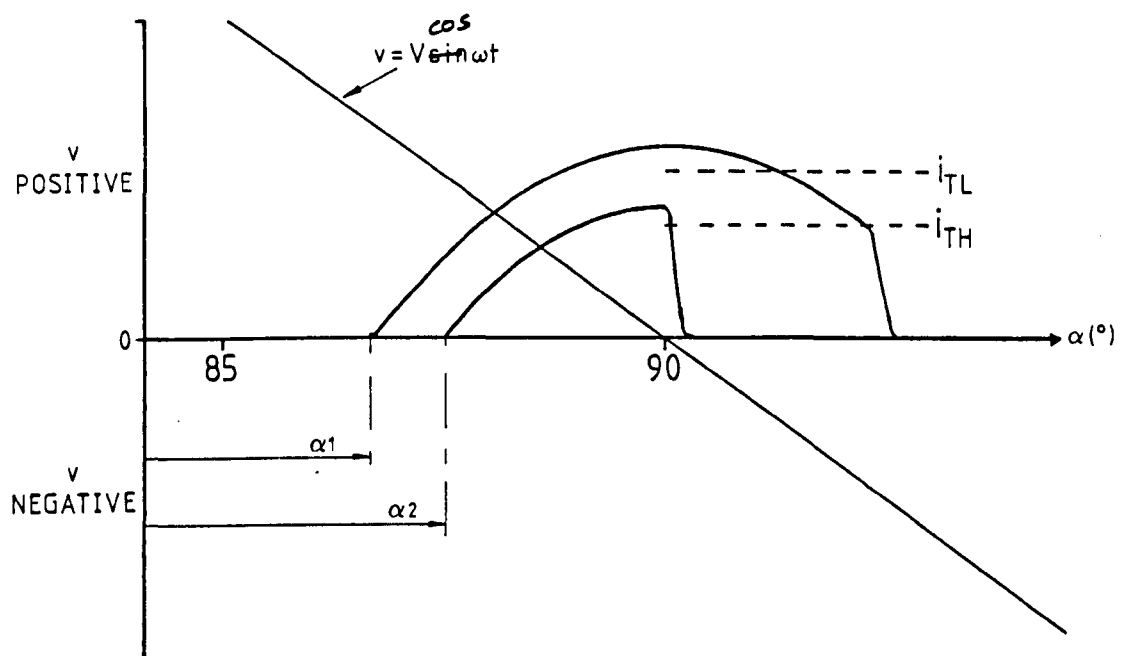


Fig. 4.8 : Thyristor conduction near to voltage zero

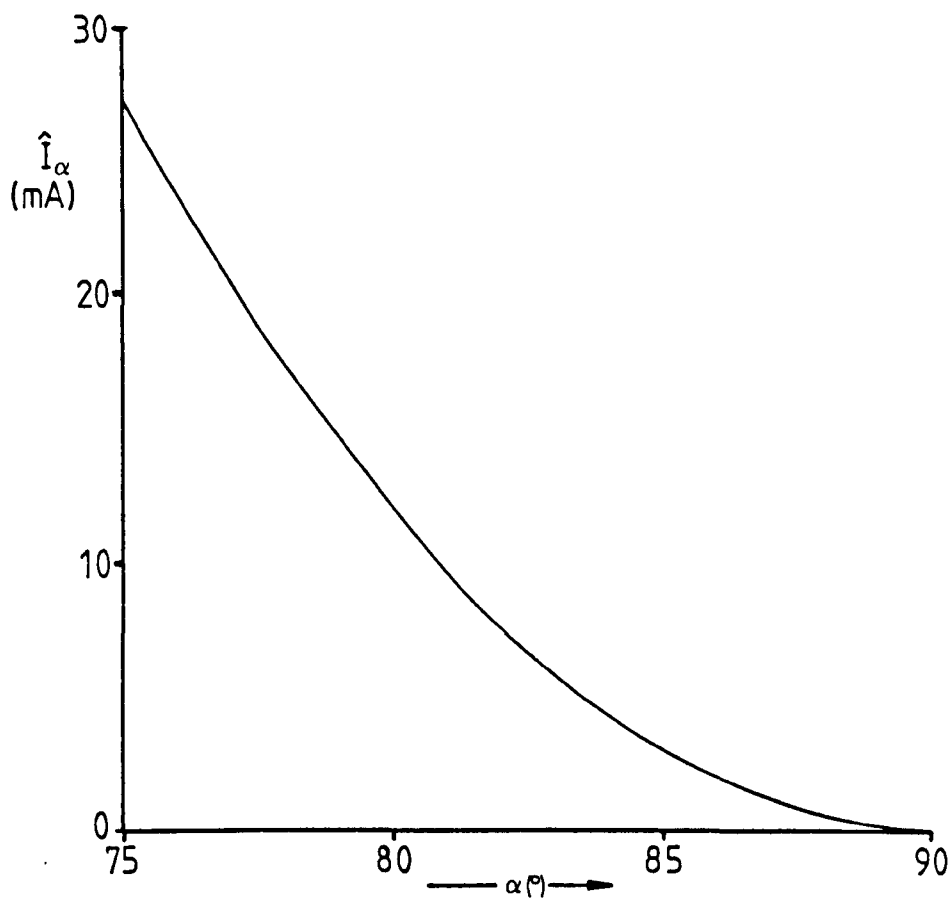


Fig. 4.9 : Peak inductive current for ' α ' near to 90°

The thyristors used in the early models were Mullard BT 152-400 and intermittent firing late in the half cycle was eventually traced to the high values of:

$$\text{and } \begin{array}{l} i_{TL} < 80 \text{ mA} \\ i_{TH} < 60 \text{ mA} \end{array} \quad [105]$$

$I = 80 \text{ mA}$ is only reached for $\alpha < 64^\circ$

The thyristor used in all later studies was the Mullard BTX 18-500 having:

$$\text{and } \begin{array}{l} i_{TL} < 10 \text{ mA} \\ i_{TH} < 5 \text{ mA} \end{array} \quad [106]$$

With the compensator branch inductance, L_c , of 1.0 Henry the confidence limit for firing is $\alpha = 82.52^\circ$. In practice intermittent firing was found to occur at approximately $\alpha = 86^\circ$.

4.1.2 Control Requirements

Section 3.4.3 identified the general control requirements for different types of shunt reactive compensator. The particular system for controlling a 6-pulse TCR was required to have an equivalent delay in control response of less than 10 milliseconds. Cooper and Hussayni^[41] studied practicable TCR control methods and highlighted the advantages of 'Integral of Voltage' control methods whilst commenting on the inadequacy of systems which restricted thyristor firing to $60^\circ \leq \alpha \leq 90^\circ$.

It was decided at an early stage that an investigation of integral of voltage control should be included in this research project, with the possibility of studying TCR response times shorter than those achieved elsewhere.

Implementing control schemes using a digital processor offered definite advantages:

- (i) Ease of changing the control algorithm.
- (ii) Standard compensator hardware, including all signal conditioning circuits.
- (iii) The possibility of adaptive or 'intelligent' control.
- (iv) Simple inclusion of a data logging facility.

Digital sampling of the analogue system variables introduces two possible major sources of error^[107]:

- (a) Quantisation noise.
- (b) Aliasing distortion.

The former arises from the discretisation process employed by all analogue-to-digital converters and occurs when the analogue quantity does not exactly correspond to one of the 'N' defined levels within the span of the device.

Aliasing distortion will arise when the sampling rate is too low, and higher frequency components in the sampled signal corrupt the information that can reliably be recovered from the sampling process.

The Nyquist Frequency, F_N , is the sampling frequency necessary to recover all of the information in a continuous signal with frequency components below the frequency f_{MAX} ,

Where
$$F_N = 2 f_{MAX}$$

The highest frequency component able to be reconstructed from the CEGB recordings by the arc furnace model is then half the sampling frequency, F_{SM} .

$$f_{MAX} = F_{SM}/2 = \frac{1}{2} \left[\frac{1}{800 \cdot 10^{-6}} \right] = 625\text{Hz}$$

The spline interpolation process (Section 2.3.2 and Appendix C) will introduce higher spurious frequency components up to

$$f'_{MAX} = 4 F_{SM} = 5000\text{Hz}$$

but, these will be attenuated by the low-pass filters in the power amplifier input circuits.

The TCR data sampling frequency, F_{sc} , should then be:

$$F_{sc} \geq 1250\text{Hz or } \Delta t \leq 800 \text{ microseconds}$$

The control system should perform a 'real time' process, therefore the calculation of whether thyristor firing is required or not must be completed within this time period, before the next sample. It follows that if one processor is controlling all three of the compensator branches, it is required to perform three times as many calculations as each of three separate processors each dedicated to the operation of one branch.

The structure of the Intel 8088 processor made it suitable for its application as an independent controller for each compensator branch (Figure 4.10(a)) and for the later development of a supervisory system whereby each of the three processors would be controlled from a central processor via interrupts and a common bus structure. (Figure 4.10(b)).

Both arrangements offered advantages in processing speed over other microprocessors and minicomputers, and the Intel 8088 was used in the form of the SDK-88 microcomputer^[108].

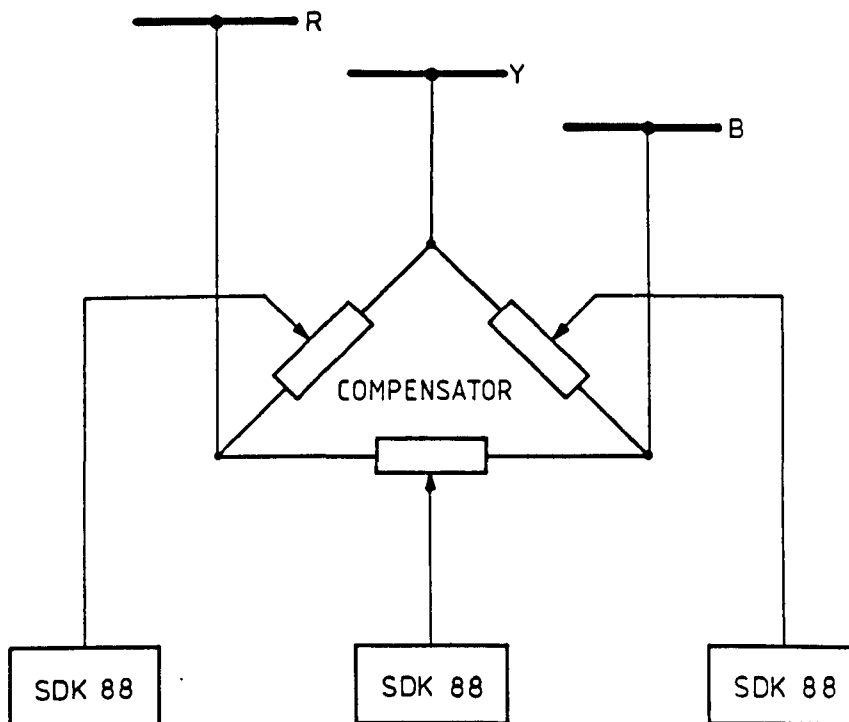


Fig. 4.10(a) : Independent phase control of compensator branches

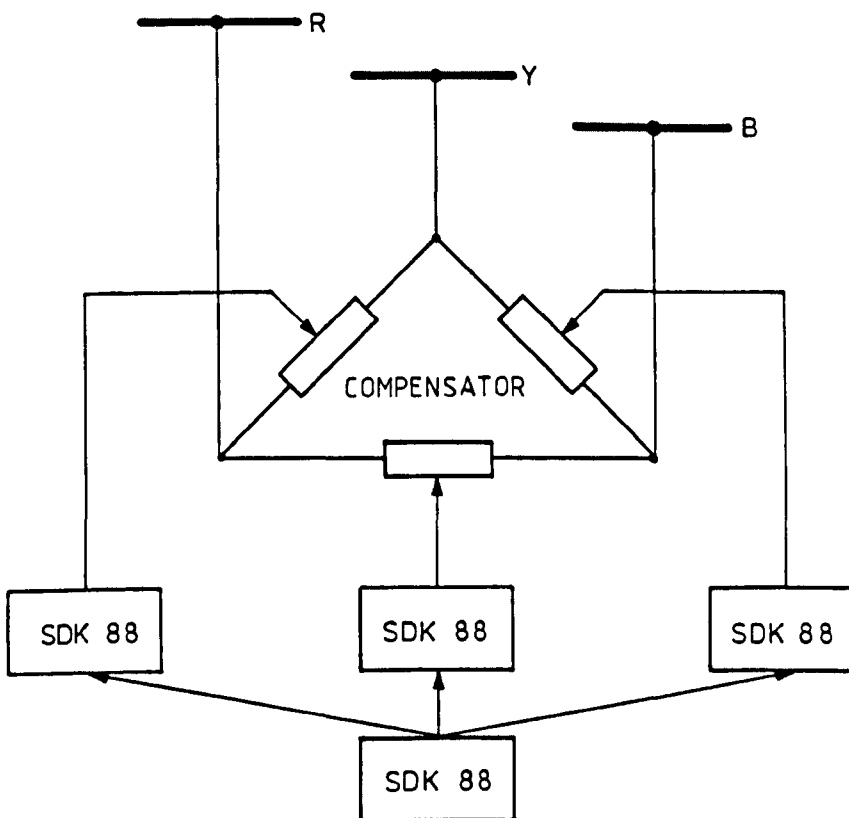


Fig. 4.10(b) : Development to supervisory control

4.2 MICROPROCESSOR CONTROL

Three separate SDK-88 microcomputer systems were installed in the laboratory for the control of the 6-pulse TCR. Each system contained rack-mounted analogue to digital converters fed from identical signal conditioning circuits, for measurement of the three-phase system parameters.

Control programs could be written locally using a ROM-resident monitor and keyboard routine, or remotely using a high level development system in Liverpool University's Microprocessor Laboratory.

Local program control was used for fault finding and the study of program operation. Variables within the program machine code could be adjusted for the control of the individual compensator branches.

4.2.1 System Operation

A Video Display Unit (VDU) and keyboard was sited adjacent to the laboratory equipment allowing individual control of each SDK-88 via the ROM-resident monitor routine. This could also be connected to act as a remote terminal of a Tektronix 8650 Multi-User System Development Unit (MUSDU)^[110]. The MUSDU supported file storage under the TNIX operating system and allowed high level language programs to be compiled and linked with assembler language programs. The final machine code could be stored in a file, ready to be downloaded from the MUSDU to the SDK-88 RAM at any time.

Figure 4.11 illustrates the system operating principles. In practice the high-level PASCAL programming language was used for 'supervisory' functions, such as text manipulation and program flow control apart from the compensator control algorithm. The control algorithm was written in Intel ASM-86 Assembler language for increased speed and simpler fault-finding.

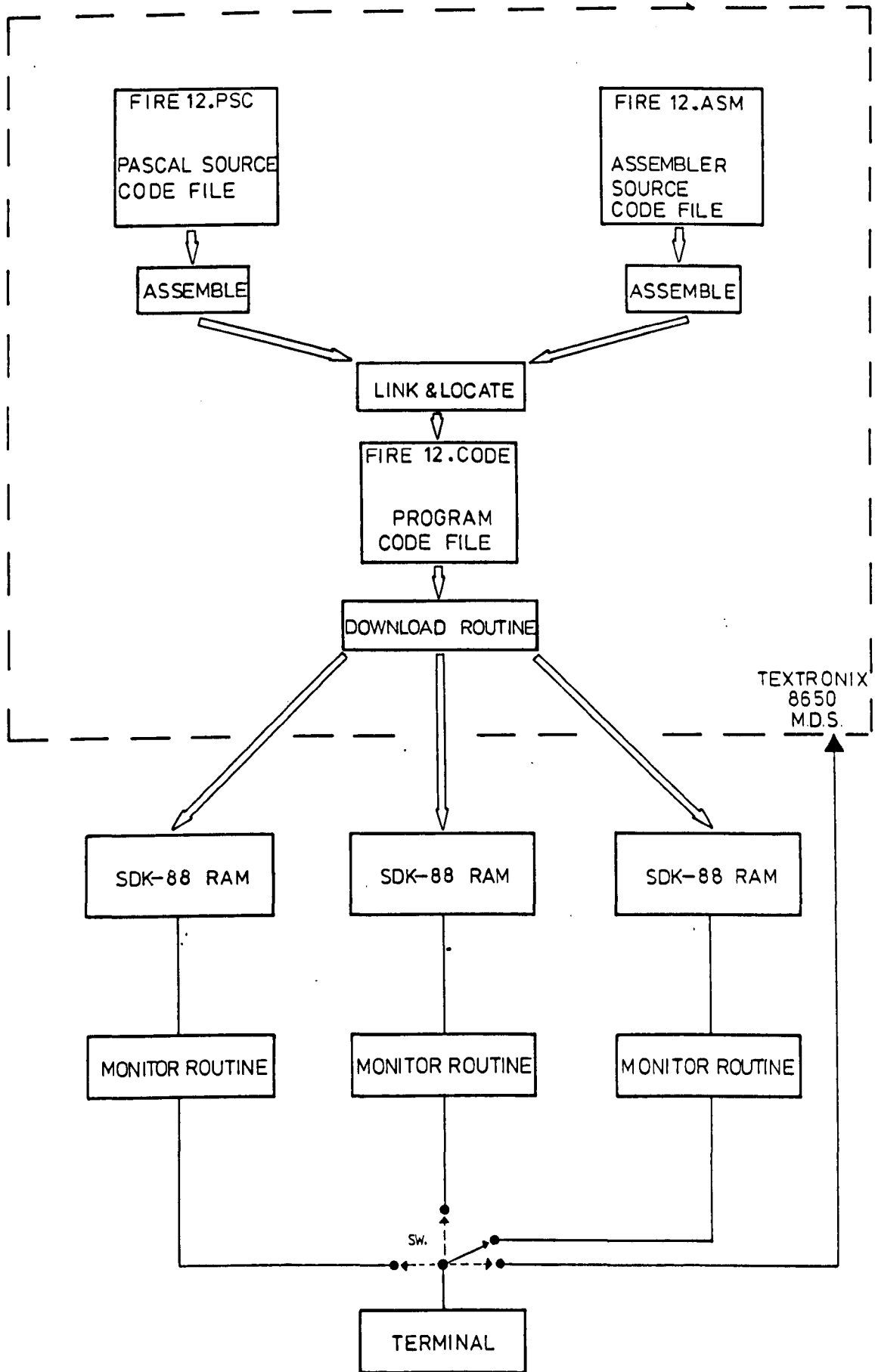


Fig. 4.11 : SDK-88 microprocessor programming arrangements

4.2.2 Sampling

Each of the three SDK-88s used the signal conditioning circuit shown in Figure 4.12 to feed the sample and hold circuit and analogue to digital converter (ADC) shown in Figure 4.13. The logic timing diagram in Figure 4.14 illustrates the sequence of events required to get data on to the Intel 8088 data bus.

From the program environment, a data sample is initiated by an OUT DX instruction, where DX is the data register containing the ADC address. After time has been allowed for the sampling process the digital word may be read to the accumulator, AL, using the IN DX instruction.

Typical instruction times for the 8088 processor with 4.9MHz clock are less than 10 microseconds^[108,109], therefore some delay needed to be incorporated between the OUT DX and IN DX instructions to allow the 12 microseconds ADC conversion^[111].

For the ADC located at address a F800 the assembler code required is then:

```

MOV DX, @ OF800H      ;      Load address of ADC
OUT DX, AX            ;      Initiate conversion
MOV CL, @ OFH         ;      Conversion -
SHR CL, CL            ;      delay
XOR AH, AH            ;      Set accumulator word to zero
IN AL, DX             ;      Input sample to accumulator low
                        ;      byte

```

The time between successive samples will be dictated by the amount of code required by the control algorithm. N-bit sampling of the model supply voltage gives 2^N possible quantisation levels, and therefore a maximum signal to noise ratio of:

$$20 \log_{10} \left[\frac{1}{2^N} \right] \text{ dB} = -6N \text{ dB}$$

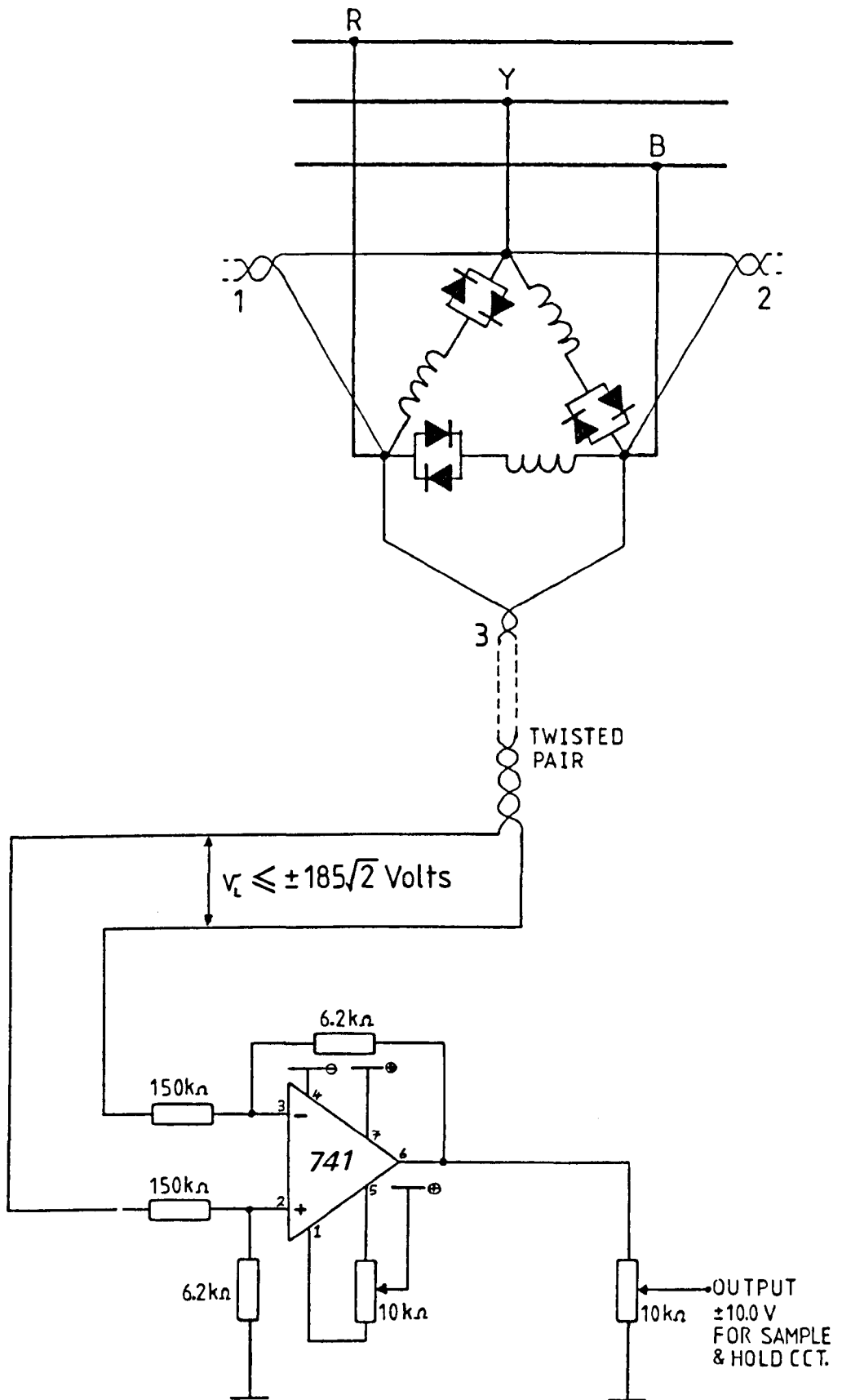


Fig. 4.12 : Signal conditioning circuit for voltage measurement

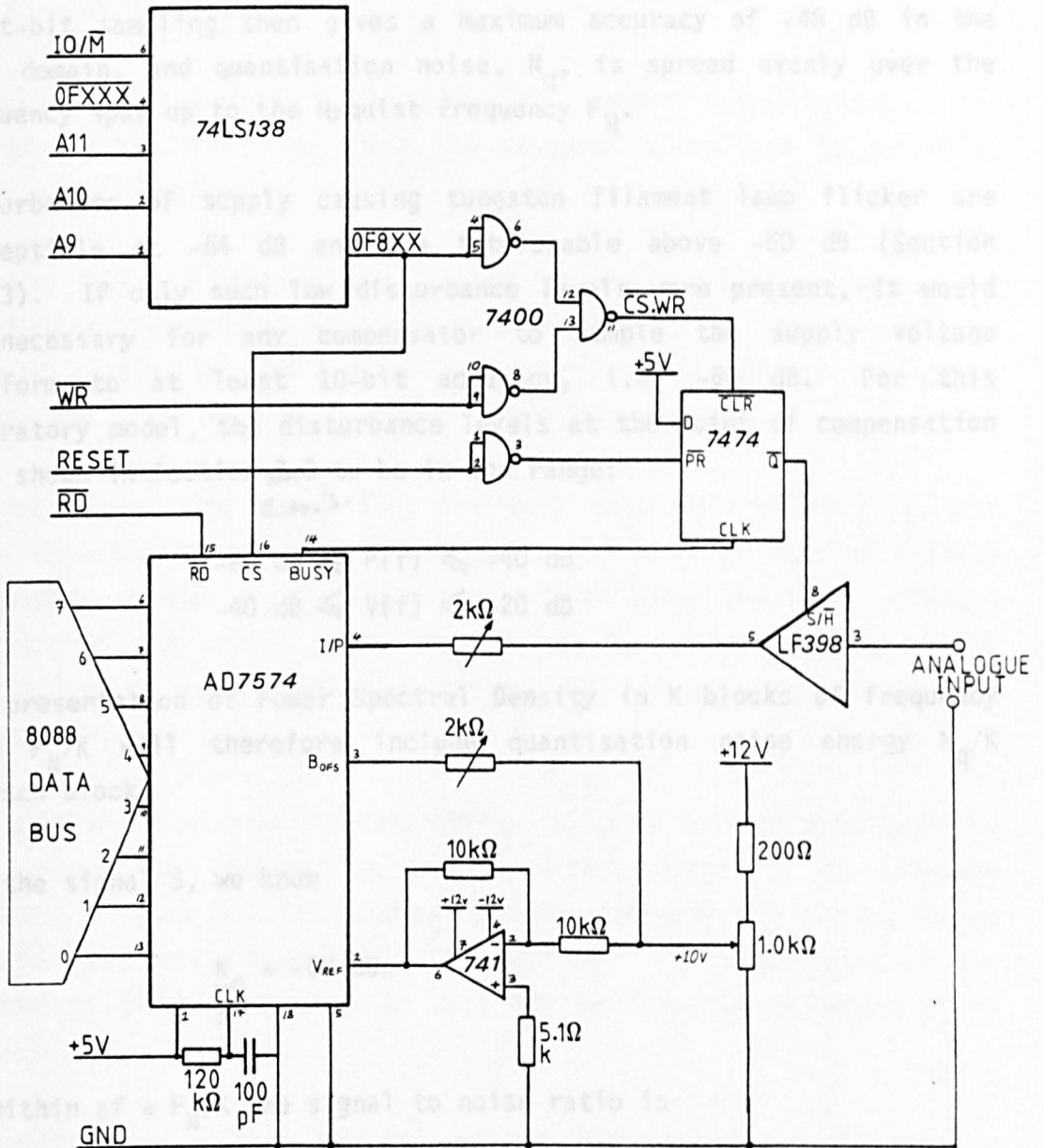


Fig. 4.13 : Sample and hold circuit for voltage measurement

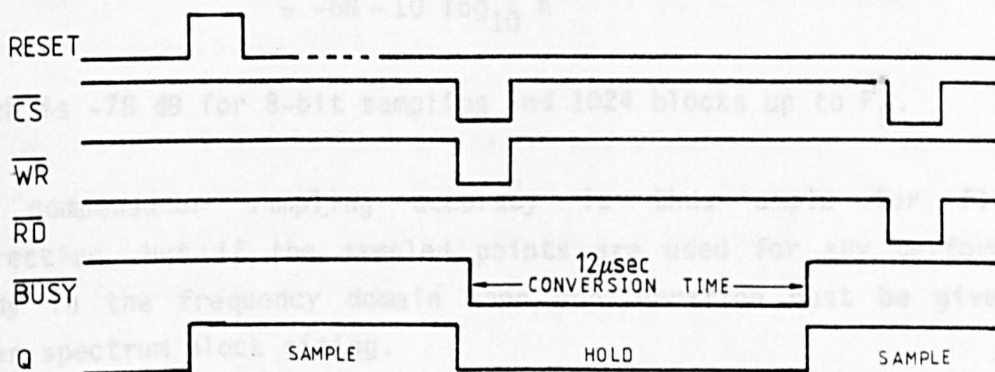


Fig. 4.14 : Logic timing diagram for sample and hold circuit

Eight-bit sampling then gives a maximum accuracy of -48 dB in the time domain, and quantisation noise, N_q , is spread evenly over the frequency span up to the Nyquist frequency F_N .

Disturbances of supply causing tungsten filament lamp flicker are perceptible at -54 dB and are intolerable above -50 dB (Section 3.1.3). If only such low disturbance levels were present, it would be necessary for any compensator to sample the supply voltage waveform to at least 10-bit accuracy, i.e. -60 dB. For this laboratory model, the disturbance levels at the point of compensation were shown in Section ~~2.3~~ to be in the range:

2.4.3.

$$-80 \text{ dB} \leq P(f) \leq -40 \text{ dB}$$

then
$$-40 \text{ dB} \leq V(f) \leq -20 \text{ dB}$$

The presentation of Power Spectral Density in K blocks of frequency span F_N/K will therefore include quantisation noise energy N_q/K in each block.

For the signal S , we know

$$\frac{N_q}{S} = -6N \text{ dB}$$

So within $\Delta f = F_N/K$ the signal to noise ratio is

$$\begin{aligned} 10 \log_{10} \frac{N_q}{KS} &= 10 \log_{10} \frac{N_q}{S} - 10 \log_{10} K \\ &= -6N - 10 \log_{10} K \end{aligned}$$

which is -78 dB for 8-bit sampling and 1024 blocks up to F_N .

The compensator sampling accuracy is thus ample for flicker correction, but if the sampled points are used for any performance study in the frequency domain then consideration must be given to power spectrum block sizing.

4.2.3 The Control Algorithm

Section 4.1.2 briefly discussed TCR control requirements, and introduced the method of using the integral of voltage to determine thyristor firing angles.

V_f , the 'flicker voltage', is evident as the modulation envelope of the 50Hz supply voltage waveform (Figures 2.3, 3.1). The severity of this modulation may be reduced by attempting to minimise variations of the RMS value of each half-cycle of supply voltage.

Evaluating $\int v^2(t)dt$ or $\int v(t)dt$ for each half-cycle suffers in that small departures in $v(t)$ from the sinusoidal will produce only small percentage changes in the integral sum. An algorithm that initiates thyristor firing when a given integral sum is reached would thus lack sensitivity to small voltage variations if the full integral were to be employed.

A method of increasing the sensitivity to small voltage variations is to perform the integration process with respect to a reference sinusoid. Figure 4.15 illustrates how the integral sum may be formed using a reference sinusoid $v_R(\omega t) = R\sin\omega t$. The sensitivity of the process to given variations in $v(t)$ may be lessened by making $|V-R|$ larger.

The undistorted voltage waveform $v(\omega t) = V\sin\omega t$ may be disturbed by additional components $v_f(\omega t)$. Figures 4.15(a) and (b) indicate how the point in the half cycle at which a given integral sum is reached will vary for $\int v_f(\omega t)dt$ negative and positive respectively. This variation may be used by a control algorithm to determine a firing angle α for thyristors in a TCR.

Turning on the TCR applies a sudden additional load to the supply system and the voltage at the point of TCR connection will fall accordingly. It will remain depressed throughout the period of thyristor conduction as shown in Figure 4.16.

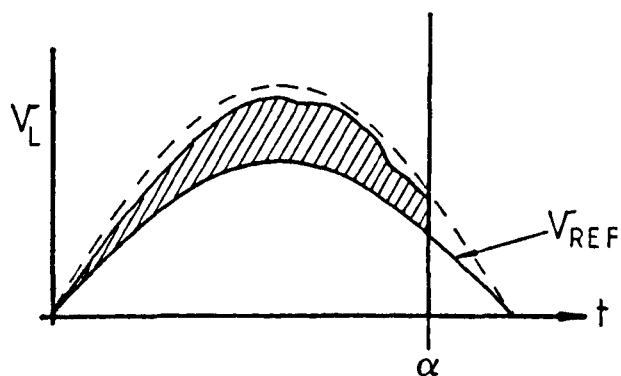


Fig. 4.15(a) : Integral of voltage difference - late firing

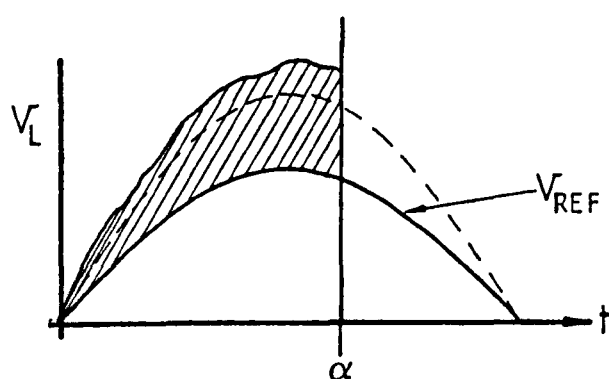


Fig. 4.15(b) : Integral of voltage difference - early firing

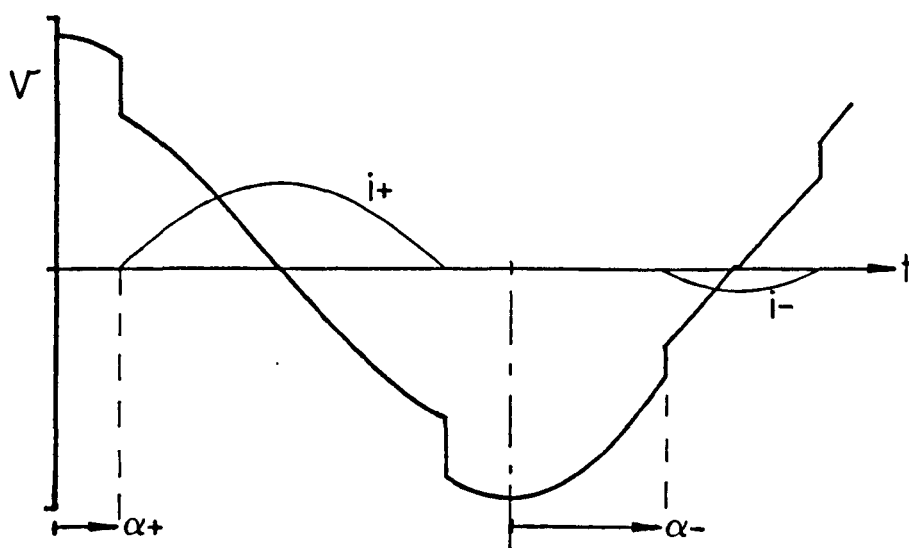


Fig. 4.16 : Voltage depression due to shunt TCR conduction

The principle of the control algorithm is now established:

A voltage waveform that is overall greater than some nominal reference within one half cycle will cause earlier switching of the TCR compensator. This will depress the voltage for the remainder of the half cycle.

Conversely, a voltage waveform lower than nominal will cause later switching of the TCR, causing less depression of the voltage waveform within the half cycle.

Thus it is intended to balance supply voltage variations with those impressed by the TCR. This is of course the principle of shunt compensation whereby the compensator inversely balances the varying load characteristics.

Cooper and Hussayni^[41] surmised that the use of a reference sine wave integration process may present difficulties in the synchronisation of the reference sinusoid $v_R(\omega t)$ to the distorted voltage

$$v'(\omega t) = v(\omega t) + v_f(t)$$

The relative size of the reference sinusoid is also of obvious importance, and is related to the process by which a thyristor firing angle is decided. Fortunately, where this process is determined by a computer program, numerical techniques may be used to investigate and experiment with the control method. Figure 4.17(a) and (b) give the full flow chart for the control algorithm. The full program compiler listing is given in Appendix F.

The integration procedure begins after each zero-crossing of the supply voltage waveform, each digital sample is added to give a cumulative sum. When the sum exceeds a pre-set value, a short pulse is output to cause the thyristor that is correctly biased to turn on. Thyristor turn-off follows naturally at the next current zero, approximately $180-2\alpha$ degrees later.

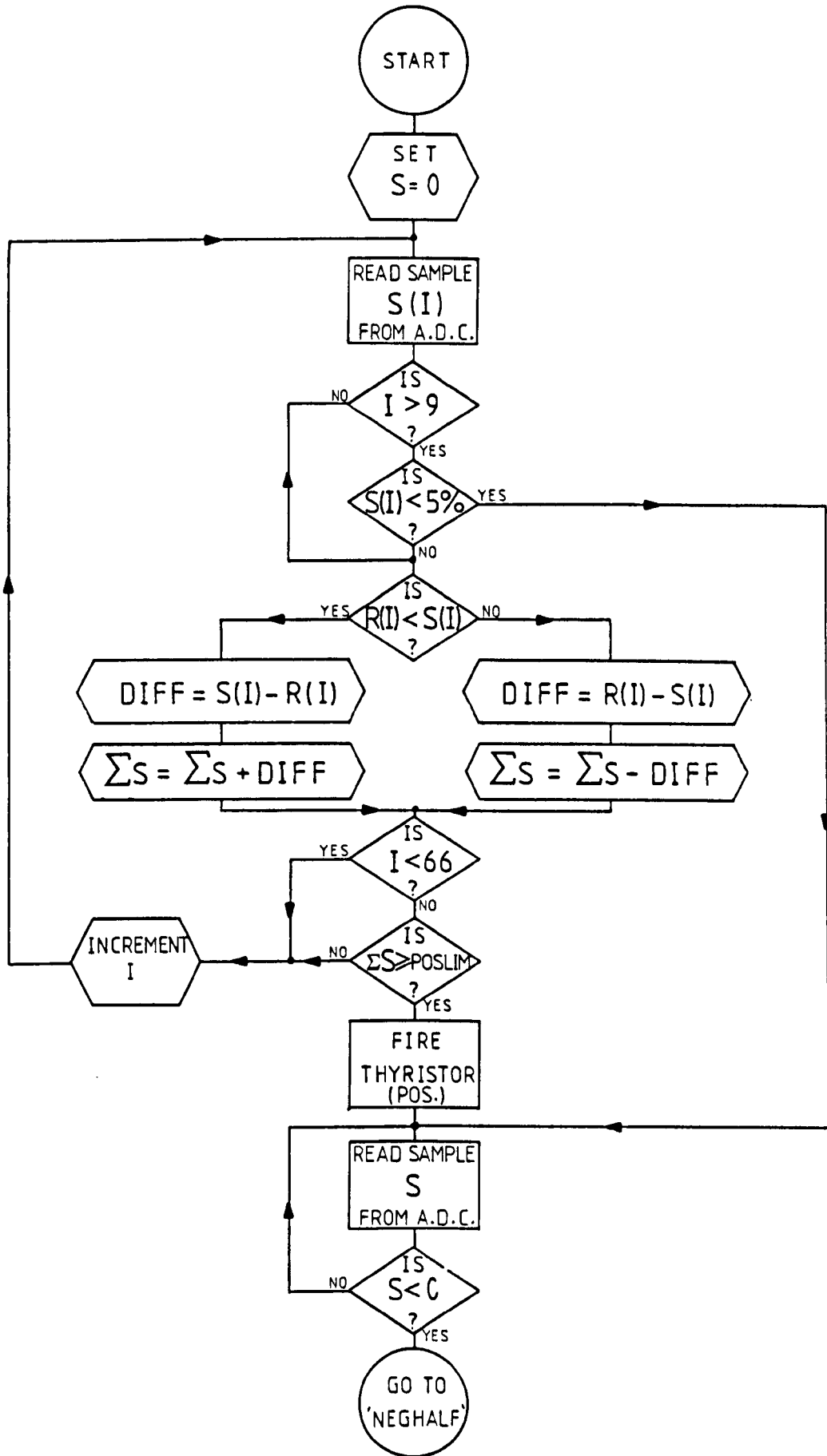


Fig. 4.17(a) : 6-pulse TCR compensator control algorithm flow chart

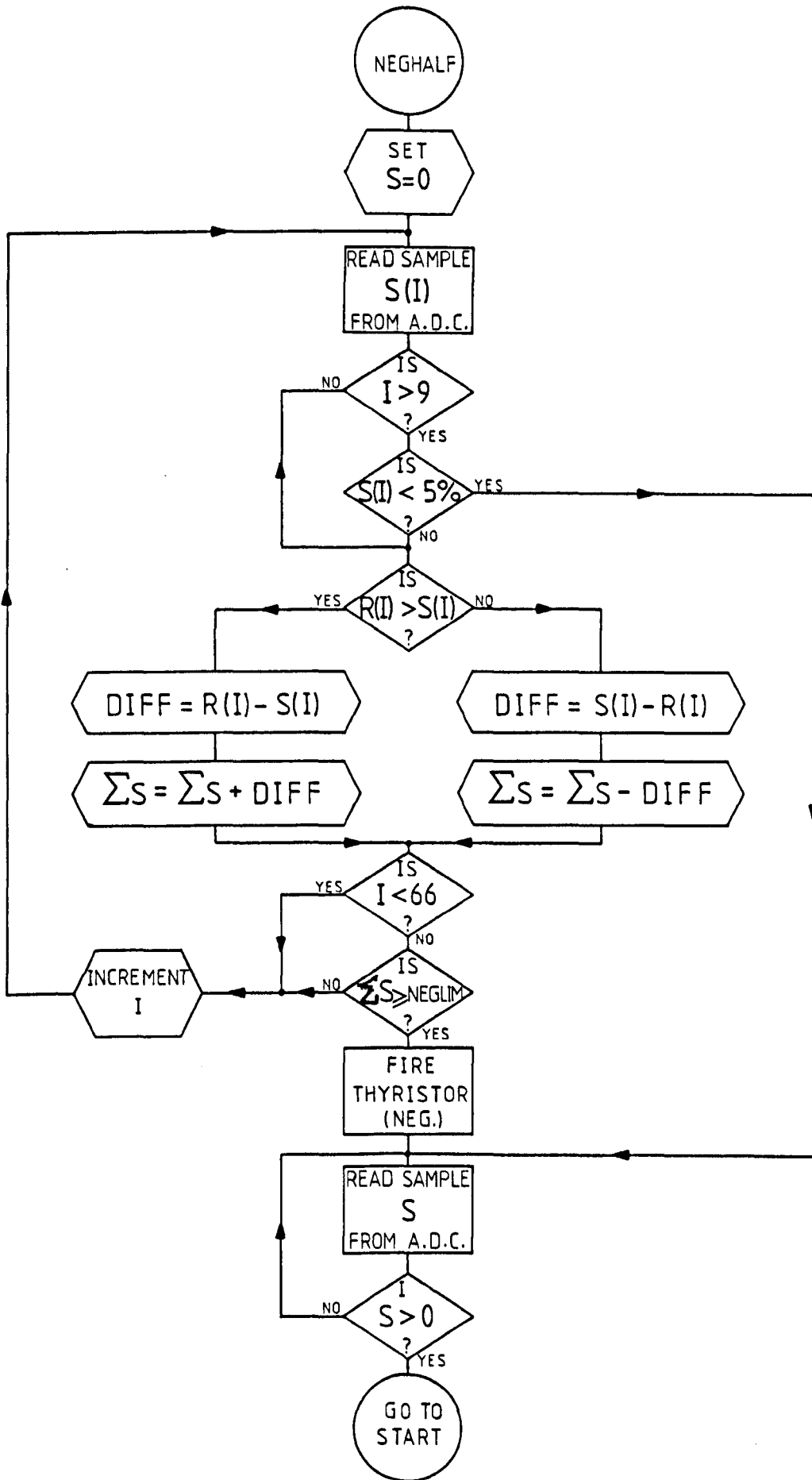


Fig. 4.17(b) : 6-pulse TCR compensator control algorithm flow chart (cont'd)

This procedure therefore performs the discrete equivalent of the continuous integral

$$\int_0^{a/\omega} v'(\omega t) dt$$

where a is measured from the preceding voltage zero-crossing.

The machine code was stored in a file on the Tectronix 8560 MUSDU and downloaded in turn to each of the three SDK-88s. Small differences between the three SDK-88 systems necessitated that changes be made once the code was in the processors RAM.

All variables in the program could be changed via the terminal and SDK-88 Monitor routine, those requiring attention are considered below, together with reasoning for their values.

4.2.4 Control Variables

The variables in the control program that require consideration are:

- (i) The sample loop delay, D .
- (ii) The reference sine wave, $v_R(\omega t)$.
- (iii) The integration limit, LIMIT

and these are now considered in turn.

(i) Sample Loop Delay, D

It was found that free running of the program, with no additional delays inserted, gave consecutive ADC read pulses approximately every 65 microseconds. This time, Δt , varied slightly between the three SDK-88 systems:

- System 1, Δt approximately 63 μ seconds
- System 2, Δt approximately 66 μ seconds
- System 3, Δt approximately 64 μ seconds

Although small, these differences would mean that a particular integration limit would be reached at different times in different processors.

For example, 7.5 milliseconds would contain 119, 113, 117 samples by 1,2,3 respectively, giving approximately 0.4 milliseconds difference between the firing times in two different branches of the TCR.

In order to balance the three systems as best as possible, a software 'sample loop delay', D, was inserted in the program using the software:

```
-----
MOV CL,'D'
SHR CL, CL
-----
```

(See Appendix F for full program listing.)

Δt was fixed close to 74.0 microseconds using the following values of D:

System 1, positive half cycle, D = 9 @ 09 : $\Delta t = 74.4 \mu\text{secs}$
 negative half cycle, D = 8 @ 08 : $\Delta t = 74.2 \mu\text{secs}$
 System 2, positive half cycle, D = 6 @ 06 : $\Delta t = 74.1 \mu\text{secs}$
 negative half cycle, D = 4 @ 04 : $\Delta t = 74.6 \mu\text{secs}$
 System 3, positive half cycle, D = 8 @ 08 : $\Delta t = 74.1 \mu\text{secs}$
 negative half cycle, D = 6 @ 06 : $\Delta t = 74.6 \mu\text{secs}$

The final location of bytes representing 'D' in RAM were 14 and 116 bytes respectively from the start of the 'fireASub' object code program block.

(11) The Reference Sine Wave, $v_R(\omega t)$

The signal conditioning circuits and ADCs were carefully adjusted so that ± 262 volts for the model supply line voltage, v_L , would just be within the range of the 8-bit ADCs. This ± 262 volt range allowed the nominal supply line voltage to rise by 5p.c. and just be within the extreme range of the ADC.

Figure 4.18 shows how use of the ADC in its unipolar mode results in:

$v_L = -262$ Volts is sampled as (a) 00 or (a) 01

$v_L = 0$ Volts is sampled as (a) 7F or (a) 80

$v_L = +262$ Volts is sampled as (a) FE or (a) FF

Ajustment enabled the underlined values to be repeatedly obtained with a test 262v dc supply.

Thus the least significant bit (LSB) of the data byte represents 2.063 volts of the model supply v_L .

The nominal model line voltage of $V_{RMS} = 175$ volts will then give an equivalent sampled sine wave of:

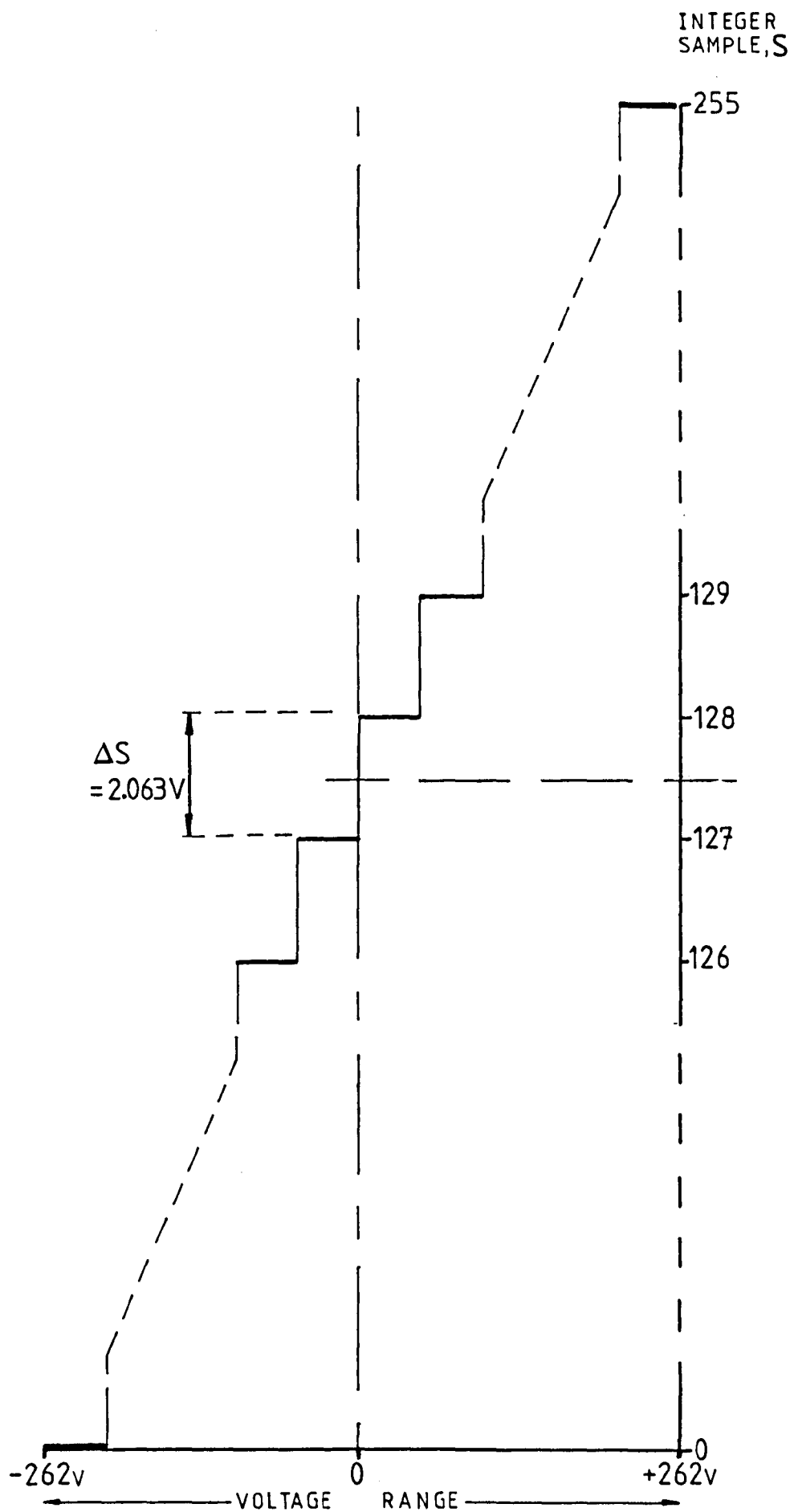
$$v_S = 127 + 120 \sin \omega t$$

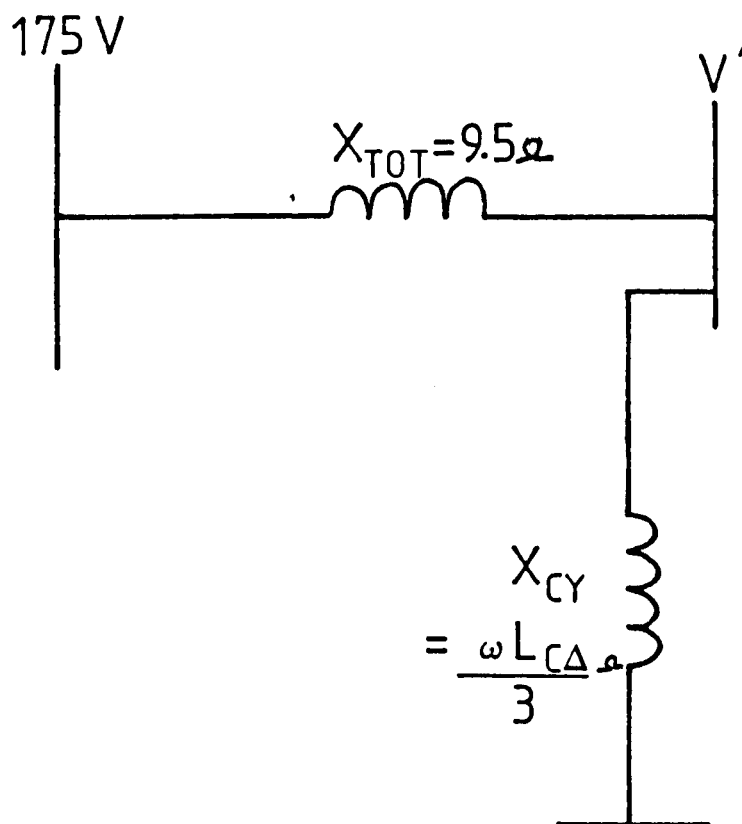
Similarly $v_S = 127 + 116 \sin \omega t$ for $V_{RMS} = 179$ Volts

and $v_S = 127 + 113 \sin \omega t$ for $V_{RMS} = 165$ Volts

Full conduction of the TCR with 1.0 Henry inductances in each branch would produce the equivalent circuit shown in Figure 4.19, and the model busbar voltage will fall to

$V_{RMS} = 160.44$ Volts.

**Fig. 4.18 : ADC range and span**



FOR $L_{C\Delta} = 1.0$ HENRY, $V' = 160.4$ VOLTS

Fig. 4.19 : RMS Voltage depression for full compensator conduction

This would be represented by an equivalent sampled sine wave of:

$$v_S = 127 + 110 \sin \omega t$$

Making the reference sinusoid equal to this ensured that most sampled points would be greater than or equal to the 'reference' values:

$$\text{ie } \underline{v_R = 127 + 110 \sin \omega t}$$

With the knowledge that the sampling interval, Δt , is approximately 74.0 microseconds, it would be a simple matter to calculate values for v_R to correspond to each of the sampled data points v_S . Close examination of the ADC sample circuitry, however, revealed that the first sample was being made 100 microseconds after voltage zero, instead of 74 microseconds. This occurred because of a 25 microsecond delay introduced by the section of the program that detected the voltage-zero crossing.

A nominal supply frequency of 50Hz allows 133 reference points to be calculated for each half cycle.

$$t_0=0, t_1=100, t_2=175, t_3=250 \dots\dots t_{133}=10,000 \text{ usecs}$$

The points for the positive half-cycle v_R were stored in a look-up table beginning at the memory location labelled 'sine1'. Similarly, 'sine2' located the negative half-cycle of v_R . All were individually calculated for unipolar operation to eliminate the maximum amount of real time processing.

iii) Integration limit, LIMIT

Section 4.2.3 described how a digital integration process decided the TCR firing angle in each half-cycle of the supply voltage waveform, $v = V\sin\omega t$, for an equivalent reference sinusoid $v_R = R\sin\omega t$.

The continuous integral to be evaluated would be:

$$E = \int_0^{\frac{\alpha}{\omega}} (V\sin\omega t - R\sin\omega t) dt$$

$$= \frac{(V - R)}{\omega} [1 - \cos\alpha]$$

Where

- E = The summated error of $v - v_R$.
- α = The phase angle, after the voltage zero-crossing, at which E is reached.
- V = The sinusoidal peak value of v .
- R = The sinusoidal peak value of v_R .

The discretised equivalent of this continuous integral may be written:

$$\sum \Delta t S = \frac{(V' - R')}{\omega} [1 - \cos\alpha]$$

Where

- Δt = The sampling interval
- S = A single digital sample of the difference $(v - v_R)$
- V' = The equivalent digital value of V
- R' = The equivalent digital value of R

and $\sum S$ is the LIMIT value set in RAM to fix the firing angle α w.r.t. voltage zero crossing
or α w.r.t. voltage peak

The units of S and $\sum S$ are simply Volts, although scaling of the digital sample values are required to obtain Volts since:

$$1 \text{ bit} = 2.063 \text{ Volts (Figure 4.18)}$$

Then the relationship between E and $\sum S$ or LIMIT is:

$$\begin{aligned} E &= S \times 2.063 \times \Delta t \\ &= S \times 2.063 \times 74.0 \times 10^{-6} \\ &= S \times 152.7 \times 10^{-6} \\ &= \text{LIMIT} \times 152.7 \times 10^{-6} \quad \text{Volt Seconds} \end{aligned}$$

$$\text{i.e.} \quad \text{LIMIT} = \frac{E}{152.7 \times 10^{-6}} \quad \text{Volt Seconds}$$

$$\text{Let} \quad v'_R = 127 + 110 \sin \omega t$$

Then for the digital value 127 = 0 Volts,

$$v_R = 226.9 \sin \omega t \quad \text{Volts}$$

$$\text{i.e.} \quad R = 226.9 \quad \text{Volts}$$

If v is typically 175V RMS, then

$$V = 247.5$$

thus for $\theta = \pi$ radians,

$$\begin{aligned} E_{\text{MAX}} &= \frac{[V - R]}{\omega} \times 2 \\ &= 0.131 \end{aligned}$$

$$\text{and } \text{LIMIT}_{\text{MAX}} = 858 \text{ dec.} = 35\text{D hex.}$$

This is the maximum value of integration limit to be expected for $R = 226.9$ Volts, and it has been calculated assuming a perfectly sinusoidal supply voltage waveform.

For $\alpha = \pi/2$ radians, LIMIT will be 429 dec. = 1AE hex. These values are clearly dependent upon the choice of reference sinusoid and the distortion of the supply voltage waveform. A theoretical approach will be able to show how combinations of v_R and LIMIT will influence the compensator performance. This is explored further in Section 4.3.3 in the study of steady state reactive compensation.

The compensator performance for different combinations of the control variables above was studied. A 'steady-state' analysis is given in Section 4.3.3, and Chapter V presents the results of experiments using the three-phase compensator with the laboratory arc furnace model.

4.3 STEADY STATE TUNING AND PERFORMANCE

Having established the control variables that would affect the TCR compensator performance, studies were made with an un-modulated 50Hz supply voltage. Varying the RMS value of the voltage illustrated the range of voltage control that the TCR compensator could effect.

These early experiments, with the three-phase TCR arrangement drawing current from the supply for the first time, highlighted the need for careful 'tuning' of the three compensator phases. The more important aspects are now presented.

4.3.1 Thyristor Firing and Conduction Limits

Thyristor turn-on was initiated with a logic '1' applied to the relevant bit of the 8-bit output port at address ^(a) 0F000H. This signal was latched for 100 microseconds and logically ANDed with a 21kHz square wave to produce a 100 microsecond 21kHz burst for application to the thyristor gate through a transistor and isolating pulse transformer. Figure 4.20 gives the firing circuit for each inverse-parallel pair of thyristors switched from the microprocessor output port A. The 5V d.c. supply to the transistor circuits was separate from the 5V d.c. logic supply, and was only energised when firing was required.

The latching circuit meant that the processor was only committed for a very short time at each pulse output, timing and pulse turn-off being executed in hardware rather than software.

The 8088 microprocessor 'SI' register was used to hold the incremented address for each successive reference sinusoid sample, and could thus be used to calculate the number of samples taken after voltage-zero crossing. Each pre-programmed reference sinusoid, 'sine1' and 'sine2' are given in Appendix F.

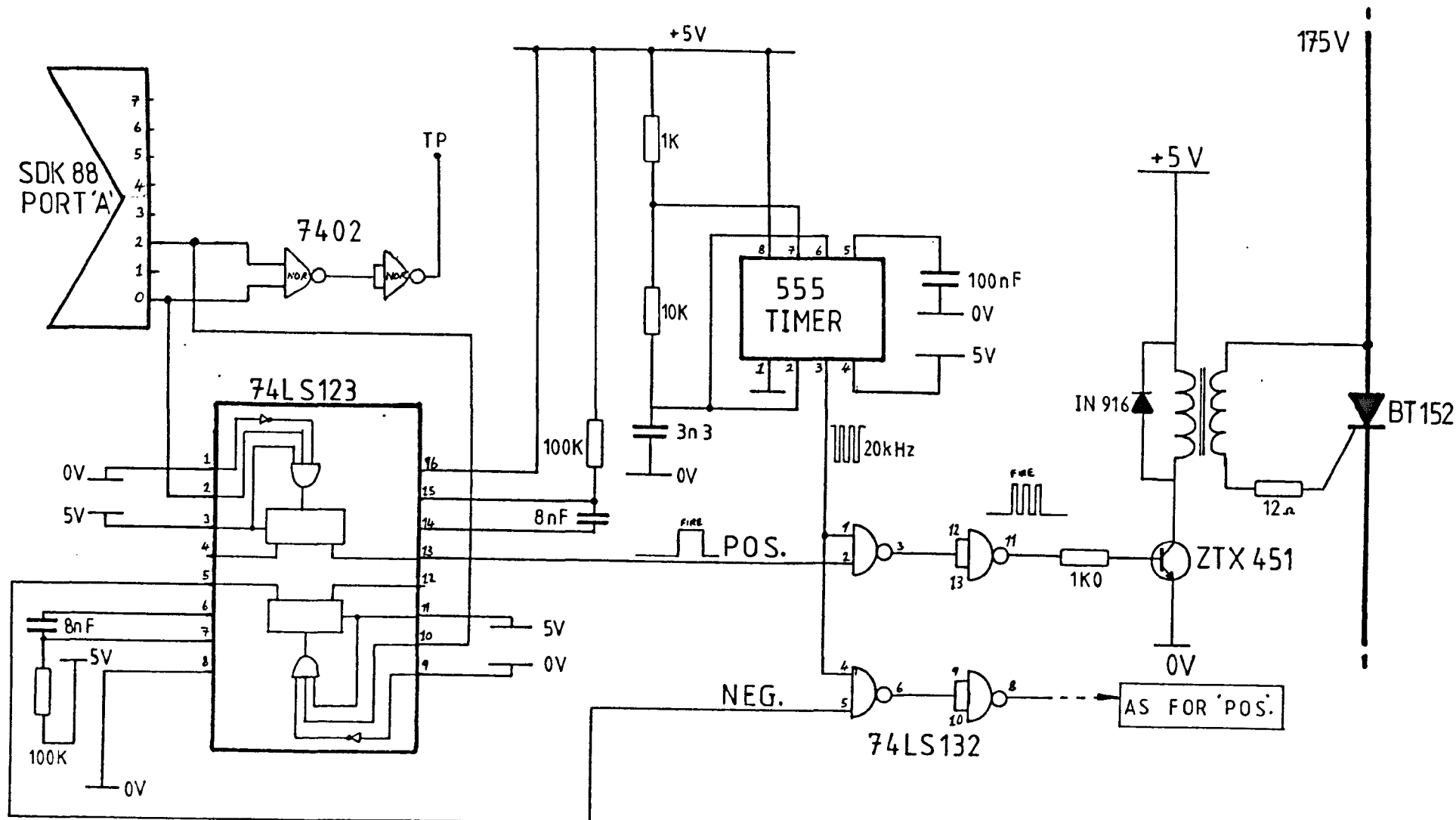


Fig. 4.20 : Thyristor firing circuit for laboratory TCR thyristors

Figure 4.3 shows how the start of conduction for each thyristor must be $0^\circ \leq \alpha \leq 90^\circ$, where $\alpha = 0^\circ$ is 90° after the relevant voltage zero-crossing.

This range corresponds to:

$$\begin{aligned} \text{sine1} \leq \text{SI} \leq \text{sine1} + @ 42 & \quad \text{for the positive 1/2-cycle} \\ \text{sine2} \leq \text{SI} \leq \text{sine2} + @ 42 & \quad \text{for the negative 1/2-cycle} \end{aligned}$$

The program flow chart (Figure 4.17) shows that even if the integral limit is reached, the thyristor firing pulse is not allowed until $\text{SI} = @ 109\text{A}$ or $@ 111\text{F}$ for positive and negative half-cycles respectively.

The control system was also prevented from initiating thyristor firing pulses at the very end of each half cycle of the voltage waveform. This ensured that the program flow proceeded to the section where rapid sampling detects a voltage zero-crossing necessary before the integration process in the following half-cycle may proceed. The program flow chart (Figure 4.17) shows that integration is abandoned if the sampled voltage falls below 14 volts. This is reasonable since thyristor conduction is only prevented beyond $\alpha \approx 87^\circ$, where compensation effects are a minimum.

4.3.2 Phase Balancing

Small differences in offset and gain in the sampling circuitry for each branch of the compensator, coupled with the slight variance in the sampling rate, resulted in a slightly different firing angle α when identical values of LIMIT were set.

The integration sum LIMIT was then adjusted for the positive and negative half-cycle firing pulse of each compensator branch to achieve totally balanced operation under given conditions.

This required values of LIMIT which varied from each other by up to $\pm 10\text{p.c.}$, the exact values are given with corresponding theory and results in Section 4.3.3 and Chapter 5.

4.3.3 Steady State Reactive Compensation Theory

Theory will predict the interaction between LIMIT and the reference sinusoid v_R for reactive compensation under sinusoidal conditions. Part 5.1 then presents comparable results obtained in the laboratory, and a choice of control variables may be made before proceeding with laboratory studies for non-sinusoidal conditions.

Figure 4.21 shows the one line diagram and voltage waveform for a three-phase TCR compensator connected to the infinite busbar through an inductance L_S . The single phase equivalent of the delta connected compensator inductance $L_{C\Delta}$ is $L_{CY} = L_{C\Delta}/3$.

When the TCR is OFF, $v_2 = v_1$

When the TCR is ON, $v_2 = Kv_1$

$$\text{Where } K = \frac{L_{CY}}{L_S + L_{CY}}$$

Thyristor conduction occurs for $\sigma \geq \omega t \geq a$, $\sigma = \frac{\pi-a}{2}$ radians

The resulting RMS value of the waveform is then:

$$V_{RMS} = \sqrt{\frac{\omega}{\pi} \left\{ \int_0^{\sigma} (Kv_1)^2 dt + \int_{\frac{\sigma}{\omega}}^{\frac{a}{\omega}} (v_1)^2 dt + \int_{\frac{a}{\omega}}^{\frac{\pi}{\omega}} (Kv_1)^2 dt \right\}}$$

$$= \sqrt{\frac{K^2 v_1^2}{\pi} \left[\pi - a + \frac{\sin 2a}{2} \right] + \frac{v_1^2}{2\pi} \left[2a - \pi - \sin 2a \right]}$$

.....Equation I

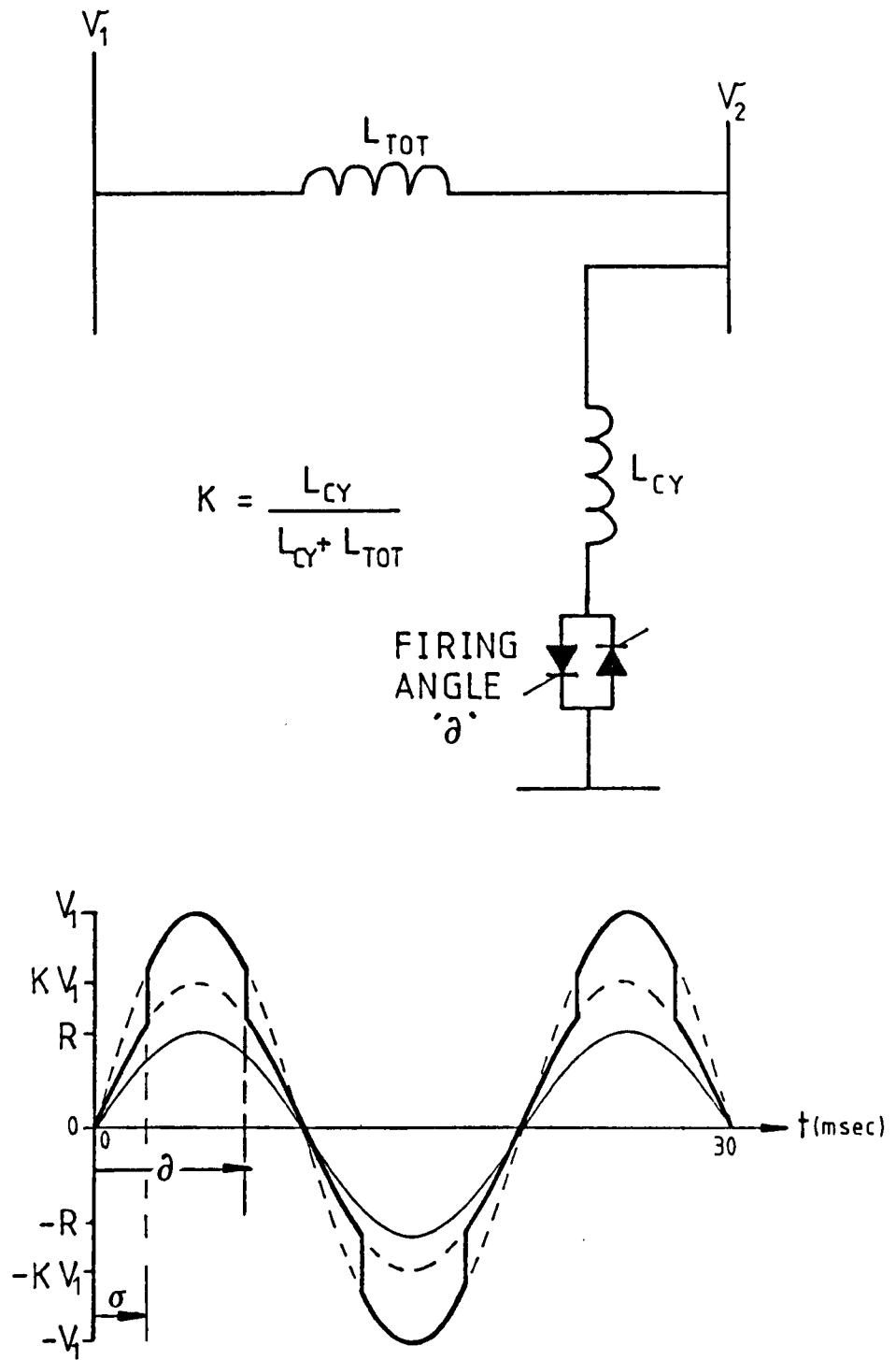


Fig. 4.21 : One line diagram for 'open circuit' TCR compensation equations

The continuous integral sum, from the voltage zero crossing to firing angle α , is:

$$\begin{aligned}
 E &= \int_0^{\alpha} (KV_1 - R) \sin \omega t \, dt + \int_{\alpha}^{\frac{\pi}{2}} (V_1 - R) \sin \omega t \, dt \\
 &= \frac{KV_1}{\omega} - \frac{R}{\omega} - \cos \alpha \left[\frac{KV_1 + R - 2V_1}{\omega} \right] \quad \text{Volt Seconds} \\
 \alpha &= \cos^{-1} \left[\frac{\omega E + R - KV_1}{R - V_1(2-K)} \right] \quad \text{radians}
 \end{aligned}$$

.....Equation II

For a given value of LIMIT (and hence E), the values of V_1 , K and R may be set as required, and α from Equation II substituted into Equation I to give V_{RMS} .

V_1 is nominally 247.5 Volts corresponding to 175 Volts RMS.

$$R = 110 \times 2.063 = 226.9 \text{ Volts}$$

$$L_S = 30.4 \text{ millihenries}$$

$$\text{For } L_{C\Delta} = 1.0H \quad ; \quad L_{CY} = 0.333H \text{ and } K = 0.916$$

The variation of α versus LIMIT for $K = 0.916$ is shown in Figure 4.22.

Three steady-state values of the firing angle α were chosen for experiments with the laboratory TCR. These are shown in Figure 4.22, $\alpha_1 \approx 100^\circ$, $\alpha_2 \approx 135^\circ$ and $\alpha_3 \approx 170^\circ$. They represent only a lower mid and upper setting for $90^\circ \leq \alpha \leq 180^\circ$, with the greatest range of VAR control occurring from $\alpha_1 \approx 100^\circ$. However, including three values of the integration limit will highlight its effects in the control scheme.

Figure 4.22 gives:

$$\text{LIMIT1} = 150 \text{ dec. for } \alpha_1$$

$$\text{LIMIT2} = 610 \text{ dec. for } \alpha_2$$

$$\text{LIMIT3} = 843 \text{ dec. for } \alpha_3$$

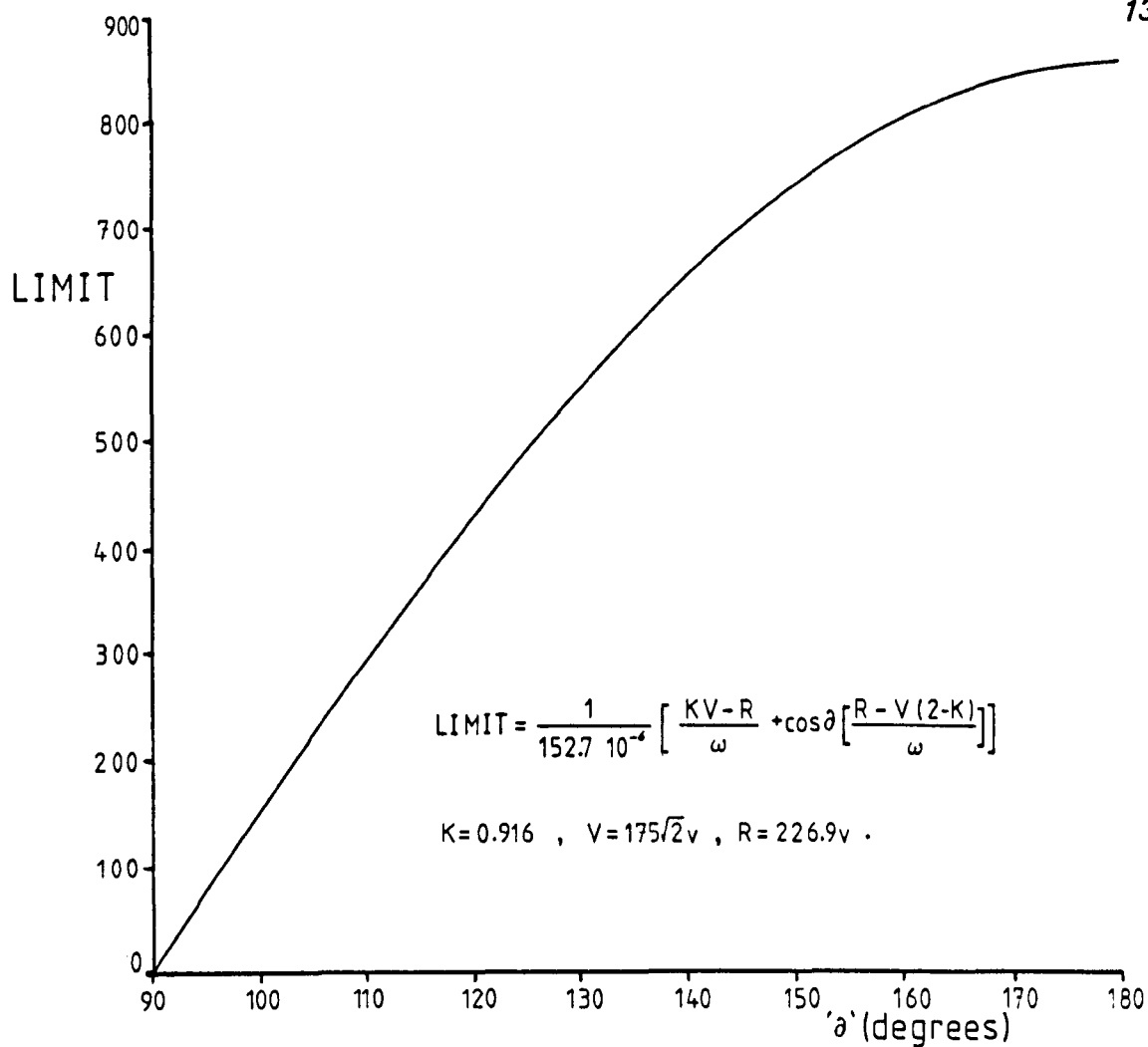


Fig. 4.22 : Theoretical variation of LIMIT versus 'θ'

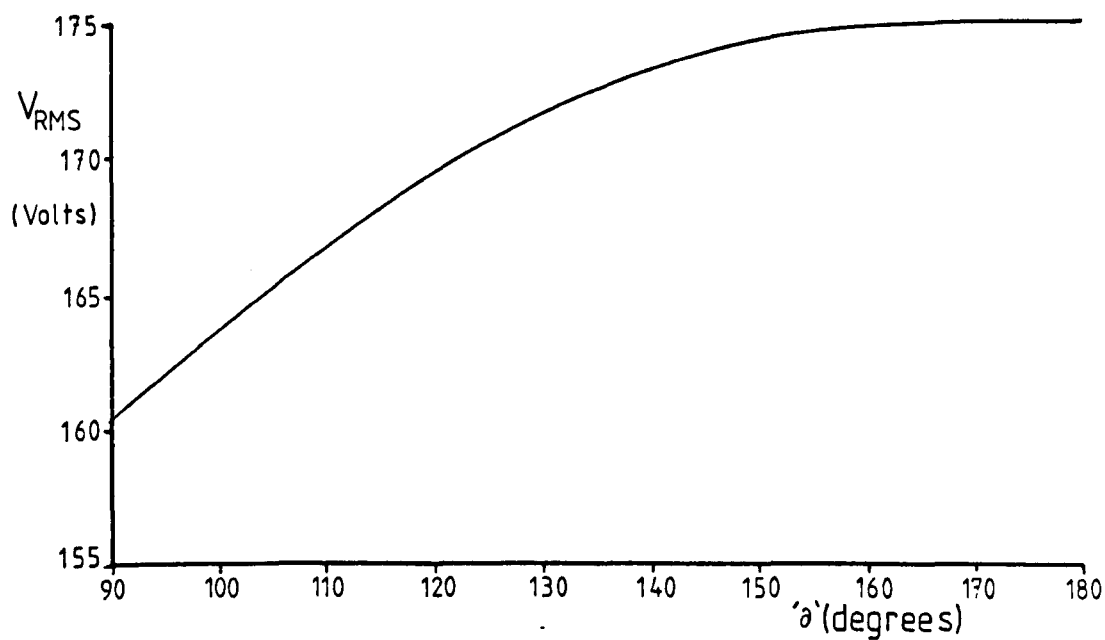


Fig. 4.23 : Theoretical variation of RMS voltage versus 'θ'

For a fixed value of V_1 , V_{RMS} can be plotted as a function of α only. This is shown in Figure 4.23.

Once the parameters D , v_R and LIMIT have been set for a constant supply voltage peak V_1 , it is sensible to undertake a study of the effects of varying V_1 for a set combination of control variables. This will allow the compensator performance to be evaluated as a function of the control parameters.

A simple investigation of the TCR compensator's ability to control the voltage at its point of connection may be carried out using the circuit representation of Figure 4.24. This will give results for open-circuit voltage control. Shunt load TCR compensation may then be studied using the circuit representation of Figure 4.25.

(i) Open Circuit Voltage Control

Open-circuit voltage control describes the function of the TCR compensator when there is no other load connected in parallel to the point of TCR connection (Figure 4.24).

With a fixed reference sinusoid, v_R , V_1 may be varied over a set range. V_{2RMS} may then be calculated using equations I and II, provided that a suitable value for LIMIT is set. Figure 4.26 shows the effect of using LIMIT1, LIMIT2 and LIMIT3 above for fixed $R = 226.9$ Volts.

The flatter portions of each curve indicate the full range of TCR control, with α progressing from 180° to 90° as V_1 increases. Figure 4.25 shows clearly that the lower value of integration limit will give the flattest voltage control region. The linear portions above the range of control have gradient $K = 0.916$ since here $V_2 = KV_1$. The linear portions below the range of voltage control are of gradient 1 since $V_2 = V_1$ before conduction in the TCR.

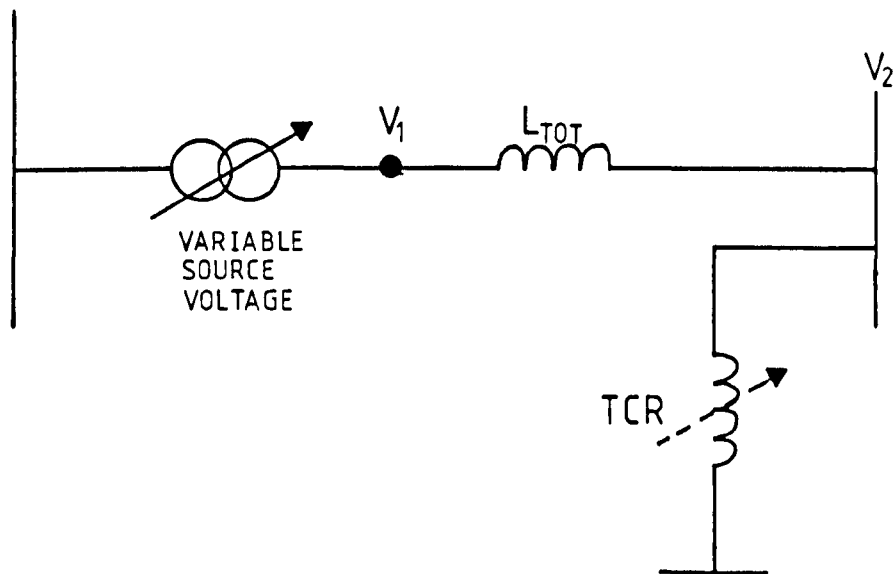


Fig. 4.24 : Experimental circuit for steady state 'open circuit' compensation

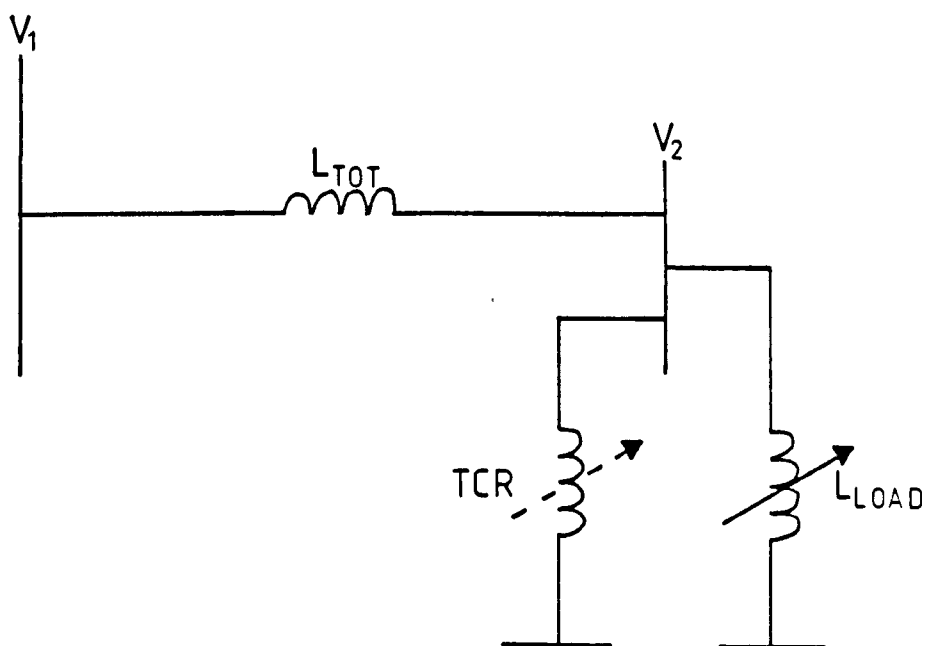


Fig. 4.25 : Experimental circuit for steady state shunt load compensation

$$R = 227 \text{ V} \quad K = 0.916$$

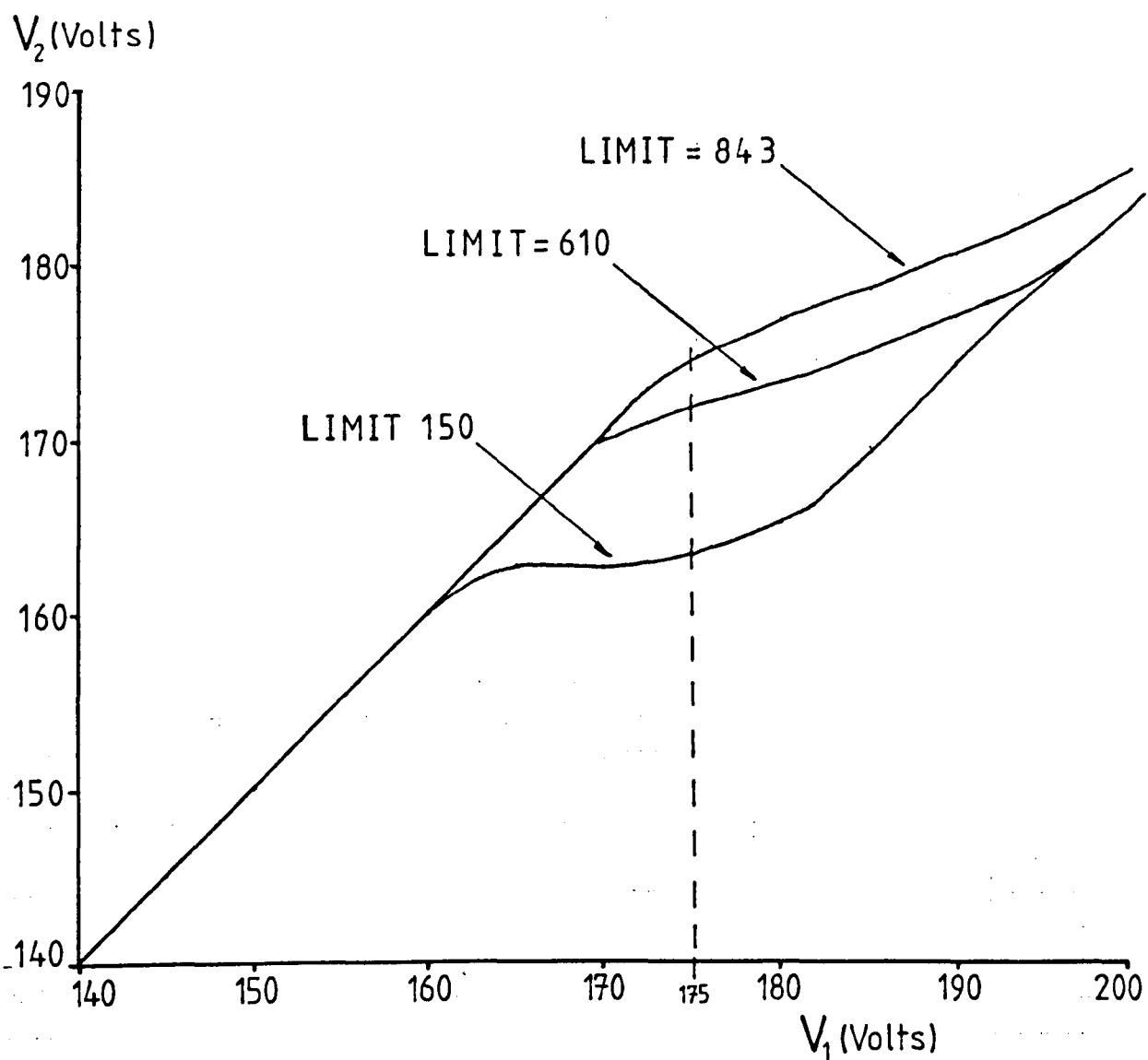


Fig. 4.26 : Theoretical 'open circuit' TCR voltage control characteristics for varying LIMIT

Having established that LIMIT1 is most likely to give the best TCR performance, we may investigate the effect of varying the value of the reference sinusoid $v_R(\omega t) = R \sin \omega t$, whilst keeping LIMIT constant at LIMIT1.

Figure 4.27 shows how the calculated level of the flat, controlled region, of V_{2RMS} is proportional to the magnitude of the reference sinusoid, typically within one percent of $R/\sqrt{2}$ Volts, and that voltage fluctuations up to the operating level of 175 Volts are best controlled with a value of $R = 226.9$ Volts.

Figure 4.28 shows how the calculated characteristics are changed by higher ratings of shunt TCR compensators, using values of $K = 0.915$, $K = 0.861$, $K = 0.731$, representing TCR three-phase ratings of $L_C = 1.01, 0.57$ and 0.25 Henries respectively. The flat control region is extended for increased TCR rating.

(ii) Shunt Load TCR Compensation

With a variable load shunt-connected with the TCR compensator (Figure 4.25), the value of v_2 becomes:

While the TCR is not conducting: $v_2 = K_1 v_1$

$$\text{where: } K_1 = \frac{L_L}{L_L + L_S}$$

While the TCR is conducting: $v_2 = K_2 v_1$

$$\text{where: } K_2 = \frac{L_{CY}}{L_{CY} + L_S + \frac{L_S L_{CY}}{L_L}}$$

as illustrated in Figure 4.29.

The equations for firing angle α and V_{2RMS} are now:

$$V_{2RMS} = \sqrt{\frac{(K_2 V_1)^2}{\pi} \left[\pi - \alpha + \frac{\sin 2\alpha}{2} \right] + \frac{(K_1 V_1)^2}{2\pi} \left[2\alpha - \pi - \sin 2\alpha \right]}$$

.....Equation III

$$\alpha = \cos^{-1} \left[\frac{\omega E + R - K_2 V_1}{R - V_1 (2K_1 - K_2)} \right]$$

.....Equation IV

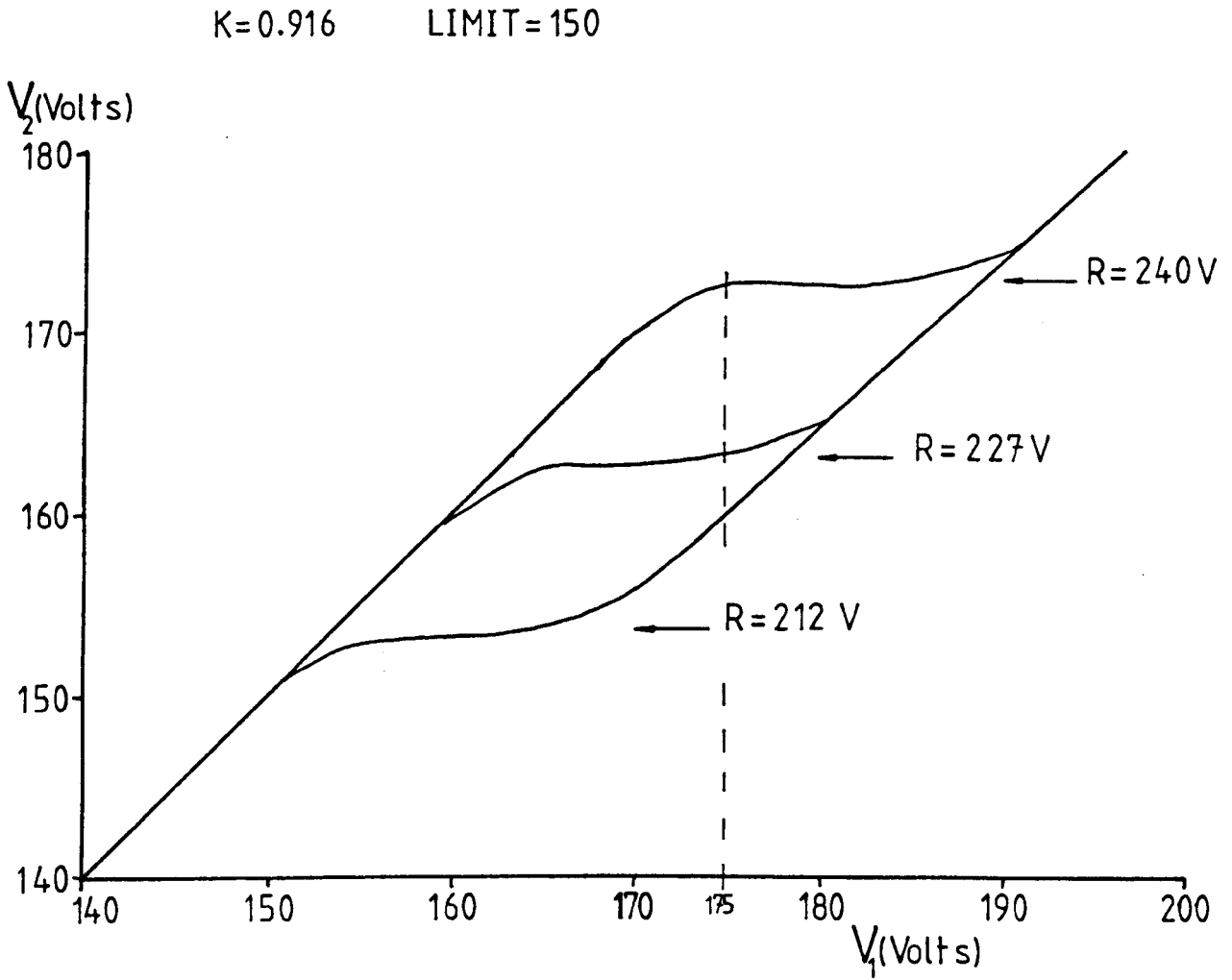


Fig. 4.27 : Theoretical 'open circuit' TCR voltage control characteristic for varying V_{ref}

LIMIT = 150 R = 227 V

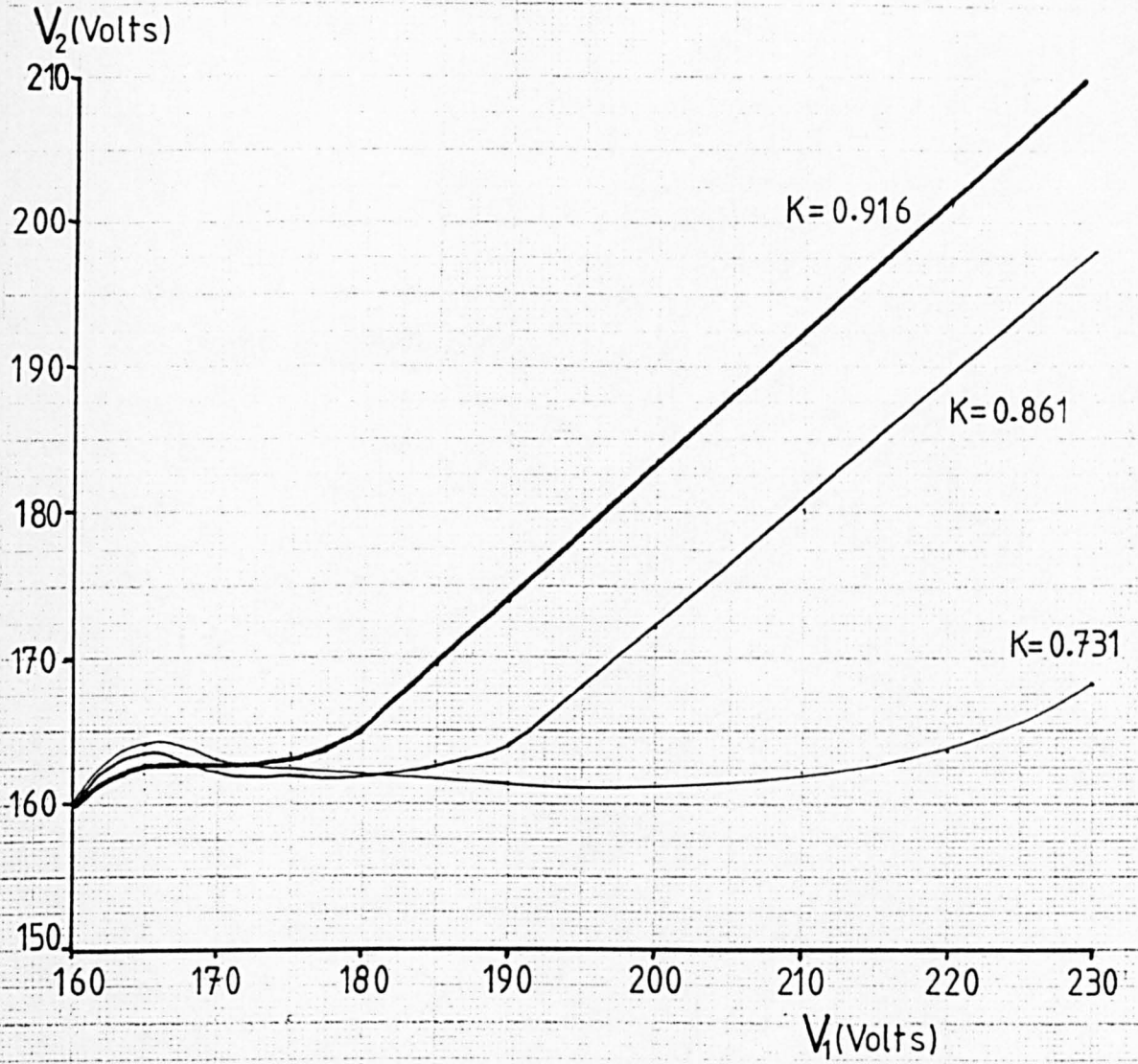


Fig. 4.28 : Theoretical 'open circuit' TCR voltage control characteristics for varying TCR rating

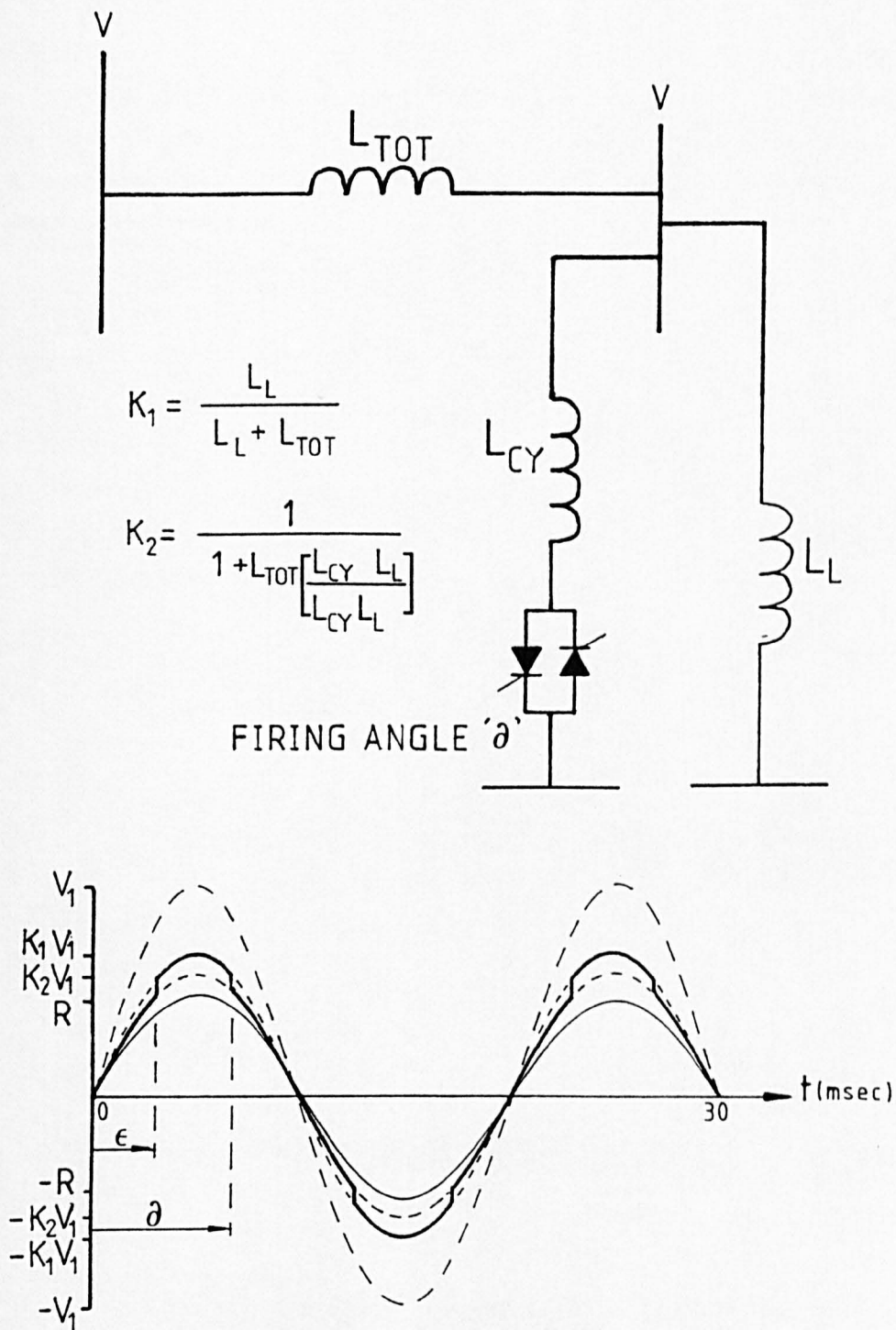


Fig. 4.29 : Theoretical voltage depression for shunt load TCR compensation

v_1 may now remain fixed at 175V RMS, and v_2 will vary as a function of the load current, i_L . Varying i_{LRMS} over the range 0 to 2.5 Amps will cause uncompensated linear voltage depression from 0 to -14p.c.

Figure 4.30 shows the calculated effect of varying LIMIT with fixed reference sinusoid $v_R = R\sin\omega t$. It can again be seen that the compensation span calculated for LIMIT1 is flatter than that for higher integration limits.

The calculated effects of varying V_{REF} for fixed LIMIT = LIMIT1 are shown in Figure 4.31, and the curves for fixed LIMIT and V_{REF} are shown in Figure 4.32 for three values of TCR compensator branch inductance.

These theoretical results suggest the optimum values for control algorithm parameters

- (a) Set the integration limit to be as low as possible for a given TCR compensator rating.

then (b) Adjust the peak reference sinusoid value, R , to be such that firing angle control is obtained over the full range from $90^\circ \leq \alpha \leq 180^\circ$ as near as possible to the operating voltage.

The complementary results from laboratory experiments are presented in Chapter V.

R = 227 V K = 0.916

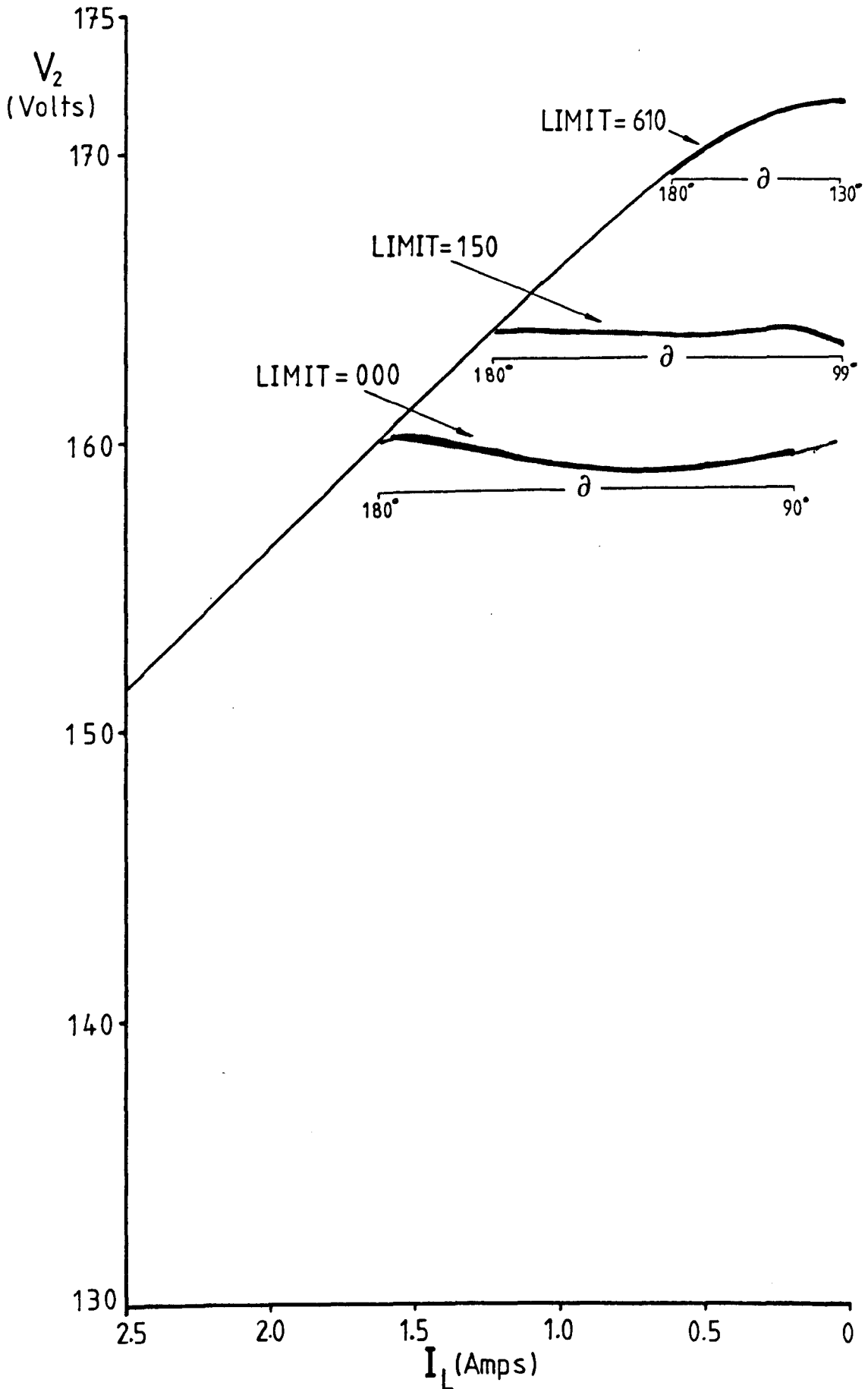


Fig. 4.30 : Theoretical shunt load compensation TCR voltage control characteristics for varying LIMIT

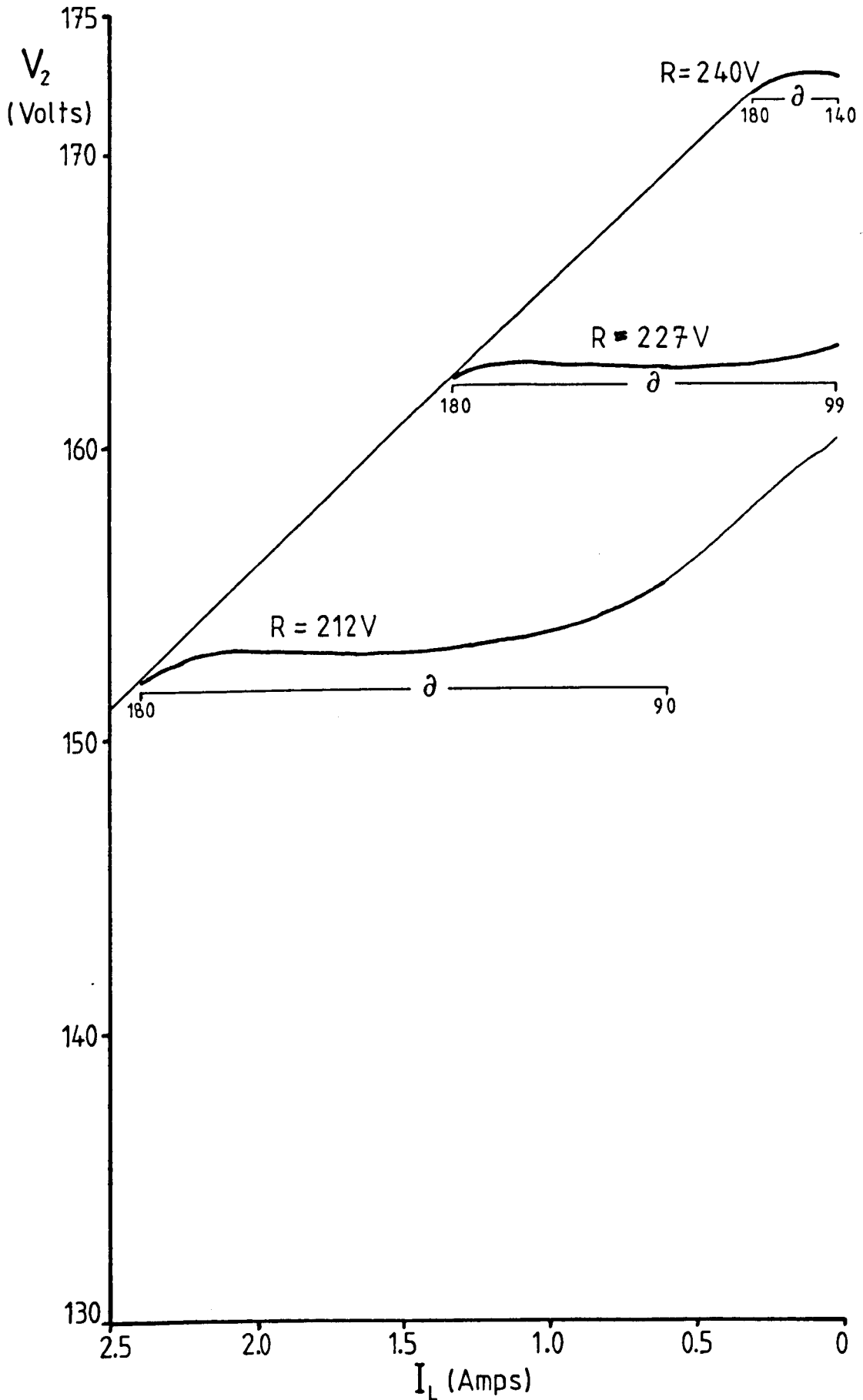
$K = 0.916$ $LIMIT = 150$


Fig. 4.31 : Theoretical shunt load compensation TCR voltage control characteristics for varying V_{ref}

LIMIT = 150 R = 227V

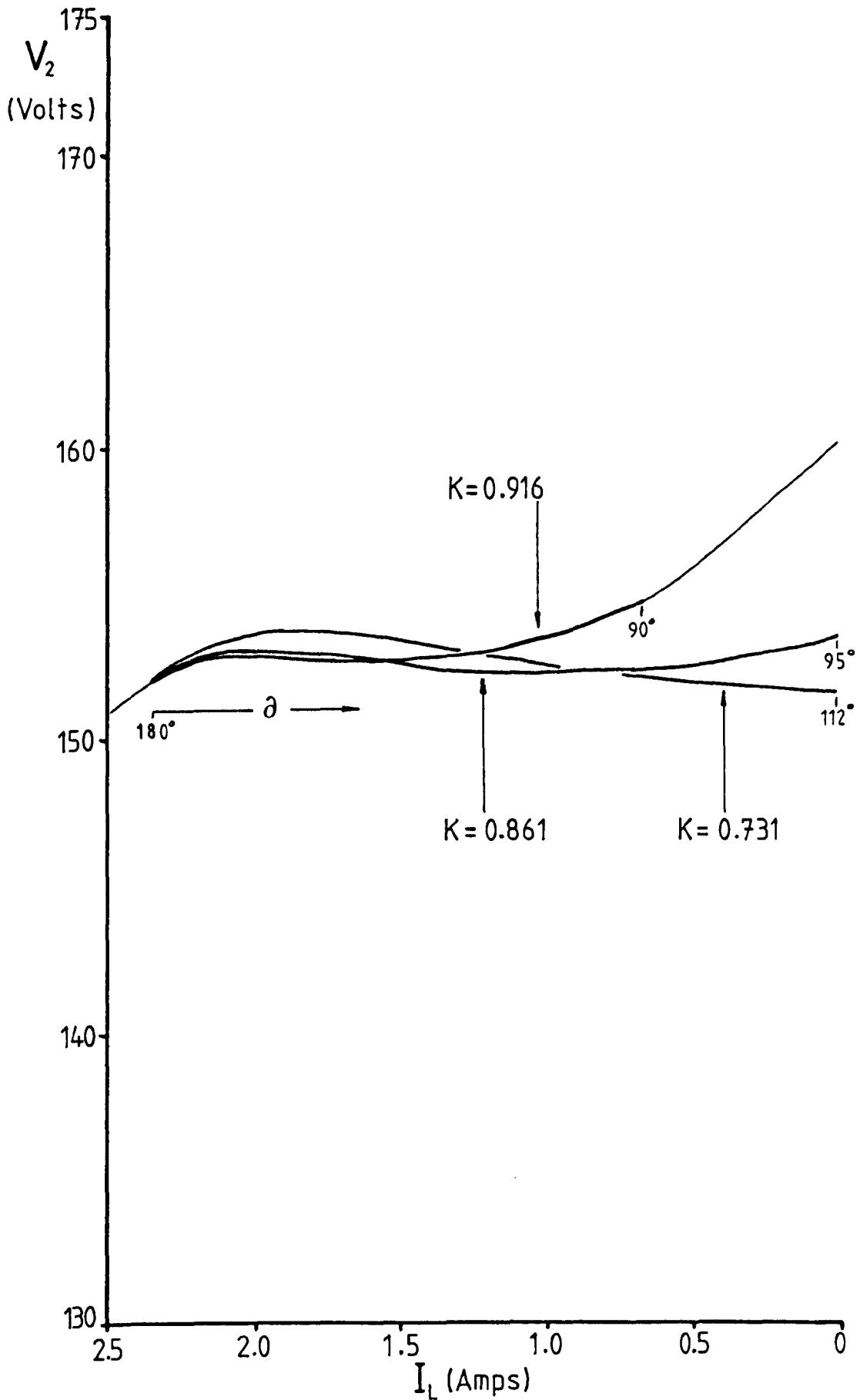


Fig. 4.32 : Theoretical shunt load compensation TCR voltage control characteristics for varying TCR rating

4.4 USE OF THE TCR UNDER NON-SINUSOIDAL CONDITIONS

When the principles behind the control and operation of the laboratory TCR compensator were understood, it was connected to the arc furnace model (Part 2.3) as shown in Figure 4.33:

With the arc furnace model's feedback gain set to zero, no 'furnace' current was drawn from the laboratory supply, and the TCR compensator currents caused all of the observed line voltage distortion (Section 4.3.3). Values of the integration sum LIMIT1 at which firing occurred, was carefully set to give a firing angle of $\alpha_1 \approx 100^\circ$. The gain in the arc furnace model feedback circuit was then increased to its normal operating level. Peaks in furnace current caused α to increase proportionally, up to the maximum of 180° .

The values of the integration sum LIMIT used in the model TCR compensator control system are tabulated in Chapter V, with a range of results showing the compensator performance as a function of the control parameters.

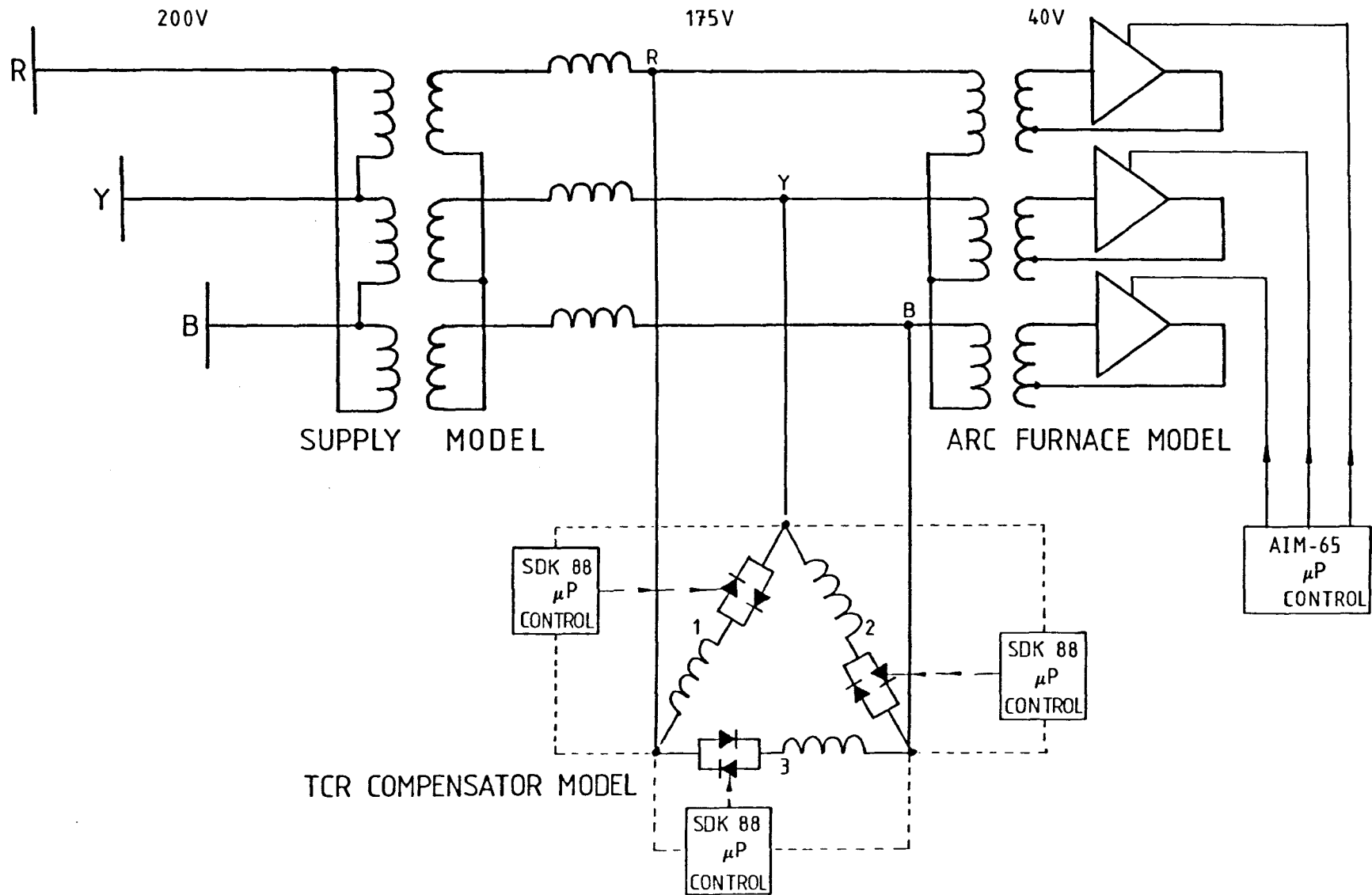


Fig. 4.30 : Connection of the 6-pulse TCR compensator to the arc furnace model

CHAPTER FIVE
SIX PULSE TCR RESULTS

5.1 STEADY STATE TCR COMPENSATOR PERFORMANCE

5.1.1 Open Circuit Voltage Control

5.1.2 Shunt Load Compensation

5.2 ANALYSIS OF VOLTAGE DISTORTION

5.2.1 Spectral Analysis

5.2.2 Data Logging

5.3 TCR PERFORMANCE WITH THE ARC FURNACE MODEL

5.3.1 Frequency Domain Study of Compensator Action

5.3.2 Time Domain Study of Compensator Action

5.4 ESI FLICKERMETER STUDIES

5.4.1 The Use of the Digital Flickermeter

5.4.2 Arc Furnace Model without TCR Compensator

5.4.3 Arc Furnace Model with TCR Compensator

CHAPTER FIVE

SIX PULSE TCR RESULTS

A 'steady state' performance analysis was carried out in Section 4.3.3 to show the theoretical voltage regulation characteristics of the TCR under sinusoidal conditions. The corresponding laboratory measurements were in agreement with theory, and the TCR was then used with the laboratory arc furnace model.

The method of spectral analysis was used to judge the performance of the laboratory models and the TCR control. A reduction in the power spectral density components of modulating frequencies up to 30Hz was achieved.

The TCR rating was then increased, and a further set of results taken for comparison with those from the original TCR rating.

Finally, measurements were taken with the CEGB/Electricity Council 'flickermeter'[14,16] to allow the disturbance levels on the laboratory model to be related to those elsewhere.

5.1 STEADY STATE TCR COMPENSATOR PERFORMANCE

The two circuit configurations studied computationally in Section 4.3.3 are shown in Figures 4.22 and 4.23. Both studies were repeated using laboratory equipment and the TCR.

5.1.1 Open Circuit Voltage Characteristics

Figure 5.1 shows the voltage characteristics for the TCR compensator only connected to the supply having an equivalent source inductance of $L_s = 30.4$ millihenries. V_1 and V_2 are the voltages at the source and at the compensator respectively.

V_1 was varied using a three-phase variable transformer with a maximum output line voltage of 240V for 200V input. V_2 is not equal to V_1 before TCR conduction because the source impedance is that of the 200/175V Y- Δ transformer. Any measured gradients should therefore be multiplied by the factor $200/175 = 1.143$ to take account of this.

The corrected gradient of the linear region before TCR conduction is 1.006, after full conduction it is 0.869. The theoretical values are 1.000 and 0.916 respectively.

The effect of varying the integration limit can be seen clearly - a flatter but shorter control region results from the lower integration limits. The hexadecimal and decimal LIMIT values are given in Table 5.1.

The tests were repeated for a higher TCR rating of 512VA corresponding to a value of $C/F = 1.13$. This uses $L_c = 0.56$ Henries giving $K = 0.860$.

Figure 5.2 gives the open circuit voltage characteristics for the higher rating TCR for three values of LIMIT giving steady state firing angles of $\alpha = 110^\circ$, 135° and 170° respectively. The corrected gradient of the linear region before TCR conduction is 0.976, with 0.853 after full conduction.

$$K = 0.916 \quad R = 227V$$

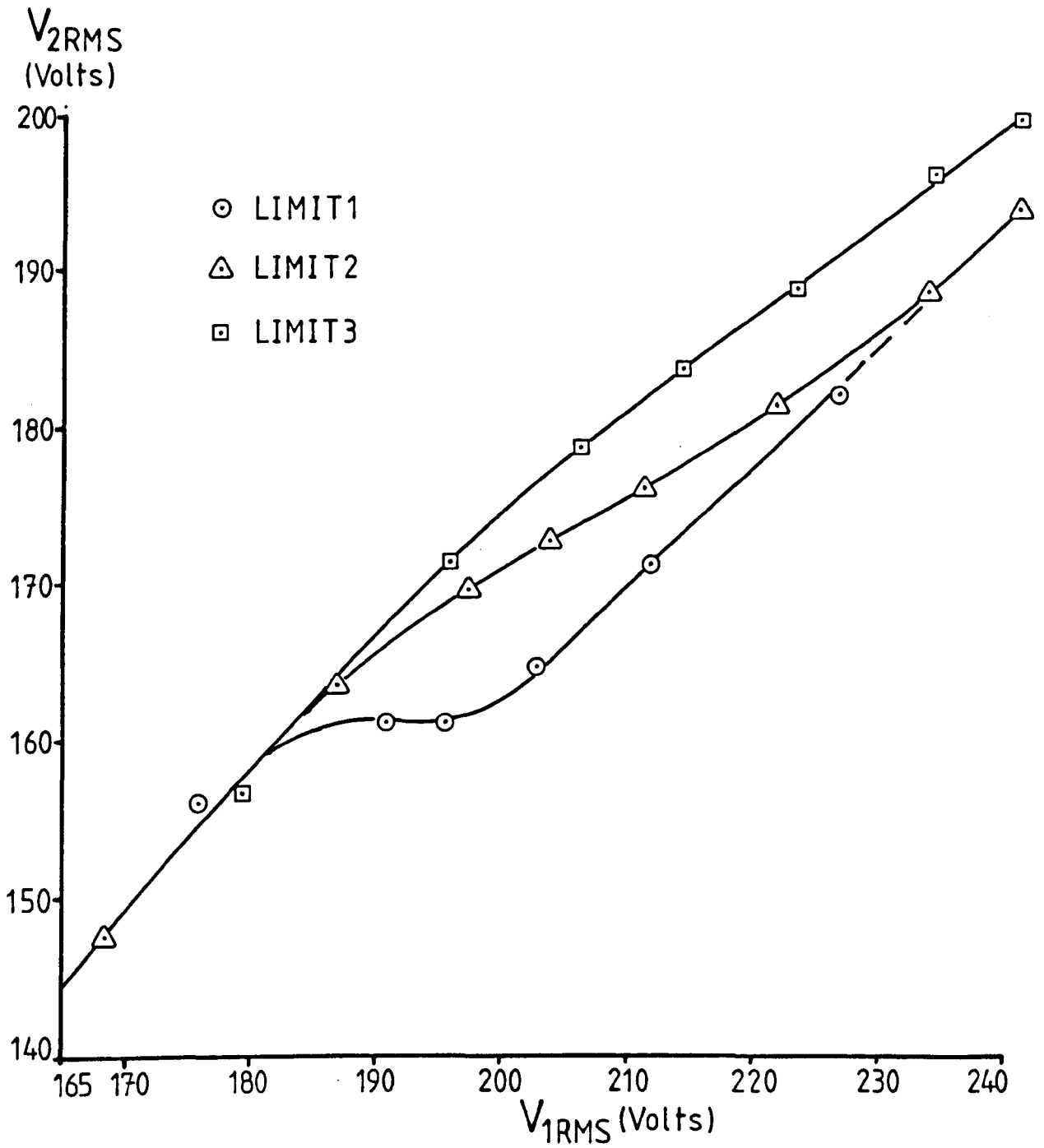


Fig. 5.1 : Measured open circuit TCR voltage characteristic for $K=0.916$ and varying LIMIT

		Compensator Branch	POSLIM (Hexadecimal)	NEGLIM
LIMIT 1	$\alpha \approx 100^\circ$	Branch 1	0018	0020
		Branch 2	0040	0040
		Branch 3	0040	0040
LIMIT 2	$\alpha \approx 135^\circ$	Branch 1	01A0	0250
		Branch 2	0220	0230
		Branch 3	01F0	0280
LIMIT 3	$\alpha \approx 170^\circ$	Branch 1	03D0	0570
		Branch 2	0440	04C0
		Branch 3	0380	0480

Table 5.1 Integration limits set for 6-pulse TCR compensator performance studies

$K = 0.860$ $R = 227V$

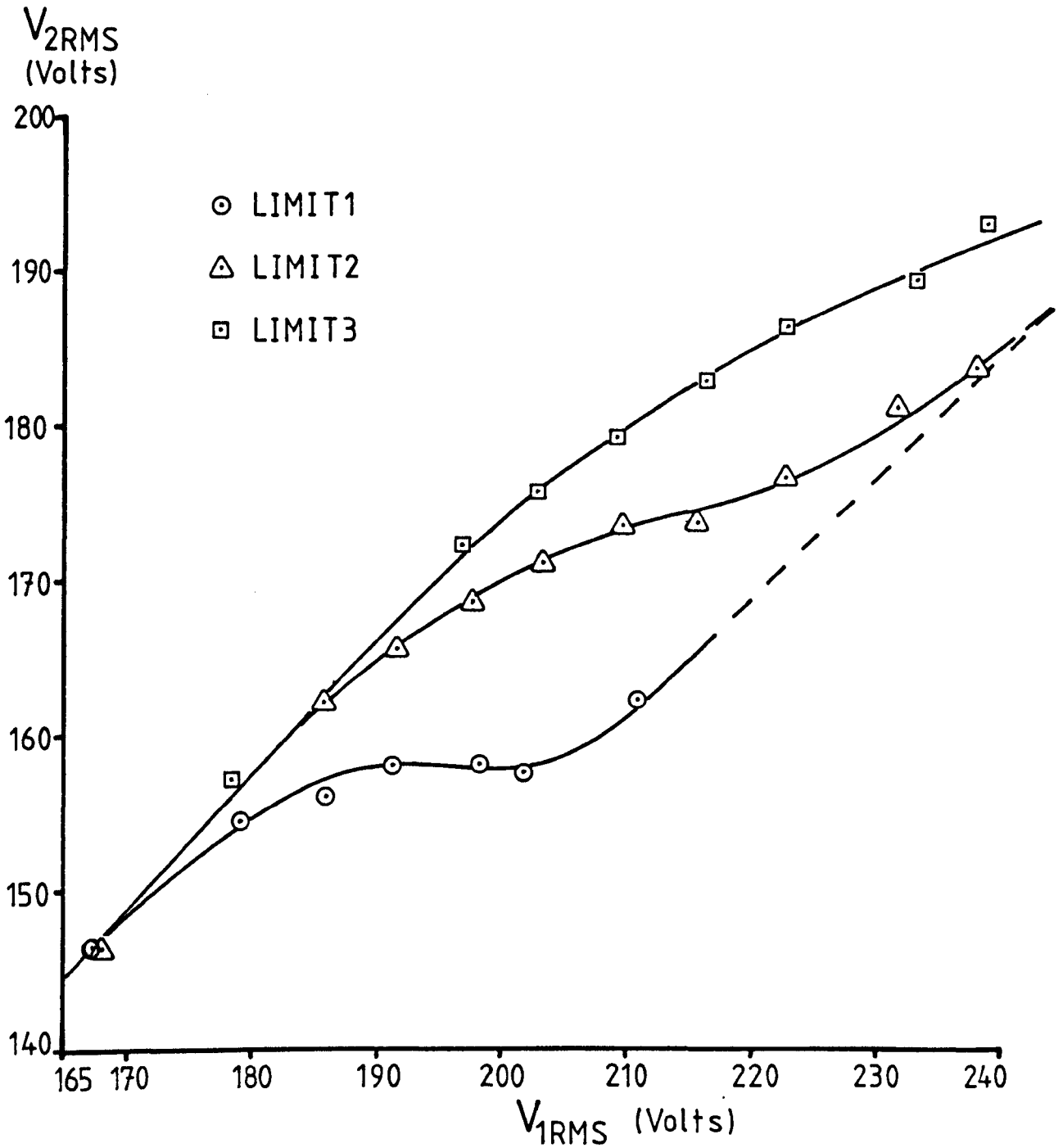


Fig. 5.2 : Measured open circuit TCR voltage characteristics for $K = 0.860$ and varying LIMIT

The corresponding theoretical values are 1.000 and 0.860, and the results show that increasing the TCR rating affects the control region of the curves such that:

- (a) Where the gradient is not zero it is decreased.
- (b) Where the gradient is zero, the span of the flat region is increased.

5.1.2 Shunt Load Compensation

A variable three-phase inductance was connected in parallel with the TCR compensator. Varying this load current between zero and approximately 1.4 Amps would act to vary V_2 linearly in the range

$$161 \leq V_2 \leq 175 \text{ Volts}$$

if there were no TCR compensator acting. The results of connecting the compensator are shown in Figure 5.3. Characteristics are again plotted for each of three values of LIMIT. At $I_2 = 0$, the TCR firing angle α is at a minimum which is set by the value of LIMIT.

i.e. For $I_2 = 0$ and LIMIT = LIMIT1, $\alpha = \alpha_1 \approx 100^\circ$
 For $I_2 = 0$ and LIMIT = LIMIT2, $\alpha = \alpha_2 \approx 135^\circ$
 For $I_2 = 0$ and LIMIT = LIMIT3, $\alpha = \alpha_3 \approx 170^\circ$

As I_2 is increased, V_2 is depressed and α increases, thus I_{COMP} inversely balances I_2 .

Figure 5.3 shows once again that the smaller value of LIMIT is of maximum benefit for voltage control. The shape of the characteristic in the control region is approximately $3.5\text{V}/-1.0\text{A} = -3.5\text{V/A}$, although the characteristic is far from linear.

$K=0.916$ $R=227V$

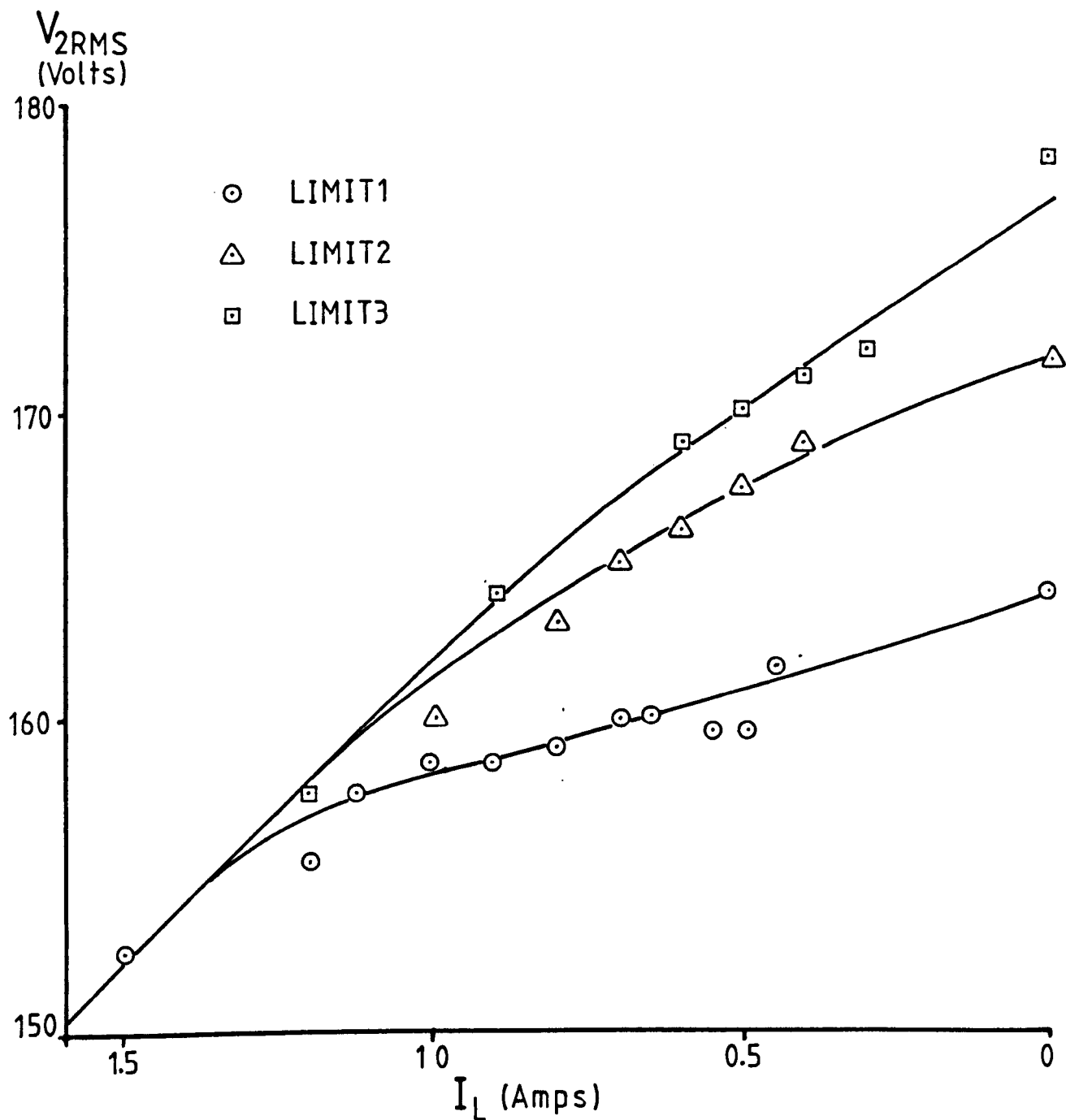


Fig. 5.3 : Measured shunt compensation TCR characteristics for $K=0.916$ and varying LIMIT

The tests were repeated with the higher rating compensator used in the previous section. The results are given in Figure 5.4, and the main effect of increasing the TCR rating is to decrease the slope of each characteristic in the control region.

The curve for $LIMIT = LIMIT1$ has an approximate gradient of $2.8V/-1.3A = -2.2V/A$. The characteristic within the control region is again far from linear. It was observed that even after careful 'tuning' of each compensator branch, firing angles would vary between each branch by up to ± 10 degrees. This imbalance between the three TCR control systems may contribute to the non-linearities observed in the ideally 'flat' controlled region of the characteristics.

$K=0.860$ $R=227V$

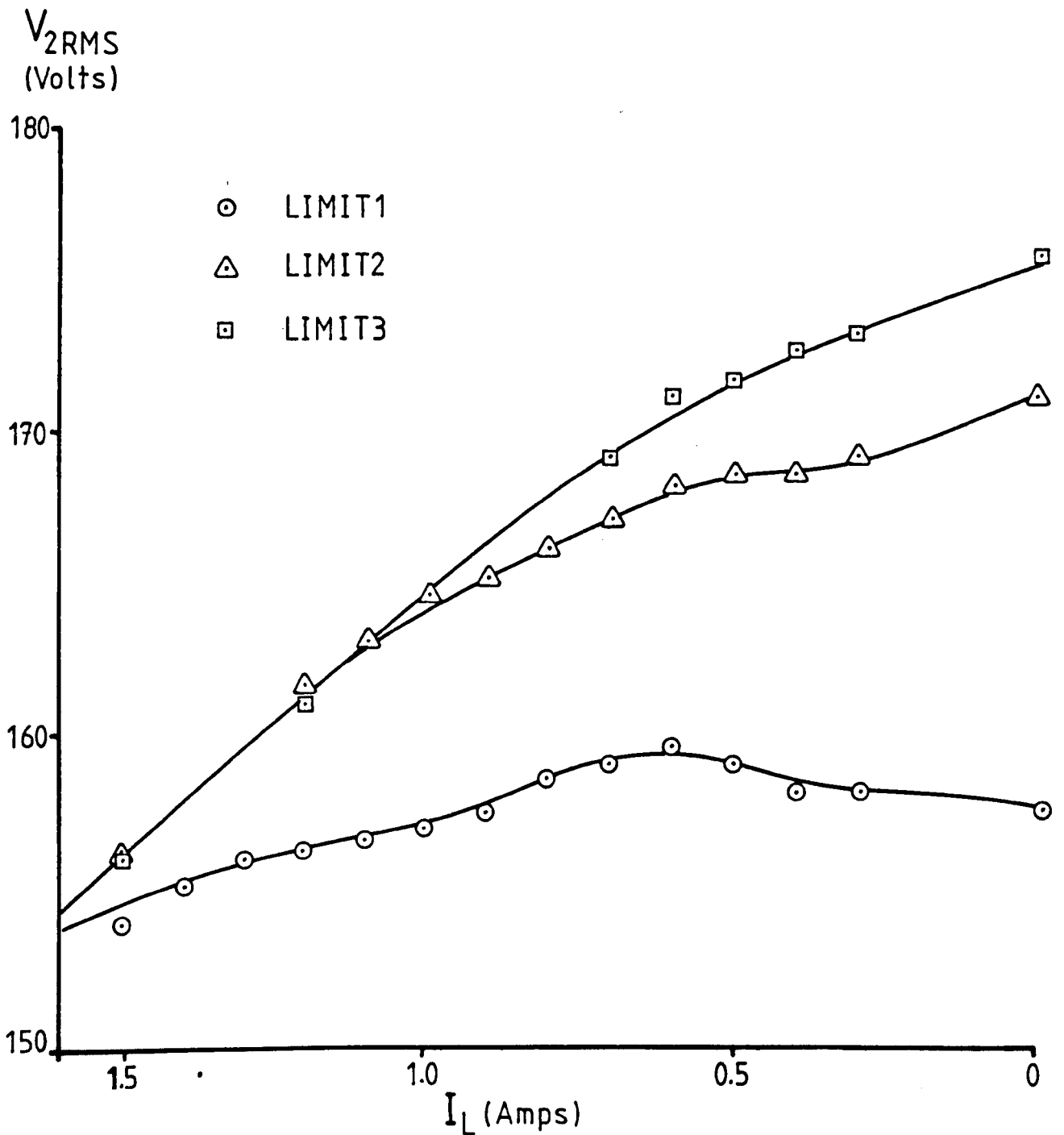


Fig. 5.4 : Measured shunt compensation characteristics for $K=0.860$ and varying LIMIT

5.2 ANALYSIS OF VOLTAGE DISTORTION

Chapter III used the concept of a 'flicker voltage', V_f , when discussing the distortion of the 50Hz supply voltage waveform. Section 3.1.2 in particular showed how the annoyance effect of V_f was frequency dependent.

The laboratory arc furnace model has been shown to reproduce successfully the wide range of frequency components impressed upon the 50Hz supply waveform at the levels encountered at a real installation (2.4.3).

The laboratory TCR compensator aims to reduce the annoyance effect of the arc furnace model load currents by shunt compensation, thus reducing the magnitude of components of V_f . It is then essential that the results of TCR compensator operation are clear, and that a reliable method for evaluating annoyance levels can be used to demonstrate some improvement factor.

These final points are now discussed in turn.

5.2.1 The Use of Spectral Analysis

The technique of spectral analysis enables the power components of a wide range of frequencies to be evaluated simultaneously. This is particularly useful in the study of the 'flicker voltage', V_f , where the magnitudes of a range of frequency components of the real time signal are of interest.

Methods of obtaining a power spectrum include direct estimation, recursive and non-recursive digital filtering^[112], mean-lagged products^[113], complex demodulation and the discrete Fourier transform. Direct estimation involves the use of special purpose analogue devices such as harmonic analysers, wave analysers and filter banks. Early generations of computers made possible the use of

digital filtering techniques and complex demodulation algorithms. The larger workspace capacity of later computers made the discrete Fourier transform (DFT) practicable, enabling the Fourier series coefficients to be calculated at discrete frequencies^[114]. The fast Fourier transform (FFT) is simply an efficient method of computing the DFT of time series data^[115,116].

A suite of FORTRAN programs, for the calculation of a Fourier power spectrum, was made available to the author by the Speech Research Group of Liverpool University. Although primarily intended for use in the 20-20,000Hz frequency band, the method of operation allowed them to be modified for use around 50Hz. Appendix G describes the method and gives program listings where necessary. The necessary workspace was only available on Liverpool University's mainframe IBM 4341 computer; data acquisition and transfer was therefore necessary before computational analysis could be carried out (see 5.2.2).

Bogert^[117] identifies two important requirements for the use of computational techniques for power spectrum analysis as a laboratory tool. The first is a set of subroutines to enable parameters to be varied at will. The second is adequate display of the output.

Although the mainframe computer more than satisfied both of these requirements, it was found that a commercial power spectrum analyser^[118] offered the advantage of an immediate and variable display from an automatic data acquisition process. The digital technology employed in the instrument gave 167 blocks of data in the frequency domain for storage and display. The bandwidth therefore varied as the frequency span was altered. The bandwidth here is the frequency band that contributes to a single point of the discrete power spectrum.

Increasing the bandwidth contributing to each point requires a correspondingly larger block of time series data for analysis. With a fixed sampling frequency the time span for which each power spectrum was calculated would vary between 10 milliseconds and 250 seconds.

The data repetition rate for the arc furnace model was 1.78 seconds, giving a high probability that individual blocks of time series data would differ, with corresponding differences in the power spectrum.

Welch^[119] describes an averaging process that may be used for successive power spectra. The Hewlett Packard spectrum analyser allowed such averages to be performed - the displayed power spectrum then being the average of 2^N samples. Using the RMS value of eight successive spectral analyses ensured that the variations within the 1.78 seconds of repeated data would not cause confusing discrepancies in the presentation of the power spectrum.

The Hewlett Packard spectrum analyser included the facility for the output of stored digital data to an X-Y plotter, and the results presented in Section 5.3 were produced by this method.

5.2.2 Data Logging

For analysis of data from the laboratory, it was necessary to transfer recordings from the laboratory equipment to the University's mainframe computer. Here large amounts of data could be stored, retrieved and analysed at will. The spectral analysis package described in Section 5.2.1 was set to operate on 2048 ($=2^{11}$) time series data points from the CEGB recordings. To allow a common analysis routine to be used for computational and laboratory data the time between samples for all time series data for input was set at 800 microseconds - corresponding to the sampling interval used for the CEGB measurements.

This sampling rate gives a Nyquist limit frequency of 625Hz, which more than covers the flicker frequency band. Harmonic frequencies up to the eleventh harmonic of 50Hz will also be recorded accurately. A further SDK-88 microprocessor system was used to undertake all data logging from the laboratory equipment.

Such a system was used because it could easily be incorporated into the system established for programming the TCR control SDK-88s from the Departmental Microprocessor Laboratory's development system. The 8088 processor possessed a 16-bit data highway, allowing high accuracy data handling, and the 20-bit address bus could give access to up to 1M 16-bit words.

Twelve-bit analogue to digital converters (ADCs) were used, giving a quantisation noise threshold of -72dB in the time domain. This would enable high-accuracy studies of recorded data to be carried out on the mainframe computer. The program listings for the sampling program is given in Appendix H.

The sampling process was initiated by a 10 microsecond pulse output from the AIM-65 system (Appendix D) in synchronism with the first point in the 1.78 second data cycle. The sampling SDK-88 detected this pulse on 8-bit ADC addressed at F800, and then executed a 3-channel, 800 microsecond sampling loop 2225 times.

The stored data could then be uploaded from the SDK-88 memory to a data file on the Tektronix 8650 MUSDU, for transfer by IBM 3470 format floppy disc to the IBM mainframe computer.

The 12-bit ADCs proved to be more susceptible to temperature effects than were the 8-bit ADCs used for the TCR control scheme. Re-calibrating the sampling circuitry proved to be time consuming and tedious. The problem was solved by preceeding the sampling program by a short block which interactively sampled each ADC three times for each of three externally applied voltages: Positive Full Scale Deflection (FSD), ZERO and Negative FSD. Thus each block of data would always be accompanied by digital samples of known reference voltages - enabling absolute sampled values to be calculated computationally.

The 12-bit ADC and sampling circuitry are shown in Appendix H after the sampling program.

5.3 TCR PERFORMANCE WITH THE ARC FURNACE MODEL

The TCR compensator was connected in parallel with the laboratory arc furnace model - at the point shown as 'B' in Figure 3.8. Disturbances of the line voltage waveform at the point of coupling produced varying firing angles in each branch of the TCR. The effect of the TCR compensator operation may be studied both in the frequency domain and in the time domain.

The values of integration limit, LIMIT, set for different sets of results were given in Table 5.1.

5.3.1 Frequency Domain Study of Compensator Action

Section 5.2 showed the advantages of using spectral analysis techniques for the examination of distorted waveforms where a range of frequency components are of interest.

Figures 2.26, 2.27 and 2.28 gave the power spectral density of the supply voltage with and without the arc furnace model operating. The power levels of frequencies modulating the 50Hz 'carrier' are obtained by the summation of the components in the upper and lower sidebands. The arithmetic sum of the power in all modulating frequencies is then the power component of the 'flicker voltage' V_f . The frequency components of V_f that are of primary interest are those in the range 0-30Hz. These then occur in the absolute frequency range $50\text{Hz} \pm 30\text{Hz}$, i.e. $20\text{Hz} \leq f \leq 80\text{Hz}$. For some flicker improvement factor to be obtained, it was necessary that the TCR compensator reduce the level of disturbances within this particular frequency band.

The results show the power spectra of the distorted voltage waveforms in dB. A change in level of 6dB at a particular frequency represents a change in voltage ratios by a factor of two. -6dB is therefore one half of the relative voltage level, and +6dB is double the relative voltage level, at the chosen frequency.

All plots of power spectra showing TCR compensator action are shown with the uncompensated distorted voltage plotted on the same axes. The compensated power spectrum is shown as a fine line, to be compared with the heavier line plotted to show the uncompensated spectrum.

The areas where a reduction in power was achieved by the TCR compensator are shaded so that the regions of attenuation may be more easily compared with any regions of amplification. This form of presentation also highlights the 'cross-over' frequency between amplification and attenuation.

Figure 5.5 gives a comparison of the line voltage power spectral density with and without the operation of the TCR compensator. All results presented in this form give the uncompensated line voltage power spectrum as a heavy line, and the compensated line voltage as the lighter line.

If the plots are studied in isolation from each other, differences between them are not immediately clear. Presenting dual plots on the same axes allows comparisons to be made, and the effects of changing TCR compensator control parameters are now studied.

(i) LIMIT = LIMIT1, R = 226.9, K = 0.916

Figure 5.5 shows the power spectrum of the line voltage $V_R - V_Y$.

A reduction in the power of components in the absolute frequency range 20Hz-90Hz is evident, but the details of such improvement lack clarity.

Figure 5.6 shows only the lower sideband of Figure 5.5. The power in modulation frequencies 0-30Hz (absolute frequencies 50-20Hz) is reduced by the compensator by between 0 and -6dB.

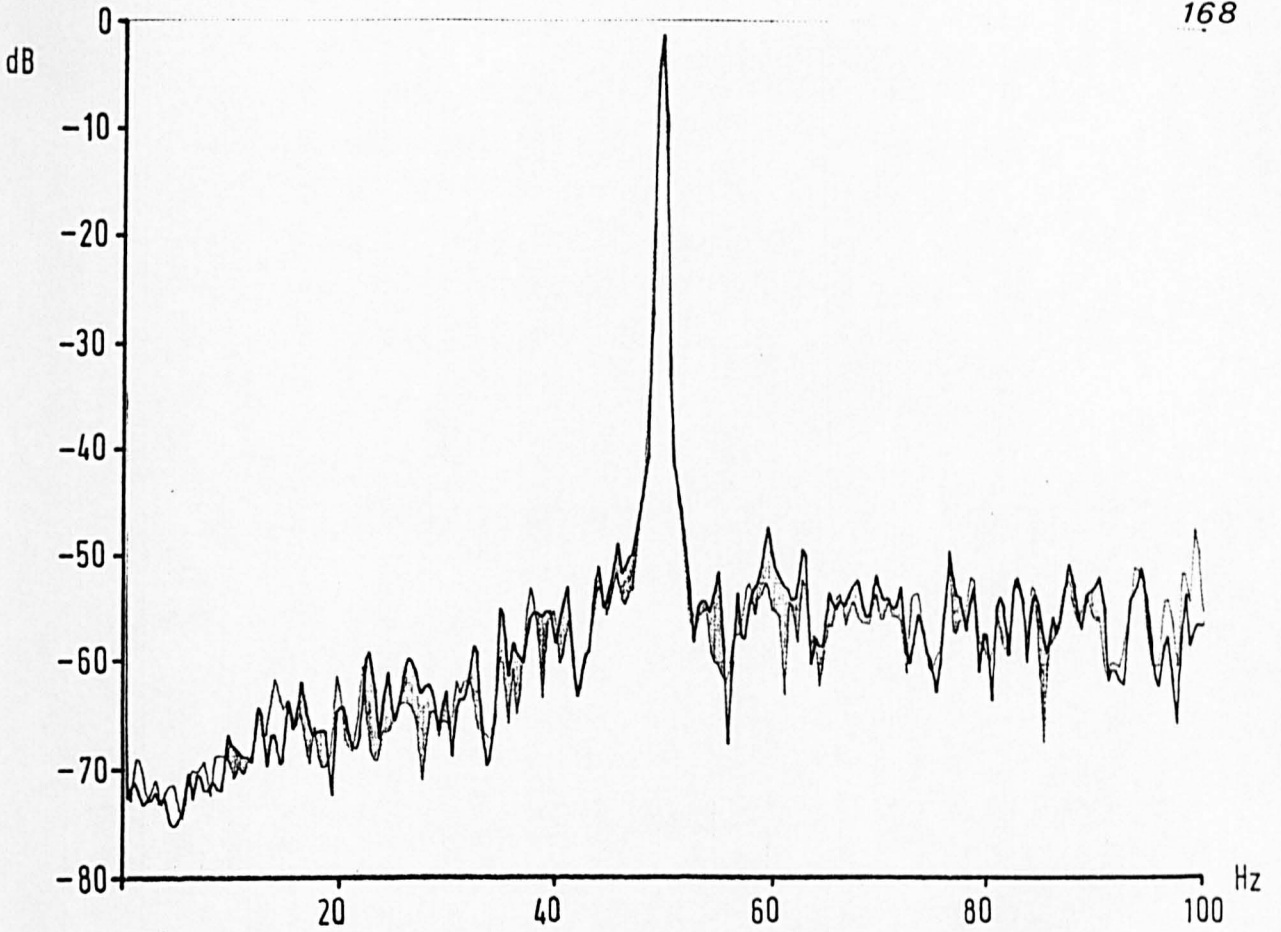


Fig. 5.5 : 0-100Hz power spectrum of Vry for K = 0.916, LIMIT 1

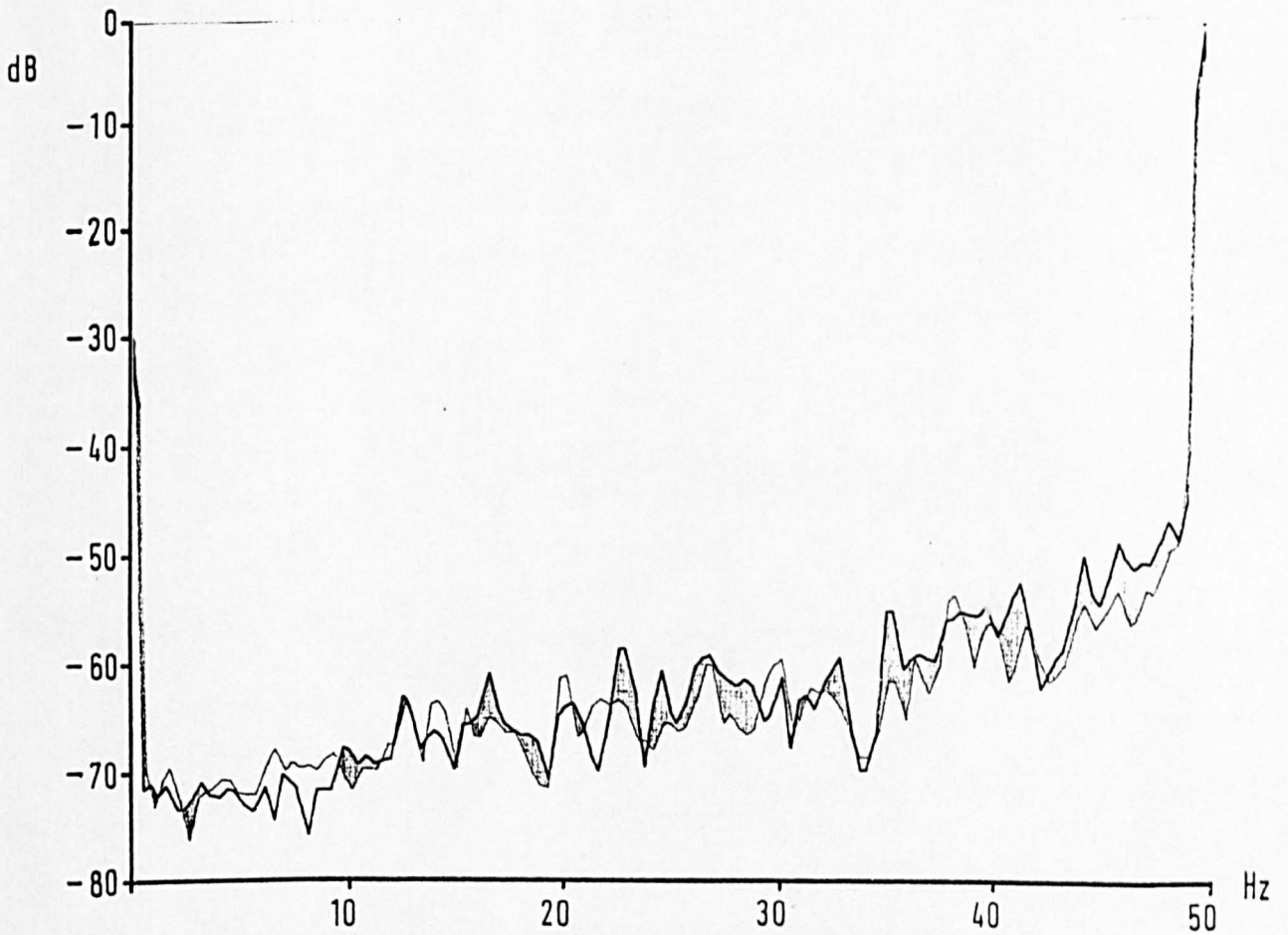


Fig. 5.6 : 0-50Hz power spectrum of Vry for K = 0.916, LIMIT 1

The 'cross-over frequency' where the compensator acts to increase rather than attenuate is at a modulation frequency of approximately 35Hz (15Hz and 85Hz absolute). What can be seen from the upper sideband in Figure 5.5 would suggest a similar if not better performance. The higher frequency effects are shown in Figure 5.7 with the V_{RY} line voltage power spectrum to 500Hz.

The changes in harmonic power amplitudes due to the TCR compensator are:

3rd Harmonic : +4dB
 5th Harmonic : -4dB
 7th Harmonic : +2.5dB

(ii) LIMIT = LIMIT2, R = 226.9 Volts, K = 0.916

The reduction in the power of frequency components in the 0-30Hz modulation band was far less for this value of LIMIT corresponding to a steady state $\alpha \approx 135^\circ$.

Figure 5.8 shows the lower 50Hz modulation sideband in detail - the sharper appearance is due to the use of a 300mHz bandwidth, giving higher resolution in the frequency domain. Any improvement due to the TCR compensator operation is always less than 4dB.

The corresponding power spectrum to 500Hz is shown in Figure 5.9. This shows a marked increase in the power of frequency components in the 200Hz-500Hz band for TCR operation.

The effects on harmonic amplitudes of TCR operation are:

3rd Harmonic : 0dB
 5th Harmonic : +3dB
 7th Harmonic : +3dB

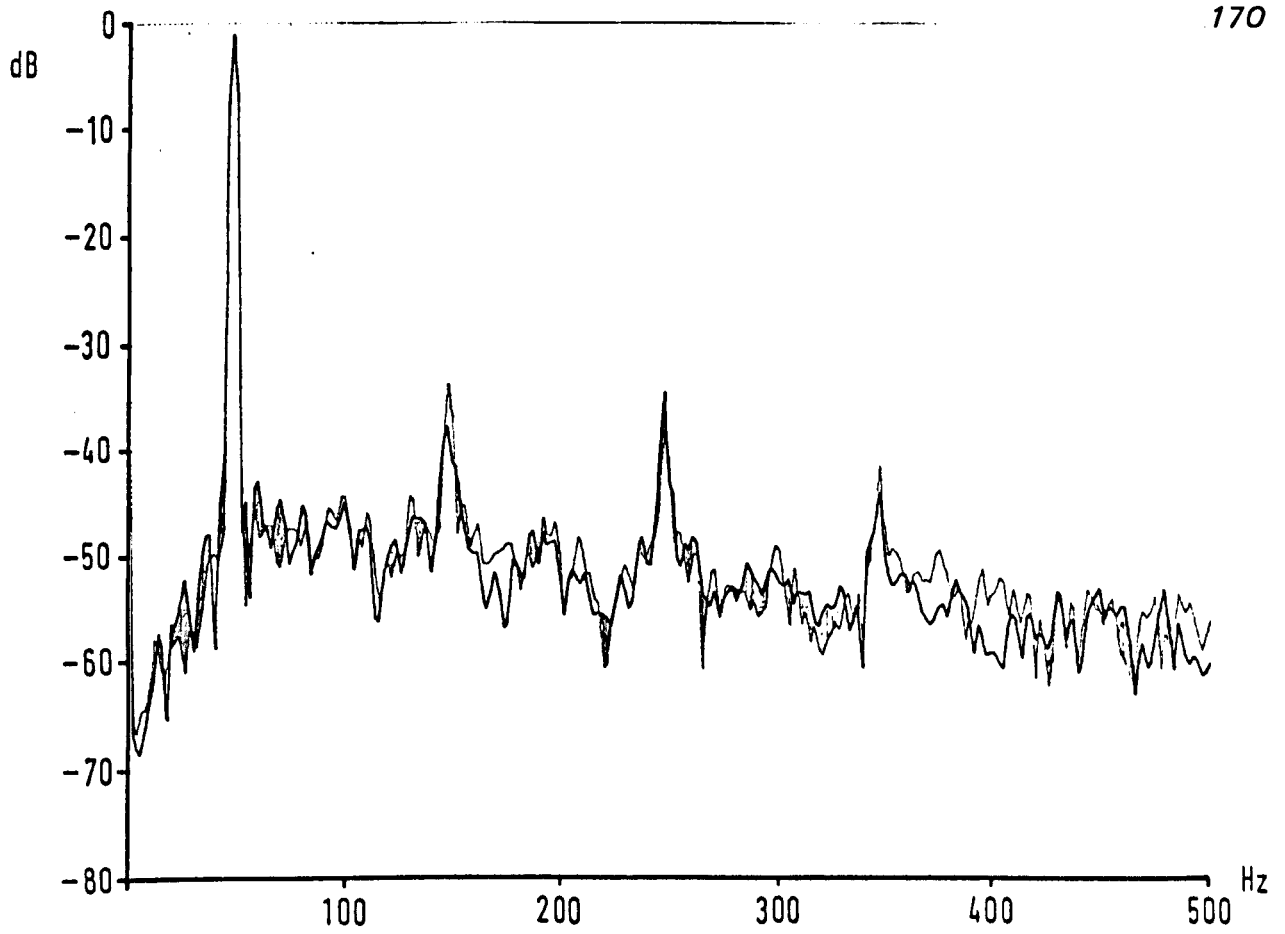


Fig. 5.7 : 0-500Hz power spectrum of Vry for $K = 0.916$, LIMIT 1

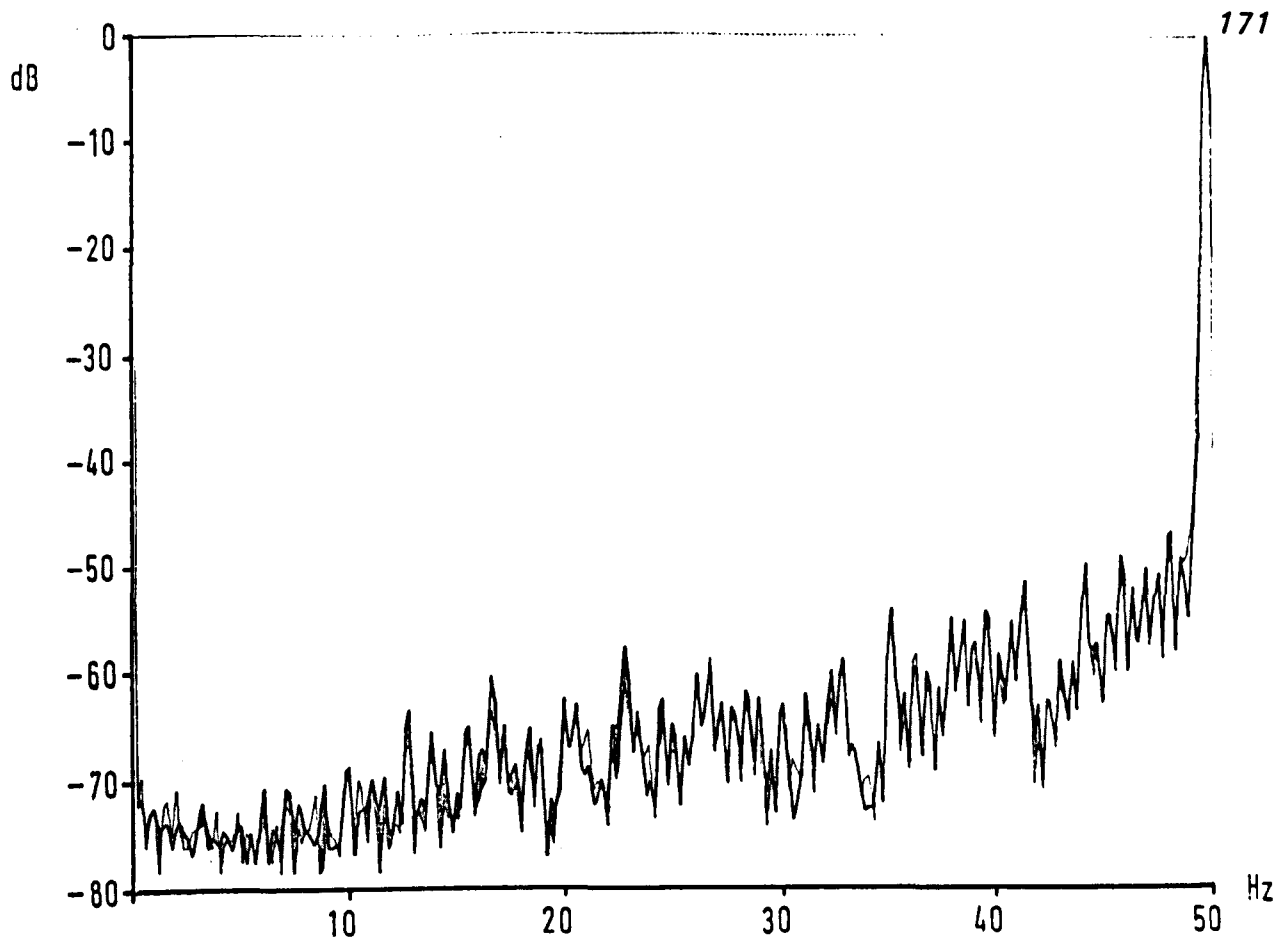


Fig. 5.8 : 0-50 z power spectrum of V_{ry} for $K=0.916$, $LIMIT2$

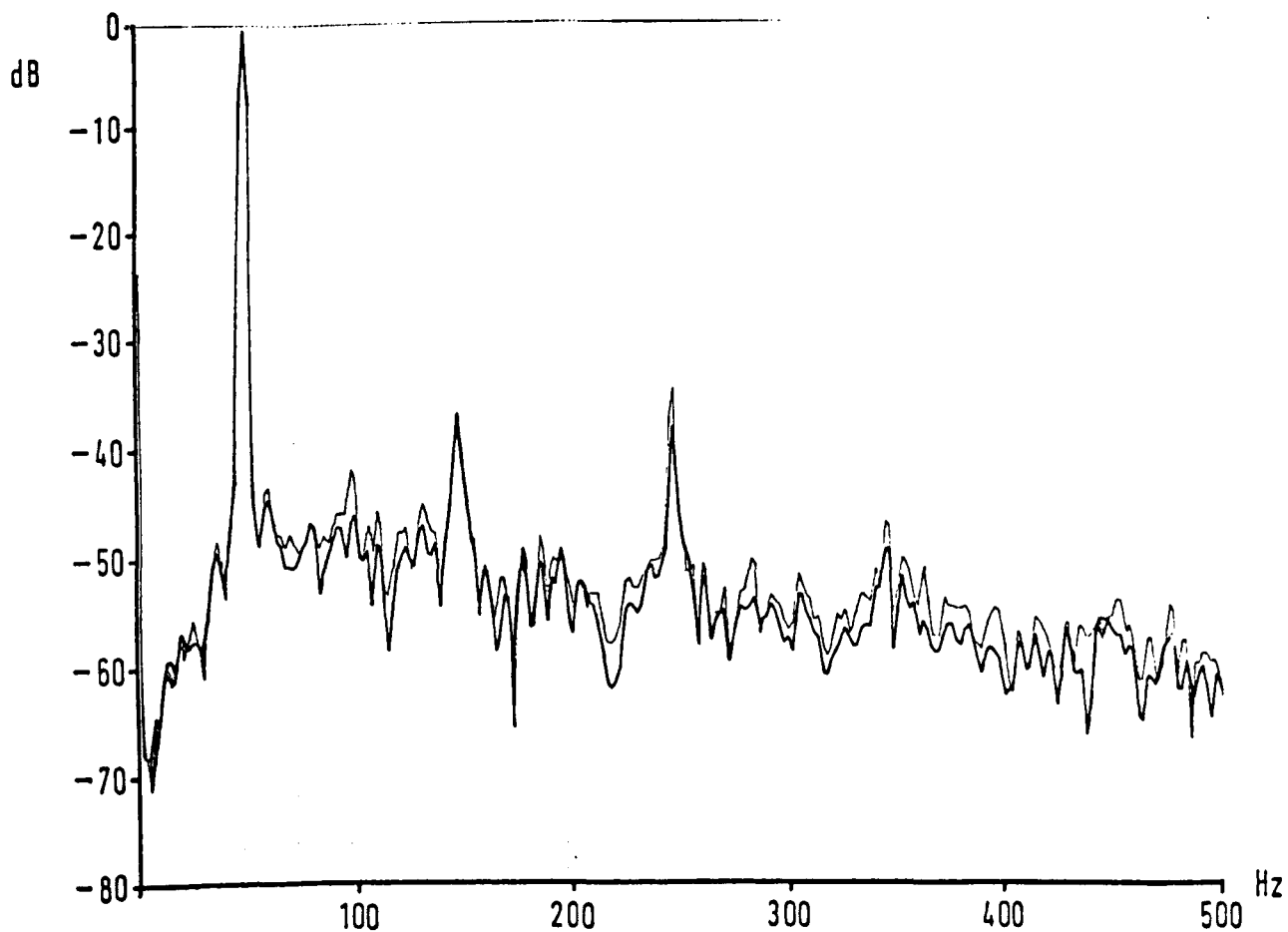


Fig. 5.9 : 0-500Hz power spectrum of V_{ry} for $K=0.916$, $LIMIT2$

(iii) LIMIT = LIMIT3, R = 226.9 Volts, K = 0.916

Steady-state sinusoidal tests (5.1) indicate that this value of LIMIT, giving a steady-state $\alpha \approx 170^\circ$, will offer poor shunt reactive compensation.

This is borne out by the results for operation with the arc furnace model, presented in Figures 5.10 and 5.11.

(iv) LIMIT = LIMIT1, R = 226.9 Volts, K = 0.860

This increased rating of the TCR compensator corresponds to that used for the later 'steady state sinusoidal' tests in Sections 5.1.1 and 5.1.2. The three phase rating is 512 VAR corresponding to a C/F value of 1.11 (see Section 5.1.1).

Figure 5.12 shows the line voltage spectrum to 100Hz. Compensator action is particularly marked in the upper modulation sideband, and the cross-over frequency is approximately 20Hz. Figure 5.13 shows that increasing the compensator rating has increased the amplification of frequencies above 100Hz - there are particularly noticeable peaks in the power spectrum at 100Hz and 200Hz, where the amplification is approximately 10dB.

Figures 5.14 and 5.15 indicate some improvement in the attenuation of modulation frequencies up to approximately 25Hz (i.e. $25 \leq f \leq 75$ Hz absolute), but with greater amplification of modulating frequencies between 40 and 50Hz relative to the 50Hz carrier.

(v) LIMIT = LIMIT2, R = 226.9 Volts, K = 0.860

Increasing the integration limit from LIMIT1 to LIMIT2 (see Table 5.2) can be seen from Figures 5.16 and 5.17 to give a large increase in the amplification of modulation frequencies between 40Hz and 50Hz relative to the 50Hz carrier.

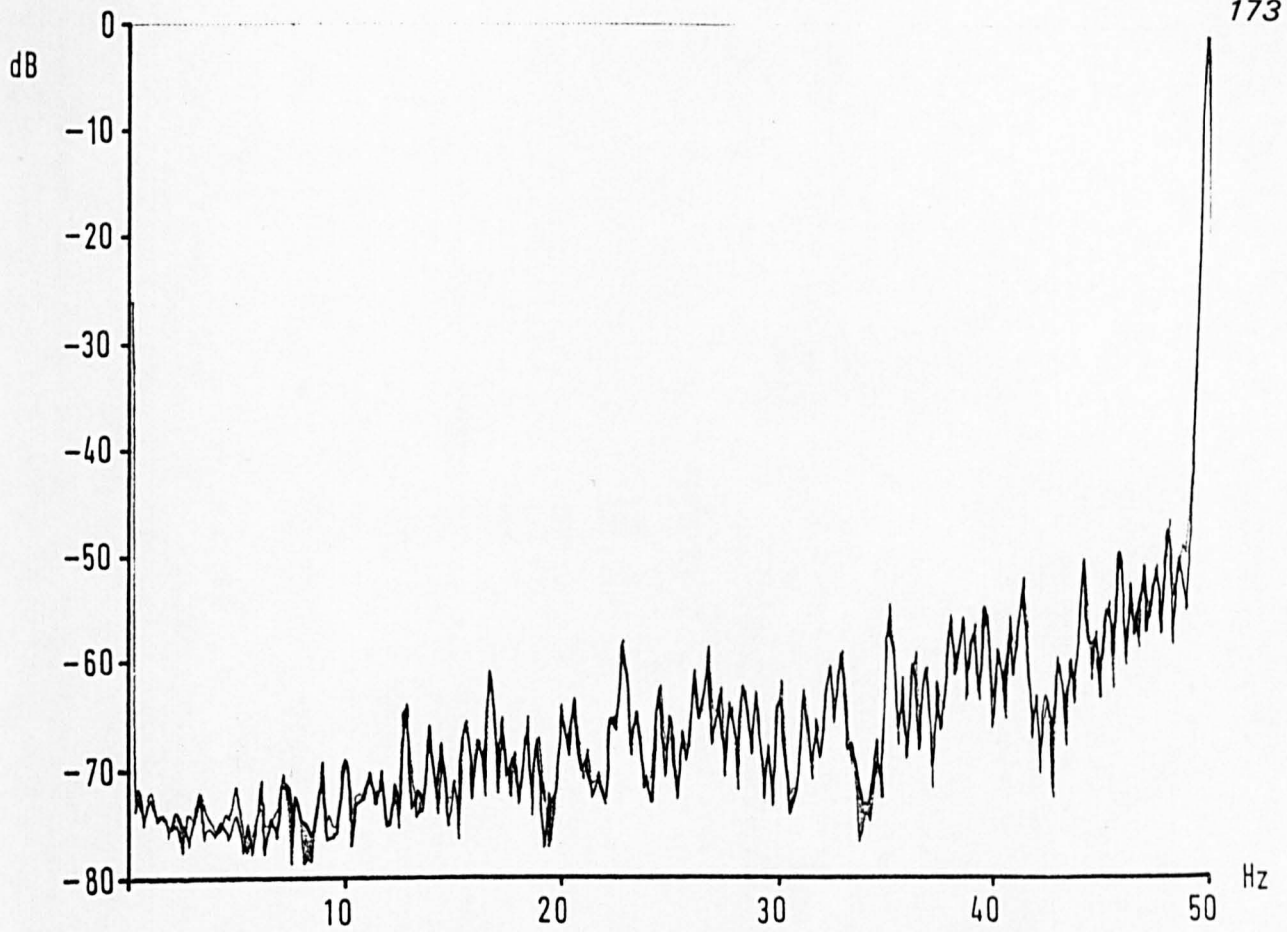


Fig. 5.10 : 0-50Hz power spectrum of V_{ry} for $K=0.916$, LIMIT3

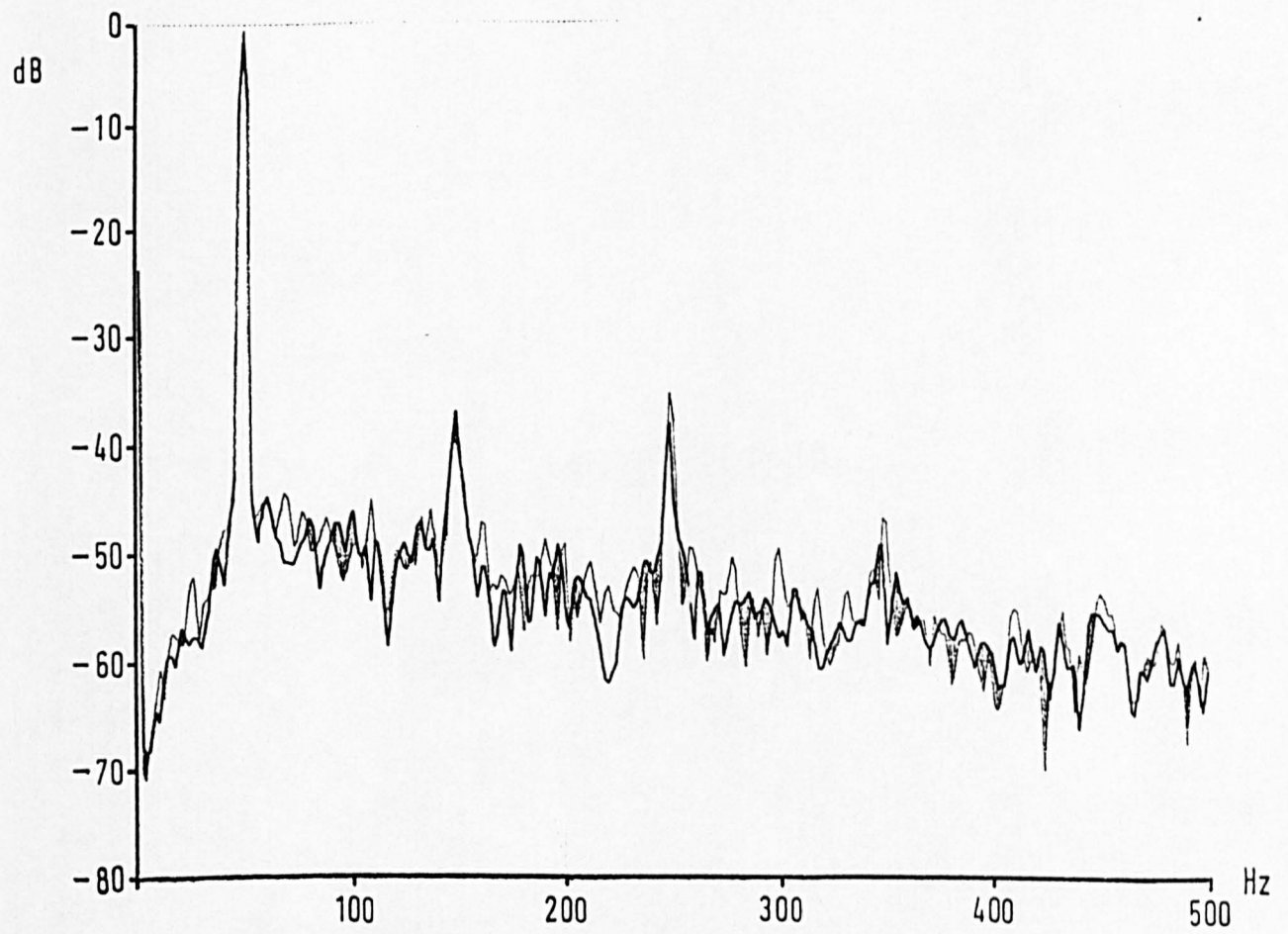


Fig. 5.11 : 0-500Hz power spectrum of V_{ry} for $K=0.916$, LIMIT3

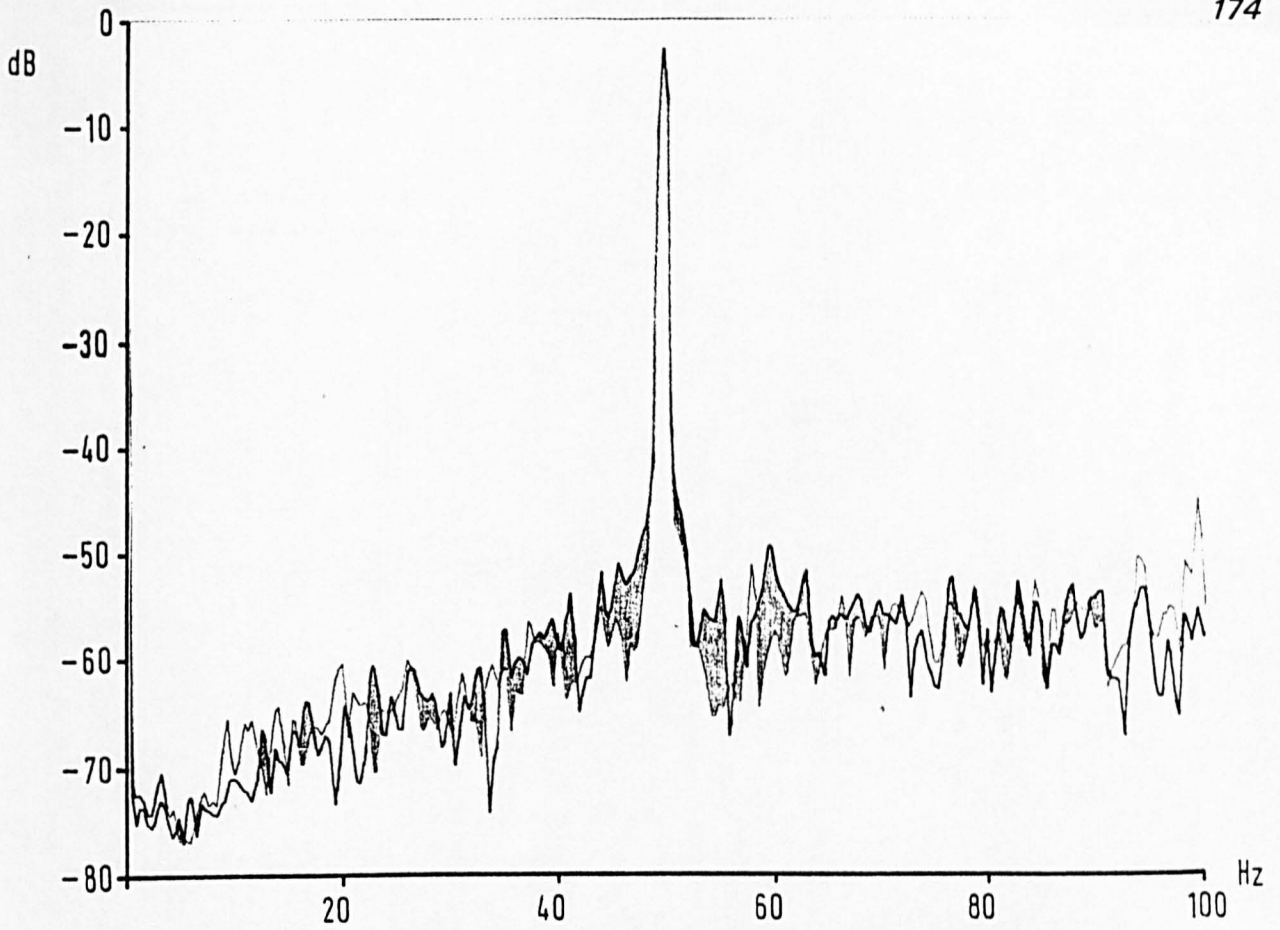


Fig. 5.12 : 0-100Hz power spectrum of Vry for K=0.860, LIMIT1

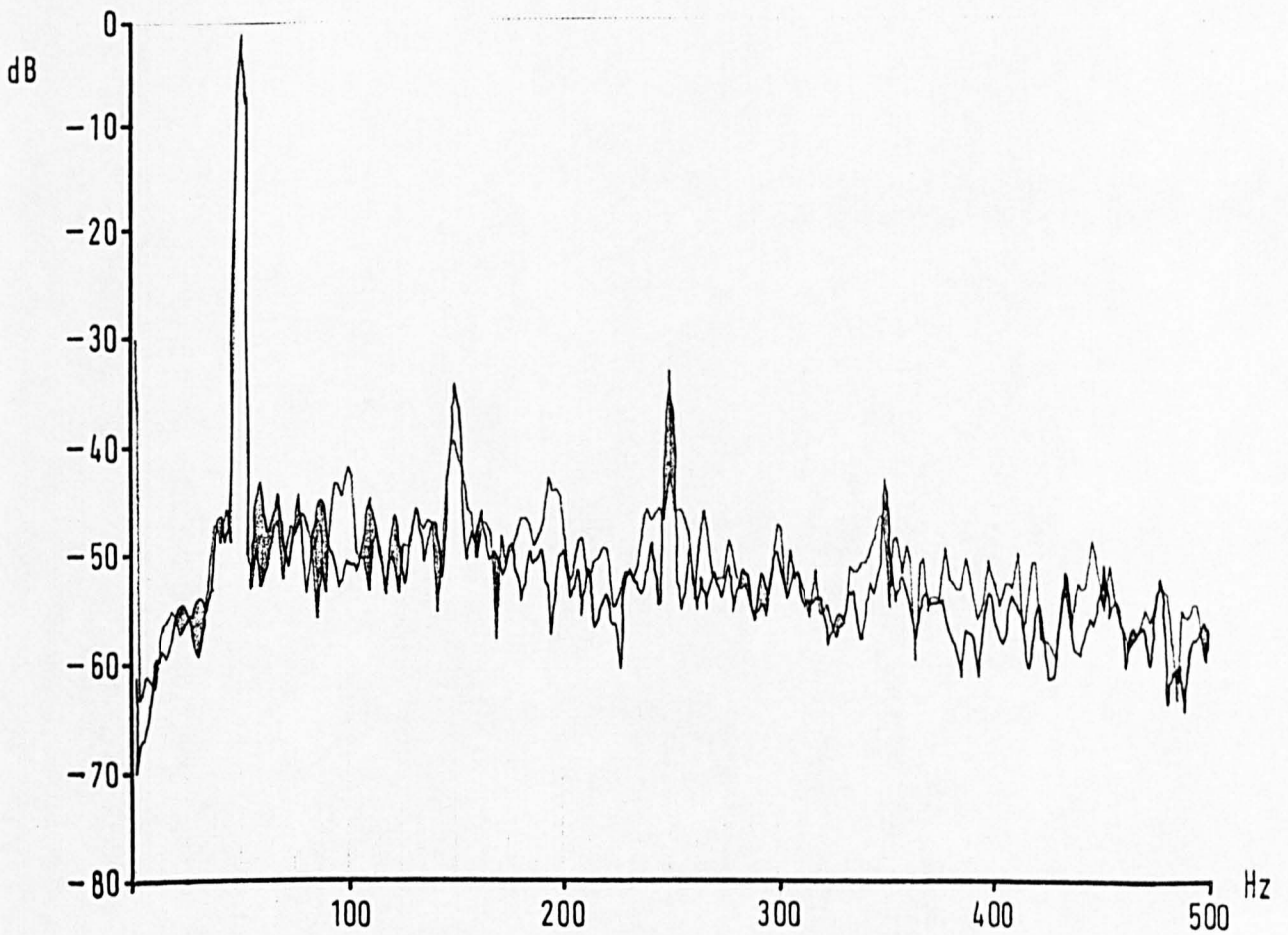


Fig. 5.13 : 0-500Hz power spectrum of Vry for K=0.860, LIMIT1

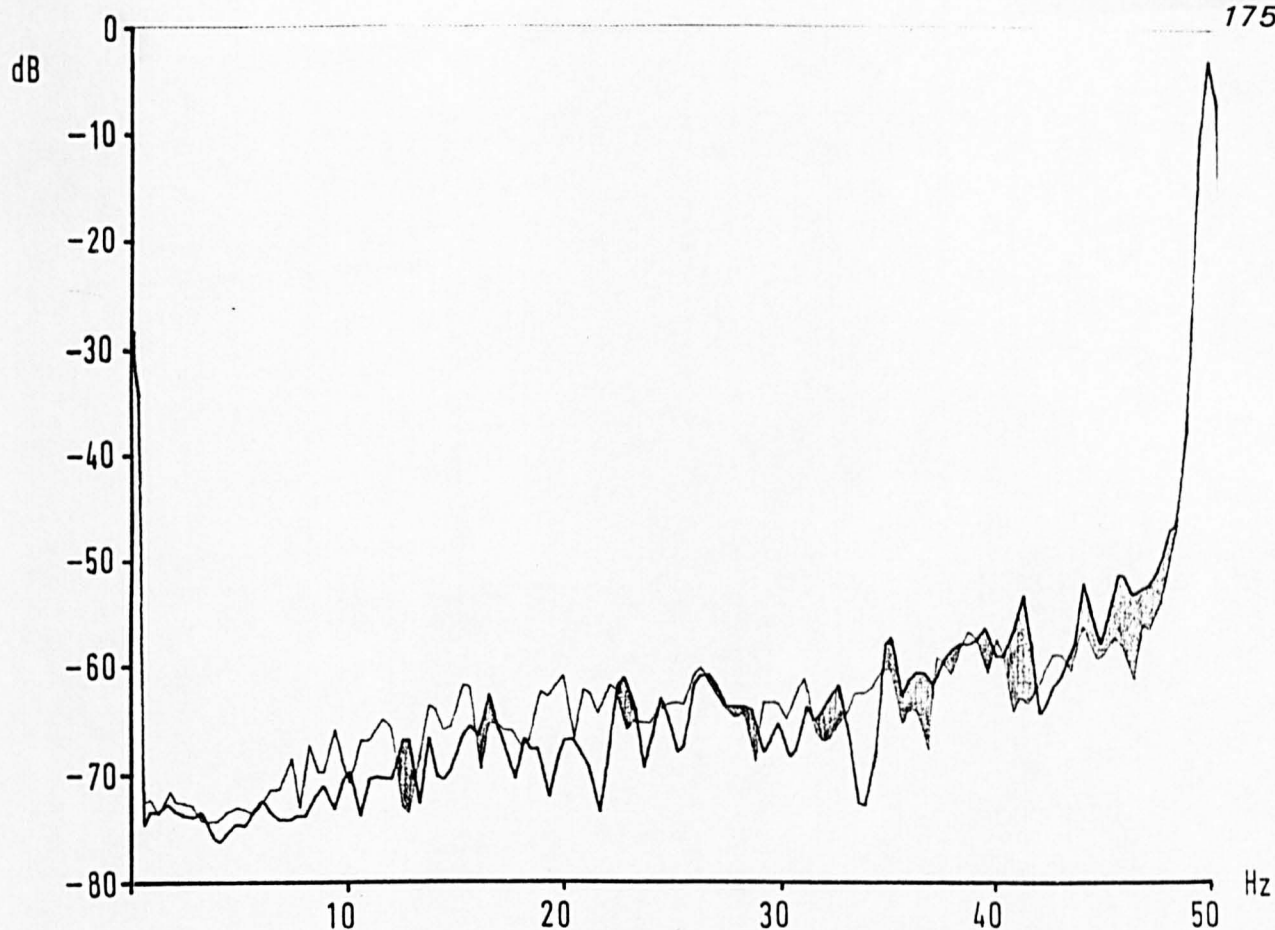


Fig. 5.14 : 0-50Hz power spectrum of V_{ry} for $K=0.860$, LIMIT 1

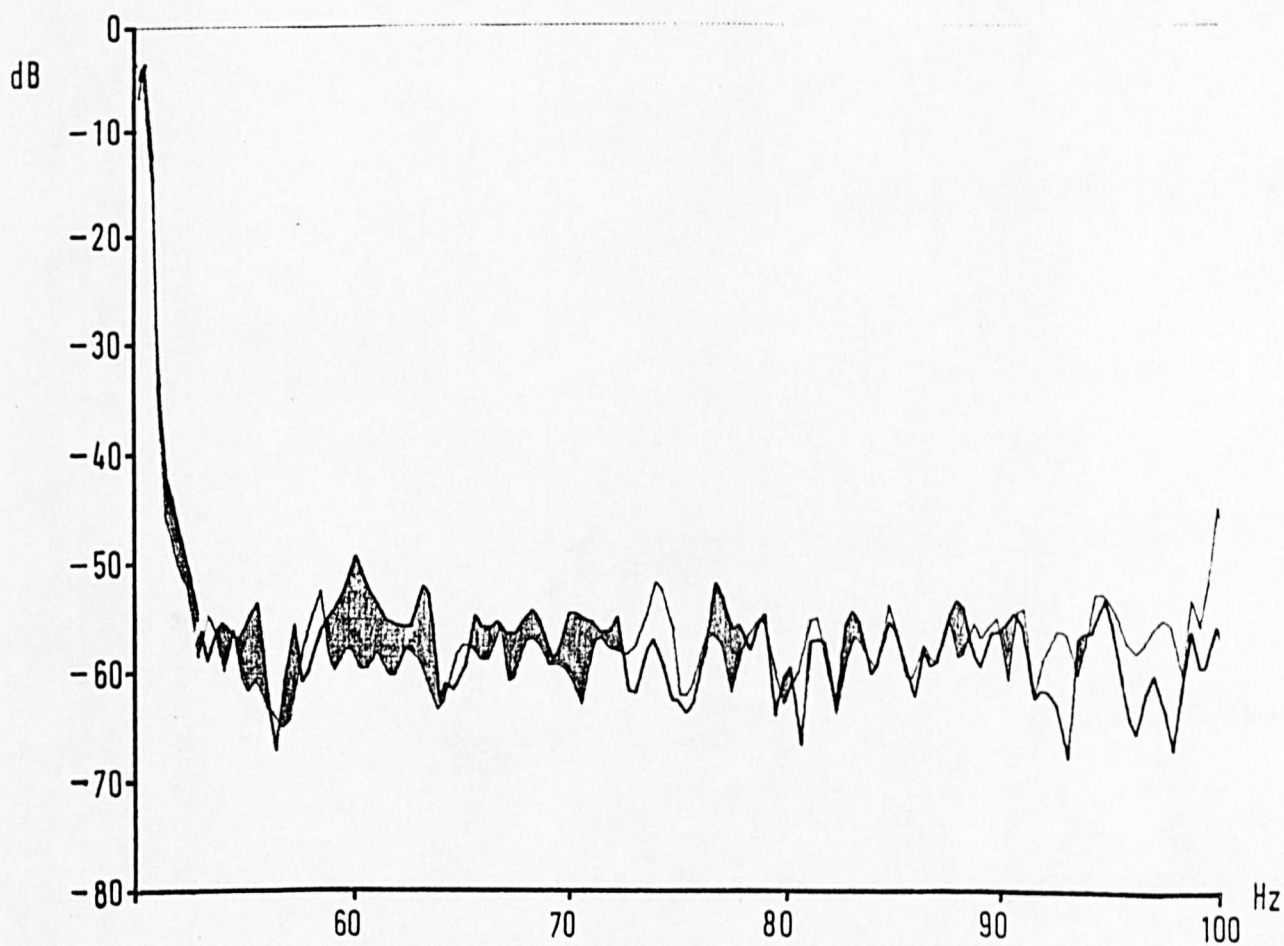


Fig. 5.15 : 50-100Hz power spectrum of V_{ry} for $K=0.860$, LIMIT 1

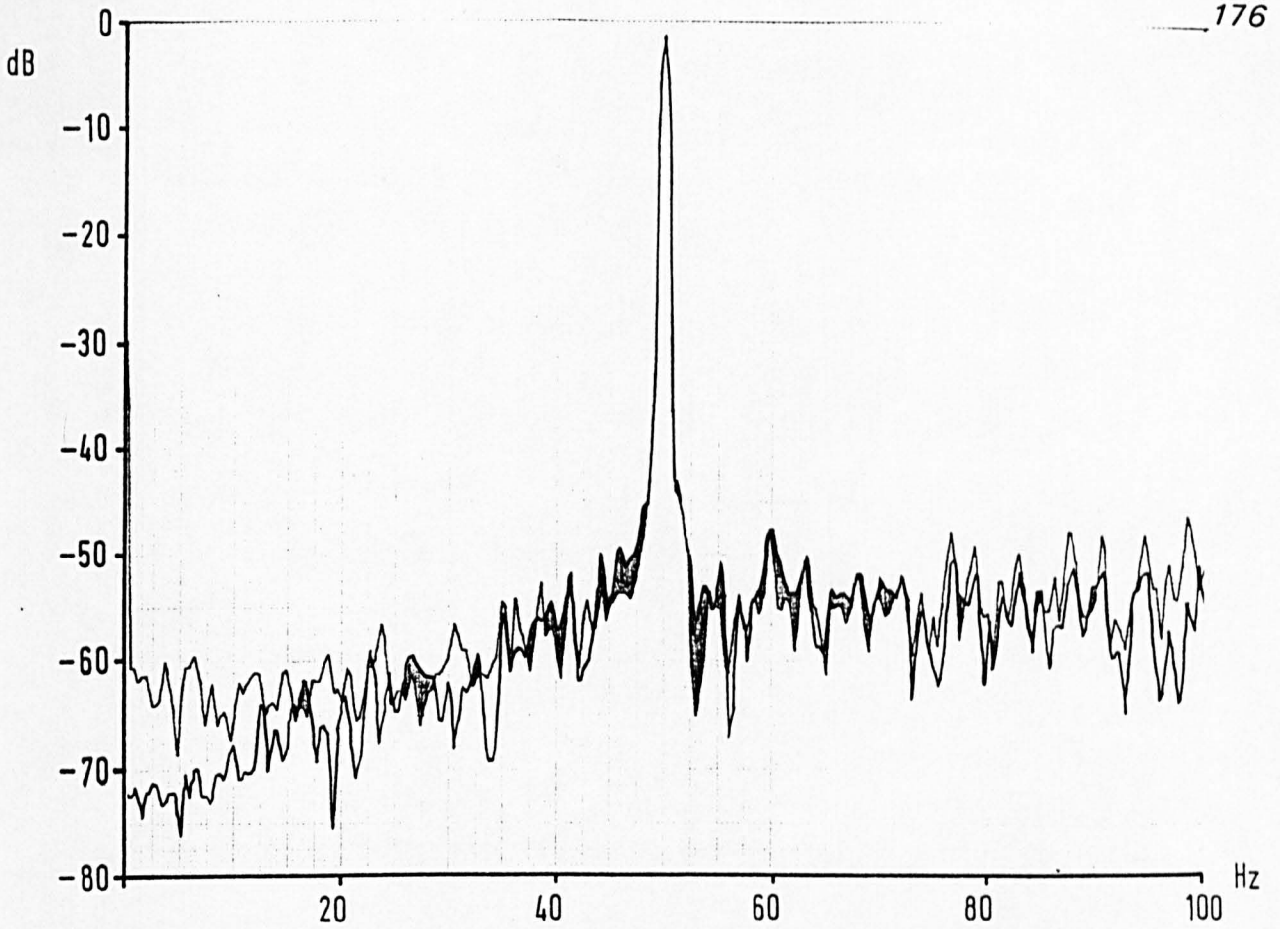


Fig. 5.16 : 0-100Hz power spectrum of Vry for K=0.860, LIMIT2

The cross-over frequency is unchanged at approximately 25Hz. The 'flicker band' attenuation is lessened but it is still noticeably better than that obtained with $K = 0.916$ (Figure 5.8).

The power spectrum to 500Hz in Figure 5.18 highlights the amplification at 100Hz and 200Hz absolute, and shows general broadband amplification similar to that found for $K = 0.916$ (Figure 5.9).

(vi) LIMIT = LIMIT3, R = 226.9 Volts, K = 0.860

The change in the power spectrum due to TCR operation is once again extremely slight for the large integration limit. Figures 5.19 and 5.20 show an almost identical power spectrum to that obtained with $K = 0.916$ (Figures 5.10 and 5.11), with possibly greater amplification of absolute frequencies less than 10Hz.

5.3.2 Time Domain Study of Compensator Action

The depression of the line voltage due to TCR operation is illustrated in Figure 5.21. The three line voltage waveforms at the point of compensator connection are shown, but the plots are not synchronous and aim only to show the distortion of the 50Hz supply waveform due to TCR conduction. The varying firing angle is shown clearly for one branch of the compensator in Figure 5.22, and the corresponding laboratory line voltage, $V_B - V_R$, at the point of compensator connection is shown above the current trace. The time $t = 0$ for Figure 5.22 is fixed by the pulse output from the AIM-65 system at the start of each furnace model data cycle.

The same pulse fixed $t = 0$ for each trace of Figure 5.23 which shows the TCR compensator branch currents when connected in parallel with the arc furnace model.

Only 0.2 seconds of the full 1.78 second data cycle are shown in the interests of clarity. However, the independent phase angle control of each TCR branch is clear, with variation of the conduction angle over the full working range.

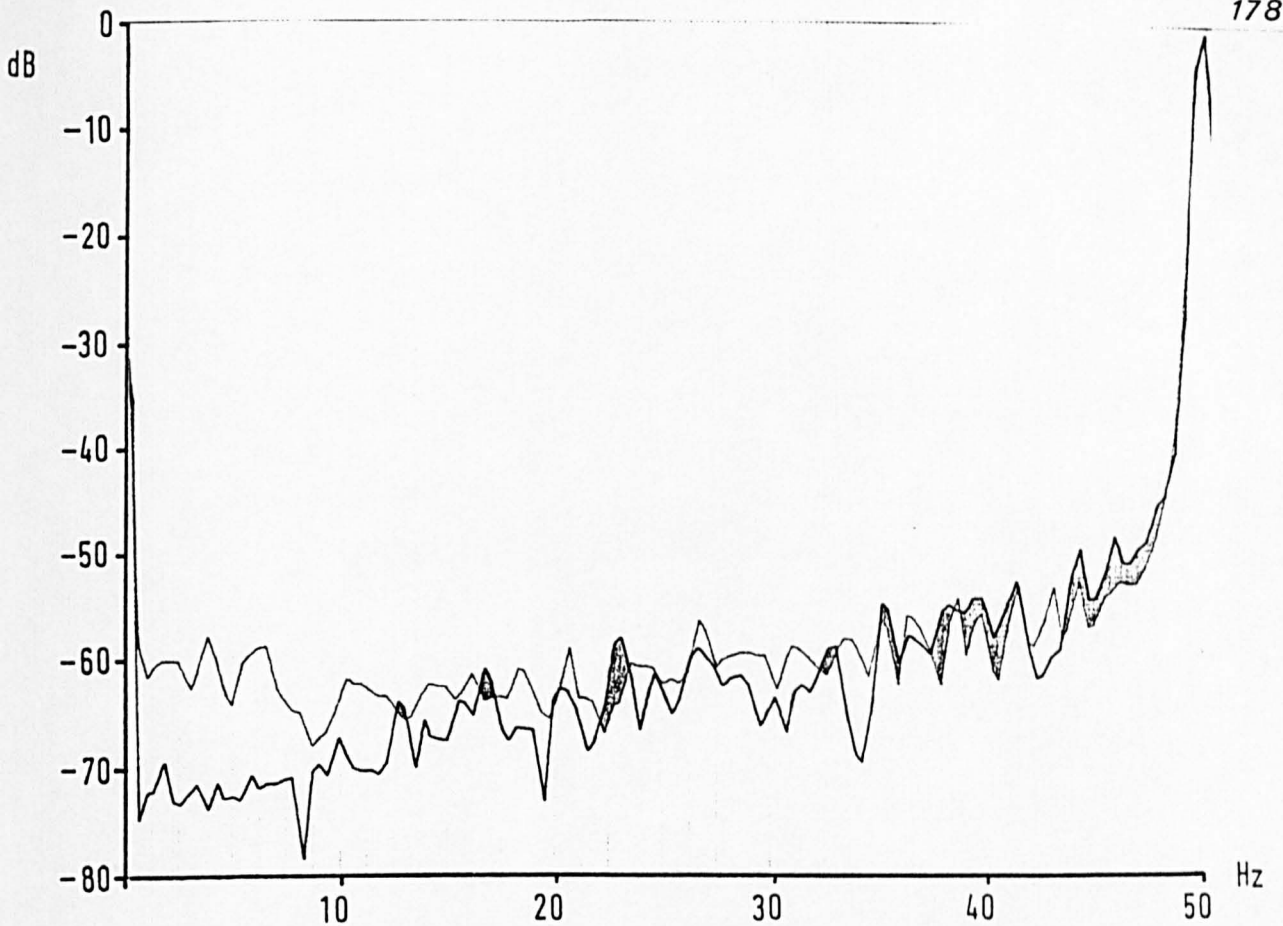


Fig. 5.17 : 0-50Hz power spectrum of V_{ry} for $K=0.860$, LIMIT2

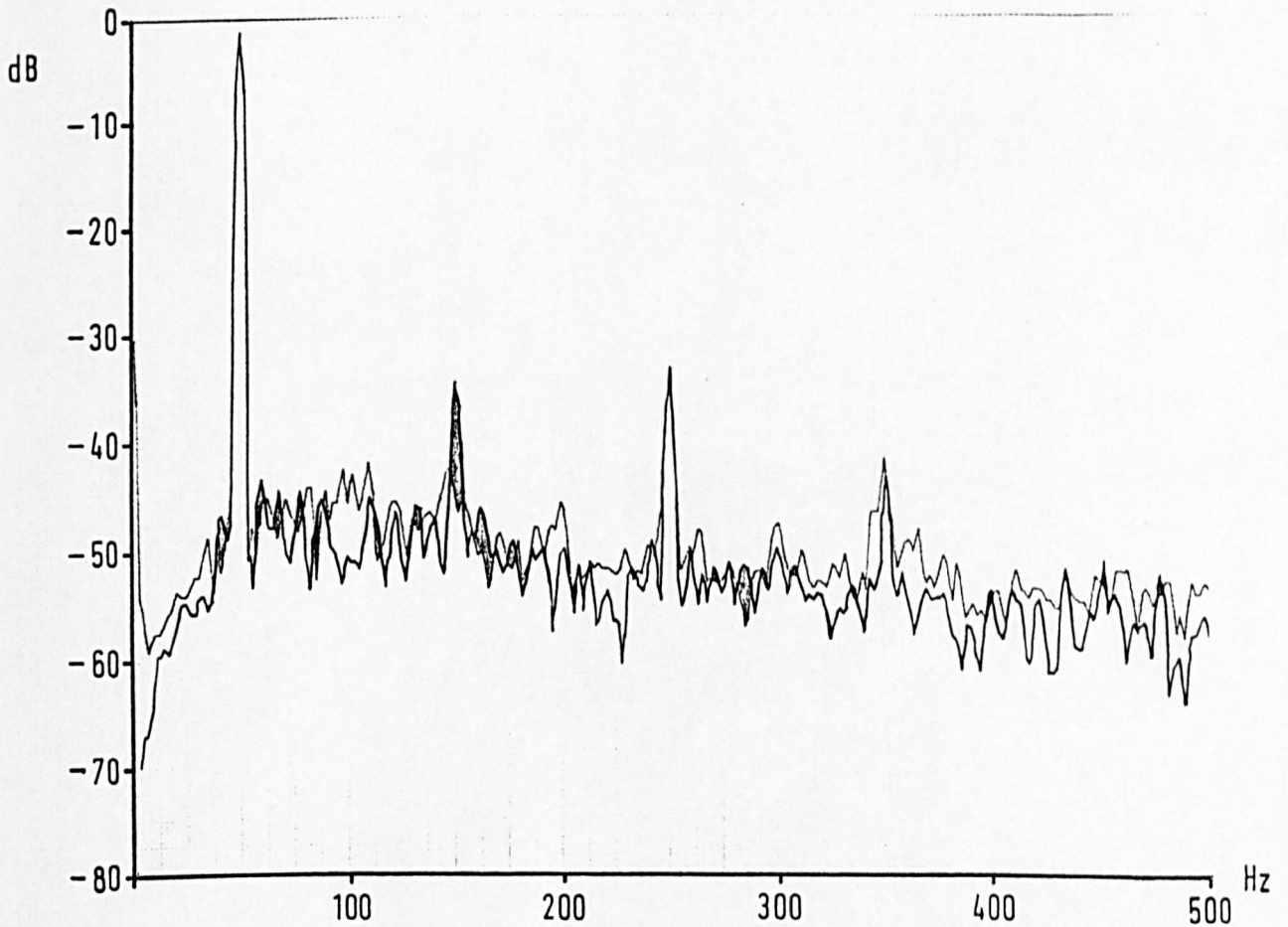


Fig. 5.18 : 0-500Hz power spectrum of V_{ry} for $K=0.860$, LIMIT2

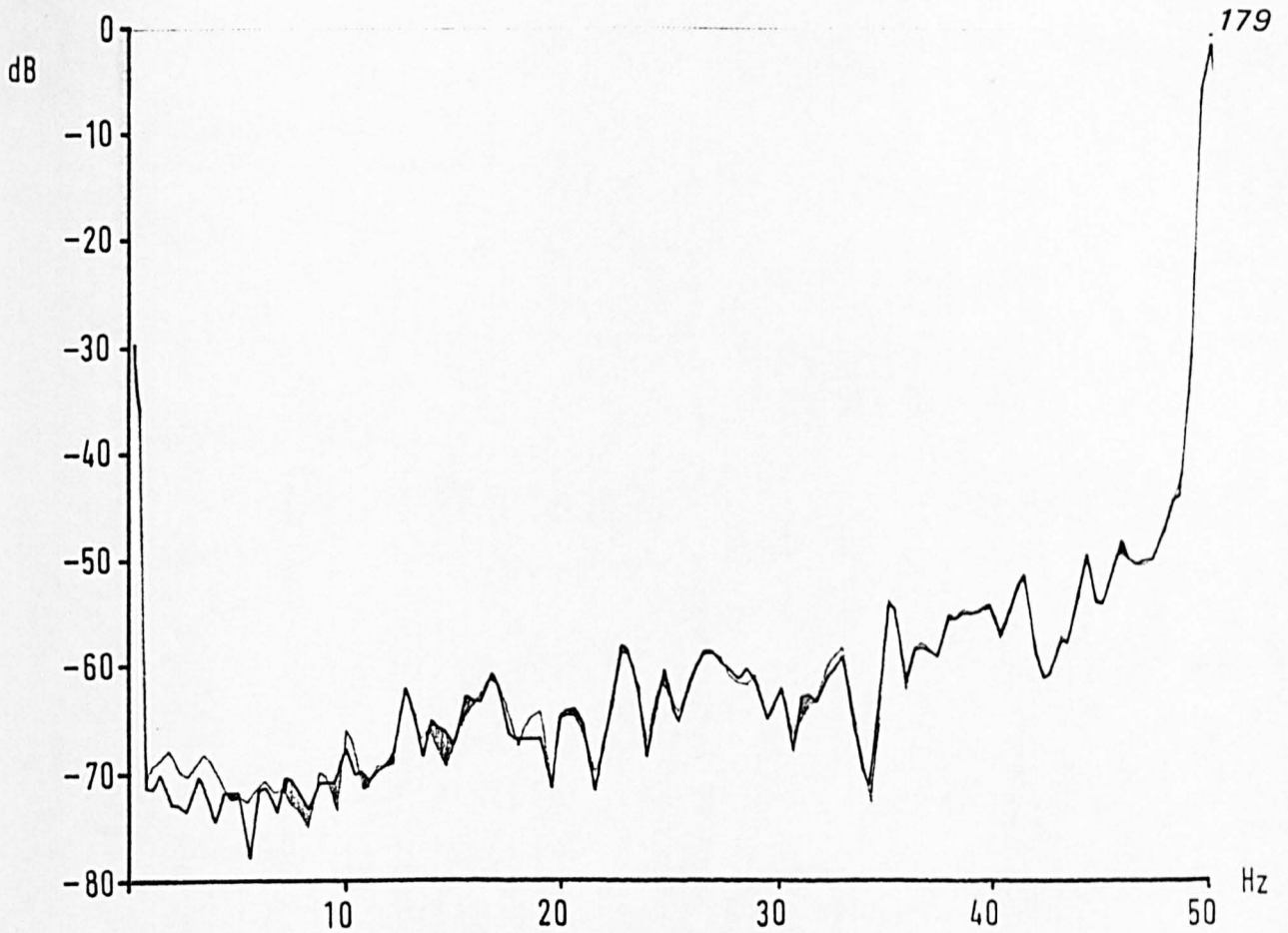


Fig. 5.19 : 0-50Hz power spectrum of V_{ry} for $K=0.860$, LIMIT3

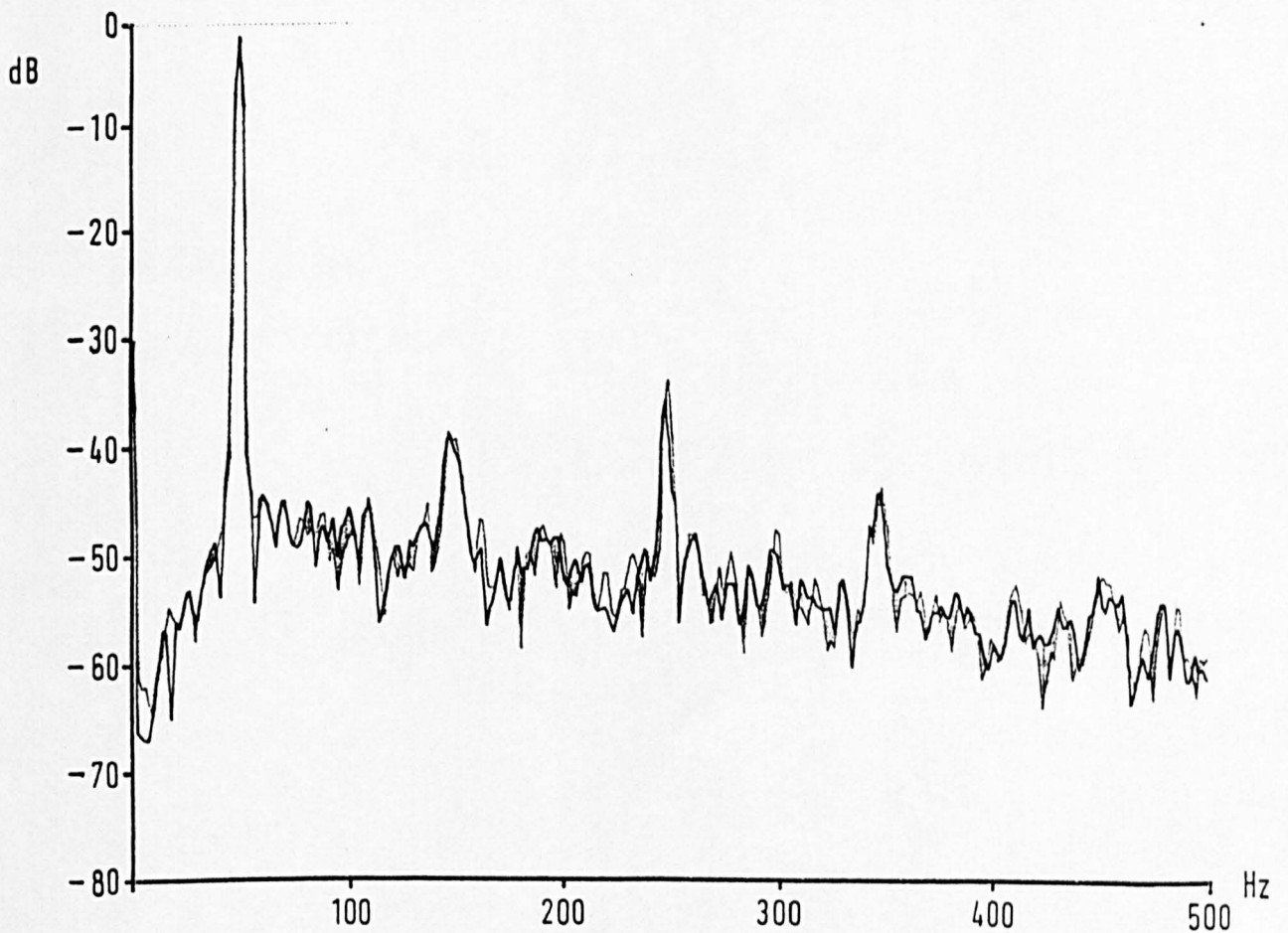


Fig. 5.20 : 0-500Hz power spectrum of V_{ry} for $K=0.860$, LIMIT3

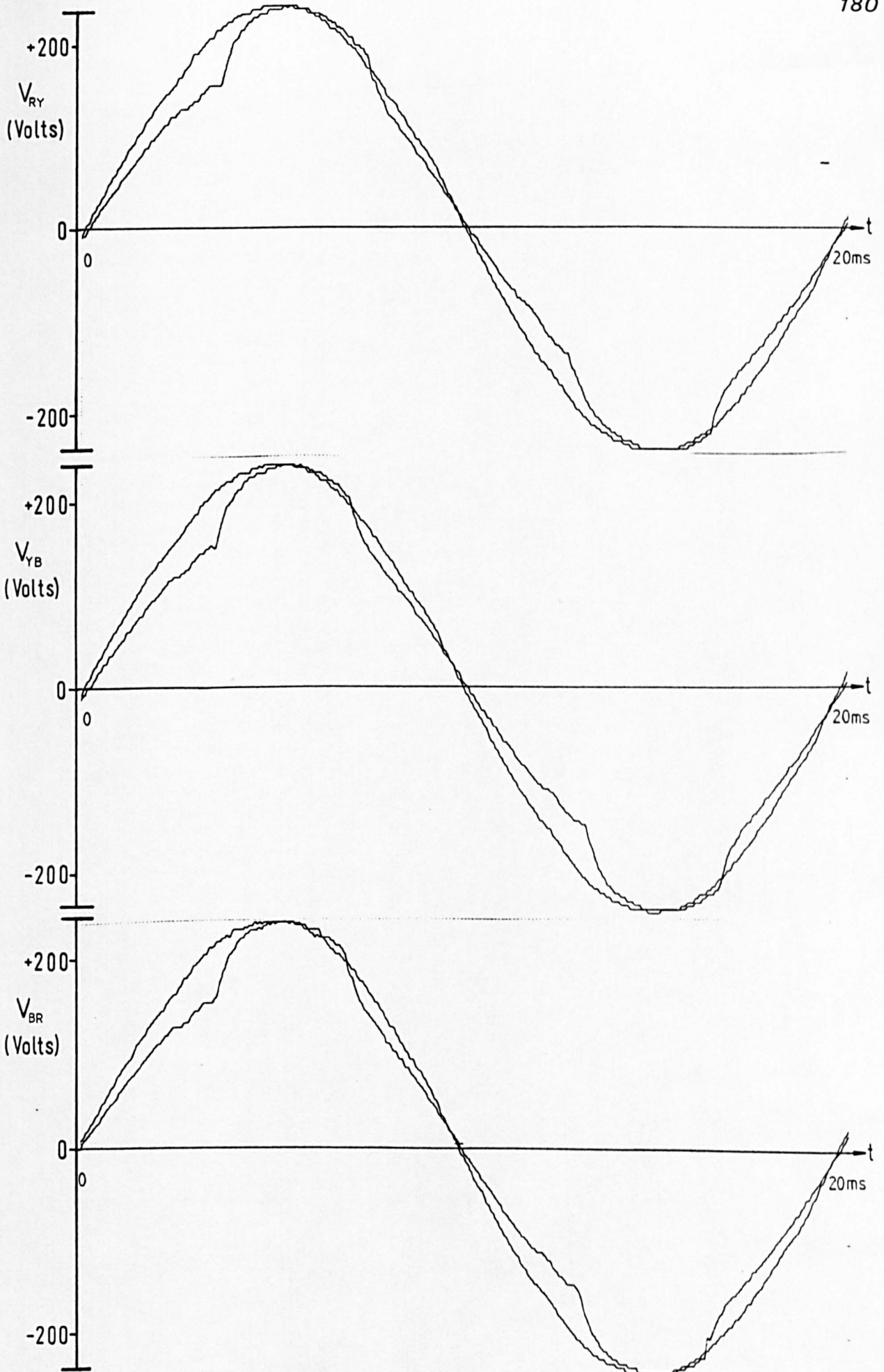


Fig. 5.21 : 3-phase line voltage depression due to TCR switching

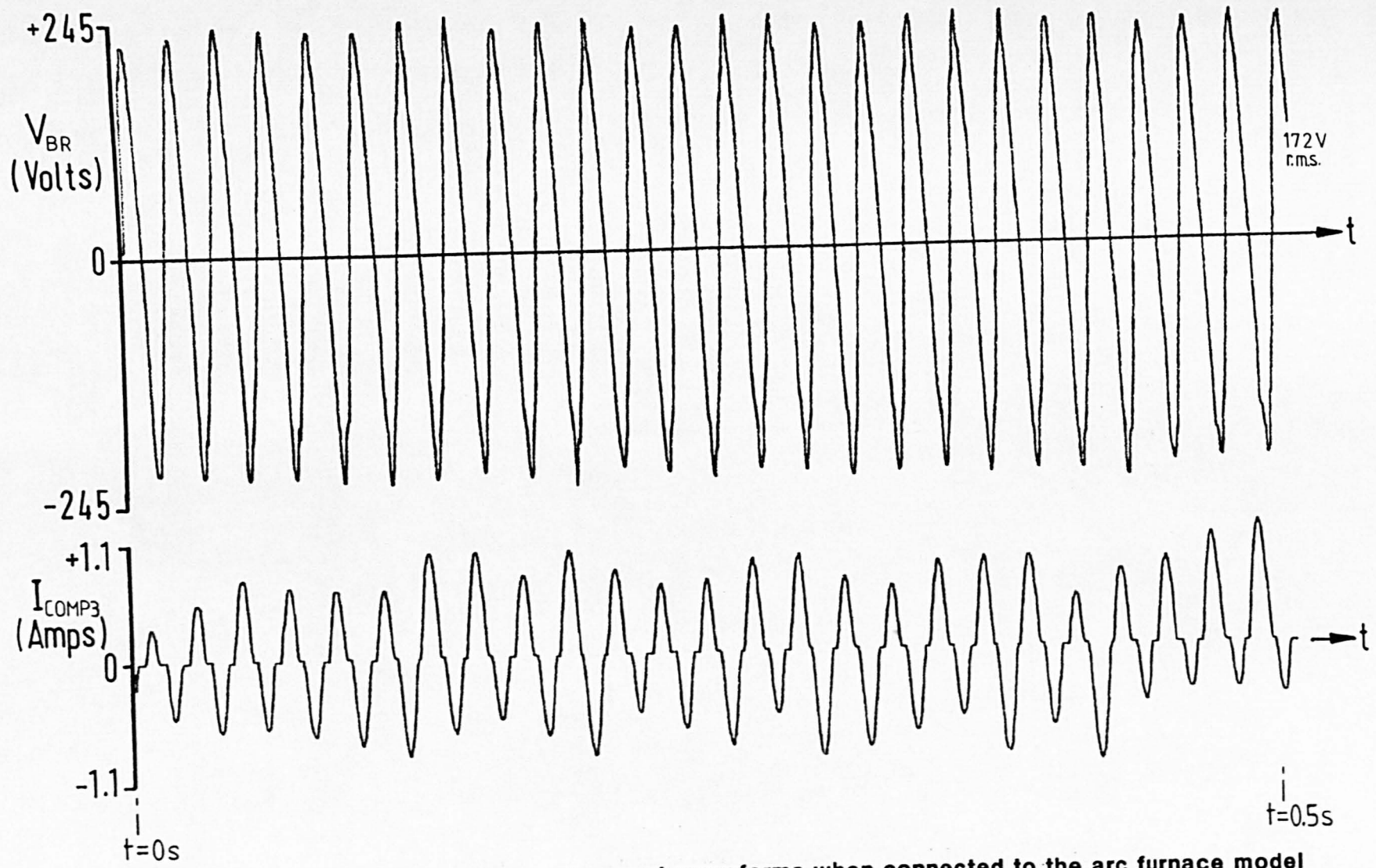
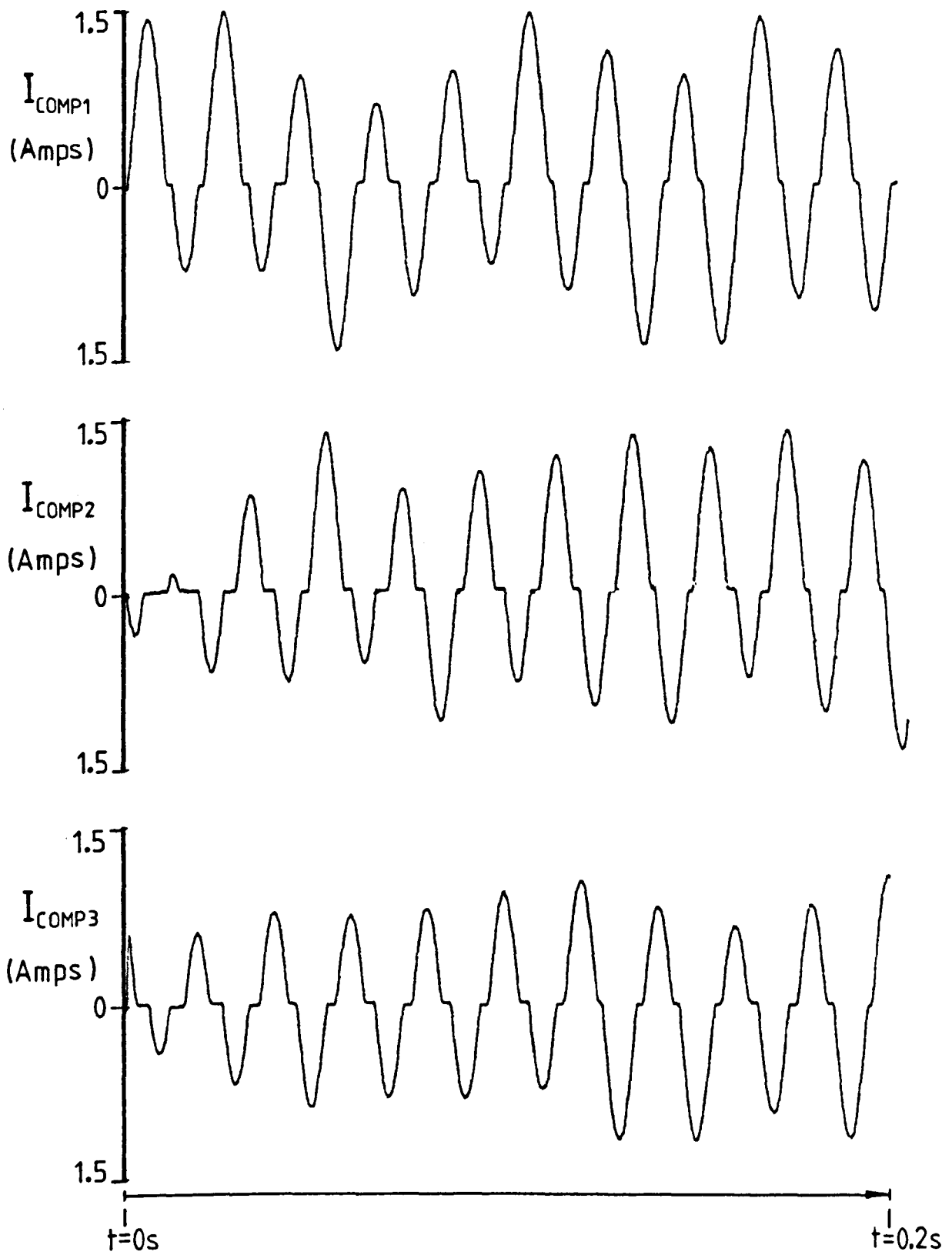


Fig. 5.22 : TCR branch voltage and current waveforms when connected to the arc furnace model



**Fig. 5.23 : TCR three-phase branch currents
when connected to the arc furnace model**

5.4 ESI FLICKERMETER STUDIES

Spectrum analysis has been shown to be a suitable tool for the comparison of compensator performance in different frequency bands (see Section 5.3.1). However, this thesis has not yet related the measured magnitudes of frequency components to the 'annoyance level' described in Section 3.1.3. A comparative study in the laboratory must at some stage be judged in absolute terms.

5.4.1 The Use of the Digital Flickermeter

In the United Kingdom the CEGB and the Electricity Council worked closely with the UIE disturbances committee to find a method for accurately assessing the flicker annoyance factor of a distorted supply voltage waveform. The result of this work was a UIE digital flickermeter, first shown and described at the IEE Third International Conference on Sources and Effects of Power System Disturbances in May 1982.

Its measurement method has been accepted as a standard^[20], and it is now being used widely for monitoring both flicker and voltage harmonics. Only a brief description of its operating method will be given here - more detailed treatments are available elsewhere^[16].

A Digital Equipment Corporation (DEC) LSI 11/23 minicomputer controls all sampling, digital processing and outputs. Fourteen-bit digital samples are made at the rate of 300 per second. Analogue signal conditioning circuits demodulate the supply waveform and weight V_f to simulate the lamp and eye response. The time series output is sampled 75 times each second.

A cumulative probability function (CPF) is then constructed for the selected one of five ranges. Each range spans 200 classified levels, thus:

Range 1 constructs a CPF from 0.05-10

Range 2 constructs a CPF from 0.5-100

Range 3 constructs a CPF from 5-1,000

Range 4 constructs a CPF from 50-10,000

The CPF is evaluated after each ten minutes, and also as a running average.

Thus probability levels

e.g. $P_{0.1}$, $P_{1.0}$, $P_{3.0}$, $P_{10.0}$

may be evaluated, giving the classified level that was exceeded for 0.1, 1.0, 3.0, 10.0 per cent of the time.

The Electricity Council's Engineering Recommendation P7/2 used only $P_{1.0}$ to give a 'guage point fluctuation voltage' V_{fg} . The UIE Disturbances Study Committee has since agreed that a combination of different probability levels is required to give a representation of the 'flicker severity factor' P_f [19,20].

P_f is calculated for three levels of flicker severity:

- (a) Annoyance
- (b) Perceptible
- (c) Visible

A factor of 1.0 for one of these levels would indicate that the measured disturbances were JUST annoying, perceptible or visible. A factor of 10.0 would indicate that the disturbances were ten times worse than just annoying, perceptible or visible.

5.4.2 Arc Furnace Model without TCR Compensator

In order to obtain 'reference' disturbance levels for the effect of the laboratory arc furnace model operating without a compensator, the ESI flickermeter was left connected to the point corresponding to point B in Figure 3.9. The arc furnace model was continuously operated at its normal rating, and the TCR compensator was disconnected.

The displayed results are given in Table 5.2. The values tabulated opposite probability levels P_{xx} are the classified levels described in Section 5.4.1. The values P_{MEAN} and P_{SD} have no meaning for flicker severity, but P_{MEAN} may be treated as a number representative of power.

The important values are those opposite 'annoyance', 'perception' and 'visible'. Thus the flicker voltage at point B (see Figure 3.9) is 10 times more severe than 'just annoying', and 15 times worse than 'just perceptible' or 'just visible'. The measured values do not change between calculations for the 1 minute, 10 minute or overall levels because the model is repeating identical data every 1.78 seconds. Thus even the 10 second upperpercentile level is constant.

5.4.3 Arc Furnace Model with TCR Compensator

The compensator control was set to have parameters identical to those which indicated the best performance from Section 5.3.2.

These parameters were:

LIMIT = LIMIT1 (see Table 5.1)

R = 226.9

K = 0.860

as reviewed in Section 5.3.2 (iv), Figures 5.12, 5.13, 5.14 and 5.15. The four Figures, 5.12 to 5.15, were produced at the same time as the flickermeter results were taken.

CHANNEL 2
RANGE 3

	1 MINUTE LEVEL	10 MINUTE LEVEL	OVERALL LEVEL
P _{MAX}	230	230	230
P _{0.1}	230	230	230
P _{1.0}	225	225	225
P _{3.0}	215	215	215
P _{10.0}	200	200	200
P _{MEAN}	142	141	141
P _{SD}	42	42	42
Annoyance	10	10	10
Perception	15	15	15
Visible	15	15	15

Previous 10 second upperpercentile level 225

Table 5.2 Flickermeter results for the arc furnace model only

Table 5.3 shows the displayed results. The classified levels for each probability value are less than half those for the uncompensated model, and the annoyance factor has been reduced from 10 times worse to 6 times worse than 'just annoying'.

It was encouraging to note that the flickering of a tungsten filament lamp connected at the point of measurement was also visibly reduced.

CHANNEL 2
RANGE 3

	1 MINUTE LEVEL	10 MINUTE LEVEL	OVERALL LEVEL
P _{MAX}	105	105	105
P _{0.1}	100	100	100
P _{1.0}	90	90	90
P _{3.0}	85	85	85
P _{10.0}	75	75	75
P _{MEAN}	57	57	57
P _{SD}	13	13	13
Annoyance	6	6	6
Perception	10	10	10
Visible	10	10	10

Previous 10 second upperpercentile level 90

Table 5.3 Flickermeter results for the compensated arc furnace model

CHAPTER SIX

A TWELVE-PULSE THYRISTOR-CONTROLLED REACTOR

6.1 MODELLING AND CONTROL

6.1.1 Modelling Requirements

6.1.2 Conduction Patterns

6.1.3 Control Requirements

6.1.4 Control Variables

- (i) Sample Loop Delay
- (ii) Reference Sinusoid
- (iii) Integration Limit

6.2 STEADY-STATE TUNING

6.2.1 Thyristor Firing and Conduction Limits

6.2.2 Steady-State Reactive Compensation Results

6.3 TWELVE-PULSE TCR PERFORMANCE WITH THE ARC FURNACE MODEL

6.3.1 Frequency Domain Study of Compensator Action

6.3.2 Time Domain Study of Compensator Action

CHAPTER SIXA TWELVE-PULSE THYRISTOR-CONTROLLED REACTOR

Twelve-pulse schemes have been successfully used in rectifier equipment^[127] to reduce the harmonic current generation. Such schemes use different sets of three-phase secondary windings on the same transformer core to achieve current cancellation at harmonic frequencies greater than the third.

Miller^[95] concludes his study of TCR compensator harmonics by presenting a twelve-pulse arrangement. Such a scheme will be investigated here, with a study of control methods and their application for voltage flicker reduction.

6.1 MODELLING AND CONTROL

The six-pulse TCR compensator described in Chapters IV and V was shown to give a reduction in the flicker frequency components of an arc furnace supply voltage waveform. The same laboratory modelling techniques were then applied to the construction of a twelve-pulse TCR compensator, for application with the arc furnace model described in Chapter II.

6.1.1 Modelling Requirements

A twelve-pulse thyristor scheme will consist of two equally rated six-pulse units connected in parallel. Phase displacement of one unit from the other may be obtained using different three-phase transformer secondary winding arrangements for each six-pulse unit, the primary windings being connected at the same point. This is more easily accomplished by using a single transformer with two secondary sets of windings sharing the same magnetic circuit with only one primary. Such a transformer is shown in Figure 6.1 together with the relevant voltage and current relationships.

The twelve-pulse TCR compensator three-phase rating was required to be equal to the rating of the six-pulse compensator which gave the best flicker improvement results in Chapter V. The rating for full conduction was then 579VA, with the rating equally divided between the two six-pulse secondary circuits of the Δ - Δ /Y transformer. Each compensator branch was constructed as a 'unit' of 1.00H inductance, connected in series with a BTX 18-500^[106] thyristor and 0.50hm resistor for branch current measurement. Firing circuits were constructed to be identical to those used for the six-pulse TCR.

The short circuit impedance of the Δ - Δ /Y transformer was approximately $0.5 + j0.20$ hms, considered to be negligible compared to the reactance of the compensator inductances. The transformer magnetising current was approximately 0.4A, and slight distortion of the supply voltage waveform was observed because of this.

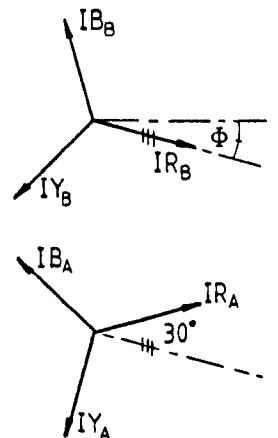
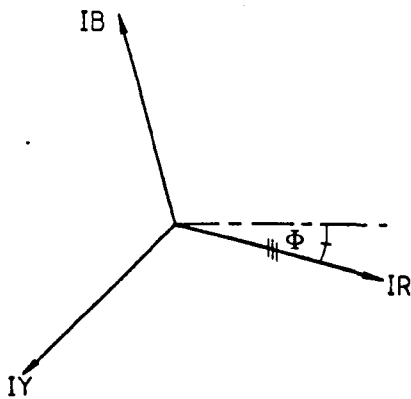
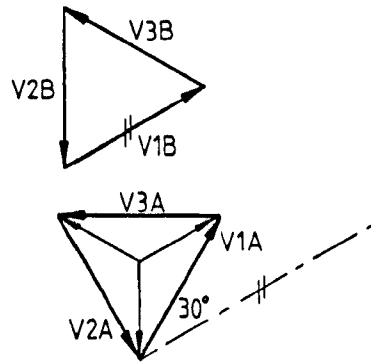
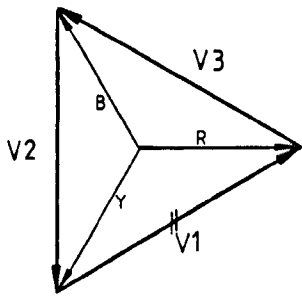
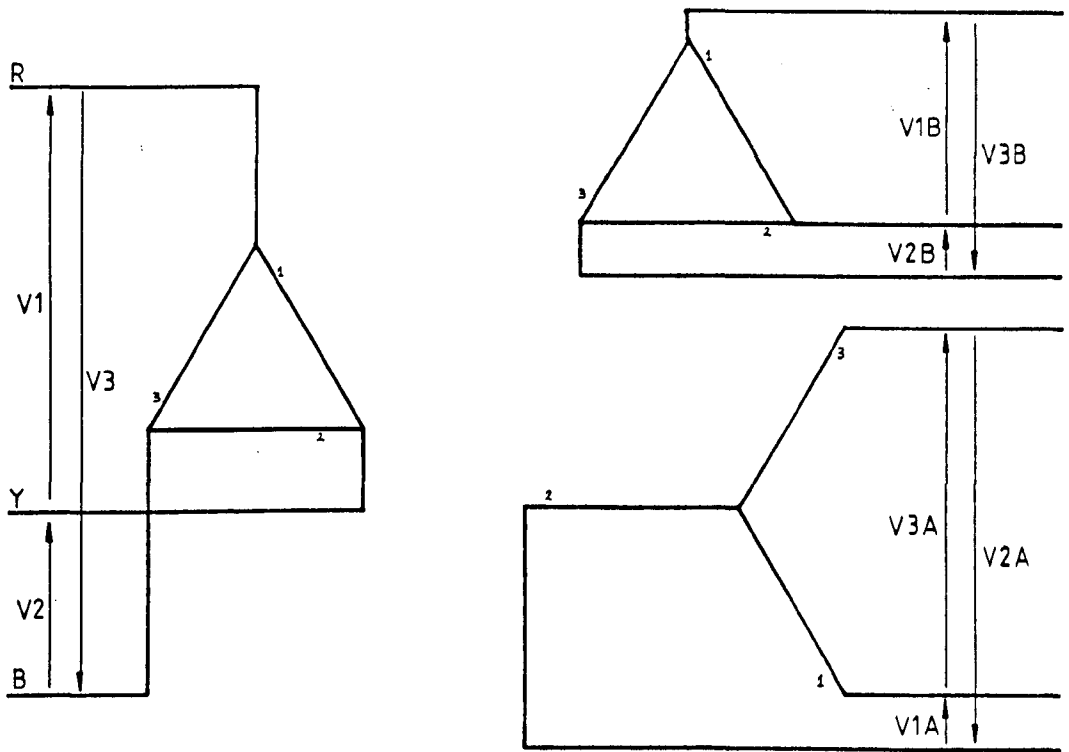


Fig. 6.1 :Y-Δ/Y transformer winding connections with voltage and current relationships

6.1.2 Conduction Patterns

Both the transformer Y and Δ secondaries were connected to identical Δ -connected three-phase TCR units. The definition of circuit parameters is given in Figure 6.2. The conduction patterns within each of the Δ -connected TCR units are identical to those shown in Chapter IV, but to a common time reference all voltages and currents in the arrangement connected to the Y secondary lead those connected to the Δ secondary by a phase angle of 30° as shown in Figure 6.1.

The sum of the currents drawn by the two secondary circuits is then drawn from the supply by the transformer primary. Conduction patterns are best studied for each secondary six-pulse TCR arrangement operating in isolation from the other, then the principle of superposition may be used to obtain the combined effect on the primary circuit. Figure 6.3 shows the current conduction patterns for thyristor firing delayed at 100, 135 and 170 degrees after the respective voltage zero crossing. Figure 6.4 shows how the currents add in the primary circuit.

6.1.3 Control Requirements

An advantage of the Y-Y/ Δ twelve-pulse TCR system is that thyristor conduction in the relevant branch of the Δ -connected secondary circuit may lead the conduction in the Y-connected secondary circuit by a phase angle of 30° . The flexibility of the microprocessor-based control equipment allowed it to be easily adapted for use with the twelve-pulse scheme. Each of the three microprocessors continued to sample separate line voltages, and decide on thyristor firing angles using an 'integral of voltage difference' calculation similar to that described in Chapter IV.

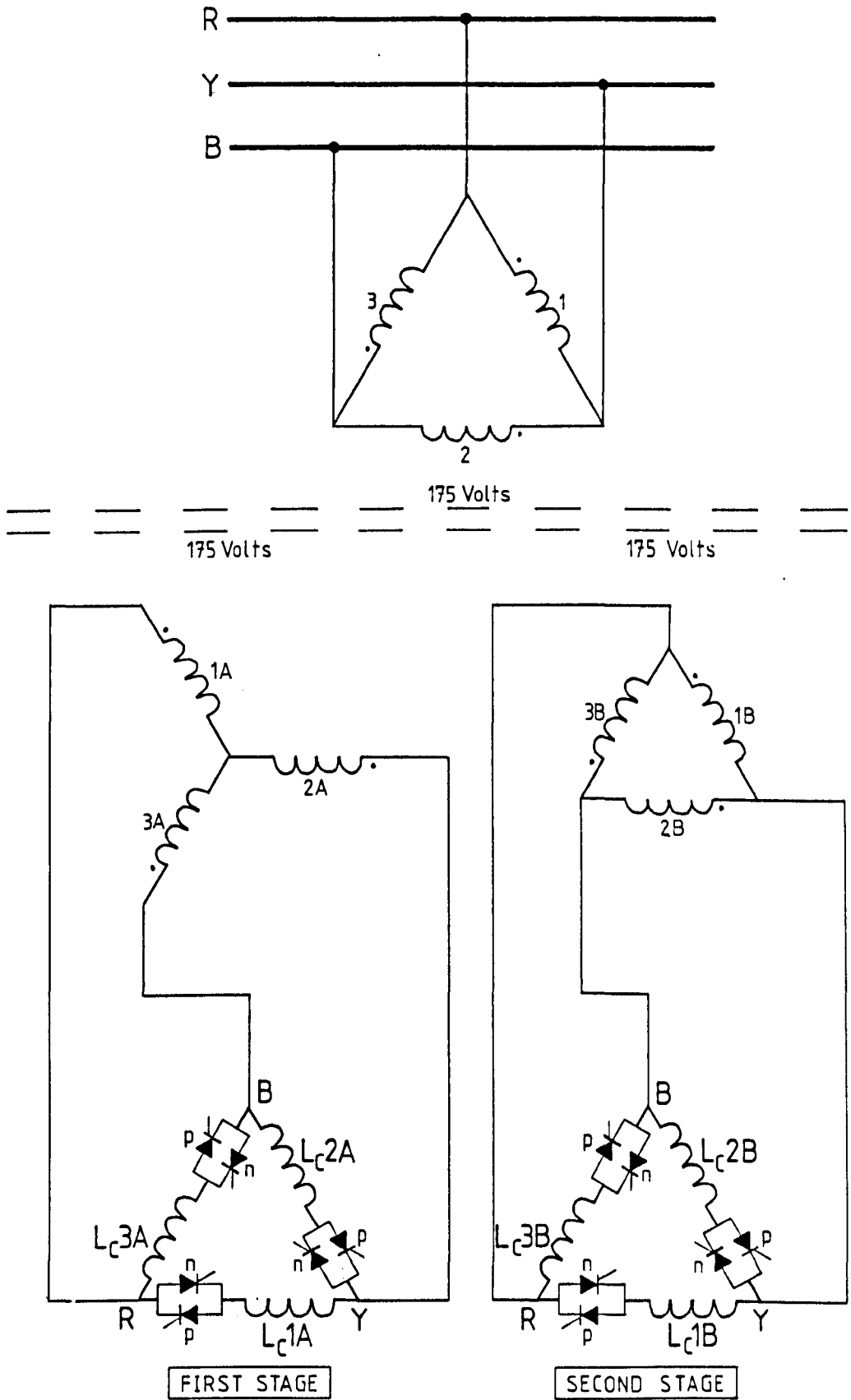


Fig. 6.2 : Connection diagram of 12-pulse TCR compensator

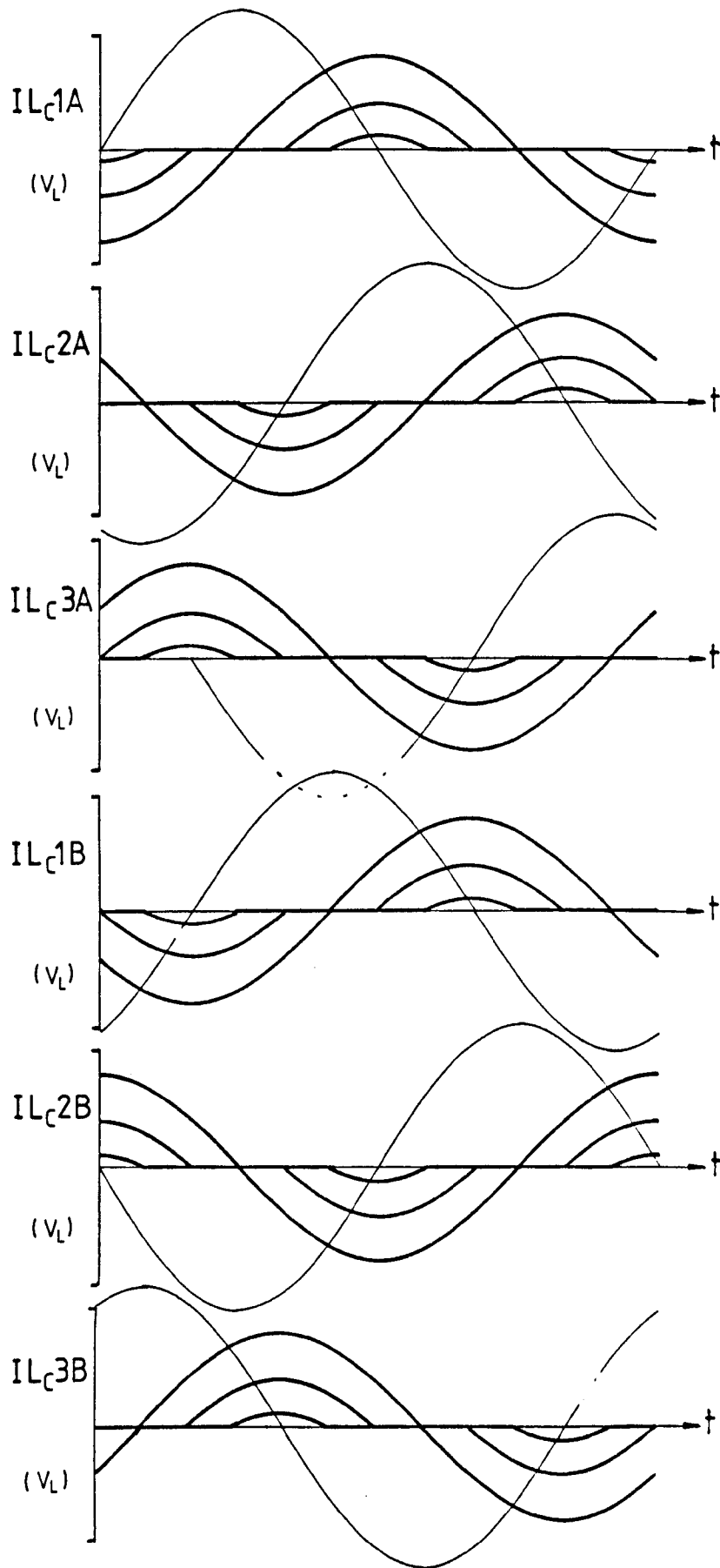


Fig. 6.3 : Y-Δ/Y Transformer secondary current conduction patterns

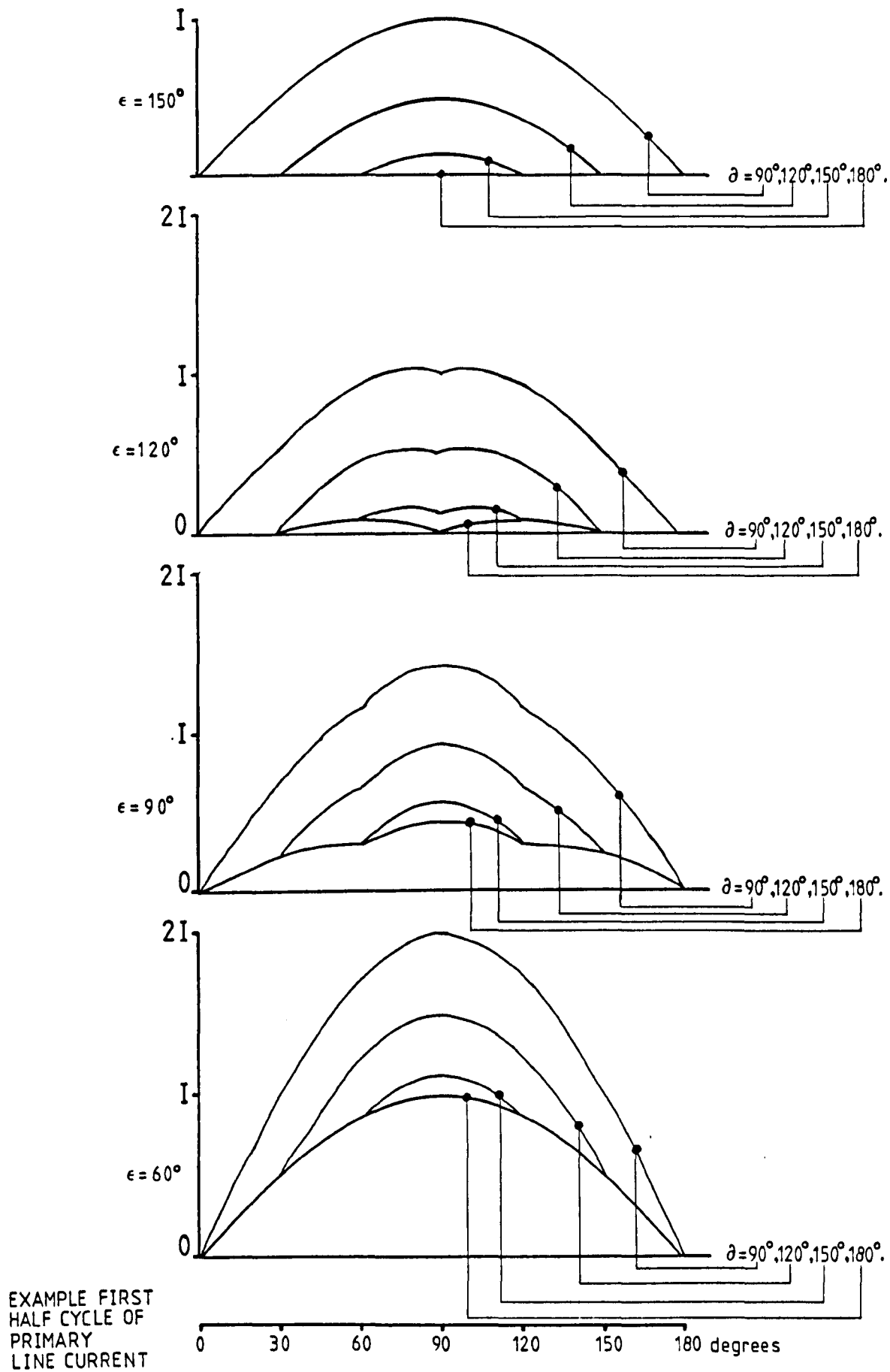


Fig. 6.4 : $Y-\Delta/Y$ Transformer primary current conduction patterns

Figure 6.5 shows the allowable conduction angles for both of the secondary circuits, with respect to the primary line voltage that is sampled by the control system. We define the period when current is flowing in the 30 degrees phase advanced six-pulse unit as 'first stage conduction', and that period when current is flowing in the in-phase six-pulse unit as 'second stage conduction'. It is clear from Figure 6.5 that if the voltage-zero crossing is retained for initiation of the integration procedure (see Section 4.2.3), then the earliest firing angle for first-stage conduction is preceded by an integration period of only 3.33 milliseconds. This shorter integration period could easily have been overcome, but the control philosophy for the twelve-pulse system did not demand such action.

It was intended that the speed of response of the TCR compensator could be improved by having the ability to initiate first-stage firing as soon as possible.

It was highly likely that such shortening of the integration period would result in some loss of accuracy in the compensation system, and therefore the second-stage conduction period would be used for slower and more accurate control.

The microprocessor systems required modification of the control programs to achieve the following items in both positive and negative half-cycle sections of the control routine:

- (a) Integration from voltage zero-crossing to a lower integration limit, LIMIT1, set to initiate first-stage conduction. Integration then to continue to a higher integration limit, LIMIT2, for second-stage conduction.
- (b) Restriction of first-stage firing pulse output to between 3.33 and 8.33 milliseconds after primary voltage zero-crossing.

The assembler language program, 'FirBsub.asm', is listed in full in Appendix K.

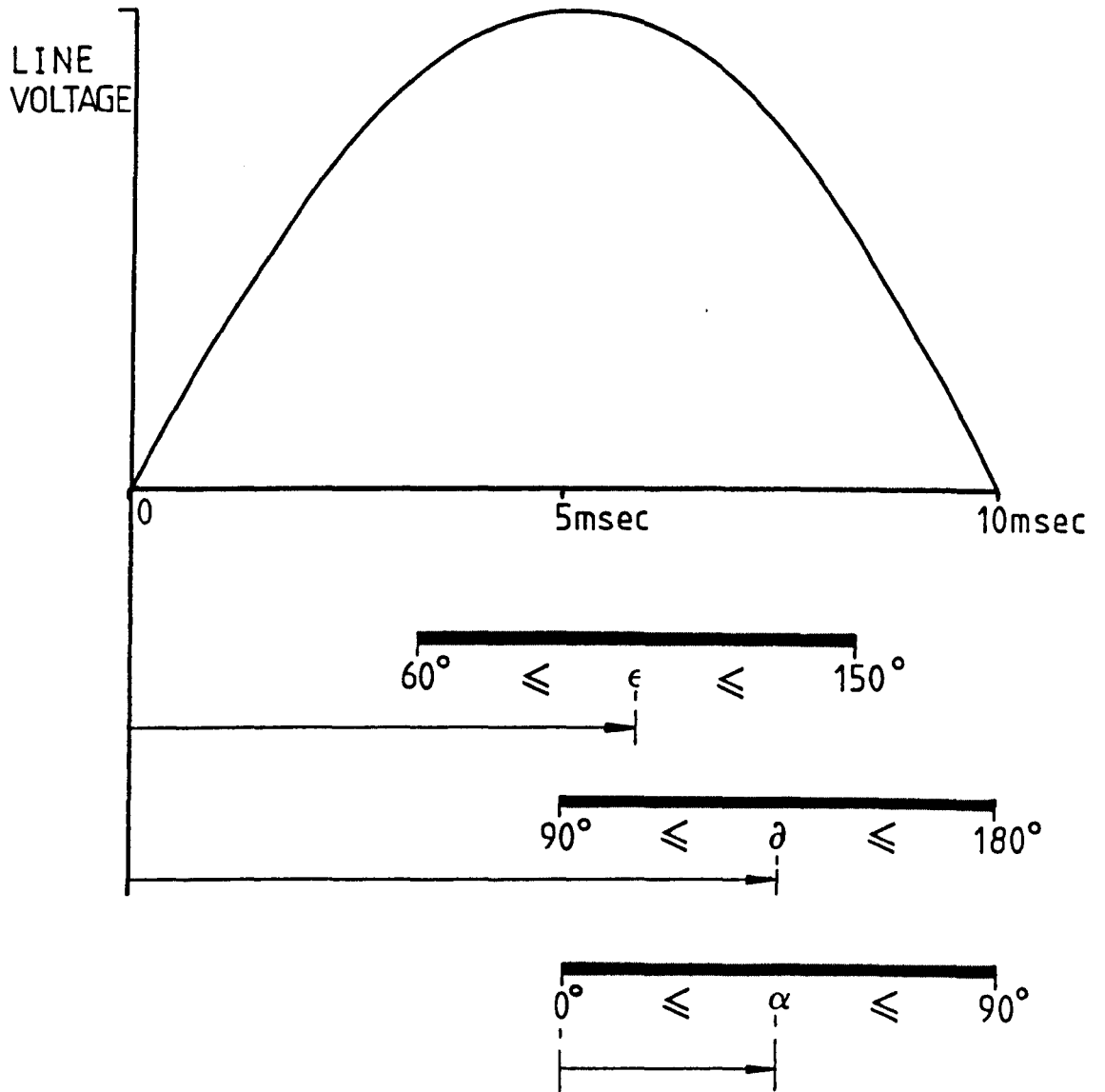


Fig. 6.5 : $Y-\Delta/Y$ transformer primary line voltage with secondary current conduction angles

6.1.4 Control Variables

The variables in the twelve-pulse TCR control algorithm are similar to those treated in Section 4.2.4 for the six-pulse version:

- i.e. (i) The sample loop delay, D .
- (ii) The reference sinusoid $v_R(\omega t)$.
- (iii) The integration limit, LIMIT.

and these are once again considered in turn.

(i) Sample Loop Delay, D

The same block of program code as given in Section 4.2.4 was used to allow a variable hexadecimal value, D , to be inserted into every sampling loop. There are now four such sampling loops in the program, covering the integration periods before the first and second stage firing for positive and negative half cycles.

The sample loop delay time, Δt , was thus adjusted to be as near as 74.0 microseconds as possible, and the times obtained were:

System 1, positive half cycle, first stage : $\Delta t = 74.1 \mu\text{secs}$
 positive half cycle, second stage : $\Delta t = 74.5 \mu\text{secs}$
 negative half cycle, first stage : $\Delta t = 74.1 \mu\text{secs}$
 negative half cycle, second stage : $\Delta t = 74.3 \mu\text{secs}$
 System 2, positive half cycle, first stage : $\Delta t = 74.1 \mu\text{secs}$
 positive half cycle, second stage : $\Delta t = 73.9 \mu\text{secs}$
 negative half cycle, first stage : $\Delta t = 74.1 \mu\text{secs}$
 negative half cycle, second stage : $\Delta t = 73.6 \mu\text{secs}$

System 3, positive half cycle, first stage : $\Delta t = 74.1 \mu\text{secs}$
 positive half cycle, second stage : $\Delta t = 73.4 \mu\text{secs}$
 negative half cycle, first stage : $\Delta t = 73.3 \mu\text{secs}$
 negative half cycle, second stage : $\Delta t = 73.9 \mu\text{secs}$

The final location of bytes representing 'D' in RAM were 20, 101, 194 and 275 bytes respectively from the start of the 'FirBsub' object code program block.

(ii) The Reference Sinusoid, $v_R(\omega t)$

The ADCs and sampling circuitry was left as set for the six-pulse TCR compensator.

The open circuit line voltage of the laboratory model was nominally 175 volts, and it was found that the magnetising current of the Δ - Δ /Y transformer depressed this voltage to approximately 171 volts.

Full three-phase TCR conduction, in both first and second stage units, further depressed the line voltage to approximately 149 volts. The reference sinusoid values were set in RAM to be equivalent to a sine wave with an RMS value of 146 volts.

The LSB of the data byte represents 2.063 volts, therefore

$$\underline{v_R = 127 + 100 \sin \omega t}$$

With the sampling frequency at approximately 74 microseconds, there were once again 133 reference points calculated for each half cycle. These were stored in look-up tables 'sine1' and 'sine2' in RAM and are given in Appendix K.

(iii) Integration Limit, LIMIT

Each of the three controllers required four integration limits to be set in RAM to determine the position of the four thyristor firing pulses through each 50Hz voltage cycle.

POSLIM1 - Determined the position of the first-stage firing pulse in the positive half-cycle.

POSLIM2 - Determined the position of the second-stage firing pulse in the positive half-cycle.

NEGLIM1 - Determined the position of the first-stage firing pulse in the negative half-cycle.

NEGLIM2 - Determined the position of the second-stage firing pulse in the negative half-cycle.

The most successful thyristor firing angles for the six-pulse TCR were shown in Chapter V to be those giving $\alpha = 100^\circ$; allowing the greatest range of control as the model arc furnace current increases toward the short-circuit value.

The integration limits were set in the twelve-pulse TCR to correspond to $\alpha = 100^\circ$

i.e. $\epsilon = 70^\circ$ and $\alpha = 100^\circ$

Part 6.2 details how these integration limits were set for a steady-state study, and Part 6.3 gives the results of applying the system to the fluctuating model arc furnace load.

6.2 STEADY-STATE TUNING AND PERFORMANCE

The studies performed for the six-pulse TCR compensator in Part 4.3 gave an appreciation of the effects of changing different control variables. The most useful of these was judged to be the 'shunt load TCR compensation' experiment (4.3.3 (ii)) and this was repeated in various forms for the twelve-pulse scheme.

6.2.1 Thyristor Firing and Conduction Limits

The thyristor firing circuitry and isolation transformers were identical to those used for the six-pulse TCR compensator described in Section 4.3.1. The same 8-bit output port was used to transfer firing commands to the pulse stretching and amplification circuitry. The latching circuitry was particularly important for this application, where to apply a long output pulse from the processor would have inhibited integration following first-stage firing.

The SDK88 'SI' register was again used as a counter and incremented through 133 steps, one for each analogue to digital conversion made in the half-cycle. Tables of the reference sinusoids 'sine1' and 'sine2' are not presented here, but may be found at the end of the 'FirBsub.asm' program listing in Appendix K.

This counter 'SI' was again used as a reference for the program to determine whether firing should be allowed, and the values were used to limit ϵ and α to:

$$\begin{aligned} & 60^\circ \leq \epsilon \leq 150^\circ \\ \text{and} & 90^\circ \leq \alpha \leq 180^\circ \end{aligned}$$

The limiting values appear in the program listing (Appendix K).

6.2.2 Steady-State Reactive Compensation Results

The step changes and depression of the model supply line voltage waveform varied according to the firing angles ϵ and α .

Figure 6.6 shows how the open circuit line voltage is depressed by operation of the first-stage unit, with the second stage unit disconnected. The limits required for this steady-state 'open circuit' condition were:

POSLIM1 = 256 dec, @ 0100 NEGLIM1 = 192 dec, @ 00C0

for each of the three systems, giving $\epsilon \approx 70^\circ$.

The corresponding waveforms for second-stage conduction only are given in Figure 6.7. A value of $\alpha \approx 110^\circ$ was obtained with limits set at:

POSLIM2 = 448 dec, @ 01C0 NEGLIM2 = 384 dec, @ 0180

Further tests were performed with the first and second stages acting in isolation from each other to compare the shunt compensation effects of the separate halves of the twelve-pulse TCR system before both stages were used together.

Figure 6.8 shows the steady-state inductive load compensation test circuit, and the V-I characteristics obtained.

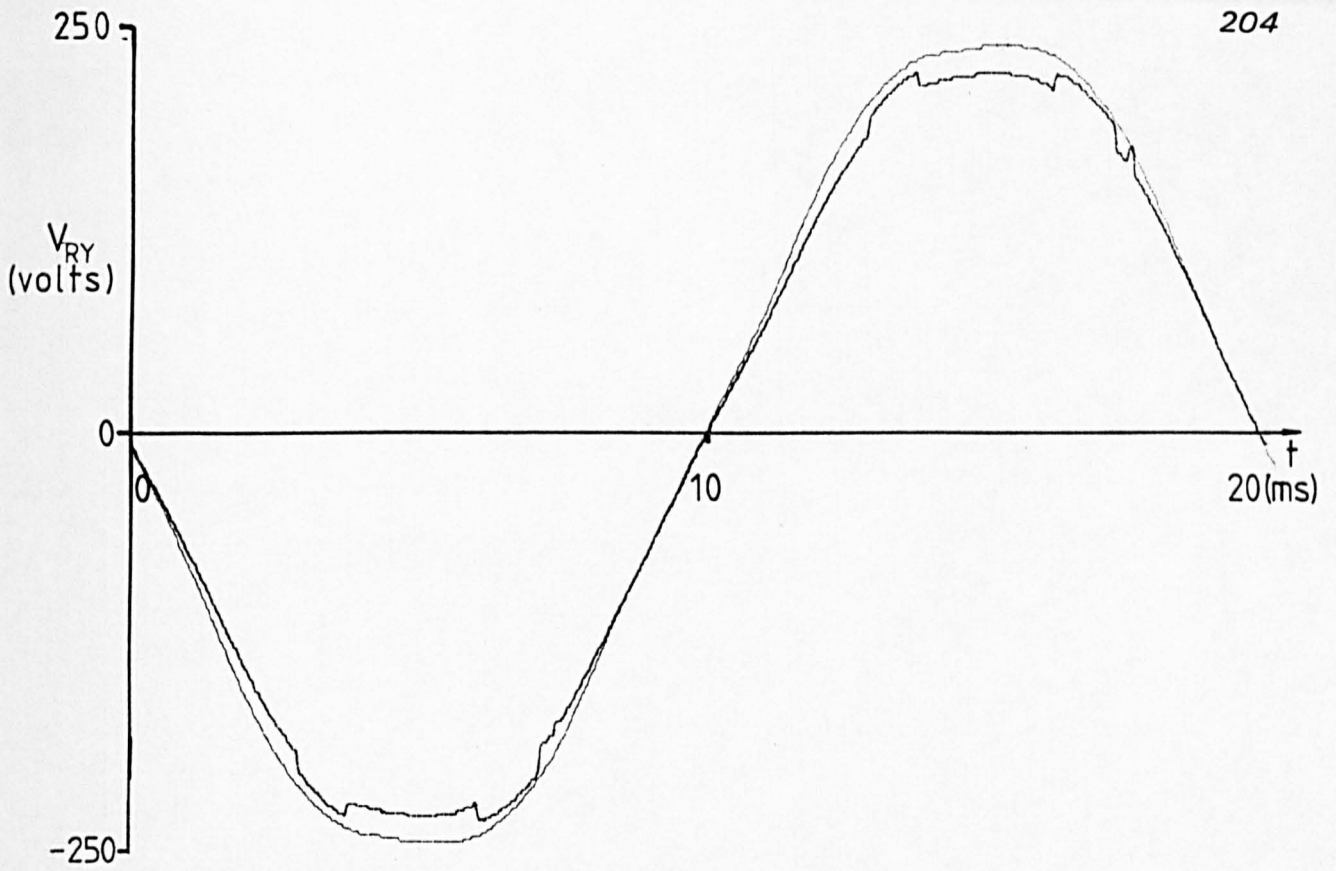


Fig. 6.6 : Line voltage depression for 12-pulse TCR first stage operation

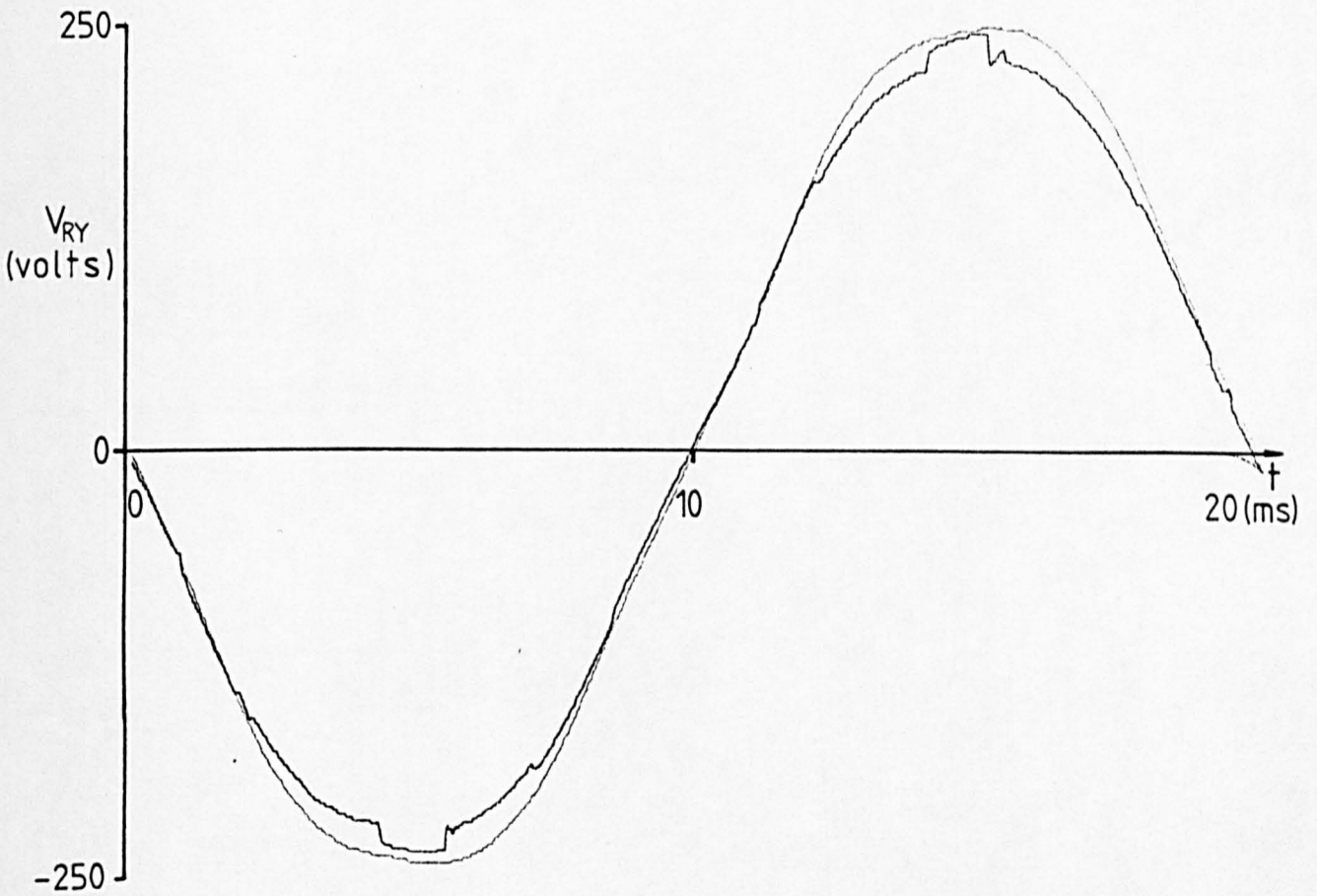


Fig. 6.7 : Line voltage depression for 12-pulse TCR second stage operation

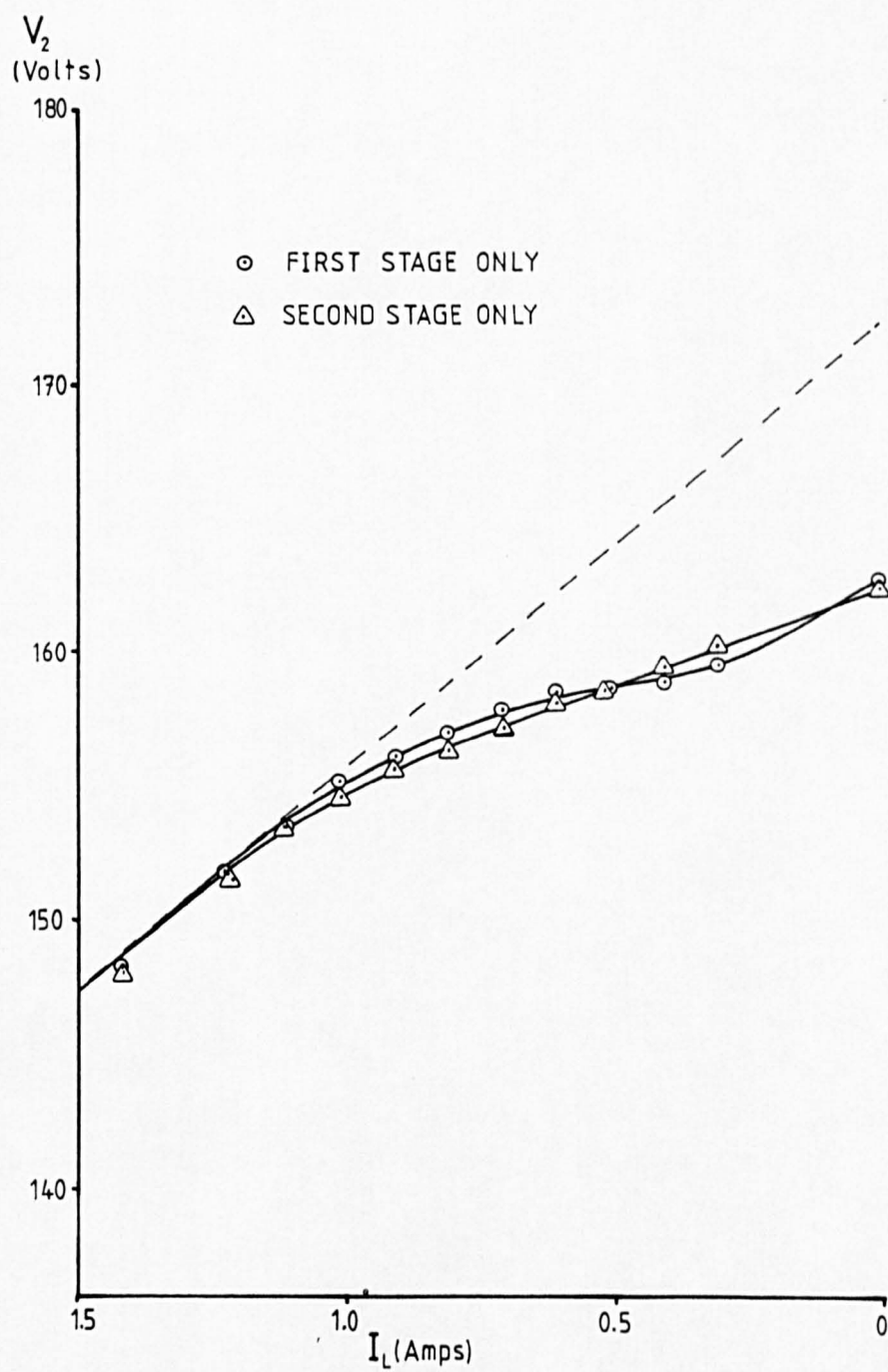


Fig. 6.8 : 12-pulse TCR steady state inductive load shunt compensation V-I characteristic

6.3 TWELVE-PULSE TCR PERFORMANCE WITH THE ARC FURNACE MODEL

Before attempting to operate both stages of the twelve-pulse compensator together, each stage was connected in turn to the laboratory arc furnace model.

The integration limits given in Section 6.2.2 remain applicable, since they were set for the condition where the inductive test load current was zero.

The arc furnace model was operated at its rated value as described in Chapter II, causing the TCR conduction angles to change cycle-by-cycle.

Figures 6.9, 6.10, 6.11 and 6.12 show the change in the line voltage power spectrum caused by operation of only the first-stage of the twelve-pulse TCR. Figures 6.13, 6.14, 6.15 and 6.16 show the spectra corresponding to operation of the second-stage only.

Both stages give a reduction in the 0-50Hz modulation frequency sidebands similar to the results presented for the six-pulse TCR compensator in Chapter V.

Operating both the first- and second-stage units of the twelve-pulse TCR system together required that the integration limits be adjusted in order to keep $\epsilon \approx 70^\circ$ and $\alpha \approx 110^\circ$ for the three-phase system.

The limits set to achieve these firing angles, with no model arc furnace current flowing, are shown in Table 6.1.

Figures 6.17, 6.18, 6.19 and 6.20 show the change in power spectra caused by operation of both stages of the twelve-pulse TCR compensator.

It is apparent that the twelve-pulse system as operated did not achieve as great a reduction in low frequency modulation power as the six-pulse TCR compensator showed. The reasons for the disappointing results may possibly lie in the control strategy used, and this is discussed further in Section 8.1.2.

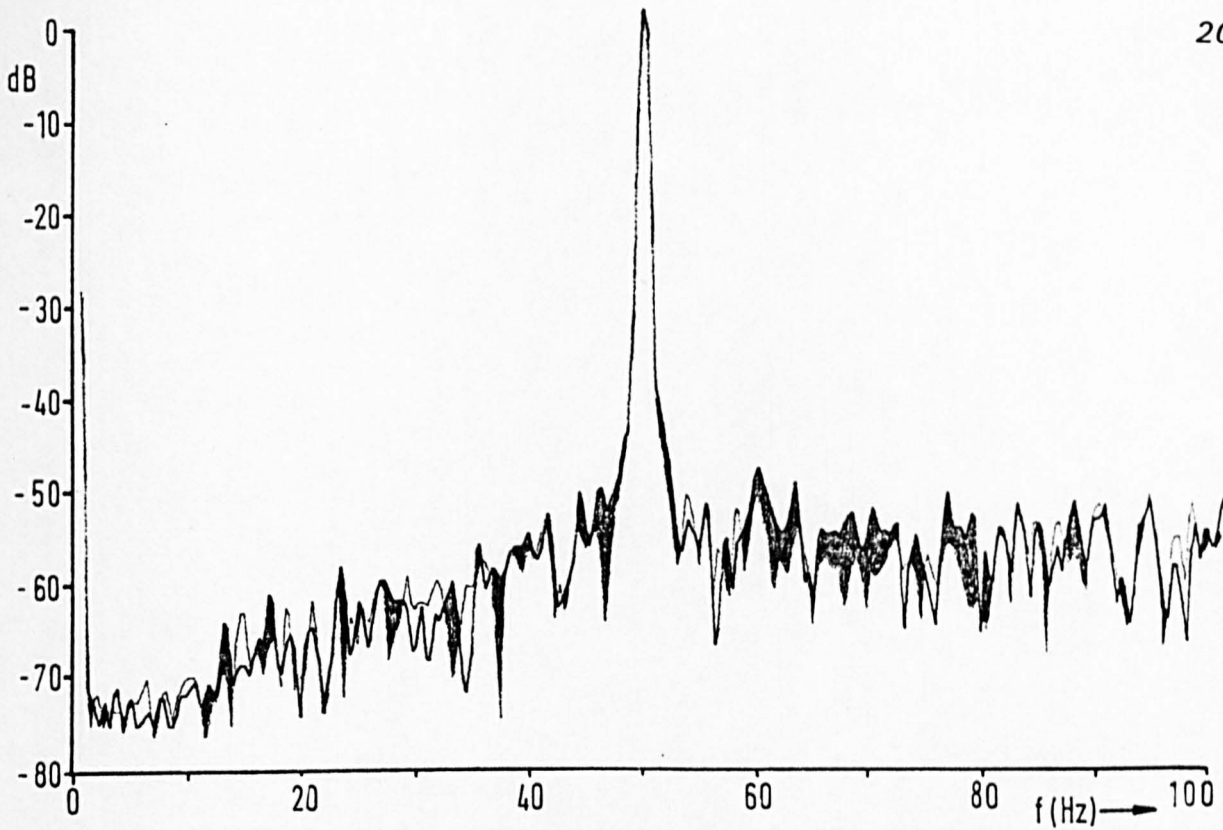


Fig. 6.9 : 0-100Hz power spectrum of Vry showing effect of 12-pulse TCR first stage operation

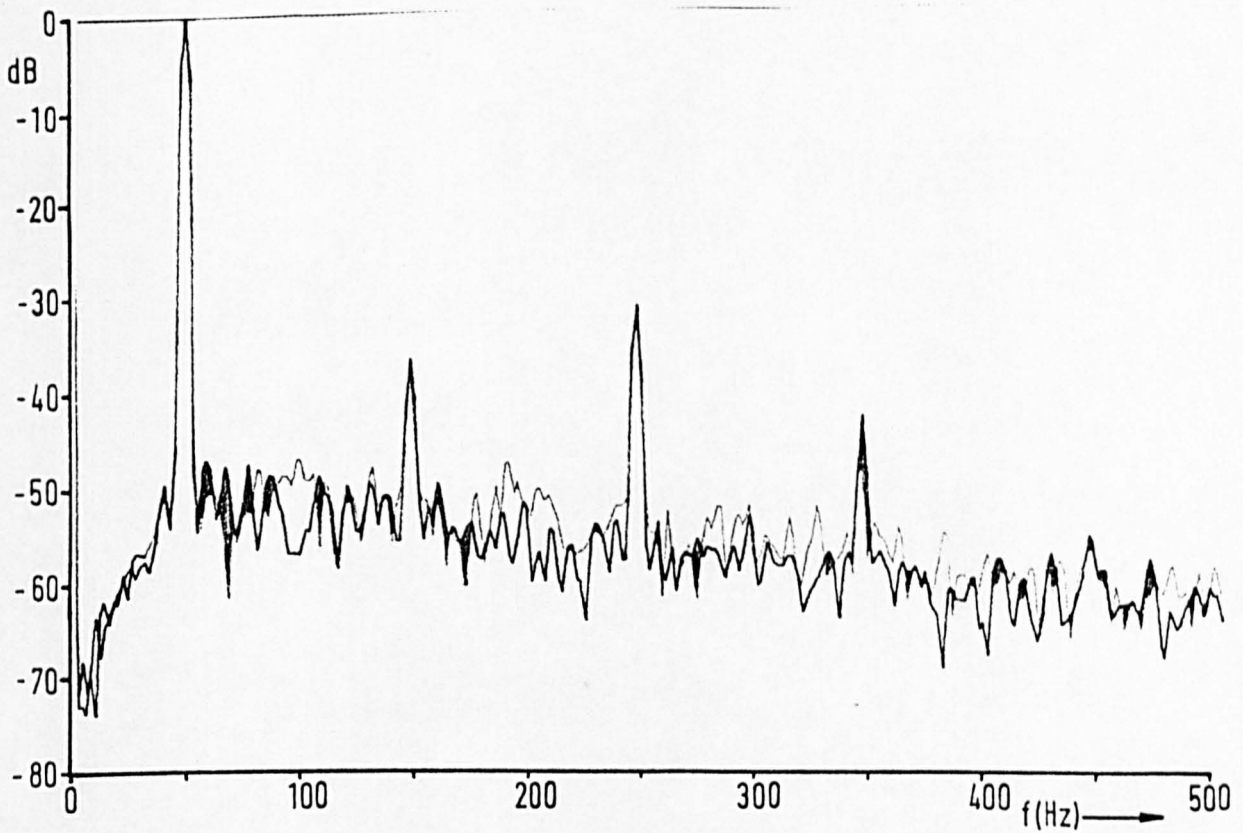


Fig. 6.10 : 0-500Hz power spectrum of Vry showing effect of 12-pulse TCR first stage operation

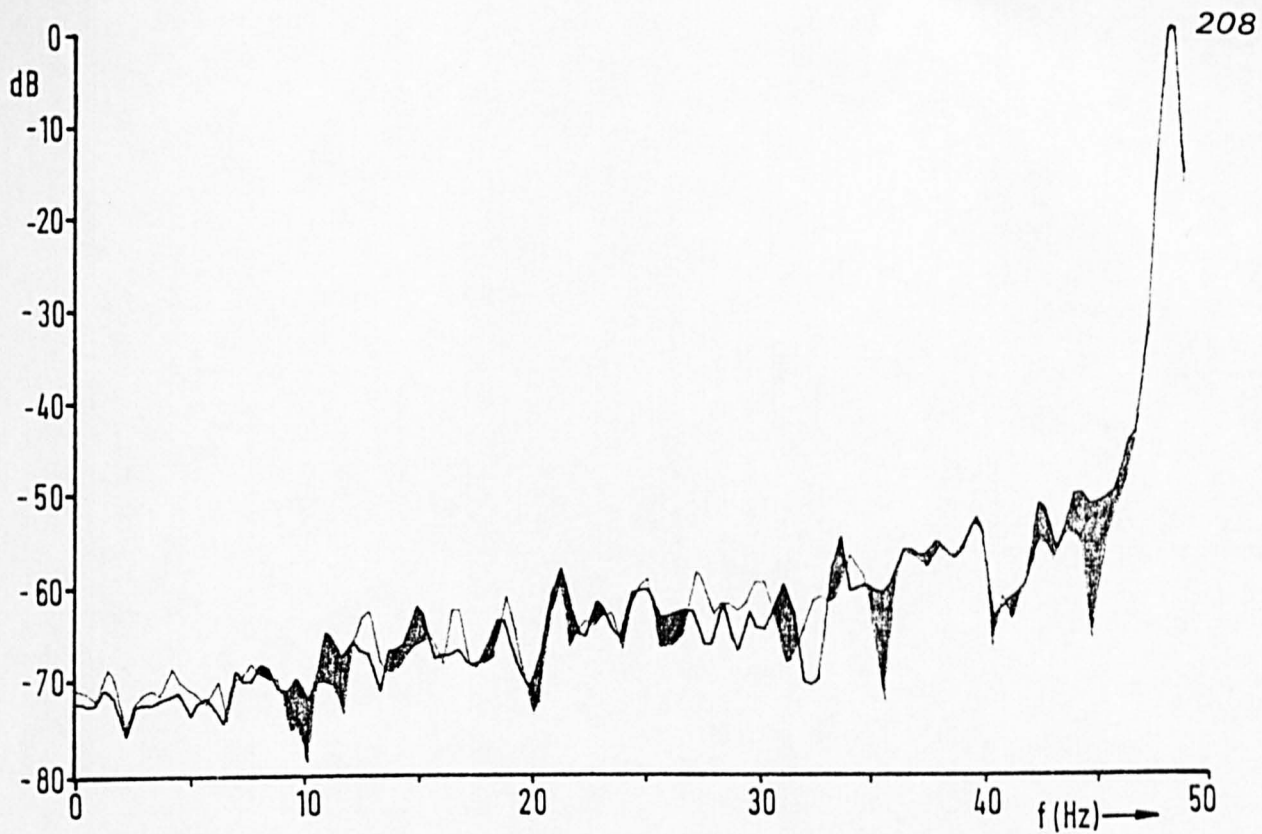


Fig. 6.11 : 0-50Hz power spectrum of Vry showing effect of 12-pulse TCR first stage operation

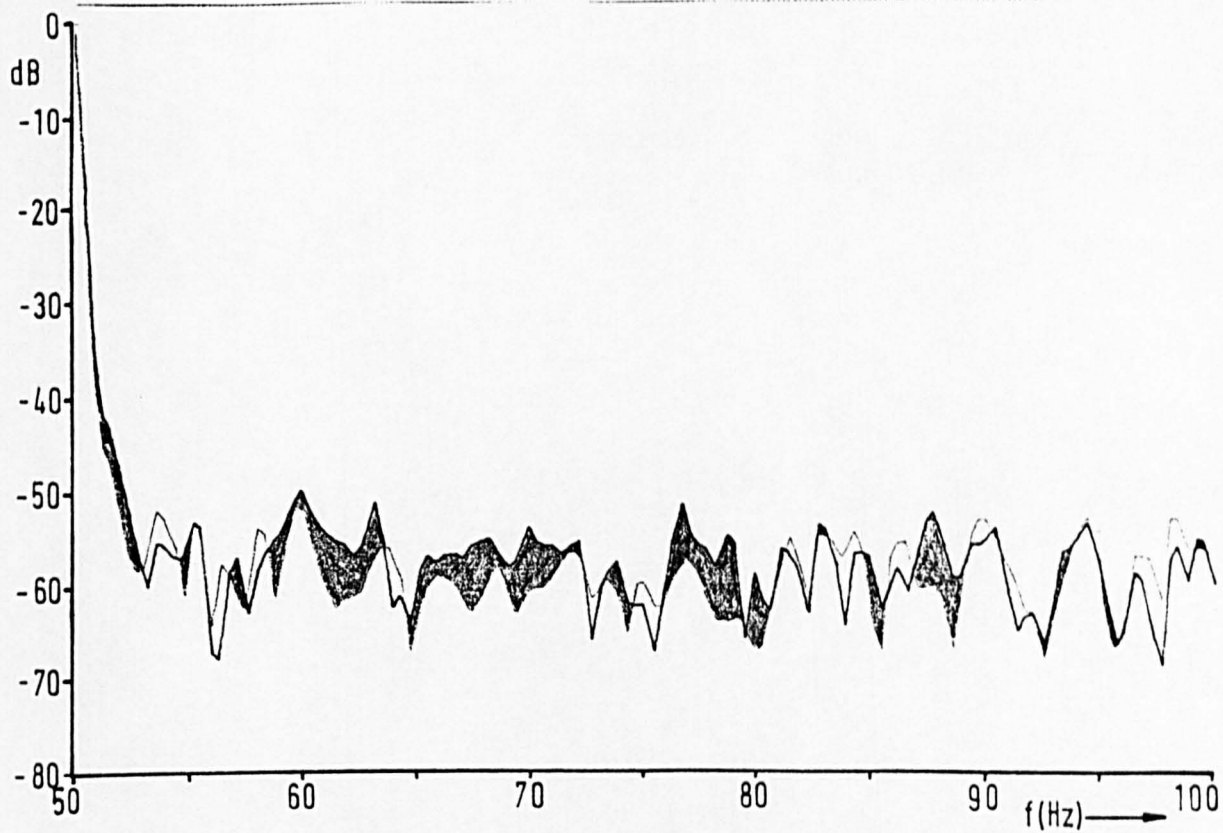


Fig.6.12 : 50-100Hz power spectrum of Vry showing effect of 12-pulse TCR first stage operation

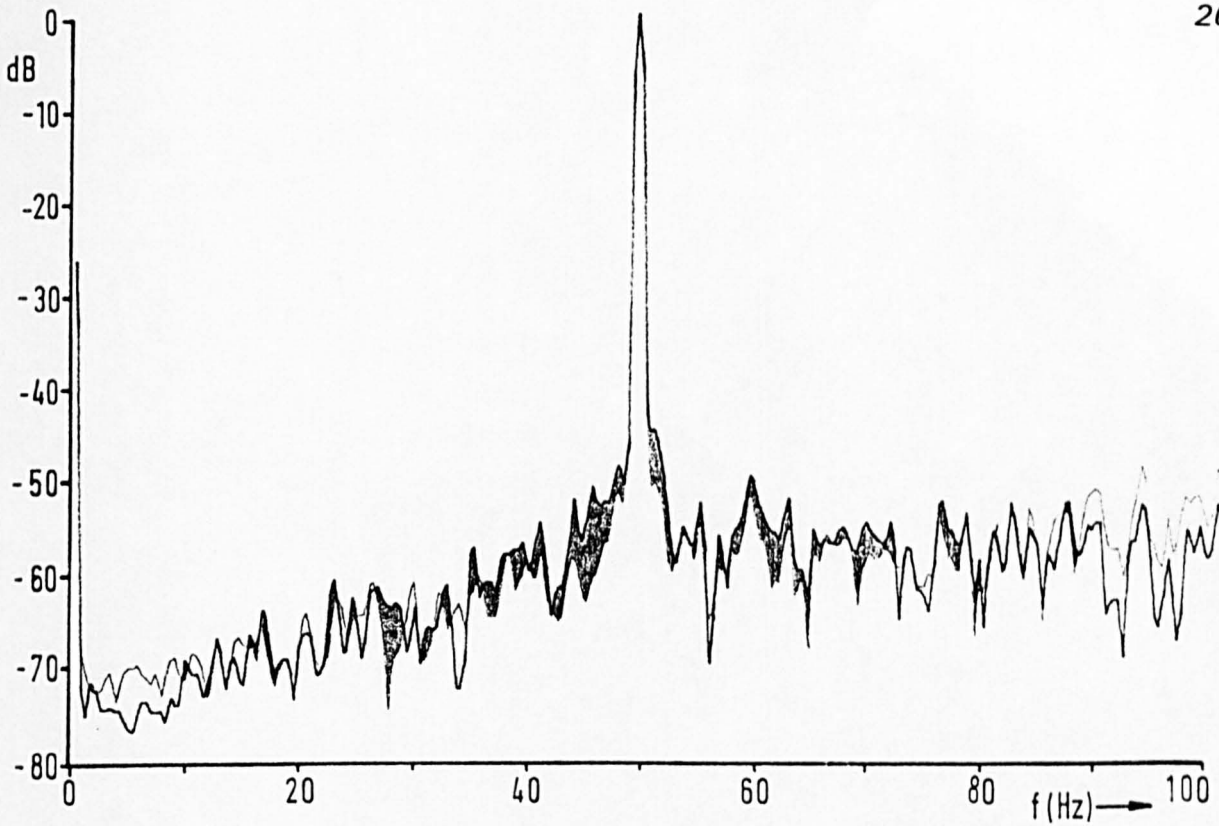


Fig. 6.13 : 0-100Hz power spectrum of Vry showing effect of 12-pulse TCR second stage operation

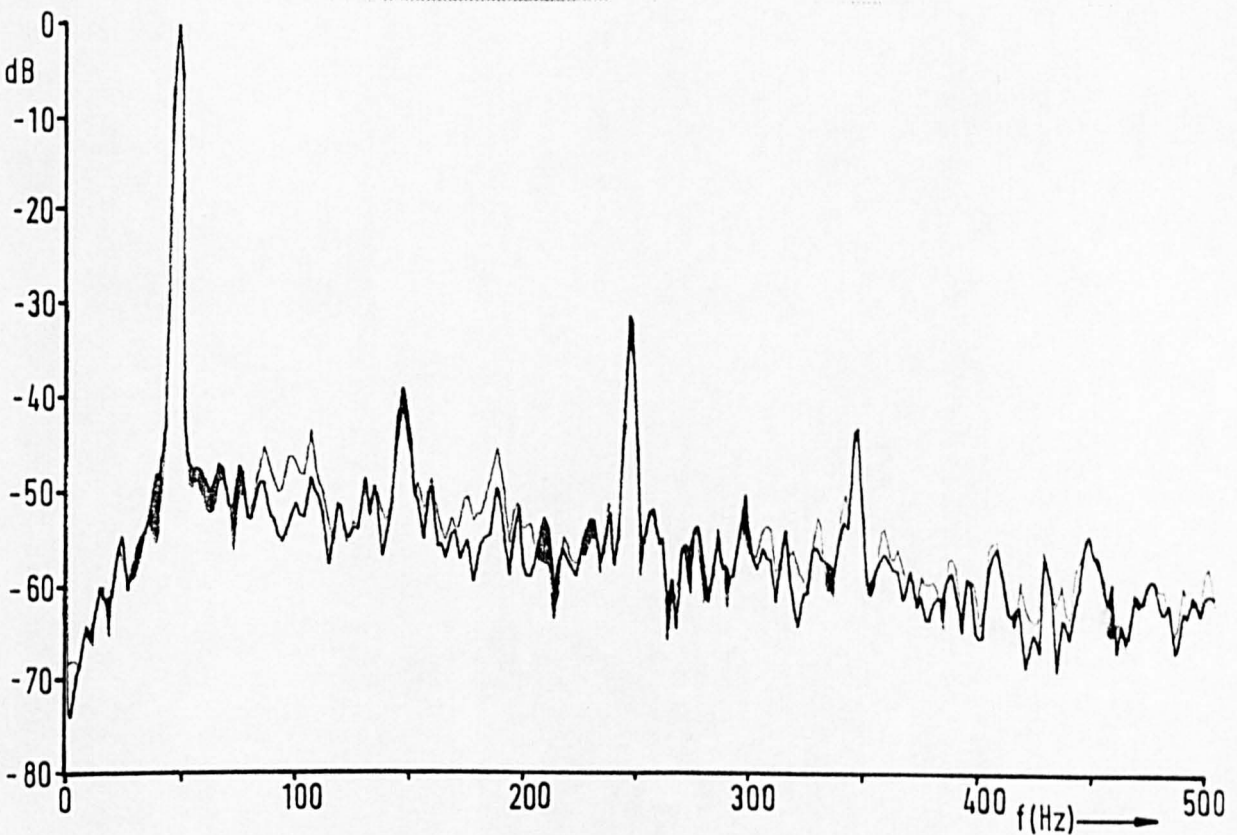


Fig. 6.14 : 0-500Hz power spectrum of Vry showing effect of 12-pulse TCR second stage operation

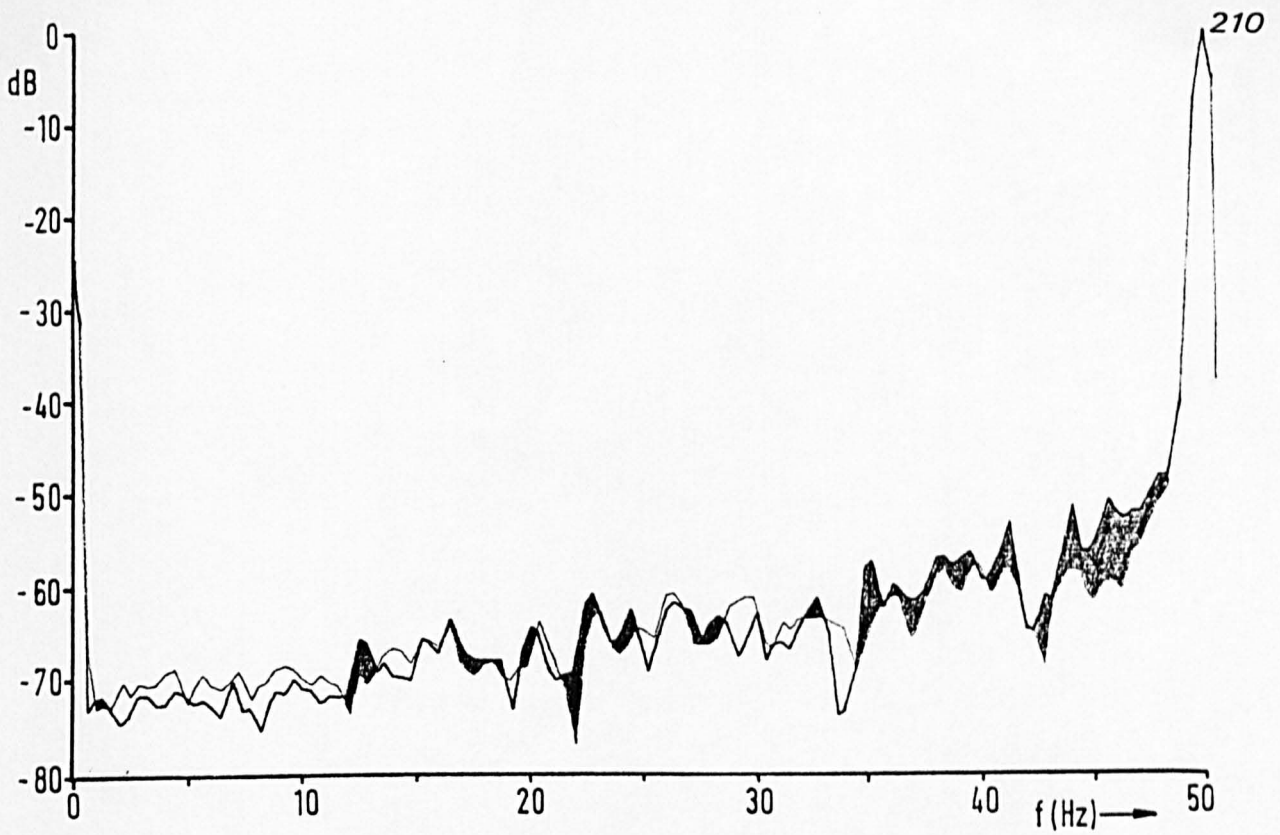


Fig. 6.15 : 0-50Hz power spectrum of Vry showing effect of 12-pulse TCR second stage operation

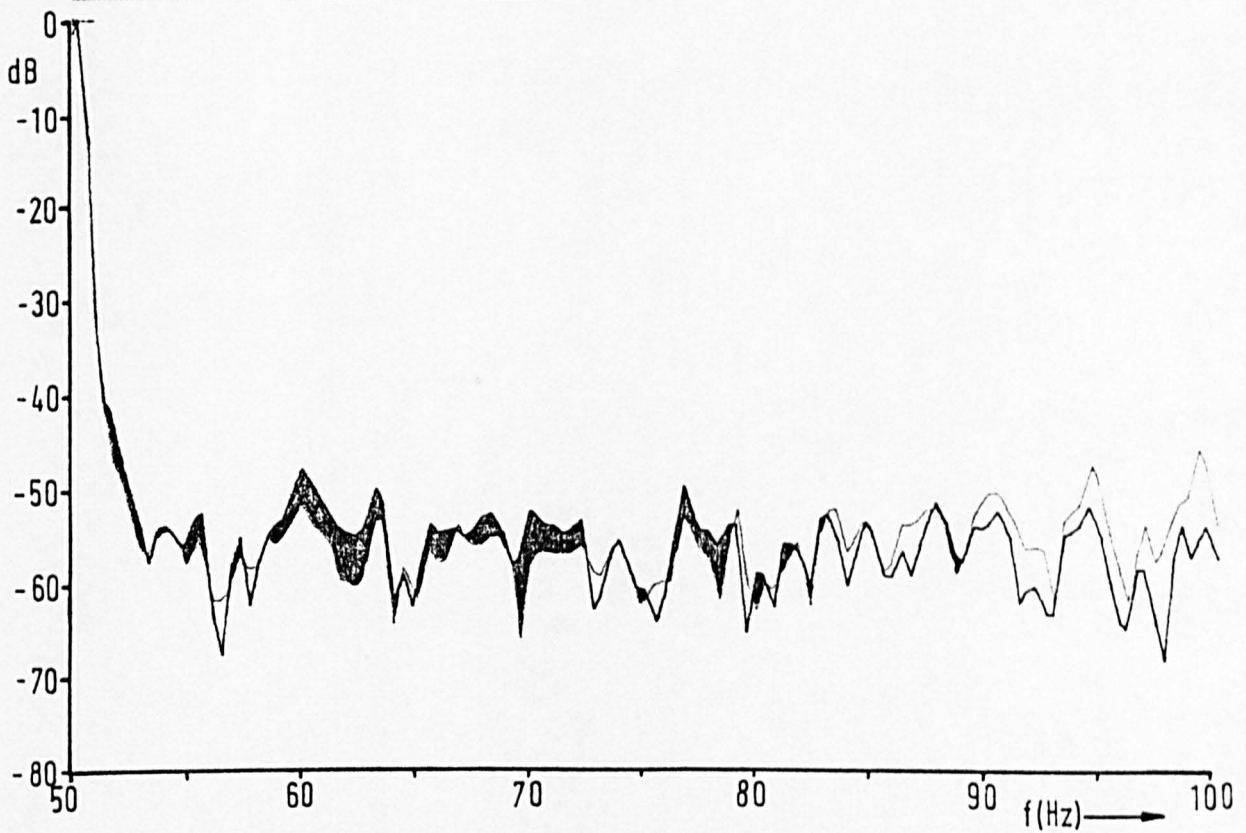


Fig. 6.16 : 50-100Hz power spectrum of Vry showing effect of 12-pulse TCR second stage operation

	SYSTEM 1	SYSTEM 2	SYSTEM 3
POSLIM1	0080	0080	0060
POSLIM2	0120	0120	00B0
NEGLIM1	0060	0020	0020
NEGLIM2	00C0	00B0	0040

Table 6.1 Hexadecimal Integration Limits for the twelve-pulse TCR Compensator

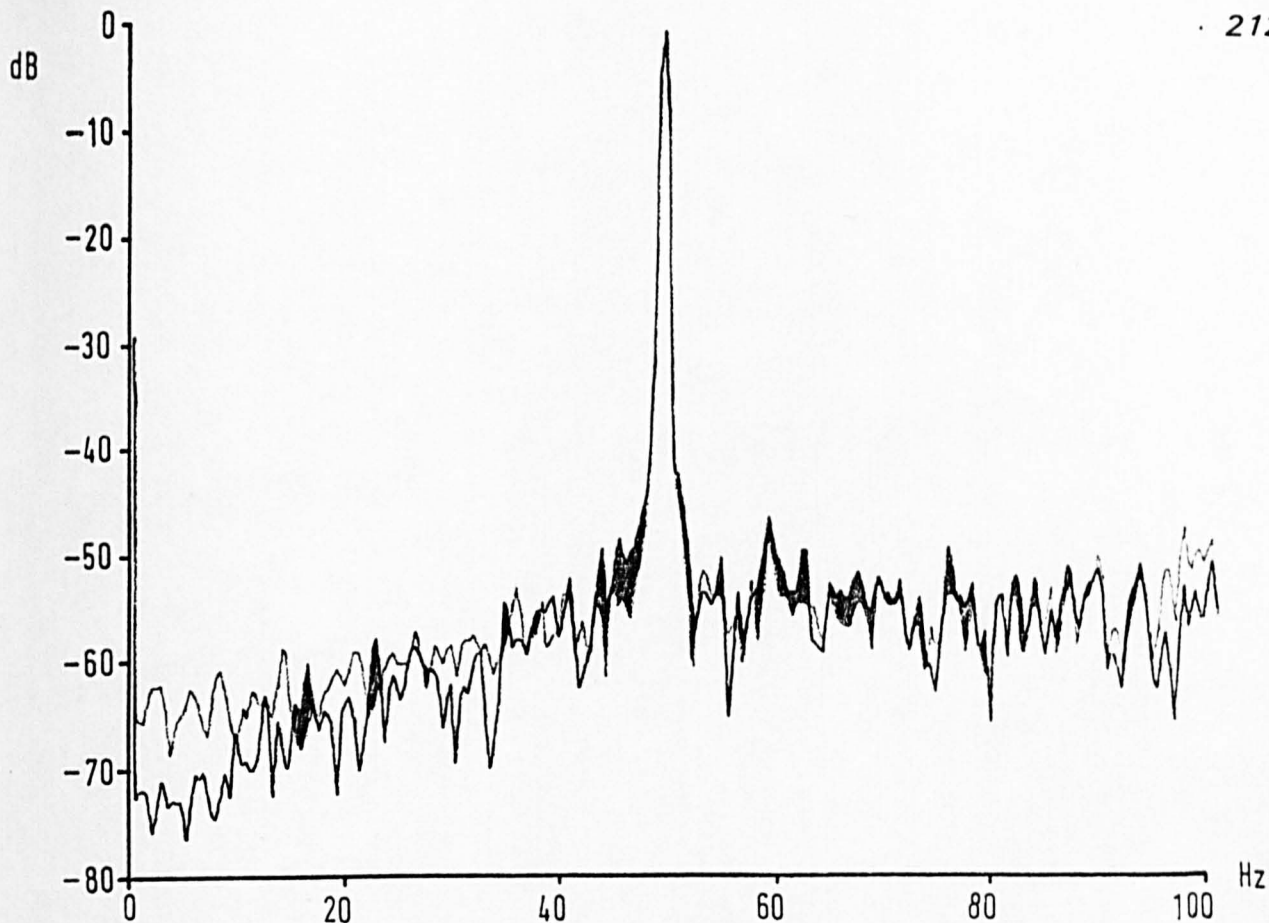


Fig. 6.17 : 0-100Hz power spectrum of Vry showing effect of 12-pulse TCR full operation

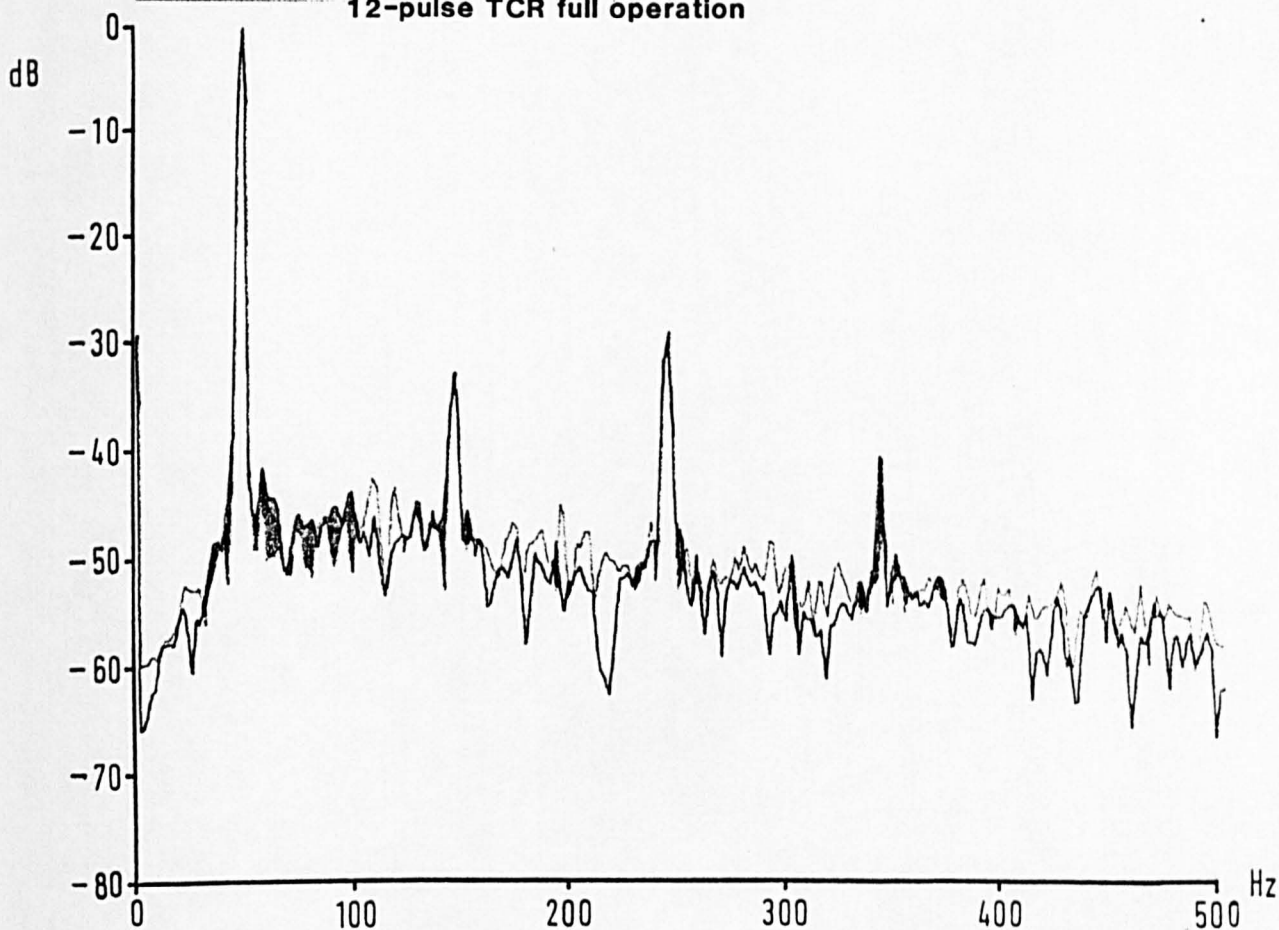


Fig. 6.18 : 0-500Hz power spectrum of Vry showing effect of 12-pulse TCR full operation

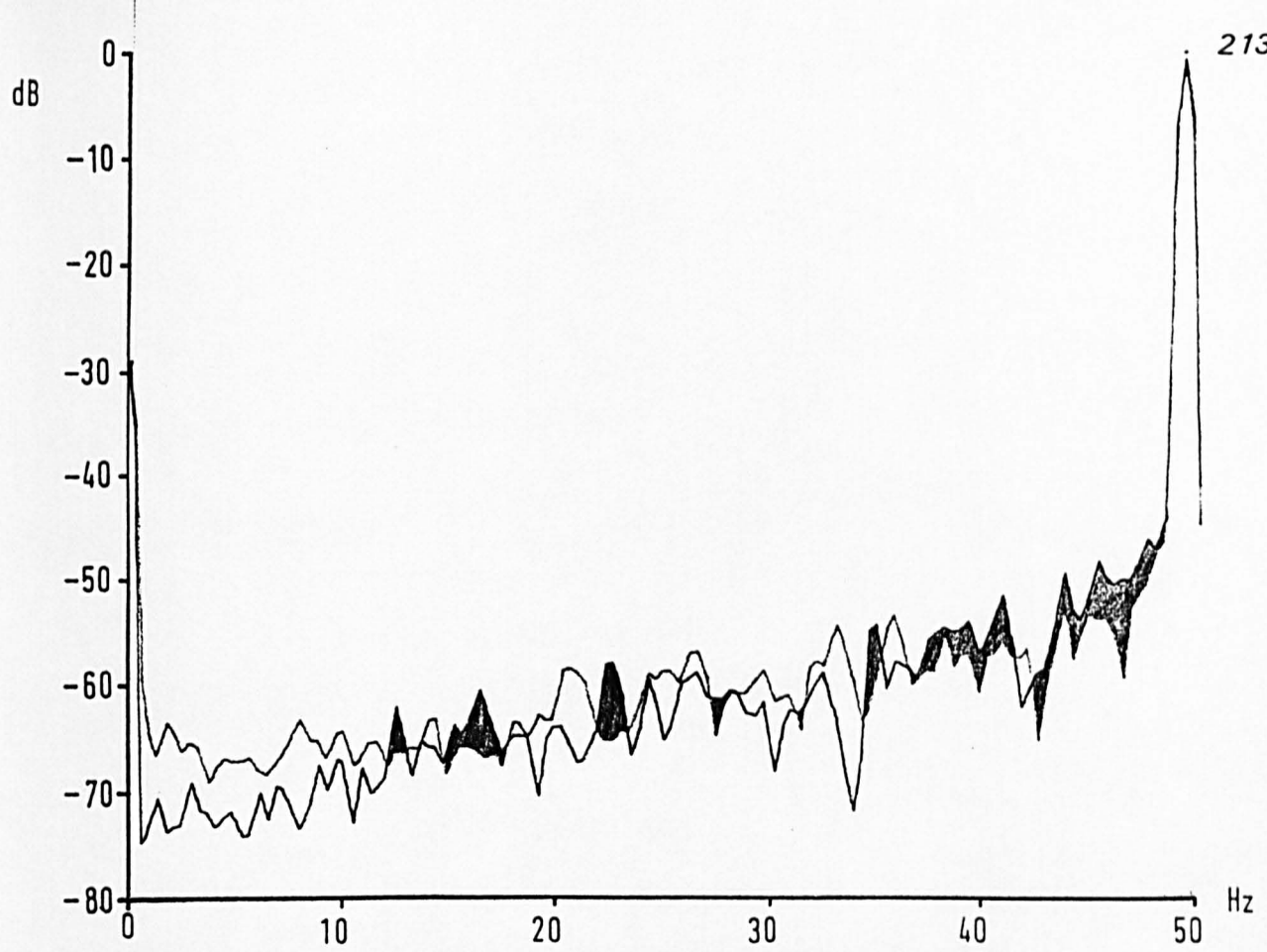


Fig. 6.19 : 0-50Hz power spectrum of Vry showing effect of 12-pulse TCR full operation

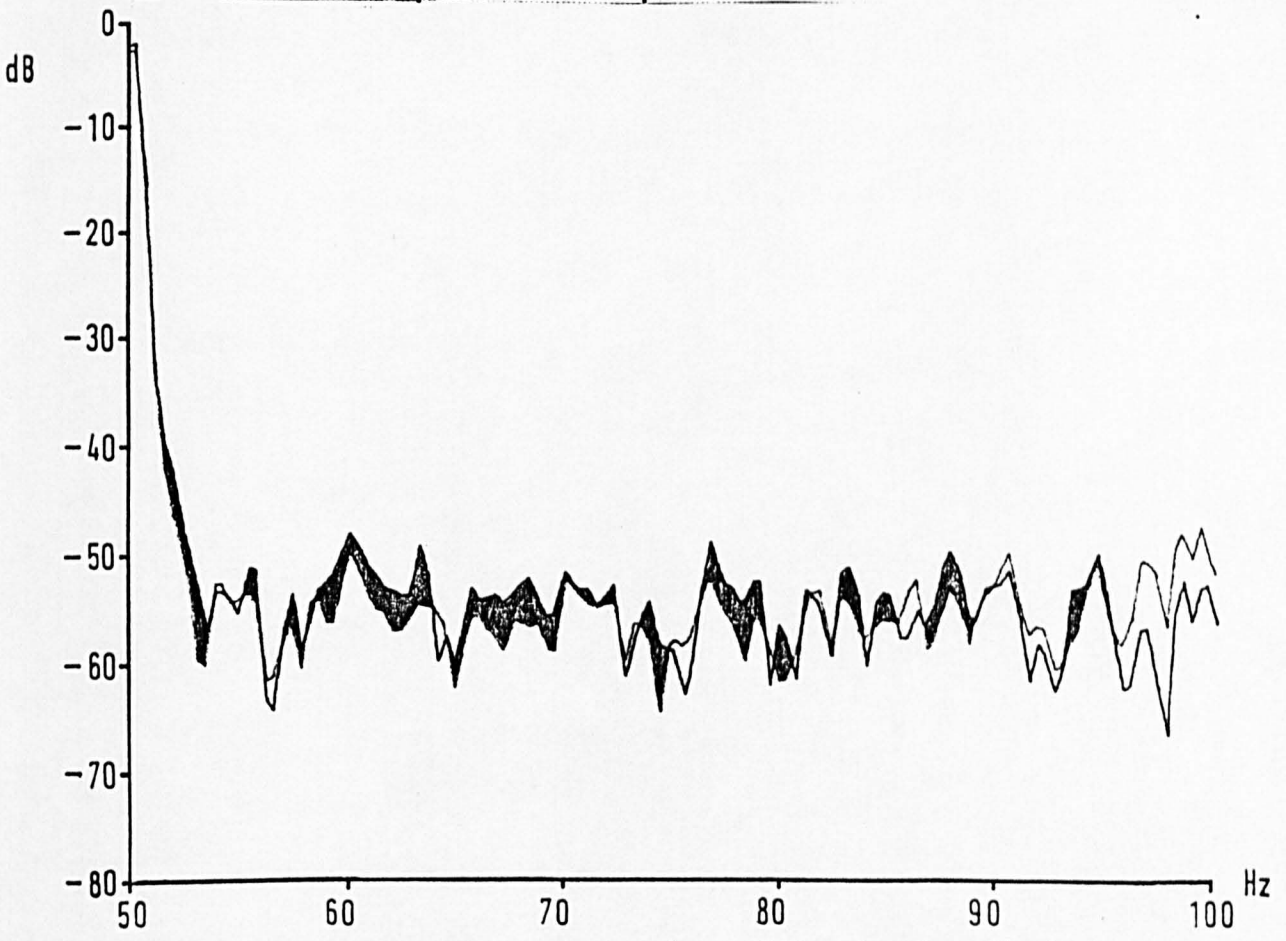


Fig.6.20 : 50-100Hz power spectrum of Vry showing effect of 12-pulse TCR full operation

CHAPTER SEVENCOMPUTATIONAL MODELLING AND ANALYSIS7.1 THE PRINCIPLE OF THE COMPUTATIONAL MODEL

7.1.1 The System to be Modelled

7.1.2 Measured and Calculated Currents and Voltages

7.1.3 Inputs to the Arc Furnace Model

7.1.4 Phase Angle ' δ '7.2 Y- Δ TRANSFORMER CURRENT AND VOLTAGE TRANSFORMATIONS

7.2.1 Current Transformation

7.2.2 Voltage Transformation

7.2.3 Current Derivative Transformation

7.3 PERFORMANCE OF THE COMPUTATIONAL ARC FURNACE MODEL

7.3.1 Results Comparison Using Power Spectra

7.3.2 Results Comparison in the Time Domain

7.3.3 Demodulation

7.4 COMPUTATIONAL MODELLING OF A TCR COMPENSATOR

7.4.1 TCR Compensator Circuit Definitions

7.4.2 The Differential Equations of Compensator Currents

7.4.3 Step-by-Step Solution of Compensator Differential Equations

7.4.4 Compensator Control

7.4.5 Results from the Computer Model Compensator

7.1 THE PRINCIPLE OF THE COMPUTATIONAL MODEL

As the Templeborough arc furnace installation and its supply (Part 2.2) were modelled physically in the laboratory (Part 2.3), it was a parallel aim of this research project to construct a digital model. The main benefits of such a model would be found in the study of various compensator arrangements and their control. This could be achieved prior to the construction of such systems in the laboratory.

The approach to the digital modelling was essentially simple: Values of current measured at the installation would be used to calculate volt-drops across known impedances. The voltage at any point in the network would thus be known with respect to some reference. Additional currents due to compensator connection would suitably modify the calculated voltages.

The details of such a technique are studied below.

7.1.1 The System to be Modelled

Chapter II, Part 2, describes the Templeborough system in detail, and shows how the impedance of the supergrid transformer SGT4 dominates in the supply impedance to the 33kV furnace busbar. The transformer windings were connected Y primary and Δ secondary. If per unit (p.u.) values are maintained the transformer voltage ratio need not concern us.

The form of the measured current waveforms is extremely non-sinusoidal (Figure 2.3), and a step-by-step solution of circuit equations required instantaneous circuit equations rather than a treatment for RMS quantities.

The impedances for the supply system were given in Section 2.2.1 as percentage values to a 100MVA base. Referring all impedances to 33kV gives $Z_{\text{base}} = 10.89$ Ohms and the following ohmic impedances for the supply system at 50Hz:

$$\begin{aligned}
 Z_{\text{tot}} &= (0 \quad + j0.1307) \text{ Ohms} && 275\text{kV Supply} \\
 &+ (0.0565 \quad + j2.595) \text{ Ohms} && \text{SGT4} \\
 &+ (0.00218 \quad + j0.01089) \text{ Ohms} && 33\text{kV Cable}
 \end{aligned}$$

$$\therefore Z_{\text{tot}} = 0.0587 + j2.737 \text{ Ohms}$$

The total 50Hz inductance of the system is then 8.711 millihenries.

The three phase resistance and inductance network is shown in Figure 7.1. For balanced sinusoidal conditions the RMS values of i_1, i_2, i_3, i_4, i_5 , and i_6 would be equal, and a one-line diagram would suffice. For this study of instantaneous unbalanced currents, all three primary and secondary circuits must be considered.

7.1.2 Measured and Calculated Currents and Voltages

The line currents corresponding to i_R, i_Y and i_B in Figure 7.1, and the phase voltages at those points, were measured and recorded by the CEGB (see Section 2.2.2 and Appendix B). The Δ -Y transformation described in Section 7.2 yields i_1, i_2 and i_3 . The knowledge of these current values allows resistive volt drop to be calculated, and the value of di/dt at the same instant (see Section 8.3.2) may be used to obtain the values of voltages at all points in the network using:

$$\Delta V = Ri + L \frac{di}{dt}$$

for each branch.

Figure 7.2 gives the notation used to refer to currents and voltages at different points of the network. At this stage i_4, i_5, i_6 and derivatives are equal to i_R, i_Y, i_B and derivatives.

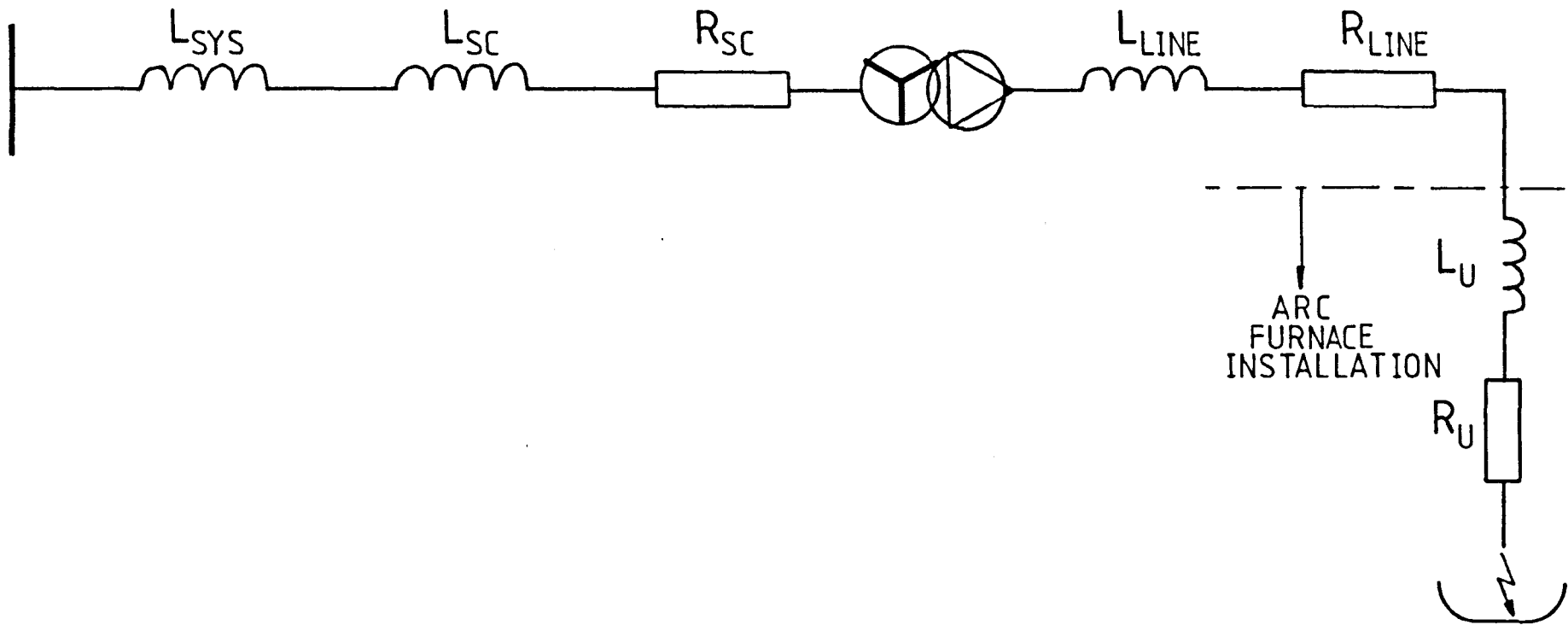


Fig. 7.1 : The resistance and inductance network for the computational model

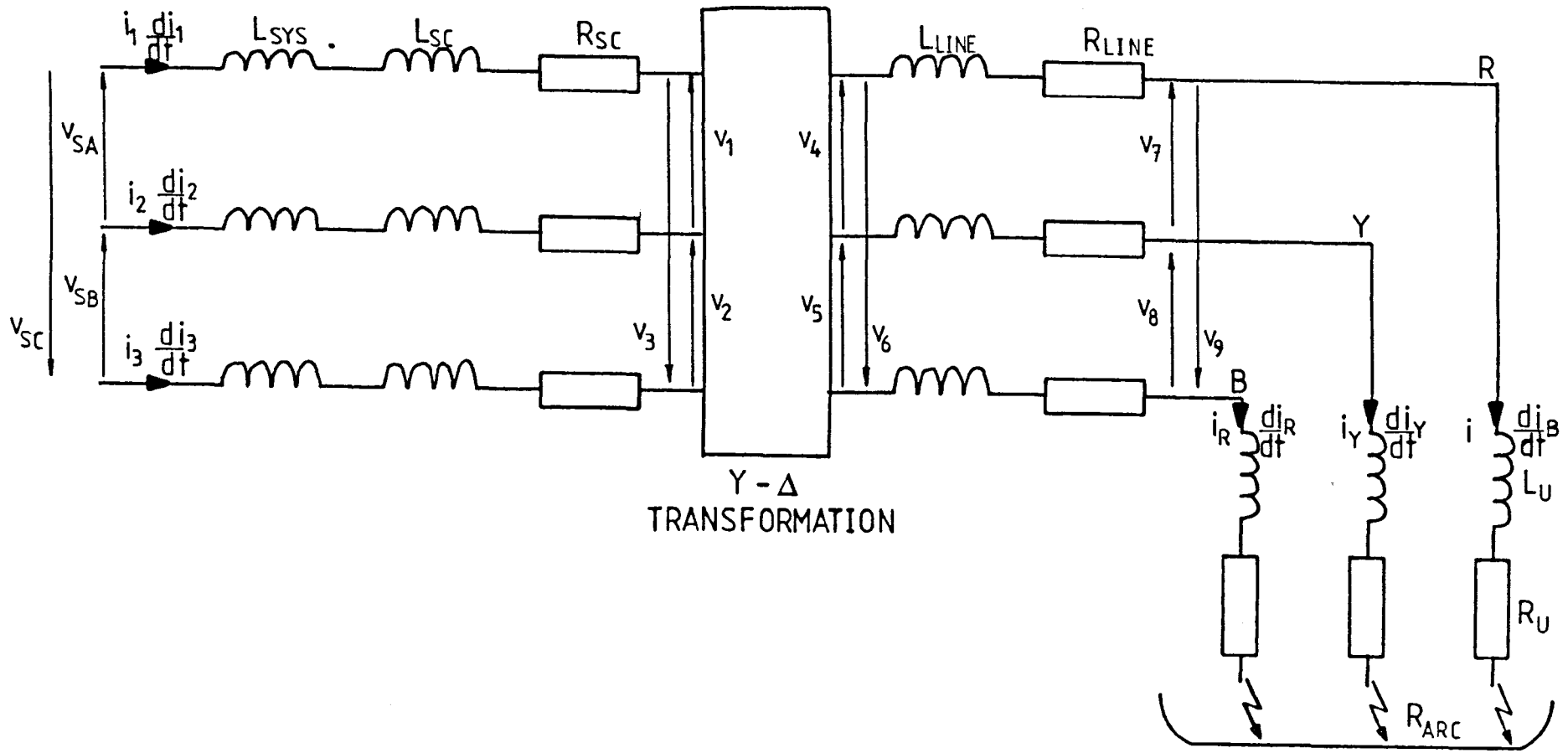


Fig. 7.2 : Definition of network voltages and currents

A step-by-step computational process was then used with the recorded furnace currents as the driving function. The same span of data as used for the physical laboratory model was used, without cubic spline interpolation between recorded values of current. The currents i_1, i_2, i_3 and their derivatives may be calculated from i_4, i_5, i_6 and their derivatives, via the Δ -Y current transformation (see Section 7.2). Then the voltages v_1, v_2, v_3 may be found at each step by subtracting a calculated voltage drop from the sinusoidal infinite busbar voltages v_{S1}, v_{S2} and v_{S3} .

$$\text{i.e. } \begin{bmatrix} v_1 \\ v_2 \\ v_3 \end{bmatrix} = \begin{bmatrix} v_{S1} \\ v_{S2} \\ v_{S3} \end{bmatrix} - R_{SC} \begin{bmatrix} i_1 \\ i_2 \\ i_3 \end{bmatrix} - (L_S + L_{SC}) \frac{d}{dt} \begin{bmatrix} i_1 \\ i_2 \\ i_3 \end{bmatrix}$$

$$\begin{aligned} \text{Where } v_{S1} &= V_S \sin \omega t \\ v_{S2} &= V_S \sin(\omega t + 2\pi/3) \\ v_{S3} &= V_S \sin(\omega t - 2\pi/3) \end{aligned}$$

$$\text{and } \omega = 100\pi$$

The Y- Δ voltage transformation from Section 7.2 then yields v_4, v_5 and v_6 , and:

$$\begin{bmatrix} v_7 \\ v_8 \\ v_9 \end{bmatrix} = \begin{bmatrix} v_4 \\ v_5 \\ v_6 \end{bmatrix} - R_{CAB} \begin{bmatrix} i_4 \\ i_5 \\ i_6 \end{bmatrix} - L_{CAB} \frac{d}{dt} \begin{bmatrix} i_4 \\ i_5 \\ i_6 \end{bmatrix}$$

It is the 'flicker voltage' component of v_7, v_8 and v_9 that may be reduced by the addition of a suitable compensating network to modify i_4, i_5 and i_6 . This is studied further in Part 7.4.

The computational process was carried out for each of the 2225 sequential samples in the 89 cycles used. The real time sampling interval of 800 microseconds was not relevant to the computational process.

The program to model the supply system carrying arc furnace currents was written in the FORTRAN language, and the full program listing is given in Appendix J. Comment statements within the listing explain its operation.

7.1.3 Inputs to the Arc Furnace Model

The main FORTRAN program, SYSMOD6 (Appendix J) was stored in compiled form, and run repeatedly with varying input parameters read from files of data set up for input to the program. The system, and files used, is described further in Appendix J.

The main requirement for the operation of the arc furnace numerical model is the accurate time-series data for arc furnace three-phase line currents and their first derivatives. A further three channels were used to input the recorded three-phase voltages for comparison with calculated values, giving:

CHANNEL:	1	2	3	4	5	6	7	8	9
INPUT:	v_R	v_Y	v_B	i_B	i_R	i_Y	$\frac{di_B}{dt}$	$\frac{di_R}{dt}$	$\frac{di_Y}{dt}$

The first derivatives of line current were calculated using the cubic spline fitting routines described in Appendix C. A further input file, 'SYSMOD OPTION', contained the required settings for program flow bit settings, results formats and iteration loop limits.

7.1.4 The Phase Angle ' δ '

When the current drawn by the arc furnace installation is low, the voltages $v_{7,8,9}$ will be practically in phase with the supply voltages $v_{S1,S2,S3}$. The circuit impedance is dominantly inductive, and as the current drawn from the supply increases so $v_{7,8,9}$ will lag $v_{S1,S2,S3}$ by an increasing amount.

The CEGB recordings of current, $i_{R,Y,B}$, were accompanied by simultaneous recordings of phase voltage, $v_{R,Y,B}$. The voltage recordings were used to generate line voltage values $v_{RY,YB,BR}$ for comparison with the calculated values $v_{7,8,9}$. The recordings alone give no indication of the phase of the recorded currents relative to infinite busbar voltage. The varying phase angle which may be observed between $i_{R,Y,B}$ and $v_{R,Y,B}$ is a function of the changing value of the unknown impedance Z_U (see Figure 3.10).

where
$$Z_U = R_{ARC} + R_U + jX_U$$

The values of $i_{R,Y,B}$ and $v_{7,8,9}$ will both vary in phase relative to $v_{S1,S2,S3}$; and a nominal angle of ' δ ' radians may be attached to the difference between the first zero crossings of i_R and v_{S1} .

Running the full program for each of the 2225 points will generate the calculated values of $v_{7,8,9}$ for 89 cycles. If ' δ ' has been set incorrectly then $v_{7,8,9}$ will be out of phase with the voltage $v_{RY,YB,BR}$ obtained from the recordings. This phase error was used to adjust ' δ ' iteratively until the error magnitude was reduced below a set average limit of 0.1 radians per cycle, giving

$$' \delta ' = -0.235 \text{ radians}$$

which is a phase angle of 14 degrees.

7.2 Y-Δ TRANSFORMER CURRENT AND VOLTAGE TRANSFORMATIONS

Figure 7.3(a) shows the primary and secondary currents and voltages at the terminals of a Y-Δ transformer, and gives a notation to be used for the winding voltages and currents where necessary.

Figure 7.3(b) shows the coil sense notation to be used.

7.2.1 Current Transformation

The star point of the load on the secondary windings is the arc furnace melt pool. The melt pool is insulated from surrounding metal work by refractory brick, and there is no 'neutral' return to the Δ winding. Therefore there can be no zero sequence component in the secondary circuit, and:

$$\begin{aligned} i_X + i_Y + i_Z &= 0 \\ \text{and} \quad i_4 + i_5 + i_6 &= 0 \end{aligned}$$

$$\text{If} \quad v_1 = Nv_4$$

Then $v_4 = \frac{\sqrt{3}}{N} v_B$ and $i_Y = \frac{N}{\sqrt{3}} i_2$, where N is the turns ratio.

For the secondary circuit:

$$\begin{aligned} i_4 &= i_Y - i_X \\ i_5 &= i_Z - i_Y \\ i_6 &= i_X - i_Z \end{aligned}$$

Giving,

$$i_X = \frac{i_6 - i_4}{3}; \quad i_Y = \frac{i_4 - i_5}{3}; \quad i_Z = \frac{i_5 - i_6}{3}$$

Using the vectors

$$I_{XYZ} = \begin{bmatrix} i_X \\ i_Y \\ i_Z \end{bmatrix} \quad \text{and} \quad I_{456} = \begin{bmatrix} i_4 \\ i_5 \\ i_6 \end{bmatrix}$$

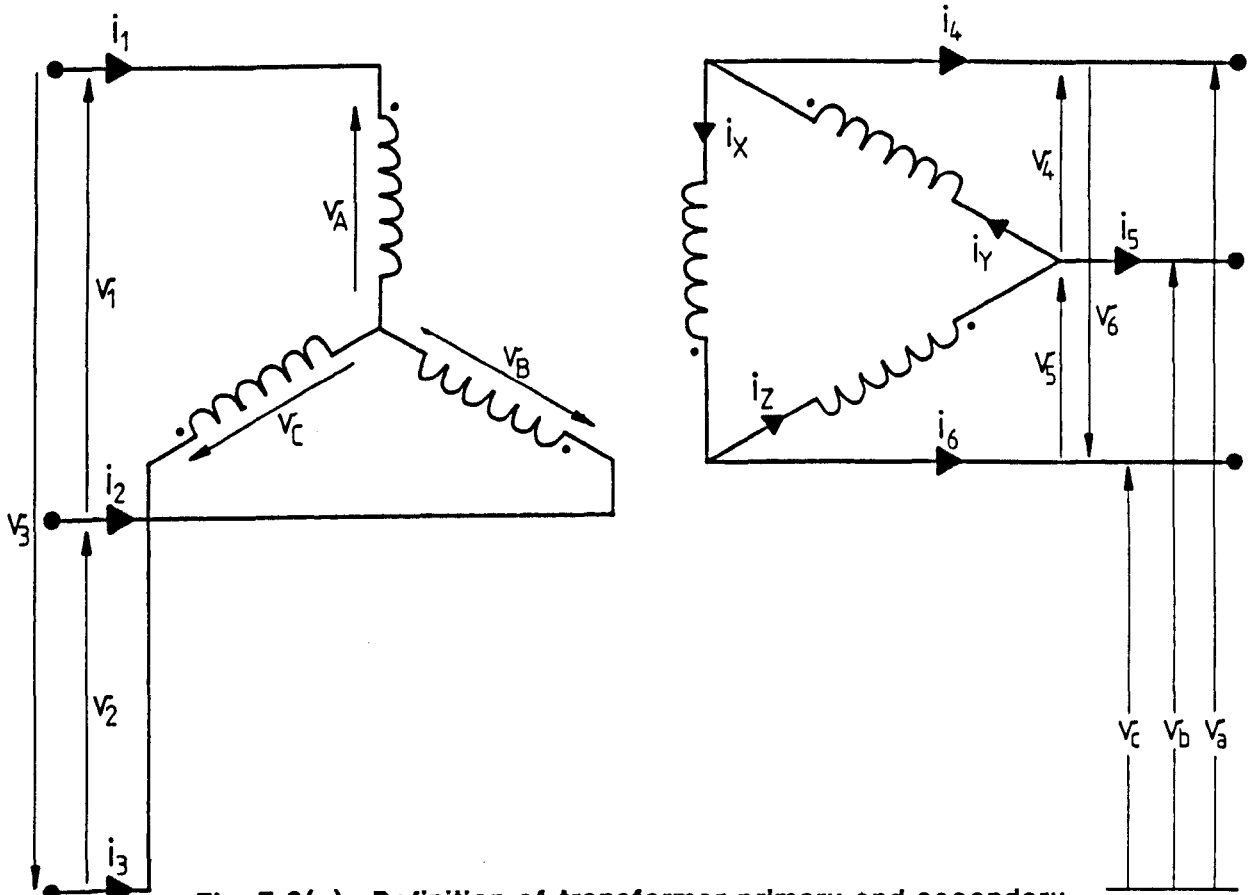


Fig. 7.3(a) : Definition of transformer primary and secondary winding voltages and currents

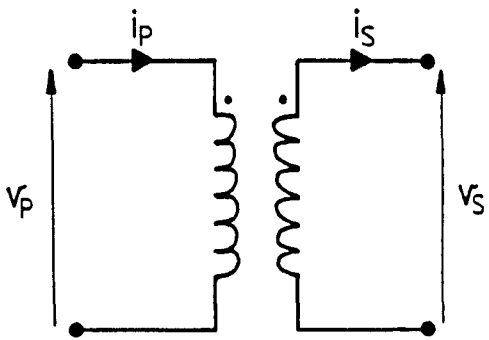


Fig. 7.3(b) : Transformer winding voltage - current conventions

We have,

$$I_{XYZ} = \frac{1}{3} [C] I_{456}$$

where [C] is the matrix
$$\begin{bmatrix} -1 & 0 & 1 \\ 1 & -1 & 0 \\ 0 & 1 & -1 \end{bmatrix}$$

But, $I_{123} = \frac{\sqrt{3}}{N} I_{XYZ}$, where N is the turns ratio.

Then, for $N = 1$,

$$\underline{I_{123} = \frac{1}{\sqrt{3}} [C] I_{456}}$$

It may also be shown that, for $N = 1$,

$$I_{456} = [C_t] I_{123}$$

where $[C_t]$ is the transposed matrix of [C].

7.2.2 Voltage Transformation

Using the vector and matrix notation for

$$V_{ABC} = \begin{bmatrix} v_A \\ v_B \\ v_C \end{bmatrix}, \quad V_{123} = \begin{bmatrix} v_1 \\ v_2 \\ v_3 \end{bmatrix} \quad \text{and} \quad V_{645} = \begin{bmatrix} v_6 \\ v_4 \\ v_5 \end{bmatrix}$$

then,

$$V_{ABC} = \frac{1}{3} [C] V_{123}$$

But,

$$V_{645} = \frac{\sqrt{3}}{N} V_{ABC} \quad \text{where N is the turns ratio.}$$

Then, for $N = 1$,

$$\underline{V_{645} = \frac{1}{\sqrt{3}} [C] V_{123}}$$

It may also be shown that, for $N = 1$,

$$V_{123} = -\sqrt{3} [C_t] V_{645}$$

$$V_{abc} = \frac{1}{\sqrt{3}} [C_t] V_{ABC}$$

and $V_{ABC} = \sqrt{3} [C] V_{abc}$

where $[C_t]$ is the transposed matrix of $[C]$.

7.2.3 Current Derivative Transformation

For each of the primary-secondary coil pairs as shown in Figure 7.3(b) the mutual inductance, M , relates voltage and current such that:

$$V_p = -M \frac{dI_s}{dt} \quad \text{and} \quad V_s = -M \frac{dI_p}{dt}$$

Giving,

$$\frac{-V_p}{dI_s/dt} = \frac{-V_s}{dI_p/dt} = M$$

For $N = 1$, $I_s = I_p$

$$V_s = V_p$$

and $\frac{dI_s}{dt} = \frac{dI_p}{dt}$

The current transformations established in Section 7.2.1 therefore hold for the first order differentials of I_{123} , I_{456} and I_{XYZ} .

7.3 PERFORMANCE OF THE COMPUTATIONAL ARC FURNACE MODEL

Comparisons of measured voltage waveform distortion have been made (Sections 2.4.3 and 5.3.1) by studying the distribution of each signal's power spectral density. The modulation frequencies of particular interest for a 'flicker' analysis are contained in the 0-30Hz sidebands of the 50Hz supply voltage power spectrum.

The computational model, described in this Chapter, used measured values of line current and its first derivative to calculate a distorted supply waveform. The comparisons between real and calculated distorted voltages are now presented, firstly in the frequency domain and secondly in the time domain. Finally, the results of demodulating the supply voltage waveform are shown to require careful interpretation.

7.3.1 Results Comparison using Power Spectra

Only the phase voltages at the Templeborough 33kV busbars were measured and recorded by the CEBG. Section 2.2.2 showed how the study of line voltages calculated from these phase voltages is valid. The line voltages derived from the phase voltage recordings are denoted MVRY MUYB MVBR, and their power spectra are given in Figure 7.4(a)(b)(c).

The computational model described in 7.1.2. and listed in Appendix J, produced the line voltages CVRY CVYB CVBR representing those occurring at the 33kV busbar. The power spectra of MVRY and CVRY are given in Figure 7.5(a) and (b) respectively. The equivalent comparisons for MUYB/CVYB and MVBR/CVBR are not presented, because the red-yellow line voltage spectra compared in Figure 7.5 are representative of the three-phase voltages.

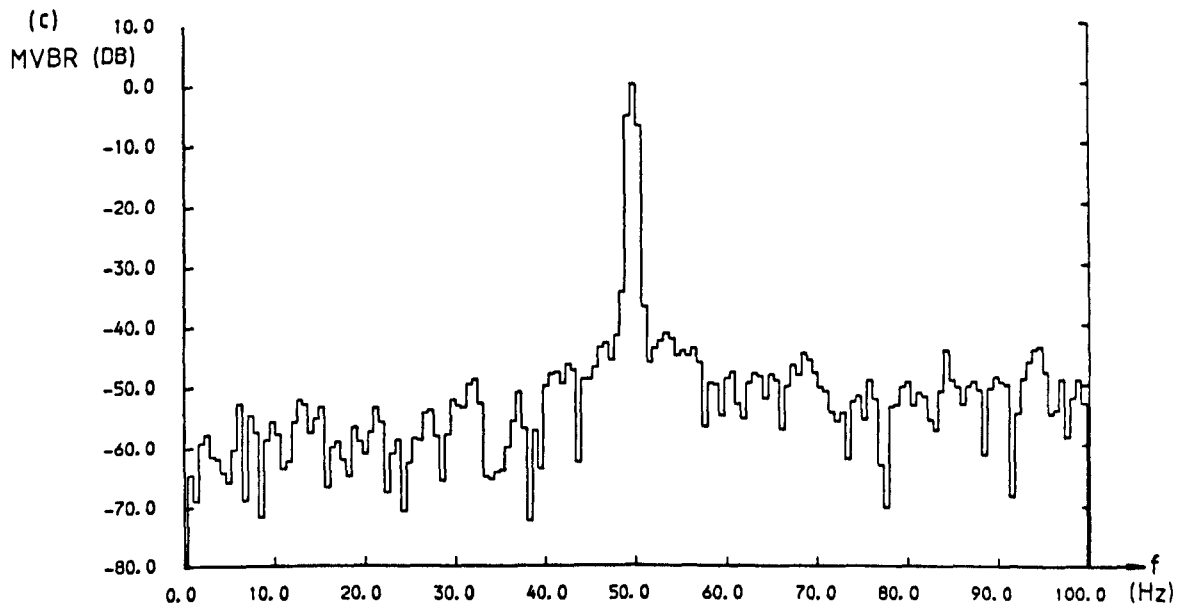
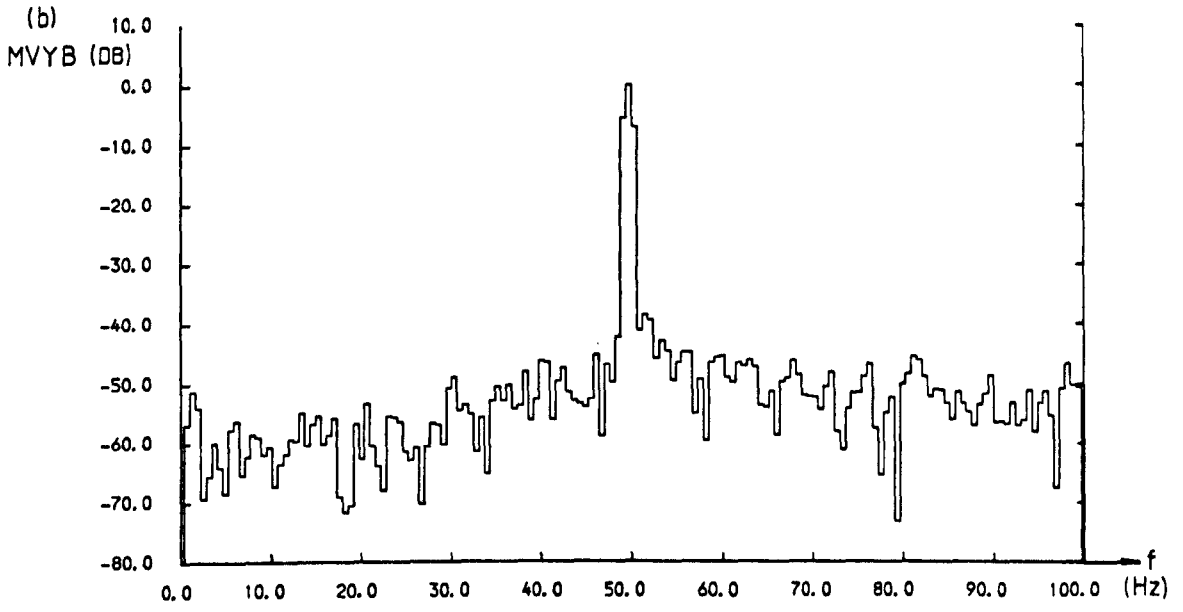
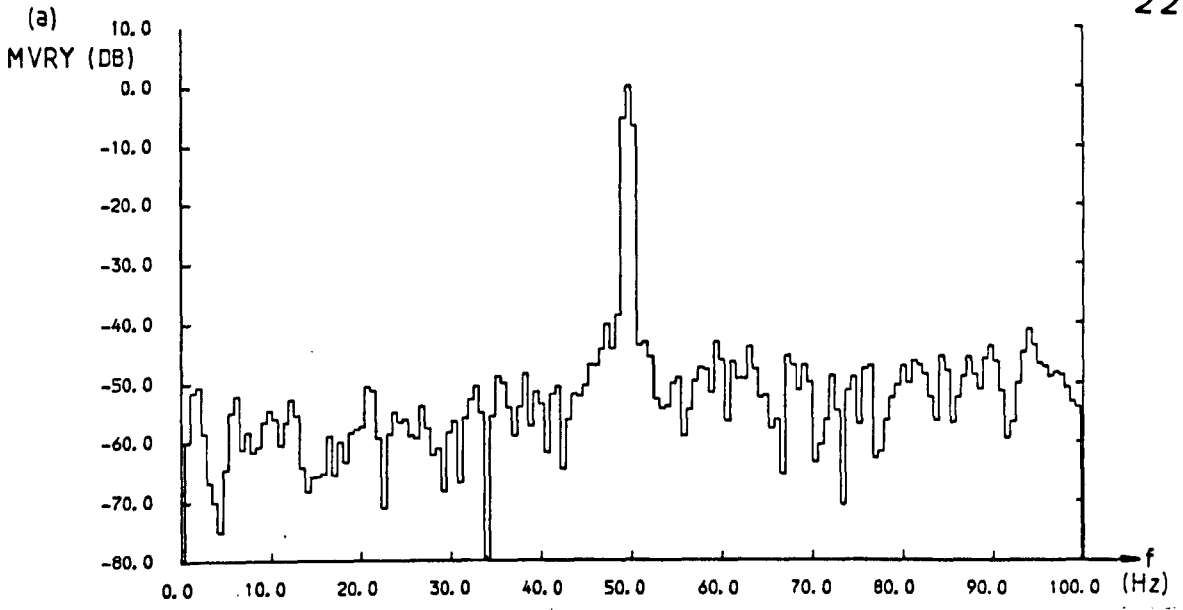


Fig. 7.4 : 0-100Hz power spectrum of line voltages derived from measured phase voltages

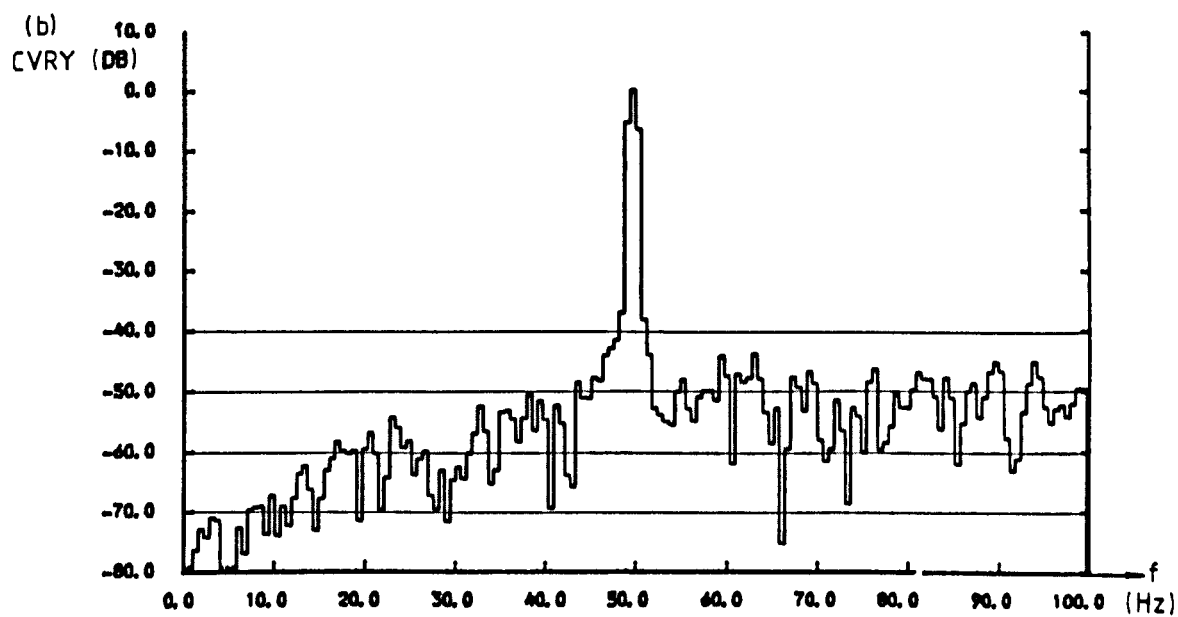
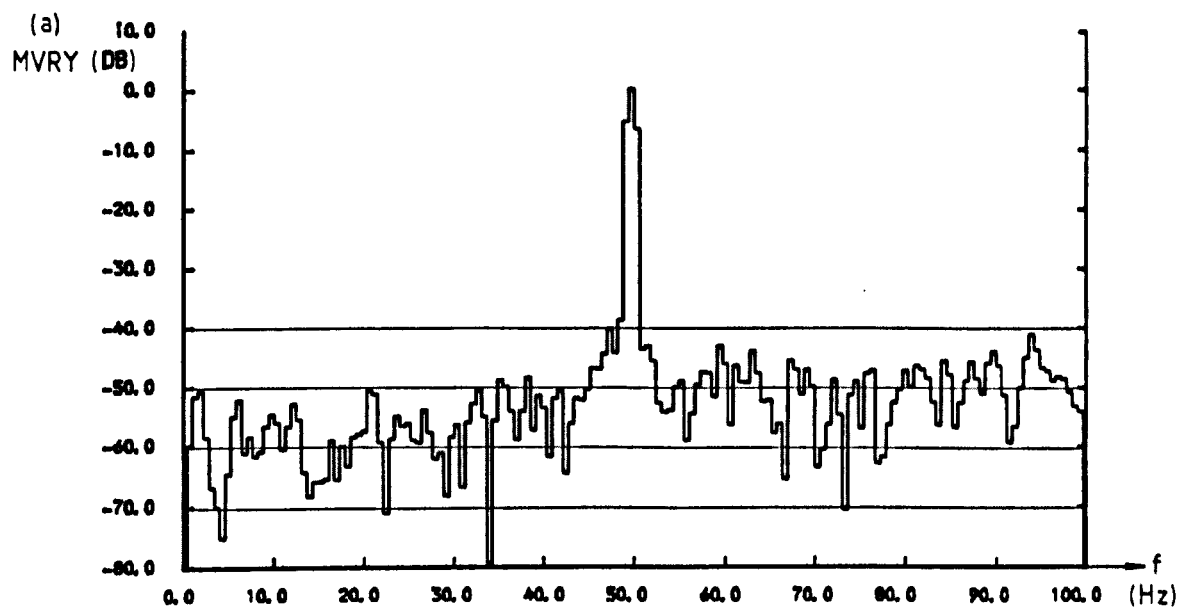


Fig. 7.5 : Comparison of power spectra of measured and calculated arc furnace line voltages MVRY and CVRY

Points arising from a study of Figure 7.5 are:

- (i) The upper modulation sideband of CVRY has a power spectral density distribution very close to that of MVRV. The 'peak and trough' formation of the spectrum in this band is almost identical, with the most obvious differences being in the absolute power levels of a few frequency blocks (e.g. 57Hz, 66.5Hz, 77Hz, 92Hz).
- (ii) The lower modulation sideband of CVRY is far less in agreement with that of MVRV. The most striking difference occurs in the absolute frequency range 1Hz to 20Hz. Here the power spectral components are, on average, some 20dB lower for CVRY than those in MVRV.
- (iii) Modulation frequencies that are most important for any 'flicker' study have been calculated with reasonable accuracy. There are some discrepancies, but it is not necessary for CVRY exactly to equal MVRV. CVRY will be a perfectly satisfactory reference distorted voltage from which to proceed with a study of reactive compensation. Reactive compensation will modify the power spectrum of CVRY and allow changes in the powers of the modulating frequencies to be assessed for a relative improvement factor.

7.3.2 Results Comparison in the Time Domain

Early work placed greater significance on the distorted voltage waveform rather than its power spectrum^[8,66]. The 33kV phase voltages from the recorded Templeborough data were shown in Figure 2.3 as MVR, MVY and MVB. Each of these voltages shows severe distortion from the sinusoidal form, and the distortion is particularly noticeable about the voltage peaks.

The computational model described in Section 7.1.2 and listed in Appendix J, produced the line voltages CVRY CVYB CVBR representing those occurring at the 33kV busbar. MVRV is repeated for comparison with CVRY over ninety 50Hz cycles in Figure 7.6. The corresponding waveforms for MVYB/CVYB and MVBR/CVBR are not presented, because the red-yellow voltage is representative of the form of the other line voltages.

A cursory study of Figure 7.6 shows that the sudden and severe voltage changes for MVRV are absent from CVRY, and suggests that the modulation voltage, V_f , is far lower for CVRY.

The first four 50Hz cycles of MVRV and CVRY are presented in more detail in Figure 7.7, which clearly shows the greater magnitude of MVRV's departures from a sinusoidal form.

The disagreement between these measured and calculated line voltages is then most pronounced for high frequency disturbances of the sinusoidal waveform. Lower frequency modulation of the 50Hz supply voltage cannot be discerned from Figure 7.7, but closer inspection of Figure 7.6 shows that the sub-harmonic modulation is of a similar magnitude for both waveforms. This is highlighted when MVRV and CVRY are given in the time-compressed form of Figure 7.8. The quantitative study in Section 7.3.1 shows that the power levels of modulating frequencies between 1 and 30Hz are almost identical.

7.3.3 Demodulation

Modulating frequencies causing lamp flicker may be seen in greater detail in the time domain if the 50Hz fundamental 'carrier' waveform is removed from the time series data.

Such a process was easily accomplished on the mainframe computer for the 90 cycles of data used by both the physical and computational model.

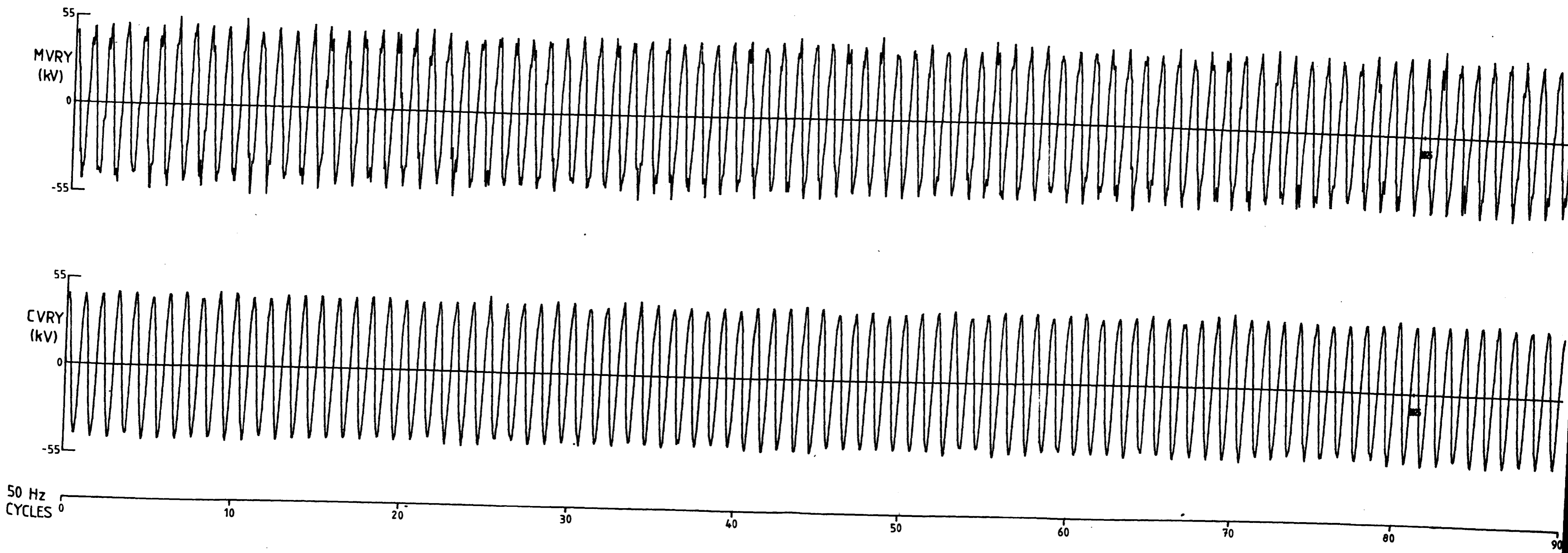
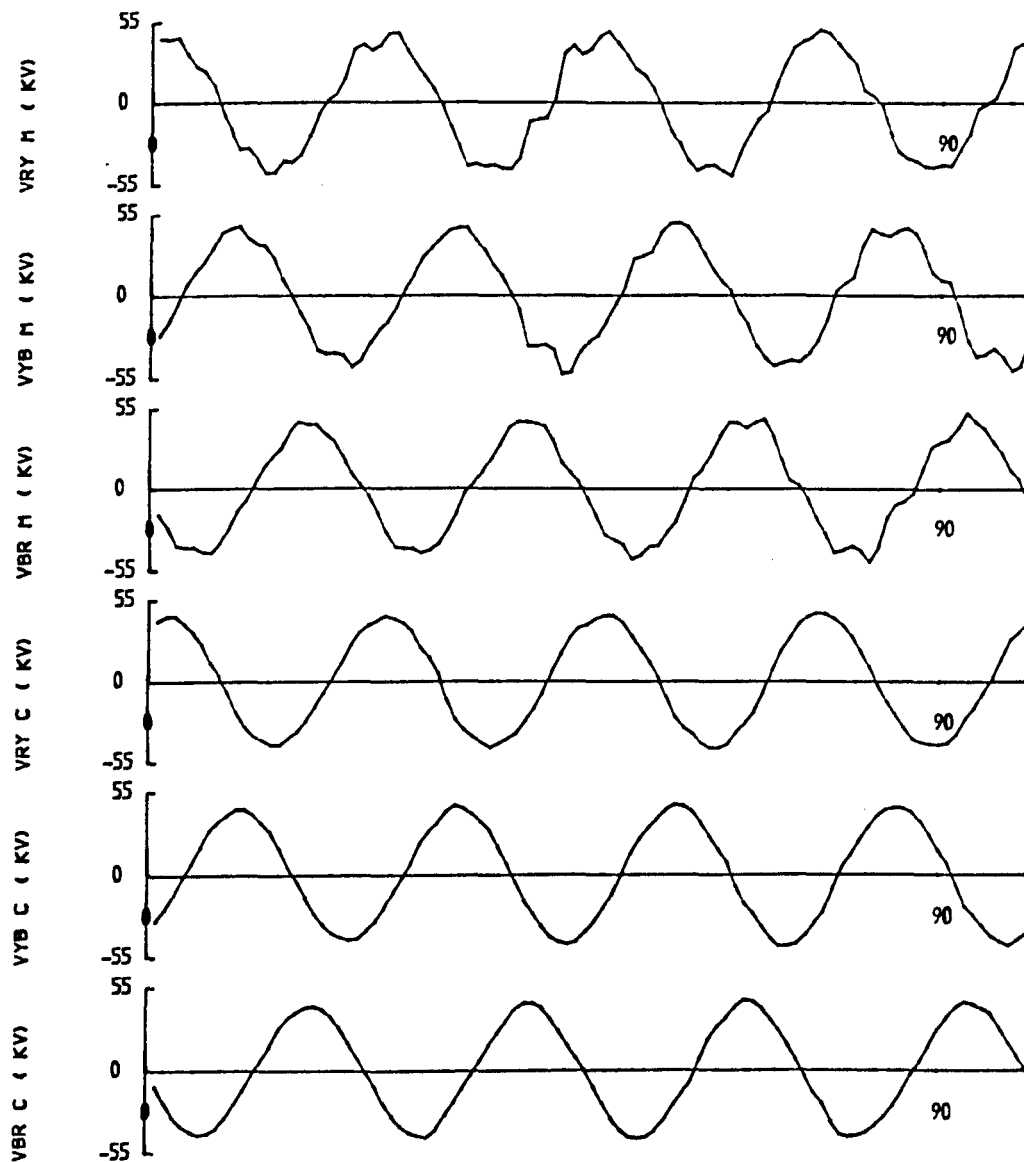


Fig. 7.6 : Comparison of-MVRV and CVRY over 90 cycles

MEASURED AND CALCULATED LINE VOLTAGES



•• COMPENSATOR DETAILS ••

LC=1.2000 POSLIM=400 NEGLIM=-400 ICON=2245 ICOFF=2248

Fig. 7.7 : Comparison of MVRV and CVRY over 4 cycles

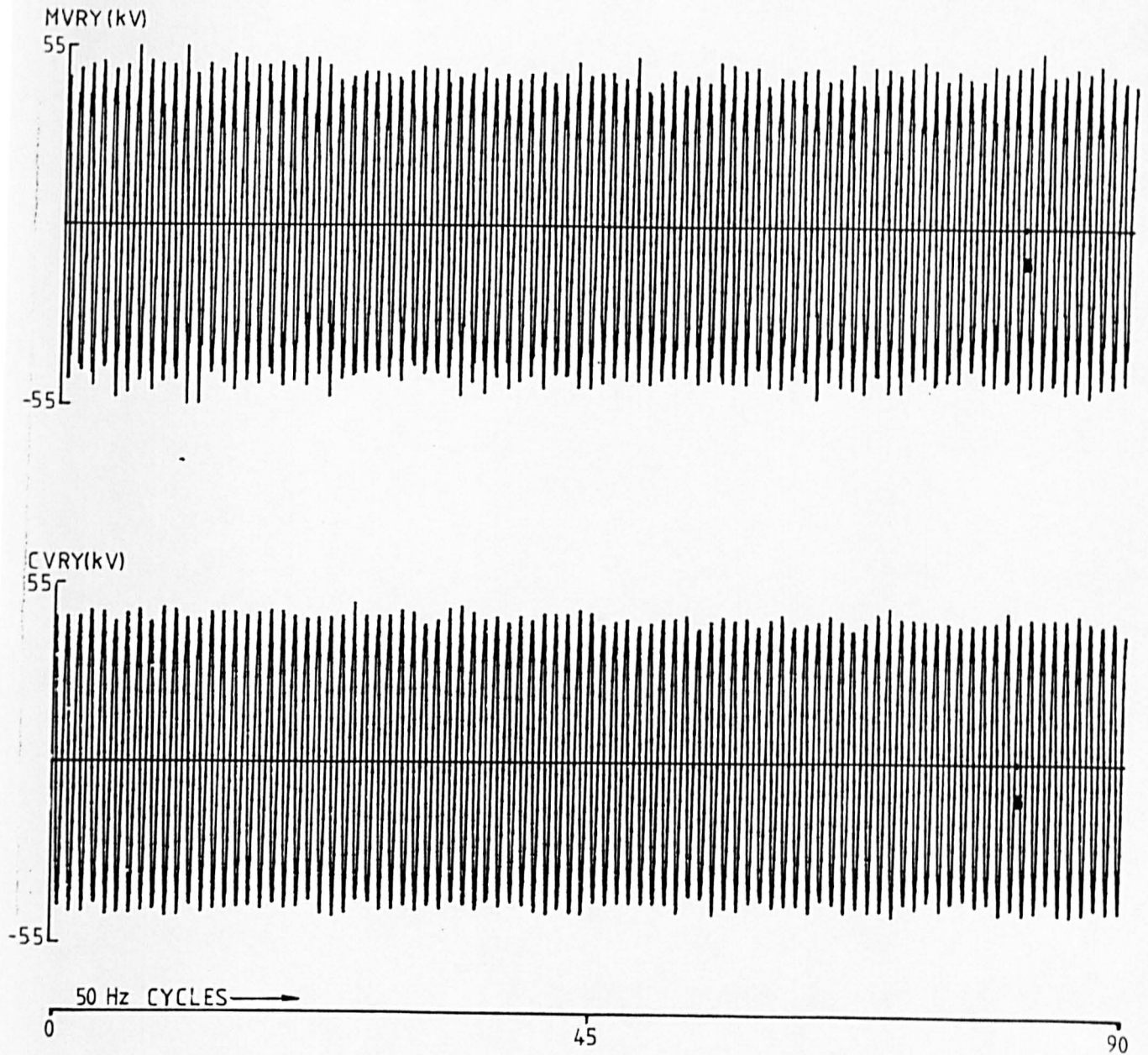


Fig. 7.8 : Comparison of MVRY and CVRY over compressed 90 cycles

The FORTRAN subroutine DEMOD called from the main SYSMOD6 program effected numerical demodulation of any waveform with a dominant fundamental frequency. The listing of DEMOD, together with all other subroutines called from SYSMOD6 is given in Appendix J.

Figure 7.9 presents the original and calculated line voltage as for Figure 7.6, except that a 50.06Hz sinusoid with RMS value 33.41kV has been subtracted from MVRY and CVRY to give the demodulated voltages DMVRY and DCVRY. The greater magnitude of distortions for MVRY is once again emphasised by this time-domain presentation. The time-compressed plots in Figure 7.10 begin to show how the lower frequency fluctuations are not dissimilar for DMVRY and DCVRY.

Finally the power spectral density plots for DMVRY and DCVRY in Figure 7.11 show that the numerical demodulation process has succeeded in removing only the 50Hz 'carrier' frequency. The remaining sidebands in the 1 to 100Hz band are identical to those presented in Figure 7.5, except that they are presented in dBs relative to the 3rd harmonic component rather than the 50Hz fundamental.

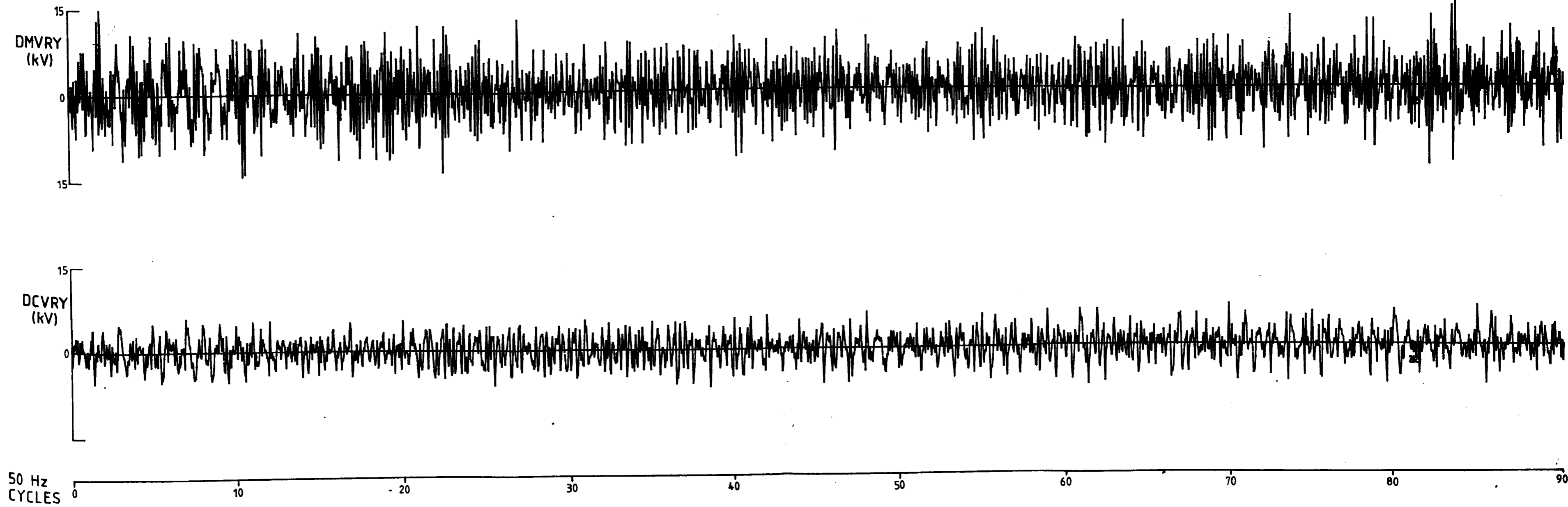


Fig. 7.9 : Comparison of demodulated measured and calculated voltages DMVRY, DCVRY over 90 cycles

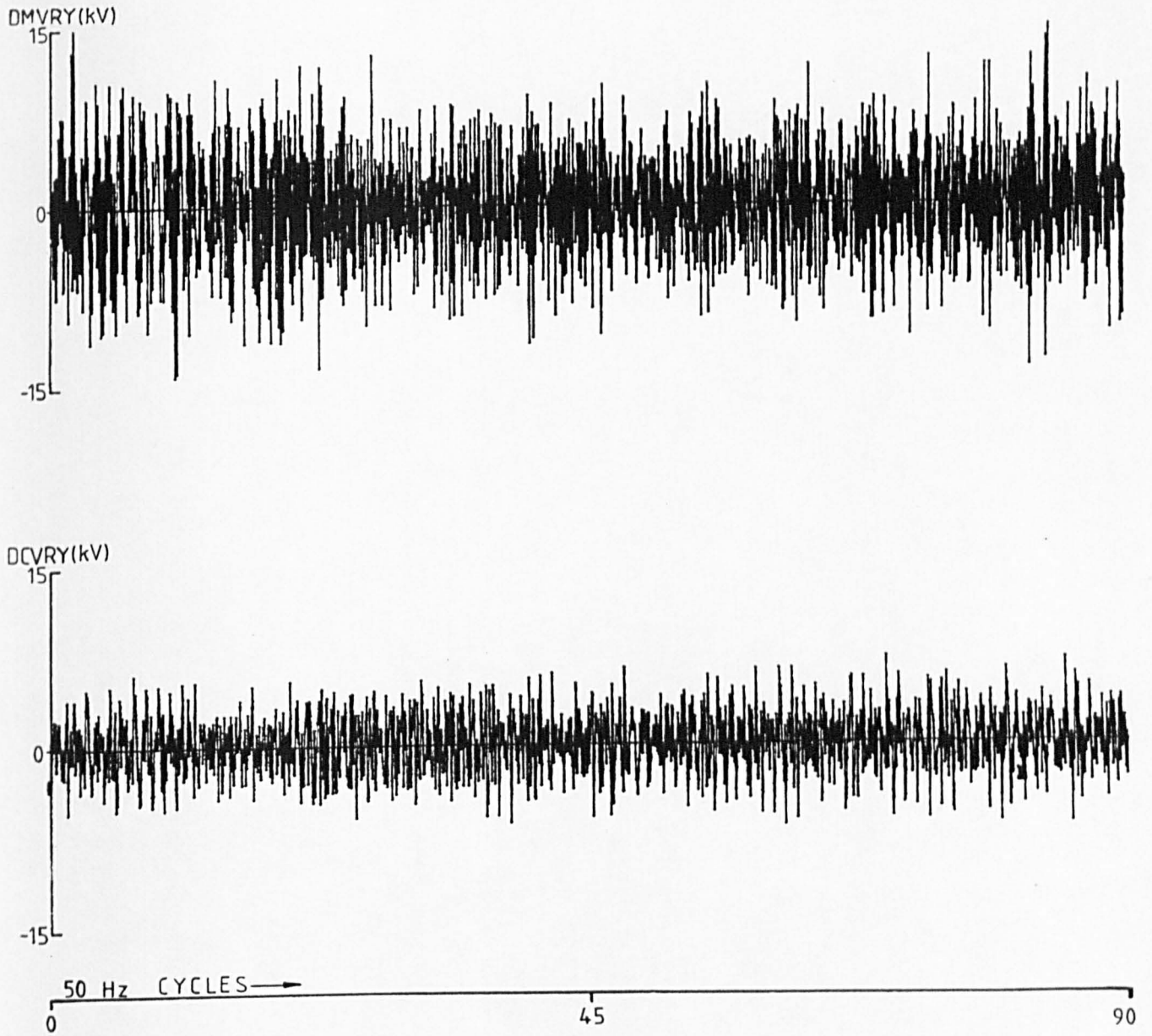


Fig. 7.10 : Comparison of DMVRY and DCVRY over compressed 90 cycles

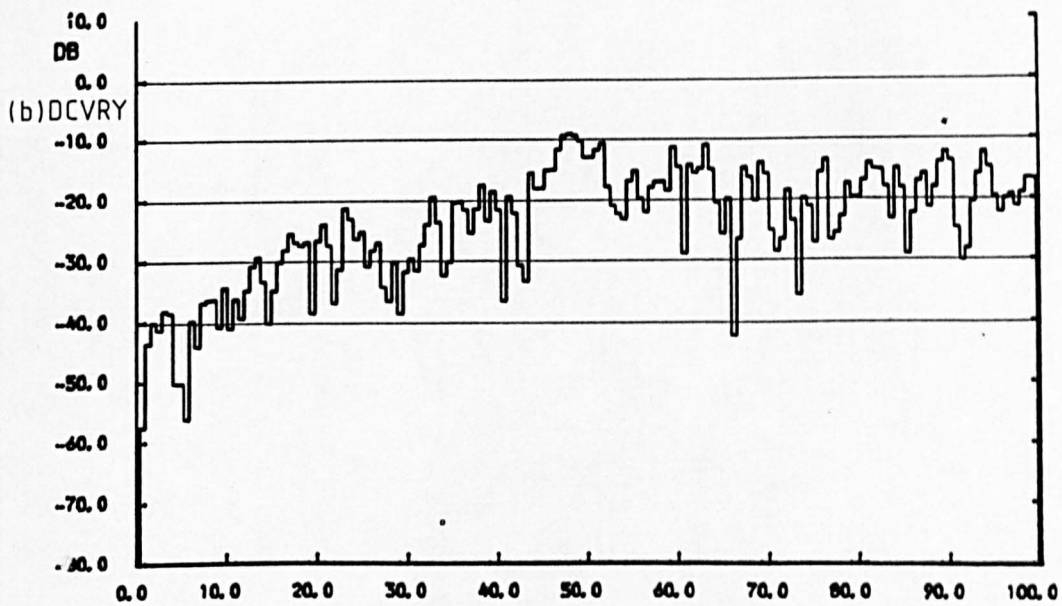
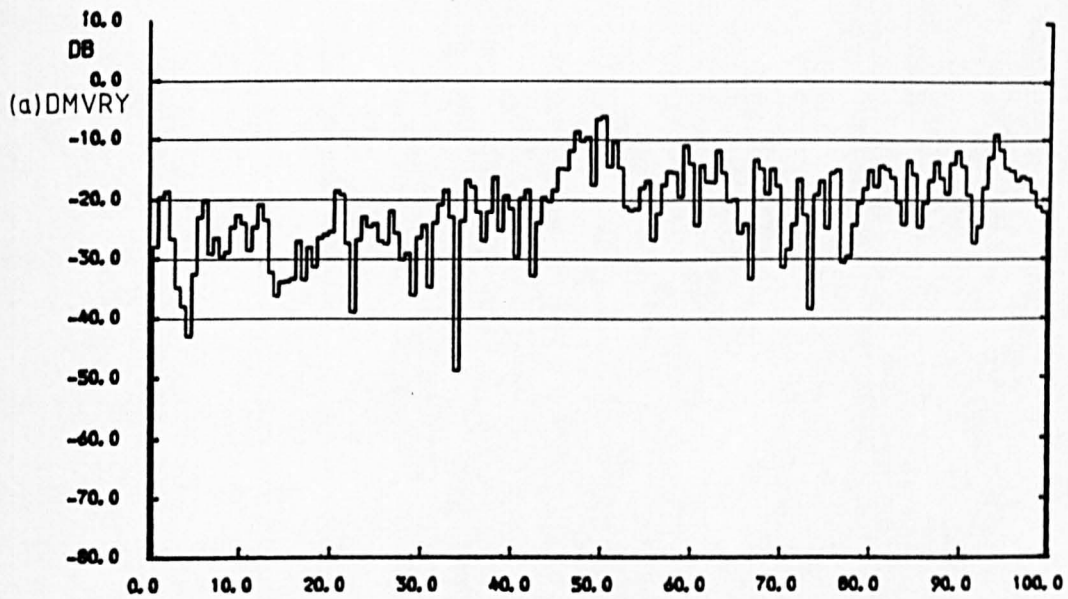


Fig. 7.11 : Comparison of power spectra of DMVRY and DCVRY

7.4 COMPUTATIONAL MODELLING OF A TCR COMPENSATOR

Adding a compensating shunt inductance to the computational arc furnace model described above will modify the line currents drawn from the source.

An algorithm to calculate the required conduction angles for a TCR compensator is easily constructed on this totally digital model. Then, when inductive conduction in the compensator has been initiated, a first order differential equation must be solved using a step-by-step approach as part of the digital model's function.

Correct solution of the differential equation shows the expected compensator branch current waveforms, and modification of the line currents drawn from the system. An improvement factor may then be calculated for different combinations of TCR compensator ratings and control algorithm.

7.4.1 TCR Compensator Circuit Definitions

The compensator is shunt connected with the arc furnace load. The line voltages applied to the compensator are then v_7 , v_8 and v_9 (the vector V_{789}). The currents drawn through the supply impedances will no longer be just I_{RYB} , since they will have been modified by the compensator line currents.

Figure 7.12 defines the computational model parameters when a shunt-connected compensator is included. The currents i_4 , i_5 and i_6 are therefore defined, using vector notation, as:

$$\begin{aligned} I_{456} &= I_{RYB} + I_{LCRYB} \\ \text{also } I_{LCRYB} &= -[C] I_{LC123} \end{aligned}$$

the same algebraic equations apply to the derivatives of the currents above.

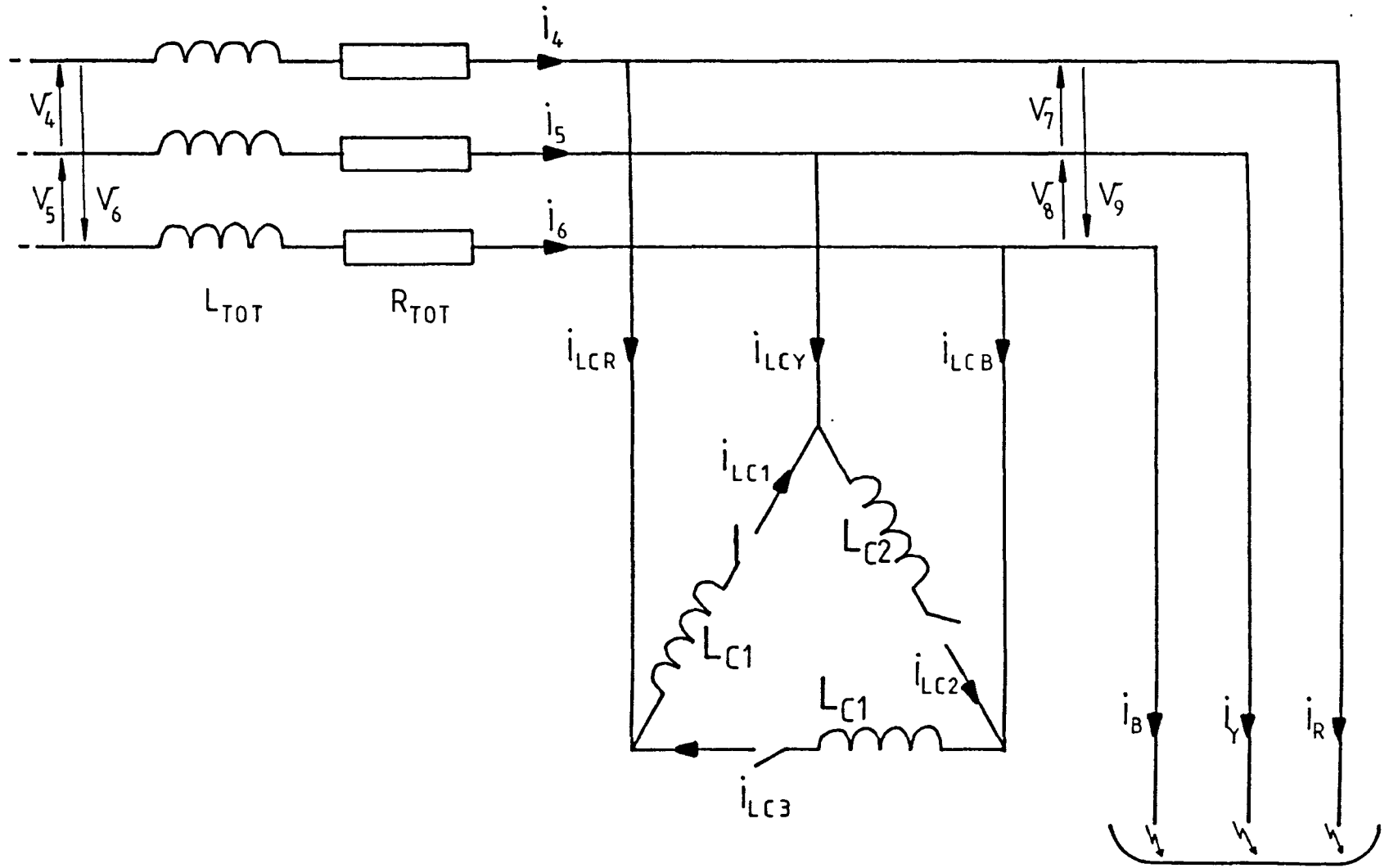


Fig. 7.12 : Definition of computational model voltages and currents when a shunt TCR compensator is included

7.4.2 The Differential Equations of Compensator Currents

Simple circuit theory gives the relationship between the parameters defined in Figure 7.12:

$$v_7 = v_4 - \left[R_{\text{sum}} (i_R - i_Y + i_{LCR} - i_{LCY}) + L_{\text{sum}} \left(\frac{di_R}{dt} - \frac{di_Y}{dt} + \frac{di_{LCR}}{dt} - \frac{di_{LCY}}{dt} \right) \right] \quad \text{.....Equation 7A}$$

$$v_8 = v_5 - \left[R_{\text{sum}} (i_Y - i_B + i_{LCY} - i_{LCB}) + L_{\text{sum}} \left(\frac{di_Y}{dt} - \frac{di_B}{dt} + \frac{di_{LCY}}{dt} - \frac{di_{LCB}}{dt} \right) \right] \quad \text{.....Equation 7B}$$

$$v_9 = v_6 - \left[R_{\text{sum}} (i_B - i_R + i_{LCB} - i_{LCR}) + L_{\text{sum}} \left(\frac{di_B}{dt} - \frac{di_R}{dt} + \frac{di_{LCB}}{dt} - \frac{di_{LCR}}{dt} \right) \right] \quad \text{.....Equation 7C}$$

But $v_{789} = L_c \frac{di_{LC123}}{dt}$ and $i_{LCRYB} = -[C] i_{LC123}$

Therefore

$$\frac{di_{LC1}}{dt} = \frac{1}{L_c} \left\{ v_4 - R_{\text{sum}} [i_R - i_Y + (2i_{LC1} - i_{LC2} - i_{LC3})] - L_{\text{sum}} \left[\frac{di_R}{dt} - \frac{di_Y}{dt} \right] \right\} - \frac{L_{\text{sum}}}{L_c} \left[2 \frac{di_{LC1}}{dt} - \frac{di_{LC2}}{dt} - \frac{di_{LC3}}{dt} \right] \quad \text{.....Equation 7D}$$

$$\frac{di_{LC2}}{dt} = \frac{1}{L_c} \left\{ v_5 - R_{\text{sum}} [i_Y - i_B + (-i_{LC1} + 2i_{LC2} - i_{LC3})] - L_{\text{sum}} \left[\frac{di_Y}{dt} - \frac{di_B}{dt} \right] \right\} - \frac{L_{\text{sum}}}{L_c} \left[- \frac{di_{LC2}}{dt} + 2 \frac{di_{LC2}}{dt} - \frac{di_{LC3}}{dt} \right] \quad \text{.....Equation 7E}$$

and

$$\begin{aligned} \frac{di_{LC3}}{dt} = \frac{1}{L_c} \left\{ V_6 - R_{sum} \left[i_B - i_R + (-i_{LC1} - i_{LC2} + 2i_{LC3}) \right] \right. \\ \left. - L_{sum} \left[\frac{di_B}{dt} - \frac{di_R}{dt} \right] \right\} \\ - \frac{L_{sum}}{L_c} \left[-\frac{di_{LC1}}{dt} - \frac{di_{LC2}}{dt} + \frac{2di_{LC3}}{dt} \right] \end{aligned}$$

.....Equation 7F

The equations above have the following solutions for

$\frac{di_{LC1}}{dt}$, $\frac{di_{LC2}}{dt}$ and $\frac{di_{LC3}}{dt}$:

$$\begin{aligned} \frac{di_{LC1}}{dt} = \frac{1}{L_c + 3L_{sum}} \left\{ V_4 - R_{sum} \left[i_R - i_Y + (2i_{LC1} - i_{LC2} - i_{LC3}) \right] \right. \\ \left. - L_{sum} \left[\frac{di_R}{dt} - \frac{di_Y}{dt} \right] \right\} \end{aligned}$$

.....Equation 7G

$$\begin{aligned} \frac{di_{LC2}}{dt} = \frac{1}{L_c + 3L_{sum}} \left\{ V_5 - R_{sum} \left[i_Y - i_B + (-i_{LC1} + 2i_{LC2} - i_{LC3}) \right] \right. \\ \left. - L_{sum} \left[\frac{di_Y}{dt} - \frac{di_B}{dt} \right] \right\} \end{aligned}$$

.....Equation 7H

$$\begin{aligned} \frac{di_{LC3}}{dt} = \frac{1}{L_c + 3L_{sum}} \left\{ V_6 - R_{sum} \left[i_B - i_R + (-i_{LC1} - i_{LC2} + 2i_{LC3}) \right] \right. \\ \left. - L_{sum} \left[\frac{di_B}{dt} - \frac{di_R}{dt} \right] \right\} \end{aligned}$$

.....Equation 7I

Provided that

$$V_4 + V_5 + V_6 = 0,$$

$$i_R + i_Y + i_B = 0$$

$$\text{and } \frac{di_R}{dt} + \frac{di_Y}{dt} + \frac{di_B}{dt} = 0$$

Equations 7G, 7H and 7I above apply only to the circuit shown in Figure 7.12. In the arc furnace model described in Part 7.1 and 7.2, this circuit only included voltages, currents and impedances from the secondary terminals of the super grid transformer (SGT).

Voltage and current transformations (Part 7.2) were necessary to include the transformer short circuit impedance and the system impedance in the model, since they were positioned in the transformer primary circuit.

To incorporate primary circuit impedances into the differential equations 7G, 7H and 7I above would bring many more terms into the equations, requiring proportionally greater computing effort. To avoid this, the SGT short circuit impedance was transferred to its secondary circuit.

The secondary circuit parameters were then lumped as

$$R_{\text{sum}} = R_{\text{SC}} + R_{\text{LINE}}$$

and
$$L_{\text{sum}} = L_{\text{SC}} + L_{\text{LINE}}$$

Treating v_4, v_5 and v_6 as the infinite busbar then ignored L_{SYS} and eliminated the need to perform the voltage and current transformations.

This simplified computational model of the arc furnace and supply system produced distorted '33kV equivalent' voltage waveforms and power spectra that were almost indistinguishable from those produced by the complete model described in Part 7.1 and 7.2.

7.4.3 Step-by-Step Solution of Compensator Differential Equations

In equations 7G, 7H and 7I above, i_R , i_Y , i_B , $\frac{di_R}{dt}$, $\frac{di_Y}{dt}$ and $\frac{di_B}{dt}$

are known variables - as they form the input to the arc furnace model described in Parts 7.1 and 7.2. R_{sum} and L_{sum} are the resistance and inductance shown in Figure 7.4. For each computational step both i_{LC123} and $\frac{di_{LC123}}{dt}$ must be found before V_{789} may be obtained from equations 7A, 7B and 7C.

For the first step at which current flows in a compensator branch,

$$i_{LC}(n) = 0 \quad \text{and} \quad \frac{di_{LC}(n)}{dt} = \frac{v_L}{L_C}$$

For the next step-by-step calculation,

$i_{LC}(n+1)$ and $\frac{di_{LC}(n+1)}{dt}$ can only be calculated from $i_{LC}(n)$

and $\frac{di_{LC}(n)}{dt}$.

Equations 7G, 7H and 7I are first-order differential equations in the explicit form such that

$$y' = f(x,y)$$

Step-by-step numerical solution of such an equation evaluates y at

$$\begin{aligned} t &= t_0 \\ t &= t_1 = t_0 + \Delta t \\ t &= t_2 = t_1 + \Delta t \end{aligned}$$

' Δt ' is the step size, and here is fixed on the data sampling interval of 800 microseconds.

The Euler-Cauchy method^[120] crudely calculates

$$y(n+1) = y + \Delta ty'$$

This first order method results in truncational errors of the order h^2 per step. An improved Euler-Cauchy method reduces these errors to order h^3 , and the important Runge-Kutta method gives truncation errors of order h^5 per step^[120].

Four auxiliary values, A,B,C and D, are calculated for each step of the numerical process, and they combine to give

$$y(n+1) = y(n) + \frac{1}{6} [A(n) + 2B(n) + 2C(n) + D(n)]$$

The values for A(n), B(n), C(n) and D(n) are described generally in the literature^[120] and are shown for this particular application in the FORTRAN program listing in Appendix J.

Where variables at $t(n)$ are required, the known values of i_R , i_Y , i_B , $\frac{di_R}{dt}$, $\frac{di_Y}{dt}$ and $\frac{di_B}{dt}$ are used. Similarly, values for $t(n+1)$

will use the next set of values from the input data. However, the half-step values at $t(n+\Delta t/2)$ are always unknown, and these are calculated at each stage by simple linear interpolation between $t(n)$ and $t(n+1)$.

7.4.4 Compensator Control

A separate input file to the SYSMOD6 program contained details of the required compensator parameters. These controlled the compensator rating and conduction angle.

Control of conduction in the compensator branch inductances followed an integration procedure. The line voltage zero-crossing points were used to initiate integrations and conduction in the relevant compensator branch was allowed when a pre-set limit was reached. The equations given in Section 7.4.2 were then used to calculate the compensator currents until 'commutation' at current-zero.

The integration procedure used to calculate 'firing angle' in the computer model was first set up as a simple integration of line voltage. Ideally this control method would have been extended to model the system used for the laboratory analogue model, but further work is required to achieve this.

The file 'SYSCOMP OPTION' contained the following parameters defining the TCR compensator.

L_C - The compensator branch inductance (Henries)
 POSLIM - The positive integration limit (Volt seconds)
 NEGLIM - The negative integration limit (Volt seconds)

The compensator branch inductance was set to give a three-phase compensator rating corresponding to the C/F value of 1.13 as used in Chapters IV, V and VI of this thesis. For the 56MVA numerically modelled furnace, this demanded a compensator rating of 63.4MVA, with the compensator branch inductance, $L_{C\Delta}$, equal to 0.164 Henries.

The integration limits were set to approximate to those obtained from simple integration theory, such that for

$\alpha_1 \approx 100^\circ$; POSLIM = NEGLIM = 174kV secs
 $\alpha_2 \approx 135^\circ$; POSLIM = NEGLIM = 253kV secs
 $\alpha_3 \approx 170^\circ$; POSLIM = NEGLIM = 294kV secs

7.4.5 Results from the Computer Model Compensator

(i) Compensator Currents

The calculation of conduction angles was first tested over only four cycles of input data to avoid the use of excessive computational effort. The values ICON and ICOFF set the step value 'N' at which the compensator is judged to be on and off respectively.

Figure 7.13(a) shows the three-phase compensator branch currents calculated for an integration limit of 200 units. This value initiates 'conduction' at a point corresponding to $\alpha = 100^\circ$.

Also shown in Figure 7.13(a) is the compensator branch voltage waveform from ICON onwards.

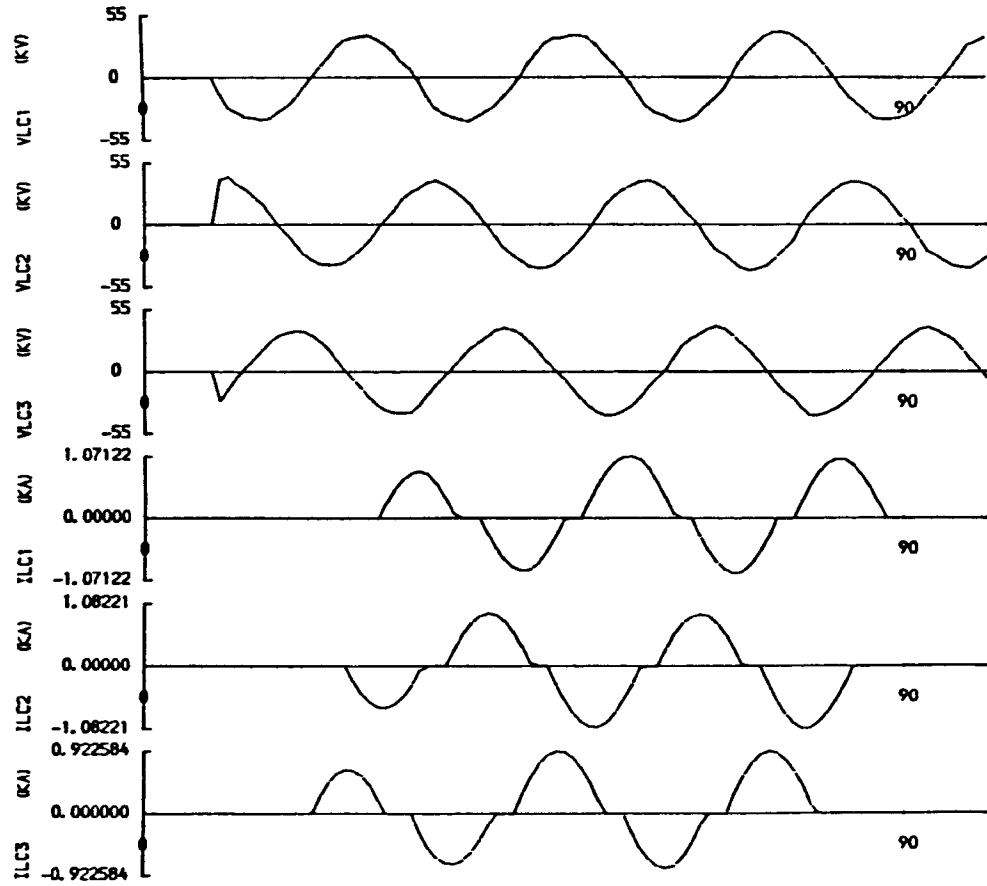
Figure 7.13(b) shows how the delta-connected compensator branch currents combine on three-phase line currents, and compares them with the fixed arc furnace line currents.

The effect of varying the integration limit is shown in Figures 7.14 and 7.15, where conduction angles decrease for limits of 250 and 385 respectively. The compensator current peaks are always plotted to fill the scale available, and the scales show that current peaks decrease with decreasing conduction angle as expected.

(ii) Compensator Voltages

Study of the calculated compensator branch voltages presented in Figures 7.13(c), 7.14(a) and 7.15(a) shows that the characteristic form of voltage depression is apparently missing from the line voltage waveforms.

COMPENSATOR BRANCH VOLTAGES AND CURRENTS

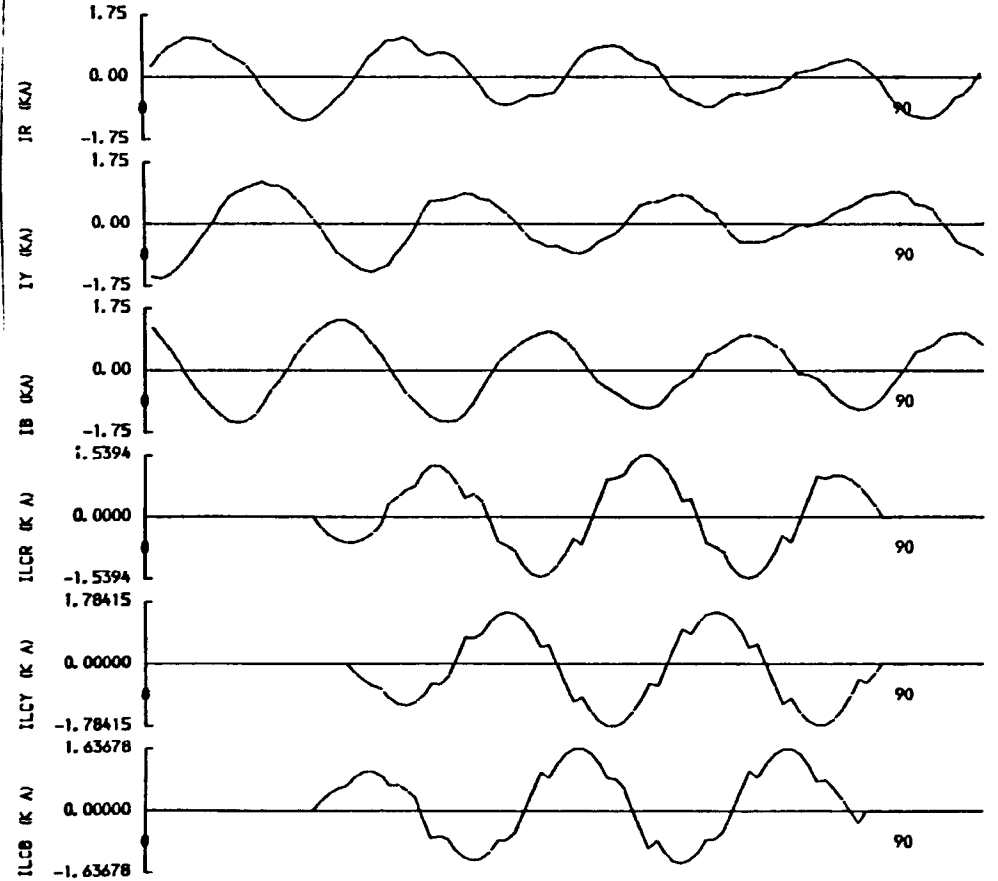


↔ COMPENSATOR DETAILS ↔

LC=0.1600 POSLIN=200 NEGLIM=200 ICON= 10 ICOFF= 80

Fig. 7.13(a) : Computed 6-pulse TCR branch voltages and currents with *LIMIT = 200*

FURNACE & COMPENSATOR LINE CURRENTS

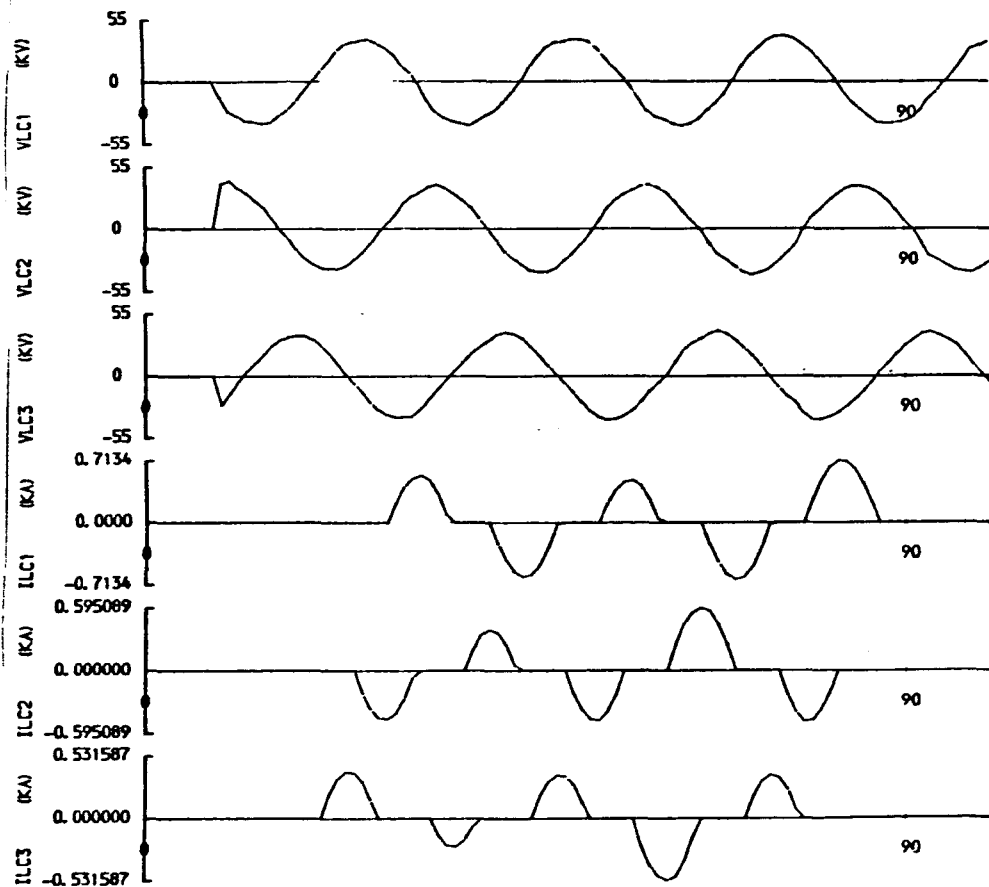


↔ COMPENSATOR DETAILS ↔

LC=0.1600 POSLIN=200 NEGLIM=200 ICON= 10 ICOFF= 80

Fig. 7.13(b) : Computed line currents for arc furnace and TCR with *LIMIT = 200*

COMPENSATOR BRANCH VOLTAGES AND CURRENTS

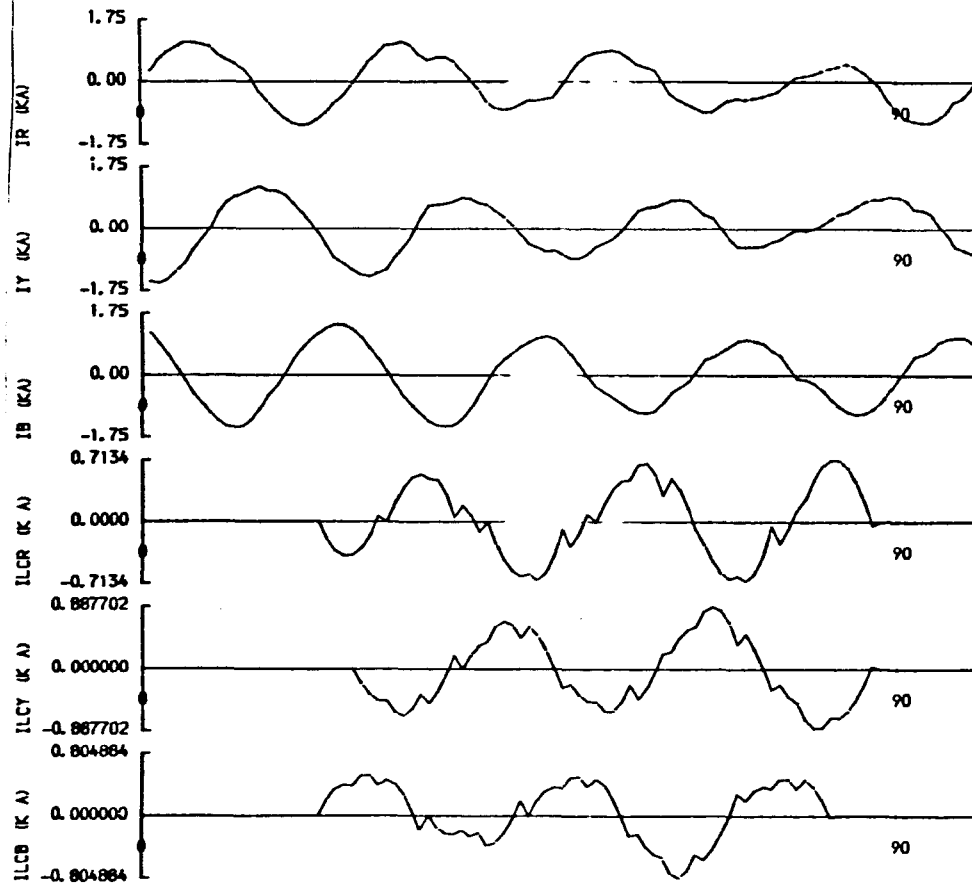


COMPENSATOR DETAILS

LC=0.1600 POSLIN=250 NEGLIM=250 ICON= 10 ICOFF= 80

Fig. 7.14(a) : Computed 6-pulse TCR branch voltages and currents with *LIMIT = 250*

FURNACE & COMPENSATOR LINE CURRENTS

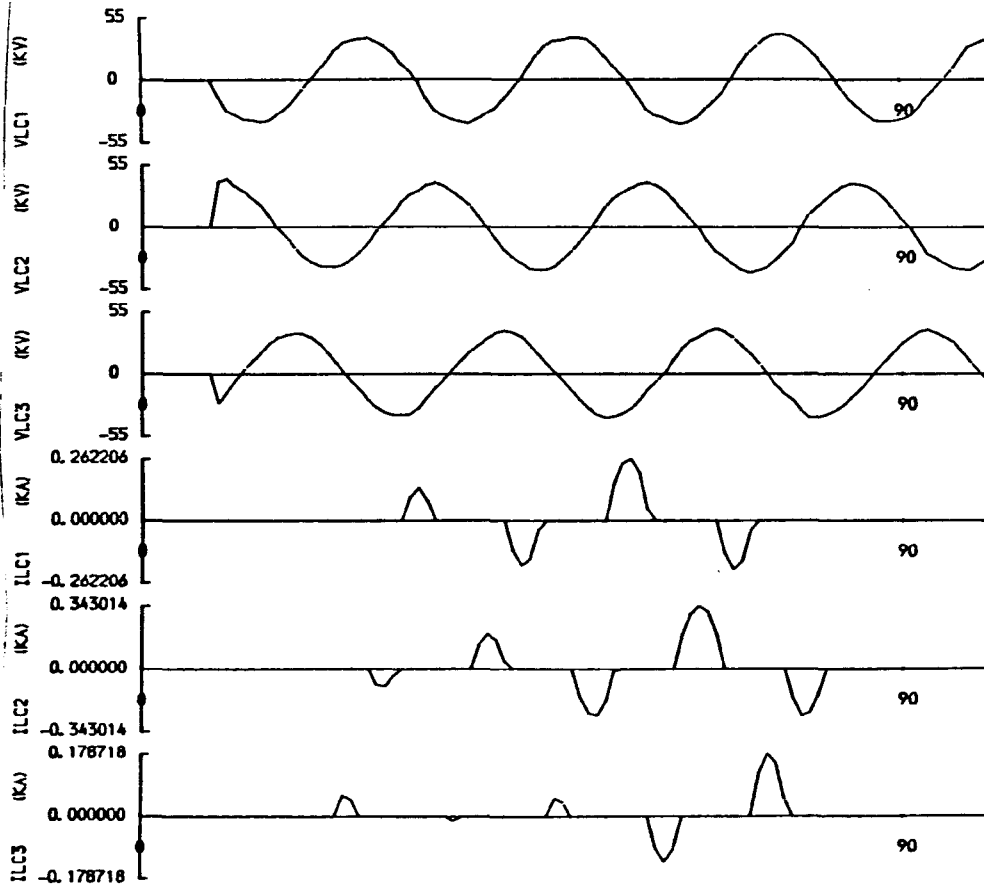


COMPENSATOR DETAILS

LC=0.1600 POSLIN=250 NEGLIM=250 ICON= 10 ICOFF= 80

Fig. 7.14(b) : Computed line currents for arc furnace and TCR with *LIMIT = 250*

COMPENSATOR BRANCH VOLTAGES AND CURRENTS

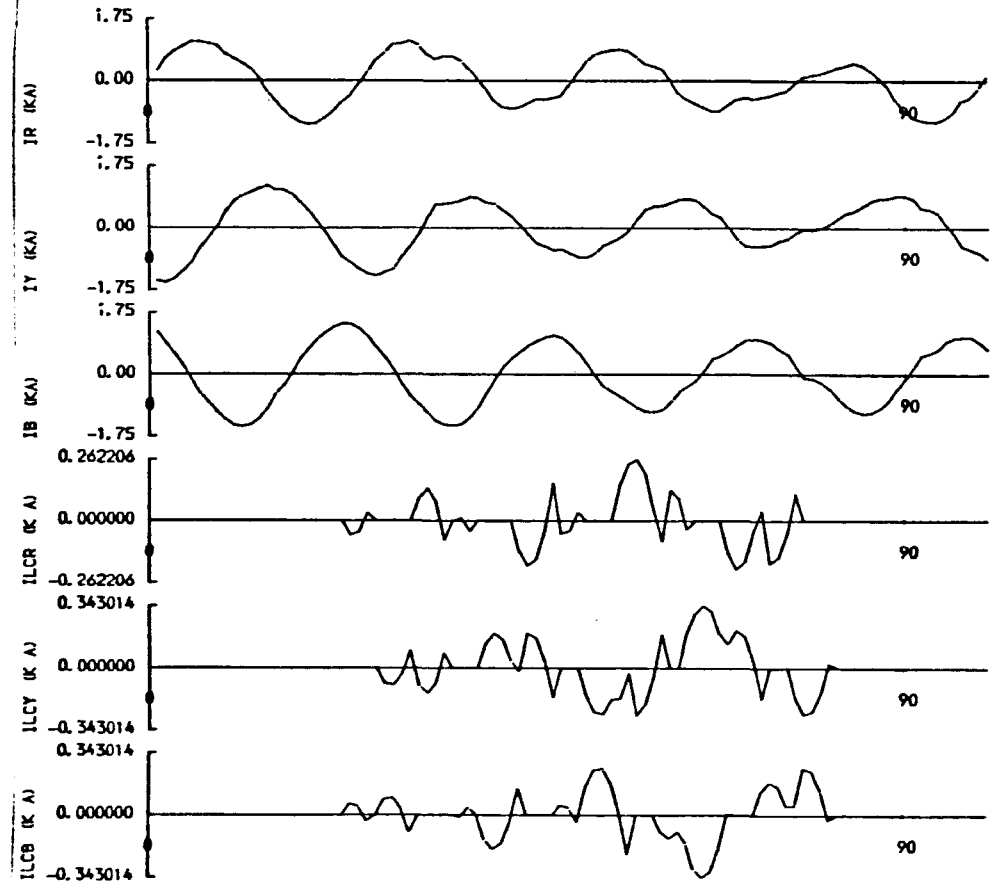


COMPENSATOR DETAILS

LC=0.1600 POSLIM=285 NEGLIM=285 ICON=10 ICOFF=80

Fig. 7.15(a) : Computed 6-pulse TCR branch voltages and currents with LIMIT = 285

FURNACE & COMPENSATOR LINE CURRENTS



COMPENSATOR DETAILS

LC=0.1600 POSLIM=285 NEGLIM=285 ICON=10 ICOFF=80

Fig. 7.15(b) : Computed line currents for arc furnace and TCR with LIMIT = 285

Since this is the means by which the compensator would achieve voltage flicker reduction, further investigation was carried out into the effect of the compensator's calculated 'shunt compensation'.

Figure 7.16(a) gives the first 4 cycles of three-phase line voltages calculated by the 'uncompensated' computational arc furnace model together with the 'demodulated' flicker voltage. Figure 7.16(b) then shows, for comparison, the equivalent three-phase line voltages calculated for the 'compensated' computational arc furnace model.

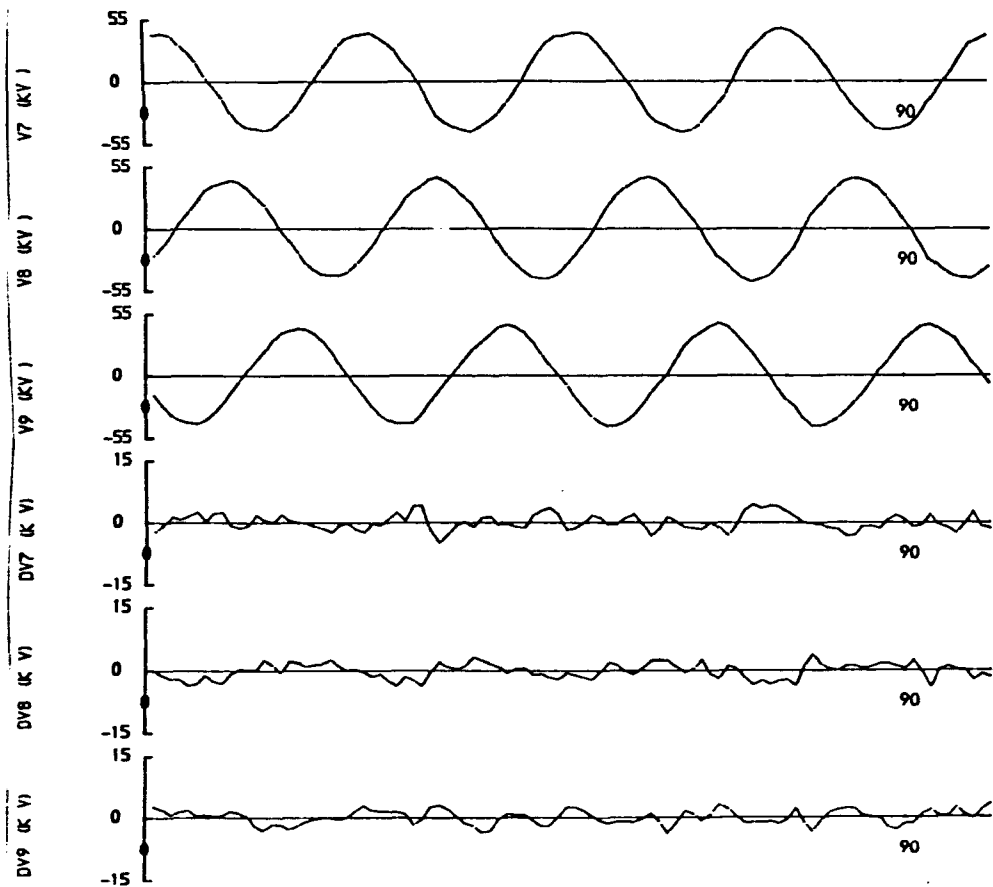
The demodulated 'compensated' line voltage waveforms show a greater 50Hz component than the corresponding 'uncompensated' waveform, and this is due to the slight voltage depression due to compensator branch conduction.

The two demodulated three-phase waveforms are compared on a larger scale in Figure 7.17 where the 50Hz component is more visible.

The power spectrum of the compensated line voltage time series data was obtained for comparison with the uncompensated form, but the results were disappointing and showed hardly any improvement in the 0-100Hz frequency band.

Possible reasoning for this is given in the discussion in Section 8.1.4, and further work is suggested in Part 8.3.

CALCULATED LINE VOLTAGES WITHOUT TCR

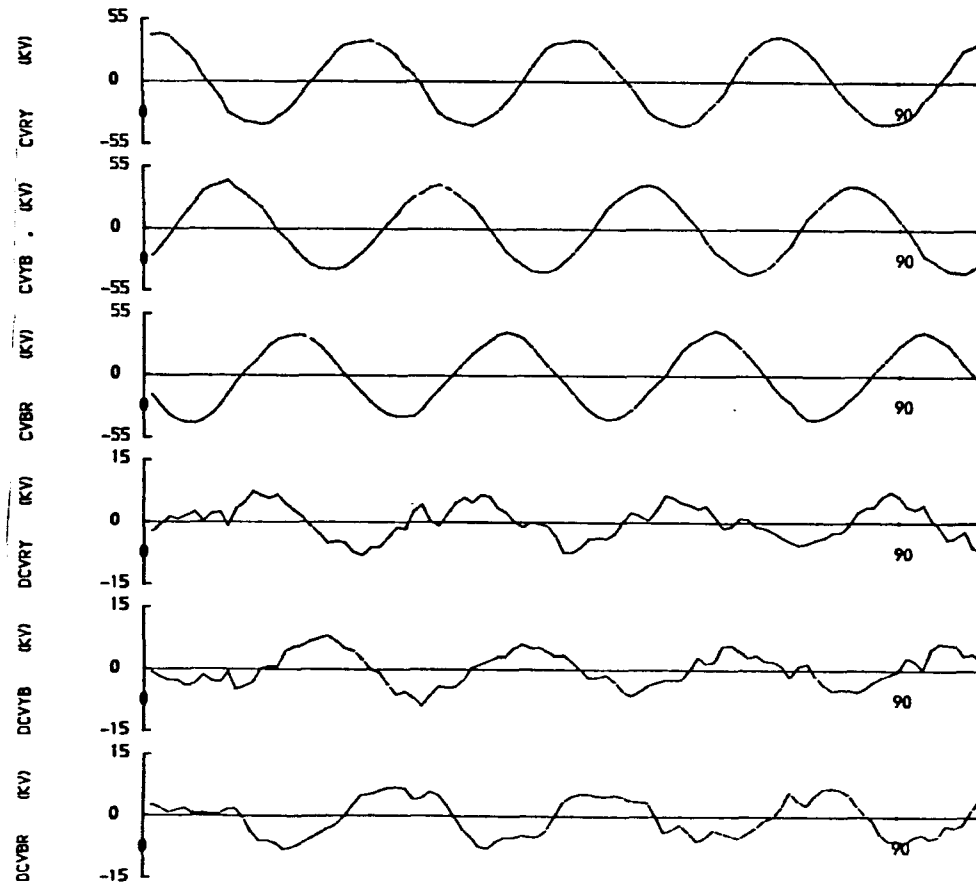


COMPENSATOR DETAILS

LC=0.1600 POSLIM=200 NEGLIM=-200 ICON= 10 ICOFF= 80

Fig. 7.16(a) : Computed uncompensated arc furnace line voltages

CALCULATED LINE VOLTAGES WITH TCR

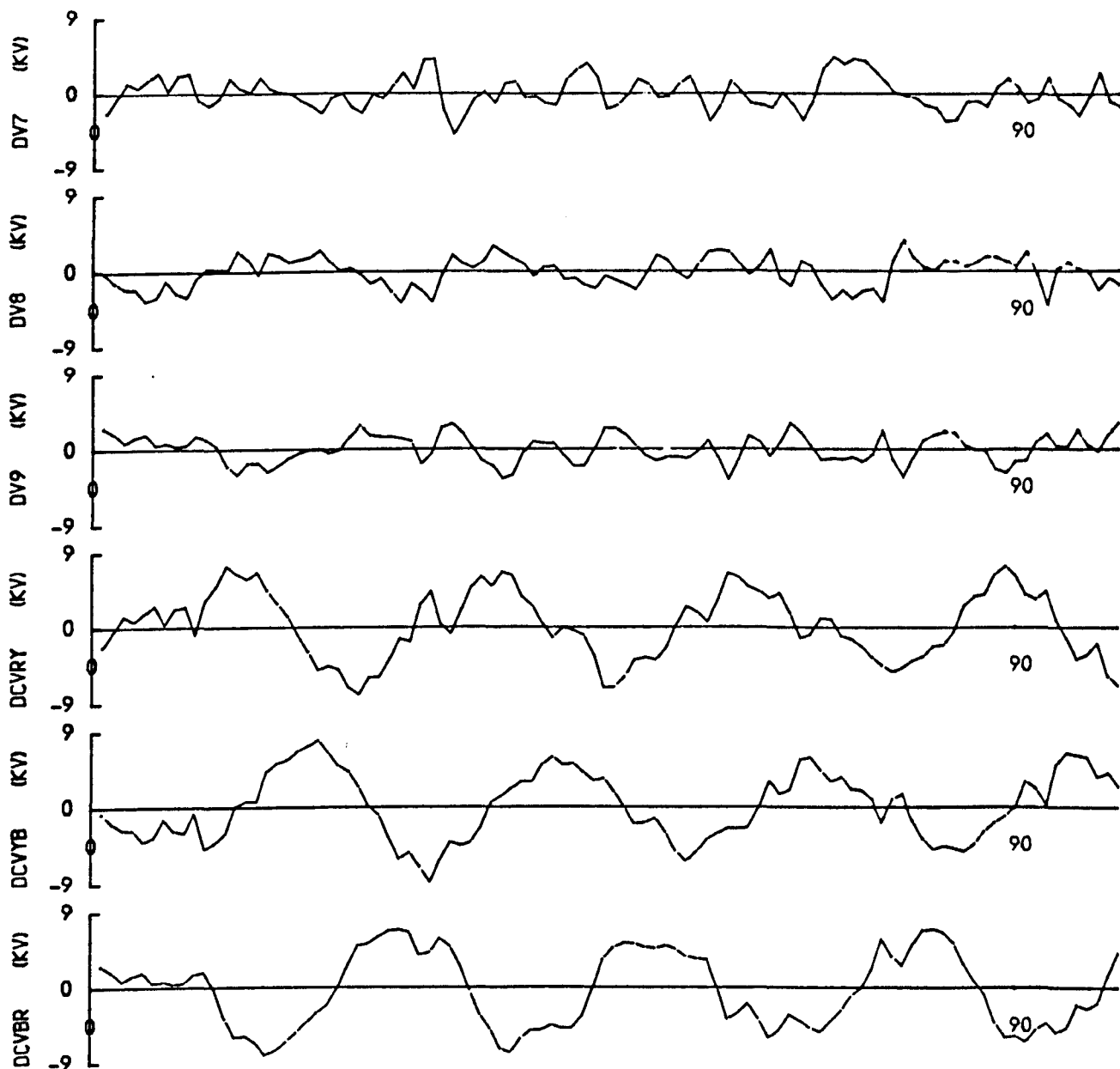


COMPENSATOR DETAILS

LC=0.1600 POSLIM=200 NEGLIM=-200 ICON= 10 ICOFF= 80

Fig. 7.16(b) : Computed compensated arc furnace line voltages

DEMOMULATED LINE VOLTS WITHOUT/WITH TCR



** COMPENSATOR DETAILS **

LC=0.1600 POSLIM=200 NEGLIM=-200 ICON= 10 ICOFF= 80

Fig. 7.17 : Computed compensated and uncompensated demodulated arc furnace line voltages

CHAPTER EIGHTDISCUSSION, CONCLUSIONS AND FURTHER WORK8.1 DISCUSSION

8.1.1 The Laboratory Arc Furnace Model

- (i) Current Waveform Reproduction
- (ii) Voltage Waveform Reproduction

8.1.2 The Laboratory TCR Compensator Models

- (i) The Six-Pulse TCR Compensator
- (ii) The Twelve-Pulse TCR Compensator

8.1.3 Data Analysis

8.1.4 Mathematical Modelling

8.2 CONCLUSIONS8.3 FURTHER WORK

8.1 DISCUSSION

The summary of this thesis describes briefly the areas of work covered, and it is felt that the work was successful in the following areas:

- (a) The establishment of laboratory and numerical models of an arc furnace and supply system that gave repeatable results for use with different compensation studies.
- (b) The presentation of a detailed description and results from the use of a six-pulse TCR compensator. Its success was demonstrated with a very simple but fast control method.

This discussion will now present aspects of the research work that have not been covered in the preceding chapters, and will attempt to assess the suitability of techniques used in the work to obtain the results.

8.1.1 The Laboratory Arc Furnace Model

(i) Current Waveform Reproduction

Using the AIM-65 microcomputer system imposed a number of restrictions upon small-signal current waveforms generated to drive the power amplifiers. It was apparent at an early stage that the storage capacity of a machine with only 28 kbytes of available addressable RAM would restrict the cycling period of the data to be output in its analogue form. The dynamic expansion RAM was continually refreshed, and would not operate reliably at the higher clock rate of 6MHz used instead of the 4MHz standard.

Data transfer to the model from the mainframe computer was laborious, using punch tape output from old equipment. Errors in reading to the AIM-65 microcomputer were frequent, and early plans to have a selection of data spans available for reproduction were dropped in favour of one set span stored in EPROM.

The data output frequency of 5kHz was more than sufficient for a study of flicker voltages, but the 8-bit resolution could not make full use of the accuracy of the 15-bit recording equipment used by the CEGB. The data cycling period of eighty-nine 50Hz cycles allowed only a reproduction of frequency components above 1.8Hz. Frequencies below this value have a low weighting on the flicker sensitivity curve, but ideally should they not be neglected.

The Y-connected commercial power amplifiers driven by the small analogue signals were a success. The voltage feedback method of driving their inputs gave reliable fine control, and established a useful technique for current reproduction at frequencies other than 50Hz.

After the arc furnace model had been constructed, it was clear that the power amplifiers were only being used at less than one third of their full current rating. This was because of the original safety margin used in deciding the base operating levels of the model. The real operating current levels were then less than the base level and the safety margin excessive. Increasing the gain of the control feedback loop caused the model to draw currents of identical form, and greater than twice the normal magnitude, without ill-effect. The base values for the model were by then fixed by the modelling impedances; the compensator ratings were established, and increasing the VA rating of the model would have lost much time.

Establishment of the current waveform reproduction data in EPROM and the provision of separate AC supplies for laboratory technical equipment meant that the arc furnace model became reliable and simple to use.

(ii) Voltage Waveform Reproduction

The early stages of the physical model design worked towards a small scale reproduction of the Templeborough system as a whole. Only at a later stage was it decided that the very small voltage fluctuations occurring on the 'system' side of the Y- Δ transformer would not be included as part of a reactive compensation study. With the bulk of the model supply impedance appearing in the 'line inductances', it is now apparent that the Y- Δ transformer could be removed from the model. Such a step, however, would detract from the generality of the system modelling approach and would preclude any measurement of primary parameter at a later date.

The X/R value obtained in the model was approximately 11, compared with 40 for the real system. This disparity could have been reduced by using physically larger components, but for a laboratory model it was felt that 91p.c. reactance compared reasonably with the 98p.c. reactance of the real system. Resistive losses or dampening effects did not give difficulties in any part of the arc furnace modelling.

It was noticeable that the distorted line voltages in the time domain did not show the same sudden instantaneous departures from the sinusoidal as those recorded at 33kV. This lack of agreement was at first disappointing, but subsequent comparison of power spectra in the relevant frequency bands showed that the power frequency distribution was very similar. This firstly showed that sudden voltage changes do not contribute significantly to low frequency power, and secondly suggested that the sudden voltage changes may not have been attributable to the measured arc furnace load but rather to loads elsewhere on the supply system.

The flicker level at the point of application of shunt reactive compensation was considerably higher than that defined as 'just perceptible' by the UIE. This was judged to be useful for comparative studies of compensator performance. Varying the feedback gain to the power amplifier inputs could greatly change the percentage voltage distortion obtained, and it would be simple to undertake an investigation of compensator performance for very different flicker levels.

8.1.2 The Laboratory TCR Model

(i) The Six-Pulse TCR Compensator

The rating of the first laboratory TCR compensator was intended to give effective compensation of the flicker voltages found in the normal operating range of the arc furnace model. The results obtained with this compensator were disappointing, and the rating was duly increased to allow for the full change in demand between furnace open- and short-circuit.

Some thought must be given to why the design calculations for the original TCR compensator had to be modified. The answer may lie in the method used for control of thyristor firing angles: The efficacy of the control method will depend on the level of success in each of the following:

- (a) Sensitivity
- (b) Accuracy
- (c) Speed of response

The sensitivity of the system was determined by adjustment of the magnitude of the 'reference' sinusoid used in all half-cycle integrations. This was carefully set to be as close as possible to the sampled distorted sinewave, whilst being less than the sampled values at all times. If the reference

sinusoid is made too large in an attempt to gain greater sensitivity, then it can be shown that the control algorithm begins to give an effect opposite to that desired and the sensitivity is duly impaired. Attempts for maximum sensitivity may have brought the sampled values of the depressed line voltage waveform below those values stored as the reference sinusoid, although calculations show that this condition should not occur.

The accuracy of the equipment is determined by a number of elements of the system, both in hardware and software. Most important is the accuracy to which the line voltage is sampled, and this is a function of both the ADC bit number and the sampling rate. The sampling rate was software-timed, and therefore subject to 'float' due to device temperature effects. The decision to use 8-bit ADCs was based on a brief study of noise levels together with the limited availability of suitable 10- and 12-bit devices. The 8-bit device was shown to give reasonable results on the model arc furnace supply system with relatively high flicker levels. Nevertheless, it must be noted that the resolution of an 8-bit sampling system is 0.4 percent of full scale, which is greater than the 'just perceptible' limit of 0.2 percent peak-to-peak that is widely recognised. This compensator system was thus applied, with limited accuracy, to a supply system with flicker levels high enough to be detected and compensated. The lower levels of voltage fluctuation, still sufficient to cause annoyance, could not be detected by an 8-bit sampling system and therefore remained uncompensated.

The speed of response of the system may be estimated by considering the times between start of sampling and subsequent initiation of the thyristor firing pulse. This time will always be within one half-cycle, and it may be after one quarter-cycle. This suggests a speed of response between 5 and 10 milliseconds. No studies were conducted to attempt to measure the speed of response of the control system used, although such an investigation would have been relatively easily conducted with the equipment available.

An advantage of the laboratory system used was that the same compensator control system could be applied to a TCR compensator with different rating, with only minimal changes to the system software. A second six-pulse TCR compensator, of higher rating than the first, was successfully used for the same equipments, and proved considerably more successful. The flicker improvement factor of 0.4 and the cross-over frequency of 25Hz compare very favourably with the published results of work elsewhere.

It is accepted, however, that this model shunt reactive compensator is not a full model of any particular system in service, or likely to be in service, on a full scale supply system. No attempt was made to filter harmonic frequencies, and the flicker levels compensated were of a high level. It is hoped that the work on the six-pulse TCR compensator scheme will encourage the presentation of comparable results from work elsewhere, in order to promote the objective assessment of this subject in greater depth.

(ii) The Twelve-Pulse TCR Compensator

The twelve-pulse TCR compensator scheme was developed in order to obtain a compensator with a faster speed of response for given rating, sensitivity and accuracy. The system functioned adequately, but failed to achieve results to improve on the six-pulse scheme.

The control algorithm used was a simple extension of that used successfully for the six-pulse compensator, and it is possible that a superior scheme could have been developed, given more time. A particular improvement may have been to increase the rating of the 'first stage' TCR unit to give fast, coarse control of voltage, to be followed by the conduction of a smaller rating 'second stage' for finer control.

Higher pulse numbers could be accommodated by the control scheme if necessary, and this is an obvious development of this aspect of the work. An eighteen-pulse TCR compensator design could give even earlier 'coarse' control, with finer control spaced over two following stages per half-cycle.

Such control schemes, of greater complexity, may benefit from the type of 'supervisory' control suggested in Chapter IV of this thesis. The response of the individual phase TCR controllers could be tuned by a master controller acting from a longer response time constant or from prior information on the furnace melt cycle.

Such a scheme could be applied to this laboratory model by enabling a 'master controller' to select the control variables to be used by each of the three-phase controllers. In this way the phase controllers would be dedicated to a fast response, whilst the master controller calculated the necessary values of reference sinusoid, sampling time and LIMIT.

8.1.3 Data Analysis

The bulk storage of the recorded Templeborough arc furnace voltages and currents on a mainframe computer gave fast and simple access, and enabled many different studies of sections of data to be made using modern graphical output programs.

Logging of results from the laboratory models, and subsequent transfer of this data to the mainframe computer, provided a very large storage facility for blocks of data obtained from different experimental conditions.

It must be noted that the work towards providing such data transfer facilities was, although apparently straightforward, very time consuming; transfer of data from one format through three other formats was not unusual. The ability to transfer experimental results from the laboratory to mainframe computer files was not achieved until the very final stage of the research project, and in fact little use was made of this facility.

The bulk of the laboratory modelling results were then obtained from benchtop equipment such as the spectrum analyser, two-channel storage oscilloscope and flat bed plotter. Careful measurement techniques allowed these to be used to good effect, and they saved many hours of programming effort which would have been required to obtain the same results via the mainframe computer.

Where the modelling was itself carried out on the computer, standard spectral analysis and graphical output routines were written and tailored to suit exactly the needs and interests of this research project.

One analysis method which was not achieved, even though the facilities were available, was the mainframe computer modelling of the UIE digital flickermeter. Applying such a facility to the results from arc furnace and TCR compensator models would have completed the link between simple observation and comparison of power spectra on the one hand, and the knowledge of a 'flicker severity factor' on the other.

8.1.4 Mathematical Modelling

It was an early aim of the research project to develop a numerical model of the arc furnace installation, in parallel with modelling work undertaken in the laboratory. This would have allowed investigative work to be done computationally in advance of capital expenditure on different arrangements of equipment.

The computational arc furnace model has been shown to successfully reproduce the flicker frequency disturbances found in the real system, although there is still some disparity between the observed time domain line voltages produced. Sudden severe voltage fluctuations are absent from the modelled line voltage, and it was suggested that such fluctuations may not be an effect of the arc furnace load currents measured by the CEGB, but rather are caused by other loads on the 275kV system.

This explanation rapidly solves the problem, but the disturbance levels observed would then indicate that the 275kV 'Sheffield ring' supply had large transient voltage changes regularly impressed upon it for the duration of the measurement period.

The numerical model was eventually developed at a stage after results had been obtained from the laboratory model, and there was in fact little parallel development carried out. The two areas of study progressed separately, and far more work is still required on the mathematical modelling of the TCR compensator. The program listings show that considerably more computational effort was involved for the compensator modelling than was required for the arc furnace model, and the control algorithm used was not subjected to sufficient investigation once the TCR compensator equations were established. The control algorithm described in Chapter VII was even simpler than that used in the laboratory, and it is possible that further development to integral of voltage difference or 'voltage difference squared' may yet produce results to assist in the understanding of TCR compensator control schemes.

8.2 CONCLUSIONS

The work carried out shows that recordings of arc furnace current waveforms may be used to reproduce successfully the voltage fluctuations appearing on the real supply system. The numerical model allows this to be undertaken in an environment where supply system parameters may be rapidly changed to suit different investigative approaches.

The laboratory model provided a facility for obtaining voltage fluctuations with frequency components accurately representing those found on the real arc furnace supply network, and the magnitude of these fluctuations relative to the 50Hz 'carrier' amplitude was easily changed.

The disturbances produced by the models formed an excellent reference for studies aiming for their reduction by shunt compensation techniques, and the reproduction of low frequency disturbances in particular allowed shunt compensation for voltage flicker reduction to be carried out in the laboratory.

The compensation studies employed a thyristor controlled reactor configuration commonly used in the industry, and it was shown how a simple, low-cost microcomputer system could be used to achieve effective reduction in the frequency components of the voltage fluctuations that cause tungsten filament lamp voltage flicker.

8.3 FURTHER WORK

The models now established form an excellent facility for the research and testing of other types of TCR compensator control algorithm. A common assessment method, and presentation of the results obtained from each scheme, would contribute much to the industry's understanding of the benefits of different TCR control strategies.

The twelve-pulse TCR compensator design requires further development of its control algorithm to achieve results comparable with those already presented for the six-pulse scheme, and it is possible that the computer modelling methods described may be extended towards the study of a twelve-pulse scheme. The two stage conduction patterns of the twelve-pulse arrangement allow a wide range of control strategies to be investigated, which will be new to the field of research in this subject.

Improvement of the laboratory model may be obtained by increasing its VA rating to allow greater levels of current to be drawn by the thyristor controlled reactances.

The presentation of the results of TCR compensator schemes would be considerably strengthened by the application of an internationally recognised digital flickermeter, such as that now recommended by the UIE.

REFERENCES

- [1] Subcommittee Report, 1957 'Survey of Arc Furnace Installations on Power Systems and Resulting Lamp Flicker'
AIEE Trans., Applications and Industry, Vol 76, Pt II, pp 170-183, 1957.
- [2] Langman R D and Walker R W:
'Factors Influencing the Control and Supply of Power to Three-Phase Electric Arc Furnaces'
IEE Conference Publication No 8, Abnormal Loads on Power Systems, February 1963.
- [3] Thomas R J:
'The Characteristics of Voltage Fluctuations Caused by Arc Furnaces'
IEE Conference Publication No 8, Abnormal Loads on Power Systems, 1964.
- [4] Thomas R J and Kendall P G:
'Effect of Small Voltage Fluctuations on the Light Output of Lamps'
IEE Conference Report No 8, 1964, pp 122-124.
- [5] Thomas R J and Kendall P G:
'Perception and Toleration of Some Kinds of Regular Lamp Flicker'
IEE Conference Report No 8, pp 125-131.
- [6] The Electricity Council:
'Supply to Arc Furnaces'
Engineering Recommendation p 7/2, July 1970.
- [7] The Electricity Council:
'Report on Supply to Arc Furnaces'
ACE Report No 26, 1970.
- [8] Dixon G F L and Kendall P G:
'Supply to Arc Furnaces: Measurement and Prediction of Supply Voltage Variation'
Proceedings of the IEE, 1972, Vol. 119, pp 456-465.
- [9] Kendall P G:
'Light Flicker in Relation to Power System Voltage Fluctuation'
Proceedings of the IEE, 1966, Vol 113 pp 471-479.
- [10] Coates R and Brewer G L:
'The Measurement and Analysis of Waveform Distortion Caused by a Large Multi-Furnace Arc Furnace Installation'
IEE Conference Publication No 110, Sources and Effects of Power System Disturbances, April 1974.
- [11] Kauferle J and Jahn H H:
'Measuring and Evaluating Current Fluctuations of Arc Furnaces'
IEE Conference Publication No 110, Sources and Effects of Power System Disturbances, April 1974.
- [12] Kirkby H J A and Langman R D:
'Measuring Voltage Fluctuations Caused by Electric Arc Furnaces'
IEE Conference Publication No 110, Sources and Effects of Power System Disturbances, April 1974.

- [13] Granstrom S:
'Computer Studies of Voltage Fluctuations Caused by Arc Furnaces'
UIE 9th International Congress, Cannes, October 1981.
- [14] Jervis W B:
'An Assessment of Power System Voltage Disturbances in Terms of Lamp Flicker Perception'
IEE Conference Publication No 210, 1982, pp 71-76.
- [15] Franklin P J:
'The assessment of Flicker from Groups of Supergrid Connected Arc Furnaces'
IEE Conference Publication No 210, 1982, pp 1-5.
- [16] Ashmole P H and Cornfield G:
'Design and Use of a Digital Meter for Monitoring System Voltage Flicker and Harmonics'
IEE Conference Publication No 210, 1982, pp 160-165.
- [17] Hamoaki Y:
'Present State and Future of the Methods for Estimating Lamp Flicker caused by Arc Furnaces'
UIE 9th International Congress, Cannes, October 1980.
- [18] Aoki M:
'Standard Method for Measurement of Voltage Fluctuations'
UIE 9th International Congress, Cannes, October 1980.
- [19] UIE Disturbances Study Committee:
'Arc Furnace Disturbances - State of the Art'
- [20] Ashmole P H:
'The 'UIE' Digital Flicker Meter'
The Electricity Council, Distribution Developments, September 1982.
- [21] Kelela J and Firestone L:
'Under-Excited Operation of Generators'
IEEE Transactions, Vol PAS-83, pp 811-817, 1964.
- [22] Chang N E:
'Locating Shunt Capacitors on Primary Feeders for Voltage Control and Loss Reduction'
IEEE Transactions, Vol PAS-88, pp 1574-1577.
- [23] Illiceto F and Cinieri E:
'Comparative Analysis of Series and Shunt Compensation Schemes for AC Transmission Systems'
IEEE Transactions, Vol PAS-96, pp 1819-1830.
- [24] Oliver J A, Ware B J and Carruth R C:
'345MVA Fully Water Cooled Synchronous Condenser; Application Considerations'
IEEE Transactions, Vol PAS-90, pp 2758-2764, 1971.

- [25] Dixon G F L, Friedlander E, Seddon F and Young D J:
'Static Shunt Compensation for Voltage-Flicker Suppression'
IEE Conference Publication No 8, Abnormal Loads on Power Systems, pp
45-61, 1964.
- [26] Friedlander E:
'Voltage-Flicker Compensation with AC Saturated Reactors'
GEC Journal of Science and Technology, Vol 29 No 2, pp 107-114, 1962.
- [27] Friedlander E, Telehum A and Young D J:
'Arc Furnace Flicker Compensation in Ethiopia'
GEC Journal of Science and Technology, Vol 32 No 1, pp 2-10, 1965.
- [28] Clegg E, Heath A J and Young D J:
'The Static Compensator for the BSC Anchor Project'
IEE Conference Publication 110, Sources and Effects of Power System
Disturbances, 1974.
- [29] Kennedy M W, Loughran J and Young D J:
'Application of a Static Suppressor to Reduce Voltage Fluctuations
Caused by a Multiple Arc Furnace Installation'
IEE Conference Publication 110, Sources and Effects of Power System
Disturbances, pp 130-134, 1974.
- [30] Berry D H, Clarke C D, Goldsmith D S and Young D J:
'Saturated Reactor Compensator Achieves Major Reduction of Flicker
Caused by Arc Furnace Installation'
Paper presented to CEA Spring Meeting, Toronto, 22-24 March 1976.
- [31] The Electricity Council:
'Compensators for Arc Furnaces'
ACE Report No 58 (1977).
- [32] Ashmole P H, Murray B E, Young D J:
'An Assessment of Compensation Equipment for Arc Furnace Supplies'
UIE 9th International Congress, Cannes, October 1981.
- [33] IEE Proceedings Part C; Special Section:
'Static Compensation for AC Power Systems'
IEE Proceedings, Vol 128, Part C, No 6 pp 362-406, November 1981.
- [34] Byerly R T, Poznaniak D T and Taylor E R:
'Static Reactive Compensation for Power Transmission Systems'
IEEE Transactions, Vol PAS-101, No 10, pp 3997-4005, October 1982.
- [35] Gavriolic A, Heath A J and Williams W P:
'Reduction of Flicker by Alternative Types of Static Compensator'
IEE Conference Publication CIREN '81, pp 86-90, 1981.
- [36] IEEE Substations Committee, Working Group 79.2:
'Bibliography of Static VAR Compensators'
IEEE Paper 83WM 105-4 presented at the IEEE PES Winter Meeting, January
1983.

- [37] Gyugi L and Otto R A:
'Static Shunt Compensation for Voltage Flicker Reduction and Power Factor Correction'
Proceedings of the American Power Conference, 1976, pp 1271-1286.
- [38] Gyugi L, Otto R A and Putman T H:
'Principles and Applications of Static, Thyristor-Controlled Shunt Compensators'
IEEE Transactions, Vol PAS-97, No 5 September/October 1978 pp 1935-1945
- [39] Brehler R and Kleinsorge N:
'Static Compensators - VAR Control Using Thyristors'
Siemens 30th Annual Power Distribution Conference, University of Texas, October 1977.
- [40] Ashmole P H:
'Fundamental Reactive Power Control Requirements'
IEE Technical Seminar on Control of Reactive Compensation for AC Power Systems, September 1980. pp 2/1-2/9.
- [41] Cooper C B and Hussayani S A:
'Thyristor Switched Reactors for Distribution Systems'
IEE Technical Seminar on Control of Reactive Compensation for AC Power Systems, September 1980. pp 4/1-4/8.
- [42] Young D J:
'Frequency Response of Arc Furnace Compensators'
Electrical Review, Vol 204, No 11, pp 41-43 1979.
- [43] Seki A, Nishidai J and Murotani K:
'Suppression of Flicker due to Arc Furnaces by a Thyristor-controlled VAR Compensator'
IEEE PES Summer Meeting, Los Angeles CA July 1978.
- [44] Ritamaki P and Saarelainness E:
'New Low-loss Static Compensator Improves Steel Production and Quality of Power System'
Electricity in Finland, Sahko 51 (1978) 5-6 pp 197-187.
- [45] Hosono I, Yano M, Takeda M and Yuya S:
'Suppression and Measurement of Arc Furnace Flicker with a Large Static VAR Compensator'
IEEE Transactions 1979, Vol PAS-98, No 6, pp 2276-2283.
- [46] Bergeal J:
'Thyristors Controlled Static Compensators and Arc Furnaces'.
Paper presented to the 1979 CIRED Conference, Liege.
- [47] Kumar A and Koch G:
'Microprocessor-Based Integrated Protection and Control of MV Substations - A Practical Approach to Substation Automation'
IEE Conference Publication No 250, CIRED 1985, pp 122-131.

- [48] Sucena Paiva J P, Pinto de Sa J L and Barruncho L:
'Distribution Substation Automated Controller'
IEE Conference Publication No 250, CIREC 1985, pp 292-296.
- [49] Alegria, C M:
'Microcomputer Control of Power Converters'
IEEE Transactions, Vol PAS-65, pp 2011-2017, 1984.
- [50] Thorp J S and Phadke A G:
'A Microprocessor-Based Three-Phase Transformer Differential Relay'
IEEE Transactions, Vol PAS-101 No 2, pp 426-432, 1982.
- [51] Reeve J and Giesbrecht W J:
'Microprocessor Control for HVDC Converters'
IEE Conference Publication No 205, International Conference on Thyristor and Variable Static Equipment for AC and DC Transmission, pp 186-189, 1981.
- [52] Tso S K and Ho P T:
'Dedicated Microprocessor Scheme for Thyristor Phase Control of Multiphase Converters'
IEE Proceedings, Vol 128, Part B, No 2, pp 101-108, 1981.
- [53] Dewan S B and Dunford W G:
'A Microprocessor-Based Controller for a Three-Phase Controlled Rectifier Bridge'
IEEE Transactions, Vol IA-19, No 1, pp 113-119, 1983.
- [54] Tso S K and Leung C C:
'Microprocessor Control of Triac Cycloconverter'
IEE Proceedings, Vol 130, Part B, No 3, pp 193-200, 1983.
- [55] Lowry L R and Gyugyi L:
'Field Testing of Light-Triggered Thyristors in an Electric Utility Application'
IEE Conference Publication 205, International Conference on Thyristor and Variable Static Equipment for AC and DC transmission, pp 92-95, 1981.
- [56] Temple V A K:
'Thyristor Devices for Electric Power Systems'
IEEE Transactions, Vol PAS-101, No 7, pp 2286-2291, 1982.
- [57] Imai K, Kobayashi S, Senda T:
'Behaviour of HVDC Thyristor Valve on the Critical Turn-Off Condition and Optimised Gate Firing System'
IEEE Transactions, Vol PAS-101 No 11, pp 4419-4427, 1982.
- [58] Nilsson A, Eklund L and Hogberg K E:
'Design and Testing of an HVDC Thyristor Valve'
IEE Conference Publication 205, International Conference on Thyristor and Variable Static Equipment for AC and DC transmission, pp 154-157, 1981.

- [59] Lips H P:
'Optimisation of High Power Thyristor Valves'
IEE Conference Publication 205, International Conference on Thyristor and Variable Static Equipment for AC and DC transmission, pp 164-166, 1981.
- [60] Woodhouse M L, Ballard J P, Haddock J L and Rowe B A:
'The Control and Protection of Thyristors in the English Terminal Cross Channel Valves, Particularly During Forward Recovery'
IEE Conference Publication 205, International Conference on Thyristor and Variable Static Equipment for AC and DC transmission, pp 158-163, 1981.
- [61] Cooper C B and Yacamini R:
'Choice of Analytical and Modelling Methods for Reactive Compensation Equipment'
IEE Proceedings, Vol 128, Part C, No 6 pp 402-406, 1981.
- [62] Ritamaki P and McGranaghan M F:
'Static Compensator Control Systems and their Simulation on a TNA'
IEE Conference Publication 205, 'International Conference on Thyristor and Variable Static Equipment for AC and DC Transmission' pp 52-55, 1981.
- [63] Borgonovo G, Baggini L, Santagostino G and Nicola G:
Studies Concerning the Possible Application of SVS's on the Future UHV Transmission System of ENEL'
Proceedings of the EPRI/Hydro-Quebec International Symposium on Controlled Reactive Compensation, Varennes, 1979.
- [64] Engberg K and Ivner S:
'Static VAR Systems for Voltage Control During Steady-State and Transient Conditions'
Proceedings of the EPRI/Hydro-Quebec International Symposium on Controlled Reactive Compensation, Varennes, 1979.
- [65] Gavriolic M M, Sybille G, Do V Q and Lemay J Y:
'Controlled Reactive Compensation Modelling on the IREQ Power System Simulator'
Proceedings of the EPRI/Hydro-Quebec International Symposium on Controlled Reactive Compensation, Varennes, 1979.
- [66] Turner D R, Watkinson P and Davis I C:
* 'Modelling of an Electric Arc Furnace'
IEE Conference Publication 210, 'Sources and Effects of Power System Disturbances, pp 237-242, 1982.
- [67] Holmes J and Wright A:
'A Laboratory High Speed Reactive Power Compensator'
IEE Conference Publication 210, 'Sources and Effects of Power System Disturbances, pp 237-242, 1982.
- [68] Dommel H W:
'Digital Computer Solution of Electromagnetic Transients in Single and Multiphase Networks'
IEEE Transactions, Vol PAS-88, No 4 pp 388-399, 1969.

- [69] Dommel H W:
'Non-linear and Time Varying Elements in Digital Simulation of Electromagnetic Transients'
Paper Presented at the PICA Conference, Boston, Mass, 1971.
- [70] Dommel H W and Sato N:
'Fast Transient Stability Solutions'
Paper Presented at the IEEE PES Winter Meeting, New York, 1972.
- [71] Dommel H W and Scott Meyer W:
'Computation of Electromagnetic Transient'
IEEE Proceedings, Vol 62, No 7, pp 983-993, 1974.
- [72] Budner A:
'Introduction of Frequency-Dependent Line Parameters into an Electromagnetic Transients Program'
IEEE Transactions, Vol PAS-89, No 1, pp 88-97, 1970.
- [73] Marti J R:
'Accurate Modelling of Frequency-Dependent Transmission Lines in Electromagnetic Transient Simulations'
IEEE Transactions, Vol PAS-101, No 1, pp 147-155, 1982.
- [74] Feero W E, Juves J A and Long R W:
'Circuit Breaker and Transformer Models for the Solution of Wavy Propagation in Distributed Parameter Systems'
Paper Presented at the IEEE Summer Power Meeting, July 1970.
- [75] Lasseter R H and Lee S Y:
'Digital Simulation of Static VAR System Transients'
IEEE Transactions, Vol PAS-101, No 10 pp 4070-4177, 1982.
- [76] Cornfield G:
'The Performance of Switched Reactor Arc Furnace Compensators'
IEE Conference Publication 210, 'Sources and Effects of Power System Disturbances', May 1982.
- [77] Turner D R and Davis I C:
* 'The Computational Modelling of an Electric Arc Furnace'
Paper presented at the 17th Universities Power Engineering Conference (UPEC), 1982.
- [78] Billings S A and Nicholson H:
'Modelling a Three-Phase Electric Arc Furnace: A Comparative Study of Control Strategies'
Applied Mathematical Modellings, Vol 1, pp 355-361, 1977.
- [79] Dugan R C:
'Simulation of Arc Furnace Power Systems'
IEEE Transactions, Vol IA-16, No 6, pp 813-818, 1980.
- [80] Columbo L B, Profumo F and Valfre L:
'Digital Model to Evaluate the Flicker Level in an Industrial Plant: Application to Steelworks with Arc Furnaces'
IEE Conference Publication 250, CIRED 1985, pp 344-351, 1985.

- [81] Hensman G O, Levy A and Mogridge L:
'DREAM - Digital recording and measuring equipment for power system data acquisition. Summary guide to equipment'
CEGB System Technical Branch Report PL-ST/11/80 June 1980.
- [82] Hensman G O:
'A digital recording and measurements system for power system studies'
European Conference on Precise Electrical Measurements (EUROMEAS), IEE September 1977.
- [83] Rockwell International Corporation:
'AIM-65 Microcomputer users guide' 1979.
- [84] Rockwell International Corporation:
'R6511 Microcomputer System Hardware Manual' 1978.
- [85] Rockwell International Corporation:
'R6511 Microcomputer System Programming Manual' 1979.
- [86] The Computerist Incorporated:
Guide to "DRAM PLUS multi-purpose expansion board' 1980.
- [87] 'Crown M-600 Power Amplifier Handbook'
Crown International Inc, USA.
- [88] Macedo F X:
'Power System Harmonic Impedance Measurement using Natural Disturbances'
IEE Conference Publication 210, pp 183-188, 1982.
- [89] Unpublished CEGB results:
'HARPO3' Harmonic Analysis package.
- [90] Gould OS-4100 Oscilloscope Handbook.
- [91] Jenkins G and Watts D:
'Spectral Analysis and its Applications'
Holden Day, 1968.
- [92] Lathi B P:
'Modern Digital and Analog Communication Systems'
Holt Sanders, 1983.
- [93] Robiette A G E:
'Electric Melting Practice'
Griffin 1972.
- [94] Morris A S and Sterling M J H:
'Identification and Direct Digital Control of an Electric Arc Furnace Controller'
IEE Proceedings, Part D, 1981, Vol 128 pp 123-217.
- [95] Miller T J E (Ed):
'Reactive Power Control in Electric System'
J Wiley, New York 1982.

- [96] De Mello E P, Johnson B K, Hannett L N, Birfet D and Toulemond J:
'Thyristor - Controlled Reactors, Analysis of Fundamental Frequency and Harmonic Effects'
IEEE PES Winter Meeting, New York, January 1978.
- [97] Reichert K, Terens L, Durr J and Pfyl W:
'Harmonic Interactions between Static VAR Systems and the Network: Problems, Analysis and Solutions'
pp 142-173.
- [98] Granstrom S and Sundberg Y:
'Harmonics and their Suppression in a 48/40MVA Arc Furnace Plant'
Elektrowarme International 36 (1978) B5 - October, pp 264-269.
- [99] Ravenscroft J:
'The determination of the Electrical Characteristics of an Arc Furnace'
IEE Paper No 3328 U, September 1960.
- [100] Schwabe W E:
'Electrical and Thermal Factors in UHP Arc Furnace Design Operation'.
Paper presented at the 9th International UIE Congress, Cannes. October 1980.
- [101] Schweickardt H and Romegialli G:
'The Static VAR Source in EHV Transmission Systems and its Control'
Brown Boveri Review 9-78, 1978.
- [102] Czech P, Hung S Y M, Huynh N H and Scott G:
'TNA Study of Static Compensator Performance on the 1982-1983 James Bay System, Results and Analysis'
Proceedings of the IREQ Conference, Varennes, September 19-21, 1979.
- [103] Dorf R C:
'Modern Control Systems'
Addison-Wesley Publishing Company, 1974.
- [104] Chee Hing D J and Julien K S:
'A New Static Watt Compensator for the Iron and Steel Company of Trinidad and Tobago'
IEEE Transactions 1982, Vol PAS-101, No 8, pp 2982-2987.
- [105] Mullard BT 152-400 Data Sheet.
- [106] Mullard BTX 18-500 Data Sheet.
- [107] Ziemer R E and Tranter W H:
'Principles of Communications - System, Modulation and Noise'
Houghton Mifflin, 1976.
- [108] 'Microprocessor Laboratory 8088 System Development Kit Users Manual'
University of Liverpool Internal Document, 1982.

- [109] Morse S P:
'The 8086/8088 Primer'
Hayden Book Company Inc, 1982.
- [110] Tektronix 8560 MUSDU Handbook.
- [111] Analogue Devices AD7574 Data Sheet (8-bit ADC).
- [112] Liu B (Ed):
'Digital Filters and the Fast Fourier Transform'
Halsted Press, 1975.
- [113] Blinichikov H J and Zverev A I:
'Filtering in the Time and Frequency Domains'
J Wiley, New York, 1976.
- [114] IEEE G-AE Subcommittee on Measurement Concepts:
'What is the Fast Fourier Transform'
IEEE Trans on Audio and Electroacoustics, Vol AU-15, No 2, June 1967
pp 45-56.
- [115] Bendat J S:
'Engineering Applications of Correlation and Spectral Analysis'
J Wiley, New York 1980.
- [116] Bingham C, Godfrey M D and Tukey J W:
'Modern Techniques of Power Spectrum Estimation'
IEEE Trans on Audio and Electroacoustics, Vol AU-15, No 2, June 1967
pp 56-66.
- [117] Bogert B P:
'Informal Comments on the Uses of Power Spectrum Analysis'
IEEE Trans on Audio and Electroacoustics, Vol AU-15, No 2, June 1967
pp 74-75.
- [118] Hewlett Packard HP 3582A Power Spectrum Analyser Handbook.
- [119] Welch P D:
'The Use of Fast Fourier Transform for the Estimation of Power Spectra: A Method Based on Time Averaging over Short, Modified Periodograms'
IEEE Trans on Audio and Electroacoustics, Vol AU-15, No 2, June 1967
pp 70-73.
- [120] Kreyszig E:
'Advanced Engineering Mathematics'
J Wiley, New York, 1972.
- [121] Davis I C:
'Notes on Arc Furnace Operation'
Unpublished Report to the CEGB System Technical Branch.

- [122] 'NAG FORTRAN Library Manual Mark 10 - Application Notes for Subroutine E02BAF'
Numerical Algorithms Group Ltd, Oxford, 1983.
- [123] 'NAG FORTRAN Library Manual Mark 10 - Application Notes for Subroutine E02BCF'
Numerical Algorithms Group Ltd, Oxford, 1983.
- [124] Cox M G:
'A Data Fitting Package for the Non-Specialist User'
In Software for Numerical Mathematics (D J Evans, Ed)
Academic Press, London, 1974.
- [125] Cox M G:
'The Numerical Evaluation of B-Splines'
J Inst Maths Applics, Vol 10, pp 134-149, 1972.
- [126] Schweickardt H E, Romegialli G and Reichert K:
'Closed Loop Control of Static VAR Sources on EHV Transmission Lines'
Paper submitted to the IEEE PES Winter Meeting, 1978.

APPENDIX A

SHORT CIRCUIT POWER OF A 56MVA ARC FURNACE AT TEMPLEBOROUGH

The arc furnace installation is supplied from the 275kV busbar as shown in Figure 2.2.

Define X_s' , X_b' and X_a' as:

X_s' = Source Reactance - between PCC and infinite busbar

X_b' = Any reactance between furnace transformer and PCC

X_a' = Reactance of furnace transformer, supplementary reactors and arc furnaces

as illustrated in Figure 3.7.

X_a' is often unknown, and typical values based on furnace nameplate rating can be consulted^[6].

Thus $X_a' = 50\text{p.c.}$ on 56MVA base for a 56MVA furnace

and $X_a' = 50\text{p.c.} \times \frac{100}{56}$ on 100MVA base

= 89.3p.c. on 100MVA base

For this network (see Figure 2.2):

$X_s' = 1.18\text{p.c.}$ on 100MVA base

and $X_b' = 23.933\text{p.c.}$ on 100MVA base

Then:

$$S_t = \frac{100}{X_a' + X_b' + X_s'} \quad \text{MVA}$$

$$\underline{S_t = 87.46 \text{ MVA}}$$

SGT4 incorporates an on-load tap changer with taps between +10p.c. and -20p.c. in 13 steps. For a constant primary voltage of 275kV, the SGT4 secondary voltage may vary between $29.7\text{kV} \leq V_2 \leq 39.6\text{kV}$. The percentage impedance, X_{33} , given for those components at 33kV will then vary with the true voltage V_2 as: $X = X_{33} \times \frac{33^2}{V_2^2}$. Thus X_a' may vary from the nominal value of 0.893 per unit between 0.52 per unit and 1.102 per unit. These impedance values then show how S_t may vary from the nominal value given above, depending on SGT4 tap position:

$$S_{t\text{MAX}} = 114.8\text{MVA}$$

$$S_{t\text{MIN}} = 73.9\text{MVA}$$

The CEGB measurements were made at point B, between the impedances X_b' and X_a' , therefore the measured short circuit MVA will be proportionally less than the theoretical value from the infinite busbar by the factor

$$\frac{X_a'}{X_a' + X_b' + X_s'}$$

Then:

$$S_{t\text{MAX}} = 81.71\text{MVA}$$

$$S_t = 68.21\text{MVA Nominal}$$

$$S_{t\text{MIN}} = 61.19\text{MVA}$$

APPENDIX B

RECOVERY OF DATA FROM CEGB MAGNETIC TAPE STORAGE

Recordings were made over a period of 3 days at the Templeborough 275kV/33kV substation. Six arc furnaces were supplied from this substation, with a collective nameplate rating of 360MVA.

Up to 8 channels of data could be sampled using the DREAM recording equipment^[81,82]. Studies of oscillograms for the bulk of the recorded data revealed trends in the recordings which would not be so apparent for a cycle by cycle analysis. On the basis of these visual studies two different sections of data were selected for further use at Liverpool University. Blocks of selected data were transferred to magnetic tape number LSN201, to be held in the Liverpool University Computer Centre tape library.

Each block or record of data contains 2048 bytes of information:

8 bytes - block number and time GMT at start of block

2032 bytes - data. 2 bytes x 8 channels x 127 lines

8 bytes - spare at end of each block

Each line of 8 channels is time-spaced from the next line by 800microseconds. Thus each block contains approximately 5 cycles of data.

Each 2-byte channel gives a 16-bit signed integer value in the range -32767 to +32767 which needs to have a small offset removed before a scale factor is applied to give values of kV or kA.

Recording details and comments on the data content are now given:

(i) First 600 Blocks on LSN201

From RF07, tape No 3, blocks 60 to 660 inclusive.

16.11.00 hours to 16.21.30 hours 28/6/1977

Furnace No 2 operating in isolation. (Furnace No 1 off and bus section switch open - see Figure 2.1.)

Start-up of Furnace No 2 occurs in block 60.

This 'start-up' data is the same as that used by CEGB STB for various studies^(REFS).

See table B1 for scaling and offset values.

(ii) Blocks 600 to 1500 on LSN201

From RF18, tape No 2, blocks 2600 to 3500 inclusive.

Furnace No 5 and Furnace No 6 on. Severe low frequency oscillations in furnace No 6 line current peaks. Furnace No 6 becomes almost open circuit for several seconds before returning to full power during melt-down.

See table B2 for scaling and offsets.

CHANNEL	1	2	3	4	5	6	7	8
ADD TO INTEGER VALUE	-2	-5	-1	+71	+80	-109	+32	-12
MULTIPLY BY	3.404	3.393	3.411	0.3364	0.3360	0.3452	0.3374	0.3382
QUANTITY (UNITS)	VR1 kV	VY1 kV	VB1 kV	IR1 kA	IY1 kA	IB2 kA	IR2 kA	IY2 kA

Table B1 Scaling and Offsets for RF07

CHANNEL	1	2	3	4	5	6	7	8
ADD TO INTEGER VALUE	-145	-128	-150	-111	-72	-72	-49	-
MULTIPLY BY	3.390	3.394	3.387	0.3836	0.3748	0.3787	0.3790	-
QUANTITY (UNITS)	VR6 kV	VY6 kV	VB6 kV	IR5 kA	IB5 kA	IR6 kA	IB6 kA	-

Table B2 Scaling and Offsets for RF18

APPENDIX C

CUBIC SPLINE CURVE FITTING AND ITS APPLICATION

C.I Introduction

The time series data obtained from the CEGB (see Appendix B) gave only the measured instantaneous three-phase voltages and currents with a sampling interval of 800 microseconds.

The modelling work undertaken in this Thesis used the measured three-phase currents as the 'driving signal' in physical and mathematical models to reproduce voltage distortion.

In each model, some additional information was required from this data, namely:

- (i) In the physical model (Chapter 2), interpolation between points was used to increase the number of points output in each cycle to give smoother waveforms.
- (ii) In the mathematical model (Chapter 8), the value of di/dt was required for each value of measured current, i .

All large-scale data handling was performed on a mainframe computer, and numerical techniques were used to obtain the data required by (i) and (ii) above. The Numerical Algorithms Group (NAG) Library^[122,123] subroutine E02BAF was used to compute a weighted least-squares approximation to the original data by a cubic spline. The same subroutine was then used for interpolation to satisfy (i) above. NAG subroutine E02BCF was then used to evaluate derivatives from the B-spline to satisfy (ii) above.

C.II Applications Programs

Cox^[124,125] describes how the set of N data points (x_r, y_r) may be used to calculate a cubic spline approximation

$$S(x) = \sum_{i=1}^{N+3} C_i N_i(x)$$

where the coefficients are c_j , and the normalised B-spline is $N_j(x)$. The B-spline $N_j(x)$ is defined upon 'knots' K_{j-4} , K_{j-3} , K_{j-2} , K_{j-1} and K_j .

Once $N_j(x)$ has been calculated from $y(x)$, the B-spline parameters can then be passed to NAG subroutine E02BCF, which may be used to evaluate $S(x)$ or its derivatives at any value of x . At those values of x where the input parameters $y(x)$ is known, then

$$E(x) = S(x) - y(x)$$

may be calculated to show the error magnitudes due to use of the B-spline rather than use of original data at this point.

This procedure was followed for each of the four channels i_R , i_Y , i_B , v_R (see Section 2.3.2) in sequence. Each channel consisted of 2250 time-series data points, corresponding to ninety 50Hz cycles. Attempting B-spline evaluation for 2250 points involved large computational effort, and program failures were frequent. The process was therefore restricted to data blocks of 780 points - representing one-third of the total span, plus 15 points at each end of the block.

The FORTRAN program to perform the interpolation process for the analogue model is shown in C.III and comment statements within the program explain the program flow.

The FORTRAN program to obtain values of di/dt for all values of 'i' is shown in C.IV.

C.III SPLI30M FORTRAN Program Listing

FILE: SPLI30M FORTRAN A1 (EE68)

```

C          DOUBLE PRECISION FIRST(1),LAST(1),SECOND(1),THIRD(1),FOURTH(1),
+WORK1(800),WORK2(4,800),C(800),K(800),W(800),SS,
+VR(800),VY(800),VB(800),IP(800),IQ(800),
+IR(800),IY(800),IB(800),X(800),Y(800),
+OUT1(4000),OUT2(4000),OUT3(4000),OUT4(4000),
+T(4000),TIME(4000),T1(4000,8),TIME1(4000),
+XTOT,XSTART,XFIN,XVAR,XARG,RES,FIT(4)
  INTEGER I,NCAP,NCAP7,J,IFAIL,J2,M,L,N,R,M1,M2,M3,LEFT,
+KOUNT,RESULT,ITIME,Z,ENDNOT
  LOGICAL AMIDPT
  DATA FIRST/8H   FIRST/
  DATA LAST/8H   LAST/
C  DATA SECOND/8H SECOND/
C  DATA THIRD/8H  THIRD/
C  DATA FOURTH/8H FOURTH/
C
C.....SPLINE30M....SAME AS SPLINE10M BUT FOR 30 CYCLES OF DATA
C      INSTEAD OF 10 CYCLES.
C      (ONLY GIVES IR,IY,IB,VR FOR THE ANALOGUE MODEL)
C
C      THE PROGRAM WILL INTERPOLATE 'EXTRA' EXTRA POINTS
C      BETWEEN DATA POINTS.
C
C      SINCE OUTPUT OF A DETAILED RESULTS LIST FOLLOWED BY A
C      CONTINUOUS LISTING FOR USE AS INPUT DATA IS OFTEN EXCESSIVE,
C      'RESULTS' SHOULD BE SET AT :
C          1 -FOR BOTH LISTINGS
C          2 -FOR ONLY THE 'DETAILED' LISTING
C          3 -FOR ONLY THE 'CONTINUOUS' LISTING
C
C      TSTEP IS THE TIME STEP OF INPUT DATA .
C
C      M=780
C      NCAP=M-7
C      RESULT=1
C      TSTEP=0.0008
C      EXTRA=3.0
C      IXTRA=IFIX(EXTRA)+1
C
C      THE FOLLOWING LOOP READS ALL EIGHT CHANNELS OF DATA,
C      SPECIFIES THE DEPENDANT VARIABLE TO BE USED,
C      SETS ALL WEIGHTS TO 1.0 AND SPECIFIES KNOTS K(5) TO
C      K(NCAP+3) TO BE AT THE SAME ORDINATES AS X(5) TO
C      X(NCAP+3). THE X-AXIS IS SCALED SUCH THAT THERE IS
C      AN INPUT DATA VALUE AT EVERY FOURTH INTEGER POINT.
C
C      T1(1,1)=0.0000
C      T1(1,2)=0.0000
C      T1(1,3)=0.0000
C      T1(1,4)=0.0000
C      T1(1,5)=0.0000
C      T1(1,6)=0.0000
C      T1(1,7)=0.0000
C      T1(1,8)=0.0000
C      READ(5,996)VR(1),VY(1),VB(1),IP(1),IQ(1),IB(1),IR(1),IY(1)
C      W(1)=1.0
C      DO 10 R=2,M
C          READ(5,996)VR(R),VY(R),VB(R),IP(R),IQ(R),IB(R),IR(R),IY(R)
C          IF(VR(R).EQ.0.0.AND.VY(R).EQ.0.0)GOTO 555
C          DO 9 ICHAN=1,8
C              T1(R,ICHAN)=T1(R-1,ICHAN)+TSTEP
C          9      CONTINUE
C      W(R)=1.0
C  10 CONTINUE

```

```

SPL00010
SPL00020
SPL00030
SPL00040
SPL00050
SPL00060
SPL00070
SPL00080
SPL00090
SPL00100
SPL00110
SPL00120
SPL00130
SPL00140
SPL00150
SPL00160
SPL00170
SPL00180
SPL00190
SPL00200
SPL00210
SPL00220
SPL00230
SPL00240
SPL00250
SPL00260
SPL00270
SPL00280
SPL00290
SPL00300
SPL00310
SPL00320
SPL00330
SPL00340
SPL00350
SPL00360
SPL00370
SPL00380
SPL00390
SPL00400
SPL00410
SPL00420
SPL00430
SPL00440
SPL00450
SPL00460
SPL00470
SPL00480
SPL00490
SPL00500
SPL00510
SPL00520
SPL00530
SPL00540
SPL00550
SPL00560
SPL00570
SPL00580
SPL00590
SPL00600
SPL00610
SPL00620
SPL00630
SPL00640
SPL00650
SPL00660
SPL00670
SPL00680
SPL00690

```

```

C
C      THE NEXT LOOP VARIES 'KOUNT' , SPECIFYING WHICH
C      CHANNEL THE SPLINE IS FITTED FOR.
C
C      ORIGINALLY THESE WERE IB,IR,IY,VR, BUT SINCE
C      IB IS DERIVED ON THE PHYSICAL MODEL THE SEQUENCE
C      HAS BEEN MODIFIED TO IR,IY,VR.
C      ( IB CAN BE OBTAINED SIMPLY BY CHANGING THE
C      FOLLOWING 'DO' LOOP TO 4 PASSES ...REMEMBER
C      THAT OUTPUT STATEMENTS MAY REQUIRE CHANGING
C      TOGETHER WITH RELEVANT FORMAT STATEMENTS ).
C
      DO 1111 KOUNT=1,3,1
      IF(KOUNT.EQ.1)GOTO 12
      DO 11 R=1,M
          K(R)=0.0
          C(R)=0.0
11  CONTINUE
      SS=0.0
12  CONTINUE
      ENDNOT=M-4
      DO 14 R=1,M,1
          IF(KOUNT.NE.1)GOTO 124
          Y(R)=IR(R)
          IF(R.GT.4.AND.R.LE.ENDNOT)K(R)=T1(R,7)
          TIME1(R)=T1(R,7)
          GOTO 14
124  IF(KOUNT.NE.2)GOTO 125
          Y(R)=IY(R)
          IF(R.GT.4.AND.R.LE.ENDNOT)K(R)=T1(R,8)
          TIME1(R)=T1(R,8)
          GOTO 14
125  IF(KOUNT.NE.3)GOTO 126
          Y(R)=VR(R)
          IF(R.GT.4.AND.R.LE.ENDNOT)K(R)=T1(R,1)
          TIME1(R)=T1(R,1)
          GOTO 14
126  IF(KOUNT.NE.4)GOTO 13
          Y(R)=IB(R)
          IF(R.GT.4.AND.R.LE.ENDNOT)K(R)=T1(R,6)
          TIME1(R)=T1(R,6)
          GOTO 14
13  WRITE(6,979)KOUNT
      GOTO 888
14  CONTINUE
C
C      AFTER PRINTING RESPECTIVE HEADINGS , THE FIRST TEN
C      CHOSEN DATA VALUES ARE WRITTEN , TOGETHER WITH
C      VALUES OF R , X(R) AND K(R).
C
C
C      IF(KOUNT.EQ.1)YNUM=FIRST(1)
C      IF(KOUNT.EQ.2)YNUM=SECOND(1)
C      IF(KOUNT.EQ.3)YNUM=THIRD
C      IF(KOUNT.EQ.4)YNUM=FOURTH
C      IF(RESULT.GT.2)GOTO 30
      WRITE(6,997)M,NCAP
      WRITE(6,995)FIRST
      DO 20 R=1,20,1
          WRITE(6,994)R,TIME1(R),Y(R),K(R)
20  CONTINUE
      L=M-20
      WRITE(6,995)LAST
      DO 30 R=L,M,1
          WRITE(6,994)R,TIME1(R),Y(R),K(R)
30  CONTINUE
C
C      NCAP7 IS THE HIGHEST DIMENSION OF K TO BE GENERATED
C      BY THE SUBROUTINE EQ2BAF. THIS SUBROUTINE GENERATES
C      A B-SPLINE REPRESENTATION OF A FUNCTION REPRESENTED
C      BY THE CHOSEN DATA VALUES .
C
      NCAP7=NCAP+7
      IFAIL=0
      CALL MYBAF(M,NCAP7,TIME1,Y,W,K,WORK1,WORK2,C,SS,IFAIL)
      IF(IFAIL.NE.0)GOTO 777

```

SPL00700
 SPL00710
 SPL00720
 SPL00730
 SPL00740
 SPL00750
 SPL00760
 SPL00770
 SPL00780
 SPL00790
 SPL00800
 SPL00810
 SPL00820
 SPL00830
 SPL00840
 SPL00850
 SPL00860
 SPL00870
 SPL00880
 SPL00890
 SPL00900
 SPL00910
 SPL00920
 SPL00930
 SPL00940
 SPL00950
 SPL00960
 SPL00970
 SPL00980
 SPL00990
 SPL01000
 SPL01010
 SPL01020
 SPL01030
 SPL01040
 SPL01050
 SPL01060
 SPL01070
 SPL01080
 SPL01090
 SPL01100
 SPL01110
 SPL01120
 SPL01130
 SPL01140
 SPL01150
 SPL01160
 SPL01170
 SPL01180
 SPL01190
 SPL01200
 SPL01210
 SPL01220
 SPL01230
 SPL01240
 SPL01250
 SPL01260
 SPL01270
 SPL01280
 SPL01290
 SPL01300
 SPL01310
 SPL01320
 SPL01330
 SPL01340
 SPL01350
 SPL01360
 SPL01370
 SPL01380
 SPL01390
 SPL01400
 SPL01410
 SPL01420
 SPL01430
 SPL01440
 SPL01450
 SPL01460
 SPL01470
 SPL01480

```

C
C
C      IN THE FOLLOWING SECTION IF 'AMIDPT' IS .TRUE. THEN
C      THE RESPECTIVE VALUE OF X LIES INBETWEEN KNOT
C      ( AND INPUT DATA ) POSITIONS AND A Y VALUE MUST BE
C      FOUND . M2 AND M3 SET THE START AND FINISH POINTS
C      FOR THE FITTING AND THE FINAL DATA LISTING .
C
C      AMIDPT=.TRUE.
C      LEFT=1
C      M1=IXTRA*M
C      M2=14*IXTRA+1
C      M3=M1-((14*IXTRA)+1)
C
C      'STEP' IS THE TIME BETWEEN EACH OF THE
C      INTERPOLATED POINTS.
C
C      THE FOLLOWING 'DO LOOP' SETS UP AN ARRAY
C      T(IXTRA),T(IXTRA+1),T(IXTRA+2)...ETC.
C      CONTAINING ALL VALUES OF TIME AT WHICH A
C      VALUE IS REQUIRED FROM THE SPLINE FIT.
C
C      STEP=TSTEP/IXTRA
C      DO 60 L=IXTRA,M1,IXTRA
C          J=L/IXTRA
C          Z=0
58      IF(KOUNT.EQ.1) T(L+Z)=T1(J,6)+0.0000086+STEP*Z
C          IF(KOUNT.EQ.2) T(L+Z)=T1(J,7)+0.0000150+STEP*Z
C          IF(KOUNT.EQ.3) T(L+Z)=T1(J,8)+0.0000214+STEP*Z
C          IF(KOUNT.EQ.4) T(L+Z)=T1(J,1)+0.0000288+STEP*Z
C          Z=Z+1
C          IF(Z.GT.EXTRA)GOTO 59
C          GOTO 58
59      CONTINUE
60      CONTINUE
C
C      J=0
C      I=0
C      ITIME=0
C      IF(RESULT.EQ.1.OR.RESULT.EQ.2) WRITE(6,992)
C      DO 40 N=M2,M3
C          XVAR=T(N)
C          IFAIL=1
C          CALL MYBCF(NCAP7,K,C,XVAR,LEFT,FIT,IFAIL)
C          IF(IFAIL.NE.0)GOTO 320
C          IF(N.GT.M2+30.AND.N.LT.M3-30) GOTO 295
C          IF(RESULT.EQ.1.OR.RESULT.EQ.2) WRITE(6,990)XVAR,T(N),FIT(1),
C          + FIT(2)
295      IF(KOUNT.EQ.1)OUT1(N)=FIT(1)
C          IF(KOUNT.EQ.2)OUT2(N)=FIT(1)
C          IF(KOUNT.EQ.3)OUT3(N)=FIT(1)
C          IF(KOUNT.EQ.4)OUT4(N)=FIT(1)
C          I=I+1
C          IF(I.NE.IXTRA) GOTO 340
300      I=0
C          AMIDPT=.NOT.AMIDPT
C          IF(KOUNT.EQ.1) T(N)=T(N)-0.0000086
C          IF(KOUNT.EQ.2) T(N)=T(N)-0.0000150
C          IF(KOUNT.EQ.3) T(N)=T(N)-0.0000214
C          IF(KOUNT.EQ.4) T(N)=T(N)-0.0000288
C          XVAR=T(N)
C          IFAIL=0
C          CALL MYBCF(NCAP7,K,C,XVAR,LEFT,FIT,IFAIL)
C          IF(IFAIL.NE.0)GOTO 320
C          R=N/IXTRA
C          RES=FIT(1)-Y(R)
C          IF(N.GT.M2+30.AND.N.LT.M3-30) GOTO 340
C          IF(RESULT.EQ.1.OR.RESULT.EQ.2)WRITE(6,991)XVAR,T(N),
C          + FIT(1),RES,FIT(2)
C          GOTO 340
320      WRITE(6,989)XVAR
C          J=J+1
C          IF(J.GE.50) GOTO 1111
340      CONTINUE
40      CONTINUE
1111      CONTINUE
C          IF(RESULT.EQ.2) GOTO 1113
C          WRITE(6,981)
C          M4=M2
C          DO 1112 R=M2,M3,1
C              WRITE(6,980) OUT1(R),OUT2(R),OUT3(R),OUT4(R)
1112      CONTINUE

```

SPL01490
 SPL01500
 SPL01510
 SPL01520
 SPL01530
 SPL01540
 SPL01550
 SPL01560
 SPL01570
 SPL01580
 SPL01590
 SPL01600
 SPL01610
 SPL01620
 SPL01630
 SPL01640
 SPL01650
 SPL01660
 SPL01670
 SPL01680
 SPL01690
 SPL01700
 SPL01710
 SPL01720
 SPL01730
 SPL01740
 SPL01750
 SPL01760
 SPL01770
 SPL01780
 SPL01790
 SPL01800
 SPL01810
 SPL01820
 SPL01830
 SPL01840
 SPL01850
 SPL01860
 SPL01870
 SPL01880
 SPL01890
 SPL01900
 SPL01910
 SPL01920
 SPL01930
 SPL01940
 SPL01950
 SPL01960
 SPL01970
 SPL01980
 SPL01990
 SPL02000
 SPL02010
 SPL02020
 SPL02030
 SPL02040
 SPL02050
 SPL02060
 SPL02070
 SPL02080
 SPL02090
 SPL02100
 SPL02110
 SPL02120
 SPL02130
 SPL02140
 SPL02150
 SPL02160
 SPL02170
 SPL02180
 SPL02190
 SPL02200
 SPL02210
 SPL02220
 SPL02230
 SPL02240
 SPL02250
 SPL02260
 SPL02270
 SPL02280
 SPL02290
 SPL02300
 SPL02310


```

1113 CONTINUE
      GOTO 888
555 WRITE(6,988)R
      GOTO 888
777 GOTO(360,380,400,420,440),IFAIL
360 WRITE(6,987)
      GOTO 888
380 WRITE(6,986)
      GOTO 888
400 WRITE(6,985)
      GOTO 888
420 WRITE(6,984)
      GOTO 888
440 WRITE(6,983)
      GOTO 888
999 FORMAT(6A4)
998 FORMAT(4(1X/),1H ,6A4)
997 FORMAT(2(1X/),30H      M = NO. OF DATA POINTS = ,I4,
+ //52H NCAP = NO. OF INTERPOLATED INTERVALS BETWEEN INTERN,
+ 11HAL KNOTS = ,I4)
C 996 FORMAT(1H ,8(F8.4,1X))
996 FORMAT(1H ,8(F12.8,1X))
995 FORMAT(2(1X//),2H ,A8,29H 20 LINES OF DATA FOR FIT AND,
+ 15H KNOT POSITIONS,
+ /52H -----//,
+ /58H      R          T1(R)          Y(R)          K(R)//)
994 FORMAT(1X/,4H      ,I4,8X,F10.5,8X,F8.4,8X,F10.5)
993 FORMAT(3(1X/),16H      OUTPUT DATA,1X/,17H -----)
992 FORMAT(2(1X//),48H      X          TIME          FITTED Y          RESIDUE,
+16H      GRADIENT,
+ /53H -----,
+18H-----,
+ /53H -----,
+18H-----//)
991 FORMAT(1H ,2X,F9.6,2X,F9.6,3X,F8.4,4X,E12.4,4X,F12.4)
990 FORMAT(1H ,2X,F9.6,2X,F9.6,3X,F8.4,20X,F12.4)
989 FORMAT(/1X,27HARGUMENT OUTSIDE RANGE      ,E20.5)
988 FORMAT(1X/,15H NO MORE DATA , ,I4,11H LINES READ//)
987 FORMAT(/47H KNOTS DISORDERED OR NOT INTERIOR TO DATA INTER,
+3HVAL)
986 FORMAT(/20H NON-POSITIVE WEIGHT)
985 FORMAT(/46H DISORDERED VALUES OF THE INDEPENDANT VARIABLE)
984 FORMAT(/42H TOO MANY KNOTS FOR TKE NUMBER OF DISTINCT,
+35H VALUES OF THE INDEPENDANT VARIABLE)
983 FORMAT(/42H NO UNIQUE SOLUTION SINCE SHOENBURG-WITNEY,
+20H CONDITIONS VIOLATED)
982 FORMAT(6(1X/),22H      ***** KOUNT = ,I2,6H *****)
981 FORMAT(6(1X/),40H      COMPLETE LISTING OF OUTPUT NOW FOLLOWS,
+ /41H -----,
+ /41H -----,
+ //55H      TIME          CHANNEL1----GRADIENT          CHANNEL2----
+8HGRADIENT//)
980 FORMAT(1H ,4(F12.4,1X))
979 FORMAT(///40H      INVALID VALUE OF 'KOUNT', KOUNT = ,I3,///)
888 STOP
      END

```

```

SPL02320
SPL02330
SPL02340
SPL02350
SPL02360
SPL02370
SPL02380
SPL02390
SPL02400
SPL02410
SPL02420
SPL02430
SPL02440
SPL02450
SPL02460
SPL02470
SPL02480
SPL02490
SPL02500
SPL02510
SPL02520
SPL02530
SPL02540
SPL02550
SPL02560
SPL02570
SPL02580
SPL02590
SPL02600
SPL02610
SPL02620
SPL02630
SPL02640
SPL02650
SPL02660
SPL02670
SPL02680
SPL02690
SPL02700
SPL02710
SPL02720
SPL02730
SPL02740
SPL02750
SPL02760
SPL02770
SPL02780
SPL02790
SPL02800
SPL02810
SPL02820
SPL02830
SPL02840
SPL02850
SPL02860
SPL02870

```

C.IV SPLI30C FORTRAN Program Listing

C		SPL00710
C	THE NEXT LOOP VARIES 'KOUNT' ,SPECIFYING WHICH	SPL00720
C	CHANNEL THE SPLINE IS FITTED FOR.	SPL00730
C		SPL00740
C		SPL00750
C	KOUNT=1	SPL00760
	DO 1111 KOUNT=1,6	SPL00770
	IF(KOUNT.EQ.1)GOTO 12	SPL00780
	DO 11 R=1,M	SPL00790
	K(R)=0.0	SPL00800
	C(R)=0.0	SPL00810
	11 CONTINUE	SPL00820
	SS=0.0	SPL00830
	12 CONTINUE	SPL00840
	DO 14 R=1,M,1	SPL00850
	IF(KOUNT.NE.1)GOTO 124	SPL00860
	Y(R)=IR(R)	SPL00870
	IF(R.GT.4.AND.R.LE.NCAP3)K(R)=T(R)	SPL00880
	GOTO 14	SPL00890
124	IF(KOUNT.NE.2)GOTO 125	SPL00900
	Y(R)=IY(R)	SPL00910
	IF(R.GT.4.AND.R.LE.NCAP3)K(R)=T(R)	SPL00920
	GOTO 14	SPL00930
125	IF(KOUNT.NE.3)GOTO 126	SPL00940
	Y(R)=IB(R)	SPL00950
	IF(R.GT.4.AND.R.LE.NCAP3)K(R)=T(R)	SPL00960
	GOTO 14	SPL00970
126	IF(KOUNT.NE.4)GOTO 127	SPL00980
	Y(R)=VR(R)	SPL00990
	IF(R.GT.4.AND.R.LE.NCAP3)K(R)=T(R)	SPL01000
	GOTO 14	SPL01010
127	IF(KOUNT.NE.5)GOTO 128	SPL01020
	Y(R)=VY(R)	SPL01030
	IF(R.GT.4.AND.R.LE.NCAP3)K(R)=T(R)	SPL01040
	GOTO 14	SPL01050
128	IF(KOUNT.NE.6)GOTO 13	SPL01060
	Y(R)=VB(R)	SPL01070
	IF(R.GT.4.AND.R.LE.NCAP3)K(R)=T(R)	SPL01080
	GOTO 14	SPL01090
	13 WRITE(6,979)KOUNT	SPL01100
	14 CONTINUE	SPL01110
C		SPL01120
C		SPL01130
C	AFTER PRINTING RESPECTIVE HEADINGS , THE FIRST TEN	SPL01140
C	CHOSEN DATA VALUES ARE WRITTEN , TOGETHER WITH	SPL01150
C	VALUES OF R , X(R) AND K(R).	SPL01160
C		SPL01170
C		SPL01180
C	IF(KOUNT.EQ.1)YNUM=FIRST	SPL01190
C	IF(KOUNT.EQ.2)YNUM=SECOND	SPL01200
C	IF(KOUNT.EQ.3)YNUM=THIRD	SPL01210
C	IF(KOUNT.EQ.4)YNUM=FOURTH	SPL01220
C	IF(RESULT.GT.2)GOTO 30	SPL01230
	WRITE(6,997)M,NCAP	SPL01240
	WRITE(6,995)FIRST	SPL01250
	WRITE(6,994)((R,T(R),Y(R),K(R)),R=1,20)	SPL01260
	L=M-20	SPL01270
	WRITE(6,995)LAST	SPL01280
	WRITE(6,994)((R,T(R),Y(R),K(R)),R=L,M)	SPL01290
	30 CONTINUE	SPL01300
C		SPL01310
C		SPL01320
C	NCAP7 IS THE HIGHEST DIMENSION OF K TO BE GENERATED	SPL01330
C	BY THE SUBROUTINE E02BAF. THIS SUBROUTINE GENERATES	SPL01340
C	A B-SPLINE REPRESENTATION OF A FUNCTION REPRESENTED	SPL01350
C	BY THE CHOSEN DATA VALUES .	SPL01360
C		SPL01370
C		SPL01380
	NCAP7=NCAP+7	SPL01390
	IFAIL=1	SPL01400
	CALL MYBAF(M,NCAP7,T,Y,W,K,WORK1,WORK2,C,SS,IFAIL)	SPL01410
	IF(IFAIL.NE.0)GOTO 777	SPL01420

```

C
C
C      IN THE FOLLOWING SECTION IF 'AMIDPT' IS .TRUE. THEN
C      THE RESPECTIVE VALUE OF X LIES INBETWEEN KNOT
C      ( AND INPUT DATA ) POSITIONS AND A Y VALUE MUST BE
C      FOUND . M2 AND M3 SET THE START AND FINISH POINTS
C      FOR THE FITTING AND THE FINAL DATA LISTING .
C
C
C      AMIDPT=.FALSE.
C      LEFT=1
C      M1=IXTRA*M
C      M2=14*IXTRA
C      M3=M1-((14*IXTRA)+1)
C
C      'STEP' IS THE TIME BETWEEN EACH OF THE
C      INTERPOLATED POINTS.
C
C      THE FOLLOWING 'DO LOOP' SETS UP AN ARRAY
C      T(IXTRA),T(IXTRA+1),T(IXTRA+2)...ETC.
C      CONTAINING ALL VALUES OF TIME AT WHICH A
C      VALUE IS REQUIRED FROM THE SPLINE FIT.
C
C
C      STEP=TSTEP/IXTRA
C      DO 60 L=IXTRA,M1,IXTRA
C          J=L/IXTRA
C          Z=0
C      58  T1(L+Z)=T(J)+STEP*Z
C          Z=Z+1
C          IF(Z.GT.EXTRA)GOTO 59
C          GOTO 58
C      59  CONTINUE
C      60  CONTINUE
C
C      I=0
C      J=0
C      ITIME=0
C      IF(RESULT.EQ.1.OR.RESULT.EQ.2) WRITE(6,992)
C      DO 40 N=M2,M3,1
C          IF(AMIDPT) GOTO 290
C          GOTO 300
C      290  XVAR=T1(N)
C          IFAIL=1
C          CALL MYBCF(NCAP7,K,C,XVAR,LEFT,FIT,IFAIL)
C          IF(IFAIL.NE.0)GOTO 320
C          IF(N.GT.M2+30.AND.N.LT.M3-30) GOTO 295
C          IF(RESULT.EQ.1.OR.RESULT.EQ.2) WRITE(6,990)XVAR,T1(N),FIT(1),
C      +  FIT(2)
C      295  IF(KOUNT.EQ.1)OUT4(N)=FIT(1)
C          IF(KOUNT.EQ.1)OUT7(N)=FIT(2)
C          IF(KOUNT.EQ.2)OUT5(N)=FIT(1)
C          IF(KOUNT.EQ.2)OUT8(N)=FIT(2)
C          IF(KOUNT.EQ.3)OUT6(N)=FIT(1)
C          IF(KOUNT.EQ.3)OUT9(N)=FIT(2)
C          IF(KOUNT.EQ.4)OUT1(N)=FIT(1)
C          IF(KOUNT.EQ.5)OUT2(N)=FIT(1)
C          IF(KOUNT.EQ.6)OUT3(N)=FIT(1)
C          I=I+1
C          IF(I.EQ.IXTRA-1) AMIDPT=.FALSE.
C          GOTO 340
C      300  I=0
C          IF(IXTRA.NE.1) AMIDPT=.NOT.AMIDPT
C          XVAR=T1(N)
C          IFAIL=1
C          CALL MYBCF(NCAP7,K,C,XVAR,LEFT,FIT,IFAIL)
C          IF(IFAIL.NE.0)GOTO 320
C          R=N/IXTRA
C          RES=FIT(1)-Y(R)
C          IF(N.GT.M2+30.AND.N.LT.M3-30) GOTO 310
C          IF(RESULT.EQ.1.OR.RESULT.EQ.2)WRITE(6,991)XVAR,T1(N),
C      +  FIT(1),RES,FIT(2)
C      310  IF(KOUNT.EQ.1)OUT4(N)=FIT(1)
C          IF(KOUNT.EQ.1)OUT7(N)=FIT(2)
C          IF(KOUNT.EQ.2)OUT5(N)=FIT(1)
C          IF(KOUNT.EQ.2)OUT8(N)=FIT(2)
C          IF(KOUNT.EQ.3)OUT6(N)=FIT(1)
C          IF(KOUNT.EQ.3)OUT9(N)=FIT(2)
C          IF(KOUNT.EQ.4)OUT1(N)=FIT(1)
C          IF(KOUNT.EQ.5)OUT2(N)=FIT(1)
C          IF(KOUNT.EQ.6)OUT3(N)=FIT(1)
C          GOTO 340
C      320  WRITE(6,989)XVAR

```

```

SPL01430
SPL01440
SPL01450
SPL01460
SPL01470
SPL01480
SPL01490
SPL01500
SPL01510
SPL01520
SPL01530
SPL01540
SPL01550
SPL01560
SPL01570
SPL01580
SPL01590
SPL01600
SPL01610
SPL01620
SPL01630
SPL01640
SPL01650
SPL01660
SPL01670
SPL01680
SPL01690
SPL01700
SPL01710
SPL01720
SPL01730
SPL01740
SPL01750
SPL01760
SPL01770
SPL01780
SPL01790
SPL01800
SPL01810
SPL01820
SPL01830
SPL01840
SPL01850
SPL01860
SPL01870
SPL01880
SPL01890
SPL01900
SPL01910
SPL01920
SPL01930
SPL01940
SPL01950
SPL01960
SPL01970
SPL01980
SPL01990
SPL02000
SPL02010
SPL02020
SPL02030
SPL02040
SPL02050
SPL02060
SPL02070
SPL02080
SPL02090
SPL02100
SPL02110
SPL02120
SPL02130
SPL02140
SPL02150
SPL02160
SPL02170
SPL02180
SPL02190
SPL02200
SPL02210
SPL02220
SPL02230
SPL02240

```

```

          J=J+1
          IF(J.GE.50) GOTO 1111
340      CONTINUE
40       CONTINUE
1111    CONTINUE
          IF(RESULT.EQ.2) GOTO 1113
          WRITE(6,981)
          DO 1112 R=M2,M3,1
            IF(OPWIDE) WRITE(6,978) OUT1(R),OUT2(R),OUT3(R),OUT4(R),
+           OUT5(R),OUT6(R),OUT7(R),OUT8(R),OUT9(R)
            IF(.NOT.OPWIDE) WRITE(6,980) OUT1(R),OUT2(R),OUT3(R),OUT4(R),
+           OUT5(R),OUT6(R),OUT7(R),OUT8(R),OUT9(R)
1112    CONTINUE
1113    CONTINUE
          GOTO 888
555     WRITE(6,988)R
          GOTO 888
777     GOTO(360,380,400,420,440),IFAIL
360     WRITE(6,987)
          GOTO 888
380     WRITE(6,986)
          GOTO 888
400     WRITE(6,985)
          GOTO 888
420     WRITE(6,984)
          GOTO 888
440     WRITE(6,983)
          GOTO 888
999     FORMAT(6A4)
998     FORMAT(4(1X/),1H ,6A4)
997     FORMAT(2(1X/),30H      M = NO. OF DATA POINTS = ,I4,
+ //52H NCAP = NO. OF INTERPOLATED INTERVALS BETWEEN INTERN,
+ 11HAL KNOTS = ,I4)
C 996     FORMAT(1H ,8(F8.4,1X))
996     FORMAT(1H ,8(F12.8,1X))
995     FORMAT(2(1X//),2H ,A6,29H 20 LINES OF DATA FOR FIT AND,
+ 15H KNOT POSITIONS,
+ /52H -----//,
+ /58H      R          T1(R)          Y(R)          K(R)//)
994     FORMAT(1X/,4H      ,I4,8X,F10.5,8X,F8.4,8X,F10.5)
993     FORMAT(3(1X/),16H      OUTPUT DATA,1X/,17H -----)
992     FORMAT(2(1X/),48H      X          TIME          FITTED Y          RESIDUE,
+16H      GRADIENT,
+ /53H -----,
+18H-----,
+ /53H -----,
+18H-----//)
991     FORMAT(1H ,2X,F9.6,2X,F9.6,3X,F8.4,4X,E12.4,4X,F12.4)
990     FORMAT(1H ,2X,F9.6,2X,F9.6,3X,F8.4,20X,F12.4)
989     FORMAT(/1X,27HARGUMENT OUTSIDE RANGE      ,E20.5)
988     FORMAT(1X/,15H NO MORE DATA      ,I4,11H LINES READ//)
987     FORMAT(/47H KNOTS DISORDERED OR NOT INTERIOR TO DATA INTER,
+3HVAL)
986     FORMAT(/20H NON-POSITIVE WEIGHT)
985     FORMAT(/46H DISORDERED VALUES OF THE INDEPENDANT VARIABLE)
984     FORMAT(/42H TOO MANY KNOTS FOR TKE NUMBER OF DISTINCT,
+35H VALUES OF THE INDEPENDANT VARIABLE)
983     FORMAT(/42H NO UNIQUE SOLUTION SINCE SHOENBURG-WITNEY,
+20H CONDITIONS VIOLATED)
982     FORMAT(6(1X/),22H      ***** KOUNT = ,I2,6H *****)
981     FORMAT(6(1X/),40H      COMPLETE LISTING OF OUTPUT NOW FOLLOWS,
+ /41H -----,
+ /41H -----,
+ ///55H      TIME          CHANNEL1----GRADIENT          CHANNEL2----
+8HGRADIENT//)
980     FORMAT(1H ,3(F6.2,1X),3(F7.4,1X),3(F8.3,1X))
979     FORMAT(///40H      INVALID VALUE OF 'KOUNT', KOUNT = ,I3,///)
978     FORMAT(1H ,3(F10.6,1X),2X,3(F10.7,1X),2X,3(F10.4,1X))
888     STOP
          END

```

```

SPL02250
SPL02260
SPL02270
SPL02280
SPL02290
SPL02300
SPL02310
SPL02320
SPL02330
SPL02340
SPL02350
SPL02360
SPL02370
SPL02380
SPL02390
SPL02400
SPL02410
SPL02420
SPL02430
SPL02440
SPL02450
SPL02460
SPL02470
SPL02480
SPL02490
SPL02500
SPL02510
SPL02520
SPL02530
SPL02540
SPL02550
SPL02560
SPL02570
SPL02580
SPL02590
SPL02600
SPL02610
SPL02620
SPL02630
SPL02640
SPL02650
SPL02660
SPL02670
SPL02680
SPL02690
SPL02700
SPL02710
SPL02720
SPL02730
SPL02740
SPL02750
SPL02760
SPL02770
SPL02780
SPL02790
SPL02800
SPL02810
SPL02820
SPL02830
SPL02840
SPL02850
SPL02860
SPL02870
SPL02880
SPL02890
SPL02900
SPL02910
SPL02920
SPL02930
SPL02940

```

C.V Results and Error Magnitudes

The results output from application of the programs to consecutive blocks of 750 time series data points overlapped slightly due to the extra 15 points at each end of the data span. When the three interpolated output files were combined, the overlapping was carefully eliminated, to give output files of:

(i) For input to the physical model:

9000 time-series data records with
 I_R, I_Y, I_B on each record.
 Record step length = 100 microseconds.

(ii) For input to the computational model:

2250 time-series data records, with
 $I_R, I_Y, I_B, \frac{dI_R}{dt}, \frac{dI_Y}{dt}, \frac{dI_B}{dt}$ on each record.
 Record step length = 800 microseconds.

The error magnitudes were estimated by calculation of the quantity,

$$E(x) = S(x) - y(x)$$

and were always less than 10^{-8} percent over the non-overlapping region of the B-spline fit. The end regions of the B-spline were slightly less accurate, with always less than 10^{-4} percentage error.

APPENDIX D

AIM-65 MICROCOMPUTER OPERATION, INTERFACE
AND PROGRAM LISTINGS

D.I Overview

The Rockwell R6500 Advanced Interactive Microcomputer^[83,84,85,86], (AIM-65), was used in the laboratory for the small signal reproduction of arc furnace installation current waveforms, using data loaded from punch-tape.

A block diagram of the AIM-65 system is given in Figure D.1. An extra 16K bytes of dynamic RAM, and two R6522 versatile Interface Adapters were added using the expansion connector.

The memory map for the 64K bytes of addressable I/O and memory was given in Table 2.1 (Section 2.3.2).

D.II Monitor, Editor and Assembler

The monitor program occupied 8K bytes in ROM between addresses E000 and FFFF hex. Application programs could be entered and changed using the text edit facility of the monitor. Programs written in R6502 assembler language source code could then be assembled into object code using the assembler software located in a separate 4K bytes ROM package.

D.III Program Storage

Once assembled, the programs were stored on magnetic tape using the tape input/output facilities of the monitor routine. When programs were correct, there was no need for them to be stored in their source code form, nor for the assembler chip to occupy memory space.

All programs written for use in this research project were stored and run from the 4K byte on-board RAM at address 0000-00FF.

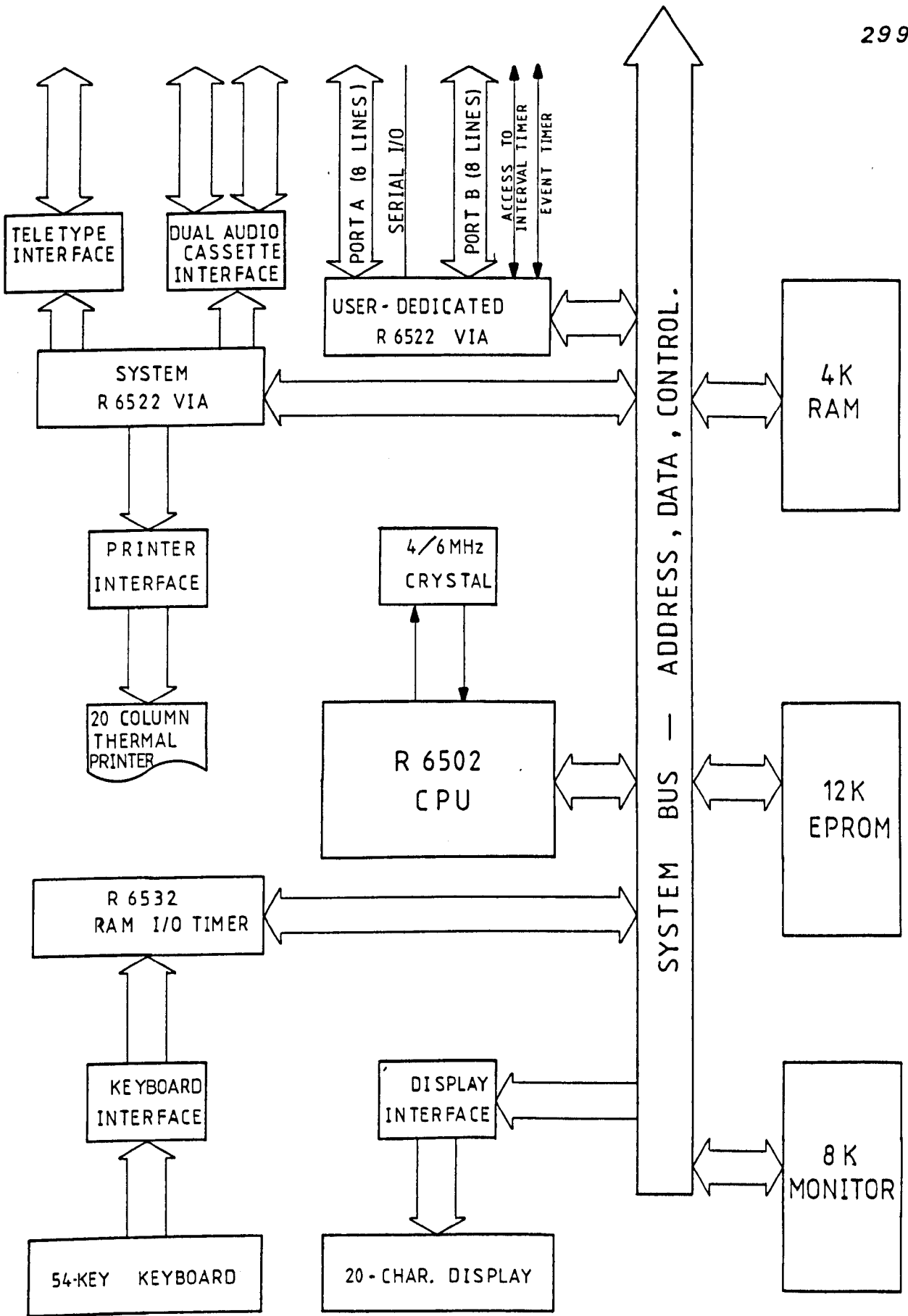


FIG. D1 : AIM-65 BLOCK DIAGRAM

D.IV System Operation

The 'function' keys F1, F3 gave immediate program 'jumps' to memory locations at the start of the program blocks 'START' and 'TAPE READER' respectively.

(a) 'START' The source code listing for this program is given in Section D.V. Once entered, its timing was controlled by a hard wired phase-locked loop outputting a 200kHz square wave in synchronism with the a.c. mains (red phase) voltage. The circuit used to generate the controlling interrupts CA1 and CB1 is shown in Figure D2.

(b) 'TAPE READER' The source code listing this program is given in Section D.VI. The program reads a series of 8-bit values from a punch-tape reader connected at input port A, finishing when a given number of cycles are complete. Data read from the tape is stored in RAM.

When the data output program from 'START' was operating, clock frequency of 6MHz was used to allow a minimum time between consecutive channel outputs (I_R , I_Y , I_B) of 20 microseconds to be achieved. Every 200 microseconds the 8-bit data word for each of channels I_R , I_Y , I_B was sent to port A, with a bit number on Port B selecting a particular DAC to receive the 8-bit word. This value was then held by the DAC until the new value was received 200 microseconds later. The DAC circuit is given in Figure D3, and the analogue outputs fed the low-pass filter circuits shown in Chapter II, Figure 2.5(c).

An additional pulse was output at the start of each repeated 'N' cycles of data, ($N = 89$ for most applications), to allow measuring and data logging equipment to have a common 'start' time reference. This pulse was output to bit 4 of port B, and was software-timed for a duration of 10 microseconds as shown in the program listing (Section DV).

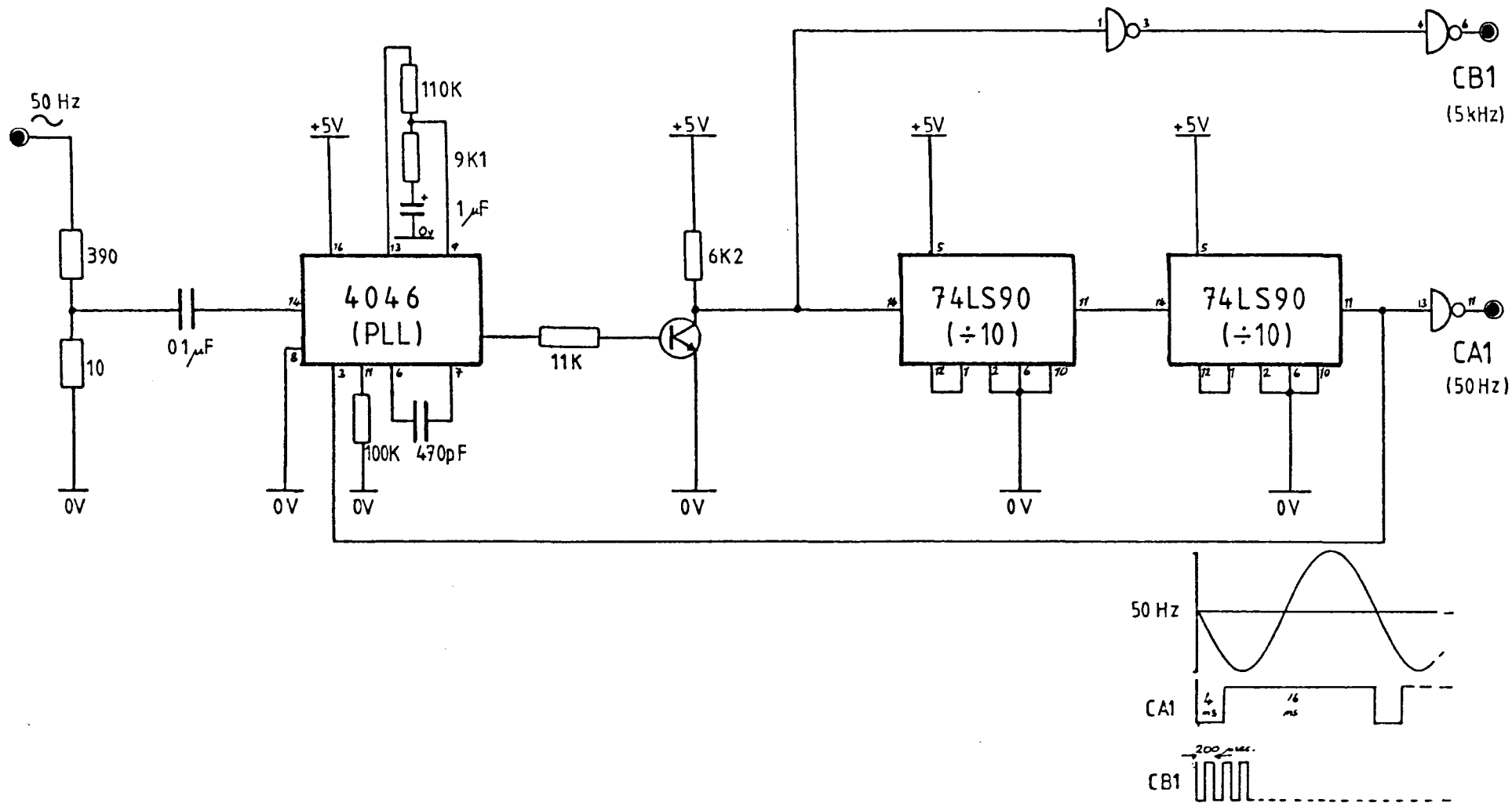
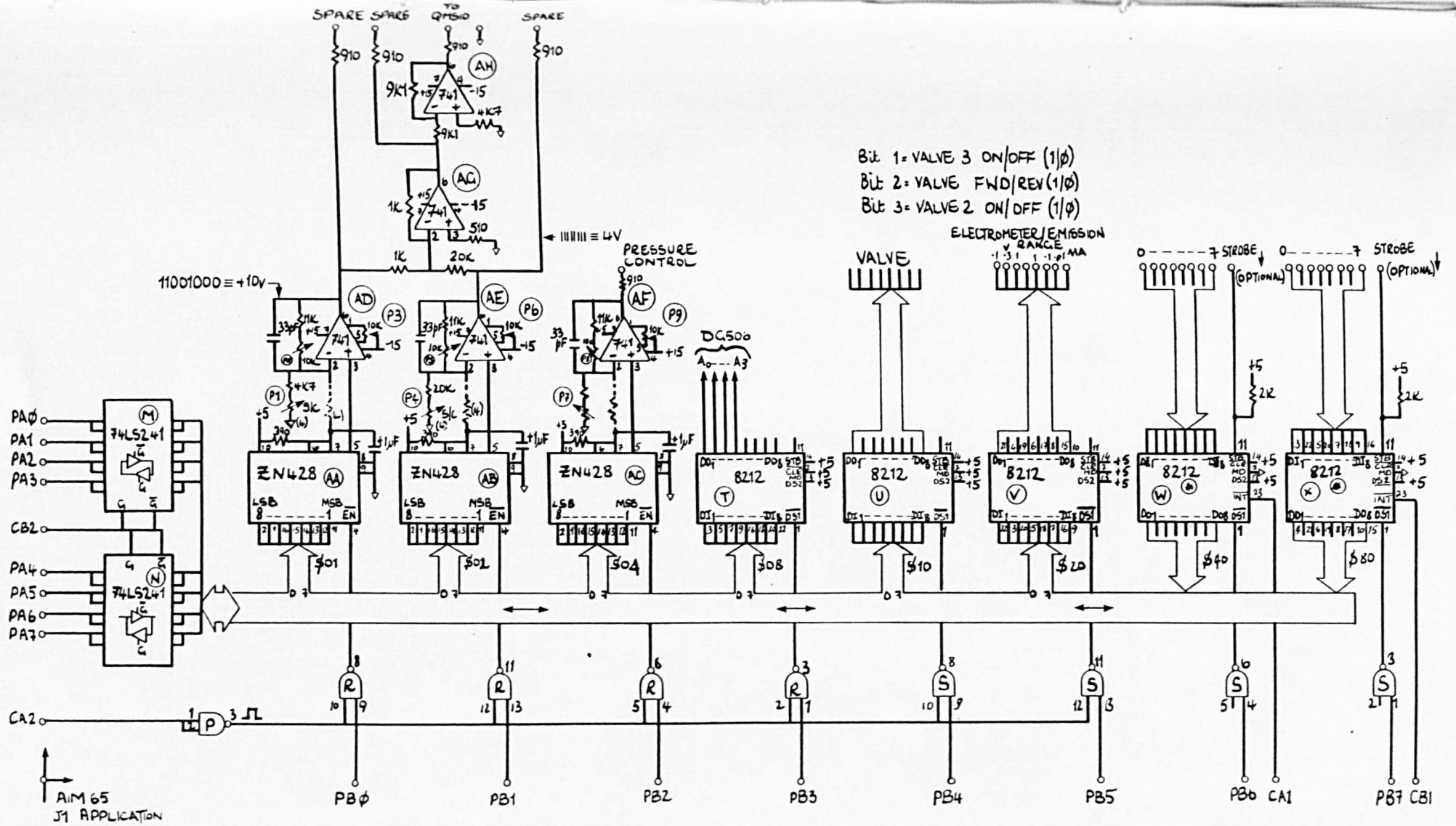


FIG. D2 : Phase-locked loop generation of d ta synchronising pulses



Bit 1 = VALVE 3 ON/OFF (1/0)
 Bit 2 = VALVE FWD/REV (1/0)
 Bit 3 = VALVE 2 ON/OFF (1/0)

- NOTE
1. ITEMS (⊙) NOT FITTED
 2. CB2 IN STATIC MODE, LO → DATA OUT
HI → DATA IN
 - CA2 IN PULSE MODE
 3. CA1 & CB1 - VE EDGE INTERRUPT IF REQ'D
 4. FITTED FOR BU POLAR OPERATION ONLY

FIG. D3 : Digital to analogue converters for AIM-65

THE UNIVERSITY OF LIVERPOOL ELECTRICAL ENGINEERING AND ELECTRONICS DEPT.	
TITLE 16CHANNEL ADC / I/O	DATE JOB NO 20/2/81 982

D.V Waveform Regeneration Program Listing


```

RERUN;
LDA    #04           ;Store interrupt vector.
STA    $A404
LDA    #$08
STA    $A405
LDA    #$CA         ;Set interrupt sense.
STA    PCR
LDA    #$FF         ;Set ports A & B to output.
STA    DDRA
STA    DDRB
LDY    #00
LDA    #$92         ;Allow interrupts.
STA    IER
CLI

IDLE;
NOP
JMP    IDLE

*=$0800

OUTPUT;
.BYTE  16,4,2,1     ;Set bits to define output channels.
;      VR,R,Y,B

INRPT;
LDA    IFR           ;Any interrupt.
AND    #$10         ;CB1 flag bit.
BEQ    CA1FLG       ;Branch if not CB1.
LDA    #$80         ;Reset CB1 interrupt latch.
STA    $A000
LDA    #00
STA    $A000

CA1FLG;
LDA    IFR           ;Interrupt type.
AND    #$02         ;CA1 flag bit.
BEQ    DATOUT       ;Branch if not CA1.
LDA    #$40         ;Reset CA1 interrupt latch.
STA    $A000
LDA    #00
STA    $A000
DEC    NCYCLE        ;Branch if no. of
BPL    DATOUT        ; - cycles not complete
LDA    LADDR         ;Reload start address for output data.
STA    BAL
LDA    HADDR
STA    BAH
LDA    NUM
STA    NCYCLE
LDA    #08           ;Configure synch. pulse - bit 4 of B.
STA    $A000
LDA    #FF           ;Output pulse to port A.
STA    $A001
NOP                 ;Synch. pulse duration 10 usecs.
NOP
NOP
NOP
NOP
NOP
LDA    #00           ;End synch. pulse.
STA    A001

```



```

DATOUT;
    LDX    #03                ;Set 'X' as no. of output channels.
    LDY    #00                ;Reset address offset.
LOOP;
    DEX
    BPL    CONT                ;Branch if more channels to be output.
    RTI
CONT;
    LDA    OUTPUT,X           ;Select relevant output DAC.
    STA    DEVICE
    LDA    (BAL),Y           ;Select correct data byte.
    STA    OUT                 ;Output byte.
    INC    BAL
    BNE    LOOP
    INC    BAH
    LDA    #$A0
    CMP    BAH                 ;Skip address block A0 in memory.
    BNE    LOOP
    LDA    #$B0
    STA    BAH
    JMP    LOOP                ;Continue loop.

```

```

;*****

```

```

;
```

UTILITIES

```

PRIFLG  = $A411                ;Define variables.
CRCK    = $EA24
RBYTE   = $E3FD
NUMA    = $EA46
BLANK2  = $E83B
DEBK1   = $ED2C
BAL     = $01
BAH     = $02
NUM     = $03
TEMP    = $04
OUTDP   = $EEFC
LL      = $E8FE
REDOUT  = $E973
PACK    = $EA84
M1      = $0500
M2      = $050F
MSG     = $063F
GETVAL  = $064E
BCDBIN  = $0666
NCYCLE  = $00
PORTA   = $5801
DDRA    = $5803
PCR     = $580C
ACR     = $580B
DELAY   = $ED2C

```

D.VI Tape Reader Program Listing

TAPE READER

```

*=$0112
JMP      TREAD          ;Start 'TREAD' program if 'F3' key pressed.

*=$0500
M1              ;Messages.
.BYTE 'START ADDRESS,'
M2
.BYTE 'NO.OF CYCLES=,'

TREAD;
LDA      #01
STA      PRIFLG
JSR      CRCK
LDX      #M1-M1
JSR      MSG
JSR      RBYTE
STA      BAH
JSR      RBYTE
STA      BAL
LDY      #00
JSR      CRCK
LDX      #M2-M1
JSR      GETVAL
JSR      BCDBIN
ASL      A
STA      NCYCLE
LDA      #00
STA      DDRA
STA      ACR
LDA      #$C0
LDY      #00

LOOP1;
LDX      #200

LOOP2;
LDA      #$E0
STA      PCR
LDA      #$C0
STA      PCR
JSR      DELAY
JSR      DELAY
LDA      PORTA
STA      (BAL),Y
INC      BAL
BNE      STEST
INC      BAH

STEST;
DEX
BNE      LOOP2
DEC      NCYCLE
BNE      LOOP1
JMP      TREAD

```

```

DELAY;      JSR      DEBK1          ;Delay loop used in 'TREAD'
            DEX
            BNE      DELAY
            JMP      LOOP

MSG;        LDA      M1,X          ;Loop to output message no. 1.
            CMP      #' ','
            BEQ      EXIT
            JSR      OUTDP
            INX
            JMP      MSG

EXIT;       RTS

GETVAL;     JSR      MSG          ;Reads a 4-byte hex. value
            JSR      LL          ; -from keyboard.
            JSR      REDOUT
            JSR      PACK
            JSR      REDOUT
            JSR      PACK
            PHA
            JSR      CRCK
            PLA
            RTS

BCDBIN;     PHA                  ;BCD to binary subroutine.
            AND      #$0F
            STA      TEMP
            LDX      #04

J1;         PLA
            DEX
            BMI      ANSWER
            PHA
            AND      MASK,X
            BEQ      J1
            LDA      BINEQV,X
            CLC
            ADC      TEMP
            STA      TEMP
            JMP      J1

ANSWER;     LDA      TEMP
            RTS
            MASK
            .BYTE $80,$40,$20,$10 ;BCD to binary masks.
            BINEQV
            .BYTE 80,40,20,10
            .END

```

APPENDIX E

SAFE START SEQUENCE FOR THE LABORATORY MODEL

Figure E1 gives a schematic of the complete laboratory model. The safe-start sequences to be followed for the protection of equipment and personnel was then:

- (i) Ensure all switches and contactors open, GAIN and LEVEL adjust potentiometers set at zero, and VARIAC wound to zero secondary volts.
- (ii) Start microprocessor cycling of stored data.
- (iii) Close MAIN ISOLATOR.
- (iv) Close SAFETY CONTACTOR.
- (v) Increase GAIN adjust to maximum on power amplifiers.
- (vi) Slowly increase VARIAC secondary voltage until $\Delta V = 0$.
- (vii) Close SHORTING SWITCH.
- (viii) Increase LEVEL adjust until line current is of correct value.

The procedure is reversed for stopping the model's operation. Rapid isolation of all equipment could be achieved by pressing the emergency stop button.

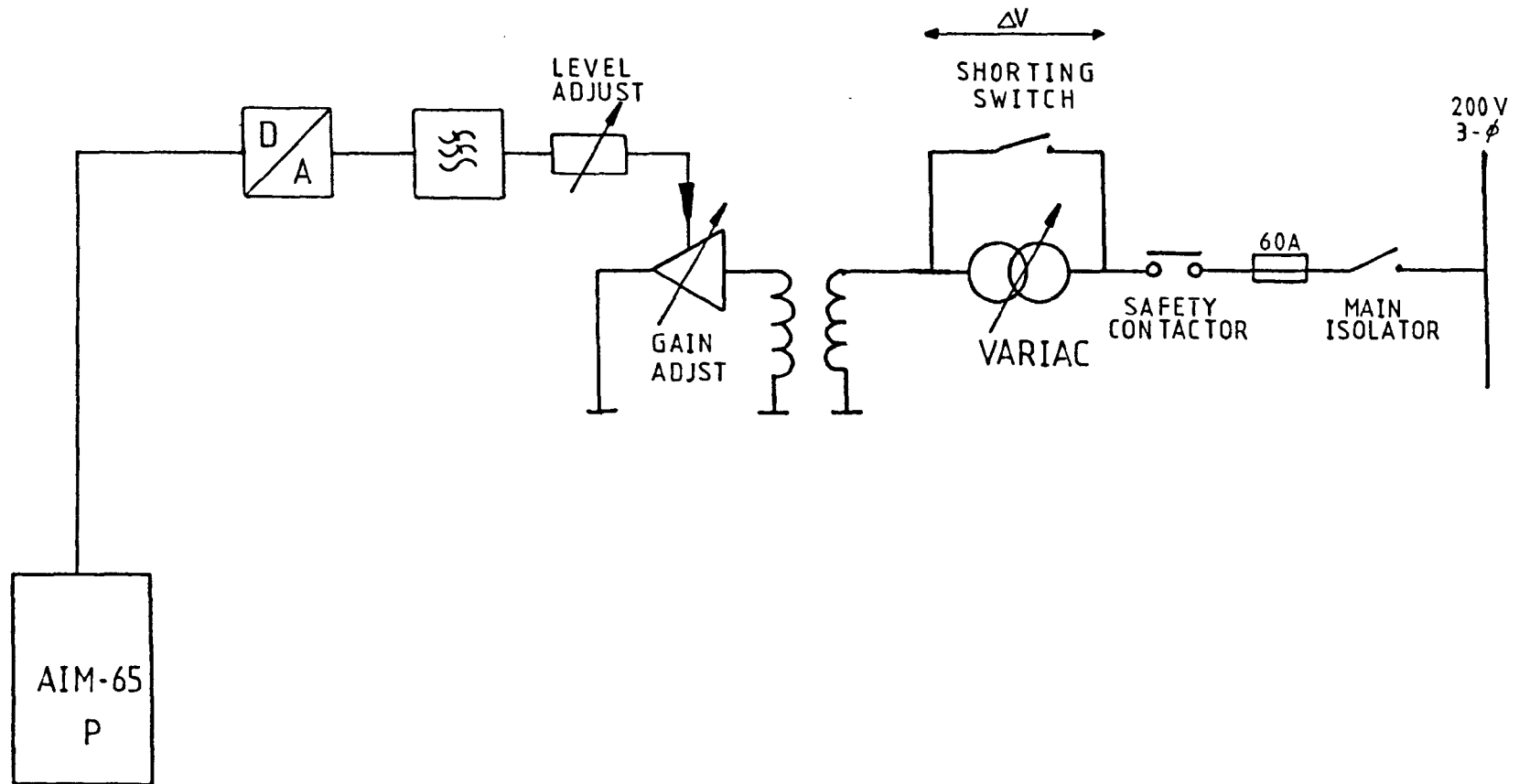


FIG. E1: Laboratory model schematic

APPENDIX F

SIX-PULSE TCR CONTROL PROGRAM

F.I FireAsub.asm - Control Algorithm
Compiler Listing

1
 2
 3
 4
 5
 6
 7
 8
 9
 10
 11
 12
 13
 14
 15
 16
 17
 18
 19
 20
 21
 22
 23
 24
 25
 26
 27
 28
 29
 30
 31
 32
 33
 34
 35
 36
 37
 38
 39
 40
 41
 42
 43
 44
 45
 46
 47
 48
 49
 50
 51
 52

NAME thyristor_firing_routine
 NOLIST ON

 GLOBAL firAsub
 GLOBAL CODEBASEEQ, DATABASEEQ, CONSTBASEEQ

 ASSUME DS:DATABASEEQ

 SECTION pascalprocedure, CLASS=INSTRQQ

```

;XXXXXXXXXXXXXXXXXXXXXXXXXXXXXXXXXXXXXXXXXXXXXXXXXXXXXXXXXXXXXXXXXXXXXXXXXXXX
;assembly routine to fire thyristor=
;called from main prog after voltage zero detected
;algorithm subtracts sine value from measured value and integrates
;testing value against a limit, fires thy. when limit reached
;
;only outputs a short pulse for thyristor firing
;
;loop delay values set to values suitable for ncl compensator. Values
;for the other two compensators must be set in RAM after download
;
;
;positive half cycle
;
firAsub ;thyristor firing routine
fire1 ;positive half cycle section
    LEA SI, sine1
    XOR BX, BX
    MOV CH, 009H
start1  MOV DX, 00F800H ;load address of adc
        OUT DX, AX ;initiate conversion
        MOV CL, 00FH ;conversion delay
        SHR CL, CL
        XOR AH, AH ;set ah to zero
        IN AL, DX ;input sample
        MOV CL, 009H ;loop delay to adjust sampling frequency
        SHR CL, CL ;sine curve based on 74 usecs sample time
        CMP CH, 000H ;test whether one of first nine samples
        JNE tsta ;jump to tsta if after nine samples
        DEC CH
        JMP tsta1
tsta 1  CMP AL, 007H ;test sample to check if near end of 1/2 cycle
        JB end1
lab1  MOV CL, 151H ;now current value of sine curve from memory
        CMP AL, CL ;decide whether?sample & sine, jmp to neg1 if?
        JB neg1 ;if it is.
        SUB AL, CL ;subtract sine from sample
        ADD BX, AX ;add difference to summation store
add1  ADD BX, AX
        JNF add1
neg1  SUB CL, AL ;if AL, subtract AL from CL
        MOV AL, CL ;put difference into AL
  
```

```

53 00002036 3E08          CMP BX,AX          ;test AX against BX--if AX>BX make AX=BX so
54 00000038 7702          JA sub1           ;that BX is set to zero in the subtraction
55 0000003A 8BC3          MOV AX,BX
56 0000003C 2E08          sub1  SUB BX,AX
57 0000003E 81FE9A10      cont  CMP SI,109AH      ;test SI for > 1/4 cycle
58 00000042 7206          JB next          ;sample again if si < 1/4 cycle
59 00000044 81FB0003      CMP BX,0300H     ;test BX against limit
60 00000048 7703          JA firea        ;jump to firea when limit exceeded
61 0000004A 46          next  INC SI          ;update pointer to sine curve
62 0000004B EBBB          JMP start1
63 0000004D BA00F0      firea MOV DX,00F000H   ;fire thyristor...one short pulse
64 00000050 8001          MOV AL,201H
65 00000052 EE          OUT DX,AL
66 00000053 B110          MOV CL,101H
67 00000055 D2E9          SHR CL,CL
68 00000057 B000          MOV AL,000H
69 00000059 EE          OUT DX,AL
70 0000005A BA00F8      end1  MOV DX,00F800H   ;load adc address and input sample
71 0000005D EF          OUT DX,AX
72 0000005E B10F          MOV CL,00FH
73 00000060 D2E9          SHR CL,CL
74 00000062 EC          IN AL,DX
75 00000063 3C80          CMP AL,80H      ;check for zero crossing
76 00000065 77F3          JA end1
77 00000067 8D368500 R      fire2 LEA SI,sine2    ;neg half cycle routine Basically same as---
78 0000006B 3308          XOR BX,BX        ;--positive half cycle routine except--
79 0000006D 8509          MOV CH,09H      ;--a positive contribution to summation--
80 0000006F BA00F8      start2 MOV DX,00F800H  ;--store results from AL being ---
81 00000072 EF          OUT DX,AX        ;--numerically smaller than sine curve--
82 00000073 B10F          MOV CL,00FH     ;--to allow for fact that zero volts---
83 00000075 D2E9          SHR CL,CL       ;--corresponds to an adc output of 128.
84 00000077 32E4          XOR AH,AH
85 00000079 EC          IN AL,DX
86 0000007A B108          MOV CL,08H      ;loop delay to adjust sampling frequency
87 0000007C D2E9          SHR CL,CL       ;sine curve based on 74usecs sample time
88 0000007E 80FD00      CMP CH,100H
89 00000081 7405          JE tab
90 00000083 FECD          DEC CH
91 00000085 E90481      jmp tab
92 00000088 3C73          tab  CMP AL,73H
93 0000008A 7735          JA end2
94 0000008C 8A0C          tab2 MOV CL,0C1H
95 0000008E 3AC1          CMP AL,C1
96 00000090 720D          JB pos2
97 00000092 2AC1          SUB AL,C1
98 00000094 3E08          CMP BX,AX
99 00000096 7702          JA sub1
100 00000098 8BC3          MOV AX,BX
101 0000009A 2E08          sub1  SUB BX,AX
102 0000009C E90600      jmp cont2
103 0000009F 2AC8          pos2  SUB CL,C8
104 000000A1 8AC1          MOV AL,C1

```

```

105 000000A3 0308      add2  ADD BX, AX
106 000000A5 81FE1F11   cont2 CMP SI, 111FH
107 000000A7 7264              JB next2
108 000000AB 81FBC003          CMP BX, 1003C0H
109 000000AF 7703              JA fireb
110 000000B1 46              next2 INC SI
111 000000B2 EB88              JMP start2
112 000000B4 BA00F0   fireb MOV DX, 10F000H ; fire thyristor...one short pulse
113 000000B7 B002              MOV AL, 02H
114 000000B9 EE              OUT DX, AL
115 000000BA B110              MOV CL, 10H
116 000000BC D2E9              SHR CL, CL
117 000000BE B000              MOV AL, 00H
118 000000C0 EE              OUT DX, AL
119 000000C1 BA00F0   end2  MOV DX, 10F000H ; load adc address and input sample
120 000000C4 EF              OUT DX, AX
121 000000C5 B10F              MOV CL, 0FH
122 000000C7 D2E9              SHR CL, CL
123 000000C9 EC              IN AL, DX
124 000000CA 3C80              CMP AL, 80H ; check for pos going zero crossing--
125 000000CC 72F3              JB end2
126 000000CE E92FFF          JMP fire1 ;--cycle routine.
127 000000D1 C20400          RET 4

```

128
 129
 130
 131
 132
 133
 134
 135
 136
 137
 138

SECTION sdr88.const, CLASS=DATA00

```

; reference sine wave ... zero = 127
; plus/minus 115
; first sample at 100us
; subsequent dt = 75us
; pt.s per 1/2 cyc = 132

```

```

139 00000000 8285888A   sine1 BYTE 130, 133, 136, 138, 141, 143, 146, 148, 151, 154, 156, 159, 161
      808F92Y4
      777A9C9F
      A1
140 00000000 A3A6A8AB   BYTE 163, 166, 168, 171, 173, 175, 178, 180, 182, 184, 187, 189, 191
      ADAFB2C4
      B6B8B6BD
      BF
141 0000001A C1C5C5C7   BYTE 193, 195, 197, 199, 201, 203, 205, 207, 208, 210, 212, 213, 215
      C9C8C5CF
      0002D4D5
      D7
142 00000027 D8DAD8DD   BYTE 216, 218, 219, 221, 222, 223, 225, 226, 227, 228, 229, 230, 231
      DEDF71E2
      E3E4E5E6
      E7
143 00000034 E8E8E9EA   BYTE 232, 232, 233, 234, 234, 235, 235, 236, 236, 237, 237, 237
      EAEBEBEC

```

		ECECEDED		
		ED		
144	00000041	EDEDEDED EDECECEC EBEBEAEA	BYTE	237, 237, 237, 237, 237, 236, 236, 236, 235, 235, 234, 234, 233
		E9		
145	0000004E	E8E7E6E6 E5E4E3E1 E0DFDEDC	BYTE	232, 231, 230, 230, 229, 228, 227, 225, 224, 223, 222, 220, 219
		DB		
146	0000005B	D9D8D6D5 D3D2D0CE CCCAC8C6	BYTE	217, 216, 214, 213, 211, 210, 208, 206, 204, 202, 200, 198, 196
		C4		
147	00000068	C2C0BEBC EAB8B6B3 B1AFACAA	BYTE	194, 192, 190, 188, 186, 184, 182, 179, 177, 175, 172, 170, 167
		A7		
148	00000075	A5A3A09E 9E999694 918E8C89	BYTE	165, 163, 160, 158, 155, 153, 150, 148, 145, 142, 140, 137, 135
		87		
149	00000082	84827F	BYTE	132, 130, 127
150				
151				
152	00000085	7C797674 716F6C6A 6764625F 5D5A	BYTE	124, 121, 118, 116, 113, 111, 108, 106, 103, 100, 98, 95, 93, 90
		5D5A		
153	00000093	58565351 4F4C4A40 4643413F	BYTE	88, 86, 83, 81, 79, 76, 74, 72, 70, 67, 65, 63, 61
		3D		
154	000000A0	3B393735 33312F2E 2C2A2927	BYTE	59, 57, 55, 53, 51, 49, 47, 46, 44, 42, 41, 39, 38
		26		
155	000000AD	24232120 1F1B1C1B 1A191817	BYTE	36, 35, 33, 32, 31, 29, 28, 27, 26, 25, 24, 23, 22
		16		
156	000000BA	16151414 13131212 12111111	BYTE	22, 21, 20, 20, 19, 19, 18, 18, 17, 17, 17, 17
		11		
157	000000C7	11111111 12121213 13141415	BYTE	17, 17, 17, 17, 18, 18, 18, 19, 19, 20, 20, 21, 22
		16		
158	000000D4	17181819 1A1B1C1E 1F202223	BYTE	23, 24, 24, 25, 26, 27, 29, 30, 31, 32, 34, 35, 37

ASM 8086/8088 SYMBOL TABLE
V01.18-38 (8560)

Page 6
29-Sep-83 12:30:53

Section = SDK88.CONST, Class = DATA00, Aligned to 00000010, Size = 0000010A

SINE1-----00000000 SINE2-----00000085

Section = PASCALPROCEDURE, Class = INSTR00, Aligned to 00000010, Size = 000000D4

ADD1-----0000002D	ADD2-----000000A3	CONT-----0000003E	CONT2-----000000A5
END1-----0000005A	END2-----000000C1	FIRASUB-----00000000 6	FIRE1-----00000020
FIRE2-----00000067	FIREA-----0000004D	FIREB-----00000064	LAB1-----00000025
LAB2-----0000008C	NEG1-----00000032	NEXT-----0000004A	NEXT2-----000000B1
POS2-----0000009F	START1-----00000003	START2-----0000006F	SUB1-----0000003C
SUB2-----0000009A	TSTA-----00000021	TSTR-----00000088	

Section = %FIREA0BJ, Aligned to 00000010, Size = EMPTY

Unbound Globals

CODEBASE00-----00000000 CONSTRASE00-----00000000 DATABASE00-----00000000

167 Lines Read
167 Lines Processed
0 Errors

Sample No.	Address dec.	vr dec.	cont'd			cont'd			cont'd		
			dec.	hex.	dec.	dec.	hex.	dec.	dec.	hex.	dec.
0	1058	130	35	107B	210	70	109E	236	105	10C1	192
1	1059	133	36	107C	212	71	109F	236	106	10C2	190
2	105A	136	37	107D	213	72	10A0	236	107	10C3	188
3	105B	138	38	107E	215	73	10A1	235	108	10C4	186
4	105C	141	39	107F	216	74	10A2	235	109	10C5	184
5	105D	143	40	1080	218	75	10A3	234	110	10C6	182
6	105E	146	41	1081	219	76	10A4	234	111	10C7	179
7	105F	148	42	1082	221	77	10A5	232	112	10C8	177
8	1060	151	43	1083	222	78	10A6	232	113	10C9	175
9	1061	154	44	1084	223	79	10A7	231	114	10CA	172
10	1062	156	45	1085	225	80	10A8	230	115	10CB	170
11	1063	159	46	1086	226	81	10A9	230	116	10CC	167
12	1064	161	47	1087	227	82	10AA	229	117	10CD	165
13	1065	163	48	1088	228	83	10AB	228	118	10CE	163
14	1066	166	49	1089	229	84	10AC	227	119	10CF	160
15	1067	168	50	108A	230	85	10AD	225	120	10D0	158
16	1068	171	51	108B	231	86	10AE	224	121	10D1	155
17	1069	173	52	108C	232	87	10AF	223	122	10D2	153
18	106A	175	53	108D	232	88	10B0	222	123	10D3	140
19	106B	178	54	108E	233	89	10B1	220	124	10D4	148
20	106C	180	55	108F	234	90	10B2	219	125	10D5	145
21	106D	182	56	1090	234	91	10B3	217	126	10D6	142
22	106E	184	57	1091	235	92	10B4	216	127	10D7	130
23	106F	187	58	1092	235	93	10B5	214	128	10D8	137
24	1070	189	59	1093	236	94	10B6	213	129	10D9	135
25	1071	191	60	1094	236	95	10B7	211	130	10DA	132
26	1072	193	61	1095	236	96	10B8	210	131	10DB	130
27	1073	195	62	1096	237	97	10B9	208	132	10DC	127
28	1074	197	63	1097	237	98	10BA	206			
29	1075	199	64	1098	237	99	10BB	204			
30	1076	201	65	1099	237	100	10BC	202			
31	1077	203	66	109A	237	101	10BD	200			
32	1078	205	67	109B	237	102	10BE	198			
33	1079	207	68	109C	237	103	10BF	196			
34	107A	208	69	109D	237	104	10C0	194			

F.II SINE1: Positive half-cycle reference sinusoid

Sample No.	Address dec.	vr hex.	cont'd			cont'd			cont'd		
			dec.	hex.	dec.	dec.	hex.	dec.	dec.	hex.	dec.
0	10DD	124	35	1110	44	70	1133	13	105	1156	62
1	10DE	121	36	1111	42	71	1134	236	106	1157	64
2	10DF	118	37	1112	41	72	1135	236	107	1158	66
3	10E0	116	38	1113	39	73	1136	235	108	1159	68
4	10E1	113	39	1114	38	74	1137	235	109	115A	70
5	10E2	111	40	1115	36	75	1138	234	110	115B	72
6	10E3	108	41	1116	35	76	1139	234	111	115C	75
7	10E4	106	42	1117	33	77	113A	232	112	115D	77
8	10E5	103	43	1118	32	78	113B	232	113	115E	79
9	10E6	100	44	1119	31	79	113C	231	114	115F	82
10	10E7	98	45	111A	29	80	113D	230	115	1160	84
11	10E8	95	46	111B	28	81	113E	230	116	1161	87
12	10E9	93	47	111C	27	82	113F	229	117	1162	89
13	10EA	90	48	111D	26	83	1140	228	118	1163	91
14	10EB	88	49	111E	25	84	1141	227	119	1164	94
15	10EC	86	50	111F	24	85	1142	225	120	1165	96
16	10ED	83	51	1120	23	86	1143	224	121	1166	99
17	10EE	81	52	1121	22	87	1144	223	122	1167	101
18	10EF	79	53	1122	22	88	1145	222	123	1168	104
19	1100	76	54	1123	21	89	1146	220	124	1169	106
20	1101	74	55	1124	20	90	1147	219	125	116A	109
21	1102	72	56	1125	20	91	1148	217	126	116B	112
22	1103	70	57	1126	19	92	1149	216	127	116C	114
23	1104	67	58	1127	19	93	114A	214	128	116D	117
24	1105	65	59	1128	18	94	114B	213	129	116E	122
25	1106	63	60	1129	18	95	114C	211	130	116F	124
26	1107	61	61	112A	18	96	114D	210	131	1170	130
27	1108	59	62	112B	17	97	114E	208	132	1171	127
28	1109	57	63	112C	17	98	114F	206			
29	110A	55	64	112D	17	99	1150	204			
30	110B	53	65	112E	17	100	1151	202			
31	110C	51	66	112F	17	101	1152	200			
32	110D	49	67	1130	17	102	1153	198			
33	110E	47	68	1131	17	103	1154	196			
34	110F	46	69	1132	17	104	1155	194			

F.III SINE2: Negative half-cycle reference sinusoid

APPENDIX G

SPECAN.FORTRAN - A SPECTRUM ANALYSIS PACKAGE
PROGRAM LISTING

G.I Spectral Analysis Program Overview

The main SPECAN program is used for handling and manipulation of data to enable it to be used as a general program suited to input data with varying characteristics.

The number of time-series data samples was required to be 2^N , and an equivalent number of frequency blocks were returned from the FFT subroutine 'FRXFM' within the range $0 - F_s$ Hz, where $F_s = 1/\Delta t$, the sampling frequency. Only the lower half of this frequency domain data could be used - that below the Nyquist frequency $F_N = 1/2\Delta t$.

The frequency range of power spectral density that could be studied was therefore simply a function of the input data sampling frequency F_s .

Δt for most of the data studied was fixed at 800 microseconds, giving $F_N = F_s/2 = 625$ Hz.

The resolution into frequency blocks within this range was then a function of the total number of time series samples input to the program.

Table G1 shows how the output frequency range and resolution vary with input time series data sampling frequency F_s , and total number of samples 2^N .

2048 samples were always used, giving $N = 11$ and a resolution of 0.6 Hz per block in the output frequency range to 625 Hz.

Figure G1 shows how the main 'SPECAN' program utilised a run-time library of compiled subroutines 'FRXFM', 'BLOCK' and 'HAN'.

'BLOCK' rearranges the frequency components output from 'FRXFM' into their correct consecutive sequence.

Sampling Frequency F_s	Hertz		
	2500	1250	625
frequency span resulting	0 - 1250	0 - 625	0 - 312
Number of samples N_s			
1024	2.44	1.22	0.61
2048	1.22	0.61	0.31
4096	0.61	0.31	0.15
	Resolution bandwidth		

TABLE G1 : FFT output frequency range and resolution.

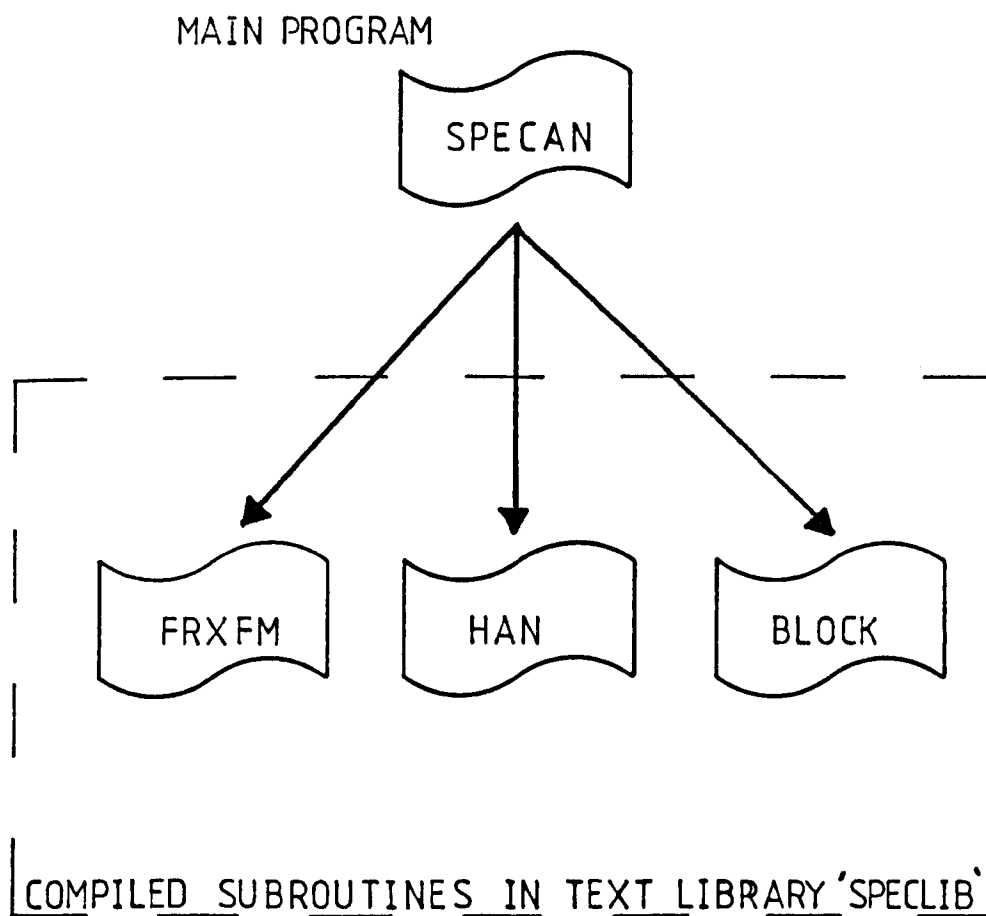


FIG. G1 : SPECTRUM ANALYSIS
PROGRAM STRUCTURE

'HAN' introduces a Hanning smoothing window which takes the form of a cosine 'half-bell' at each end of the data span. This reduces errors over the whole frequency span which may be caused by end-effects from the start and end of the time-series data.

The FORTRAN program listings for SPECAN, FRXFM, BLOCK and HAN are given in Sections G.II, G.III, G.IV and G.V respectively.

G.II 'SPECAN' Program Listing

```

      DIMENSION V(2048),T(2048),X(2048),Y(2048),XV(2048),YV(2048),
+ XHZ(20),YHZ(20),XDB(20),YDB(20),TITLE(8)
      INTEGER I,J,K,K1,K2,LINES,IDB,NBLK,NBLK50,NBLKH,ENDBLK
      LOGICAL LIST,HANFIL
C      READ(5,100) N2TOT,N2SAM,NBLK,ITST,IDYN,IHAN,IPRINT,ISQ,IWAVE
C      WRITE(6,100) N2TOT,N2SAM,NBLK,ITST,IDYN,IHAN,IPRINT,ISQ,IWAVE
C
C.....THIS SPEC50 PROGRAM IS A MODIFICATION OF THE GENERAL
C      SPECAN PROGRAM FOR SPECTRAL ANALYSIS.
C
C      THE MODIFICATIONS ONLY ALLOW ONE 'SEGMENT' TO BE
C      PLOTTED FROM THE INPUT DATA.
C      THUS:
C      'ITST' MUST BE 1 (TEST SEGMENT IS THE FIRST)
C      'ISQ' NEED ONLY BE 1
C      'N2SAM'='N2TOT' (SAMPLES PER SEGMENT
C      = TOTAL NO. OF SAMPLES)
C      ALSO:
C      'NTOT' MUST BE 2048 DATA POINTS HERE
C      'NBLK' IS SET SO THAT ALL SPECTRAL LINES ARE
C      CALCULATED - NO AVERAGING OCCURS
C      'IDYN' IS SET TO 90 BECAUSE THIS APPLICATIONS
C      REQUIRES DETAILS DOWN TO -80DB
C
C      THERE IS NO LONGER ANY FACILITY FOR PLOTTING THE
C      INPUT TIME-SERIES DATA.
C
      IDYN=90
      N2TOT=11
      N2SAM=11
      NBLK=(2.0**N2SAM)/2.0
      ITST=1
      ISQ=1
      HANFIL=.TRUE.
C
C.....THE RANGE OF FREQUENCY TO BE PRESENTED IS DEFINED
C      BY SETTING THE NO. OF BLOCKS TO BE PLOTTED,
C      REMEMBERING THAT (NO. OF SAMPLES X 0.5) WILL GIVE
C      UP TO THE NYQUIST FREQUENCY.
C
C      THUS FOR 2048 SAMPLES AT 800US SAMPLING INTERVAL...
C      82 BLOCKS GIVES 0 - 50 HZ
C      983 BLOCKS GIVES 0 - 600 HZ.
C
      NBLK50=82
      NBLKC=165
      NBLKH=983
      IDYN=IDYN-10
      NTOT=2**N2TOT
      NSAM=2**N2SAM
      NSAM2=NSAM/2
      FSAMSQ=FLOAT(NSAM)*FLOAT(NSAM)
      NSEG=NTOT/NSAM2 - 1
      NLPB=NSAM2/NBLK
C
C.....READ ALPHANUMERIC DATA AT HEAD OF DATA FILE
C
      READ(5,111) TITLE
C
C.....READ THE INPUT DATA AND ATTACH TO EACH POINT AN
C      ARBITRARY TIME VALUE
C
      LINES=NTOT/8
      IF(LIST)WRITE(6,104)
      DO 2 J=1,LINES
        K1=J*8-7
        K2=J*8
        READ(5,102)(V(K),K=K1,K2,1)
        DO 1 K=K1,K2,1
          T(K)=FLOAT(K)
          IF(LIST) WRITE(6,105) K,T(K),V(K)
1        CONTINUE
          IF(LIST) WRITE(6,110)
          IF(LIST) WRITE(6,102) (V(K),K=K1,K2,1)
2        CONTINUE
C
C.....DRY RUN TO ESTIMATE MAX POWER
C
      I1=(ITST-1)*NSAM2 + 1
      I2=(ITST+1)*NSAM2
      DO 5 I=I1,I2
        K=I-I1+1
        X(K)=V(I)
        Y(K)=0.0

```



```

5 CONTINUE                                     SPE00860
  CALL FRXFM(N2SAM,NSAM,X,Y)                   SPE00870
  IF(.NOT.HANFIL) GO TO 6                      SPE00880
  CALL HAN(NSAM,X,Y)                           SPE00890
  SCALE=16.0/(3.0*FSAMSQ)                     SPE00900
  GO TO 7                                       SPE00910
6 SCALE=2.0/FSAMSQ                             SPE00920
7 X(1)=0.0                                     SPE00930
  DO 8 I=2,NSAM2                              SPE00940
8 X(I)=SCALE*(X(I)*X(I) + Y(I)*Y(I))         SPE00950
  CALL BLOCK(X,Y,NSAM2,NBLK)                  SPE00960
  XMX=X(1)                                     SPE00970
  DO 9 I=2,NBLK                               SPE00980
9 IF(X(I).GT.XMX) XMX=X(I)                   SPE00990
C                                               SPE01000
C.....COMPUTE AND PLOT SPECTRA                SPE01010
C                                               SPE01020
C                                               SPE01030
C.....J IS INVARIANT BECAUSE THERE IS ONLY ONE SEGMENT
C                                               SPE01040
C                                               SPE01050
  J=1                                          SPE01060
  I1=(J-1)*NSAM2+1                          SPE01070
  I2=(J+1)*NSAM2                            SPE01080
  DO 12 I=I1,I2                              SPE01090
  K=I-I1+1                                   SPE01100
  X(K)=V(I)                                  SPE01110
12 Y(K)=0.0                                  SPE01120
  CALL FRXFM(N2SAM,NSAM,X,Y)                 SPE01130
  IF(LIST) WRITE(6,106)                      SPE01140
  IF(LIST) WRITE(6,101) (I,X(I),Y(I),I=1,NSAM)
  IF(.NOT.HANFIL) GO TO 13                   SPE01150
  CALL HAN(NSAM,X,Y)                         SPE01160
  IF(LIST) WRITE(6,107)                      SPE01170
  IF(LIST) WRITE(6,101) (I,X(I),Y(I),I=1,NSAM)
  IF(LIST) WRITE(6,109)                      SPE01180
  SCALE=16.0/(3.0*FSAMSQ)                   SPE01190
  GO TO 14                                    SPE01200
13 SCALE=2.0/FSAMSQ                          SPE01210
14 X(1)=0.0                                  SPE01220
  DO 16 I=2,NSAM2                            SPE01230
16 X(I)=SCALE*(X(I)*X(I) + Y(I)*Y(I))         SPE01240
  CALL BLOCK(X,Y,NSAM2,NBLK)                SPE01250
  IF(LIST) WRITE(6,108)                      SPE01260
  IF(LIST) WRITE(6,101)(I,X(I),Y(I), I=1,NBLK)
C                                               SPE01270
C.....PLOTTING OF SPECTRUM FOLLOWS           SPE01280
C                                               SPE01290
C                                               SPE01300
C                                               SPE01310
C                                               SPE01320
C                                               SPE01330
C                                               SPE01340
17 CONTINUE                                  SPE01350
  ENDBLK=NBLKC                               SPE01360
  CALL PAPER(1)                               SPE01370
18 CALL PSPACE(0.2,0.56,0.3,0.9)            SPE01380
  CALL CSPACE(0.0,0.0,0.0,0.0)              SPE01390
  ENDYM=0.5*(FLOAT(ENDBLK)/1024.0)          SPE01400
  WRITE(2,*) ENDBLK,ENDYM                    SPE01410
  CALL MAP(-80.0,10.0,ENDYM,0.0)            SPE01420
  CALL CTRFNT(1)                             SPE01430
  CALL CTRMAG(10)                            SPE01440
C                                               SPE01450
C                                               SPE01460
C                                               SPE01470
C                                               SPE01480
C                                               SPE01490
C                                               SPE01500
C                                               SPE01510
C                                               SPE01520
C                                               SPE01530
C                                               SPE01540
C                                               SPE01550
C                                               SPE01560
C                                               SPE01570
C                                               SPE01580
C                                               SPE01590
C                                               SPE01600
C                                               SPE01610
C                                               SPE01620
C                                               SPE01630
C                                               SPE01640
C                                               SPE01650
C                                               SPE01660
C                                               SPE01670
C                                               SPE01680
C                                               SPE01690
C                                               SPE01700
C                                               SPE01710
  XSM1=-FLOAT(80)
  XSM2=10.0
  YSM1=0.5
  YSM2=0.5*(NBLK50/1024.0)
  DEL=Y(2)-Y(1)
  CALL POSITN(XSM1,0.0)
  MARK=0
  XP=XSM1
  IF(X(1).EQ.0.0) GO TO 19
  XP=10.0*ALOG10(X(1)/XMX)
19 YP=0.0
  IF(XP.LT.XSM2) GO TO 20
  MARK=MARK+1
  XP=XSM2
  YV(1)=Y(1)
  XV(1)=XP
  GO TO 22
20 IF(XP.GT.XSM1) GO TO 22

```

```

MARK=MARK+1
XP=XSM1
YV(1)=Y(1)
XV(1)=XP
22 CALL JOIN(XP,YP)
YP=Y(1)+DEL/2.0
CALL JOIN(XP,YP)
C
C      THE LOOP TO 30 PLOTS THE BLOCKS IN THE F-DOMAIN AFTER THE
C      FIRST BLOCK.
C
C      USUALLY THE UPPER LIMIT WOULD BE SIMPLY NBLK--BUT FOR THIS
C      SPEC50 PROGRAM IT IS NBLKC AS SET ABOVE.
C
DO 30 I=2,ENDBLK
IF(X(I).GT.0.0) GO TO 23
XP=XSM1
GO TO 26
23 XP=10.0*ALOG10(X(I)/XMX)
IF(XP.LT.XSM2) GO TO 24
MARK=MARK+1
XP=XSM2
XV(MARK)=XP
YV(MARK)=Y(I)
GO TO 26
24 IF(XP.GT.XSM1) GO TO 26
MARK=MARK+1
XP=XSM1
XV(MARK)=XP
YV(MARK)=Y(I)
C 26 IF(MARK.GT.499) GO TO 34
26 CONTINUE
IF(LIST) WRITE(6,103)XP,YP
CALL JOIN(XP,YP)
YP=YP+DEL
30 CALL JOIN(XP,YP)
XP=XSM1
CALL JOIN(XP,YP)
IF(MARK.EQ.0) GO TO 40
C
C.....PLOT STARS WHERE XP IS 'OUT OF RANGE'
C
34 CALL PTPLOT(XV,YV,1,MARK,45)
40 CONTINUE
C
C      FOLLOWING SECTION LABELS AXES OF SPECTRUM PLOT
C      (ONLY IF J=1)
C
C
IF(J.GT.1) GO TO 50
CALL AXNOTA(0)
CALL XAXIS
DBMIN=-(IDYN)
DO 41 I=1,10,1
YHZ(I)=FLOAT(I)*(ENDYM/10.0)
XHZ(I)=DBMIN
41 CONTINUE
IDB=IDYN/10+1
DO 42 I=1,IDB,1
XDB(I)=10.0-(I*10.0)
YDB(I)=0.0
42 CONTINUE
CALL CTRMAG(20)
CALL PTPLOT(XHZ,YHZ,1,10,43)
CALL PTPLOT(XDB,YDB,1,IDB,43)
CALL POSITN(DBMIN,0.0)
CALL JOIN(10.0,0.0)
CALL POSITN(DBMIN,0.0)
CALL JOIN(DBMIN,ENDYM)
CALL CTRORI(270.0)
CALL PSPACE(0.0,1.0,0.0,1.0)
CALL CSPACE(0.0,0.0,0.0,0.0)
CALL MAP(0.0,1.0,0.0,1.0)
CALL CTRMAG(8)
CALL CTRORI(270.0)
XCH=0.18
YCH=0.91
CALL PLOTCS(XCH,YCH,91H0.0 10.0 20.0 30.0 40.0
+50.0 60.0 70.0 80.0 90.0 100.0,91)
XCH=XCH-0.03
YCH=YCH-0.08
SPE01720
SPE01730
SPE01740
SPE01750
SPE01760
SPE01770
SPE01780
SPE01790
SPE01800
SPE01810
SPE01820
SPE01830
SPE01840
SPE01850
SPE01860
SPE01870
SPE01880
SPE01890
SPE01900
SPE01910
SPE01920
SPE01930
SPE01940
SPE01950
SPE01960
SPE01970
SPE01980
SPE01990
SPE02000
SPE02010
SPE02020
SPE02030
SPE02040
SPE02050
SPE02060
SPE02070
SPE02080
SPE02090
SPE02100
SPE02110
SPE02120
SPE02130
SPE02140
SPE02150
SPE02160
SPE02170
SPE02180
SPE02190
SPE02200
SPE02210
SPE02220
SPE02230
SPE02240
SPE02250
SPE02260
SPE02270
SPE02280
SPE02290
SPE02300
SPE02310
SPE02320
SPE02330
SPE02340
SPE02350
SPE02360
SPE02370
SPE02380
SPE02390
SPE02400
SPE02410
SPE02420
SPE02430
SPE02440
SPE02450
SPE02460
SPE02470
SPE02480
SPE02490
SPE02500
SPE02510
SPE02520

```

```

CALL CTRMAG(10)
CALL PLOTCS(XCH,YCH,36H
CALL PLOTCS(0.54,0.95,2HDB,2)
CALL CTRMAG(10)
CALL PLOTCS(0.98,0.95,TITLE,64)
CALL CTRMAG(20)
CALL PLOTCS(0.65,0.70,13HPOWER SPECTRA,13)
CALL CTRMAG(8)
CALL PLOTCS(0.560,0.95,5H 10.0,5)
CALL PLOTCS(0.520,0.95,5H 0.0,5)
CALL PLOTCS(0.480,0.95,5H-10.0,5)
CALL PLOTCS(0.440,0.95,5H-20.0,5)
CALL PLOTCS(0.400,0.95,5H-30.0,5)
CALL PLOTCS(0.360,0.95,5H-40.0,5)
CALL PLOTCS(0.320,0.95,5H-50.0,5)
CALL PLOTCS(0.280,0.95,5H-60.0,5)
CALL PLOTCS(0.240,0.95,5H-70.0,5)
CALL PLOTCS(0.200,0.95,5H-80.0,5)
CALL CTRORI(0.0)
CALL CTRMAG(10)
50 CONTINUE
CALL GREND

C
C
C.....SECOND PLOTTING SECTION (BELOW) OUTPUTS 0 - 600HZ
C          FOR HARMONIC ANALYSIS.
C
C
C          ENDBLK=NBLKH
CALL PAPER(1)
68 CALL PSPACE(0.2,0.56,0.3,0.9)
CALL CSPACE(0.0,0.0,0.0,0.0)
ENDYM=0.5*(FLOAT(ENDBLK)/1024.0)
WRITE(2,*) ENDBLK,ENDYM
CALL MAP(-80.0,10.0,ENDYM,0.0)
CALL CTRFNT(1)
CALL CTRMAG(10)

C
C
C          THE FOLLOWING PRAMETERS SET THE MATHEMATICAL SPACE FOR THE
C          POWER SPECTRUM PLOT.
C
C          YSM DICTATES THE RANGE OF NORMALISED FREQUENCY PLOTTED--ITS
C          MAXIMUM ALLOWABLE VALUE IS 0.5. (NYQUIST LIMIT)
C
C
C          XSM1=-FLOAT(80)
C          XSM2=10.0
C          YSM1=0.5
C          YSM1=0.5*(NBLK50/1024.0)
C          YSM2=0.0
C          DEL=Y(2)-Y(1)
CALL POSITN(XSM1,0.0)
MARK=0
XP=XSM1
IF(X(1).EQ.0.0) GO TO 69
XP=10.0*ALOG10(X(1)/XMX)
69 YP=0.0
IF(XP.LT.XSM2) GO TO 70
MARK=MARK+1
XP=XSM2
YV(1)=Y(1)
XV(1)=XP
GO TO 72
70 IF(XP.GT.XSM1) GO TO 72
MARK=MARK+1
XP=XSM1
YV(1)=Y(1)
XV(1)=XP
72 CALL JOIN(XP,YP)
YP=Y(1)+DEL/2.0
CALL JOIN(XP,YP)

C
C          THE LOOP TO 80 PLOTS THE BLOCKS IN THE F-DOMAIN AFTER THE
C          FIRST BLOCK.
C
C          USUALLY THE UPPER LIMIT WOULD BE SIMPLY NBLK--BUT FOR THIS
C          PLOT IT IS NBLKH AS SET ABOVE.
C
C          DO 80 I=2,ENDBLK
C          IF(X(I).GT.0.0) GO TO 73
C          XP=XSM1
C          GO TO 76
73 XP=10.0*ALOG10(X(I)/XMX)
IF(XP.LT.XSM2) GO TO 74
MARK=MARK+1
XP=XSM2
XV(MARK)=XP
YV(MARK)=Y(I)
GO TO 76
74 IF(XP.GT.XSM1) GO TO 76

```

SPE02530
SPE02540
SPE02550
SPE02560
SPE02570
SPE02580
SPE02590
SPE02600
SPE02610
SPE02620
SPE02630
SPE02640
SPE02650
SPE02660
SPE02670
SPE02680
SPE02690
SPE02700
SPE02710
SPE02720
SPE02730
SPE02740
SPE02750
SPE02760
SPE02770
SPE02780
SPE02790
SPE02800
SPE02810
SPE02820
SPE02830
SPE02840
SPE02850
SPE02860
SPE02870
SPE02880
SPE02890
SPE02900
SPE02910
SPE02920
SPE02930
SPE02940
SPE02950
SPE02960
SPE02970
SPE02980
SPE02990
SPE03000
SPE03010
SPE03020
SPE03030
SPE03040
SPE03050
SPE03060
SPE03070
SPE03080
SPE03090
SPE03100
SPE03110
SPE03120
SPE03130
SPE03140
SPE03150
SPE03160
SPE03170
SPE03180
SPE03190
SPE03200
SPE03210
SPE03220
SPE03230
SPE03240
SPE03250
SPE03260
SPE03270
SPE03280
SPE03290
SPE03300
SPE03310
SPE03320
SPE03330
SPE03340
SPE03350
SPE03360
SPE03370
SPE03380
SPE03390
SPE03400
SPE03410
SPE03420
SPE03430

```

MARK=MARK+1
XP=XSM1
XV(MARK)=XP
YV(MARK)=Y(I)
C 76 IF(MARK.GT.499) GO TO 84
76 CONTINUE
IF(LIST) WRITE(6,103)XP,YP
CALL JOIN(XP,YP)
YP=YP+DEL
80 CALL JOIN(XP,YP)
XP=XSM1
CALL JOIN(XP,YP)
IF(MARK.EQ.0) GO TO 90
C
C.....PLOT STARS WHERE XP IS 'OUT OF RANGE'
C
84 CALL PTPLOT(XV,YV,1,MARK,45)
90 CONTINUE
C
C          FOLLOWING SECTION LABELS AXES OF SPECTRUM PLOT
C          (ONLY IF J=1)
C
IF(J.GT.1) GO TO 99
CALL AXNOTA(0)
CALL XAXIS
DBMIN=-(IDYN)
DO 91 I=1,12,1
  YHZ(I)=FLOAT(I)*(ENDYM/12.0)
  XHZ(I)=DBMIN
91 CONTINUE
IDB=IDYN/10+1
DO 92 I=1,IDB,1
  XDB(I)=10.0-(I*10.0)
  YDB(I)=0.0
92 CONTINUE
CALL CTRMAG(20)
CALL PTPLOT(XHZ,YHZ,1,10,43)
CALL PTPLOT(XDB,YDB,1,IDB,43)
CALL POSITN(DBMIN,0.0)
CALL JOIN(10.0,0.0)
CALL POSITN(DBMIN,0.0)
CALL JOIN(DBMIN,ENDYM)
CALL CTRORI(270.0)
CALL PSPACE(0.0,1.0,0.0,1.0)
CALL CSPACE(0.0,0.0,0.0,0.0)
CALL MAP(0.0,1.0,0.0,1.0)
CALL CTRMAG(8)
CALL CTRORI(270.0)
XCH=0.18
YCH=0.91
CALL PLOTCS(XCH,YCH,91H 0          100          200
+ 300          400          500          600 ,91)
XCH=XCH-0.03
YCH=YCH-0.08
CALL CTRMAG(10)
CALL PLOTCS(XCH,YCH,36H          FREQUENCY ( HZ ),36)
CALL PLOTCS(0.54,0.95,2HDB,2)
CALL CTRMAG(8)
CALL PLOTCS(0.98,0.95,TITLE,64)
CALL CTRMAG(20)
CALL PLOTCS(0.65,0.70,13HPOWER SPECTRA,13)
CALL CTRMAG(8)
CALL PLOTCS(0.560,0.95,5H 10.0,5)
CALL PLOTCS(0.520,0.95,5H 0.0,5)
CALL PLOTCS(0.480,0.95,5H-10.0,5)
CALL PLOTCS(0.440,0.95,5H-20.0,5)
CALL PLOTCS(0.400,0.95,5H-30.0,5)
CALL PLOTCS(0.360,0.95,5H-40.0,5)
CALL PLOTCS(0.320,0.95,5H-50.0,5)
CALL PLOTCS(0.280,0.95,5H-60.0,5)
CALL PLOTCS(0.240,0.95,5H-70.0,5)
CALL PLOTCS(0.200,0.95,5H-80.0,5)
CALL CTRORI(J.0)
CALL CTRMAG(10)
99 CONTINUE
CALL GREND
100 FORMAT(9I5)
101 FORMAT(//2(2X,I4,E11.4,E11.4,2X))
102 FORMAT(1H ,8(1X,F8.4))
103 FORMAT(1H ,2(2X,F10.5))
104 FORMAT(///14H DATA DETAILS: ,/27H K          T(K)          V(K),/)
105 FORMAT(2X,I4,2X,F10.4,2X,F10.4)
106 FORMAT(//25H X(I) & Y(I) AFTER FRXFM: ,/)
107 FORMAT(//23H X(I) & Y(I) AFTER HAN: ,/)
108 FORMAT(//25H X(I) & Y(I) AFTER BLOCK: ,/)
109 FORMAT(//23H POINTS TO BE PLOTTED: ,/)
110 FORMAT(//19H CONTINUOUS V(K)... ,/)
111 FORMAT(8A8)
895 FORMAT(//46H      &&&&&&&&& THIS IS THE TEST LINE &&&&&&&&&)
STOP
END

```

SPE03440
SPE03450
SPE03460
SPE03470
SPE03480
SPE03490
SPE03500
SPE03510
SPE03520
SPE03530
SPE03540
SPE03550
SPE03560
SPE03570
SPE03580
SPE03590
SPE03600
SPE03610
SPE03620
SPE03630
SPE03640
SPE03650
SPE03660
SPE03670
SPE03680
SPE03690
SPE03700
SPE03710
SPE03720
SPE03730
SPE03740
SPE03750
SPE03760
SPE03770
SPE03780
SPE03790
SPE03800
SPE03810
SPE03820
SPE03830
SPE03840
SPE03850
SPE03860
SPE03870
SPE03880
SPE03890
SPE03900
SPE03910
SPE03920
SPE03930
SPE03940
SPE03950
SPE03960
SPE03970
SPE03980
SPE03990
SPE04000
SPE04010
SPE04020
SPE04030
SPE04040
SPE04050
SPE04060
SPE04070
SPE04080
SPE04090
SPE04100
SPE04110
SPE04120
SPE04130
SPE04140
SPE04150
SPE04160
SPE04170
SPE04180
SPE04190
SPE04200
SPE04210
SPE04220
SPE04230
SPE04240
SPE04250
SPE04260
SPE04270
SPE04280
SPE04290
SPE04300
SPE04310
SPE04320
SPE04330
SPE04340
SPE04350

G.III 'FRXFM' Program Listing

FILE: FRXFM FORTRAN A1 (EE68)

```

SUBROUTINE FRXFM(N2POW,NTHPOW,X,Y)
REAL X(NTHPOW), Y(NTHPOW), I,I1,I2,I3,I4
INTEGER PASS,SEQLOC,L(13)
EQUIVALENCE (L13,L(1)),(L12,L(2)),(L11,L(3)),(L10,L(4)),
1 (L9,L(5)),(L8,L(6)),(L7,L(7)),(L6,L(8)),(L5,L(9)),
2 (L4,L(10)),(L3,L(11)),(L2,L(12)),(L1,L(13))
N4POW=N2POW/2
IF(N4POW.EQ.0) GO TO 3
DO 2 PASS=1,N4POW
NXTLTH=2**(N2POW-2*PASS)
LENGTH=4*NXTLTH
SCALE=6.283185307/FLOAT(LENGTH)
DO 2 J=1,NXTLTH
ARG=FLOAT(J-1)*SCALE
C1=COS(ARG)
S1=SIN(ARG)
C2=C1*C1-S1*S1
S2=C1*S1+C1*S1
C3=C1*C2-S1*S2
S3=C2*S1+S2*C1
DO 2 SEQLOC=LENGTH,NTHPOW,LENGTH
J1=SEQLOC-LENGTH+J
J2=J1+NXTLTH
J3=J2+NXTLTH
J4=J3+NXTLTH
R1=X(J1)+X(J3)
R2=X(J1)-X(J3)
R3=X(J2)+X(J4)
R4=X(J2)-X(J4)
I1=Y(J1)+Y(J3)
I2=Y(J1)-Y(J3)
I3=Y(J2)+Y(J4)
I4=Y(J2)-Y(J4)
X(J1)=R1+R3
Y(J1)=I1+I3
IF(J.EQ.1) GO TO 1
X(J3)=C1*(R2-I4)-S1*(I2+R4)
Y(J3)=S1*(R2-I4)+C1*(I2+R4)
X(J2)=C2*(R1-R3)-S2*(I1-I3)
Y(J2)=S2*(R1-R3)+C2*(I1-I3)
X(J4)=C3*(R2+I4)-S3*(I2-R4)
Y(J4)=S3*(R2+I4)+C3*(I2-R4)
GO TO 2
1 X(J3)=R2-I4
Y(J3)=I2+R4
X(J2)=R1-R3
Y(J2)=I1-I3
X(J4)=R2+I4
Y(J4)=I2-R4
2 CONTINUE
3 IF(N2POW.EQ.2*N4POW) GO TO 5
DO 4 J=1,NTHPOW,2
R=X(J)+X(J+1)
X(J+1)=X(J)-X(J+1)
X(J)=R
I=Y(J)+Y(J+1)
Y(J+1)=Y(J)-Y(J+1)
4 Y(J)=I
5 DO 6 J=1,13
L(J)=1
6 IF(J.LE.N2POW) L(J)=2**(N2POW+1-J)
IJ=1
DO 7 J1=1,L1
DO 7 J2=J1,L2,L1
DO 7 J3=J2,L3,L2
DO 7 J4=J3,L4,L3
DO 7 J5=J4,L5,L4
DO 7 J6=J5,L6,L5
DO 7 J7=J6,L7,L6
DO 7 J8=J7,L8,L7
DO 7 J9=J8,L9,L8
DO 7 J10=J9,L10,L9
DO 7 J11=J10,L11,L10
DO 7 J12=J11,L12,L11
DO 7 JI=J12,L13,L12
IF(IJ.GE.JI) GO TO 7
R=X(IJ)
X(IJ)=X(JI)
X(JI)=R
I=Y(IJ)
Y(IJ)=Y(JI)
Y(JI)=I
7 IJ=IJ+1
RETURN
END
FRX00010
FRX00020
FRX00030
FRX00040
FRX00050
FRX00060
FRX00070
FRX00080
FRX00090
FRX00100
FRX00110
FRX00120
FRX00130
FRX00140
FRX00150
FRX00160
FRX00170
FRX00180
FRX00190
FRX00200
FRX00210
FRX00220
FRX00230
FRX00240
FRX00250
FRX00260
FRX00270
FRX00280
FRX00290
FRX00300
FRX00310
FRX00320
FRX00330
FRX00340
FRX00350
FRX00360
FRX00370
FRX00380
FRX00390
FRX00400
FRX00410
FRX00420
FRX00430
FRX00440
FRX00450
FRX00460
FRX00470
FRX00480
FRX00490
FRX00500
FRX00510
FRX00520
FRX00530
FRX00540
FRX00550
FRX00560
FRX00570
FRX00580
FRX00590
FRX00600
FRX00610
FRX00620
FRX00630
FRX00640
FRX00650
FRX00660
FRX00670
FRX00680
FRX00690
FRX00700
FRX00710
FRX00720
FRX00730
FRX00740
FRX00750
FRX00760
FRX00770
FRX00780
FRX00790
FRX00800
FRX00810
FRX00820
FRX00830
FRX00840
FRX00850

```

G.IV 'BLOCK' Program Listing

```

SUBROUTINE BLOCK(X,Y,N,NBLK)
C SPLITS ARRAY X, LENGTH N, INTO NBLK BLOCKS. X(1) IS SET TO
C ZERO AVERAGES OF X(I) IN EACH BLOCK ARE EVALUATED AND RETURNED
C IN THE FIRST NBLK POSITIONS OF X.
C FOR FRXFMS, THE FIRST NBLK POSITIONS OF Y CARRY MEAN BLOCK
C FREQUENCIES. N AND NBLK INTEGER POWERS OF TWO.
  DIMENSION X(N), Y(N)
  NLPB=N/NBLK
  KLST=N-NLPB+1
  X(1)=0.0
  NF=0
  DO 1 K=1,KLST,NLPB
  NF=NF+1
  Y(NF)=0.0
  DO 1 J=1,NLPB
  I=K+J-1
1 Y(NF)=Y(NF)+X(I)
  IF (NBLK.EQ.N) GO TO 3
  X(1)=Y(1)/FLOAT(NLPB-1)
  DO 2 K=2,NBLK
2 X(K)=Y(K)/FLOAT(NLPB)
  GO TO 5
3 DO 4 K=1,NBLK
4 X(K)=Y(K)
5 DO 6 K=1,NBLK
6 Y(K)=FLOAT((2*K-1)*NLPB-1)/FLOAT(4*N)
  RETURN
  END

```

BLO00010
BLO00020
BLO00030
BLO00040
BLO00050
BLO00060
BLO00070
BLO00080
BLO00090
BLO00100
BLO00110
BLO00120
BLO00130
BLO00140
BLO00150
BLO00160
BLO00170
BLO00180
BLO00190
BLO00200
BLO00210
BLO00220
BLO00230
BLO00240
BLO00250
BLO00260
BLO00270
BLO00280

G.V 'HAN' Program Listing

```

SUBROUTINE HAN(NTHPOW,X,Y)
C HANS FRXFM COEFFS IN ARRAYS X,Y GIVEN IN USUAL FORM ABOUT
C FOLDING FREQUENCY. SIGNAL POWER REDUCED BY 3/8.
  DIMENSION X(NTHPOW), Y(NTHPOW)
  X1=0.5*(X(1)-X(2))
  Y1=0.5*Y(1)
  XN=0.5*X(NTHPOW) - 0.25*(X(NTHPOW-1)+X(1))
  YN=0.5*Y(NTHPOW) - 0.25*(Y(NTHPOW-1)+Y(1))
  JLST=NTHPOW-1
  XB=X(1)
  YB=Y(1)
  DO 1 J=2,JLST
  XA=X(J)
  YA=Y(J)
  X(J)=0.5*X(J) - 0.25*(XB+X(J+1))
  Y(J)=0.5*Y(J) - 0.25*(YB+Y(J+1))
  XB=XA
1 YB=YA
  X(1)=X1
  Y(1)=Y1
  X(NTHPOW)=XN
  Y(NTHPOW)=YN
  RETURN
  END

```

HAN00010
HAN00020
HAN00030
HAN00040
HAN00050
HAN00060
HAN00070
HAN00080
HAN00090
HAN00100
HAN00110
HAN00120
HAN00130
HAN00140
HAN00150
HAN00160
HAN00170
HAN00180
HAN00190
HAN00200
HAN00210
HAN00220
HAN00230
HAN00240

APPENDIX H

DATA LOGGING

H.I Twelve-Bit Data Logging

It was required that the mainframe computer could be used for storage and subsequent analysis of the test results obtained using the laboratory compensator. Section 4.2.2 showed that 8-bit digital sampling of voltage waveforms would not be able to accurately measure the small level of voltage disturbances that would just cause annoying lamp flicker.

To be able to measure the compensator's performance more effectively, a three channel data-logger incorporating three 12-bit ADCs was constructed. Sampling and immediate storage of data was controlled by an SDK-88 microprocessor development kit similar to that used in the TCR compensators (Part 4.2).

Data logging for any particular cycle of the arc furnace model's operation was initiated by the 10 microsecond synchronising pulse output from the AIM-65 microcomputer system.

A software sample loop delay time was incorporated into the controlling assembler language program 'sampsb', fixing the sampling interval for all three channels to 800 microseconds. The full program listing is given in H.II.

H.II 12-Bit ADC Sampling Program

MODEL synchronised_sampling_routine
NOLIST OFF

GLOBAL sampsub
GLOBAL CODEBASEQQ, DATABASEQQ, CONSTBASEQQ

ASSUME DS:DATABASEQQ

SECTION pascalprocedure, CLASS=INSTRQQ

XX
; assembler routine to sample from 3 12-bit adcs at addresses FA00, FC00
; and FE00. sampling is initiated by a 5v level on l.s.b. of PORT A of
; 8255 PPI. the 5v level should last for at least 200us.

; the code for text strings is stored in the CONST RAM segment so the
; results are offset from the beginning of this segment by 500 bytes.

; pascal call :- sampsub

; condition of stack on entry to this routine

RETURN ADDRESS (---SP

sampsub

30	00000000 B400	MOV AH, 00H	; zero AH
31	00000002 B000	MOV AL, 00H	;
32	00000004 BA03F0	MOV DX, 00F003H	; set address of 8255 control port
33	00000007 1F	OUT DX, AL	; set ports as inputs
34	00000008 BA00F0	MOV DX, 00F000H	; set address of PORT A
35			
36			
37	00000008 EC	IN AL, DX	; read byte from PORT A into AL
38	0000000C 3C00	CMP AL, 00H	; a '1' for any bit will initiate sampling
39	0000000E 74FB	JC idle	; all bits zero perpetuates idle loop
40			
41	00000010 B50F	MOV CH, 00FH	; set number of loops
42	00000012 B80000	MOV BX, 000500H	; set start address for data storage
43			
44	00000015 BA00FA	MOV DX, 00FA00H	; set address of adc1
45	00000018 0	OUT DX, AL	; start conversion for 12-bit adc1
46	00000019 BA00FC	MOV DX, 00FC00H	; set address of adc2
47	0000001C 0	OUT DX, AL	; start conversion for 12-bit adc2
48	0000001D BA00FE	MOV DX, 00FE00H	; set address of adc3
49	00000020 0	OUT DX, AL	; start conversion for 12-bit adc3
50			
51	00000021 B12F	MOV BL, 02FH	; conversion delay 200us
52	00000023 B200	SHR BL, 1	

```
53  
54 00000025 BA00FA      MOV DX, 00FA00H      ;set address for high byte of 12-bit adc1  
55 00000028 00      IN AL, DX            ;read high byte of adc1  
56 00000029 8807      MOV EBXJ, AL         ;store high byte  
57 0000002B 43      INC DX              ;set address for low nibble of 12-bit adc1  
58 0000002C EC      IN AL, DX          ;read low nibble (left justified)  
59 0000002D 43      INC BX             ;next memory location for data storage  
60 0000002E 8807      MOV EBXJ, AL         ;and store  
61  
62 00000030 BA00FC      MOV DX, 00FC00H      ;repeat for adc2  
63 00000033 EC      IN AL, DX          ;  
64 00000034 43      INC BX             ;  
65 00000035 8807      MOV EBXJ, AL         ;  
66 00000037 42      INC DX             ;  
67 00000038 EC      IN AL, DX          ;  
68 00000039 43      INC BX             ;  
69 0000003A 8807      MOV EBXJ, AL         ;  
70  
71 0000003C BA00FE      MOV DX, 00FE00H      ;repeat for adc3  
72 0000003F EC      IN AL, DX          ;  
73 00000040 43      INC BX             ;  
74 00000041 8807      MOV EBXJ, AL         ;  
75 00000043 42      INC DX             ;  
76 00000044 EC      IN AL, DX          ;  
77 00000045 43      INC BX             ;  
78 00000046 8807      MOV EBXJ, AL         ;  
79 00000048 43      INC BX             ;  
80  
81 00000049 FECB      DEC CH              ;decrement loop counter  
82 0000004B 80FDH      CMP CH, 00FDH  
83 0000004E 7765- EA    JA again  
84 00000050 C3      RET                  ;return to calling pascal program  
85  
86      END
```

APPENDIX J

SYSMOD6.FORTRAN - COMPUTATIONAL ARC FURNACE MODEL
PROGRAM LISTING

FILE: SYSMOD6 FORTRAN A1 (EE68)

```

C
C      SYSMOD6 FORTRAN..... SAME AS SYSMOD5 EXECPT CALLING SY500010
C      SUBROUTINES FROM TEXT LIBRARY 'SYSLIB'          SY500020
C                                                    SY500030
C                                                    SY500040
C                                                    SY500050
C                                                    SY500060
C      EXTERNAL VZEROS,DEM0D,GRAF6,FOSPEC            SY500070
      REAL VR(2300),VY(2300),VB(2300),IB(2300),IR(2300),IY(2300),
+     DIB(2300),DIR(2300),DIY(2300),                SY500080
+     I1(2300),I2(2300),I3(2300),DI1(2300),DI2(2300),DI3(2300),
+     V1(2300),V2(2300),V3(2300),V4(2300),V5(2300),V6(2300),
+     V7(2300),V8(2300),V9(2300),VSA(2300),VSB(2300),VSC(2300),
+     MVRV(2300),MVB(2300),MVBR(2300),              SY500090
+     CVRY(2300),CVYB(2300),CVBR(2300),T(2300),
+     RTZERO(200),YTZERO(200),BTZERO(200),           SY500100
+     CRTZ(200),CYTZ(200),CBTZ(200),
+     VSPEAK,W,DELTA,PI,LLINE,LSYS,LSC,LTOT,RSC,RLINE,RSUM,RTOT,
+     RERROR,YERROR,BERROR,RERSUM,YERSUM,AVSUM,AVFREQ,TUSED,
+     RFREQ,YFREQ,BFREQ,CRFREQ,CYFREQ,CBFREQ,RADERR,DEGERR,LIMIT,
+     DMVRY(2300),DMVYB(2300),DMVBR(2300),DCVRY(2300),DCVYB(2300),
+     DCVBR(2300)                                     SY500110
      REAL TITLA(5),TITLB(5),TITLC(5),TITLD(5),TITLE(5),TITLF(5),
+     TITLG(5),TITLH(5),                              SY500120
+     GINFOB(4),
+     GINFO1(4),GINFO2(8),GINFO3(8),                 SY500130
+     TITL1A(2),TITL2A(2),TITL3A(2),TITL4A(2),TITL5A(2),TITL6A(2),
+     TITL1B(2),TITL2B(2),TITL3B(2),TITL4B(2),TITL5B(2),TITL6B(2),
+     TITL1C(2),TITL2C(2),TITL3C(2),TITL4C(2),TITL5C(2),TITL6C(2),
+     TITL1D(2),TITL2D(2),TITL3D(2),TITL4D(2),TITL5D(2),TITL6D(2),
+     TITL1E(2),TITL2E(2),TITL3E(2),TITL4E(2),TITL5E(2),TITL6E(2),
+     TITL1F(2),TITL2F(2),TITL3F(2),TITL4F(2),TITL5F(2),TITL6F(2),
+     TITL1G(2),TITL2G(2),TITL3G(2),TITL4G(2),TITL5G(2),TITL6G(2),
+     TITL1H(2),TITL2H(2),TITL3H(2),TITL4H(2),TITL5H(2),TITL6H(2),
C     FIRST(1),SECOND(1),THIRD(1),FOURTH(1),FIFTH(1),SIXTH(1),
+     STRNG1(2),STRNG2(2),STRNG3(2),STRNG4(2),STRNG5(2),STRNG6(2)
+     REAL SUM1,SUM2,SUM3,PLIM1,PLIM2,PLIM3,NLIM1,NLIM2,NLIM3,
+     HVSA,HVSB,HVSC,HIR,HIY,HIB,HDIR,HDIY,HDIH,
+     LC,KL1,A1,A2,A3,B1,B2,B3,C1,C2,C3,D1,D2,D3,
+     VLC1(2300),VLC2(2300),VLC3(2300),POSLIM,NEGLIM,
+     ILC1(2300),ILC2(2300),ILC3(2300),
+     DILC1(2300),DILC2(2300),DILC3(2300),
+     ILCR(2300),ILCY(2300),ILCB(2300),
+     DILCR(2300),DILCY(2300),DILCB(2300)
      INTEGER I,J,K,L,M,N,POINTS,CHECK,LOOP,LOOPS,NPERSQ,
+     RKROS(200),YKROS(200),BKROS(200),
+     CRKROS(200),CYKROS(200),CBKROS(200),
+     RCYCLS,YCYCLS,BCYCLS,CRCYCS,CYCYCS,CBCYCS,
+     RZEROS,YZEROS,BZEROS,CRZS,CYZS,CBZS
      INTEGER ICON,ICOFF,K1,K2,K3,QCYC,QUART1,QUART2,QUART3
      LOGICAL PLOT,NOPLOT,LONG,DMOD,NODMOD,LIST,NOLIST,DMOD2,SPEC,SPEC3,
+     CYC10
      LOGICAL NOCOMP,COMPON,INT1P,INT2P,INT3P,INT1N,INT2N,INT3N,
+     ON1,ON2,ON3,NEGI1,NEGI2,NEGI3,POS11,POS12,POS13
      COMMON/COM1/LIST,NOLIST,POINTS/COM2/TSTEP,PI,ROOT2
C
C.....READ THE LINES CONTAINING EXPLANATORY CHARACTERS SY500150
C      AT THE BEGINNING OF THE 'OPTION' DATA FILE . SY500160
C                                                    SY500170
C                                                    SY500180
C      READ(3,800)                                     SY500190
      READ(3,800)                                     SY500200
      READ(3,800)                                     SY500210
C                                                    SY500220
C.....READ THE COMPENSATOR OPTIONS FOR THIS RUN OF THE SY500230
C      PROGRAM:                                        SY500240
C                                                    SY500250
C      LC : VALUE IN HENRIES OF COMPENSATOR            SY500260
C      BRANCH INDUCTANCE SY500270
C      POSLIM : INTEGRATION LIMIT FOR A +'VE HALF CYCLES SY500280
C      NEGLIM : INTEGRATION LIMIT FOR A -'VE HALF CYCLES SY500290
C      ICON : FIRST VALUE OF 'I' FOR COMPENSATOR 'ON' SY500300
C      ICOFF : LAST VALUE OF 'I' FOR COMPENSATOR 'ON' SY500310
C                                                    SY500320
      READ(3,795) LC,POSLIM,NEGLIM,ICON,ICOFF         SY500330
      READ(3,794) GINFO2                               SY500340
      READ(3,794) GINFO3                               SY500350

```

```

C
C.....READ THE LINES CONTAINING EXPLANATORY CHARACTERS
C          AT THE BEGINNING OF THE 'OPTION' DATA FILE .
C
C          READ(4,800)
C          READ(4,800)
C          READ(4,800)
C          READ(4,800)
C
C.....READ OPTIONS FOR THIS RUN OF THE PROGRAM.
C          TSTEP : TIME INTERVAL BETWEEN SUCCESSIVE DATA PTS.
C          LIMIT : ERROR LIMIT FOR EVALUATING DELTA.
C          LOOPS : MAX. NO. OF LOOPS TO TRY FOR 'LIMIT' ABOVE
C          LIST : T/F (T IF FULL LISTING REQUIRED IN O/P)
C          PLOT : T/F (T IF PLOTTING IS REQUIRED)
C          LONG : T/F (T IF LONG CALCOMP PLOTS WILL BE USED)
C          SPEC : T/F (T IF OUTPUT REQUIRED FOR SPECTRAL
C                   ANALYSIS)
C          SPEC3 : T/F (T IF OUTPUT FOR SPECTRAL ANALYSIS OF
C                   3 CHANNELS IS REQUIRED)
C          DMOD : T/F (T IF DEMODULATION IS REQUIRED)
C          DMOD2 : T/F (T FOR SAME SINE WAVE TO BE
C                   SUBTRACTED FROM BOTH MEASURED
C                   AND CALCULATED VOLTAGE WAVEFORMS)
C
C          *** NOTE *** ..... DMOD.AND.DMOD2 IS ILLEGAL
C                   SPEC.AND.SPEC3 = SPEC3
C
C          READ(4,897)TSTEP,LIMIT,LOOPS,LIST,PLOT,LONG,SPEC,SPEC3,DMOD,DMOD2
C
C.....THE OPTIONS USED ARE ALWAYS PRINTED
C
C          WRITE(6,896)TSTEP,LIMIT,LOOPS,LIST,PLOT,LONG,SPEC,SPEC3,DMOD,DMOD2
C          WRITE(6,793) LC,POSLIM,NEGLIM,ICON,ICOFF
C          WRITE(6,792) (GINFO2(I),I=1,8),(GINFO3(I),I=1,8)
C
C.....CHECK FOR ILLEGAL INPUT COMBINATION
C
C          IF(DMOD.AND.DMOD2) GOTO 160
C
C.....USING INVERSE LOGICAL VARIABLES IMPROVES THE
C          'READABILITY' OF THE PROGRAM.
C
C          NOLIST=.NOT.LIST
C          NOPLOT=.NOT.PLOT
C          NODMOD=.NOT.DMOD
C
C.....DEFINE CERTAIN CONSTANTS THAT ARE FREQUENTLY
C          USED IN THE PROGRAM.
C
C          PI=3.1415926536
C          ROOT2=SQRT(2.0)
C          ROOT3=SQRT(3.0)
C
C.....THE SYSTEM PARAMETERS ARE SET HERE WHILE THEY
C          ARE NOT LIKELY TO BE CHANGED.
C
C          ALL VALUES ARE IN OHMS.
C
C          RLINE=0.00218
C          XLINE=0.01089
C          XSYS=0.1307
C          XSC=2.595
C          RSC=0.0565
C          RTOT=RSC+RLINE
C          QCYC=7
C          VSPEAK=33.0*ROOT2
C
C....CERTAIN VARIABLES ARE SET HERE TEMPORARILY INSTEAD OF BEING READ
C          FROM THE OPTIONS FILE
C
C          NOCOMP=.FALSE.
C          PLIM1=POSLIM
C          PLIM2=POSLIM
C          PLIM3=POSLIM
C          NLIM1=NEGLIM
C          NLIM2=NEGLIM
C          NLIM3=NEGLIM

```

```

SYS00750
SYS00760
SYS00770
SYS00780
SYS00790
SYS00800
SYS00810
SYS00820
SYS00830
SYS00840
SYS00850
SYS00860
SYS00870
SYS00880
SYS00890
SYS00900
SYS00910
SYS00920
SYS00930
SYS00940
SYS00950
SYS00960
SYS00970
SYS00980
SYS00990
SYS01000
SYS01010
SYS01020
SYS01030
SYS01040
SYS01050
SYS01060
SYS01070
SYS01080
SYS01090
SYS01100
SYS01110
SYS01120
SYS01130
SYS01140
SYS01150
SYS01160
SYS01170
SYS01180
SYS01190
SYS01200
SYS01210
SYS01220
SYS01230
SYS01240
SYS01250
SYS01260
SYS01270
SYS01280
SYS01290
SYS01300
SYS01310
SYS01320
SYS01330
SYS01340
SYS01350
SYS01360
SYS01370
SYS01380
SYS01390
SYS01400
SYS01410
SYS01420
SYS01430
SYS01440
SYS01450
SYS01460
SYS01470
SYS01480
SYS01490
SYS01500
SYS01510
SYS01520
SYS01530

```

```
C
C.....THE FOLLOWING ALPHANUMERIC STRINGS ARE USED
C          TO IDENTIFY PRINTED OUTPUT PRODUCED FROM SEVERAL
C          CALLS TO THE SAME SECTION
C
C DATA FIRST/' FIRST '/
C DATA SECOND/' SECOND '/
C DATA THIRD/' THIRD '/
C DATA FOURTH/' FOURTH '/
C DATA FIFTH/' FIFTH '/
C DATA SIXTH/' SIXTH '/
C
C.....'GINFO' ALPHANUMERIC INFORMATION IS FOR
C          INCLUSION IN PLOTTED OUTPUT.
C
C DATA GINFOB/'
C DATA GINFO1/'*** COM','MON DEM','ODULATIO','N *** '/
C
C.....'STRNG' ALPHANUMERIC DATA IS COMMON TO
C          SEVERAL PLOTTING SUBROUTINES
C
C DATA STRNG1/' MEASUR','ED VR '/
C DATA STRNG2/' MEASUR','ED VY '/
C DATA STRNG3/' MEASUR','ED VB '/
C DATA STRNG4/' CALCULA','TED VR '/
C DATA STRNG5/' CALCULA','TED VY '/
C DATA STRNG6/' CALCULA','TED VB '/
C
C.....SKIP THE FIRST LINE OF THE DATA FILE
C          (DESCRIPTIVE TEXT)
C
C READ(5,800)
C
C.....THE FOLLOWING LOOP FOR 'I' READS DATA
C          UNTIL A BLANK LINE IS ENCOUNTERED
C
C I=0
C 20 I=I+1
C READ(5,999) VR(I),VY(I),VB(I),IB(I),IR(I),IY(I),DIB(I),
C +DIR(I),DIY(I)
C T(I)=FLOAT(I)*TSTEP
C IF(I.LT.5)WRITE(6,998)VR(I),VY(I),VB(I),IB(I),IR(I),IY(I),
C +DIB(I),DIR(I),DIY(I)
C MVR(I)=VR(I)-VY(I)
C MVYB(I)=VY(I)-VB(I)
C MVRB(I)=VB(I)-VR(I)
C IF(VR(I).NE.0.0.OR.VY(I).NE.0.0) GOTO 20
C POINTS=I-1
C CYC10=.TRUE.
C IF(POINTS.GE.300) CYC10=.FALSE.
C
C.....'POINTS' IS THE NUMBER OF LINES OF INPUT DATA.
C
C WRITE(6,992)POINTS
C
C.....INITIALISE WHERE NECESSARY
C
C RERROR=0.0
C RERSUM=0.0
C YERROR=0.0
C YERSUM=0.0
C BERROR=0.0
C BERSUM=0.0
C AVSUM=0.0
C AVFREQ=0.0
C DEGERR=0.0
C RADEERR=0.0
C DO 40 I=1,POINTS,1
C   VLC1(I)=0.0
C   VLC2(I)=0.0
C   VLC3(I)=0.0
C   DILC1(I)=0.0
C   DILC2(I)=0.0
C   DILC3(I)=0.0
C 40 CONTINUE
C
```

```
SYS01540
SYS01550
SYS01560
SYS01570
SYS01580
SYS01590
SYS01600
SYS01610
SYS01620
SYS01630
SYS01640
SYS01650
SYS01660
SYS01670
SYS01680
SYS01690
SYS01700
SYS01710
SYS01720
SYS01730
SYS01740
SYS01750
SYS01760
SYS01770
SYS01780
SYS01790
SYS01800
SYS01810
SYS01820
SYS01830
SYS01840
SYS01850
SYS01860
SYS01870
SYS01880
SYS01890
SYS01900
SYS01910
SYS01920
SYS01930
SYS01940
SYS01950
SYS01960
SYS01970
SYS01980
SYS01990
SYS02000
SYS02010
SYS02020
SYS02030
SYS02040
SYS02050
SYS02060
SYS02070
SYS02080
SYS02090
SYS02100
SYS02110
SYS02120
SYS02130
SYS02140
SYS02150
SYS02160
SYS02170
SYS02180
SYS02190
SYS02200
SYS02210
SYS02220
SYS02230
SYS02240
SYS02250
SYS02260
SYS02270
SYS02280
```



```

CALL VZEROS (POINTS,MVRY,T,RTZERO,RZEROS,RCYCLS,RFREQ,RKROS,VRRMS, SYS02290
+CHECK,STRNG1) SYS02300
IF(CHECK.EQ.0) WRITE(6,997) SYS02310
CALL VZEROS (POINTS,MVYB,T,YTZERO,YZEROS,ICYCLS,YFREQ,YKROS,VYRMS, SYS02320
+CHECK,STRNG2) SYS02330
IF(CHECK.EQ.0) WRITE(6,996) SYS02340
CALL VZEROS (POINTS,MVBR,T,BTZERO,BZEROS,BCYCLS,BFREQ,BKROS,VBRMS, SYS02350
+CHECK,STRNG3) SYS02360
IF(CHECK.EQ.0) WRITE(6,995) SYS02370
WRITE(6,993) RZEROS,YZEROS,BZEROS,RCYCLS,ICYCLS,BCYCLS, SYS02380
+ RFREQ,YFREQ,BFREQ SYS02390
RSUM=RLINE+RSC SYS02400
W=2.0*PI*RFREQ SYS02410
DELTA=-0.2 SYS02420
LOOP=0 SYS02430
50 LOOP=LOOP+1 SYS02440
IF(LOOP.GT.LOOPS)GOTO 140 SYS02450
IF(CYC10) DELTA=DELTA-1.0*RADERR SYS02460
IF(.NOT.CYC10) DELTA=DELTA-0.1*RADERR SYS02470
RERSUM=0.0 SYS02480
YERSUM=0.0 SYS02490
BERSUM=0.0 SYS02500
60 CONTINUE SYS02510
LLINE=XLINE/W SYS02520
LSYS=XSYS/W SYS02530
LSC=XSC/W SYS02540
LTOT=LSYS+LSC+LLINE SYS02550
KL1 = 1.0/(LC*(3.0*LTOT+LC)) SYS02560
DO 100 I=1,POINTS,1 SYS02570
C SYS02580
C.....EVALUATE PRIMARY CIRCUIT LINE CURRENTS SYS02590
C FROM SECONDARY CIRCUIT LINE CURRENTS SYS02600
C (CURRENT TRANSFORMATION) SYS02610
C SYS02620
C SYS02630
I1(I)=(IB(I)-IR(I))/ROOT3 SYS02640
I2(I)=(IR(I)-IY(I))/ROOT3 SYS02650
I3(I)=(IB(I)-IB(I))/ROOT3 SYS02660
C SYS02670
C.....SIMILARLY FOR CURRENT FIRST DERIVATIVES SYS02680
C (CURRENT TRANSFORMATION) SYS02690
C SYS02700
C SYS02710
DI1(I)=(DIB(I)-DIR(I))/ROOT3 SYS02720
DI2(I)=(DIR(I)-DIY(I))/ROOT3 SYS02730
DI3(I)=(DIY(I)-DIB(I))/ROOT3 SYS02740
80 CONTINUE SYS02750
C SYS02760
C.....SET-UP SYSTEM VOLTAGES, SYS02770
C THREE PHASE SINUSOIDAL ADVANCED BY PHASE ANGLE SYS02780
C 'DELTA' WITH RESPECT TO VOLTAGES AT THE SYS02790
C FURNACE BUSBAR (V7,V8,V9) SYS02800
C SYS02810
VSA(I)=VSPEAK*COS(W*T(I)+DELTA) SYS02820
VSB(I)=VSPEAK*COS(W*T(I)-2.0*PI/3.0+DELTA) SYS02830
VSC(I)=VSPEAK*COS(W*T(I)+2.0*PI/3.0+DELTA) SYS02840
C SYS02850
C.....CALCULATE TRANSFORMER PRIMARY VOLTAGES SYS02860
C USING VOLT-DROPS. SYS02870
C SYS02880
V1(I)=VSA(I) - RSC*(I1(I)-I2(I)) - (LSYS+LSC)*(DI1(I)-DI2(I)) SYS02890
V2(I)=VSB(I) - RSC*(I2(I)-I3(I)) - (LSYS+LSC)*(DI2(I)-DI3(I)) SYS02900
V3(I)=VSC(I) - RSC*(I3(I)-I1(I)) - (LSYS+LSC)*(DI3(I)-DI1(I)) SYS02910
C SYS02920
C.....PRIMARY TO SECONDARY SYS02930
C VOLTAGE TRANSFORMATION SYS02940
C SYS02950
V4(I)=(V1(I)-V2(I))/ROOT3 SYS02960
V5(I)=(V2(I)-V3(I))/ROOT3 SYS02970
V6(I)=(V3(I)-V1(I))/ROOT3 SYS02980
C SYS02990
C.....ALLOW FOR CABLE VOLT-DROP SYS03000
C SYS03010
V7(I)=V4(I) - RLINE*(IR(I)-IY(I)) - LLINE*(DIR(I)-DIY(I)) SYS03020
V8(I)=V5(I) - RLINE*(IY(I)-IB(I)) - LLINE*(DIY(I)-DIB(I)) SYS03030
V9(I)=V6(I) - RLINE*(IB(I)-IR(I)) - LLINE*(DIB(I)-DIR(I)) SYS03040
CVRY(I)=V7(I) SYS03050
CVYB(I)=V8(I) SYS03060
CVBR(I)=V9(I) SYS03070
IF(LOOP.NE.LOOPS)GOTO 90 SYS03080
IF(LIST) WRITE(6,994)VR(I),VY(I),VB(I), SYS03090
+ CVRY(I),CVYB(I),CVBR(I) SYS03100
90 CONTINUE SYS03110
100 CONTINUE SYS03120

```

```

IF(.NOT.LIST) GOTO 101
WRITE(6,892)
DO 101 I=1,15,1
WRITE(6,893) VR(I),VY(I),VB(I),
+           IR(I),IY(I),IB(I),
+           CVRY(I),CVYB(I),CVBR(I)
101 CONTINUE
C
C.....USE VZEROS SUBROUTINE TO GET DETAILS OF
C           ZERO CROSSING POINTS OF CALCULATED VOLTAGES
C
CALL VZEROS(POINTS,CVRY,T,CRTZ,CRZS,CRCYCS,CRFREQ,CRKROS,CVRRMS,
+CHECK,STRNG4)
CALL VZEROS(POINTS,CVYB,T,CYTZ,CYZS,CYCYCS,CYFREQ,CYKROS,CVYRMS,
+CHECK,STRNG5)
CALL VZEROS(POINTS,CVBR,T,CBTZ,CBZS,CBCYCS,CBFREQ,CBKROS,CVBRMS,
+CHECK,STRNG6)
IF(.NOT.LIST) GOTO 118
WRITE(6,991)
WRITE(6,990) (J,RKROS(J),YKROS(J),BKROS(J),
+           CRKROS(J),CYKROS(J),CBKROS(J),J=1,YZEROS,1)
WRITE(6,891)
118 CONTINUE
C
C.....CALCULATE A SUM OF DIFFERENCES BETWEEN THE
C           ZERO CROSSING POINTS OF
C           MEASURED AND CALCULATED VOLTAGES.
C
DO 120 J=1,YZEROS,1
RERROR=RTZERO(J)-CRTZ(J)
YERROR=YTZERO(J)-CYTZ(J)
BERROR=BTZERO(J)-CBTZ(J)
IF(LIST) WRITE(6,890) J,RTZERO(J),CRTZ(J),YTZERO(J),CYTZ(J),
+           BTZERO(J),CBTZ(J)
RERSUM=RERSUM+RERROR
YERSUM=YERSUM+YERROR
BERSUM=BERSUM+BERROR
120 CONTINUE
AVSUM=(RERSUM+YERSUM+BERSUM)/(3.0*YZEROS)
AVFREQ=(RFREQ+YFREQ+BFREQ)/3.0
C
C.....CALCULATE AN AVERAGE PHASE ERROR BETWEEN
C           MEASURED AND CALCULATED VOLTAGES AND RETURN
C           TO ADJUST 'DELTA' IF THE ERROR IS OUTSIDE
C           THE PRESET LIMIT.
C
DEGERR=AVSUM*AVFREQ*360.0
RADERR=1.0*PI*DEGERR/180.0
WRITE(6,895) LOOP,DELTA,RADERR,AVSUM
IF(RADERR.GT.LIMIT.OR.RADERR.LT.-LIMIT)GOTO 50
C
C.....PRINT THE FIRST 25 VALUES OF EACH ARRAY
C           TO AID FAULT FINDING
C
WRITE(6,699)
WRITE(6,666) (I1(I),I2(I),I3(I), I=1,25,1)
WRITE(6,698)
WRITE(6,666) (DI1(I),DI2(I),DI3(I), I=1,25,1)
WRITE(6,697)
WRITE(6,666) (VSA(I),VSB(I),VSC(I), I=1,25,1)
WRITE(6,696)
WRITE(6,666) (V1(I),V2(I),V3(I), I=1,25,1)
WRITE(6,695)
WRITE(6,666) (V4(I),V5(I),V6(I), I=1,25,1)
699 FORMAT(///32H FIRST 25 PRIMARY LINE CURRENTS:/)
698 FORMAT(///32H FIRST 25 PRIMARY DI/DT'S :/)
697 FORMAT(///32H FIRST 25 SYSTEM LINE VOLTAGES :/)
696 FORMAT(///32H FIRST 25 PRIMARY LINE VOLTAGES:/)
695 FORMAT(///32H FIRST 25 SECONDARY LINE VOLTS :/)
666 FORMAT(3(F12.4,5X))
SYS03130
SYS03140
SYS03150
SYS03160
SYS03170
SYS03180
SYS03190
SYS03200
SYS03210
SYS03220
SYS03230
SYS03240
SYS03250
SYS03260
SYS03270
SYS03280
SYS03290
SYS03300
SYS03310
SYS03320
SYS03330
SYS03340
SYS03350
SYS03360
SYS03370
SYS03380
SYS03390
SYS03400
SYS03410
SYS03420
SYS03430
SYS03440
SYS03450
SYS03460
SYS03470
SYS03480
SYS03490
SYS03500
SYS03510
SYS03520
SYS03530
SYS03540
SYS03550
SYS03560
SYS03570
SYS03580
SYS03590
SYS03600
SYS03610
SYS03620
SYS03630
SYS03640
SYS03650
SYS03660
SYS03670
SYS03680
SYS03690
SYS03700
SYS03710
SYS03720
SYS03730
SYS03740
SYS03750
SYS03760
SYS03770
SYS03780
SYS03790
SYS03800
SYS03810
SYS03820

```

```
CCCCCCCCCCCCCCCCCCCCCCCCCCCCCCCCCCCCCCCCCCCCCCCCCCCCCCCCCCCCCCCCCCCCCCCCCCCCCCCCCCCCCSYS03830
C                                                                                                   CSYS03840
C                                                                                                   CSYS03850
C                                                                                                   CSYS03860
C                                                                                                   CSYS03870
C.....A REPRESENTATION OF A DELTA-CONNECTED COMPENSATOR  CSYS03880
C                    FOLLOWS FROM THIS POINT.             CSYS03890
C                                                                                                   CSYS03900
C                                                                                                   CSYS03910
C                                                                                                   CSYS03920
CCCCCCCCCCCCCCCCCCCCCCCCCCCCCCCCCCCCCCCCCCCCCCCCCCCCCCCCCCCCCCCCCCCCCCCCCCCCCCCCCCCCCSYS03930
C                    I=0                                   SYS03940
C                    IF(NOCOMP) GOTO 520                 SYS03950
200 I=I+1                                                SYS03960
C                    IF(I.LT.ICON) GOTO 200             SYS03970
C                    COMON=.FALSE.                    SYS03980
C                                                                                                   SYS03990
C.....FOR THE FIRST VALUE OF 'I' FOR WHICH THE COMPENSATOR SYS04000
C                    IS 'ON' , VALUES OF V7, V8, V9 ARE USED  SYS04010
C                    AS THE VOLTAGE ACROSS EACH BRANCH OF THE COMPENSATOR SYS04020
C                                                                                                   SYS04030
C                                                                                                   SYS04040
C                    VLC1(I-1)=V7(I-1)                SYS04050
C                    VLC2(I-1)=V8(I-1)                SYS04060
C                    VLC3(I-1)=V9(I-1)                SYS04070
C                    VLC1(I)=V7(I)                    SYS04080
C                    VLC2(I)=V8(I)                    SYS04090
C                    VLC3(I)=V9(I)                    SYS04100
210 CONTINUE                                           SYS04110
C                    WRITE(6,212) I                    SYS04120
212 FORMAT(/5H I =,I3)                                  SYS04130
C                                                                                                   SYS04140
C.....IF COMON IS .FALSE. NO FURTHER INTEGRATION OR      SYS04150
C                    SWITCHING ON CAN TAKE PLACE BUT CURRENT IN CONDUCTING  SYS04160
C                    BRANCHES IS ALLOWED TO FLOW UNTIL A CURRENT ZERO  SYS04170
C                                                                                                   SYS04180
C                    IF(.NOT.COMON) GOTO 310           SYS04190
C                                                                                                   SYS04200
C.....FOR INCREMENT OF 'I' FLAGS ARE SET SHOWING WHAT STAGE  SYS04210
C                    CALCULATIONS ARE AT FOR EACH BRANCH OF THE COMPENSATOR SYS04220
C                                                                                                   SYS04230
C                    'INT1P' TRUE MEANS INTEGRATION FOR RED BRANCH IN POS.  SYS04240
C                    'INT1N' TRUE MEANS INTEGRATION FOR RED BRANCH IN NEG.  SYS04250
C                    --- - - - - HALF CYCLES           SYS04260
C                                                                                                   SYS04270
C                    'SUM1' WILL CONTAIN THE CUMULATIVE INTEGRATION VALUE  SYS04280
C                                                                                                   SYS04290
C                                                                                                   SYS04300
C                                                                                                   SYS04310
C                    IF(INT1P.OR.INT1N) GOTO 230       SYS04320
C                    IF(VLC1(I).GT.0.0.AND.VLC1(I-1).LE.0.0) GOTO 215     SYS04330
C                    INT1P=.FALSE.                    SYS04340
C                    GOTO 220                          SYS04350
215 INT1P=.TRUE.                                       SYS04360
C                    SUM1=0.0                          SYS04370
C                    QUART1=0                          SYS04380
220 IF(VLC1(I).LT.0.0.AND.VLC1(I-1).GE.0.0) GOTO 225 SYS04390
C                    INT1N=.FALSE.                    SYS04400
C                    GOTO 230                          SYS04410
225 INT1N=.TRUE.                                       SYS04420
C                    SUM1=0.0                          SYS04430
C                    QUART1=0                          SYS04440
C                                                                                                   SYS04450
C.....SIMILARLY FOR YELLOW BRANCH                      SYS04460
C                                                                                                   SYS04470
230 IF(INT2P.OR.INT2N) GOTO 250                        SYS04480
C                    IF(VLC2(I).GT.0.0.AND.VLC2(I-1).LE.0.0) GOTO 235     SYS04490
C                    INT2P=.FALSE.                    SYS04500
C                    GOTO 240                          SYS04510
235 INT2P=.TRUE.                                       SYS04520
C                    SUM2=0.0                          SYS04530
C                    QUART2=0                          SYS04540
240 IF(VLC2(I).LT.0.0.AND.VLC2(I-1).GE.0.0) GOTO 245 SYS04550
C                    INT2N=.FALSE.                    SYS04560
C                    GOTO 250                          SYS04570
245 INT2N=.TRUE.                                       SYS04580
C                    SUM2=0.0                          SYS04590
C                    QUART2=0                          SYS04600
```

C		SYS04610
C.....	SIMILARLY FOR BLUE BRANCH	SYS04620
C		SYS04630
250	IF(INT3P.OR.INT3N) GOTO 270	SYS04640
	IF(VLC3(I).GT.0.0.AND.VLC3(I-1).LE.0.0) GOTO 255	SYS04650
	INT3P=.FALSE.	SYS04660
	GOTO 260	SYS04670
255	INT3P=.TRUE.	SYS04680
	SUM3=0.0	SYS04690
	QUART3=0	SYS04700
260	IF(VLC3(I).LT.0.0.AND.VLC3(I-1).GE.0.0) GOTO 265	SYS04710
	INT3N=.FALSE.	SYS04720
	GOTO 270	SYS04730
265	INT3N=.TRUE.	SYS04740
	SUM3=0.0	SYS04750
	QUART3=0	SYS04760
270	CONTINUE	SYS04770
	WRITE(6,796) ON1,ON2,ON3,POS11,POS12,POS13,INT1N,INT2N,INT3N,	SYS04780
	+NEGI1,NEGI2,NEGI3,INT1P,INT2P,INT3P	SYS04790
C		SYS04800
C.....	CHECK FOR ATTEMPTED POS. & NEG. INTEGRATION	SYS04810
C		SYS04820
	IF(INT1P.AND.INT1N) GOTO 150	SYS04830
	IF(INT2P.AND.INT2N) GOTO 150	SYS04840
	IF(INT3P.AND.INT3N) GOTO 150	SYS04850
C		SYS04860
C.....	INTEGRATION CAN ONLY PROCEED IF THE SIGN OF THE	SYS04870
C	MEASURED POINTS REMAINS IN THE CORRECT SENSE	SYS04880
C	(CHECKING FOR END OF HALF CYCLE)	SYS04890
C	OTHERWISE THE INTEGRATION IS ABANDONED	SYS04900
C		SYS04910
C.....	FOR RED BRANCH	SYS04920
C		SYS04930
C		SYS04940
	IF(INT1P) GOTO 271	SYS04950
	IF(INT1N) GOTO 272	SYS04960
	GOTO 274	SYS04970
271	IF(VLC1(I).GT.0.0) GOTO 273	SYS04980
	INT1P=.FALSE.	SYS04990
	SUM1=0.0	SYS05000
	QUART1=0	SYS05010
	GOTO 275	SYS05020
272	IF(VLC1(I).LT.0.0) GOTO 273	SYS05030
	INT1N=.FALSE.	SYS05040
	SUM1=0.0	SYS05050
	QUART1=0	SYS05060
	GOTO 274	SYS05070
273	CONTINUE	SYS05080
	SUM1=SUM1+VLC1(I)	SYS05090
	QUART1=QUART1+1	SYS05100
274	CONTINUE	SYS05110
C		SYS05120
C.....	FOR YELLOW BRANCH	SYS05130
C		SYS05140
	IF(INT2P) GOTO 275	SYS05150
	IF(INT2N) GOTO 276	SYS05160
	GOTO 278	SYS05170
275	IF(VLC2(I).GT.0.0) GOTO 277	SYS05180
	INT2P=.FALSE.	SYS05190
	SUM2=0.0	SYS05200
	QUART2=0	SYS05210
	GOTO 278	SYS05220
276	IF(VLC2(I).LT.0.0) GOTO 277	SYS05230
	INT2N=.FALSE.	SYS05240
	SUM2=0.0	SYS05250
	QUART2=0	SYS05260
	GOTO 278	SYS05270
277	CONTINUE	SYS05280
	SUM2=SUM2+VLC2(I)	SYS05290
	QUART2=QUART2+1	SYS05300
278	CONTINUE	SYS05310

C		SYS05320
CFOR BLUE BRANCH	SYS05330
C		SYS05340
	IF(INT3P) GOTO 279	SYS05350
	IF(INT3N) GOTO 280	SYS05360
	GOTO 282	SYS05370
279	IF(VLC3(I).GT.0.0) GOTO 281	SYS05380
	INT3P=.FALSE.	SYS05390
	SUM3=0.0	SYS05400
	QUART3=0	SYS05410
	GOTO 282	SYS05420
280	IF(VLC3(I).LT.0.0) GOTO 281	SYS05430
	INT3N=.FALSE.	SYS05440
	SUM3=0.0	SYS05450
	QUART3=0	SYS05460
	GOTO 282	SYS05470
281	CONTINUE	SYS05480
	SUM3=SUM3+VLC3(I)	SYS05490
	QUART3=QUART3+1	SYS05500
282	CONTINUE	SYS05510
C		SYS05520
	WRITE(6,797) SUM1,SUM2,SUM3,QUART1,QUART2,QUART3	SYS05530
C		SYS05540
CSET FURTHER FLAGS IF THE INTEGRATION LIMITS ARE REACHED	SYS05550
C	(UNLESS THE INTEGRATION LIMITS ARE SO SMALL THAT	SYS05560
C	CONDUCTION WOULD START BEFORE THE 1/4 CYCLE POINT)	SYS05570
C		SYS05580
C	'POS11' INDICATES ALLOWANCE OF CURRENT FLOW IN RED	SYS05590
C	BRANCH OF COMPENSATOR AS RESULT OF INTEGRATIONS	SYS05600
C	IN POSITIVE HALF-CYCLE OF 'VLCR'.	SYS05610
C		SYS05620
C	'ON1' RED BRANCH ON	SYS05630
C		SYS05640
C		SYS05650
	IF(QUART1.LT.QCYC) GOTO 285	SYS05660
	IF(SUM1.LT.PLIM1) GOTO 284	SYS05670
	IF(NEG11) GOTO 285	SYS05680
	ON1=.TRUE.	SYS05690
	POS11=.TRUE.	SYS05700
	INT1P=.FALSE.	SYS05710
	SUM1=0.0	SYS05720
	QUART1=0	SYS05730
284	IF(SUM1.GT.NLIM1) GOTO 285	SYS05740
	IF(POS11) GOTO 285	SYS05750
	ON1=.TRUE.	SYS05760
	NEG11=.TRUE.	SYS05770
	INT1N=.FALSE.	SYS05780
	SUM1=0.0	SYS05790
	QUART1=0	SYS05800
C		SYS05810
CSIMILARLY FOR YELLOW BRANCH	SYS05820
C		SYS05830
285	IF(QUART2.LT.QCYC) GOTO 295	SYS05840
	IF(SUM2.LT.PLIM2) GOTO 290	SYS05850
	IF(NEG12) GOTO 295	SYS05860
	ON2=.TRUE.	SYS05870
	POS12=.TRUE.	SYS05880
	INT2P=.FALSE.	SYS05890
	SUM2=0.0	SYS05900
	QUART2=0	SYS05910
290	IF(SUM2.GT.NLIM2) GOTO 295	SYS05920
	IF(POS12) GOTO 295	SYS05930
	ON2=.TRUE.	SYS05940
	NEG12=.TRUE.	SYS05950
	INT2N=.FALSE.	SYS05960
	SUM2=0.0	SYS05970
	QUART2=0	SYS05980
C		SYS05990
CSIMILARLY FOR BLUE BRANCH	SYS06000
C		SYS06010
295	IF(QUART3.LT.QCYC) GOTO 305	SYS06020
	IF(SUM3.LT.PLIM3) GOTO 300	SYS06030
	IF(NEG13) GOTO 305	SYS06040
	ON3=.TRUE.	SYS06050
	POS13=.TRUE.	SYS06060
	INT3P=.FALSE.	SYS06070
	SUM3=0.0	SYS06080
	QUART3=0	SYS06090
300	IF(SUM3.GT.NLIM3) GOTO 305	SYS06100

```

IF(POS13) GOTO 305
ON3=.TRUE.
NEGI3=.TRUE.
INT3N=.FALSE.
SUM3=0.0
QUART3=0
305 CONTINUE
WRITE(6,796) ON1,ON2,ON3,POS11,POS12,POS13,INT1N,INT2N,INT3N,
+NEGI1,NEGI2,NEGI3,INT1P,INT2P,INT3P
IF(POS11.AND.NEGI1) GOTO 150
IF(POS12.AND.NEGI2) GOTO 150
IF(POS13.AND.NEGI3) GOTO 150
310 CONTINUE
C
C.....CALCULATE THE 'HALF STEP' VALUES NEEDED FOR
C THE RUNGE-KUTTA PROCESS
C
C SIMPLE LINEAR INTERPOLATION IS USED
C
C.....SYSTEM VOLTAGE
C
HVSA= VSA(I) + ((VSA(I+1) + VSA(I))/2.0)
HVSB= VSB(I) + ((VSB(I+1) + VSB(I))/2.0)
HVSC= VSC(I) + ((VSC(I+1) + VSC(I))/2.0)
C
C.....PER-UNIT FURNACE CURRENT
C
HIR= IR(I) + ((IR(I+1) + IR(I))/2.0)
HIY= IY(I) + ((IY(I+1) + IY(I))/2.0)
HIB= IB(I) + ((IB(I+1) + IB(I))/2.0)
C
C.....PER-UNIT FURNACE CURRENT GRADIENT
C
HDIR= DIR(I) + ((DIR(I+1) + DIR(I))/2.0)
HDIY= DIY(I) + ((DIY(I+1) + DIY(I))/2.0)
HDIB= DIB(I) + ((DIB(I+1) + DIB(I))/2.0)
C
C.....SET ZERO VALUES FOR RED BRANCH CURRENT ILC1
C & RED BRANCH DI/DT DILC1
C IF THE BRANCH IS 'OFF' OR IF THIS IS THE FIRST STEP
C FOR THE 'ON' COMPENSATOR.
C
IF(ON1) GOTO 315
DILC1(I)=0.0
ILC1(I)=0.0
GOTO 320
315 K1=K1+1
IF(K1.EQ.1) ILC1(I)=0.0
320 CONTINUE
C
C.....SIMILARLY FOR YELLOW
C
IF(ON2) GOTO 325
DILC2(I)=0.0
ILC2(I)=0.0
GOTO 330
325 K2=K2+1
IF(K2.EQ.1) ILC2(I)=0.0
C WRITE(6,895)
C WRITE(6,777) LC,I,VLC2(I),DILC2(I),ILC2(I)
C 777 FORMAT(5H LC=,F8.6,9H & FOR I=,I3,6H VLCY=,F8.5,7H DILC2=,F8.5,
C +6H ILC2=,F8.5)
330 CONTINUE
C
C.....SIMILARLY FOR BLUE
C
IF(ON3) GOTO 335
DILC3(I)=0.0
ILC3(I)=0.0
GOTO 340
335 K3=K3+1
IF(K3.EQ.1) ILC3(I)=0.0
340 CONTINUE

```

```

SYS06110
SYS06120
SYS06130
SYS06140
SYS06150
SYS06160
SYS06170
SYS06180
SYS06190
SYS06200
SYS06210
SYS06220
SYS06230
SYS06240
SYS06250
SYS06260
SYS06270
SYS06280
SYS06290
SYS06300
SYS06310
SYS06320
SYS06330
SYS06340
SYS06350
SYS06360
SYS06370
SYS06380
SYS06390
SYS06400
SYS06410
SYS06420
SYS06430
SYS06440
SYS06450
SYS06460
SYS06470
SYS06480
SYS06490
SYS06500
SYS06510
SYS06520
SYS06530
SYS06540
SYS06550
SYS06560
SYS06570
SYS06580
SYS06590
SYS06600
SYS06610
SYS06620
SYS06630
SYS06640
SYS06650
SYS06660
SYS06670
SYS06680
SYS06690
SYS06700
SYS06710
SYS06720
SYS06730
SYS06740
SYS06750
SYS06760
SYS06770
SYS06780
SYS06790
SYS06800
SYS06810
SYS06820
SYS06830
SYS06840

```

```

C
C.....CALCULATE VALUE FOR COMPENSATOR DI/DT IF THIS IS
C          THE FIRST STEP FOR CURRENT CONDUCTION
C
C.....FOR BRANCH ONE
C
  IF(.NOT.ON1) GOTO 341
  DILC1(I)= KL1*(VSA(I)
+ - RTOT*(IR(I)-IY(I)+2.0*ILC1(I)-ILC2(I)-ILC3(I))
+ - LTOT*(DIR(I)-DIY(I)))
341 CONTINUE
C
C.....FOR BRANCH TWO
C
  IF(.NOT.ON2) GOTO 342
  DILC2(I)= KL1*(VSB(I)
+ - RTOT*(IY(I)-IB(I)-ILC1(I)+2.0*ILC2(I)-ILC3(I))
+ - LTOT*(DIY(I)-DIB(I)))
342 CONTINUE
C
C.....FOR BRANCH THREE
C
  IF(.NOT.ON3) GOTO 343
  DILC3(I)= KL1*(VSC(I)
+ - RTOT*(IB(I)-IR(I)-ILC1(I)-ILC2(I)+2.0*ILC3(I))
+ - LTOT*(DIB(I)-DIR(I)))
343 CONTINUE
C
C.....CALCULATE VALUES FOR V7,V8 & V9 SINCE DILC1,2,3
C          & ILC1,2,3 ARE NOW KNOWN FOR THIS VALUE OF 'I'
C
C
  IF(I.EQ.ICON) GOTO 345
  VLC1(I) = VSA(I)-RTOT*(IR(I)-IY(I)
+           + 2.0* ILC1(I) - ILC2(I) - ILC3(I))
+           -LTOT*(DIR(I)-DIY(I)
+           + 2.0*DILC1(I) - DILC2(I) - DILC3(I))
C
C
  VLC2(I) = VSB(I)-RTOT*(IY(I)-IB(I)
+           - ILC1(I) + 2.0* ILC2(I) - ILC3(I))
+           -LTOT*(DIY(I)-DIB(I)
+           - DILC1(I) + 2.0*DILC2(I) - DILC3(I))
C
C
  VLC3(I) = VSC(I)-RTOT*(IB(I)-IR(I)
+           - ILC1(I) - ILC2(I) + 2.0* ILC3(I))
+           -LTOT*(DIB(I)-DIR(I)
+           - DILC1(I) - DILC2(I) + 2.0*DILC3(I))
C
C
C.....CALCULATE THE CONSTANT A,B,C,D FOR THE RUNGE-KUTTA
C          PROCESS WHICH CALCULATES ILC FROM D ILC/DT.
C
C          FIRST SET CALCULATED VARIABLES TO ZERO
C
345 CONTINUE
  A1=0.0
  A2=0.0
  A3=0.0
  B1=0.0
  B2=0.0
  B3=0.0
  C1=0.0
  C2=0.0
  C3=0.0
  D1=0.0
  D2=0.0
  D3=0.0

```

```

SYS06850
SYS06860
SYS06870
SYS06880
SYS06890
SYS06900
SYS06910
SYS06920
SYS06930
SYS06940
SYS06950
SYS06960
SYS06970
SYS06980
SYS06990
SYS07000
SYS07010
SYS07020
SYS07030
SYS07040
SYS07050
SYS07060
SYS07070
SYS07080
SYS07090
SYS07100
SYS07110
SYS07120
SYS07130
SYS07140
SYS07150
SYS07160
SYS07170
SYS07180
SYS07190
SYS07200
SYS07210
SYS07220
SYS07230
SYS07240
SYS07250
SYS07260
SYS07270
SYS07280
SYS07290
SYS07300
SYS07310
SYS07320
SYS07330
SYS07340
SYS07350
SYS07360
SYS07370
SYS07380
SYS07390
SYS07400
SYS07410
SYS07420
SYS07430
SYS07440
SYS07450
SYS07460
SYS07470
SYS07480
SYS07490
SYS07500
SYS07510
SYS07520
SYS07530
SYS07540
SYS07550
SYS07560
SYS07570

```

```

A1= TSTEP* DILC1(I)
A2= TSTEP* DILC2(I)
A3= TSTEP* DILC3(I)
C
  IF(.NOT.ON1) GOTO 350
  B1 = TSTEP* KL1*(HVSA
+      -RTOT*(HIR-HIY
+  +2.0*(ILC1(I)+A1/2.0) - (ILC2(I)+A2/2.0) - (ILC3(I)+A3/3.0))
+      -LTOT*(HDIR-HDIY))
  GOTO 355
350 B1 = 0.0
355 CONTINUE
C
  IF(.NOT.ON2) GOTO 360
  B2 = TSTEP* KL1*(HVSB
+      -RTOT*(HIY-HIB
+  -(ILC1(I)+A1/2.0) +2.0*(ILC2(I)+A2/2.0) - (ILC3(I)+A3/3.0))
+      -LTOT*(HDIY-HDIB))
  GOTO 365
360 B2 = 0.0
365 CONTINUE
C
  IF(.NOT.ON3) GOTO 370
  B3 = TSTEP* KL1*(HVSC
+      -RTOT*(HIB-HIR
+  -(ILC1(I)+A1/2.0) - (ILC2(I)+A2/2.0) +2.0*(ILC3(I)+A3/3.0))
+      -LTOT*(HDIB-HDIR))
  GOTO 375
370 B3 = 0.0
375 CONTINUE
C
C
C
C
  IF(.NOT.ON1) GOTO 380
  C1 = TSTEP* KL1*(HVSA
+      -RTOT*(HIR-HIY
+  +2.0*(ILC1(I)+B1/2.0) - (ILC2(I)+B2/2.0) - (ILC3(I)+B3/3.0))
+      -LTOT*(HDIR-HDIY))
  GOTO 385
380 C1 = 0.0
385 CONTINUE
C
  IF(.NOT.ON2) GOTO 390
  C2 = TSTEP* KL1*(HVSB
+      -RTOT*(HIY-HIB
+  -(ILC1(I)+B1/2.0) +2.0*(ILC2(I)+B2/2.0) - (ILC3(I)+B3/3.0))
+      -LTOT*(HDIY-HDIB))
  GOTO 395
390 C2 = 0.0
395 CONTINUE
C
  IF(.NOT.ON3) GOTO 400
  C3 = TSTEP* KL1*(HVSC
+      -RTOT*(HIB-HIR
+  -(ILC1(I)+B1/2.0) - (ILC2(I)+B2/2.0) +2.0*(ILC3(I)+B3/3.0))
+      -LTOT*(HDIB-HDIR))
  GOTO 405
400 C3 = 0.0
405 CONTINUE
C
C
C
C
  IF(.NOT.ON1) GOTO 410
  D1 = TSTEP* KL1*(VSA(I+1)
+      -RTOT*(IR(I+1)-IY(I+1)
+  +2.0*(ILC1(I)+C1) - (ILC2(I)+C2) - (ILC3(I)+C3))
+      -LTOT*(DIR(I+1)-DIY(I+1)))
  GOTO 415
410 D1 = 0.0
415 CONTINUE
C
  IF(.NOT.ON2) GOTO 420
  D2 = TSTEP* KL1*(VSB(I+1)
+      -RTOT*(IY(I+1)-IB(I+1)
+  -(ILC1(I)+C1) +2.0*(ILC2(I)+C2) - (ILC3(I)+C3))
+      -LTOT*(DIY(I+1)-DIB(I+1)))
  GOTO 425
420 D2 = 0.0
425 CONTINUE
C

```

```

SYS07580
SYS07590
SYS07600
SYS07610
SYS07620
SYS07630
SYS07640
SYS07650
SYS07660
SYS07670
SYS07680
SYS07690
SYS07700
SYS07710
SYS07720
SYS07730
SYS07740
SYS07750
SYS07760
SYS07770
SYS07780
SYS07790
SYS07800
SYS07810
SYS07820
SYS07830
SYS07840
SYS07850
SYS07860
SYS07870
SYS07880
SYS07890
SYS07900
SYS07910
SYS07920
SYS07930
SYS07940
SYS07950
SYS07960
SYS07970
SYS07980
SYS07990
SYS08000
SYS08010
SYS08020
SYS08030
SYS08040
SYS08050
SYS08060
SYS08070
SYS08080
SYS08090
SYS08100
SYS08110
SYS08120
SYS08130
SYS08140
SYS08150
SYS08160
SYS08170
SYS08180
SYS08190
SYS08200
SYS08210
SYS08220
SYS08230
SYS08240
SYS08250
SYS08260
SYS08270
SYS08280
SYS08290
SYS08300
SYS08310
SYS08320
SYS08330
SYS08340
SYS08350
SYS08360
SYS08370
SYS08380
SYS08390

```



```

      IF(.NOT.ON3) GOTO 430
      D3 = TSTEP* KL1*(VSC(I+1)
+      -RTOT*(IB(I+1)-IR(I+1)
+      -(ILC1(I)+C1) - (ILC2(I)+C2) +2.0*(ILC3(I)+C3))
+      -LTOT*(DIB(I+1)-DIR(I+1)))
      GOTO 435
430 D3 = 0.0
435 CONTINUE
C
C
C
C
C.....CALCULATE THE NEXT COMPENSATOR BRANCH CURRENTS
C      (RUNGE-KUTTA)
C
      ILC1(I+1)= ILC1(I) + (A1 + 2.0*B1 + 2.0*C1 + D1)/6.0
      ILC2(I+1)= ILC2(I) + (A2 + 2.0*B2 + 2.0*C2 + D2)/6.0
      ILC3(I+1)= ILC3(I) + (A3 + 2.0*B3 + 2.0*C3 + D3)/6.0
C
C.....CHECK THAT BRANCH CURRENTS ARE ZERO WHEN
C      FLAGS INDICATE SO
C
      IF(ON1) GOTO 440
      IF(ILC1(I+1).NE.0.0) GOTO 150
440 IF(ON2) GOTO 445
      IF(ILC2(I+1).NE.0.0) GOTO 150
445 IF(ON3) GOTO 450
      IF(ILC3(I+1).NE.0.0) GOTO 150
450 CONTINUE
C
C.....CALCULATE LINE COMPENSATOR CURRENT VALUES FROM
C      THE DELTA-CONNECTED BRANCH VALUES
C
      ILCR(I+1) = ILC1(I+1) - ILC3(I+1)
      ILCY(I+1) = ILC2(I+1) - ILC1(I+1)
      ILCB(I+1) = ILC3(I+1) - ILC2(I+1)
C
C.....ALTER FLAGS IF CURRENT ZERO CROSSINGS ARE DETECTED
C      ( ALSO IF FIRST 'ON' POINT IS THE LAST POINT IN A
C      HALF CYCLE LEADING TO CONDUCTION IN ALL OF NEXT
C      HALF CYCLE )
C
      IF(POS11) GOTO 460
      IF(ILC1(I).LE.0.0.AND.ILC1(I+1).GE.0.0) GOTO 455
      GOTO 470
455 NEGI1=.FALSE.
      ON1=.FALSE.
      K1=0
      GOTO 470
460 IF(ILC1(I).GE.0.0.AND.ILC1(I+1).LE.0.0) GOTO 465
      GOTO 470
465 POSI1=.FALSE.
      ON1=.FALSE.
      K1=0
470 CONTINUE
C
      IF(POS12) GOTO 480
      IF(ILC2(I).LE.0.0.AND.ILC2(I+1).GE.0.0) GOTO 475
      GOTO 490
475 NEGI2=.FALSE.
      ON2=.FALSE.
      K2=0
      GOTO 490
480 IF(ILC2(I).GE.0.0.AND.ILC2(I+1).LE.0.0) GOTO 485
      GOTO 490
485 POSI2=.FALSE.
      ON2=.FALSE.
      K2=0
490 CONTINUE
C
      IF(POS13) GOTO 500
      IF(ILC3(I).LE.0.0.AND.ILC3(I+1).GE.0.0) GOTO 495
      GOTO 510
495 NEGI3=.FALSE.
      ON3=.FALSE.
      K3=0
      GOTO 510
500 IF(ILC3(I).GE.0.0.AND.ILC3(I+1).LE.0.0) GOTO 505
      GOTO 510
505 POSI3=.FALSE.
      ON3=.FALSE.
      K3=0
510 CONTINUE

```

```

SYS08400
SYS08410
SYS08420
SYS08430
SYS08440
SYS08450
SYS08460
SYS08470
SYS08480
SYS08490
SYS08500
SYS08510
SYS08520
SYS08530
SYS08540
SYS08550
SYS08560
SYS08570
SYS08580
SYS08590
SYS08600
SYS08610
SYS08620
SYS08630
SYS08640
SYS08650
SYS08660
SYS08670
SYS08680
SYS08690
SYS08700
SYS08710
SYS08720
SYS08730
SYS08740
SYS08750
SYS08760
SYS08770
SYS08780
SYS08790
SYS08800
SYS08810
SYS08820
SYS08830
SYS08840
SYS08850
SYS08860
SYS08870
SYS08880
SYS08890
SYS08900
SYS08910
SYS08920
SYS08930
SYS08940
SYS08950
SYS08960
SYS08970
SYS08980
SYS08990
SYS09000
SYS09010
SYS09020
SYS09030
SYS09040
SYS09050
SYS09060
SYS09070
SYS09080
SYS09090
SYS09100
SYS09110
SYS09120
SYS09130
SYS09140
SYS09150
SYS09160
SYS09170
SYS09180
SYS09190
SYS09200
SYS09210
SYS09220

```


C		SYS10020
C		SYS10030
C		SYS10040
CANALYSIS SECTION	SYS10050
C		SYS10060
C		SYS10070
C		SYS10080
C		SYS10090
C	IF(SPEC.OR.SPEC3) CALL FOSPEC(POINTS,1,2048,CVRY)	SYS10100
C	IF(SPEC3) CALL FOSPEC(POINTS,1,2048,CVYB)	SYS10110
C	IF(SPEC3) CALL FOSPEC(POINTS,1,2048,CVBR)	SYS10120
C	IF(SPEC.OR.SPEC3) CALL FOSPEC(POINTS,1,2048,MVRY)	SYS10130
C	IF(SPEC3) CALL FOSPEC(POINTS,1,2048,MVYB)	SYS10140
C	IF(SPEC3) CALL FOSPEC(POINTS,1,2048,MVBR)	SYS10150
C	IF(NOPLOT) GOTO 125	SYS10160
C		SYS10170
CNPERSQ IS THE NO. OF CYCLES PER PLOTTING SQUARE	SYS10180
C	IF A LONG PLOT IS OUTPUT.	SYS10190
C		SYS10200
C	NPERSQ=5	SYS10210
C	LONG=.TRUE.	SYS10220
C		SYS10230
C		SYS10240
C	*****	SYS10250
C	DATA TITL/ 'FURNACE', '& COMPEN', 'SATOR LI', 'NE CURRE', 'NTS' /	SYS10260
C	DATA TITL1A/ 'IR (KA)', '/	SYS10270
C	DATA TITL2A/ 'IY (KA)', '/	SYS10280
C	DATA TITL3A/ 'IB (KA)', '/	SYS10290
C	DATA TITL4A/ 'ILCR (K', 'A)', '/	SYS10300
C	DATA TITL5A/ 'ILCY (K', 'A)', '/	SYS10310
C	DATA TITL6A/ 'ILCB (K', 'A)', '/	SYS10320
C	CALL GRAF6(POINTS,6,IR,IY,IB,ILCR,ILCY,ILCB,	SYS10330
C	+TITL1A,TITL1A,TITL2A,TITL3A,TITL4A,TITL5A,TITL6A, LONG, NPERSQ,	SYS10340
C	+GINFOB,GINFO2,GINFO3,1.75,1.75,1.75,0.00,0.00,0.00)	SYS10350
C		SYS10360
C		SYS10370
C	*****	SYS10380
C	DATA TITL/ 'MEASURED', ' AND CAL', 'CULATED', 'LINE VOL', 'TAGES' /	SYS10390
C	DATA TITL1F/ 'VRY M (', 'KV)', '/	SYS10400
C	DATA TITL2F/ 'VYB M (', 'KV)', '/	SYS10410
C	DATA TITL3F/ 'VBR M (', 'KV)', '/	SYS10420
C	DATA TITL4F/ 'VRY C (', 'KV)', '/	SYS10430
C	DATA TITL5F/ 'VYB C (', 'KV)', '/	SYS10440
C	DATA TITL6F/ 'VBR C (', 'KV)', '/	SYS10450
C	CALL GRAF6(POINTS,6,MVRY,MVYB,MVBR,CVRY,CVYB,CVBR,	SYS10460
C	+TITL1F,TITL1F,TITL2F,TITL3F,TITL4F,TITL5F,TITL6F, LONG, NPERSQ,	SYS10470
C	+GINFOB,GINFO2,GINFO3,55.0,55.0,55.0,55.0,55.0,55.0)	SYS10480
C		SYS10490
C		SYS10500
C	*****	SYS10510
C	DATA TITL/ 'COMPENSA', 'TOR BRAN', 'CH VOLTA', 'GES AND', 'CURRENTS' /	SYS10520
C	DATA TITL1E/ 'VLC1', '(KV)', '/	SYS10530
C	DATA TITL2E/ 'VLC2', '(KV)', '/	SYS10540
C	DATA TITL3E/ 'VLC3', '(KV)', '/	SYS10550
C	DATA TITL4E/ 'ILC1', '(KA)', '/	SYS10560
C	DATA TITL5E/ 'ILC2', '(KA)', '/	SYS10570
C	DATA TITL6E/ 'ILC3', '(KA)', '/	SYS10580
C	LONG=.FALSE.	SYS10590
C	CALL GRAF6(POINTS,6,VLC1,VLC2,VLC3,ILC1,ILC2,ILC3,	SYS10600
C	+TITL1E,TITL1E,TITL2E,TITL3E,TITL4E,TITL5E,TITL6E, LONG, NPERSQ,	SYS10610
C	+GINFOB,GINFO2,GINFO3,55.0,55.0,55.0,0.00,0.00,0.00)	SYS10620
C	125 CONTINUE	SYS10630
C		SYS10640
C		SYS10650

```

C
C.....THE FOLLOWING SECTION USES CALLS TO SUBPROGRAM 'DEMOD' .SYS10660
C      THIS SUBPROGRAM USES PREVIOUSLY CALCULATED VALUES OF .SYS10670
C      FREQUENCY AND RMS VALUE TO FIT A TRUE SINUSOID TO THE .SYS10680
C      ARRAY OF TIME-SERIES DATA GIVEN AS THE FIRST PARAMETER. .SYS10690
C      THE FOURTH PARAMETER SHOULD BE AN ARRAY OF ZEROS ON .SYS10700
C      ENTRY & ON EXIT SHOULD CONTAIN THE 'DEMODULATED' DATA. .SYS10710
C      THE FIFTH PARAMETER SHOULD BE ZERO ON ENTRY & ON EXITSYS10720
C      SHOULD CONTAIN A TIME VALUE USED TO GIVE SYNCHRONISATION.SYS10730
C
C      SYS10740
C      SYS10750
C      SYS10760
C      SYS10770
C      SYS10780
C      SYS10790
C      SYS10800
C      SYS10810
C      SYS10820
C      SYS10830
C      SYS10840
C      SYS10850
C      SYS10860
C      SYS10870
C      SYS10880
C      SYS10890
C      SYS10900
C      SYS10910
C      SYS10920
C      SYS10930
C      SYS10940
C      SYS10950
130 CONTINUE .SYS10960
C      IF(NOPLOT) GOTO 140 .SYS10970
C
C      SYS10980
C      SYS10990
C
C      *****
C      DATA TITL/'MEASURED', 'AND DEM', 'ODULATED', ' WAVEFOR', 'MS' /SYS11000
C      DATA TITL1B/'VRY (KV', ') //SYS11010
C      DATA TITL2B/'VYB (KV', ') //SYS11020
C      DATA TITL3B/'VBR (KV', ') //SYS11030
C      DATA TITL4B/'DVRY (K', 'V) //SYS11040
C      DATA TITL5B/'DVB (K', 'V) //SYS11050
C      DATA TITL6B/'DVBR (K', 'V) //SYS11060
C      LONG=.TRUE. .SYS11070
C      SYS11080
C      IF(DMOD2) CALL GRAF6(POINTS,6,MVRY,MVYB,MVBR,DMVRY,DMVYB,DMVBR, .SYS11090
C      +TITL,TITL1B,TITL2B,TITL3B,TITL4B,TITL5B,TITL6B, LONG,NPERSQ, .SYS11100
C      +GINFO1,GINFO2,GINFO3,55.0,55.0,55.0,15.0,15.0,15.0) .SYS11110
C      IF(.NOT.DMOD2) CALL GRAF6(POINTS,6,MVRY,MVYB,MVBR,DMVRY,DMVYB, .SYS11120
C      +DMVBR,TITL,TITL1B,TITL2B,TITL3B,TITL4B,TITL5B,TITL6B, LONG,NPERSQ, .SYS11130
C      +GINFOB,GINFO2,GINFO3,55.0,55.0,55.0,15.0,15.0,15.0) .SYS11140
C      SYS11150
C      SYS11160
C      SYS11170
C      *****
C      DATA TITLC/'CALCULAT', 'ED AND ', 'DEMODULA', 'TED WAVE', 'FORMS' /SYS11180
C      DATA TITL1C/'CVRY ', '(KV) //SYS11190
C      DATA TITL2C/'CVYB ', '(KV) //SYS11200
C      DATA TITL3C/'CVBR ', '(KV) //SYS11210
C      DATA TITL4C/'DCVRY ', '(KV) //SYS11220
C      DATA TITL5C/'DCVYB ', '(KV) //SYS11230
C      DATA TITL6C/'DCVBR ', '(KV) //SYS11240
C      LONG=.TRUE. .SYS11250
C      SYS11260
C      IF(DMOD2) CALL GRAF6(POINTS,6, CVRY, CVYB, CVBR, DCVRY, DCVYB, DCVBR, .SYS11270
C      +TITLC, TITL1C, TITL2C, TITL3C, TITL4C, TITL5C, TITL6C, LONG, NPERSQ, .SYS11280
C      +GINFO1, GINFO2, GINFO3, 55.0, 55.0, 55.0, 15.0, 15.0, 15.0) .SYS11290
C      IF(.NOT.DMOD2) CALL GRAF6(POINTS,6, CVRY, CVYB, CVBR, DCVRY, DCVYB, .SYS11300
C      +DCVBR, TITLC, TITL1C, TITL2C, TITL3C, TITL4C, TITL5C, TITL6C, LONG, NPERSQ, .SYS11310
C      +GINFOB, GINFO2, GINFO3, 55.0, 55.0, 55.0, 15.0, 15.0, 15.0) .SYS11320
C      SYS11330
C      SYS11340
C      *****
C      DATA TITLD/'BOTH DEM', 'ODULATED', ' WAVEFOR', 'MS' , ' ' /SYS11350
C      DATA TITL1D/'DMVRY ', '(KV) //SYS11360
C      DATA TITL2D/'DMVYB ', '(KV) //SYS11370
C      DATA TITL3D/'DMVBR ', '(KV) //SYS11380
C      DATA TITL4D/'DCVRY ', '(KV) //SYS11390
C      DATA TITL5D/'DCVYB ', '(KV) //SYS11400
C      DATA TITL6D/'DCVBR ', '(KV) //SYS11410
C      LONG=.TRUE. .SYS11420
C      SYS11430
C      IF(.NOT.DMOD2) CALL GRAF6(POINTS,6, DMVRY, DMVYB, DMVBR, DCVRY, DCVYB, .SYS11440
C      +DCVBR, TITLD, TITL1D, TITL2D, TITL3D, TITL4D, TITL5D, TITL6D, LONG, NPERSQ, .SYS11450
C      +GINFOB, GINFO2, GINFO3, 15.0, 15.0, 15.0, 15.0, 15.0, 15.0) .SYS11460
C      IF(DMOD2) CALL GRAF6(POINTS,6, DMVRY, DMVYB, DMVBR, DCVRY, DCVYB, DCVBR, .SYS11470
C      +TITLD, TITL1D, TITL2D, TITL3D, TITL4D, TITL5D, TITL6D, LONG, NPERSQ, .SYS11480
C      +GINFO1, GINFO2, GINFO3, 15.0, 15.0, 15.0, 15.0, 15.0, 15.0)

```

```

C
C.....CALLS TO GRAF6 BELOW OUTPUT MANY MORE CYCLES
C          THAN CAN BE PLOTTED ON THE 'IMLAC' SYSTEM.
C
C          THE PLOT CODE MUST BE SENT TO THE DRUM PLOTTER
C
C          GOTO 140
135 NPERSQ=25
      LONG=.TRUE.
C
C          *****
DATA TITLG/'MEASURED', ' AND CAL', 'CULATED', 'LINE VOL', 'TAGES',
DATA TITL1G/'VRY M (' , 'KV)
DATA TITL2G/'VRY C (' , 'KV)
DATA TITL3G/'VRY M (' , 'KV)
DATA TITL4G/'VRY C (' , 'KV)
DATA TITL5G/'VRY M (' , 'KV)
DATA TITL6G/'VRY C (' , 'KV)
CALL GRAF6(POINTS,2,MVRY,CVRY,MVRY,CVRY,MVRY,CVRY,
+TITLG,TITL1G,TITL2G,TITL3G,TITL4G,TITL5G,TITL6G, LONG, NPERSQ,
+GINFOB,GINFO2,GINFO3,55.0,55.0,55.0,55.0,55.0,55.0)
C
C          *****
DATA TITLH/'DEMODULA', 'TED LINE', 'VOLTAGES',
DATA TITL1H/'DMVRY (' , 'KV)
DATA TITL2H/'DCVRY (' , 'KV)
DATA TITL3H/'DMVRY (' , 'KV)
DATA TITL4H/'DCVRY (' , 'KV)
DATA TITL5H/'DMVRY (' , 'KV)
DATA TITL6H/'DCVRY (' , 'KV)
CALL GRAF6(POINTS,2,DMVRY,DCVRY,DMVRY,DCVRY,DMVRY,DCVRY,
+TITLH,TITL1H,TITL2H,TITL3H,TITL4H,TITL5H,TITL6H, LONG, NPERSQ,
+GINFOB,GINFO2,GINFO3,15.0,15.0,15.0,15.0,15.0,15.0)
C
C.....END OF MAIN PROGRAM EXCEPT FOR FORMAT STATEMENTS
C
C          GOTO 140
160 WRITE(6,791)
      GOTO 140
150 WRITE(6,799)
140 CONTINUE
999 FORMAT(1H ,3(F10.6,1X),2X,3(F10.7,1X),2X,3(F10.4,1X))
998 FORMAT(1H ,3(F7.3,1X),1X,3(F7.4,1X),3(1X,F8.3))
997 FORMAT(//52H***** CHECK=0 ON EXIT FROM 'VZEROS' -CHANNEL 1 *****
996 FORMAT(//52H***** CHECK=0 ON EXIT FROM 'VZEROS' -CHANNEL 2 *****
995 FORMAT(//52H***** CHECK=0 ON EXIT FROM 'VZEROS' -CHANNEL 3 *****
994 FORMAT(1H ,6(F8.3,2X))
993 FORMAT(///20H INPUT DATA DETAILS,
+//22H -----,
+//22H -----,
+//49H          RED          YELLOW          BLUE ,
+//50H          -----,
+//16H NO. OF ZEROS ,3(I10,2X),
+//16H NO. OF CYCLES ,3(I10,2X),
+//16H FREQUENCY ,3(F10.2,2X),///)
992 FORMAT(//13H POINTS =,I5,/)
991 FORMAT(//46H SENSE OF CROSSING POINTS...+1 = +'VE GRADT.,
+//46H ----- 0 = UNDEFINED ,
+//46H ----- -1 = -'VE GRADT ,
+//59H -----DATA-----CALC-----,
+//55H J          R          Y          B          R          Y          B,/)
990 FORMAT(1H ,I2,8X,I2,5X,I2,5X,I2,12X,I2,5X,I2,5X,I2)
899 FORMAT(/////9H LOOP NO.,I2,11H DELTA =,F8.4,5H RADS,
+//21H ----- ERROR=,F9.5,17H RADS AND AVSUM =,F10.5)
898 FORMAT(1H ,I4,5(F9.5))

```

```

SYS11490
SYS11500
SYS11510
SYS11520
SYS11530
SYS11540
SYS11550
SYS11560
SYS11570
SYS11580
SYS11590
SYS11600
SYS11610
SYS11620
SYS11630
SYS11640
SYS11650
SYS11660
SYS11670
SYS11680
SYS11690
SYS11700
SYS11710
SYS11720
SYS11730
SYS11740
SYS11750
SYS11760
SYS11770
SYS11780
SYS11790
SYS11800
SYS11810
SYS11820
SYS11830
SYS11840
SYS11850
SYS11860
SYS11870
SYS11880
SYS11890
SYS11900
SYS11910
SYS11920
SYS11930
SYS11940
SYS11950
SYS11960
SYS11970
SYS11980
SYS11990
SYS12000
SYS12010
SYS12020
SYS12030
SYS12040
SYS12050
SYS12060
SYS12070
SYS12080
SYS12090
SYS12100
SYS12110
SYS12120
SYS12130
SYS12140
SYS12150
SYS12160
SYS12170

```

```

897 FORMAT(1H ,F6.4,4X,F7.5,4X,I2,7(5X,L1))          SYS12180
896 FORMAT(/30X,25H *****),                      SYS12190
+30X,25H *****),                                  SYS12200
+30X,25H * PROGRAM RUN FOR *,                       SYS12210
+30X,25H * *,                                       SYS12220
+30X,15H * TSTEP =,F7.5,3H *,                       SYS12230
+30X,15H * LIMIT =,F7.5,3H *,                      SYS12240
+30X,15H * LOOPS =,I3,7H *,                          SYS12250
+30X,16H * LIST =,L1,8H *,                          SYS12260
+30X,16H * PLOT =,L1,8H *,                          SYS12270
+30X,16H * LONG =,L1,8H *,                          SYS12280
+30X,16H * SPEC =,L1,8H *,                          SYS12290
+30X,16H * SPEC3 =,L1,8H *,                         SYS12300
+30X,16H * DMOD =,L1,8H *,                          SYS12310
+30X,16H * DMOD2=,L1,8H *,                          SYS12320
+30X,25H * *,                                       SYS12330
+30X,25H * *)                                       SYS12340
895 FORMAT(/48H THIS IS THE TEST LINE $$$$$$$$$$ $$$$$$$$$$) SYS12350
894 FORMAT(/23H $$$$$$$$$$ LABEL ,I4,15H $$$$$$$$$$) SYS12360
893 FORMAT(/1H ,6(F10.4,2X),/15X,3(F10.4,5X))        SYS12370
892 FORMAT(/1H ,2X,2HVR,12X,2HVY,12X,2HVB,12X,2HIR,12X,2HIY,12X,2HIB, SYS12380
+53H V7 V8 V9 ) SYS12390
891 FORMAT(/53HJ & ZERO CROSSING TIMES ..... R,RCALC,Y,YCALC,B,BCALC)SYS12400
890 FORMAT(1H ,I2,4X,3(F9.5,2X,F9.5,4X))             SYS12410
800 FORMAT(72X)                                       SYS12420
799 FORMAT(52H ***** FLAG ERROR IN COMPENSATOR SECTION *****) SYS12430
798 FORMAT(1H ,3(F9.4,3X),3(F9.4,2X),/37X,3(F9.4,2X)) SYS12440
797 FORMAT(6H SUM1=,F9.3,6H SUM2=,F9.3,6H SUM3=,F9.3, SYS12450
+10H QUART1=,I2,8H QUART2=,I2,8H QUART3=,I2) SYS12460
796 FORMAT(10H ON1 =,L1,10H ON2 =,L1,10H ON3 =,L1,   SYS12470
+3X,10H POSI1 =,L1,10H POSI2 =,L1,10H POSI3 =,L1,   SYS12480
+10H INT1N =,L1,10H INT2N =,L1,10H INT3N =,L1,     SYS12490
+3X,10H NEGI1 =,L1,10H NEGI2 =,L1,10H NEGI3 =,L1,  SYS12500
+10H INT1P =,L1,10H INT2P =,L1,10H INT3P =,L1)     SYS12510
795 FORMAT(1H ,F7.5,4X,F7.1,4X,F7.1,4X,I5,4X,I5)    SYS12520
794 FORMAT(1H ,8A8)                                   SYS12530
793 FORMAT(30X,25H * COMPENSATOR *,                 SYS12540
+30X,25H * DETAILS: *,                               SYS12550
+30X,25H * *,                                       SYS12560
+30X,16H * LC =,F7.5,3H *,                          SYS12570
+30X,16H * POSLIM=,F7.1,3H *,                       SYS12580
+30X,16H * NEGLIN=,F7.1,3H *,                      SYS12590
+30X,16H * ICON =,I5,5H *,                          SYS12600
+30X,16H * ICOFF=,I5,5H *,                          SYS12610
+30X,25H * *,                                       SYS12620
+30X,25H * *)                                       SYS12630
792 FORMAT(/' GINFO2 : ',8A8/' GINFO3 : ',8A8//)     SYS12640
791 FORMAT(/50H ***** ILLEGAL INPUT OPTION COMBINATION *****) SYS12650
STOP
END
SYS12660
SYS12670

```

APPENDIX K

TWELVE-PULSE TCR CONTROL PROGRAM LISTING

```

1 NAME thyristor_firing_routine
2 NOLIST COM
3
4 GLOBAL firBsub
5 GLOBAL CODEBASEEQ, DATABASEEQ, CONSTBASEEQ
6
7 ASSUME DS:DATABASEEQ
8
9 SECTION pascalprocedure, CLASS=INSTRQQ
10
11
12
13 ;XXXXXXXXXXXXXXXXXXXXXXXXXXXXXXXXXXXXXXXXXXXXXXXXXXXXXXXXXXXXXXXXXXXXXXXXXXXX
14 ;assembly routine to fire thyristors..... 12-pulse
15 ;called from main prog after voltage zero detected
16 ;algorithm subtracts sine value from measured value and integrates
17 ;testing value against a limit. Fires thy. when limit reached
18 ;
19 ;only outputs a short pulse for thyristor firing
20 ;
21 ;loop delay values set to values suitable for noi compensator. Values
22 ;for the other two compensators must be set in RAM after download
23 ;
24 ;
25 ;positive half cycle
26 ;
27 firBsub ;12-pulse thyristor firing routine
28 00000000 8D360000 R fire1 LEA SI, sine1 ;positive half cycle section
29 00000004 33DB XOR BX, BX
30 00000006 B507 MOV CH, f07H
31 00000008 BA00F8 start1 MOV DX, f0FB00H ;load address of adc
32 0000000B EF OUT DX, AX ;initiate conversion
33 0000000C B10F MOV CL, f0FH ;conversion delay
34 0000000E D2E9 SHR CL, CL
35 00000010 32E4 XOR AH, AH ;set ah to zero
36 00000012 EC IN AL, DX ;input sample
37 00000013 B109 MOV CL, f09H ;loop delay to adjust sampling frequency
38 00000015 D2E9 SHR CL, CL ;sine curve based on 74 usecs sample time
39 00000017 80FD00 CMP CH, f00H ;test whether one of first nine samples
40 0000001A 7400 JE lab1 ;jump to lab1 if after nine samples
41 0000001C FECD DEC CH
42 0000001E 8A0C lab1 MOV CL, [ESI] ;mov current value of sine curve from memory
43 00000020 3AD1 CMP AL, CL ;decide whether?sample ( sine, jmp to neg1---
44 00000022 7207 JB neg1 ; -- if it is.
45 00000024 2AD1 SUB AL, CL ;subtract sine from sample
46 00000026 03DB add1 ADD BX, AX ;add difference to summation store
47 00000028 E90C00 JMP com
48 0000002B 2ACB neg1 SUB CL, AL ;CL>AL, subtract AL from CL
49 0000002D 8AD1 MOV AL, CL ;put difference into AL
50 0000002F 3BD8 CMP BX, AX ;test AX against BX--if AX>BX make AX=BX so
51 00000031 7702 JA sub1 ;that BX is set to zero in the subtraction
52 00000033 8BC3 MOV AX, BX
  
```



```

53 00000035 2E03      sub1   SUB  BX, AX
54 00000037 81FE7C10   cont   CMP  SI, 1107CH      ;test SI for > 60 degrees
55 00000038 720C           JB  next           ;sample again if SI < 60 degrees
56 0000003D 81FEBF10   CMP  SI, 110BFH     ;test SI for < 150 degrees
57 00000041 7716           JA  lab2           ;if > 150 degrees disallow 1st pulse
58 00000043 81FB0001   CMP  BX, 10100H     ;test BX against first limit
59 00000047 7703           JA  firea          ;jump to firea when limit exceeded
60 00000049 46           next   INC  SI           ;update pointer to sine curve
61 0000004A EBBC           JMP  start1
62 0000004C BA00F0   firea MOV  DX, 10F000H    ;fire thyristor...one short pulse
63 0000004F B001           MOV  AL, 1011H
64 00000051 EE           OUT  DX, AL
65 00000052 B110           MOV  CL, 1101H
66 00000054 D2E9           SHR  CL, CL
67 00000056 B000           MOV  AL, 100H
68 00000058 EE           OUT  DX, AL
69
70
71
72
73 00000059 BA00F8   lab2  MOV  DX, 10F800H    ;get next sample
74 0000005C EF           OUT  DX, AX
75 0000005D B10F           MOV  CL, 10FH
76 0000005F D2E9           SHR  CL, CL
77 00000061 32E4           XOR  AH, AH
78 00000063 EC           IN  AL, DX
79 00000064 B109           MOV  CL, 109H
80 00000066 D2E9           SHR  CL, CL
81 00000068 3CB7           CMP  AL, 107H
82 0000006A 7235           JB  end1
83 0000006C 8A0C           MOV  CL, [SI]
84 0000006E 3AC1           CMP  AL, CL
85 00000070 7207           JB  neq2
86 00000072 2AC1           SUB  AL, CL
87 00000074 03DB   add2  ADD  BX, AX
88 00000076 E90C00   neq2  JMP  cont2
89 00000079 2AC0           SUB  CL, AL
90 0000007B 8AC1           MOV  AL, CL
91 0000007D 36DB           CMP  BX, AX
92 0000007F 7702           JA  sub2
93 00000081 8BC3           MOV  AX, BX
94 00000083 2E03   sub2  SUB  BX, AX
95 00000085 81FE9310   cont2 CMP  SI, 11093H     ;test SI for > 90 degrees
96 00000087 7206           JB  next2         ;sample again if SI < 90 degrees
97 0000008B 81FB0002   CMP  BX, 10200H     ;test BX against second limit
98 0000008F 7703           JA  fireb          ;jump to fireb when 2nd limit exceeded
99 00000091 46   next2 INC  SI           ;update pointer to sine curve
100 00000092 EBBC           JMP  lab1
101 00000094 BA00F0   fireb MOV  DX, 10F000H    ;fire thyristor...one short pulse
102 00000097 B004           MOV  AL, 1041H
103 00000099 EE           OUT  DX, AL
104 0000009A B110           MOV  CL, 1101H

```

```

105 0000009C D2E9      SHR CL, CL
106 0000009E B000      MOV AL, £00H
107 000000A0 EE         OUT DX, AL
108
109 000000A1 BA00FB     end1  MOV DX, £0FB00H      ;load adc address and input sample
110 000000A4 F1         OUT DX, A)
111 000000A5 B10F      MOV CL, £0FH
112 000000A7 D2E9      SHR CL, CL
113 000000A9 EC         IN AL, DX
114 000000AA 3C80      CMP AL, £80H        ;check for zero crossing
115 000000AC 77F3      JA end1
116
117
118
119
120
121
122 000000AE 8D368500 R   fire3 LEA SI, sine2
123 000000B2 33D0      XOR BX, BX          ;--positive half cycle routine except--
124 000000B4 B509      MOV CH, £09H        ;--a positive contribution to summation--
125 000000B6 BA00FB     start3 MOV DX, £0FB00H    ;--store results from AL being ----
126 000000B9 EF         OUT DX, AX          ;--numerically smaller than sine curve--
127 000000BA B10F      MOV CL, £0FH        ;--to allow for fact that zero volts--
128 000000BC D2E9      SHR CL, CL          ;--corresponds to an adc output of 128.
129 000000BE 32E4      XOR AH, AH
130 000000C0 EC         IN AL, DX
131 000000C1 B108      MOV CL, £08H        ;loop delay to adjust sampling frequency
132 000000C3 D2E9      SHR CL, CL          ;sine curve based on 74usecs sample time
133 000000C5 80FD00     CMP CH, £00H
134 000000C8 7402      JE lab3
135 000000CA FEDD      DEC CH
136 000000CC 8A0C      lab3  MOV CL, £0C
137 000000CE 3AC1      CMP AL, CL
138 000000D0 7200      JB pos3
139 000000D2 2AC1      SUB AL, CL
140 000000D4 3BD3      CMP BX, AX
141 000000D6 7702      JA sub3
142 000000D8 8B03      MOV AX, BX
143 000000DA 2BD8      sub3  SUB BX, AX
144 000000DC E90600H     JMP cont3
145 000000DF 2AC8      pos3  SUB CL, AL
146 000000E1 8AC1      MOV AL, CL
147 000000E3 03D8      add3  ADD BX, AX
148 000000E5 81FE0111     cont3 CMP SI, £1101H     ;past 240 degrees
149 000000E9 720C      JB next3
150 000000EB 81FE3D11     CMP SI, £113DH     ;before 330 degrees
151 000000EF 7716      JB lab4
152 000000F1 81FB0001     CMI BX, £0100H     ;test BX against first limit
153 000000F3 7703      JA firec
154 000000F7 4         next3 INC SI
155 000000F8 EBBC      jmp start3
156 000000FA BA00FB     firec MOV DX, £0FB00H    ;fire thyristor...one short pulse

```

```

157 000000FD B002      MOV AL, £02H
158 000000FF EB       OUT DX, AL
159 00000100 B110      MOV CL, £10H
160 00000102 D2E9      SHR CL, CL
161 00000104 B000      MOV AL, £00H
162 00000106 EB       OUT DX, AL
163
164
165                               ;integration can continue for 2nd pulse
166                               ;in negative half-cycle
167 00000107 BA00F8      lab4 MOV DX, £0F800H      ;--store results from AL being ----
168 0000010A EF         OUT DX, AX           ;--numerically smaller than sine curve--
169 0000010B B10F       MOV CL, £0FH        ;--to allow for fact that zero volts---
170 0000010D D2E9      SHR CL, CL          ;--corresponds to an adc output of 120.
171 0000010F 32E4      XOR AH, AH
172 00000111 EB       IN AL, DX
173 00000112 B108       MOV CL, £08H        ; loop delay to adjust sampling frequency
174 00000114 D2E9      SHR CL, CL          ;sine curve based on 74usecs sample time
175 00000116 3C73      CMP AL, £73H
176 00000118 7735      JA end3             ;check for end of half-cycle
177 0000011A 8A0C      MOV CL, £SI
178 0000011C 3AC1      CMP AL, CL
179 0000011E 720D      JB pos4
180 00000120 2AC1      SUB AL, CL
181 00000122 3BD8      CMP BX, AX
182 00000124 7762      JA sub4
183 00000126 8BC3      MOV AX, BX
184 00000128 2BD0      sub4 SUB BX, AX
185 0000012A E90600     JMP cont4
186 0000012D 2AC3      pos4 SUB CL, AL
187 0000012F 8AC1      MOV AL, CL
188 00000131 03D3      add4 ADD BX, AX
189 00000133 81FE1811   cont4 CMP SI, £1118H      ;past 270 degrees ?
190 00000137 7205      JB next4
191 00000139 81FB0002   CMP BX, £0200H     ;test BX against second limit
192 0000013D 7763      JA fired
193 0000013F 46         next4 INC SI
194 00000140 EB05      JMP lab4
195 00000142 BA00F0     fired MOV DX, £0F000H    ;fire thyristor...one short pulse
196 00000145 B000      MOV AL, £00H
197 00000147 EB       OUT DX, AL
198 00000148 B110      MOV CL, £10H
199 0000014A D2E9      SHR CL, CL
200 0000014C B000      MOV AL, £00H
201 0000014E EB       OUT DX, AL
202
203
204 0000014F BA00F8      end3 MOV DX, £0F800H    ;load adc address and input sample
205 00000152 EB       OUT DX, AX
206 00000153 B10F       MOV CL, £0FH
207 00000155 D2E9      SHR CL, CL
208 00000157 EC       IN AL, DX

```

209 00000158 3C00
210 0000015A 72F3
211 0000015C E9A1F0
212 0000015F C20400

CMF AL, #00H ; check for pos going zero crossing
JB end3
JMP fire1 ; ---cycle routine.
RET #4

213
214
215
216
217
218

SECTION sdk88.const, CLASS=DATA00

*actually
100*

: reference sine wave ... zero = 127
: plus/minus 105
: first sample at 100us
: subsequent dt = 75us
: pt.s per 1/2 cyc = 132

225 00000000 82040789
BC0E9093
9597999C
9E

sine1 BYTE 130, 132, 135, 137, 140, 142, 144, 147, 149, 151, 153, 156, 158

226 00000000 A0A2A5A7
A9ABADA1
B1B3B5B7
B9

BYTE 160, 162, 165, 167, 169, 171, 173, 175, 177, 179, 181, 183, 185

227 0000001A B8B0BFC1
C2C4C6C7
C9CBCCCE
CF

BYTE 187, 189, 191, 193, 194, 196, 198, 199, 201, 203, 204, 206, 207

228 00000027 D0D2D3D4
D5D7D8D9
DADEDCDD
DD

BYTE 200, 210, 211, 212, 213, 215, 216, 217, 218, 219, 220, 221, 221

229 00000034 DEDFDFE0
E1E1E2E3
E5ECE3E3
E5

BYTE 222, 223, 223, 224, 225, 225, 226, 226, 226, 236, 227, 227, 227

230 00000041 E3E3E3E3
E3E2E2E
E111E0E0
DF

BYTE 227, 227, 227, 227, 227, 226, 226, 226, 225, 225, 224, 224, 223

231 0000004E DFDEDDDC
DEDA09D
D7D6D5D4
D3

BYTE 223, 222, 221, 220, 219, 218, 217, 216, 215, 214, 213, 212, 211

232 0000005B D1D0CECD
CCCAC0C
C5C3C2C0
BE

BYTE 209, 208, 206, 205, 204, 202, 200, 199, 197, 195, 194, 192, 190

233 0000006B BCBAB9B7
B5B3B1A
ACAABA6
A8

BYTE 180, 186, 185, 183, 181, 179, 177, 174, 172, 170, 168, 166, 164

234	00000075	A29F9D9B 9996947C 0F808E88 86		BYTE	162, 159, 157, 155, 153, 150, 148, 146, 143, 141, 139, 136, 134
235	00000082	84817F		BYTE	132, 129, 127
236					
237					
238	00000085	7C7A7775 72706E6B 69676562 60	sine2	BYTE	124, 122, 119, 117, 114, 112, 110, 107, 105, 103, 101, 98, 96
239	00000092	5E5C5957 5553514F 4D4B4947 45		BYTE	94, 92, 89, 87, 85, 83, 81, 79, 77, 75, 73, 71, 69
240	0000009F	43413F3D 3C3A3837 35333230 2F		BYTE	67, 65, 63, 61, 60, 58, 56, 55, 53, 51, 50, 48, 47
241	000000AC	2E2C2B2A 29272625 24232221 21		BYTE	46, 44, 43, 42, 41, 39, 38, 37, 36, 35, 34, 33, 33
242	000000B9	201F1F1E 1D1D1C1C 1C1C1B1B 1B		BYTE	32, 31, 31, 30, 29, 29, 28, 28, 28, 28, 27, 27, 27
243	000000C6	1B1B1B1B 1B1C1C1C 1D1D1E1E 1F		BYTE	27, 27, 27, 27, 27, 28, 28, 28, 29, 29, 30, 30, 31
244	000000D3	1F202122 23242526 2728292A 2B		BYTE	31, 32, 33, 34, 35, 36, 37, 38, 39, 40, 41, 42, 43
245	000000E0	2D2E3031 3234363 393B3C3E 40		BYTE	45, 46, 48, 49, 50, 52, 54, 55, 57, 59, 60, 62, 64
246	000000ED	42444547 494B4D54 52545658 5A		BYTE	66, 68, 69, 71, 73, 75, 77, 80, 82, 84, 86, 88, 90
247	000000FA	5C5F6163 65686A6C 6E717376 78		BYTE	92, 95, 97, 99, 101, 104, 106, 108, 111, 113, 115, 118, 120
248	00000107	7A7D7F		BYTE	122, 125, 127
249					
250					
251					

Section = SDK08.CONST, Class = DATAQQ, Aligned to 00000010, Size = 0000010A

SINE1-----00000000 SINE2-----00000085

Section = PASCALPROCEDURE, Class = INSTRQQ, Aligned to 00000010, Size = 00000162

ADD1-----00000026	ADD2-----00000074	ADD3-----000000E3	ADD4-----00000131
CONT-----00000037	CONT2-----00000085	CONT3-----000000E5	CONT4-----00000133
END1-----000000A1	END3-----0000014F	FIRBSUB-----00000000 6	FIRE1-----00000000
FIRE3-----000000AE	FIREA-----0000004C	FIREB-----00000074	FIREC-----000000FA
FIRE0-----00000142	LAB1-----0000001E	LAB2-----00000059	LAB3-----000000CC
LAB4-----00000107	NEG1-----0000002B	NEG2-----00000079	NEXT-----00000049
NEXT2-----00000091	NEXT3-----000000F7	NEXT4-----0000013F	POS3-----000000DF
POS4-----00000120	START1-----00000000	START3-----000000B6	SUB1-----00000035
SUB2-----00000083	SUB3-----000000DA	SUB4-----00000128	

Section = %FIREBOBJ, Aligned to 00000010, Size = EMPTY

Unbound Globals

CODEBASEQQ-----00000000 CONSTBASEQQ-----00000000 DATABASEQQ-----00000000

251 Lines Read
251 Lines Processed
0 Errors

APPENDIX L

PUBLISHED PAPERS

L.I Reference [66]

MODELLING OF AN ELECTRIC ARC FURNACE

D R Turner, P Watkinson and I C Davis

The University of Liverpool, UK

INTRODUCTION

Electric arc furnaces provide a clean and efficient way of melting scrap metal for the production of steel, but they are well known for the effects that they can have on the supply system, particularly voltage fluctuations and consequent tungsten filament lamp flicker. There is considerable interest in the use of shunt compensators for the control of these voltage variations, and a number of methods such as saturated reactors and thyristor controlled devices have been employed. One of the requirements of such equipment is that it should have a good speed of response^{(1),(2)} and the work on modelling described in this paper is part of an investigation of the advantages to be gained by the use of increased phase numbers for thyristor controlled shunt reactors.

It is naturally desirable in such a programme to be able to model the furnace and supply system, both experimentally and theoretically, in order to assess the merits of the different control configurations, but the random nature of the arc currents makes this a difficult task. Whilst a number of authors have described theoretical models⁽³⁾, very little is reported in the literature on the experimental modelling. Dugan⁽⁴⁾ describes a model using a transient network analyser with a harmonic current source to represent the furnace. However, as the author indicates this model does not attempt to incorporate the random nature of the current variations. Investigations by Dixon⁽⁵⁾ and others suggest that the pattern of variations produced by arc furnaces is almost independent of rating, which implies that results based on one particular furnace are likely to be applicable to others.

The model described in this paper makes use of the recorded current waveforms of a working furnace, thus introducing the necessary random current variations which are needed to judge the compensator performance.

Nature of the experimental model

The basic concept on which the model is based is that the furnace be represented by a current sink which has a terminal current characteristic similar to that of a working furnace, whilst the electrical supply is represented by a constant voltage in series with a lumped parameter system impedance. The presence of transformers in the supply network, particularly those with star-delta connections, generates a coupling⁽⁶⁾ between phases which, whilst it can be ignored for balanced sinusoidal operation, is important for the unbalanced non sinusoidal currents of the arc furnace. This is a topic for which there appears to be little information available and one which needs further work. It is incorporated into the model by the use of a star-delta connected transformer in the supply system, although it is recognised that the transformer used may well not be an accurate representation of the full sized device. This coupling between phases means that the furnace and system must be modelled as a three phase unit rather than one single phase model. The ratio of reactance to

resistance of a typical supply network (Q factor) is high and the requirement to achieve a similarly high value of Q in the model demands the use of linear iron cored inductors and suitable values of base current and voltage. These base values impose constraints on the choice of current sink, but the availability of high power electronic amplifiers, such as those used in electro-mechanical vibrators, means that these requirements can be achieved making direct coupled electronic amplifiers the most convenient form of current sink. The driving or input signal to the amplifiers could be derived in a number of ways. For example the current waveform of a furnace could be subjected to a spectral analysis and the input signal then synthesised using a random but weighted combination of the frequencies found in the waveform spectrum. The approach adopted for this work is to use waveforms recorded on a working furnace as the driving signal, and to this end records made by the CEGB with the co-operation of the steel makers have been made available to the authors, in the form of digitised data on magnetic tape. The information has been transferred to a main frame computer, enabling short sections to be chosen at will and transferred to the bench top model, described in detail in the next section. This form of data handling has been used, since it also allows computational analysis of the recorded data and easy access for comparison with the results of a computational model, work which is progressing in parallel with the experimental modelling.

The nature of this current sink means that whatever one does to the system voltage or impedance the current at the terminals of the furnace model will always be an exact copy of the recorded current. Thus when a compensator is connected to the model the arc furnace currents will remain unchanged. Since the recorded data is that of a furnace operating without a compensator this approach will neglect the small changes that will arise in furnace current due to the action of the compensator. However, the random nature of the furnace currents means that it is doubtful whether these changes could be quantified, but naturally the currents seen by the supply system, and consequently the system voltages, will change when a compensator is fitted.

Details of the model

The model is based on the Templeborough Plant of British Steel Ltd., figure 1 shows the salient features of the supply system. The recordings of phase voltage and current were taken at the 33k bus bar by the CEGB using their D.R.F.A.M.⁽²⁾ equipment and for the recordings used in this paper furnace 2 was in operation. Following transfer of this data to the main frame computer at Liverpool short sections of recording can be selected at will and transferred to the model by paper tape, where it is held in RAM (figure 2). The time span of data held in the model is dependent upon the size of the memory, and at present is limited to 10 cycles, but it is intended to extend this soon. In addition to the three phase currents one of the voltages is also held in the memory and this

can be displayed for comparison with the measured model voltage.

Synchronisation of the currents to the voltage is achieved in two stages, whilst selecting the data in the mainframe computer the values of current at the instant of red phase voltage zero are identified and subsequently loaded into known memory location in the RAM.

The phase locked loop (fig. 2) circuit generates two interrupt signals, one of which is at 50Hz and coincides with the zero crossing of the red phase voltage. This is used to output the appropriate values of phase currents. The 5KHz interrupt signal is used to output the current values between zero crossing points, giving 100 samples per cycle. The digital values of current are passed to the voltage controlled current feedback amplifiers via three digital to analogue converters. The control of the system can be arranged to give either a single shot or repetitive mode of operation.

The base voltage of the model is 100 V line, and the amplifiers are capable of sinking currents in excess of 3A. The results presented in the next section were taken when the model was initially constructed to demonstrate the feasibility of the approach. At this time the star-delta transformer was not specifically designed for the task, its impedance was such to limit the base current to a value of 1.4 A, and it does not represent the variation of system impedance with frequency (or rate of change of current). Similarly the variation of line impedance with frequency is not represented, however in this case the system impedance is dominated by the super grid transformer. The model is currently being rebuilt with components to give a base value current of 5A and a better representation of the system impedances including frequency variation.

As indicated in the introduction the model is part of an investigation of the advantages to be gained by the use of increased phase numbers for thyristor controlled shunt reactors. Such a device would normally be connected to the 33 KV bus of the supply system and it is the authors' intention to connect a compensator to the model at the terminals of the amplifiers representing the arc furnace. In order that different control strategies can be readily implemented it is intended to make full use of mode in digital techniques in the compensator control system, which provide the facility for rapid reprogramming of the control algorithms. A number of different techniques have been described⁽⁷⁾ in the literature for assessing the flicker level of voltage variations and it is proposed to implement these techniques digitally, applying them to the voltage waveforms measured on the model once these have been transferred back to the main frame computer.

Results

In order to check the suitability of the amplifiers as currents sinks the model was initially run in single phase mode using one of the recorded phase currents. Figure 3(b) shows the recorded phase current used as input to the amplifier whilst figure 3(a) shows the current waveform recorded on the model, over 5 cycles, and it is seen that they are in good agreement.

The model was then developed into the three phase form, and figure 4 and 5 show two phase currents both measured (upper trace a) and recorded (lower trace b) and again it is seen that the agreement between the two is good

Figure 6 shows one of the phase voltages, the upper trace again being the measured value from the model and the lower trace the recorded value. This latter was derived from the output of one of three voltages transformers connected in star at the 33 KV bus, whilst the former was recorded across one of three balanced resistors connected in star to the amplifier terminals. The distortions to the waveforms are evident and considering that the star-delta transformers in use when these recordings were made was not an exact representation of the super grid transformer supplying the furnace (SGT4, figure 1) the agreement between the two is encouraging.

REFERENCES

1. Friedlander, B. and Young, D.J., 1974, "Requirements and compensation methods for scrap melting arc furnaces". Proc. Int. Conf. on Sources and Effects of Power System Disturbances, London, England.
2. Ashmole, P.H., Murray, B.E., and Young, D.J., 1980, "An assessment of compensation equipment for arc furnaces". Proc. U.I.E. 9th Int. Congress, Cannes, France.
3. Granstrom, S., 1980, "Computer studies of voltage fluctuation caused by arc furnaces". Proc. U.I.E. 9th Int. Congress, Cannes, France.
4. Dugan, R.C., 1977, "Simulation of arc furnace power systems". Paper PID 77-5, IEEE Industrial Applications Society Annual Meeting, Los Angeles, U.S.A.
5. Dixon, G.F.L., and Kendall, P.G., April 1972, "Supply to arc furnaces; measurement and prediction of supply voltage fluctuation". Proc. IEE. Vol. 119 No. 4.
6. Kron, G., "Tensor analysis of networks" Wiley, New York 1938 and MacDonald, London, 1965.
7. Kirkby, H.J.A. and Langman, R.D., 1974, "Measuring voltage fluctuations caused by electric arc furnaces", Proc. Int. Conf. on Sources and Effects of Power System Disturbances, London, England.

ACKNOWLEDGMENTS

The authors wish to thank the C.E.G.B. for their support in this work and their permission to use the recorded arc furnace data, and the University of Liverpool and Professor J.H. Leck for providing the laboratory facilities.

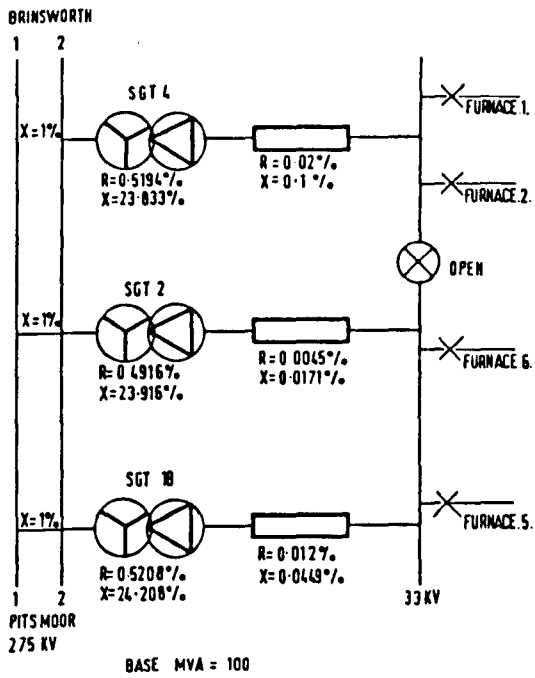


Figure 1 Supply to Templeborough Furnaces

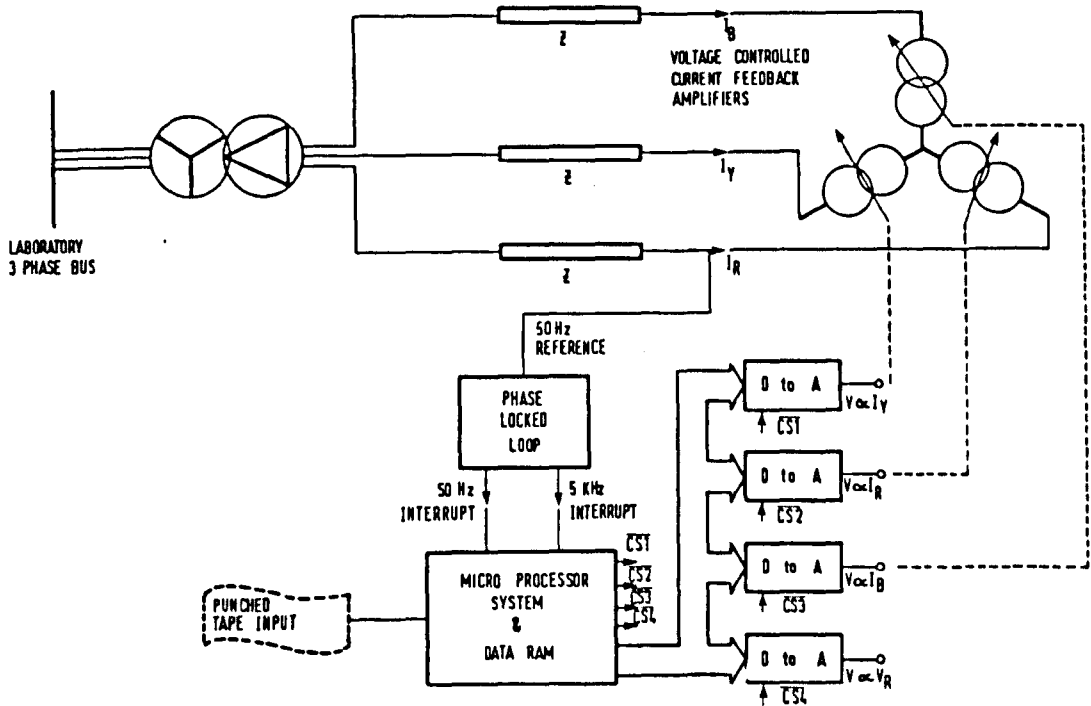
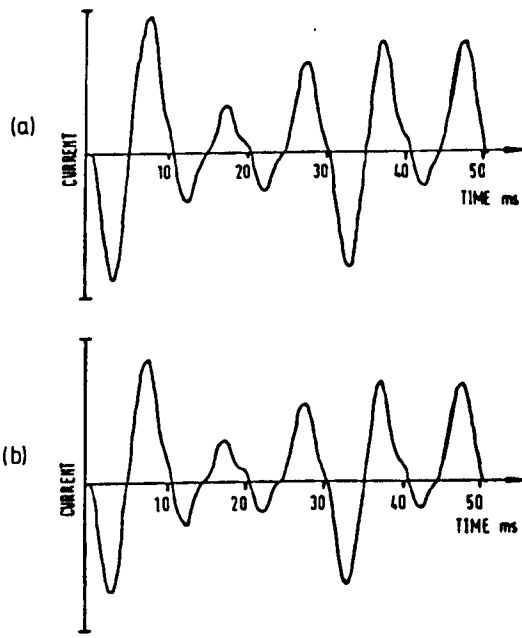
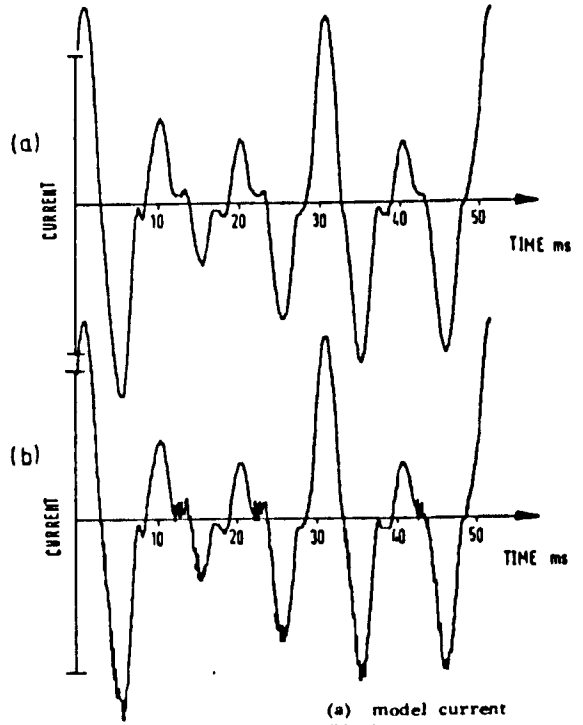


Figure 2 Block diagram of experimental model



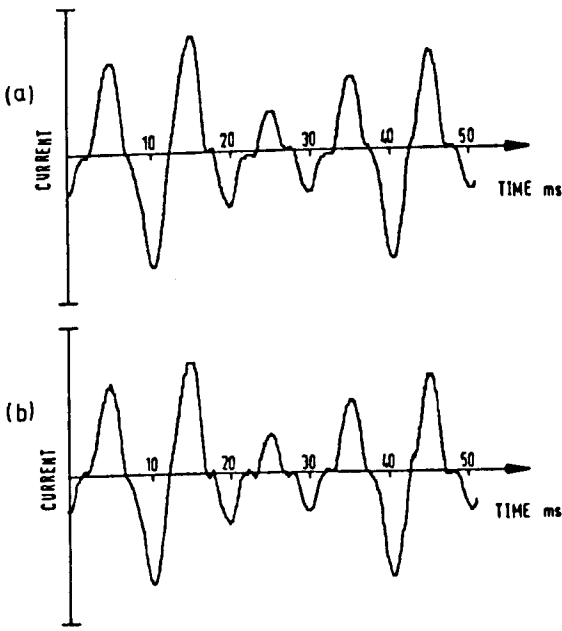
(a) model current
(b) furnace current

Figure 3 Current waveforms, single phase mode



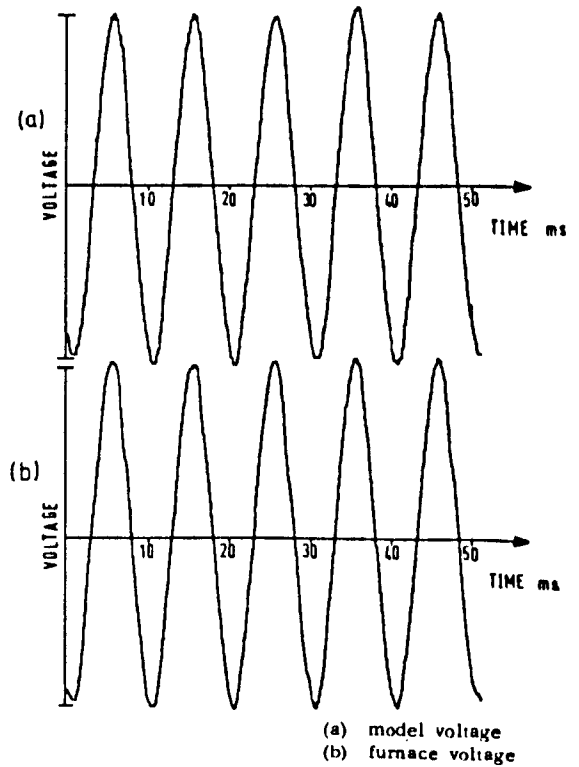
(a) model current
(b) furnace current

Figure 5 Yellow phase current waveforms, three phase model



(a) model current
(b) furnace current

Figure 4 Red phase current waveforms, three phase model



(a) model voltage
(b) furnace voltage

Figure 6 Red phase voltage waveforms, three phase model

L.II Reference [77]

The Computational Modelling of an Electric Arc Furnace

D R Turner and I C Davis

The University of Liverpool

Introduction

Residents of steel towns are frequently aware of the effects of electric arc furnaces on the supply system voltage level - as witnessed by the flicker of tungsten filament lamps. However, for certain steel making processes, this type of furnace represents the best production method, and thus there is considerable interest in possible methods of controlling voltage fluctuations. Control of voltage by shunt reactive compensators - particularly for relatively slow voltage changes, has been employed by power system authorities for some time, and following advances in solid state technology thyristor controlled static var compensators have been available for system voltage control (1). Along with saturated reactor compensators (2), thyristor controlled equipment (3) has been used by a number of installations to provide voltage and flicker control at arc furnace sites. One of the requirements of equipment used for this purpose is that it should have a fast speed of response. For thyristor controlled reactors, one possible way to reduce the response time is to increase the phase number, and the work described in this paper is part of a study of thyristor controlled reactors (T.C.R's) with higher phase numbers.

To evaluate the performance of such equipment in the laboratory it is necessary to model, either computationally or experimentally the furnace and supply system. Both methods are being used by the authors, the experimental model is described elsewhere (5), and both use a similar approach to the problem of the random nature of the furnace currents.

A number of workers have approached the modelling of arc furnaces in different ways. Granstrom (6) uses a value of arc resistance or current which is a function of time, using sinusoidal, square and random functions alone or in combination. Dugan (7) describes the use of a transient network analyser with harmonic current sources to represent the furnace, but comments that this does not represent the random nature of the furnace currents. The method described in this paper makes use of recorded values of furnace currents as the input to the model, which represents the supply system by constant resistance and inductance. Macedo (8) has shown that the system is a dynamic one and that the impedance changes with time, and it is well known that the system impedance is a more complex function of frequency than $(R + j\omega L)$ due to the capacitance of the system as well as the nature of other loads. Both these effects are ignored in the work presented in this paper but the model is to be extended to include system capacitance.

Description of the Model

Figure 1 shows the supply system to the Templeborough Plant of British Steel upon which both the computational and experimental models are based. The C.E.G.B. with the co-operation of the steel makers have recorded furnace currents and voltages at the 33 kV busbars and these records have been made available to the authors, figure 2 shows a few cycles of one phase current for the start up of a

56 MVA furnace. The aim of the model is to calculate the voltage at the 33 kV busbars given the furnace currents, thus these form an 'input' to the computer model.

Looking at figure 1, it is seen that the 33 kV busbar is supplied by star-delta transformers, and for the non-sinusoidal, unbalanced currents the delta connection introduces a coupling between phases, a topic which does not yet seem to have been considered in detail. For three phase transformers constructed on a single three limbed core there are mutual inductances between the phases which act as another source of coupling important to unbalanced operation, but these are ignored in the results presented here.

For a star-delta transformer shown in figure 3 the line currents on the delta side can be expressed simply in terms of the branch currents by the relationship:

$$[I_{\Delta L}] = [C] \cdot [I_{\Delta B}] \quad \text{where } [C] = \begin{bmatrix} 1 & 0 & -1 \\ -1 & 1 & 0 \\ 0 & -1 & 1 \end{bmatrix}$$

C is a singular matrix thus its inverse does not exist, physically this means that the branch currents $[I_{\Delta B}]$ cannot be expressed in terms of $[I_{\Delta L}]$ unless there is some additional condition, since any circulating current in the delta has no effect on the line currents. It is essential however that a relationship be derived in order to evaluate the line currents on the high voltage side of the Transformer since $[I_{\Delta L}]$ are the "driving function" of the model. It was expected that the instantaneous sum of the furnace currents would be zero and inspection of the recorded current waveforms showed this to be so within experimental error, further any circulating currents in the delta must be due to zero sequence currents flowing on the high voltage star side of the transformer, and these are most likely to be sinusoidal in nature. Thus assuming that the circulating current is zero yields:

$$[I_{\Delta B}] = \frac{1}{3} \begin{bmatrix} 1 & -1 & 0 \\ 0 & 1 & -1 \\ -1 & 0 & 1 \end{bmatrix} \cdot [I_{\Delta L}] \quad (1)$$

The line currents on the star side $[I_V]$ are related to the branch currents on the delta side $[I_{\Delta B}]$ by the transformer turns ratio.

The voltages measured at the 33kV busbars are phase values determined by three star connected voltage transformers. Assuming that these are identical and that the sum of the currents at the star point is zero then

$$[V_{\Delta p}] = \frac{1}{3} \cdot \begin{bmatrix} 1 & 0 & -1 \\ -1 & 1 & 0 \\ 0 & -1 & 1 \end{bmatrix} [V_{\Delta L}] \quad (2)$$

and it is noted that this transformation is the transpose of that for the currents, equation (1).

Using a step-by-step technique with the furnace currents of the 33kV bus-bars and their rates of change specified, the currents $[I_Y]$ can be determined by equation (1), thus referring to figure 4

$$[V_Y] = [V_B] - L_s \frac{d}{dt} [I_Y] \quad (3)$$

$[V_{\Delta L}]$ and $[V_Y]$ are related by the transformer turns ratio, thus from $[V_{\Delta L}]$ using equation (2) the voltages $[V_{\Delta P}]$ are found and then

$$[V_f] = [V_{\Delta P}] - (L_r + L_t) \frac{d}{dt} [I_f] - (R_t + R_l) [I_f]$$

As the computation continues the variation of $[V_f]$ with time is determined. It is necessary to achieve the correct phase relationship between the busbar voltage and the furnace currents. This is achieved by labelling the current values which occur at the points of measured busbar voltage zero crossing and ensuring that these coincide with the calculated voltage zero crossings by adjusting the phase of the voltage $[V_B]$.

Results

Figures 5 (a) and (b) show the predicted and measured phase voltages for the red and blue phases over $5\frac{1}{2}$ cycles, and the distortion of the voltage waveform is clearly seen. It is seen that whilst the magnitudes of the measured and predicted voltages are in reasonable agreement there is some discrepancy in the detailed shape of the waveforms, due to the limitations of the model mentioned earlier, this is obviously a topic which needs further investigation.

Acknowledgment

The authors wish to thank the C E G B for their support, help and encouragement and Professor J H Leck and the University of Liverpool for providing the laboratory and computer facilities.

References

- (1) Enberg, K., Frank, H. and Torseng, S. "Reactors and capacitors controlled by thyristor for optimum power system VAR control" EPRI Seminar, Oct 1978, Duluth, Minnesota, U S A.
- (2) Kennedy, M W., Laughran, J. and Young D J. "Application of a static suppressor to reduce voltage fluctuations caused by a multiple arc furnace installation" I E E Conf. Pub. No 110, 1974.
- (3) Seki, A., Nishidai, J. and Murotani, K. "Suppression of flicker due to arc furnaces by a thyristor-controlled VAR compensator" Paper A78 590-2 I E E E, PES summer meeting July 1978, Los Angeles, U S A

- (4) Ashmole, P. H., Murray, B. E. and Young, D J. "An assessment of compensation equipment for arc furnace supplies" Proc. U I E 9th Int. Congress, 1980, Cannes, France.
- (5) Turner, D R., Watkinson P. and Davis, I C. "Modelling of an electric arc furnace" To be presented at the I E E Int. Conf. Sources and effects of power system disturbances, London, May 1982.
- (6) Granstrom, S. "Computer studies of voltage fluctuation caused by arc furnaces". Proc U I E 9th Int. Congress, 1980, Cannes, France.
- (7) Dugan, R. C. "Simulation of arc furnace power systems" Paper P I D 77-5 I E E E Industry Applications Soc. Annual Meeting 1977 Los Angeles, U S A.
- (8) Macedo, F X. "Monitoring of system impedance using arc furnace disturbances" Proc. 16th Universities Power Engineering Conference, April 1981, Sheffield, England.
- (9) Kron, G., "Tensor analysis of networks" New York: Wiley 1938 and London: MacDonald 1965.

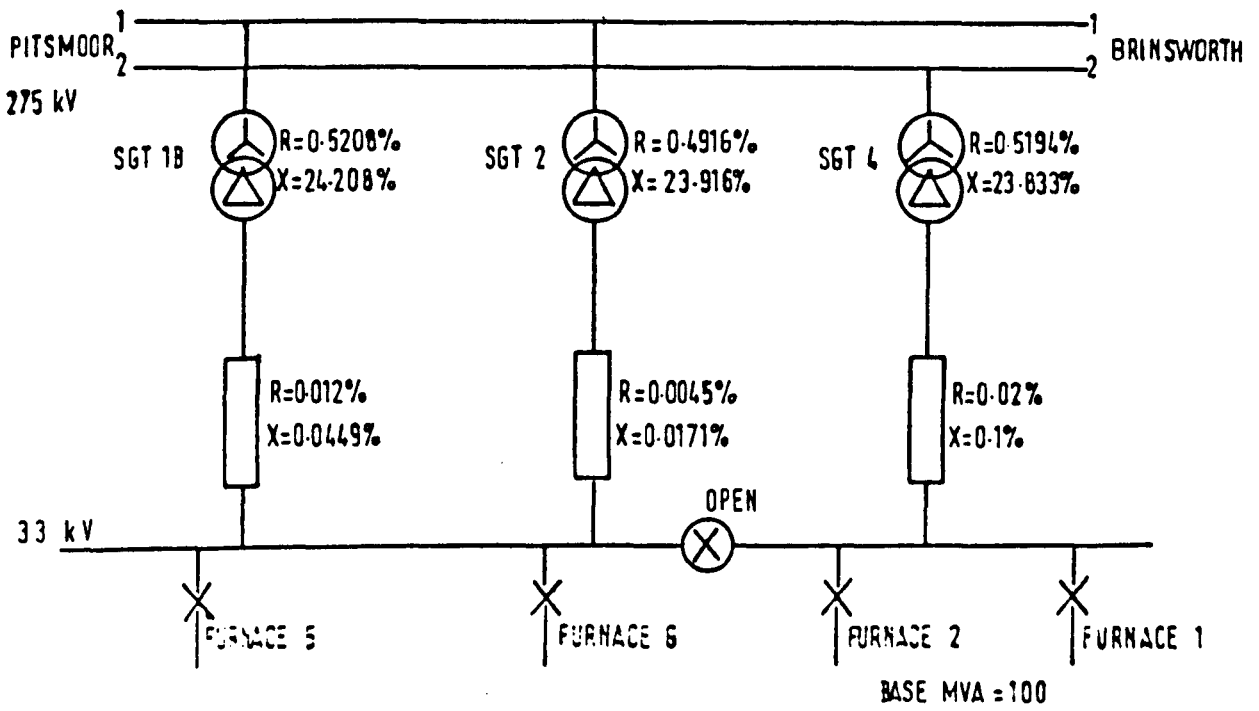


Figure 1 Supply to Templeborough Furnaces

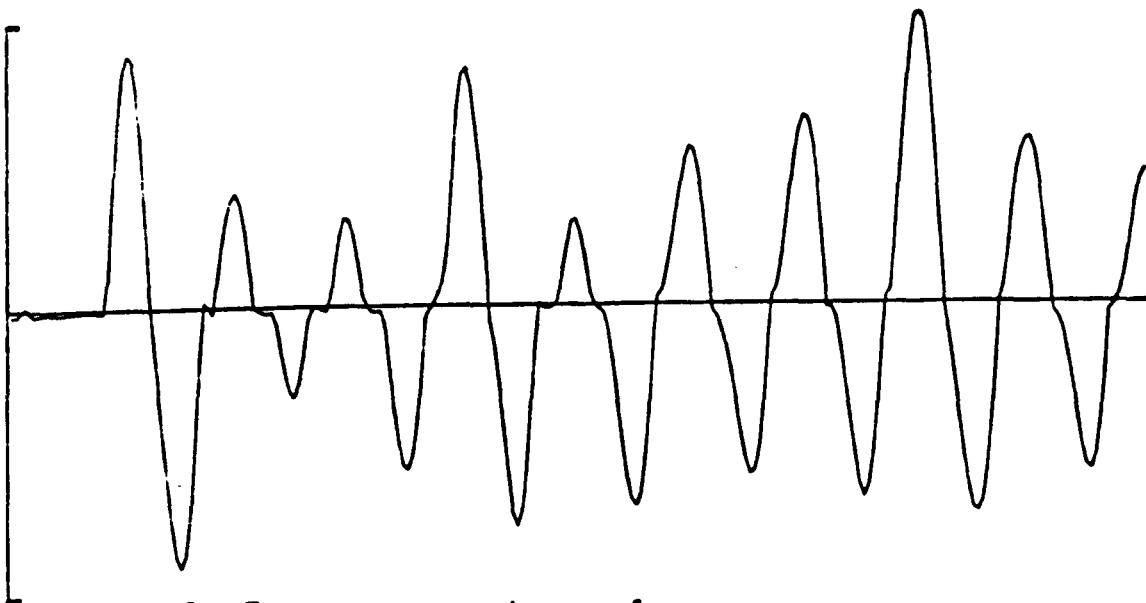


Figure 2 Furnace current waveform

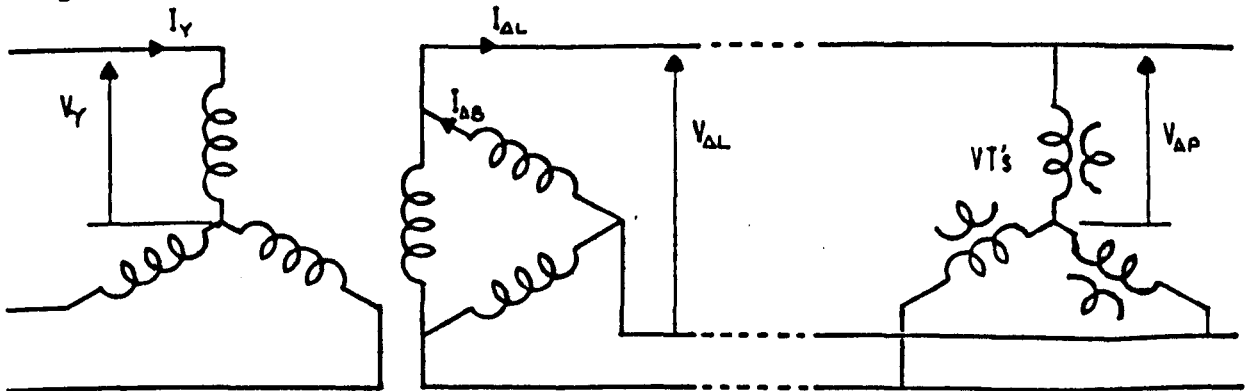


Figure 3 Star-Delta Transformer and derivation of secondary phase voltage

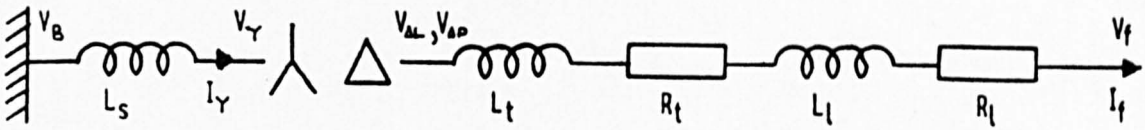
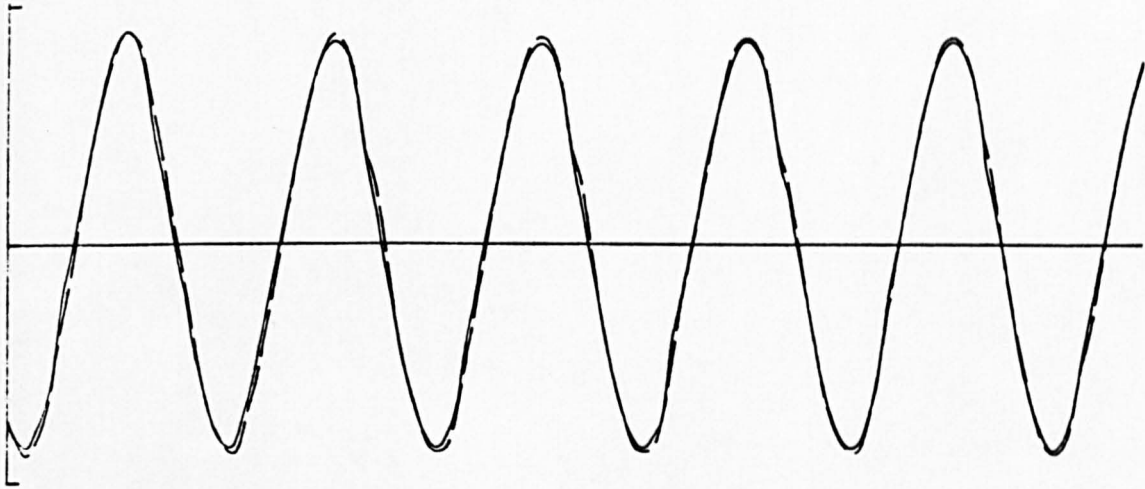
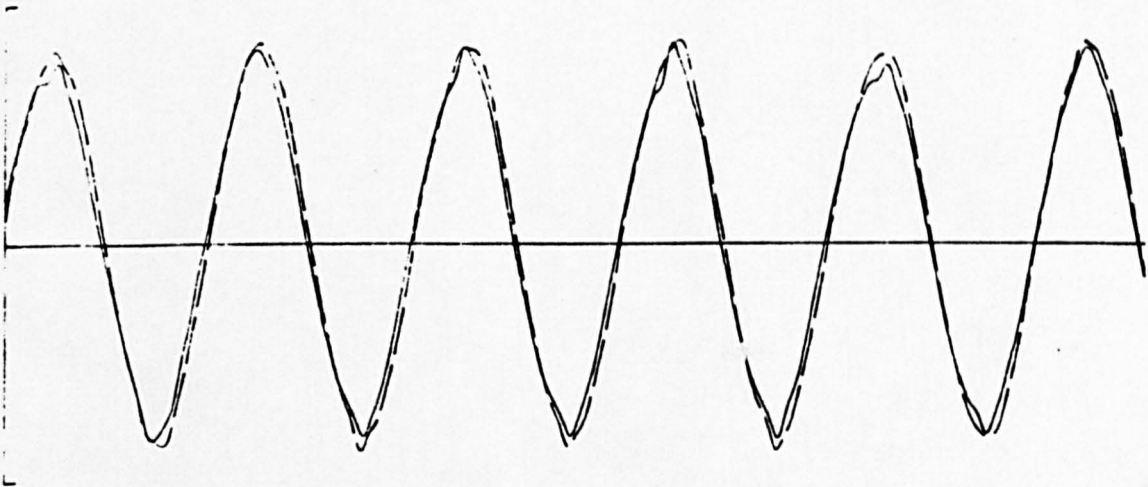


Figure 4 Equivalent Circuit



(a) Red Phase

— — recorded
 ——— calculated



(b) Blue Phase

— — recorded
 ——— calculated

Figure 5 Predicted and Measured Phase Voltage ——— 33kV Busbar